Technical Report Summary

Initial Assessment of the NORI Property, Clarion-Clipperton Zone
Deep Green Metals Inc.

In accordance with the requirements of SEC Regulation S-K (subpart 1300)

AMC Project 321012
17 March 2021

Unearth a smarter way

1 Summary

1.1 Introduction

A very large resource of polymetallic nodules, containing nickel, manganese, cobalt, and copper is located on the seafloor in the Clarion-Clipperton Zone (CCZ) of the north-east Pacific Ocean. DeepGreen Metals Inc. (DeepGreen) has identified the potential to recover metals from polymetallic nodules to support increasing demand from battery and electric vehicle production. Unlike most mining processes, the proposed mineral processing flowsheet seeks to make by-products rather than substantial waste streams and is not expected to require tailings ponds or other large-scale waste storage on-site.

Nauru Ocean Resources Inc (NORI), a wholly-owned subsidiary of DeepGreen, holds exploration rights to four areas (NORI Area A, B, C, and D, the Property) in the CCZ that were granted by the International Seabed Authority (ISA) in 2011. NORI is sponsored to carry out its mineral exploration activities in the Property by the Republic of Nauru, pursuant to a certificate of sponsorship signed by the Government of Nauru on 11 April 2011. DeepGreen commissioned AMC Consultants Pty Ltd (AMC) to undertake an Initial Assessment (IA) of the Mineral Resource contained in NORI Area D (the Project) and compile a Technical Report Summary compliant with SEC Regulation S-K (subpart 1300).

Four consortia of off-shore development companies demonstrated the technical feasibility of collecting, lifting, and converting nodules into metals in the 1970s, but development of the industry was frustrated by the absence of regulation and a governing body. In 1994 the United Nations established the ISA pursuant to the United Nations Convention on the Law of the Sea (UNCLOS). The ISA governs the development of seabed resources in the territories beyond the exclusive economic zones governed by coastal states. This international territory is known as the Area. The ISA is in the process of finalising the regulations for development of seabed resources from the CCZ and other resources in the Area. The ISA had declared a target of 2020 to have the regulations approved but the COVID-19 pandemic disrupted the ISA program.

A phased development is outlined for NORI Area D. Offshore collection systems, comprising collector vehicles on the seafloor, a riser and lift system (RALS), and a production support vessel would collect polymetallic nodules. The nodules would be transferred to transport vessels and shipped to on-shore processing facilities where established processing technology would be used to produce copper cathode, nickel sulphate and cobalt sulphate suitable for Li Ion battery cathode feedstock, nickel-copper-cobalt alloy, manganese silicate, and ammonium sulphate.

A drillship, the Hidden Gem, will be converted to undertake a pre-production Collector Test in which a collector vehicle, RALS and other systems will be tested. The first phase of commercial production (Project Zero) would then commence after the upgrading of the Hidden Gem to produce a production support vessel that can produce up to 1.3 Mtpa (wet) of nodules. The nodules would be processed through existing third-party facilities on a tolling basis. In Project One, production will be expanded with an additional converted drillship (Drill Ship 2), a second upgrade to the Hidden Gem, and construction of a bespoke production support vessel (Collector Ship 1). Ultimately, the fleet of three production support vessels, each with a dedicated seafloor collection system, would produce an average of ~12.5 Mtpa of wet nodules during steady state production. In Project One, the majority of nodules would be processed at a new facility to be constructed by NORI, with the balance of production going to toll treatment.

This phased approach to development allows for management of risk and for progressive improvement of engineering and operating systems. It will also enable NORI to adopt an adaptive management approach to environmental management.

The IA indicates a positive economic outcome. Undiscounted post-tax net cash flow of US$30.6 billion is expected. An internal rate of return of 27% has been modelled. Discounted cash flow analysis of unleveraged real cash flows, discounting at 9% per annum, indicates a current project net present value of US$6.8 billion. The analysis indicates that the Project will generate

approximately US$7.2 billion in undiscounted royalties payable to the ISA and Nauru and US$9.1 billion in on-shore corporate tax payable to the host nation of the process plant.

An IA is a conceptual study of the potential viability of Mineral Resources. This IA indicates that development of the NORI Area D Mineral Resource is potentially technically and economically viable, however, due to the preliminary nature of project planning and design, and the untested nature of the specific seafloor production systems at a commercial scale, economic viability has not yet been demonstrated.

1.2   Location

The NORI Property is located within the CCZ of the northeast Pacific Ocean (Figure 3.1). The CCZ is located in international waters between Hawaii and Mexico. The western end of the CCZ is approximately 1,000 km south of the Hawaiian island group. From here, the CCZ extends over 4,500 km east-northeast, in an approximately 750 km wide trend, with the eastern limits approximately 2,000 km west of southern Mexico. The region is well-located to ship nodules to the American continent or across the Pacific to Asian markets.

The NORI Property comprises four separate blocks (A, B, C and D) in the CCZ with a combined area of 74,830 km². These areas were previously explored by three Pioneer Investors. The NORI Area D Project covers 25,160 km² and is the easternmost of the four NORI exploration areas. Its centre point is at latitude 10° 29′ N and longitude 116° 57′ W, approximately 850 km due west of the nearest land—the uninhabited Clipperton Island.

1.3   The ISA and the NORI tenements

The international seabed area (otherwise known as the Area) is defined as the seabed and subsoil beyond the limits of national jurisdiction (UNCLOS Article 1). The principal policy documents governing the Area include:

–   The United Nations Convention on the Law of the Sea, of 10 December 1982 (The Convention).
–   The 1994 Agreement relating to the Implementation of Part XI of the United Nations Convention on the Law of the Sea of 10 December 1982 (the 1994 implementation Agreement).

Part XI of the Convention and the 1994 Implementation Agreement deals with mineral exploration and exploitation in the Area, providing a framework for entities to obtain legal title to areas of the seafloor from the ISA for the purpose of exploration and eventually exploitation of resources.

The Convention entered into force on 16 November 1994. As of 20 August 2020, the Convention had been signed by 167 states (countries) and the European Union. The United States of America is currently not a party to the Convention.

The ISA is an autonomous international organisation established under the Convention and the 1994 Implementation Agreement to organise and control activities in the Area, particularly with a view to administering and regulating the development of the resources of the Area in accordance with the legal regime established in the Convention and the 1994 Implementation Agreement.

All rules, regulations, and procedures issued by the ISA to regulate prospecting, exploration, and exploitation of marine minerals in the Area are issued within a general legal framework established by the Convention and the 1994 Implementation Agreement.

To date, the ISA has issued regulations on prospecting and exploration for polymetallic nodules in the Area. In March 2019, the Council of the ISA released the advance and unedited text (English only) of the Draft Regulations on Exploitation of Mineral Resources in the Area (ISBA/25/C/WP.1) (ISA, 2019).

In July 2011, NORI was granted a polymetallic nodule exploration contract by the ISA. The contract was granted pursuant to the Regulations on Prospecting and Exploration for Polymetallic Nodules in the Area (adopted 13 July 2000) and formalises an exploration area, a term of 15 years for the contract, and a program of activities for the first five-year period (NORI Exploration Contract). The contract also formalises the rights of NORI around tenure. Pursuant to the Regulations, NORI has the priority right to apply for an exploitation contract to exploit polymetallic nodules in the same area (Regulation 24(2)).

The NORI Exploration Contract may be extended for periods of five years at a time beyond the initial 15-year period, provided NORI has made efforts in good faith to comply with the requirements of the plan of work.

In 2020, NORI acquired the polymetallic nodule exploration contract awarded by the ISA to Tonga Off-shore Mining Limited (TOML). TOML Area F is immediately west of NORI Area D.

1.4   Geology and Mineral Resources

Seafloor polymetallic nodules occur in all oceans but the CCZ hosts a relatively high abundance of nodules. The CCZ seafloor forms part of the Abyssal Plains, which are the largest physiographic province on Earth.

The average depth of the seafloor in the Project Area is 3,800 to 4,200 m. Overall, the seafloor slopes at approximately 0.57° (1 m per km) but the Abyssal Plains are traversed by ridges, with amplitude of 50 to 300 m (maximum 1,000 m) and wavelength of 1 to 10 km. The Abyssal Plains are punctuated by extinct volcanoes rising 500 to 2,000 m above the seafloor.

Seafloor polymetallic nodules rest on the seafloor at the seawater - sediment interface. They are composed of nuclei and concentric layers of manganese and iron hydroxides and are formed by precipitation of metals from the surrounding seawater and sediment pore waters. Nickel, cobalt and copper are also precipitated and occur within the structure of the manganese and iron minerals.

Nodules are abundant in abyssal areas with oxygenated bottom waters and low sedimentation rates (less than 10 cm per thousand years). Nodules generally range from about 1 to 12 cm in their longest dimension. Nodules of 1 to 5 cm are typically the most common in NORI Area D, where they have been classified as Type 1 nodules.

The specific conditions of the CCZ (water depth, latitude, and seafloor sediment type) are considered to be the key controls for the formation of polymetallic nodules.

Information on the mineralisation within NORI Area D comprises a combination of sampling undertaken by NORI as well as free-fall grab sampler (FFG) and box core sampler (BC) data supplied by the ISA at the time of the NORI application and also supplied by the ISA to NORI in 2012. Additional regional data, assembled by the ISA as part of its Geological Model Project during 2008 to 2010 (ISA 2010), are available. The data provide significant coverage over NORI Area D and indicate a high abundance of nodules in this region, as has been confirmed by NORI's exploration.

NORI completed off-shore exploration campaigns in 2012, 2013, 2018, 2019 and 2020. During these campaigns a variety of data was collected including:

- Bathymetric mapping of the whole of NORI Area D using a hull-mounted Kongsberg Simrad EM120 12 kHz, full-ocean depth multibeam echo-sounding system (MBES). This system also provided backscatter data with which seafloor characteristics could be interpreted.
- Detailed seafloor survey work with an autonomous underwater vehicle (AUV), utilising an MBES, Side Scan Sonar (SSS), Sub-Bottom Profiler (SBP), and camera payload.
- A total of 252 box core samples collected using a 0.75 m² box corer, mainly on a 10 km by 10 km square grid.

The nodules in the box cores were collected, and their characteristics measured and recorded in detail. Samples of nodules were collected in duplicate and assayed at two reputable, well-qualified laboratories: ALS and Bureau Veritas. Certified reference material, and blank samples were inserted to provide additional levels of quality control. No significant issues were identified with the assay results.

The backscatter data and the sidescan sonar and seafloor photography indicate strong continuity of nodule abundance across NORI Area D. There is a clear relationship between nodule long axis length and nodule weight and therefore it is possible to estimate nodule abundance from photographs. Several estimation techniques were tested, and methodologies were developed that are suitable for closely packed (Type 1) and less closely packed (Type 2 and 3) nodules.

Mineral Resources were estimated using a two-dimensional block model. Estimates of nodule abundance and nickel, manganese, cobalt, and copper grades were performed using kriging. A variety of methods was used to validate the estimates, including conditional simulation. The estimates of nodule abundance were used to calculate the tonnage of the Mineral Resources.

The bathymetric mapping enabled the interpretation of parts of seafloor that are possibly too steep for recovery of nodules using the systems considered in this IA. Seafloor areas with slopes steeper than 6° were excised from the 2020 Mineral Resource estimate.

The Mineral Resource was classified on the basis of the quality and uncertainty of the sample data and sample spacing, in accordance with SEC Regulation S-K (subpart 1300).

The Measured Mineral Resource was assigned to the area within NORI Area D where box-core sampling was conducted on a nominal 7 km by 7 km spacing and infilled with estimates of nodule abundance from seafloor photography to a spacing of 3.5 km by 3.5 km.

The Indicated Mineral Resource was assigned to the area within NORI Area D where box-core sampling was conducted on a nominal spacing of 7 km by 7 km or 10 km by 10 km but without additional photo-estimates of nodule abundance.

The Inferred Mineral Resource was assigned to the areas of abyssal plain in the southeast corner of NORI Area D that are largely unsampled. The volcanic high in the southeast corner was excluded from the mineral resource estimate due to the high level of uncertainty about nodule abundance and grades in this domain.

The new Mineral Resource estimate for NORI Area D, with an effective date of 31 December 2020, is reported in Table 1.1 at a 4 kg/m^2 abundance cut-off. This cut-off is derived from the estimates of costs and revenues presented in this Initial Assessment.

Whilst the IA focusses on the development of mining operations in NORI Area D, NORI holds another three areas in the CCZ under the same title. These Areas (NORI Area A, B and C) are estimated to contain Inferred Mineral Resources of 510 Mt (wet) at 1.28% Ni, 0.21% Co, 1.04% Cu, 28.3% Mn, at an average abundance of 11 kg (wet)/m^2 at a 4 kg/m^2 abundance cut-off (Golder, 2013) (effective date of 31 December 2020). The polymetallic nodule mineralisation in Areas A, B and C has similar characteristics to NORI Area D and it is reasonable to assume that the technology proposed in the IA would be suitable for development of these additional areas.

Table 1.1   NORI 2020 Mineral Resource estimate, in situ, for NORI Area D at 4 kg/m^2 abundance cut-off

NORI Area	Category	Tonnes (Mt (wet))	Abundance (wet kg/m²)	Nickel (%)	Copper (%)	Cobalt (%)	Manganese (%)	Silicon (%)
D	Measured	4	18.6	1.42	1.16	0.13	32.2	5.13
D	Indicated	341	17.1	1.40	1.14	0.14	31.2	5.46
D	Measured + Indicated	345	17.1	1.40	1.14	0.14	31.2	5.46
D	Inferred	11	15.6	1.38	1.14	0.12	31.0	5.50

Note: Tonnes are quoted on a wet basis and grades are quoted on a dry basis, which is common practice for bulk commodities. Moisture content was estimated to be 24% w/w. These estimates are presented on an undiluted basis without adjustment for resource recovery.

1.5   Development plan

NORI proposes to implement the project in multiple phases that will allow the seafloor mining systems to be tested and then nodule production to be gradually ramped up. The phased approach will facilitate de-risking of the project for relatively low initial capital investment. Additionally, this phased development will allow for an adaptive approach to environmental management providing learning at small-scale which would be applied as the development increases scale.

The proposed seafloor production development phases are as follows:

- The Collector Test is designed to perform proof of concept for the methods of collecting and lifting the nodules while acquiring sufficient data to design a commercial system. Nodules collected during the test would be stored on the Hidden Gem and brought to shore for use in large scale process pilot testing. The Collector Test would use a converted sixth generation drillship, the Hidden Gem. The test would not demonstrate the transhipment of nodules to a shore-based facility.
- Project Zero would be an extension of the Collector Test using an upgrade of the Hidden Gem to produce a sufficient and continuous quantity of nodules to support a relatively small commercial operation of about 1.3 Mtpa (wet) nodules delivered to a shore-based facility. This operation would demonstrate a more continuous mining operation at a larger scale than the Collector test and would demonstrate the transhipment of nodules to a processing facility. It would also allow for the implementation and testing of adaptive management systems to ensure environmental compliance.
- Project One would increase production in a further three steps: 1) introduction of a second converted drillship (Drill Ship 2) with a capacity of up to 3.6 Mtpa (wet), 2) a further upgrade of the Hidden Gem to up to 3.6 Mtpa (wet) and 3) construction of a new purpose-built production support vessel (Collector Ship 1) with capacity of up to 8.2 Mtpa (wet). Project One would benefit from lessons learned on the Collector Test and Project Zero.

The processing of the polymetallic nodules would also be ramped up in phases:

- In Project Zero, NORI proposes to toll treat polymetallic nodules at existing RKEF smelters, utilizing excess industry capacity. NORI advises there is significant interest from many parties in China to utilise RKEF plants which may become stranded as a result of the Indonesian government nickel laterite ore export ban restricting supply of the nickel laterite feedstock that they currently utilise. These RKEF plants were originally built to convert nickel laterite to nickel pig iron and could be converted to smelt polymetallic nodules.
- In Project One, a purpose-built process plant would be constructed, including pyrometallurgical and hydrometallurgical circuits. Nodule production would be increased in phases by treatment in this new plant.

1.6   Mining concept

The main items of off-shore infrastructure are the nodule collector vehicles, the riser, and three production support vessels (PSV): Hidden Gem, Drill Ship 2 and Collector Ship 1. Collector Ship 1 will be supported by a collector support vessel.

The nodules will be collected from the seafloor by self-propelled, tracked, collector vehicles. No rock cutting, digging, drill-and-blast, or other breakage will be required at the point of collection. The collectors will be remotely controlled and supplied with electric power via umbilical cables from the PSV. The collectors will traverse the seabed at a speed of approximately 0.5 m/s. Suction dredge heads on each collector will recover a dilute slurry of nodules, sediment, and water from the seafloor. Each collector will yield about 254 t/hr (dry) nodules to the process plant. A hopper on each vehicle will separate sediment and excess water, which will pass out of the hopper overflow, from the nodules, which will be pumped as a higher concentration slurry via flexible hoses to a riser.

The riser is a steel pipe through which nodules will be transferred to the surface by means of an airlift. The riser will consist of three main sections. The lower section will carry the two-phase slurry of nodules and water from the collectors to the airlift injection point. The mid-section will carry a three-phase mixture of slurry and air. This section will also include two auxiliary pipes: one to carry the compressed air for the airlift system, and one to return water from dewatering of the slurry to its subsea discharge point. The upper section of riser will have a larger diameter to account for the expansion of air in the airlift.

The airlift works by lowering the average density of the slurry inside the riser to a level lower than seawater. The difference between the hydrostatic pressure of the seawater at depth and the pressure caused by the weight of the low-density three-phase slurry column inside the riser forces the slurry column to rise. The energy to achieve the lift will be supplied by compressors housed on the PSV, which will be capable of generating very high air pressures—up to 15 MPa.

The PSVs will each support a RALS and its handling equipment, and will house the airlift compressors, collector vehicle control stations, and material handling equipment. All power for off-shore equipment, including the nodule collecting vehicles, will be generated on the PSVs. The PSVs will be equipped with controllable thrusters and will be capable of dynamic positioning (DP), which will allow the vessels and risers to track the collectors. The Collector Ship 1 PSV will be similar in size to an Aframax or New Panamax class of tanker, displacing approximately 103,000 t, and housing a crew of around 120 personnel. Nodules will be discharged from the RALS to the PSVs, where they will be dewatered and temporarily stored or transferred directly to a transport vessel.

A separate collector support vessel will remain at sea to support Collector Ship 1. It will be configured as a subsea support platform, as commonly used in oil industry, with a displacement of around 17,250 t. The function of the collector support vessel will be to facilitate collector maintenance and repair.

This IA assumes transportation of nodules will be by chartered vessels, with deadweight capacities of 35,000 to 100,000 tonnes. The vessels will require dynamic positioning capability to enable them to be loaded at sea alongside the PSV. Hydraulic offloading of the nodules from the PSV to the transport ships is assumed in this IA, but future studies will confirm the offloading mechanism.

1.7   Mineral processing and metallurgical testing

A combined pyro-metallurgical and hydro-metallurgical flowsheet was evaluated for these IA. Similar flowsheets were investigated at various times over the last several decades. NORI has undertaken bench-scale test-work and is in the process of completing pilot-scale testing of the proposed flowsheet. This work has confirmed or improved the flowsheet that was initially developed from extensive information available in the literature.

Pyrometallurgical processing of nodules has been extensively studied from the early 1970s until the present day and appears to be the preferred process for most of the other currently active nodule processing research groups. Many groups including: Kennecott; Inco; Cuban / Bulgarian; German; Indian; Japanese; and Korean have studied pyrometallurgical processing of nodules at a laboratory scale. The nodule samples for these tests were collected from their respective license areas in the CCZ. The nodules used in each of the studies have similar compositions but there are subtle variations that can have significant implications for pyrometallurgical processing. Of particular importance is the ratio of $MnO:SiO_2$ in the nodules as this impacts the choice of process operating parameters for the electric furnace smelting operation.

For Project Zero, NORI proposes to toll treat polymetallic nodules at existing RKEF smelters. During Project One, NORI proposes the progressive construction and expansion of a new pyrometallurgical and hydrometallurgical process plant for the recovery of nickel, manganese, cobalt, and copper from polymetallic nodules. This will allow for the proportion of toll treatment to be reduced.

Four rotary kiln and electric furnaces lines (RKEF) and two hydrometallurgical refineries would be required to meet the production demand for the life of the project.

The pyrometallurgical front end of the plant will use RKEF lines that calcine and smelt the nodules to form an alloy. The alloy would then be sulphidised to form a matte and then partially converted in a Peirce-Smith converter operation to remove iron. The matte from the sulphidation step would then be sent to the hydrometallurgical refinery. The pyrometallurgical process is similar to that successfully used to process some nickel laterite ores.

The hydrometallurgical refinery concept is based on a sulphuric acid leach flowsheet. A two-stage leach would be used to produce copper cathode and a pregnant leach solution rich in nickel and cobalt, while low in copper. Further processing of the pregnant leach solution is based on mixed-sulphide precipitate processing flowsheets employing solvent extraction. The final production of battery-grade nickel and cobalt sulphates would use crystallisation.

The pyrometallurgical process generates a manganese silicate stream that can be sold to the manganese industry and small converter slag stream that can be sold for industrial applications. No value has been ascribed to converter slag in this IA. The hydrometallurgical plant produces an ammonium sulphate by-product for sale to the fertiliser industry. Thus, together with the ability to recycle other hydrometallurgical side-streams to the pyrometallurgical process, the flowsheet has neither tailings ponds nor permanent slag repositories and does not generate substantial waste streams.

The average targeted processing rate for the new processing plant at full capacity is 6.4 Mtpa of nodules (dry basis). The location and host country of the processing operation has not yet been determined. Engineering design has not yet been undertaken.

Expected metallurgical recoveries are summarized in Table 1.2.

Table 1.2   Metallurgical recoveries

Process Step	Nickel Recovery (%)	Cobalt Recovery (%)	Copper Recovery (%)
Final matte	94.6%	77.4%	86.5%
Hydrometallurgical products before recycle	98.9%	98.0%	96.2%
Recycled residue	94.6%	77.4%	86.5%
Overall recovery	94.6%	77.2%	86.2%

In addition to the above base metals, 98.9% of the manganese contained in the feed will be recovered to the manganese silicate product, containing 52.6% MnO. Approximately 7.3 Mt of manganese silicate will be produced per annum (from steady state operation from 2030 onwards).

1.8 Market studies

CRU International Limited (CRU) was commissioned by NORI to provide market overviews for the four main products from the NORI Area D Project: nickel sulphate ($NiSO_4$), cobalt sulphate ($CoSO_4$), copper cathode, and a manganese product (CRU, 2020).

CRU expects $NiSO_4$ and $CoSO_4$ markets to undergo extreme growth from a relatively small current level of 181 kt nickel in sulphate and 35 kt of cobalt in sulphate in 2019, with markets to increase to 138 and 178 times their 2018 sizes respectively to 1.6 Mt nickel in sulphate and 500 kt cobalt in sulphate by 2035, with much of this growth occurring post-2025. Electric vehicle production is the driver of this forecast growth.

Copper and manganese markets are forecast to grow by 25% and 20% of their 2020 sizes by 2035 respectively. Copper and manganese demand will benefit from electric vehicle penetration, however the primary driver of growth for manganese ore will be steelmaking, and a variety of end use applications generally related to economic health for copper.

CRU expects copper and $NiSO_4$ prices to rise in real terms by 2035, while manganese and $CoSO_4$ prices are forecast to remain flat, due to current prices being at or near a high point in the cycle, recent fall in prices, and expected modest growth in the global steel industry after the COVID 19 epidemic. The long-term cost of production is expected to rise for both copper and $NiSO_4$, helping to support prices.

1.9 Environmental studies, permitting, community, or social impact

Historically, a significant amount of technical work has been undertaken within the CCZ by the Contractors and a significant body of information has been acquired during the past 40 years on the likely environmental impacts of collecting nodules from the sea floor.

NORI's off-shore exploration campaigns have included sampling to support environmental studies, collection of high-resolution imagery and environmental baseline studies. A number of future campaigns are planned to collect data on ocean currents and water quality to assist plume modelling, environmental baseline studies, box core and multicorer sampling focussed on benthic ecology and sediment characteristics.

NORI has commenced the ESIA process in support of an application for an exploitation license for the commercial mining of deep-sea polymetallic nodules. A comprehensive program of metocean and biological data acquisition is in progress to characterize the baseline conditions at a designated Collector Test site and control sites in the mining lease area.

NORI intends to manage the Project under the governance of an Environmental Management System (EMS), which is to be developed in accordance with the international EMS standard, ISO 14001:2004. The EMS will provide the overall framework for the environmental management and monitoring plans that will be required.

An Environmental Monitoring Plan (EMP) will be required. The plan will specify the objectives and purpose of all monitoring requirements, the components to be monitored, frequency of monitoring, methods of monitoring, analysis required in each monitoring component, monitoring data management and reporting. The plan will be submitted to the ISA as part of the exploitation contract application. This plan will involve an ecosystem approach incorporating an adaptive management system.

The social impacts of the off-shore operation are expected to be positive. The CCZ is uninhabited by people, and there are no landowners associated with the NORI Area D nodule project. No significant commercial fishing is carried out in the area. The Project will provide a source of revenue to the sponsor country, Nauru, and to the ISA.

The on-shore environmental and social impacts have not yet been assessed because the process plant has not been designed in detail, and the location and host country (and hence regulatory

regime) not confirmed. The planned metallurgical process will not generate solid waste products, and the deleterious elements (for example, cadmium and arsenic) content of the nodules is very low, indicating that with careful management the environmental impacts of the processing operation could be very low.

1.10 Conceptual production schedule

AMC cautions that the estimates in the production case and economic analysis are preliminary and further studies and engineering design are required before technical feasibility and economic viability can be demonstrated.

The production schedule is shown in Table 1.3.

Table 1.3   Production summary

Section	Units	Total
Nodule tonnage	Mt (wet)	254
Abundance	kg/m^2	16.9
Ni Grade	%	1.39
Cu Grade	%	1.14
Co Grade	%	0.14
Mn Grade	%	31.0
Nickel recovered to Ni Sulphate	kt	2,593
Copper cathode produced	kt	1,936
Cobalt recovered to Co sulphate	kt	206
Manganese silica produced	kt	60,398
Ammonium sulphate produced	kt	7,677
Alloy product produced	kt	377
Matte product produced	kt	688

1.11 Capital cost

The capital cost estimates for the Project are summarised in Table 1.4. Pre-project items include data gathering and studies that will occur prior to construction. Off-shore project costs include the procurement and integration of the PSVs, the collector support vessel, the fabrication of the collectors, and the RALS. On-shore project costs consist principally of the construction of the minerals processing pyrometallurgical plant and hydrometallurgical refinery. Sustaining costs are for both on-shore and off-shore assets, and closure costs are principally for rehabilitation of the on-shore minerals processing site.

Table 1.4   Capital cost estimates

Section	Cost estimate (US$ million)
Pre-project costs	237
Project costs	
Off-shore project costs	
Project Zero	204
Project One	2,244
Total	2,448
On-shore project costs	
Project One	4,786
Total	4,786
Total project costs	7,234
Sustaining capital costs (on-shore and off-shore)	2,637
Closure costs	500
Total	10,607

1.12 Operating cost

Operating costs have been estimated at US$1.8 billion per annum during steady state production (from 2030 onwards). Expenditure of a total of $37.5 billion over the life of the project on operating costs is expected. On-shore processing is the most significant operating cost.

Table 1.5   Average operating cost estimates during steady state operation (from 2030 onwards)

Section	Average Operating Cost over Life of Mine (US$ million pa)	Average Unit Cost (US$/t - wet tonne nodules recovered)	Average Unit Cost (US$/t - dry tonne processed)
Off-shore	$240.74	$19.31	$25.40
Shipping	$254.37	$20.40	$26.84
On-shore	$1,286.19	$103.14	$135.71
Other	$25.00	$2.00	$2.64
Total	$1,806.31	$144.85	$190.59

1.13 Initial Assessment

The IA used product prices forecast by CRU (CRU, 2020). The averages of the forecast prices used (from 2024 onwards) are listed in Table 1.6.

Table 1.6   Average product prices assumed in IA

Parameter	Unit	Value
Ni metal	US$/t	$16,106
Ni contained Ni sulphate	US$/t	$17,711
Mn contained in SiMn product	US$/dry metric tonne unit	$4.53
Cu metal	US$/t	$6,787
Co metal	US$/t	$46,416
Co contained in Co sulphate	US$/t	$56,991
Ammonium sulphate	US$/t	$90

Note: Manganese ores are priced in dmtu (dry metric tonne units). A unit is 10 kg, or 1/100th of a tonne. For example, a tonne of material grading 45% Mn priced at US$4.00/dmtu would be worth US$180/t.

The IA indicates a positive economic outcome. Undiscounted post-tax net cash flow of US$30.6 billion is expected. An internal rate of return of 27% has been estimated from the financial model. Discounted cash flow analysis of unleveraged real cash flows, discounting at 9% per annum, indicates a pre-tax project net present value (NPV) of US$11.2 billion and a post-tax project NPV of US$6.8 billion. The discounted cash flows and progressive NPVs are shown in Figure 1.1. Excluding the inferred mineral resources from the economic analysis, the post-tax project NPV is estimated at $6.7 billion, which is not a significant difference from the economic analysis that includes the inferred mineral resources.

Figure 1.1   Project NPV$_{2021}$ and discounted cash flow
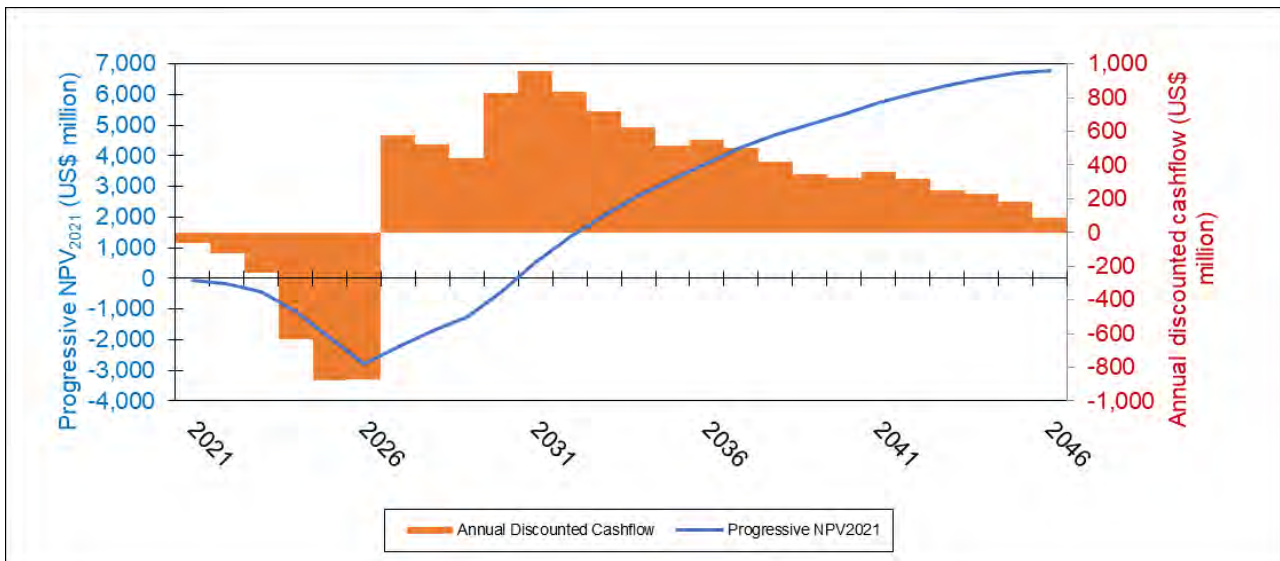
The date of the investment decision is expected to be 30 June 2023. NORI expects to spend $237 million on pre-project activities between 2021 and 2024. The future value of the project on 30 June 2023 (after the pre-project expenditure is sunk and time has elapsed) will be US$8.6 billion and the IRR from that point will be 29%.

The sensitivity of project economics to changes in the main variables was tested by selecting high and low values that represent a likely range of potential operating conditions. The variables with the biggest negative impact on NPV are all metal prices, total OPEX, collector speed, nickel sulphate price and development capex. In general, revenue drivers have the biggest impact, followed by OPEX variables and then CAPEX variables (Figure 1.2).

Figure 1.2   Tornado diagram of NPV sensitivity to variables
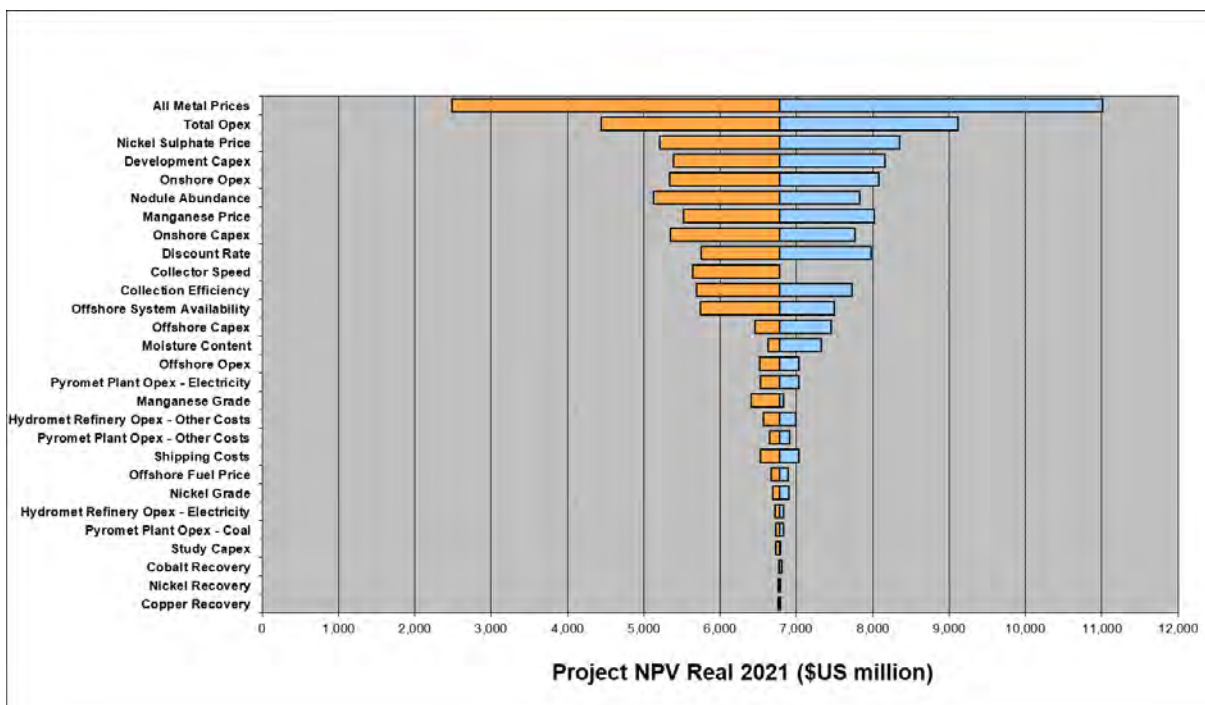
The Qualified Persons caution that this IA is preliminary in nature, and that further planning, engineering studies, design, cost estimation and seafloor tests are required before Mineral Resources can be converted to Mineral Reserves. There is no certainty that the proposals and results presented in this IA will be realized. A prefeasibility study has not yet been undertaken. Mineral Resources are not Mineral Reserves and do not have demonstrated economic viability.

Contents

Tables

Figures

Distribution list

1 e-copy to DeepGreen Metals Inc.
1 e-copy to AMC Brisbane office

List of acronyms

AAS	Atomic absorption spectroscopy
ALS	ALS Laboratory Group
AMC	AMC Consultants Pty Ltd
AMR	Arbeitsgemeinschaft Meerestechnisch Rohstoffe
APEI	Area of Particular Environmental Interest
AUV	Autonomous underwater vehicle
BC	Box core
BGR	German Federal Institute for Geosciences and Natural Resources
BV	Bureau Veritas laboratory
CCZ	Clarion-Clipperton Zone
CIM	Canadian Institute of Mining, Metallurgy and Petroleum
CV	Coefficient of variation
The Convention	United Nations Convention on the Law of the Sea 1982
DeepGreen	DeepGreen Metals Inc.
DGE	DeepGreen Engineering Pte. Ltd.
DISCOL	Disturbance and Recolonisation Experiment
DOMES	Deep Ocean Mining Environmental Study
DP	Dynamic positioning
EF	Electric furnace
EIA	Environmental Impact Assessment
EIS	Environmental Impact Statement
EMP	Environmental Management Plan
EMS	Environmental Management System
EW	Electro-winning
FFG	Free-fall grab samplers
FV	Finishing vessel
Glencore	Glencore International Ag
Golder	Golder Associates Pty Ltd.
ICP-MS	Inductively coupled plasma mass spectrometry
ID	Inside diameter
IDW	Inverse Distance Weighting – an estimation method utilising distance-weighted local averages
IFREMER	Institut Français de Recherche pour l'Exploitation de la Mer (French Research Institute for Exploitation of the Sea)
Inco	International Nickel Corporation
IOM	Interoceanmetal Joint Organisation
IRR	Internal rate of return
ISA	International Seabed Authority
IX	Ion exchange
LED	Light-emitting diode
LME	London Metal Exchange
MBES	Multi-beam echo sounder
NI 43-101	Canadian National Instrument 43-101
NOAA	National Oceanic and Atmospheric Administration
NORI	Nauru Ocean Resources Inc.
NN	Nearest neighbour estimation method
NPV	Net present value
OD	Outside diameter
OK	Ordinary kriging – an estimation method utilising distance-weighted local averages
OMI	Ocean Mining Inc.

OMCO	Ocean Minerals Company
PEA	Preliminary economic assessment
PFS	Pre-feasibility study
PLS	Pregnant liquor/leach solution
POX	Pressure oxidative leaching
PSV	Production support vessel
QAQC	Quality assurance and quality control
QP	Qualified Person, as defined by Canadian National Instrument 43-101
RALS	Riser and lift system
R-type	Rough type nodules
Regulations	Regulations on Prospecting and Exploration for Polymetallic Nodules in the Area
ROV	Remotely operated vehicle
RKEF	Rotary kiln and electric furnace
SBP	Sub-bottom profiler
S-R-type	Smooth-rough type nodules
SSS	Sidescan sonar
S-type	Smooth type nodules
SV	Sulphidation vessel
SX	Solvent extraction
TOC	Total organic carbon
TOML	Tonga Off-shore Mining Limited
UNCLOS	United Nations Convention on the Law of the Sea
USBL	Ultra-short baseline
UTM	Universal Transverse Mercator Cartesian coordinate system
UTP	Underwater transponder array
Var	Variance
WROV	Work Class remotely operated vehicle
XRF	X-ray fluorescence analysis
Yuzhmorgeologiya	State Enterprise Yuzhmorgeologiya (Russian Federation)

List of elements

Al	Aluminium
As	arsenic
Ba	barium
Ca	calcium
Cd	cadmium
Ce	cerium
Cl	chlorine
Co	cobalt
Cu	copper
Fe	iron
H_2O	hydrogen dioxide
H_2S	hydrogen sulphide
K	potassium
La	lanthanum
Mg	magnesium
Mn	manganese
MnO	manganese oxide
MnO_2	manganese dioxide
Mo	molybdenum
Na	sodium
NaHS	sodium hydro sulphide
Na_2S	sodium sulphide
Nd	neodymium
Ni	nickel
P	phosphorus
Pb	lead
REE	rare earth elements
S	sulphur
SiO_2	silicon dioxide
Sr	strontium
Ti	titanium
V	vanadium
Y	yttrium
Zn	zinc
Zr	zirconium

List of units

°	degree
°C	degrees Celsius
%	percent
% w/w	% mass/mass or weight
μm	microns
cm	centimetre
cm/s	centimetre per second
dmtu	dry metric tonne unit
G	gram
GWh	gigawatt-hours
kg	kilogram
kg/m²	kilograms per square metre (surface abundance)
km	kilometre
km²	square kilometre
kPa	kilopascal
kt	kilotonne (metric)
kt/a	kilotonnes (metric) per annum
kWh/h	kilowatt hours per hour
kWh/t	kilowatt hours per tonne
Lb	pound
M	metre
m/h	metres per hours
m/s	metres per second
m^2	square metre
m^3	cubic metre
m^3/y	cubic metres per year
mbsl	metres below sea level
mg/L	milligrams per litre
mm	millimetre
MPa	megapascal
Mt	million tonnes(metric)
Mtpa	million tonnes (metric) per annum
mV	millivolt
MW	megawatt
nm	nautical mile
Nm^3	cubic metre of gas at standard temperature and pressure
ppm	parts per million
ppmw	parts per million weight
S	second
T	tonne (metric)
t/d	tonnes (metric) per day
t/h	tonnes (metric) per hour
US$	United States dollar
y	year

2   Introduction

A very large nickel, manganese, cobalt, and copper resource occurring as polymetallic nodules is located in the Clarion-Clipperton Zone (CCZ) of the northeast Pacific Ocean between Hawaii and Mexico. The nodules are located at depths of between 4,000 to 6,000 m and have been explored with considerable success between the mid-1960s and the present day using a variety of deep-sea technologies. Successful trial extraction in the CCZ has also been carried out to demonstrate that the nodules can be collected and pumped to a surface platform and processed for recovery of metals.

Interest in seafloor mineral deposits grew through the 1960s. Several commercial and government funded organisations and consortia started exploring the oceans as part of a cooperative program known as the International Decade of Ocean Exploration. These organisations became known as Pioneer Investors.

Exploration of the seafloor in international waters is now administered by the International Seabed Authority (ISA) and regulated by the United Nations Convention on the Law of the Sea (UNCLOS). These institutions operate on the principle that the ocean floor beyond the limits of national jurisdiction, known as the Area, is the common heritage of mankind.

In July 2011, Nauru Ocean Resources Inc. (NORI), a subsidiary of DeepGreen Metals Inc. (DeepGreen), was granted an exploration contract over 74,830 km^2 (the NORI Area or the Property) in the CCZ consisting of four exploration areas (Area A, B, C and D). NORI's contract for exploration of polymetallic nodules was approved by the Council of the ISA on 19 July 2011, for a term of 15 years and then signed with the ISA on 22 July 2011.

DeepGreen commissioned AMC Consultants Pty Ltd (AMC) to undertake an Initial Assessment (IA) of the Mineral Resource contained in one of these blocks, NORI Area D, (the Project) and compile a Technical Report Summary compliant with SEC Regulation S-K (subpart 1300).

2.1   Purpose of the Technical Report Summary

AMC understands that DeepGreen may file this Technical Report Summary with Securities Exchange Commission as part of an S-4 filing to support the merger between Sustainable Opportunities Acquisition Corporation and DeepGreen Metals Inc.

2.2   Sources of information and data

This Technical Report Summary is based on information and reports supplied by NORI or in the public domain. Section 27 lists background documents that are referenced by the higher-level reports.

2.3   Field involvement

Ian Stevenson, an independent consultant trading as Margin - Marine Geoscience Innovation participated in the 2018 off-shore campaign (Campaign 3) on the Maersk Launcher which carried out surveys and sampling in the NORI Area D from 26 April - 4 June 2018. Ian Lipton, Principal Geologist, AMC, was involved in the development of sampling strategies and procedures and was in daily contact with the off-shore campaign as it was implemented, providing input as required to ensure data quality and veracity.

2.4   Personnel

The Sections that each of the Qualified Persons (QPs) were responsible for are summarised in Table 2.1. In addition, each of the QPs contributed to Sections 22 to 24, where relevant to the Sections for which they were primarily responsible.

AMC has relied upon information provided by the registrant in preparing its findings and conclusions regarding some aspects of modifying factors, as set out in Section 25.

Table 2.1   List of Qualified Persons responsible for each Section

Qualified Person	Responsible for the following report Sections:
AMC Consultants Pty Ltd	Sections 1-5, 8.2, 8.3, 8.4, 8.5, 9, 11, 12, 13.3, 13.7, 14.2, 15.1, 16, 17, 18 (except 18.3.1, 18.3.2, 18.6.1, 18.6.6), 19, 20-25
Margin - Marine Geoscience Innovation	Sections 6, 7, 8.1
Canadian Engineering Associates Ltd	Sections 10, 14.1, 14.3, 18.3.2, 18.6.6
Deep Reach Technology Inc	Section 13.1, 13.2, 13.4, 13.5, 13.6, 15.2, 18.3.1, 18.6.1

2.5 Reliance on other experts

The QPs have relied upon other experts for some sections in this report. These are summarised in Table 2.2.

Table 2.2   Reliance on other experts

Expert	Report Sections:
Picton Group Pty Ltd	Section 17

3 Property description and location

The NORI Property is located within the CCZ of the northeast Pacific Ocean Figure 3.1. The CCZ is located in international waters between Hawaii and Mexico. The western end of the CCZ is approximately 1,000 km south of the Hawaiian island group. From here, the CCZ extends over 4,500 km east-northeast, in an approximately 750 km wide trend, with the eastern limits approximately 2,000 km west of southern Mexico. The region is well-located to ship nodules to the American continent or across the Pacific to Asian markets.

Figure 3.1   Location of NORI Project and other exploration areas within the Clarion-Clipperton Zone
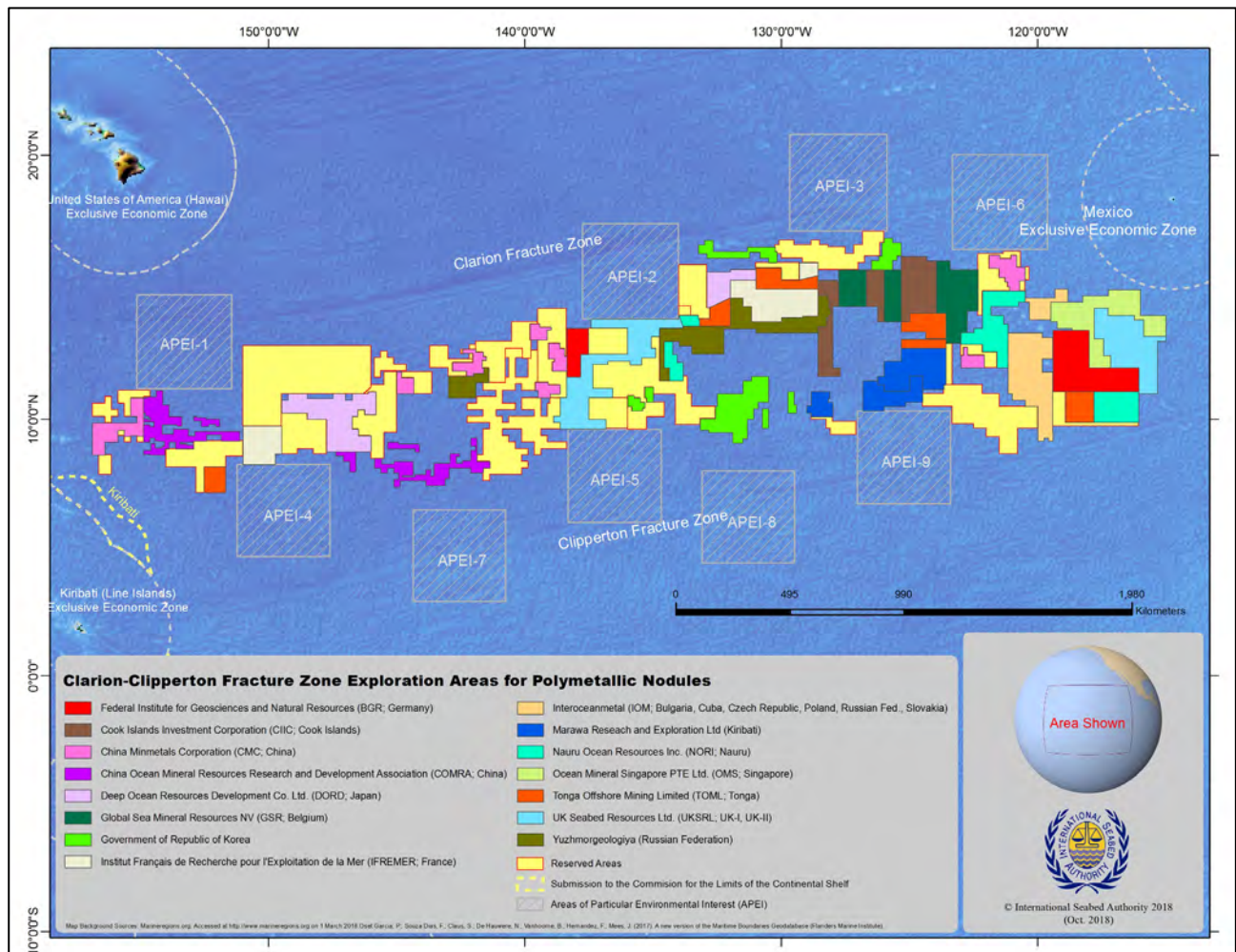
Source: https://www.isa.org.jm/map/clarion-clipperton-fracture-zone, downloaded 18 February 2021

3.1   Tenements and permits

In July 2011, NORI was granted a polymetallic nodule exploration contract by the ISA (NORI Exploration Contract). The contract was granted pursuant to the Regulations on Prospecting and Exploration for Polymetallic Nodules in the Area (adopted 13 July 2000) and formalises an exploration area, a term of 15 years for the contract, and a program of activities for the first five-year period (NORI Exploration Contract). The contract also formalises the rights of NORI around tenure. Pursuant to the Regulations, NORI has the priority right to apply for an exploitation contract to exploit polymetallic nodules in the same area (Regulation 24(2)).

The NORI Exploration Contract may be extended for periods of 5 years at a time beyond the initial 15-year period, provided NORI has made efforts in good faith to comply with the requirements of the plan of work.

The NORI contract area comprises four separate blocks (A, B, C and D) in the CCZ with a combined area of 74,830 km² Figure 3.2, Table 3.1 and Table 3.2. These areas were previously explored by three Pioneer Investors.

Figure 3.2   Detail of location of NORI Areas A, B, C and D, from Figure 4.1
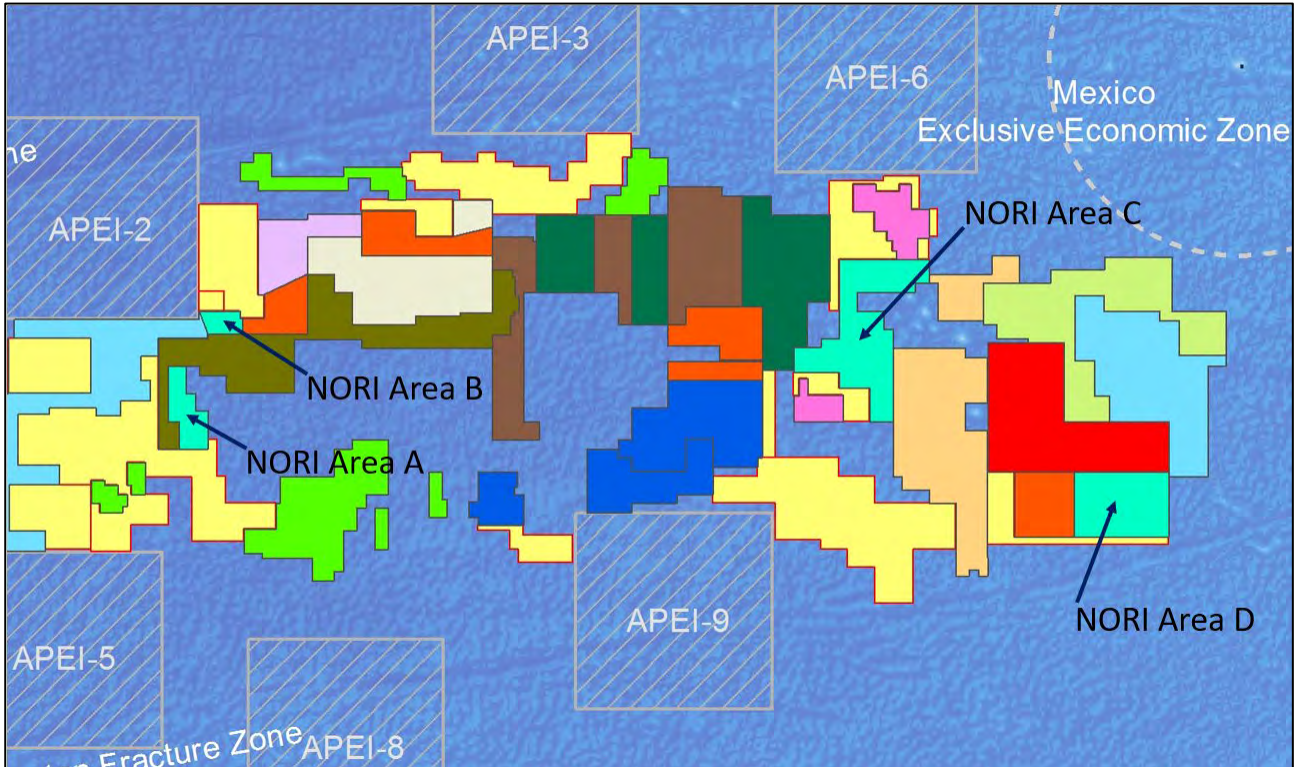
Source: https://www.isa.org.jm/map/clarion-clipperton-fracture-zone, downloaded 18 February 2021. Legend as in Figure 4.1

Table 3.1   NORI Area block details

Area	Size (km²)	ISA block number	Pioneer investor
A	8,924	13	Yuzmorgeologiya
B	3,519	15	Yuzmorgeologiya
C	37,227	22	Interoceanmetal Joint Organisation (IOM)
D	25,160	25	Arbeitsgemeinschaft Meerestechnisch Rohstoffe (AMR)

Table 3.2   NORI Area extents

Area	Minimum Latitude (DD)	Maximum Latitude (DD)	Minimum Longitude (DD)	Maximum Longitude (DD)	Minimum UTM X (m)	Maximum UTM X (m)	Minimum UTM Y (m)	Maximum UTM Y (m)	UTM Zone
A	11.5000	13.00000	-134.5830	-133.8330	545220.4	627276.0	1271339	1437255	8
B	13.5801	14.00000	-134.0000	-133.2000	607995.7	694759.8	1501590	1548425	8
C	12.0000	14.93500	-123.0000	-120.5000	500000.0	769458.3	1326941	1652649	10
D	9.8950	11.08333	-117.8167	-116.0667	410465.2	602326.1	1093913	1225353	11

DD – Decimal degrees, UTM - Universal Transverse Mercator map projection

To date, no exploitation licences for extracting minerals from the seafloor within the Area have been granted.

3.1.1   United Nations Convention on the Law of the Sea

The international seabed area (otherwise known as the Area) is defined as the seabed and subsoil beyond the limits of national jurisdiction (UNCLOS Article 1). Figure 3.3 shows a map of the Area (blue zone) as well as 200 nautical mile exclusive economic zones (grey zone) and extended

continental shelf zones (orange zone). Figure 3.4 shows the relationships between depth, distance and jurisdiction.

The principal policy documents governing the Area include:

- The United Nations Convention on the Law of the Sea, of 10 December 1982 (The Convention).
- The 1994 Agreement relating to the Implementation of Part XI of the United Nations Convention on the Law of the Sea of 10 December 1982 (the 1994 implementation Agreement).

The Convention deals with, among other things, navigational rights, territorial sea limits, exclusive economic zone jurisdiction, the continental shelf, freedom of the high seas, legal status of resources on the seabed beyond the limits of national jurisdiction, passage of ships through narrow straits, conservation and management of living marine resources in the high seas, protection of the marine environment, marine scientific research, and settlement of disputes.

Part XI of the Convention and the 1994 Implementation Agreement deals with mineral exploration and exploitation in the Area, providing a framework for entities to obtain legal title to areas of the seafloor from the ISA for the purpose of exploration and eventually exploitation of resources.

The Convention entered into force on 16 November 1994. A subsequent agreement relating to the implementation of Part XI of the Convention was adopted on 28 July 1994 and entered into force on 28 July 1996. The 1994 Implementation Agreement and Part XI of the Convention are to be interpreted and applied together as a single instrument.

As of 20 August 2020, the Convention had been signed by 167 States (countries) and the European Union. The United States of America is currently not a party to the Convention.

Figure 3.3   Map of seafloor jurisdictions
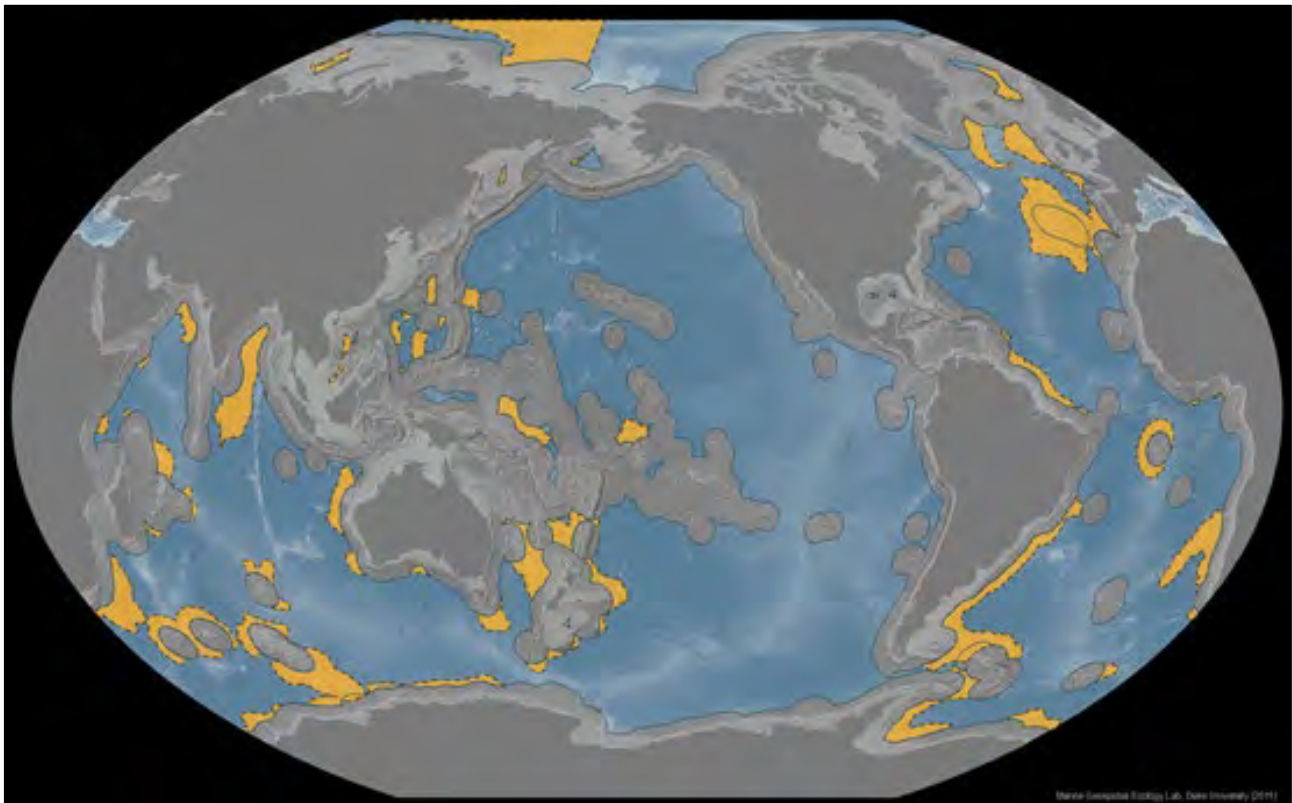
Note: International seabed area map (blue zone) as well as 200 nautical mile exclusive economic zones (grey zone) and extended continental shelf zones (orange zone). Source: Marine Geospatial Ecology Lab, Duke University (2011).

Figure 3.4   Maritime space under the 1982 UNCLOS
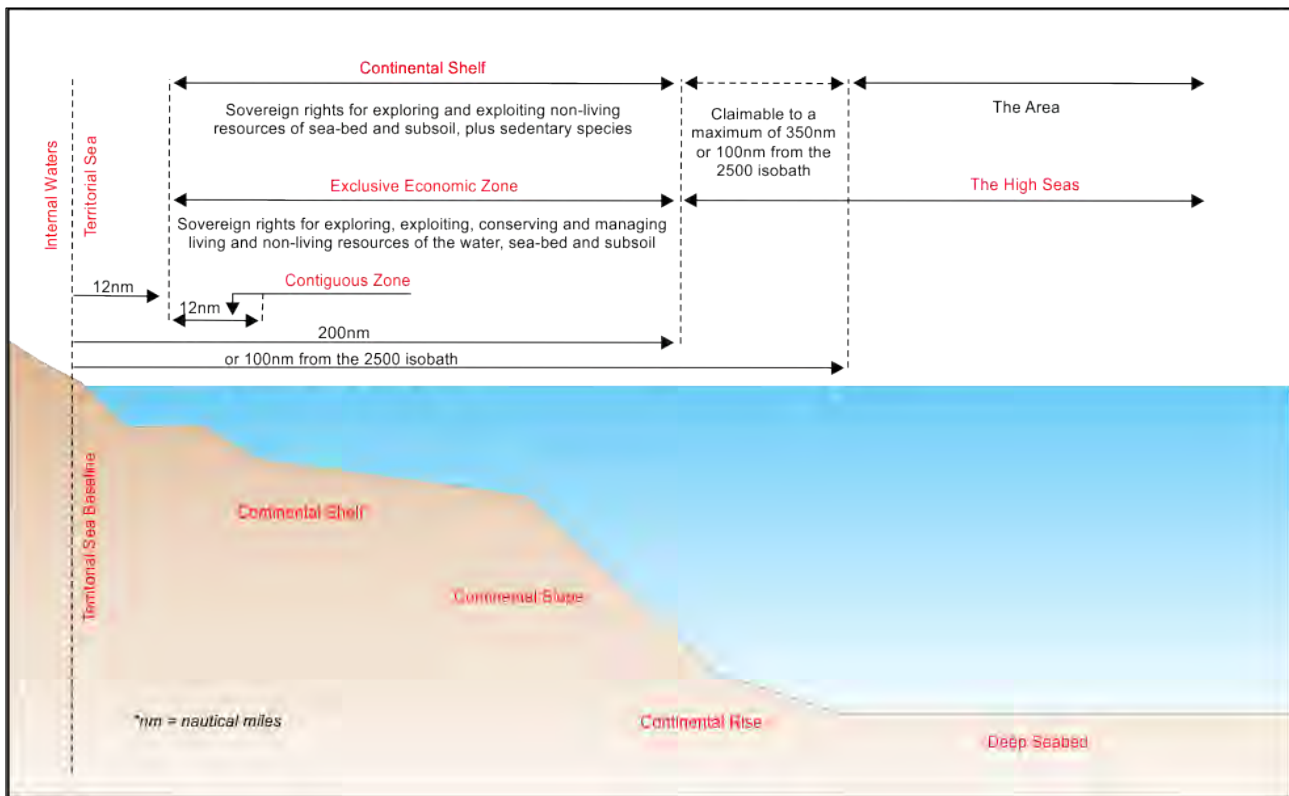
Source: DeepGreen - adapted from UNCLOS, 1982

3.1.2   International Seabed Authority

The ISA is an autonomous international organisation established under the Convention and the 1994 Implementation Agreement to organise and control activities in the Area, particularly with a view to administering and regulating the development of the resources of the Area in accordance with the legal regime established in the Convention and the 1994 Implementation Agreement.

All rules, regulations, and procedures issued by the ISA to regulate prospecting, exploration, and exploitation of marine minerals in the Area are issued within a general legal framework established by the Convention and the 1994 Implementation Agreement.

To date, the ISA has issued (https://www.isa.org.jm/mining-code/ Regulations):

•   The Regulations on Prospecting and Exploration for Polymetallic Nodules in the Area (adopted 13 July 2000; the Regulations).
•   The Regulations on Prospecting and Exploration for Polymetallic Sulphides (adopted 7 May 2010).
•   The Regulations on Prospecting and Exploration for Cobalt-Rich Ferromanganese Crusts in the Area (July 2012).

The ISA is currently working on the development of a legal framework to regulate the exploitation of polymetallic nodules in the international seabed area.

In 2014, the ISA completed a study looking at comparative extractive regulatory regimes. This was followed in March 2014 with a stakeholder survey seeking comments on what financial, environmental, and health and safety obligations should be included under the framework (ISA 2014).

In March 2019, the Council of the ISA released the advance and unedited text (English only) of the Draft Regulations on Exploitation of Mineral Resources in the Area (ISBA/25/LTC/WP.1) (ISA, 2018). The revised draft incorporated the consideration of requests addressed to the Legal & Technical Commission by the Council during the first part of the 24th Session in March 2018, comments by the Commission, and also reflected the responses to the first draft from stakeholder submissions. The ISA declared a target of July 2020 to have the regulations approved, however the July session was deferred as a result of COVID-19 pandemic.

Pursuant to paragraph 15(a) and (b) of Section 1 of the annex to the 1994 Implementation Agreement, which relates to article 162 (2)(o)(ii) of the Convention, the ISA Council must also adopt such exploitation regulations within two years of a formal request being made by any State which intends to apply for approval of a plan of work for exploitation.

3.2   NORI obligations and sponsorship

During exploration NORI, is required to, among other things:

- Submit an annual report to the ISA.
- Meet certain performance and expenditure commitments.
- Pay an annual overhead charge (currently US$60,000) to cover the costs incurred by the ISA in administering and supervising the contract.
- Implement training programs for personnel of the ISA and developing countries in accordance with a training program proposed by NORI in its licence application and five-year work plans.
- Take measures to prevent, reduce, and control pollution and other hazards to the marine environment arising from its activities in the Area.
- Maintain appropriate insurance policies.
- Establish environmental baselines against which to assess the likely effects of its program of activities on the marine environment.
- Establish and implement a program to monitor and report on such effects.

NORI is sponsored to carry out its mineral exploration activities in the Area by the Republic of Nauru, pursuant to a certificate of sponsorship signed by the Government of Nauru on 11 April 2011. Sponsorship of an entity requires the sponsoring State to certify that it assumes responsibility for the entity's activities in the Area in accordance with the Convention. NORI is a Nauruan incorporated entity and is subject to applicable Nauruan legislation and regulations.

In 2015 the Republic of Nauru enacted the International Seabed Minerals Act, which establishes the Nauru Seabed Minerals Authority to administer Nauru's sponsorship of activities carried out in the Area by companies sponsored by Nauru.

In June 2017, the Republic of Nauru and NORI entered into a Sponsorship Agreement formalising certain obligations of the parties in relation to NORI's exploration and potential exploitation of the NORI Contract Area of the CCZ.

3.2.1   Work program

As of the date of this Technical Report, NORI is in the ninth year of its exploration contract.

In 2016 NORI submitted to the ISA proposed activities for the second five-year period of its exploration contract. NORI indicated that work would focus on:

- Reducing project uncertainties and technical risks.
- Optimising the on-shore processing and off-shore production systems (including increasing performance and reliability).
- Improving project economics, including decreasing estimated capital and operating expenditure as well as increasing projected revenues.

NORI forecast estimated expenditure of US$5 million over the period 2017 to 2021, however noted the figure may be revised based upon the results of the next phase of engineering work. To date NORI has exceeded this level of expenditure on the NORI Contract Area.

3.2.2   Royalties and taxes

Royalties and taxes payable on any future production from the NORI Area will be stipulated in the ISA's exploitation regulations. While the rates of payments are yet to be set by the ISA, the 1994 Implementation Agreement (Section 8[1](b)) prescribes that the rates of payments "shall be within the range of those prevailing in respect of land-based mining of the same or similar minerals in order to avoid giving deep seabed miners an artificial competitive advantage or imposing on them a competitive disadvantage."

An ad hoc ISA working group workshop held on 21–22 February 2019 discussed a number of potential royalty and taxation regimes supported by modelling conducted by the Massachusetts Institute of Technology. No formal recommendations were forthcoming however a 2% ad valorem royalty increasing to 6% after a period of five years of production was discussed as well as a 1% ad valorem environmental levy. This is what has been included in the IA model.

Under the Sponsorship Agreement between the Republic of Nauru and NORI, upon reaching a minimum recovery level within the tenement area, NORI has agreed to pay the Republic of Nauru a seabed mineral recovery payment for polymetallic nodules recovered from the tenement area, annually adjusted (from year 5 of production) on a compounding basis based on the official inflation rate in the USA.

4 Accessibility, climate, local resources, infrastructure, and physiography

4.1 Accessibility and infrastructure

The CCZ lies between Hawaii and Mexico and is accessible by ship from various ports in the United States and South America. As the CCZ deposit does not include any habitable land and is not near coastal waters, there is no requirement to negotiate access rights from landowners for seafloor mining operations. All personnel and material will be transported to the project area by ship. The region is well located to ship nodules to the American continent or across the Pacific Ocean to Asian markets. The CCZ is generally outside major shipping lanes as indicated in Figure 4.1 which shows the global cargo shipping network, illustrating the trajectories of all cargo ships bigger than 10,000 gross tonnage during 2007.

Figure 4.1   Global cargo shipping network
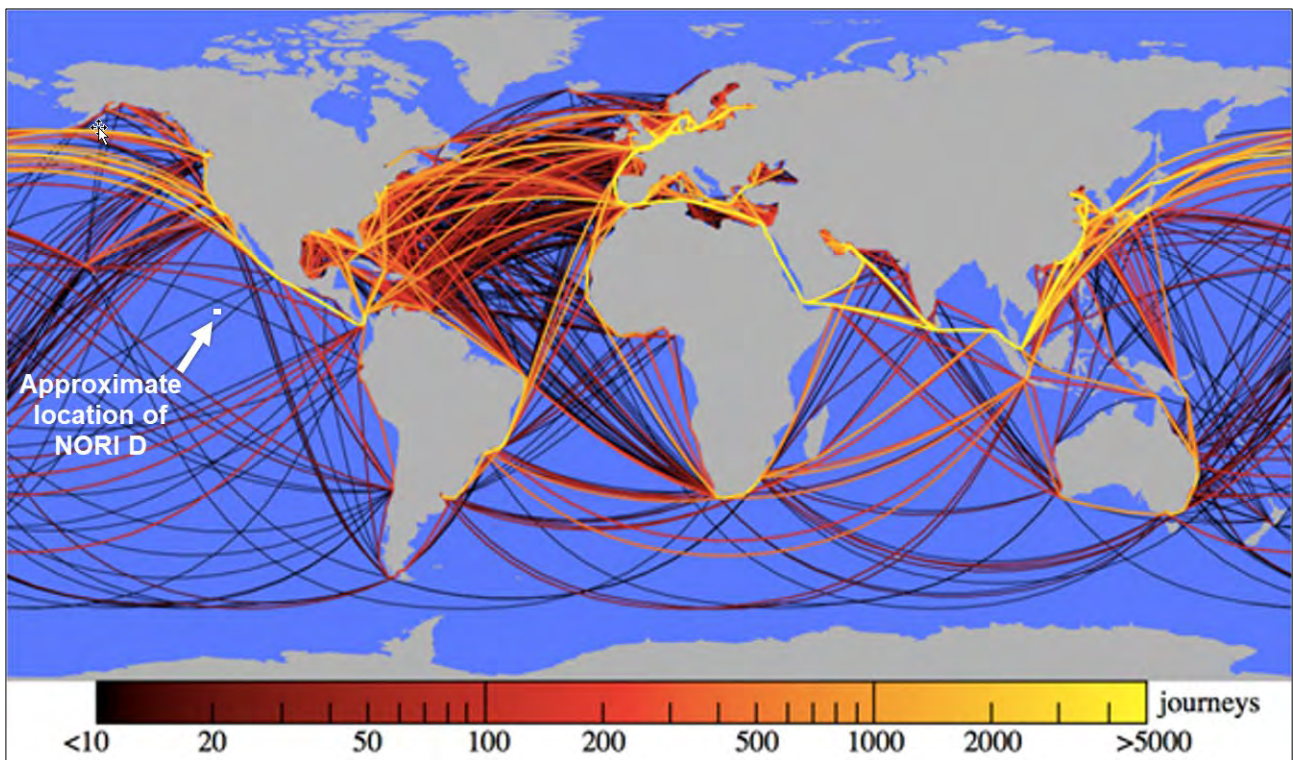
Note: The colour scale indicates the number of journeys along each route.
Source: Adapted from Kaluza et al. 2010.

4.2 Climate

The CCZ has a tropical oceanic climate, with average temperatures of from 20 to 32 °C. Minimum and maximum temperatures generally occur in March and September, respectively (ISA 2001), and the average sea surface temperature is 25 °C. The CCZ is located in open ocean and is subject to tropical weather patterns.

Off-shore operations are planned to run throughout the year, with the exception of hurricane events, which are expected to occur once every three years. Tropical hurricanes are difficult to predict due to their erratic frequency but have high intensity over short periods and occur mostly during the period from May to October (Tilot, 2006, GSR 2018).

5 History

5.1 Overview

Submarine ferromanganese concretions were first discovered in the Kara Sea off Siberia in 1868 (ISA 2010, citing Earney 1990). HMS Challenger, during its round the world expedition from 1873 to 1876, collected many small dark brown balls, rich in manganese and iron, which were named manganese nodules (ISA 2010 citing Murray and Reynard [1891], Manheim [1978], and Earney [1990]).

Since the 1960s, polymetallic nodules have been recognised as a potential source of nickel, copper, cobalt, and manganese, and have been comparatively well studied because of their potential economic importance (Mero 1965). Scientific expeditions demonstrated that polymetallic nodules have a widespread occurrence in the world's oceans although their metal content and concentration vary from region to region.

During the International Decade of Ocean Exploration and prior to the implementation of UNCLOS, many off-shore exploration campaigns were completed by international organisations and consortia. A number of at-sea trial mining operations were successfully carried out in the CCZ in the 1970s to test potential mining concepts. These system tests evaluated the performance of a self-propelled and several towed collection and mining devices, along with submersible pumps and airlift technology for lifting the nodules from the deep ocean floor to the support vessel.

The US National Oceanic and Atmospheric Administration (NOAA) monitored some of these tests as the principal effort of the Deep Ocean Mining Effects Study (DOMES II) program. The information collected during these activities provided key inputs to the impact analysis presented by NOAA in its Final Programmatic Deep-Sea Mining Environmental Impact Statement.

5.2 Pioneer Investors

For the purpose of this report the Pioneer Investors include those entities that carried out substantial exploration in the Area prior to the entry into force of the Convention, as well as those entities that inherited such exploration data. This Section describes some of the more important activities of the Pioneer Investors.

NORI Area D was originally explored by Arbeitsgemeinschaft Meerestechnisch Rohstoffe (AMR). AMR subsequently joined Ocean Management Inc. (OMI). The OMI consortium comprised Inco Ltd (Canada), AMR (Federal Republic of Germany), SEDCO Inc. (US), and Deep Ocean Mining Co. Ltd (Japan). OMI completed a successful trial mining operation in 1978. Hydraulic pumps, an air lift system, and towed collectors were tested in approximately 4,500 m of water. Approximately 800 t of nodules were recovered.

Kennecott consortium (now a division of Rio Tinto) first became seriously interested in seafloor polymetallic nodules in 1962 (Agarwal et al. 1979). In the 1970s, Kennecott developed and tested components and subsystems of a seafloor mining system, and also carried out significant polymetallic nodule metallurgical processing test work.

Using a different system to OMI, Ocean Mining Associates recovered approximately 500 t of nodules during its trial mining in the 1970s.

Between 1969 and 1974, Deepsea Ventures Inc. carried out 16 survey cruises of three to four weeks' duration each, to define the extent of the polymetallic nodule deposit discovered by them in 1969 in the CCZ. As reported by Deepsea Ventures Inc:

"These activities included the taking of some 294 discrete samples, including the bulk dredging of some 164 tons of manganese nodules from some 263 dredge stations, 28 core stations and three grab sample stations, cutting of some 28 cores, approximately 1000 lineal miles of survey of seafloor recorded by television and still photography, etc. As a result, the deposit of nodules identified with the discovery has been proved to extend generally throughout the entire area (American Society of International Law, 1975)."

Also active in the CCZ was the Ocean Minerals Company (OMCO), comprising Amoco Minerals Co. (United States), Lockheed Missiles and Space Company Inc. (United States), Billiton International Metals BV, and dredging company Bos Kalis Westminster (Netherlands). In a program lasting 16 years, OMCO collected thousands of free-fall grab and box core samples of nodules from its claim area (Spickermann 2012) and carried out trial mining. Lockheed's design efforts resulted in over 80 patents, a seafloor production system that consisted of a remote-controlled collector and crusher, a seafloor to surface slurry riser system, the first industrial scale dynamic positioning system for a vessel, and a metallurgical processing plant (Spickermann 2012).

In 1978, OMCO used a remote controlled fully manoeuvrable self-propelled miner with conveyor and crusher Figure 5.1 and Figure 5.2 to trial mine polymetallic nodules in the CCZ at approximately 4,500 mbsl. The miner used an Archimedes screw drive system to provide traction and accurate manoeuvrability on the seafloor. Nodules were picked up by the miner and transferred to the buffer, where they were to be pumped to the surface by an airlift system.

Figure 5.1   Schematic of Lockheed Group's 1970s trial mining system
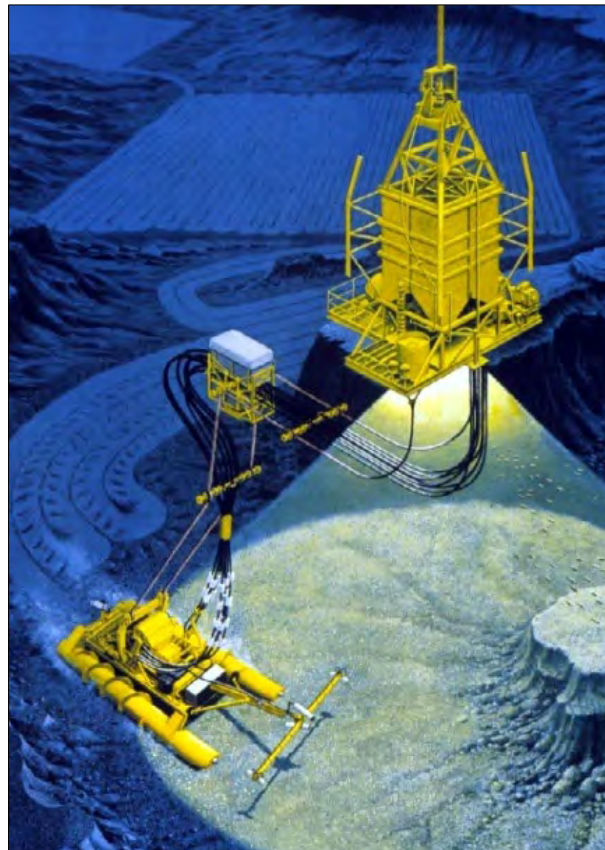
Source: DeepGreen. Used with permission of Prof. Jin Chung.

Figure 5.2   Remote operated collector used by the Lockheed Group in 1970s trial mining

Source: Spickerman 2012.

5.3   Sampling methods

Prior to NORI obtaining its exploration contract, sampling of seafloor nodules within the NORI Area was conducted by three Pioneer Investors; AMR, State Enterprise Yuzmorgeologiya of the Russian Federation and Interoceanmetal Joint Organisation (IOM), a consortium formed by Bulgaria, Cuba, the Czech Republic, Poland, the Russian Federation, and Slovakia.

Nodule samples collected by the Pioneer Investors from within the NORI Area were obtained by free-fall grab samplers (FFG) along with a few from box corers. For each sample the nodule abundance (wet kg/m^2) was derived by dividing the weight of recovered nodules by the surface area covered by the open jaws of the sampler or corer (typically 0.25 to 0.5 m^2 but in some cases as much as 1 m^2). Sample splits were dried and assayed by atomic absorption spectrophotometry (AAS) and X-ray fluorescence (XRF).

Free-fall grab samplers are currently the most productive tool available for sampling nodules. This is because a number of them can be deployed at any one time from the survey vessel allowing an order of magnitude increase in collection efficiency compared to box core sampling (i.e., approximately 10 to 20 samples per day for a FFG versus 2 to 3 samples per day for a box core (BC) that is winched to and from the seafloor). Figure 5.3 shows the operation of an FFG sampler.

Figure 5.3   Free fall grab sampler operation

(1) Free falling   (2) Photographing
(3) Bottom contact   (3) Sampling
(5) Release of ballast and start of ascent
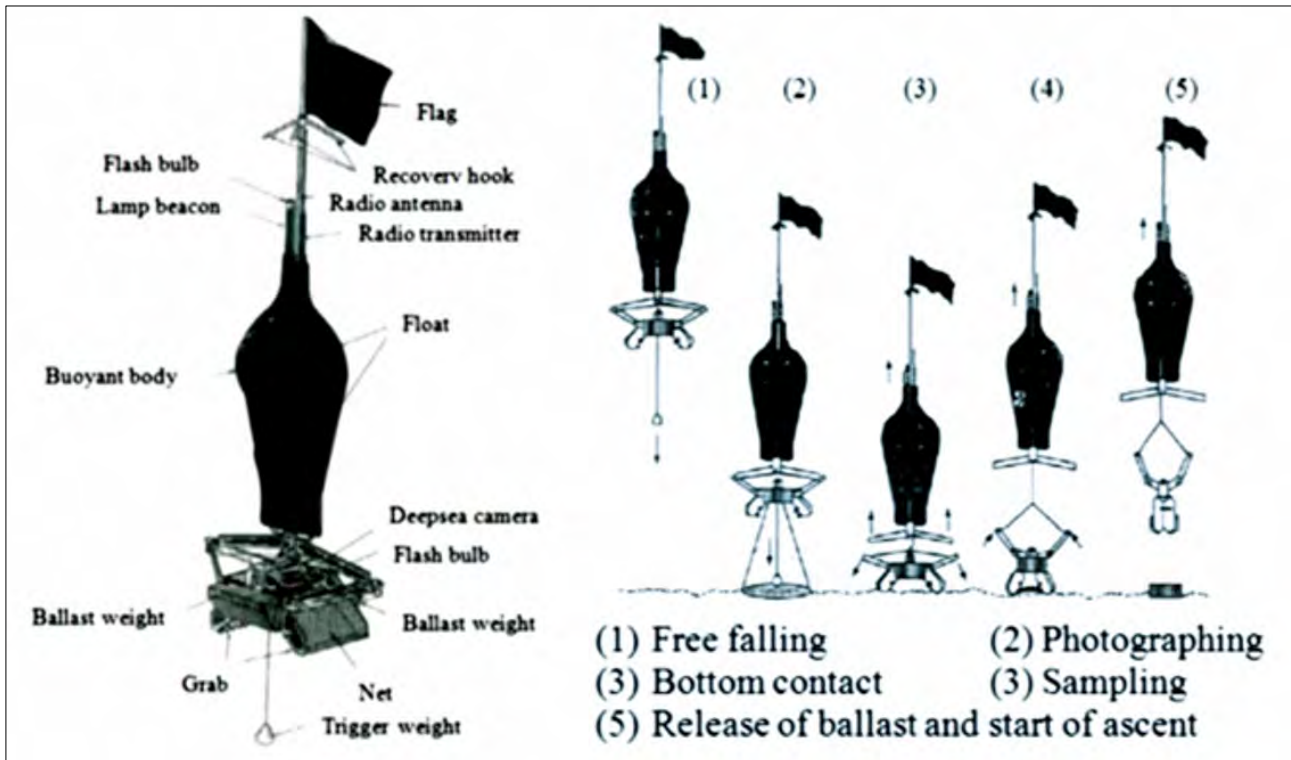
Source: ISA 1999b.

The box core is the preferred sampling method for retrieving polymetallic samples for resource evaluation and environmental studies. The box core consists of a trigger, plunger, and cutting shovel. Upon land out on the seafloor, the trigger is released which allows the plunger to push a box cutter into the substrate during retraction. Upon retraction, the cutting shovel rotates under the box while cutting into the seafloor and sealing the sample box from below Figure 5.4.

Figure 5.4   Box core sampler operation
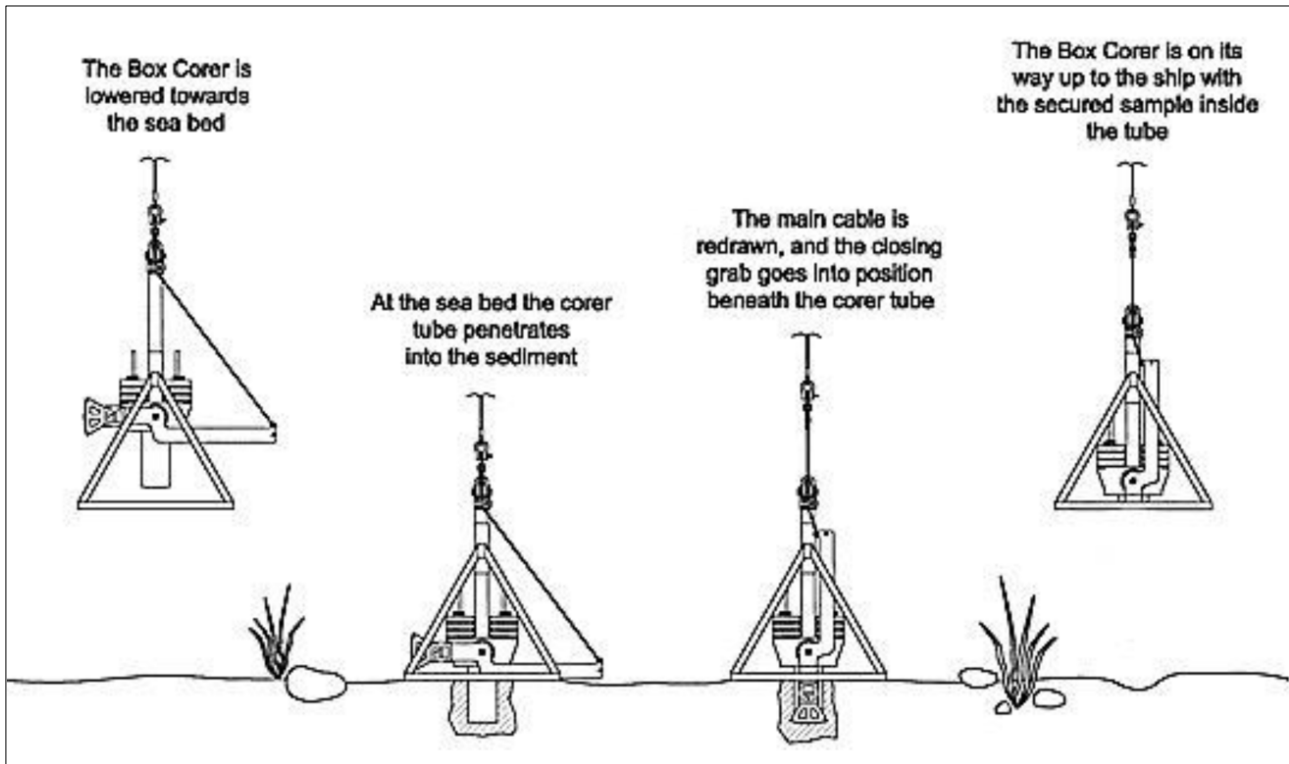
Source: KC Denmark box corer manual.

Comparison of nodule abundance measurements by free-fall grab samplers and box cores suggests that free-fall grab samplers commonly underestimate the actual abundance. This is due to smaller nodules escaping the sampler during ascent and larger nodules around the edge of the sampler being knocked out during the sampling process. Additionally, free-fall grab samplers occasionally fail to return any nodules where nodule abundance is known to be very high because the sampler fails to penetrate the layer of nodules.

Lee et al. (2008) examined correction factors between FFG and BC in some detail. They found a wide range but consistent differences with FFG under-reporting compared to BC. They recommended an overall correction factor of 1.4 to convert FFG abundance to BC abundance. However, they acknowledged that any simple factor lacks precision. One of the key issues is the size of the FFG or BC relative to the nodule diameter.

No corrections were applied to the NORI Area nodule abundance data.

5.4   Sample preparation and analysis

Information about sample preparation and analysis by the Pioneer Investors is summarised below. Additional information is provided in the Technical Report on NORI Area D, Clarion Clipperton Zone Mineral Resource Estimate, April 2019 (AMC, 2019).

5.4.1   Ocean Minerals Company

While OMCO data are not included in the datasets used for resource estimation in the NORI Area, they are discussed here as the method described below is believed to be similar to the method practised by those contractors that did contribute to the NORI Area data.

Polymetallic nodule samples were laid out separately on a white surface marked with a scaled grid and photographed to permit determination of nodule size distribution. They were then sealed in labelled fibreglass-reinforced collection bags and stored in the ship's hold for the balance of the exploration cruise. The samples were transported from the ship to the Lockheed Ocean Laboratory in San Diego.

Prior to weighing, the samples were removed from the sample bags and placed in a single layer in labelled open trays on tables in the air-conditioned laboratory for at least 12 hours to ensure a uniform degree of air drying. The samples were then weighed using a high-capacity laboratory scale and divided into two subsamples of approximately equal weight.

The second subsample was crushed using a jaw crusher to produce a product with a maximum size of less than about 1 mm. The crushed sample was then mixed and passed through a laboratory sample splitter to produce a 5 to 10 g subsample. The subsample was further ground to a fine powder using a laboratory ball mill prior to assaying.

The powdered subsample was placed in an oven at 110 °C for at least six hours to remove adsorbed water. It was then immediately transferred to a sealed desiccator to cool to ambient temperature.

A three-acid digest was used to dissolve the samples before analysis by AAS using a Hewlett-Packard instrument. Standard analysis included determination of manganese, iron, cobalt, nickel, copper, zinc, silica, calcium, and magnesium.

Analytical accuracy was confirmed by periodic introduction of standards made from crushed, mixed, and powdered bulk nodule samples that had also been sent to three independent commercial laboratories for determination of these metal contents. Additional confirmation was achieved using standards formulated by the US Geological Survey (A-1 and P-1; Flanagan and Gottfried 1980). These standards were subjected to the entire preparation procedure to ensure that no significant contamination was occurring and that no systematic analytical errors were being included in the process.

5.4.2 Yuzhmorgeologiya

The Yuzhmorgeologiya method was very similar to the method practiced by OMCO. The Yuzhmorgeologiya data cover NORI Area A and B.

The measurement of abundance of nodules at the sample site was carried out using an "enclosed" Ocean-0.25 FFG sampler with a 0.25 m^2 gripped surface and a depth of sampling of approximately 30 cm. The FFG sampler was combined with GFU-6-8 photography unit. This device took ocean bottom photos at the sampling point.

The procedure for sub-sampling was as follows:

1. Extraction of all nodules from the grab sampler.
2. Crushing of all nodules to a maximum particle size of up to 10 mm.
3. Drying (approximately 24 h) of all samples at 105°C until constant weight was achieved.
4. Crushing of all samples to 1 to 2 mm particle size and splitting of 400 to 500 g using a splitting device.
5. Pulverising of the split sample (not less than 400 g) was carried out in the vibrating grinder up to 100 mesh particle size (0.074 mm).
6. Formation of analytical sample (200 g) and its duplicate (200 g).

Chemical analyses were carried out on subsamples with an approximate weight of 0.5 g, selected from the analytical sample. Determination of nickel, copper, cobalt, and iron content was carried out by AAS and the content of manganese by a method of photometric (electrometric) titration.

5.4.3   IOM

Information regarding IOM procedures is not currently available. However, the procedures used by IOM for sample collection and assaying are likely to be similar to the sampling and assaying procedures used by the other Pioneer Investors. The results of the IOM sampling are consistent with the results obtained by other Pioneer Investors within the NORI area and within the broader CCZ.

5.4.4   Preussag

Preussag completed polymetallic nodule exploration programs in the CCZ aboard the Valdivia in the 1970s. Nodule sampling was mainly carried out using free-fall grab samplers and box corers.

After the sampling devices arrived on the working deck of the research vessel, the nodules were removed from the sediment surface (box corer) or taken from the FFG samplers and transported in plastic boxes into the geological laboratory. There, several sample treatments were carried out:

• Nodules were cleaned (if necessary) from adhering mud using filtered seawater.
• Nodules were carefully dried with paper towels.
• Nodules were photographed on a surface with a scaled grid.
• Individual nodules were measured.
• Individual nodules and the total nodules from one device were weighed with a special balance (determination of wet weight).

A detailed description including the identification of the types of nodules was conducted.

One part of the nodules was used for further investigations in the ship's laboratory. The other nodules were stored in plastic bags, which were weighed once more. Then the plastic bags were filled with seawater in order to keep the nodules in a water-saturated state. These samples were required for further studies and investigations in the home laboratories (e.g., physical properties, detailed chemical analyses, X-ray phase analysis, metallurgical tests, polished sections).

The first part of the nodules taken from one sampling device were crushed to a particle size smaller than 10 mm and then dried in an oven at ±105 °C until constant weight was achieved. Further steps of grinding in the ship's laboratory took place with a final procedure of pulverising with a ball mill producing a fine powder with a particle size of less than 100 mesh (less than 74 μm). Then the sample was passed through a laboratory sample splitter to produce several representative subsamples.

One subsample was taken as representative archive sample. Two other subsamples were dried again for at least five hours to remove the rest of adsorbed water prior to analysis.

Two methods were used to determine the key metals nickel, copper, cobalt, manganese, iron, and zinc. The first one was the AAS analysis to measure nickel, copper, zinc, and cobalt, and the second was the energy-dispersive XRF method with ratio-isotope excitation to determine manganese and iron. A sample digestion was necessary to carry out the AAS determination. For this, the dried powder was treated with a mixture of acids in a high-pressure Teflon vessel and heated for several hours to complete the digestion. The digested fluid was diluted with distilled water and analysed with the spectrometer, and the residue was weighed. The XRF analysis was performed with the powder (pressed tablets). Data quality and analytical reliability were confirmed by intermediate introduction and measurement of reference nodule samples. These reference standards consisted of powdered material which was subjected to the same procedure as described above.

5.5 QA/QC procedures

Free-fall grab samplers are considered to underestimate the actual abundance but provide adequate samples for determining the grade of the nodules (Hennigar et al. 1986).

QA/QC was known to be undertaken at the time of sampling as part of the scientific process used by each Pioneer Investor. However, no systematic quality assurance and quality control (QA/QC) information is available for these programs, as this information was not provided by the ISA. Nonetheless, the acceptance of the data by the ISA suggests the ISA was satisfied with the quality of the data.

The quality of the data was assessed (Golder 2015) using comparative measures between the different datasets (Section 9.1.2). The correlation of data from different sources, including Pioneer Investors and government scientific institutes, provides a satisfactory level of quality assurance to support Mineral Resource estimates at an Inferred level of confidence.

5.6 Pioneer Investor sample data supplied to NORI

Upon making an application, the Pioneer Investors were required to submit sufficient data and information to enable designation of a reserved area based on the estimated commercial value. These sample data provide the basis of a database held by the ISA and were used initially to define the areas of the NORI application.

The sample sites were sampled by a combination of grab samplers and box corers of different sizes and designs, with the full details of the sampling tools at a given site mostly being unavailable. As a result, sample quality, spacing, and assay reliability vary from contractor to contractor, sample to sample, and block to block. Average sample spacing (based on the data supplied by the ISA) varies across the CCZ, ranging from less than 1 km and averaging approximately 10 km within the NORI Area.

Statistics for the samples that contain both abundance and grade data inside the NORI Area are tabulated in Table 5.1 and illustrated as boxplots in Figure 5.5. The box plots show the range of grades; the box represents the range of grades in the middle 50% of the samples, centred on the median (middle value) and box width reflects number of samples. The dashed lines represent the range of the lowest 25% and highest 25% of the data.

Cobalt in NORI Area D is significantly lower than the other NORI areas, however, abundance is consistently higher in NORI Area D than the other NORI areas and the CCZ Reserved Blocks in general Figure 5.5.

The range of the assays (as summarized by the coefficient of variation) is remarkably low compared to most terrestrial Mineral Resources. Abundance values vary more widely, making abundance estimates the key variable of uncertainty in Mineral Resource estimation.

The abundance of buried nodules is poorly known at this time. Thus, buried nodules are not included in exploration information or Mineral Resource estimates.

Table 5.1   Summary of historical FFG samples in the NORI Area

NORI Area	Grade	Number	Missing	Min	Max	Mean	Median	Var	cv
A	Abundance (wet kg/m^2)	50	0	0	28.7	9.3	8.2	57.366	0.81
	Ni (%)	40	10	1.04	1.75	1.37	1.39	0.016	0.09
	Cu (%)	40	10	0.66	1.29	1.07	1.1	0.017	0.12
	Mn (%)	40	10	19.77	32.6	28.06	28.98	8.577	0.1
	Co (%)	40	10	0.16	0.28	0.22	0.22	0.001	0.11
B	Abundance (wet kg/m^2)	31	0	0	25.55	11.24	12	50.536	0.63
	Ni (%)	26	5	1.01	1.61	1.42	1.44	0.021	0.1
	Cu (%)	26	5	0.72	1.26	1.12	1.16	0.016	0.11
	Mn (%)	26	5	20.8	32.2	28.88	29.8	9.939	0.11
	Co (%)	26	5	0.21	0.31	0.25	0.25	0.001	0.09
C	Abundance (wet kg/m^2)	152	0	0	44.1	10.55	10.33	52.902	0.69
	Ni (%)	135	17	0.68	1.53	1.27	1.31	0.025	0.12
	Cu (%)	135	17	0.4	1.46	1.05	1.11	0.048	0.21
	Mn (%)	135	17	12.84	33.54	28.63	29.42	11.648	0.12
	Co (%)	135	17	0.12	0.33	0.21	0.21	0.001	0.17
D	Abundance (wet kg/m^2)	159	0	0.2	52.2	14.12	13.9	72.243	0.6
	Ni (%)	159	0	1.09	1.41	1.28	1.29	0.004	0.05
	Cu (%)	159	0	0.88	1.5	1.14	1.13	0.012	0.1
	Mn (%)	159	0	23.8	33.9	30.58	31	3.12	0.06
	Co (%)	159	0	0.05	0.2	0.12	0.11	0.001	0.26

Notes: Var = variance; CV = coefficient of variation.

Figure 5.5   Box plots of sample grades within the NORI Area compared with all other data from the Reserved Blocks
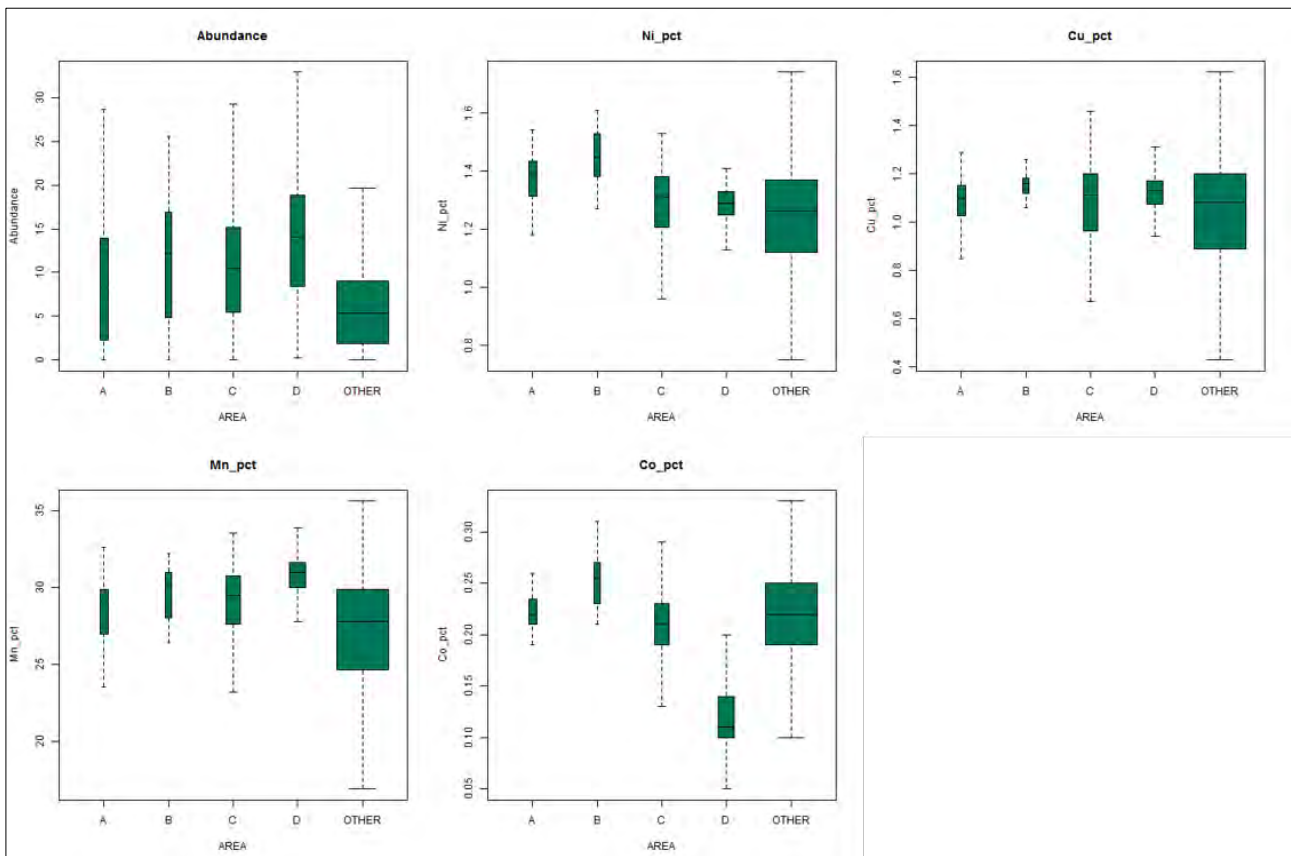
Note: Box size represents 1st and 3rd quartiles centred on the median and box width reflects number of samples.

6 Geological setting and mineralisation

6.1 Global distribution of nodules

Seafloor polymetallic nodules occur in all oceans, and the CCZ hosts a relatively high abundance of nodules. Other relatively dense zones are found in the Peru Basin in the southeast Pacific, the centre of the north Indian Ocean, and the Cook Islands Figure 6.1.

Figure 6.1   Schematic diagram of average abundance of polymetallic nodules in four major locations

Source: GRID-Arendal 2014b.

6.2 Tectonic setting and topographic features

The CCZ is defined by two major west-south-west and east-north-east trending fracture zones running through the seafloor; the Clipperton Fracture Zone to the south and the Clarion Fracture Zone to the north. These fractures zones can be seen clearly on the bathymetric map Figure 6.2. The eastern and western limits can be defined by the Mathematicians Seamounts or Ridge in the east, and the Republic of Kiribati or Line Islands in the west.

The CCZ seafloor forms part of the Abyssal Plains, which are the largest physiographic province on Earth, covering some 70% of the area of ocean basins and 30% of the Earth's surface (ISA 2004). The Abyssal Plains are traversed by ridges, believed to have formed from the process of seafloor spreading. Orientation is north-north-west to south-south-east (locally $\pm 20°$), with amplitude of 50–300 m (maximum 1,000 m; Hoffert 2008) and wavelength of 1 to 10 km. The bathymetric map of NORI Area D Figure 7.1, shows these ridges clearly. The Abyssal Plains are punctuated by extinct volcanoes rising 500 to 2,000 m above the seafloor.

Depth increases from 3,800 to 4,200 m at 115° west to 4,800 to 5,200 m at 130° west, and 5,400 to 5,600 m at 145° west.

The sediment types exhibit trends perpendicular to the fracture zones, from predominant carbonate sediments in the south-eastern extreme to predominant siliceous red clay in the west north-west.

Figure 6.2   Bathymetric map of the Clarion-Clipperton Fracture Zone
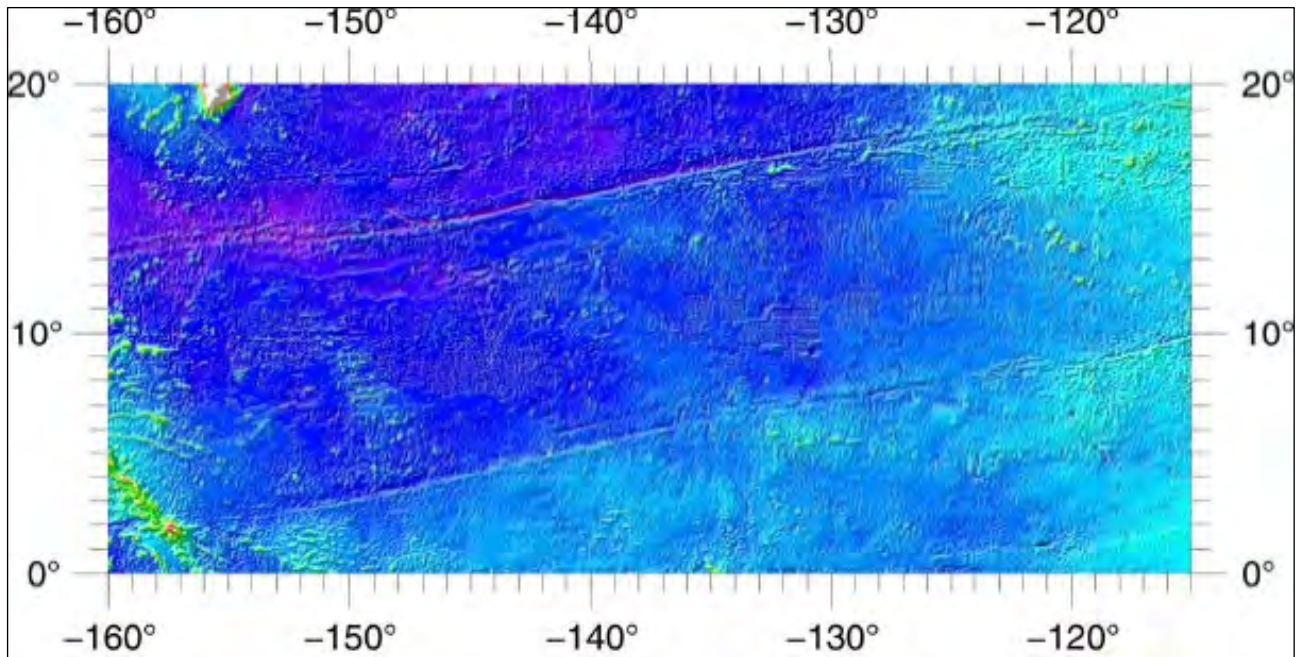
Source: ISA 2010.

6.2.1   Sedimentation and nodule formation

Seafloor polymetallic nodules are composed of nuclei and concentric layers of iron and manganese hydroxides and formed by precipitation of metals from seawater. The metal accumulation rates are slow, and it generally takes millions of years to form a nodule (ISA 2004).

Nodules are abundant in abyssal areas with oxygenated bottom waters, low sedimentation rates (less than 10 cm per thousand years), and where sources of abundant nuclei occur (Hein et al. 2013). Nodules grow on 0.1 to 1 cm nuclei (e.g., pieces of pumice and older broken nodules) and generally range from about 1 to 12 cm in their longest dimension, with the low to middle-range typically the most common (1 to 5 cm).

The specific conditions of the CCZ (water depth, latitude, and seafloor sediment type) are considered to be the key controls for its formation, along with the following factors:

•   Supply of metals to the growing surface.
•   Presence of a nucleus.
•   The corrosive / erosive forces caused by benthic currents.
•   Occurrence of semi-liquid surface layer on the seafloor (sediment water interface).
•   Bioturbation.

The highest values of metals in nodules are thought to be best developed on the seabed in the equatorial regions away from land sources of sediments. In these regions surface waters have high primary productivity. Tiny plants and animals concentrate the metals from seawater and when they die, they sink to the seafloor, dissolve, and release the metals into the pore water of seafloor sediments. It is believed that the upper portion of the nodules accumulate metals that are precipitated from seawater, while the lower portion of the nodules, partially buried in sediment, accumulate metals from pore-water in the underlying sediments.

Sediments from the CCZ consist mostly of clays and siliceous biological casts. Sands and larger sediments are not generally found so far from land, and the commonly formed carbonate biological casts dissolve on the seabed in these deep-water regions faster than they accumulate.

6.3   Polymetallic mineralisation

6.3.1   Nodule grades

Nodule chemistry varies only slightly with in the CCZ. Figure 6.3 shows that there is a general increase in combined cobalt, nickel and copper grades towards the south-east (Kazmin in ISA 2003; ISA 2010; Morgan 2009). The reason for this is not clear but may relate to proximity to metal sources from the East Pacific Rise or the American continents.

Average (mean) grades for elements of interest other than nickel, manganese, copper, and cobalt from 248 samples of nodules taken within the NORI area during the NORI 2018 and 2019 off-shore exploration campaigns are summarised as:

* Other base or alloy metals such as zinc (0.21% ZnO), titanium (0.43% TiO_2), and lead (0.03% PbO).
* Rare earth and other transition metals such as strontium (0.071% Sr), yttrium (0.009% Y), zirconium (0.033% Zr), lanthanum (0.011% La), cerium (0.022% Ce), and neodymium (0.013% Nd).
* Other elements such as iron (6.6% Fe), magnesium (3.2% MgO), aluminium (3.95% Al_2O_3), sulphur (0.28% SO_3), calcium (2.4% CaO), potassium (1.1% K_2O), sodium (2.9% Na_2O), phosphorus (0.36% P_2O_5), vanadium (0.049% V), and barium (0.43% Ba).

Analysis of 20 samples collected by NORI in 2012 showed that arsenic content is low (0.008% As).

6.3.2   Nodule abundance

Polymetallic nodules lie on the seafloor sediment, often partly buried. Some nodules are completely buried, although the frequencies of such subsurface occurrences are very poorly defined. Kotlinski and Stoyanova (2006) document up to five discrete layers of buried nodules, although all were within 45 cm of the surface despite using sediment cores of 250 to 380 cm depth (i.e., all of these nodules are near surface). Other images of box corers also suggest that all or most of the nodules are at the surface. Consequently, drilling is not required for definition of the Mineral Resources.

During the 2018 NORI campaign, 91% of nodules sampled were situated at surface. These include nodules on the surface and nodules with their top surfaces in the upper 1 cm of sediment. A few nodules were found at depth; most of these were usually clustered around the edges of the box core and are considered to have been pushed below surface by the box coring process. Significant nodule abundance below surface was only recorded in one out of 45 samples.

The nodules vary in abundance, in some cases touching one another and covering more than 70% of the seafloor. They can occur at any depth, but the highest concentrations have been found on abyssal plains between 4,000 and 6,000 mbsl.

Figure 6.4 shows estimated nodule abundance data from the ISA Geological model project. Data analysis in Section 9 shows that nodule abundance variability is significantly higher than metal grades, suggesting that abundance estimation will be the key variable in Mineral Resource estimation.

Figure 6.3   Results from ISA Geological Model Project in the CCZ - combined cobalt, nickel, and copper grades
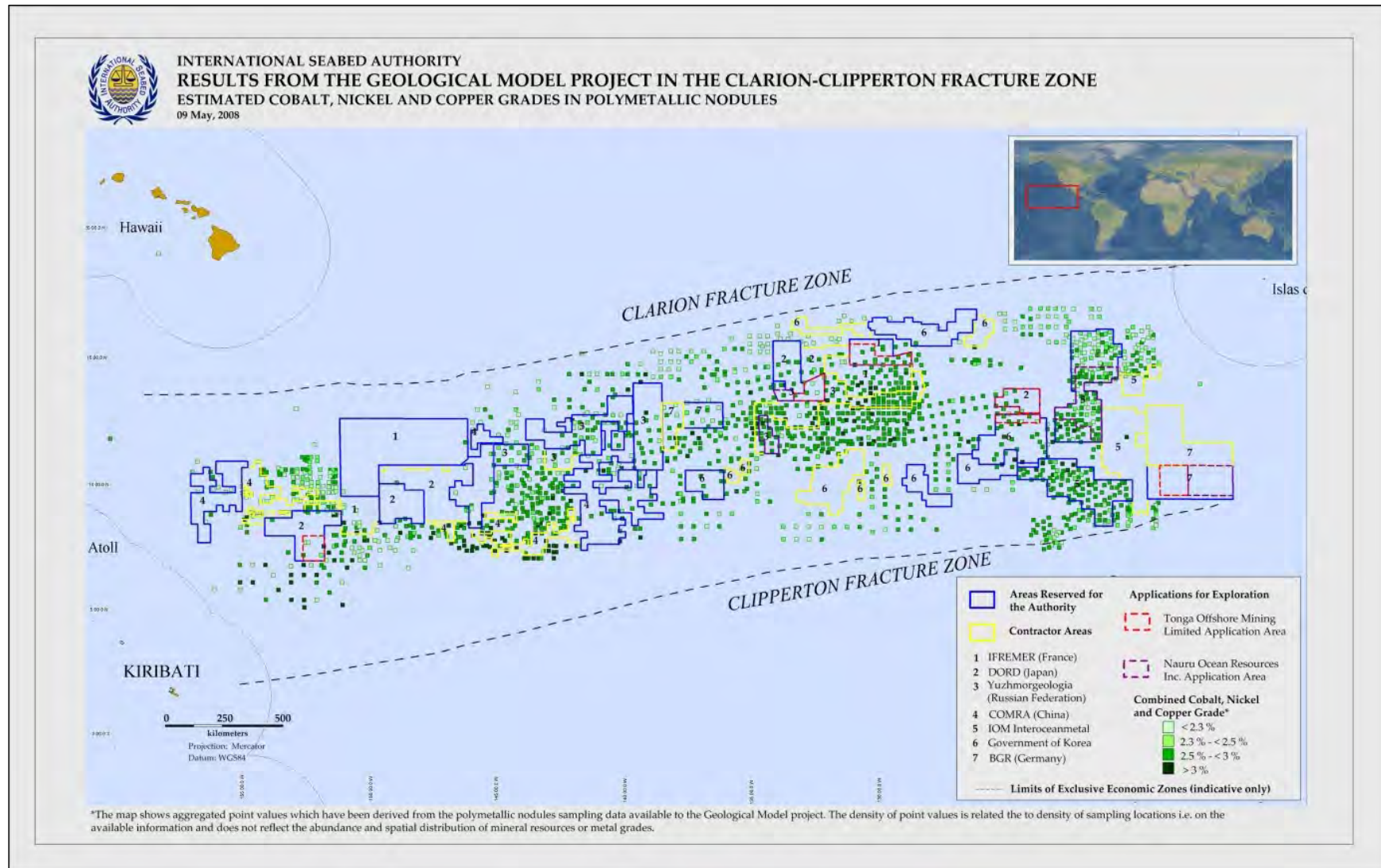
Note: The German data for NORI Area D were not included in the ISA Geological Model.
Source: provided by the ISA directly to NORI in 2008.

Figure 6.4   Results from the ISA Geological model project in the CCZ estimated nodule abundance
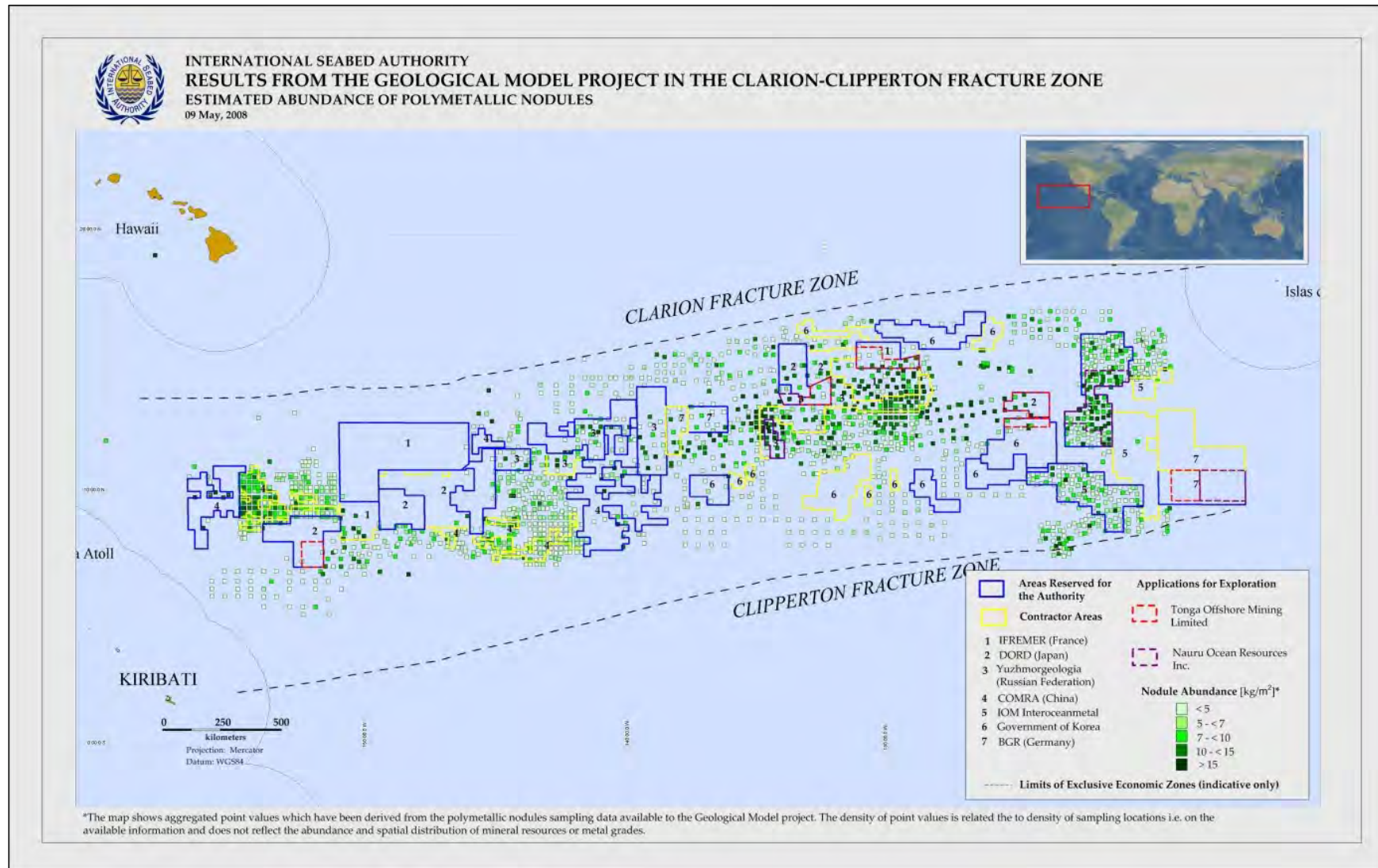
Note: The German data for NORI Area D were not included in the ISA Geological Model.
Source: ISA 2008.

6.4 Seafloor polymetallic nodule facies

Three broad classes of nodule distribution on the seafloor were identified, based on camera imagery. They are summarised in Figure 6.5.

Figure 6.5   Polymetallic nodule facies in NORI Area D

Nodule camera facies type	Description	Example
Type 1 densely packed / interconnected	>50% nodules ~1–10 cm, uncertain. Low to moderate confidence in camera imagery to resolve individual nodules	
Type 2 mostly individual / locally interconnected	~20–40% Nodules ~5–20 cm Moderate to high confidence in camera imagery to resolve individual nodules	
Type 3 mostly Individual / sparse	10–20% nodules ~5–20 cm Moderate to high confidence in camera imagery to resolve individual nodules	
Other	Volcanic outcrop - associated with NW-SE ridges	
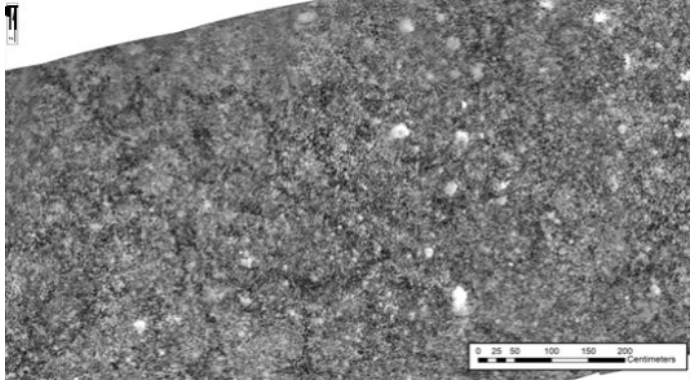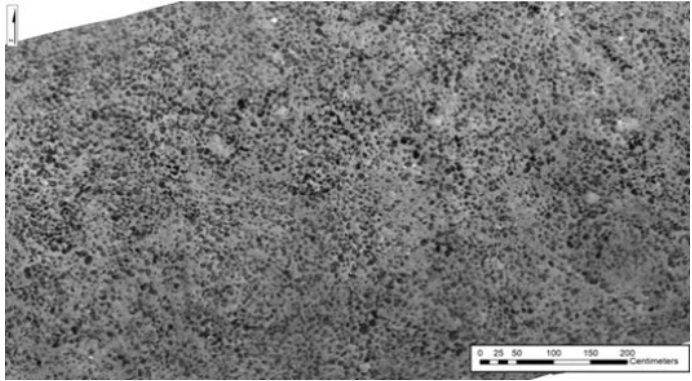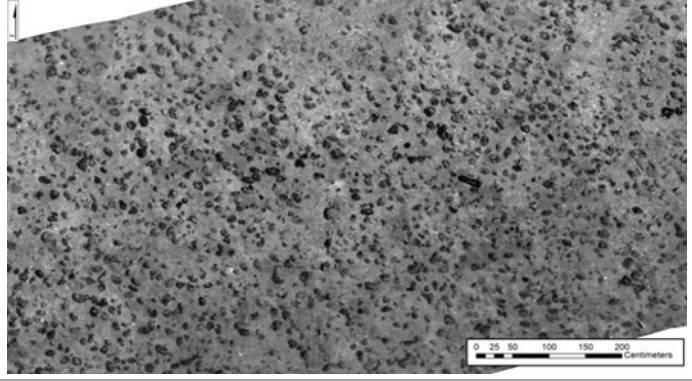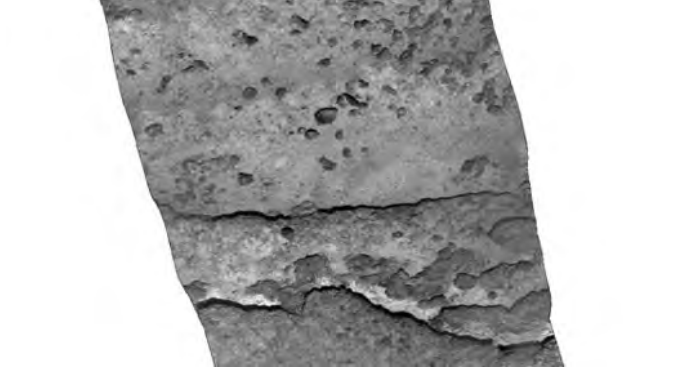
Type 1 nodule facies (distribution pattern) is typically characterised by >50% nodules (by area of coverage). The majority of these nodules are typically medium-sized and are closely packed, with many nodules in contact with their neighbours.

Types 2 and 3 are characterised by lower nodule abundance, larger nodules, and the nodules are typically separated (i.e., there are noticeable sediment gaps between individual nodules).

Facies boundaries are often well-defined (i.e., not gradational) and variable over short distances (<100 m), as illustrated in Figure 6.6.

Figure 6.6   Camera imagery showing change from Type 3 nodules (left), to Type 2 (right)
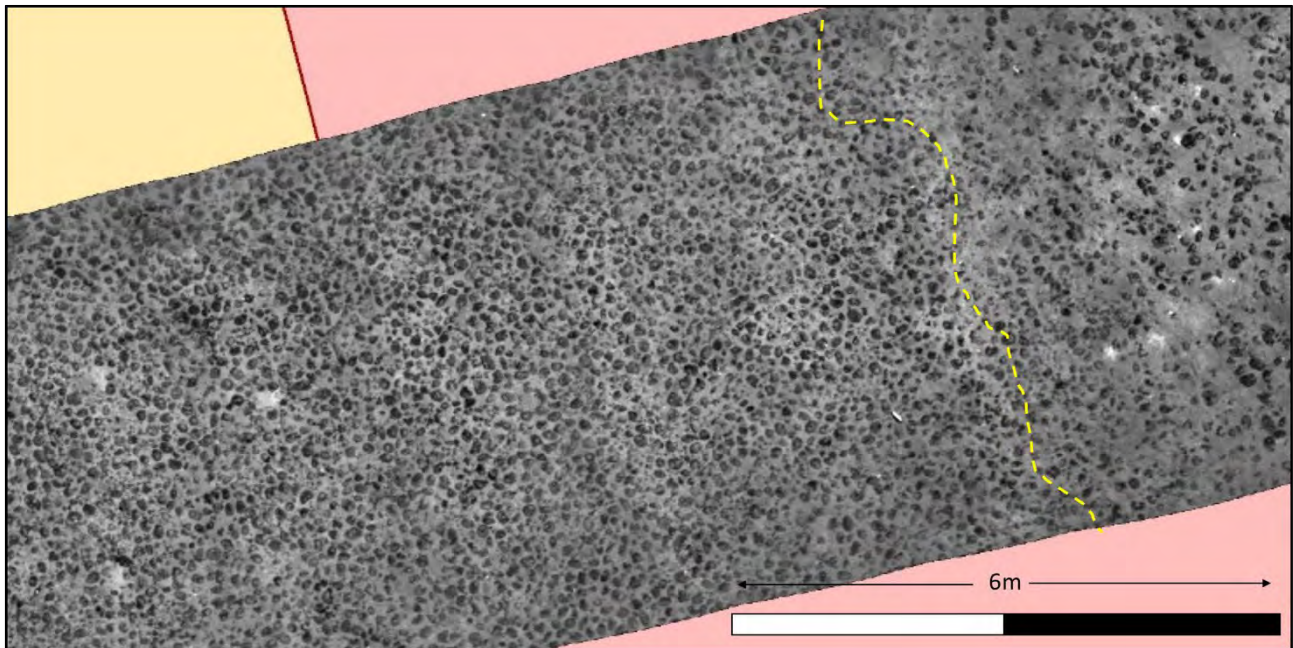
Nodule distributions can be mapped by measuring the backscatter (return signal) from multi-beam echo sounding (MBES) from vessels on the ocean surface. Type 1 nodule facies correlates with moderate-amplitude backscatter areas and is the most common facies. Type 2 and 3 nodule facies typically correlate with higher-amplitude backscatter areas. These correlations are shown in Figure 6.7 which shows nodule classification according to photographic traversing by autonomous underwater vehicle (AUV) (ribbon-track coloured: Type1 (green), Type 2 (yellow), Type 3 (red)) against a background of backscatter data. The backscatter responses are coloured by amplitude; high-amplitude areas associated with Type 2 and 3 nodule facies shown in warmer colours, with Type 1 represented by colder colours.

Figure 6.7   Map of nodule facies classification in NORI Area D
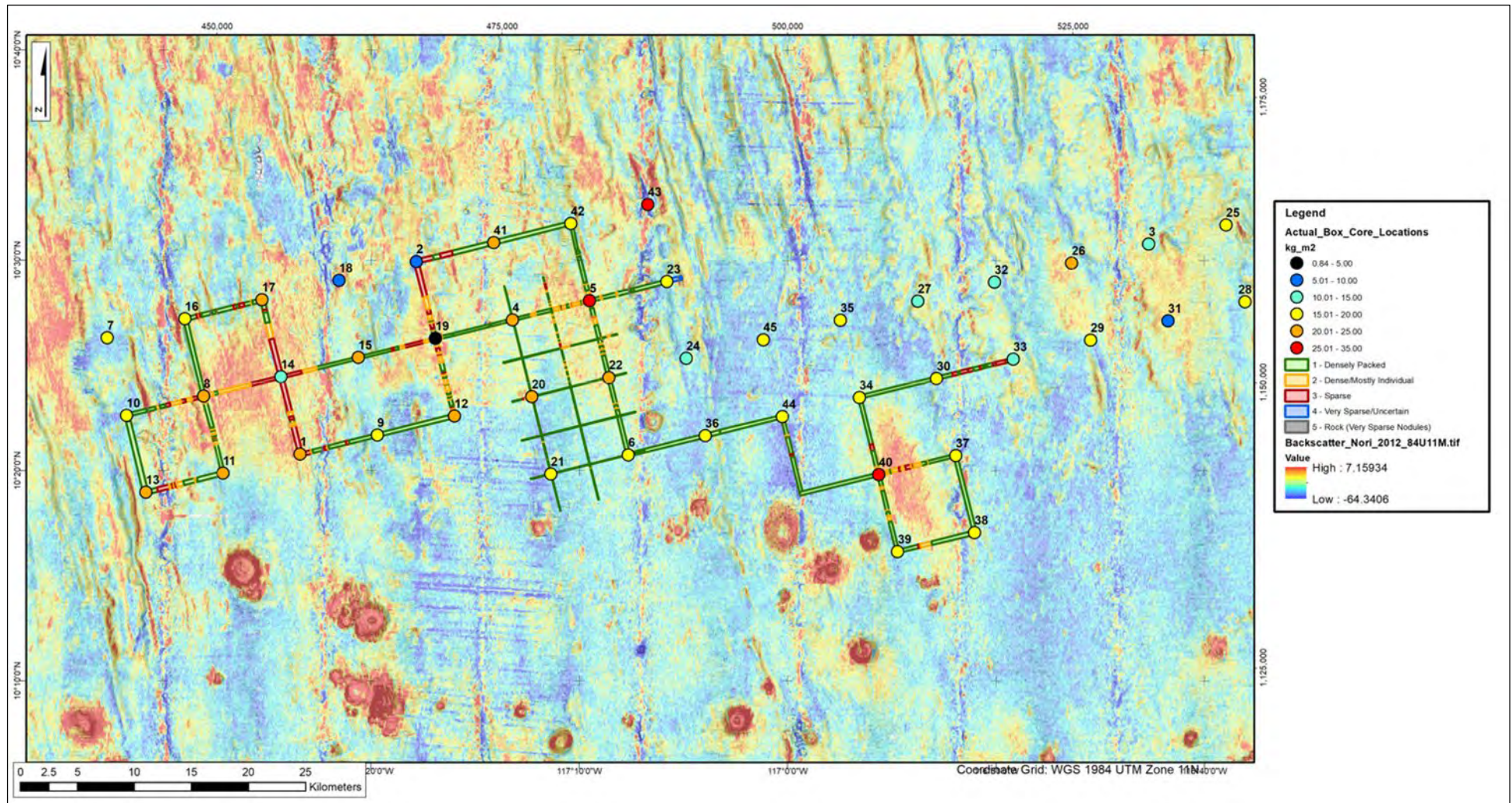
Note: Box core locations are labelled with box core number and coloured by abundance. Ribbon-track coloured by facies Type: Type1 (green), Type 2 (yellow), Type 3 (red)) against a background of backscatter data. The backscatter responses are coloured by amplitude; high-amplitude areas associated with Type 2 and 3 nodule facies shown in warmer colours, with Type 1 represented by colder colours.

6.5 Topographic / bathymetric facies

Based on analysis of bathymetric data from the 2012 and 2018 campaigns, together with the significant sampling data acquired during 2019, it was possible to refine the geological domain interpretations which characterise nodule prospectivity. Eight domains were interpreted for NORI Area D:

1. **Abyssal plains** – These constitute the majority of NORI Area D and are characterised by gentle slopes of 0° to 6°, and nodules lying on soft sediment. Nodules were observed to be ubiquitous in this domain wherever it was surveyed and sampled. It is considered a highly- prospective domain for nodules.

   The Abyssal Plains can be further divided into three sub-domains based on backscatter acoustic response and ground-truthing (box core samples and land-out video footage):

   - Areas considered indicative of Type 2 and 3 nodule facies, as determined from backscatter correlation (17% area coverage).
   - Sediment drift domains - characterised by a soft sediment ooze with low acoustic backscatter, and extremely low to no nodule abundance (1% area coverage).
   - Volcanic cones (see below) (4% area coverage).
   - The remaining area (78%) is likely indicative of Type 1 nodule facies and considered highly prospective.

2. **Abyssal Hills** – These are topographically higher features, oriented NNW-SSE, and are parallel to one another. Slopes of the hills are mostly gentle at the western side, while they are very steep at the eastern side, likely representing horsts bounded by inward-dipping normal faults and outward-dipping volcanic growth faults respectively.

3. **Abyssal Hills (hard)** – Abyssal Hills where the hill crests are associated with the occurrence of hardgrounds, caused by proximity of underlying (harder) Neogene footwall succession at seafloor, typically covered by a very thin veneer of unconsolidated sediment.

4. **Slopes ≥ 6°** – These are associated with the flanks of Abyssal Hills, where the slope is 6° or greater, and are likely associated with hardgrounds and/or volcanic debris and volcanic outcrop development typically associated with NNW trending faults. These steep slopes are considered to have low nodule prospectivity but have not been fully tested with sampling or photography.

5. **Slopes ≥ 6° (hard)** – These are associated with the flanks of Abyssal Hills where the slope is 6° or greater, and are associated with hardground development, typified by outcropping (harder) Neogene footwall succession. These steep slopes are considered to have low nodule prospectivity, based on box core sampling, AUV SBP data and photography.

6. **Volcanic Outcrop** – This is associated with volcanic growth-faults along the Abyssal Hill flanks, which trend NNW-SSE, and are elongated, narrow bodies mapped through integration of AUV SBP and camera data with EM 122 MBES data backscatter data.

7. **Volcanic Cones** – These are typically grouped in chains and follow the 'Hawaiian Trend'. Some of these features could be classed as Knolls, as they exhibit a 500–1000 m rise from the seafloor. These are isolated features and were not sampled during the 2018 or 2019 NORI Campaigns. However, because of their volcanic origin, steep slopes (>6°) and dominant high-intensity backscatter (typically associated with volcanic outcrop), they are also considered to have low nodule prospectivity.

8. **Volcanic High** – This is a macro-scale topographic feature situated in the SE corner of NORI Area D. It is interpreted as a relic volcanic intersection high, which also includes a relic transform parallel trough. Both are volcanic related features associated with the Clipperton transform zone, situated to the south of NORI Area D.

These domains are described further in Section 11.2.

6.6 Nodule morphology and formation

A variety of nodule classification systems have been used in previous studies of the CCZ (for example, Haynes et al. 1985), but the three-class system promoted by the ISA (ISA 2010) prevails today Figure 6.8. Nodules are classified according to their texture, as:

- S-type (smooth type)
- R-type (rough type)
- S-R-type (smooth-rough mixed type)

It is postulated that the different textures are related to the position of the growing nodule, relative to the seafloor, as shown in Figure 6.8.

Figure 6.8   Polymetallic nodule types (ISA 2010)
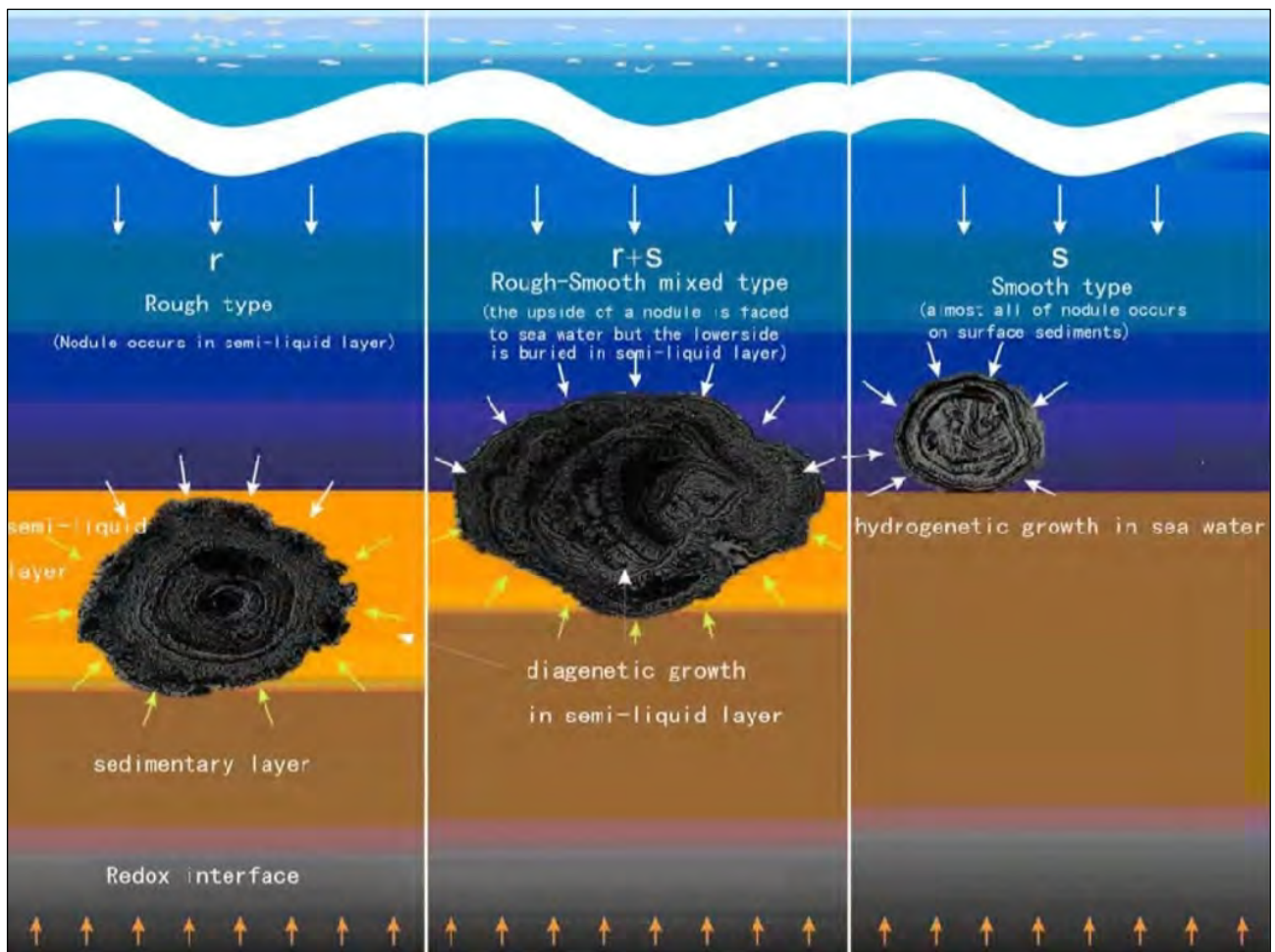
Source: ISA 2010.

7 Exploration

NORI completed off-shore exploration campaigns in July–August 2012, in 2013, May 2018, August to December 2019.

7.1 NORI 2012 campaign

The RV Mt. Mitchell, which sailed from the port of Seattle, was used for the NORI 2012 campaign. NORI conducted bathymetric mapping of the seafloor within NORI Area C and D, as well as bulk nodule sampling for metallurgical test work. Due to the nature of the bulk sampling, these samples are not suitable for use in Mineral Resource estimation.

Using a hull-mounted Kongsberg Simrad EM120 12 kHz, full-ocean depth multibeam system, approximately 25,720 km^2 was surveyed in NORI Area C and approximately 25,439 km^2 in NORI Area D. Due to swath width and vessel orientation relative to course-made-good, some data were recorded beyond the bounds of those areas. Approximately 69.1% of Area C (25,720 km^2) was surveyed. Area D was surveyed in its entirety (25,439 km^2). An image of the bathymetric data for NORI Area D, in plan view, is shown in Figure 7.1.

Figure 7.1   NORI Area D bathymetry data
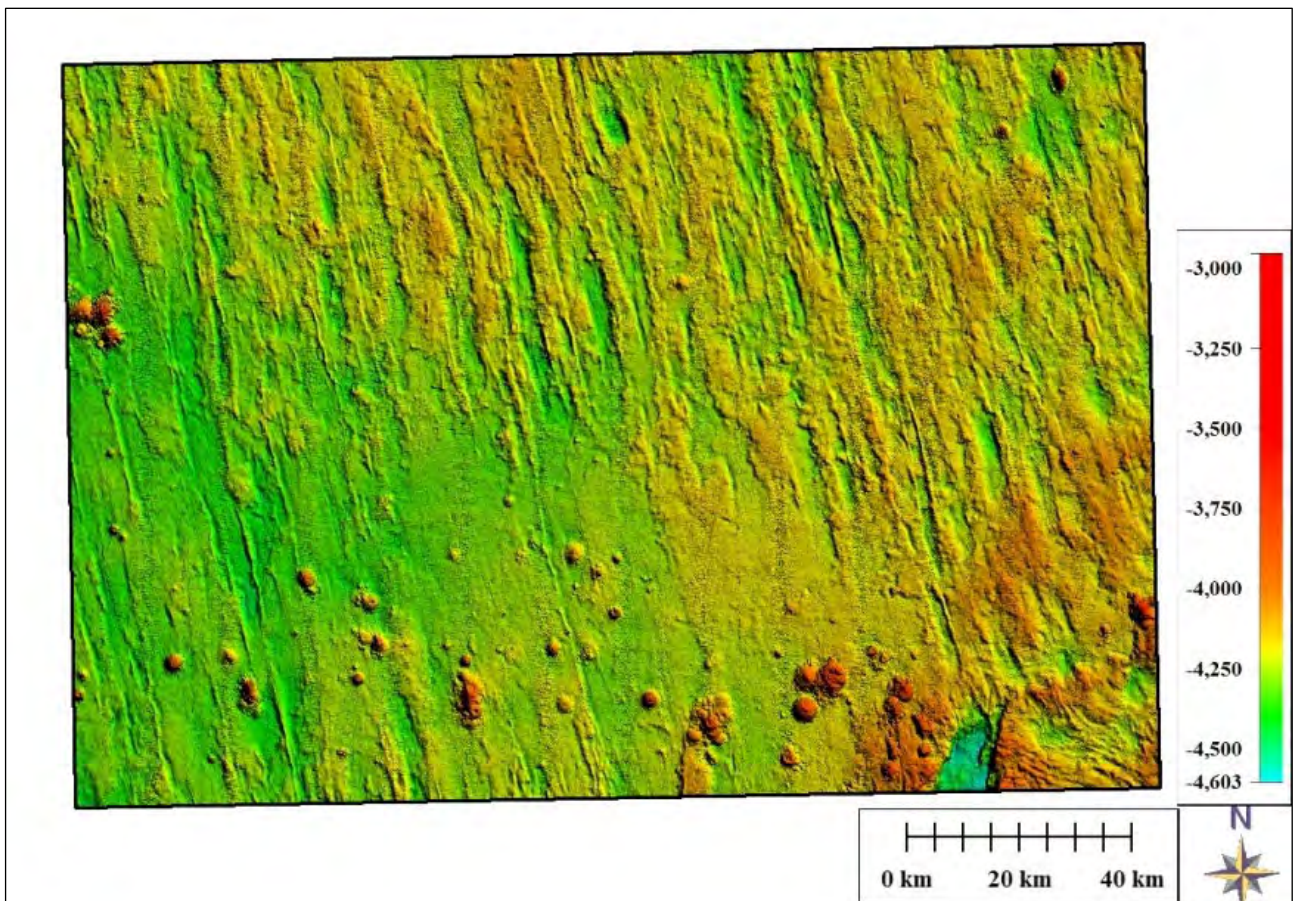
Note: The canted box is a result of projecting a large geographic area bounds (given in latitude / longitude format) into UTM 10 N, WGS 84.

MBES data was processed during the 2012 NORI Campaign and used to locate areas of high nodule density for dredge sampling, based on the bathymetric surfaces and the backscatter intensities. Overall, the geophysical interpretation of the multibeam data was remarkably successful.

Bulk samples were collected by dredging from NORI Area C (five dredge deployments) and NORI Area D (28 dredge deployments). Approximately 280 kilograms (kg) of nodules were recovered

from Area C and approximately 4,500 kg from NORI Area D. Video footage was also obtained during dredge deployments and, together with the samples recovered, provided physical verification of nodules within NORI Area C and D Figure 7.2.

Twenty (20) nodule samples (two (2) from Area C and 18 from Area D) recovered during the NORI 2012 campaign were assayed. Each sample for assaying, was a subsample of an FFG sample and weighed approximately 1 kg. Results of assaying indicated a mean grade of 1.20% nickel, 1.03% copper, 27.9% manganese, and 0.13% cobalt. These mean values are consistent with the mean grades derived from the historical grab samples within NORI Area C and D see Table 7.1. The cobalt value of 0.13% confirms the cobalt grades in the German data in Area D. A large suite of additional elements was also assayed. A drying test undertaken on a nodule sample collected during the NORI 2012 campaign indicated moisture loss of 24% at 120 °C.

Figure 7.2   Subset of nodule samples recovered during NORI's 2012 exploration campaign

7.2   NORI 2013 campaign

In 2013, NORI carried out a second exploration campaign within NORI Area A and B. This campaign was also undertaken using RV Mt. Mitchell and focused mapping bathymetry in NORI Area A and B, identifying nodule fields based on acoustic data (including interpretation of backscatter data), and recovering bulk polymetallic nodule samples.

A hull-mounted Kongsberg Simrad EM120 12 kHz, full-ocean depth multibeam system was used to survey approximately 8,924 km^2 in NORI Area A and approximately 2,911 km^2 in NORI Area B. The Applanix Pos MV 320 V4 system was used to measure vessel position and attitude, and a dual Trimble Zephyr unit was used as the Global Positioning System (GPS) system.

Dredging for bulk nodule sampling was carried out using an epibenthic sled Figure 7.3 that was designed specifically by KC-Denmark Research Equipment for seafloor polymetallic nodules sampling. The dredge in Area A was deployed at 12° 10.2'N, 134° 11.1'W. The dredge in NORI

Area B was deployed at 13° 43.5'N, 133° 35.9'W. Approximately 190 kg of nodules were recovered from NORI Area A Figure 7.4 and approximately 85 kg of nodules were recovered from NORI Area B.

Figure 7.3   Photos showing the operation of the epibenthic sled collecting nodules during the NORI 2013 campaign

After each dredge, the nodules were retrieved from the epibenthic sled on the deck of the ship. They were collected in bags and numbered. Each dredge sample was sub-sampled for laboratory analysis using a simple random scoop sampling to obtain two 2 kg samples. During the scooping the size distribution was also considered.

Figure 7.4   Photos of nodules collected from NORI Area A during the NORI 2013 campaign

The four sub-samples from NORI Area A and B were sent to ALS Laboratories in Brisbane for preparation and analysis. The samples were dried at 120 C for 12 hours then assayed using a four-acid digest specifically designed for high-manganese samples, followed by AAS (method Mn-AA62) and four-acid digest followed by ICP-MS for concentrates (ME-MS61c). The Mn-AA62 method has a claimed precision of ±5%. The results for cobalt, copper, iron, manganese, molybdenum, and nickel are included in Table 7.2, and the calculation of weight loss after drying at 120 C for 12 hours (average 28.7%) is included in Table 7.2.

Table 7.1   Assay results for NORI Area A and B nodule samples

ALS assay method code sample	ME-MS61c Co (ppm)	ME-MS61c Cu (ppm)	ME-MS61c Fe (%)	Mn-AA62 Mn (%)	ME-MS61c Mo (ppm)	ME-MS61c Ni (ppm)
NA1	2,250	10,800	5.27	29.0	589	13,600
NA2	2,240	11' 150	5.06	28.9	545	13,400
NB1	2,490	11,550	5.62	29.2	601	13,800
NB2	2,490	11' 100	5.60	28.2	590	13,750

ALS = ALS Laboratory Group; Co = cobalt; Cu = copper; Fe = iron; Mn = manganese; Mo = molybdenum; Ni = nickel; ppm = parts per million; % = percent.

Table 7.2   Weight loss of samples after drying

Sample	Wet weight (g)	Dry weight (g)	Loss (%)
NA1	536.8	374.3	30.3
NA2	574.3	396.0	31.0
NB1	616.1	452.5	26.6
NB2	588.3	431.5	26.7

7.3   NORI 2018 campaign

7.3.1   Objectives and approach

During April to June 2018, NORI conducted a successful survey and seabed sampling program in NORI Area D using the OSV *Maersk Launcher*, mobilising out of San Diego (Campaign 3). The work completed is summarised below. Additional information is provided in the Technical Report on NORI Area D, Clarion Clipperton Zone Mineral Resource Estimate, April 2019 (AMC, 2019).

The key objectives of this program were to conduct detailed bathymetric, sonar imaging – MBES backscatter, Side Scan Sonar (SSS), and photogrammetry surveys to help facilitate:

• Identification and selection of enough suitable ground for trials of a collector (the Collector Test).
• Provision of sufficient geological and geotechnical detail to ensure future sampling and Collector Test activities recovery efficiencies can be measured, and that sampling and Collector Test programs are appropriately designed.
• Provision of appropriate seafloor imagery to assist with selection of suitable environmental monitoring sites – particularly for physical oceanographic mooring studies.
• Identification of smaller environmental baseline reference zones. An important consideration is that the habitats of these reference sites are similar in character to the site that will be selected for the Collector Test.
• Demonstration of the methodology to upgrade resource confidence from Inferred to Indicated and Measured categories.

Fugro provided turnkey survey and seabed sampling support for the campaign, including:

• AUV operational support
• Hydrographic survey support.
• Data processing.
• Geoscience support for AUV survey (data compilation and preliminary data analysis).
• Geoscience support for box coring operations (core logging, nodule processing, geotechnical testing).

Biological sampling support was provided by ERIAS Group environmental consultants.

Data QA/QC, survey design and data interpretation were undertaken by Margin – Marine Geoscience Innovation, as a Client Representative on behalf of NORI.

MBES backscatter data from the 2012 MV Mt Mitchell vessel-based MBES survey was reprocessed using the time-series data. This greatly improved the image quality Figure 7.5 compared to the original beam-averaged data and enabled geological interpretations of the data to be refined. These interpretations provided the foundation for the selection of candidate Collector Test-site targets for follow-up detailed survey by AUV.

Figure 7.5   Reprocessed EM122 backscatter data from NORI Area D 2012 survey
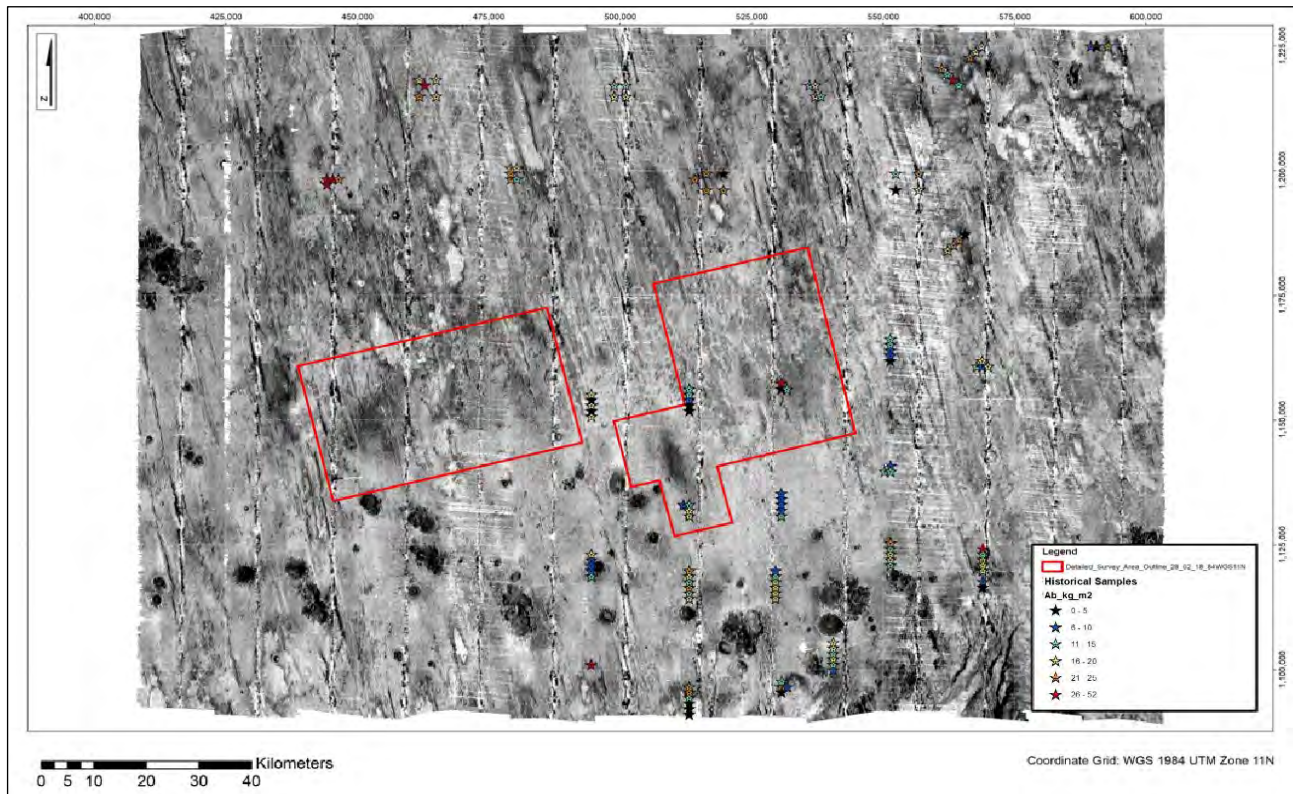
Note: NB – areas designated for AUV detailed survey are shown outlined in red, constituting targets deemed to have high-nodule potential and characterised by dominantly flat-lying topography.

7.3.2   AUV survey

AUV survey methods were identified as the best technological-fit for follow-up investigation at a site-survey scale. An AUV has the capability to provide co-registered multi-sensor datasets at the appropriate resolutions necessary to confidently select the most suitable site for a Collector Trial and provide a framework on which to build associated ongoing engineering and environmental studies.

Fugro's ESVII 4500 m-rated Kongsberg Hugin AUV was used to conduct the detailed survey work, utilising an MBES, Side Scan Sonar (SSS), Sub-Bottom Profiler (SBP) and camera payload Figure 7.6. The AUV typically navigates using a combination of Inertial Navigation System (INS) housed within the AUV and an acoustic navigation system (Kongsberg HiPAP 501 Ultra Short Base Line (USBL) system) communicating between the AUV and the support vessel. The USBL acoustically tethers the AUV to the support vessel, which follows the AUV during its survey and provides the AUV with navigation corrections to counteract drift in the INS system over time. This mode of operation was used for all reconnaissance mapping with the AUV. For survey of the Collector Test Site, the AUV was positioned within an array of transponders positioned on the seafloor – termed a UTP (Underwater Transponder Protocol) array. This enabled the AUV to be left unaided by the support vessel to compete its survey, whilst the support vessel conducted other work within the exploration license area.

Figure 7.6   Deployment ESVII Kongsberg Hugin AUV from the stern of the *Maersk Launcher*

Source: J. Croucher.

There were four main AUV survey focus areas:

- Reconnaissance lines were collected at a 35 m AUV altitude in order to assess geological and near-surface conditions prior to acquiring low-altitude camera data. These data were also used to select the Collector Test Site location and to assess the designated Preservation Reference Zones within the NORI Area D tenement.
- Camera lines were run at a 6 m AUV altitude in order to map the distribution and abundance of the nodules. These data were also used to select the Collector Test Site location.
- Within the Collector Test Site, data were collected at a 22 m altitude and were used to evaluate geologic and near-surface conditions for future Collector Test activities.
- Within the mooring sites, data were collected at a 90 m altitude and were used to evaluate geologic and near-surface conditions for future mooring locations.

Initial reconnaissance AUV traverses were conducted over the candidate Collector Test Site Figure 7.7 using MBES, SSS and SBP payloads to provide confirmation of topographic and geological features observed in the 2012 vessel-based MBES dataset, but at a higher level of detail and confidence. There was an excellent correlation between the AUV bathymetric data and that collected by hull-based multibeam methods in 2012, providing confidence in both sets of results. These traverses were then followed-up with low-altitude surveys using the AUV's camera payload to provide visual confirmation of nodule distribution.

The reconnaissance traverses were also designed in such as manner as to provide information on nodule continuity (through acquisition of sonar and camera data) between proposed sampling sites on a 7 km rectilinear sampling grid. A key component to the success of the campaign was the ability to conduct box coring simultaneously with the detailed survey by AUV of the selected Collector Test Site, through use of the UTP seafloor acoustic positioning array.

A total of 2286 line km of data was acquired with the AUV, covering an area of approximately 375 km^2 of seafloor. A summary of data types and associated data resolutions collected by the AUV during the 2018 NORI campaign is presented in Table 7.3.

Figure 7.7   AUV geosurvey data acquired during the 2018 NORI campaign
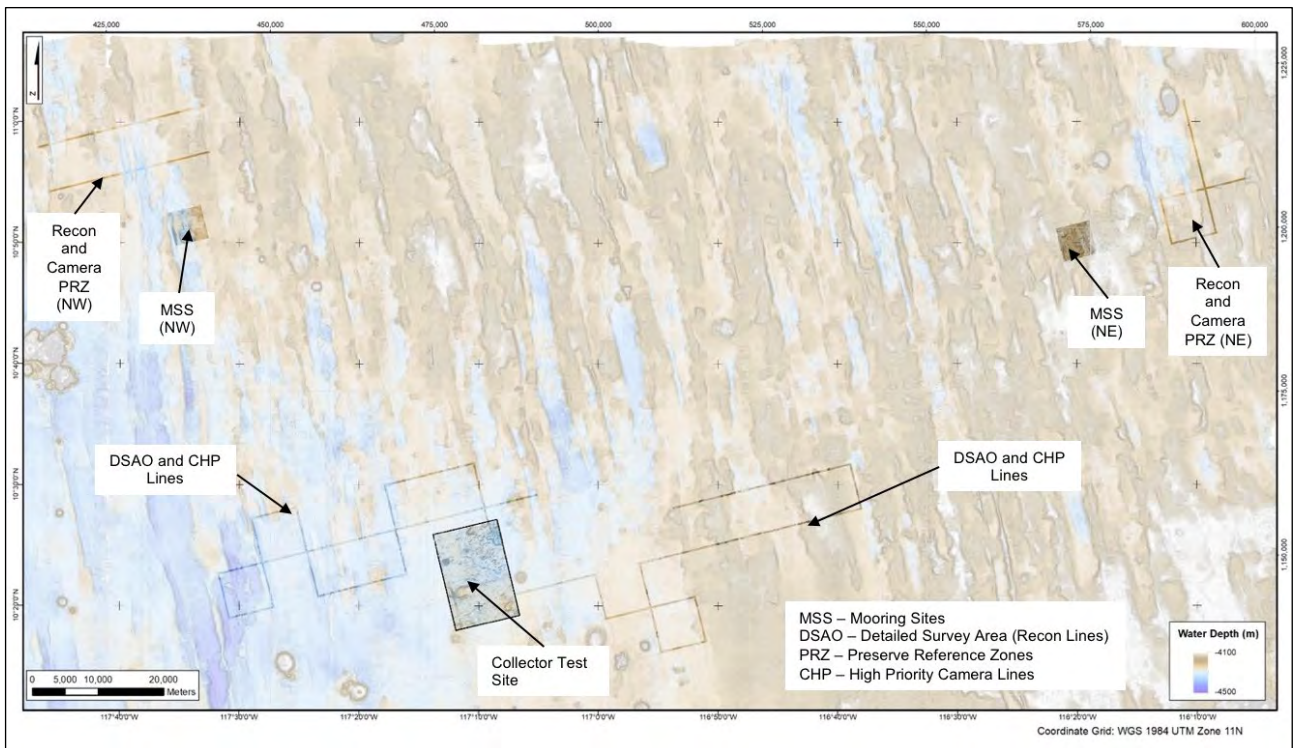
All data acquired by the AUV was processed onboard the vessel to a level where preliminary interpretation could be made on the data by the Fugro Geoscience team and NORI Client Representative onboard. This was key in enabling on-site decision making for follow-up survey optimisation, particularly with regards to selecting the most suitable Collector Test Site.

Table 7.3   Summary of data types collected by the AUV during the 2018 NORI campaign

AUV altitude			Survey area						
			90 m		35 m			22 m	6 m	
Sensor	Data item	Details	MSS (NE)	MSS (NW)	DSAO	Recon PRZ (NE)	Recon PRZ (NW)	Test mine site	CHP	Camera PRZ (NW)
MBES	Bathy	Bin size	3 m	3 m	1 m	50 cm	50 cm	27 cm	15 cm	15 cm
	Backscatter	Bin size	3 m	3 m	1 m	50 cm	50 cm	15 cm	15 cm	15 cm
Side scan sonar	SSL	Bin size	50 cm	50 cm	50 cm	25 cm	25 cm	27 cm	N/A	N/A
	SSH	Bin size	N/A	N/A	50 cm	25 cm	25 cm	15 cm	N/A	N/A
	SSX	Bin size	N/A	N/A	N/A	N/A	N/A	N/A	7 cm	7 cm
Camera	Orthos	Bin size	N/A	N/A	N/A	N/A	N/A	N/A	3 mm	3 mm
Sub bottom profiler	Sub bottom	Frequency	N/A	N/A	1-10 khz	1-10 khz	1-10 khz	1-10 khz	3.5-20.5 khz	3.5-20.5 khz

Note: MBES operated at 200 or 400 kHz, depending on survey resolution requirements. SSS was operated at 240 kHz, 540 kHz, or 1,600 kHz.

7.3.3   Box coring

Box coring was undertaken using a 0.75 m^2 box corer built by K.C. Denmark A/S, deployed from a H-frame situated amidships of the Maersk Launcher Figure 7.8.

A total of 45 box cores were acquired during the campaign. All box cores were acquired within the detailed survey area on a 7 km square grid Figure 7.9. The sampling grid was designed prior

to the mobilisation of the 2018 NORI campaign; therefore, the samples were selected without reference to any of the detailed geophysical data to avoid any bias.

Each box core site was located by positioning the vessel over the proposed box core location and acoustically monitoring the box core's position during descent using the vessel's USBL system communicating with a USBL transponder attached to the box core frame. Once the box core was lowered to approximately 30 m above the seafloor, the surveyor monitored when it was within a 35 m target circle displayed over the proposed target location on the USBL navigation workstation monitor. Once this condition was met, the instruction was given to lower the box core to bottom. Once on bottom a series of position fixes were acquired to solve the on-bottom position. The mean distance between the proposed target location and actual box core position was 18.4 m ±7.9 m.

It is important to note that the hydrographic surveyors guiding the landing out of box cores were only supplied the expected seafloor datum at the proposed core site location. They did not have access to any geophysical data (backscatter, SSS or camera etc.) during these operations. This ensured that the sampling was conducted without any bias.

Once the position fix was taken, the cutting shovel was released to seal and secure the sample and the box corer was winched up off the seafloor. Once the sample was secured on deck, the samples follow three processing paths - environmental, geotechnical, and mineralogy.

A stand-alone GoPro camera system in a pressure-rated underwater housing and LED lights were attached to the legs of the box corer. This enabled post-recovery analysis of land-outs to be made and comparison of actual box core nodule recovery and in-situ nodule distribution on seafloor.

Figure 7.8   KC Denmark 0.75 m² box corer
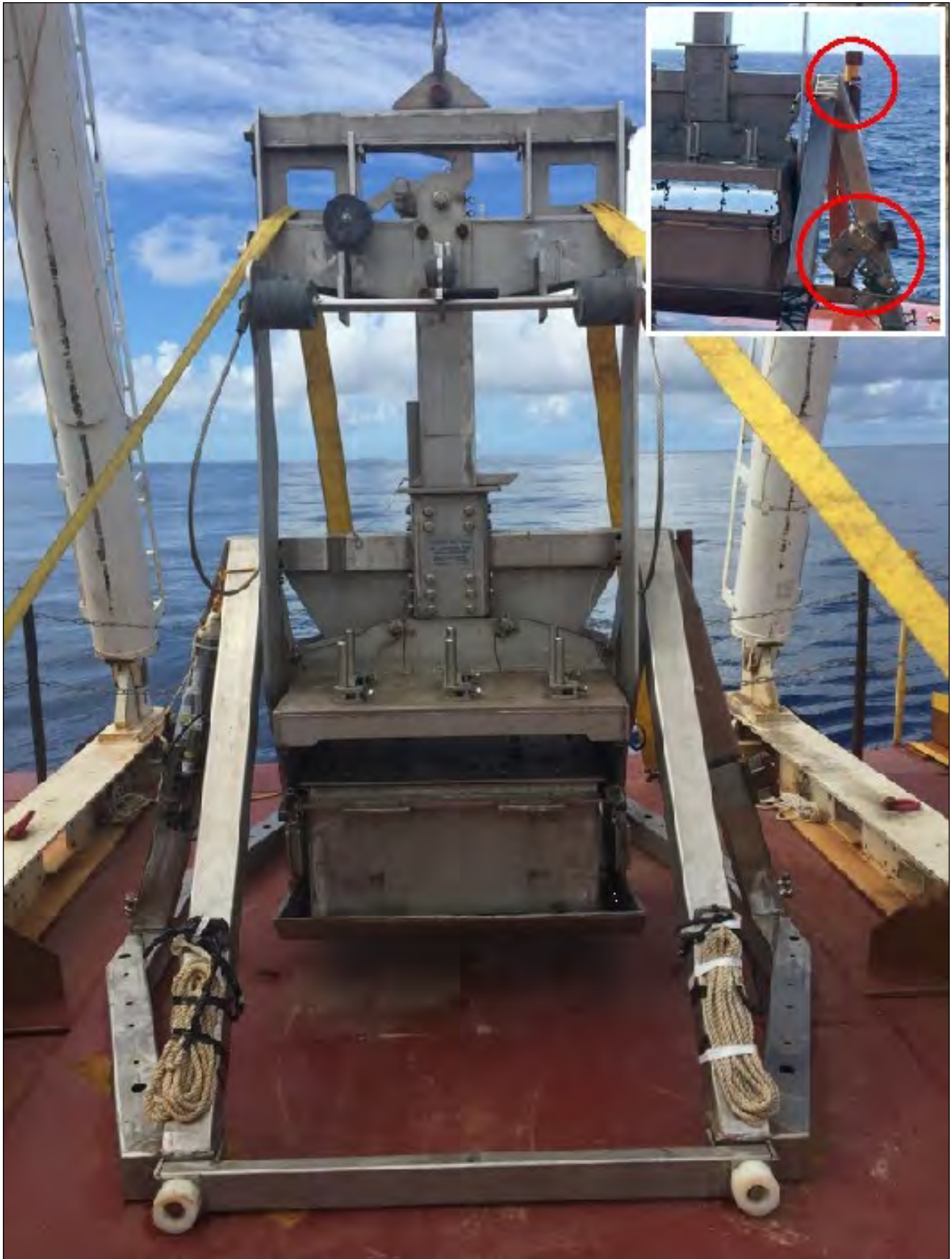
Note: Insert top right shows USBL beacon (circled top) and GoPro camera and lighting system (circled bottom).
Source: H. Hughes.

Figure 7.9   Box core locations for 2018 NORI campaign shown by green circles with black centre-dot
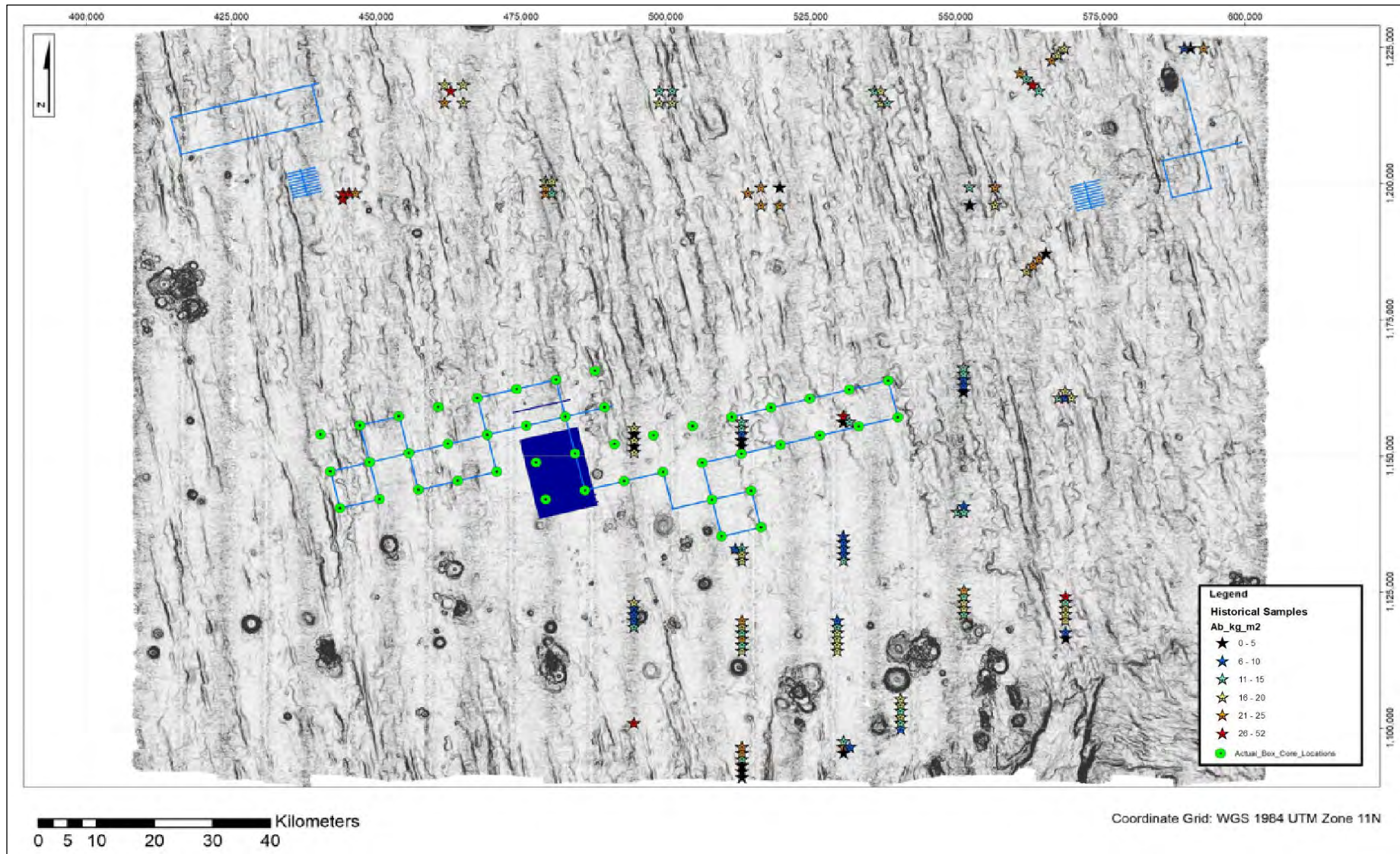
Note: Historical sampling shown by stars. NORI 2018 campaign AUV geosurvey traverses shown in blue.

Figure 7.10 shows a sequence of box core land-out footage from the GoPro camera. The top image shows the land out site visual as box core is deployed to seafloor. The middle image shows the box corer in situ on seafloor, before sample is taken (shovel open). The bottom image shows the box corer retracting from seafloor following successful closure of shovel. Loss of the laser-scale early in the campaign meant that nodule measurements could not be accurately measured from the GoPro images.

Figure 7.10   Sequence of box core land-out footage from GoPro camera

7.3.3.1 Sample processing

All samples were processed onboard post-retrieval of a box core sample to deck Figure 7.11. The vessel was equipped with a biology cold laboratory and geoscience laboratory.

Once the box core was landed out on deck and safely secured, the box was separated from the box corer frame. Three processing protocols for environmental, geotechnical, and resource began immediately after collection of each box core. The processing flow on deck was undertaken in the following sequence:

- The top of the sample with the supernatant water still in situ was photographed.
- The water was then carefully siphoned, bailed and / or suctioned off the sample and processed for biological analysis by the biological team onboard.
- The undisturbed surface of the retrieved material (nodule surface) was photographed.
- A 50 × 50 cm area of the retrieved material was cordoned for biological study.
- Three sub-samples were obtained from the undisturbed areas outside of the biology exclusion area for geotechnical purposes. All nodules except for possible buried nodules captured in the 2.638-inch push samples followed the Mineral Resource processing path.
- All surface nodules, when extracted from the box, proceeded to the biology wet laboratory where they were washed with cold seawater through a sieve.
- All buried nodules in the 50 × 50 cm area reserved for biologic sampling also proceeded to the biology wet laboratory. After washing, these nodules were returned to the geology wet laboratory.
- All buried nodules outside of the area of biologic investigation were washed of mud on deck and proceeded to the geology wet laboratory for description, measurement, photography, and sequestration in sample bags within gasket sealed pails.

Figure 7.11   On deck sample processing

Notes:
1. Sample with supernatant water photographed.
2. Water siphoned off for biological processing.
3. Box core with water removed showing GoPro camera mount and 50 × 50 cm frame demarcating area for biological study.
4. Example of GoPro top shot showing nodule distribution.
5. Geotechnical samples being taken.
6. Each layer was excavated for nodules, which were placed in collection trays for further biological processing and mineralogical logging.

7.3.4   NORI sampling

A classification system for nodules was developed by NORI prior to mobilisation to the worksite. This was largely based on guidelines set by the ISA (ISA, 2010) and work presented by TOML in their NI 43-101 resource report (AMC, 2016). Over 49,000 nodules were collected in the 45 box cores. Examples are shown in Figure 7.12. An image classification method was adopted to enable rapid measurement of each nodule for all remaining box core samples. However, descriptors such as shape, texture, and fragmentation were only recorded as the dominant types for each box core sub-sample layer, and not for each nodule.

An average nodule size of 2.95 cm (long axis measurement) was recorded for all samples recovered during the 2018 NORI Campaign. Table 7.4 presents a summary of the size distribution of the nodules within 0–1 cm of seafloor.Shape, texture and fragmentation descriptors were logged as dominant types for each box core layer. Logging was captured in a digital excel database on-board the vessel.

Table 7.4   Nodule size distribution for samples recovered during the 2018 NORI campaign

Long Axis				
<2 cm	2-5 cm			>5 cm
s (small)	sm	m (medium)	ml	l (large)
24%	37%	23%	9%	7%

Figure 7.12   Examples of nodules recovered during the 2018 NORI campaign
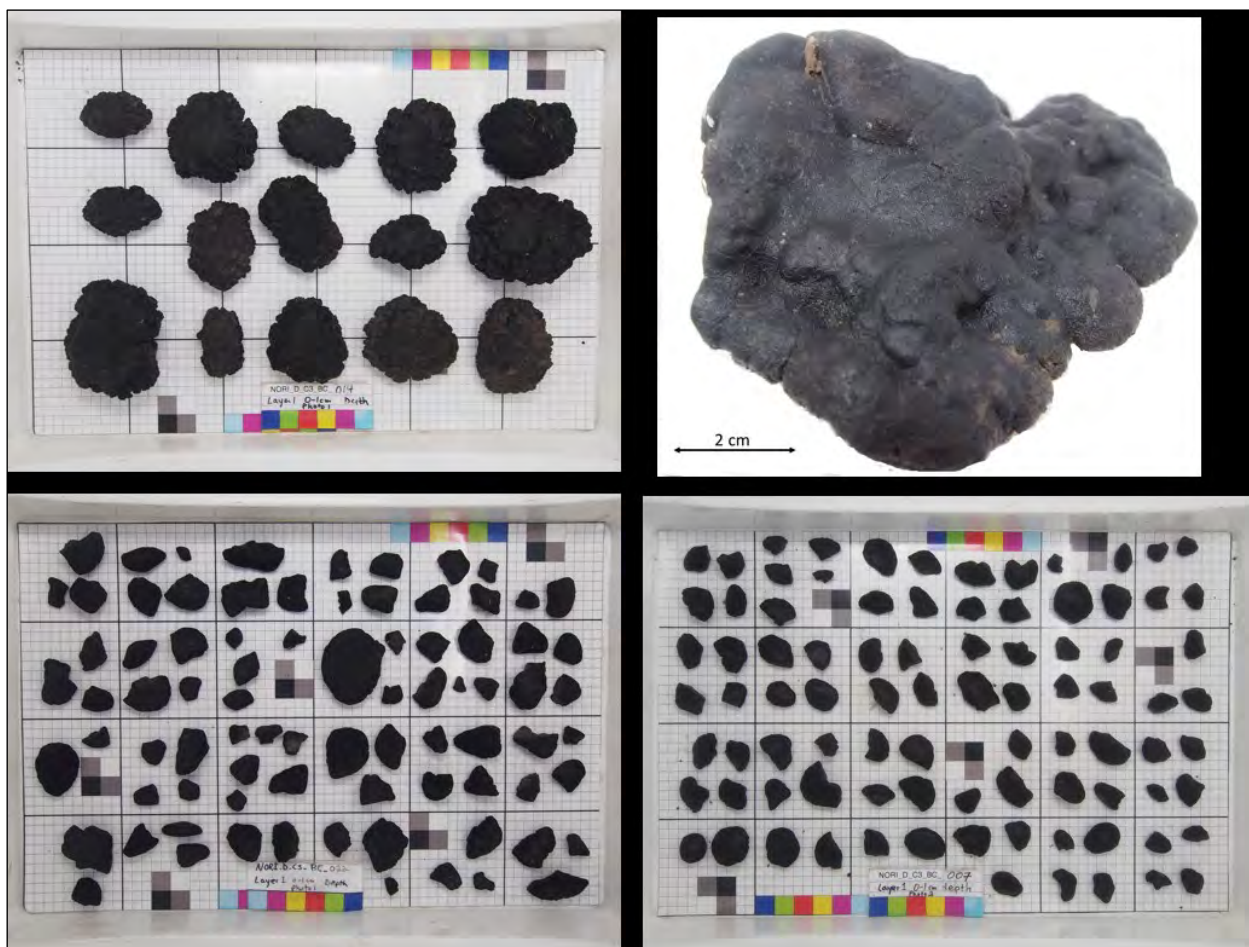
Notes: Upper left – example of large nodules with rough texture. Top right – close-up of large nodule. These nodules were the least-dominant size class. More common were nodules in the 2–5 cm range, as shown by examples in lower left and right.

Each box core was sampled by depth interval. Four intervals were used:

- 0–1 cm
- 1–5 cm
- 5–15 cm
- >15 cm

91% of nodules by weight occurred within the top layer and were exposed at seafloor and 99% occurred within the top 15 cm.

Nodules were processed through three stations - a weighing station, volume station and photography station, before division of the nodules into samples and storage in labelled, gasket-sealed 6-gallon pails. All data was collated in a series of Excel spreadsheets.

Samples for distribution to assay laboratories were prepared at sea so that the samples could be sent to their destinations upon demobilisation. The mass of nodules recovered in the box cores was generally much more than required for assaying, so it was necessary to divide the nodules in an unbiased manner, to produce samples for assay and for reference. This was done by the cone and quarter method Figure 7.13. The sampling protocol varied according to the weight of the nodules and is summarised in Table 7.5.

After samples were split, the samples were divided into series of sub-samples for marketing, primary assay, reference, duplicate primary sample and secondary primary sample. These were placed in sealed bags. Each sample was given a unique numbered zip tie placed inside the bag. Bar codes were generated from these unique numbers and adhered to the side of the bag, plus written on the side of the bag in permanent marker pen. Bar codes were linked to the Excel sampling database.

Certified blank samples were purchased from ALS laboratories in Reno, Nevada and inserted into the primary and duplicate sequence at a rate of 1 for every 10. One blank from the primary sequence and one blank in the duplicate sequence was spiked with approximately 50 g of nodules sourced from a marketing split. Certified nodule reference materials were purchased from the United States Geological Survey (USGS) and inserted randomly into the sample stream at the assay laboratory.

All samples were placed in gasket-sealed 6-gallon pails, sealed with tamper-proof tape.

Table 7.5   Sampling protocol

Total nodule weight	Procedure	Primary assay sample	Reference sample (retained)	Duplicate (primary lab)	Duplicate (secondary lab)	Marketing sample
0–4 kg	Crush oversize, cone & quarter. Combine opposite quarters to make two samples.	Yes	Yes	No	No	No
4–8 kg	Crush oversize, cone & quarter. Bag separately.	Yes	Yes	Yes	Yes	No
8–12 kg	Cone and quarter (uncrushed). Retain one quarter for marketing. Recombine the other three quarters and crush oversize, cone & quarter, bag the quarters separately.	Yes	Yes	Yes	Yes	Yes
> 12 kg	As for 8-12 kg, then combine opposite quarters, cone & quarter, bag the quarters separately.	Yes	Yes	Yes	Yes	Yes

Figure 7.13   Coning and quartering process
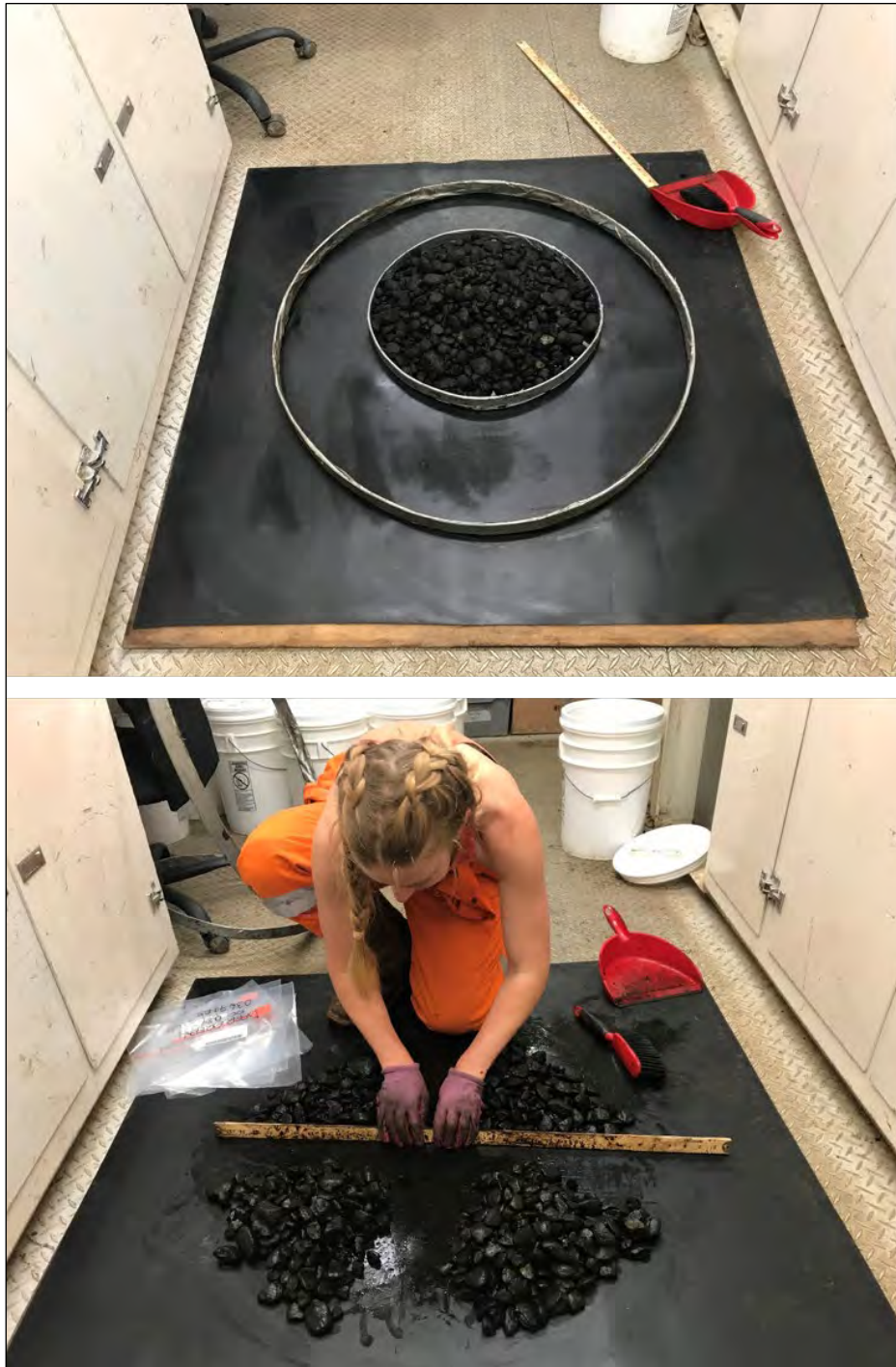
7.3.5   Image classification and size measurement

Image classification software was used to provide an alternative automated approach to measurement of nodule dimensions, using photographs. Figure 7.14 presents a comparison between the automated image processing method and hand-held calliper measurements and shows a very good correlation between the two datasets. The average (mean) lengths of the long axes of the nodules using the classification approach and the measured approach were both 3.31 cm. The mean for short axis estimation using the classification zone approach was 2.68 cm, whilst the mean for the measured approach was 2.72 cm. The test demonstrated that the image classification method was a practical, accurate method for measuring two orthogonal axes of the nodules and it was used from box core BC006 onwards.

Figure 7.14   Comparison of image classifier results vs caliper measurements
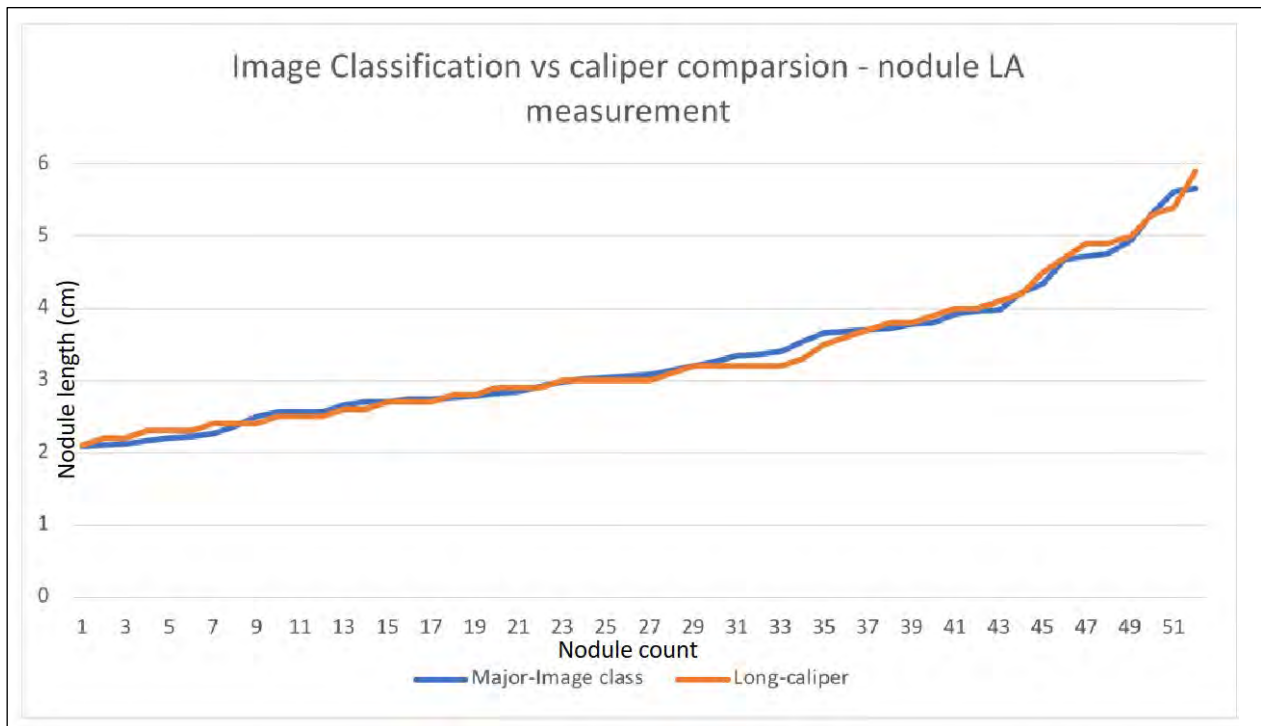
7.3.6 Biological sampling

The biological sampling was completed in 35 of the box cores Figure 7.15 and consisted of the following:

•   239 nodule biota specimens were sampled.

•   62 megafauna (>2 cm) specimens were sampled.

Samples were placed in cold storage for further analysis once ashore.

7.3.7 Geotechnical sampling

Three soil sub-samples for geotechnical study were obtained from the undisturbed areas of each box core. These consisted of one 2.125 inch inside diameter (ID) liner sampler, and two 2.638 inch ID clear polycarbonate tubes.

The focus of the geotechnical sampling was the clayey footwall sediment sequence. Basic off-shore index and strength laboratory tests, comprised of soil descriptions, wet density measurements, and undrained shear strength index tests (Torvane tests and intact and residual miniature vane tests) were conducted on the geotechnical subsamples obtained from the box cores.

Results from the field tests revealed that the shallow soil stratigraphy consists of a veneer (about 6 cm thick) of surficial, dark brown, very soft semi-liquid clay overlying very soft, dark brown clay to a maximum core penetration depth of about 0.5 m BSF. At about 0.15 m depth, typically, a colour change from dark brown to light brown occurs. Evidence of bioturbation of the light brown layer is indicated by mottling with dark brown and brown clays. It was noted on the high-resolution geophysical survey data that a reflector at about 15 cm to 20 cm depth was consistently present across all the box core sites sampled. This depth corresponds with the top of the light brown clay. Qualitative carbonate content testing typically indicates no reaction with dilute hydrochloric acid (10% concentration).

Figure 7.15 NORI Area D box core locations, showing those with biological sampling (in green)
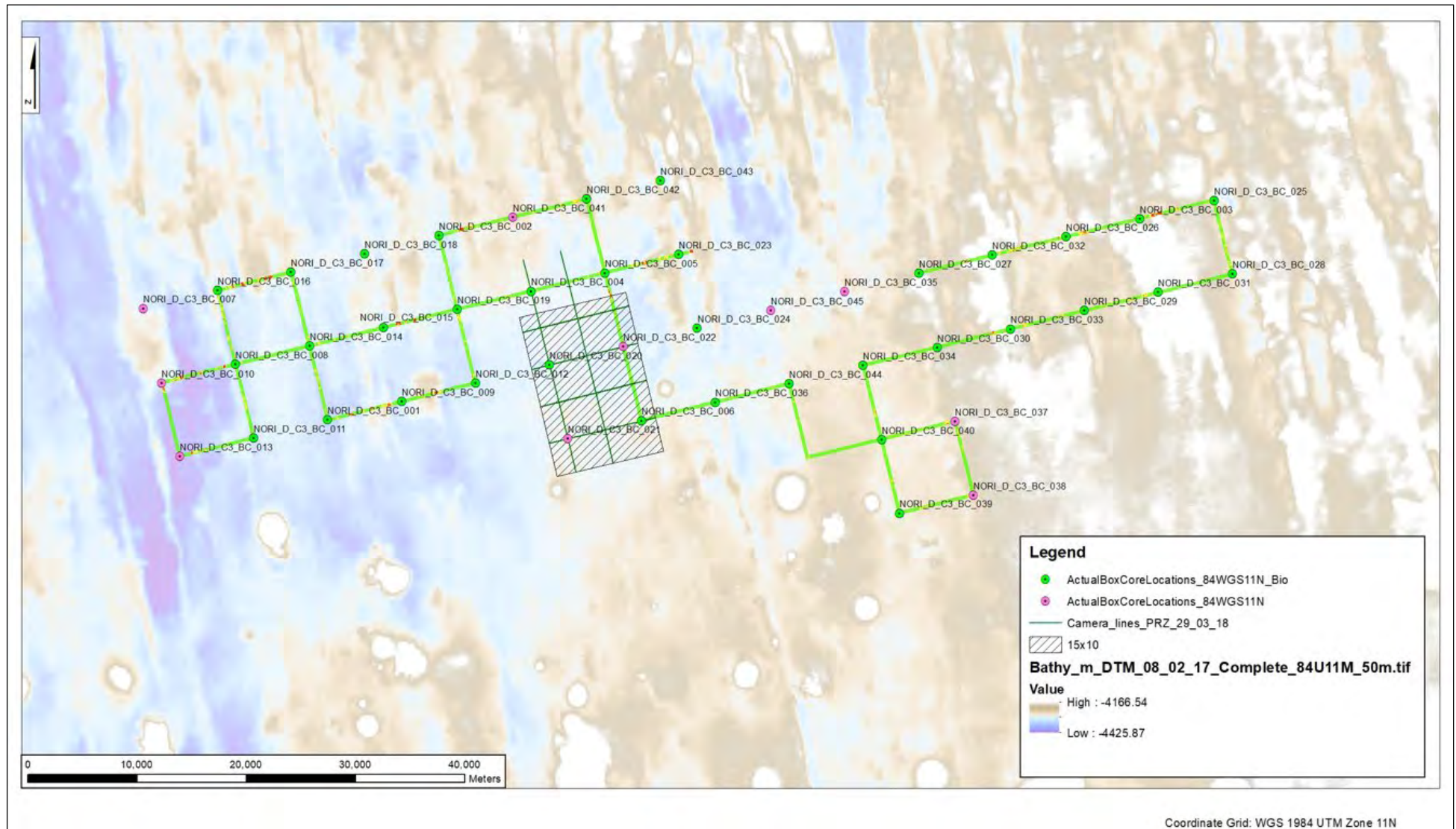
7.3.8   Exploration results

The exploration results discussed herein include all data relevant to the Mineral Resource estimate. Additional data was acquired throughout the campaign for the purposes of selecting and mapping a Collector Test Site, environmental Preservation Reference Zones and oceanographic mooring site. These results are not discussed in any detail in this report.

7.3.8.1   Box core abundance

Figure 7.16 shows the spatial distribution of nodule abundance and Figure 7.17 shows the nodule type as per the ISA system outlined in Section 6.6. The box cores had an average nodule abundance of 17.8 kg/m^2, with the highest abundance reported at 30.9 kg/m^2 (BC005). The two lowest recorded abundances are BC019 (0.8 kg/m^2) and BC031 (6.5 kg/m^2).

Figure 7.16   Box core abundance (in kg/m²)
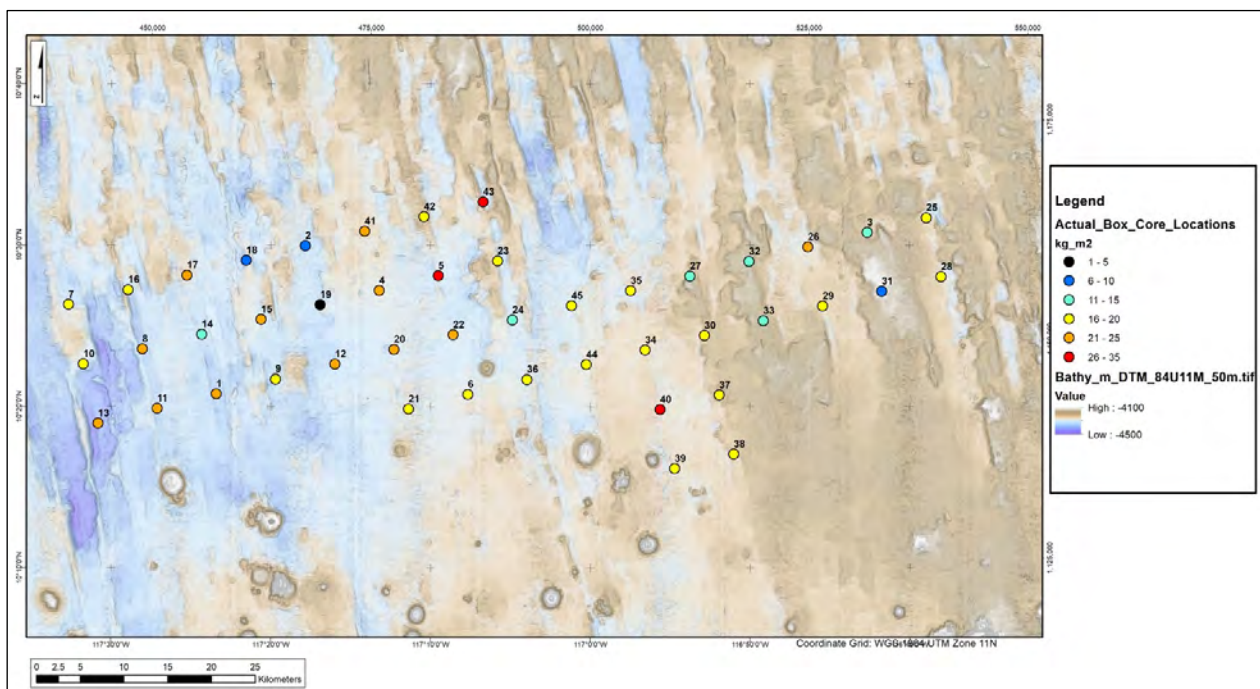
Note: Box cores labelled by box core number.

Figure 7.17   Box core size-texture classification
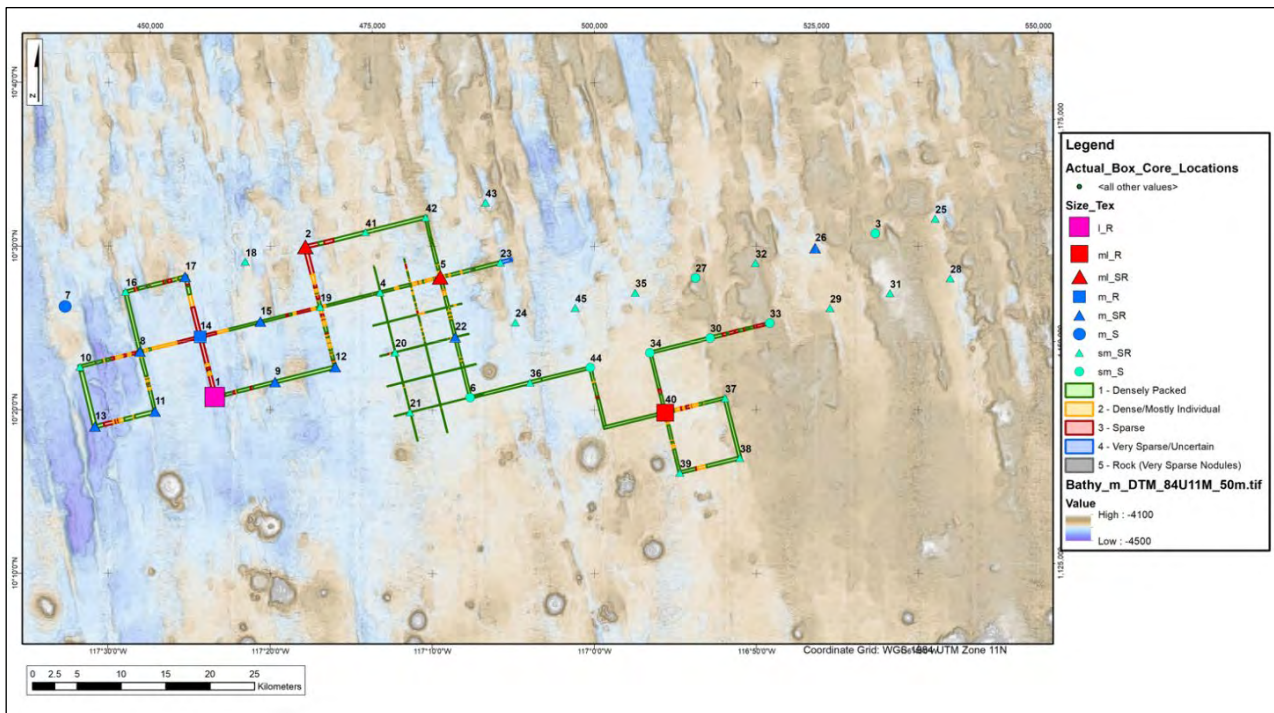
Note: ISA size classification: small (<2 cm), medium (2 – 5 cm), or large (>5 cm) grain size, and texture is smooth (S), smooth-rough (SR), or rough (R). Box cores labelled by box core number.

7.3.8.2   Buried nodules

On average, 91% of nodules by weight were located at 0–1 cm (exposed at seafloor). This is an important consideration as it implies that a representative nodule abundance can be estimated using seafloor camera imagery to map and characterise nodule surficial distribution at seafloor.

Layers 3 and 4 logged in box cores often included a few nodules pushed down deeper from upper layers by the sides of the box core, typified by accumulation along the sidewalls of the box corer. BC043 was an exception and returned a significant weight of in-situ nodules throughout the core at all levels Figure 7.18. The buried nodules were very friable.

Figure 7.18 Profile of nodule weight by depth in BC043
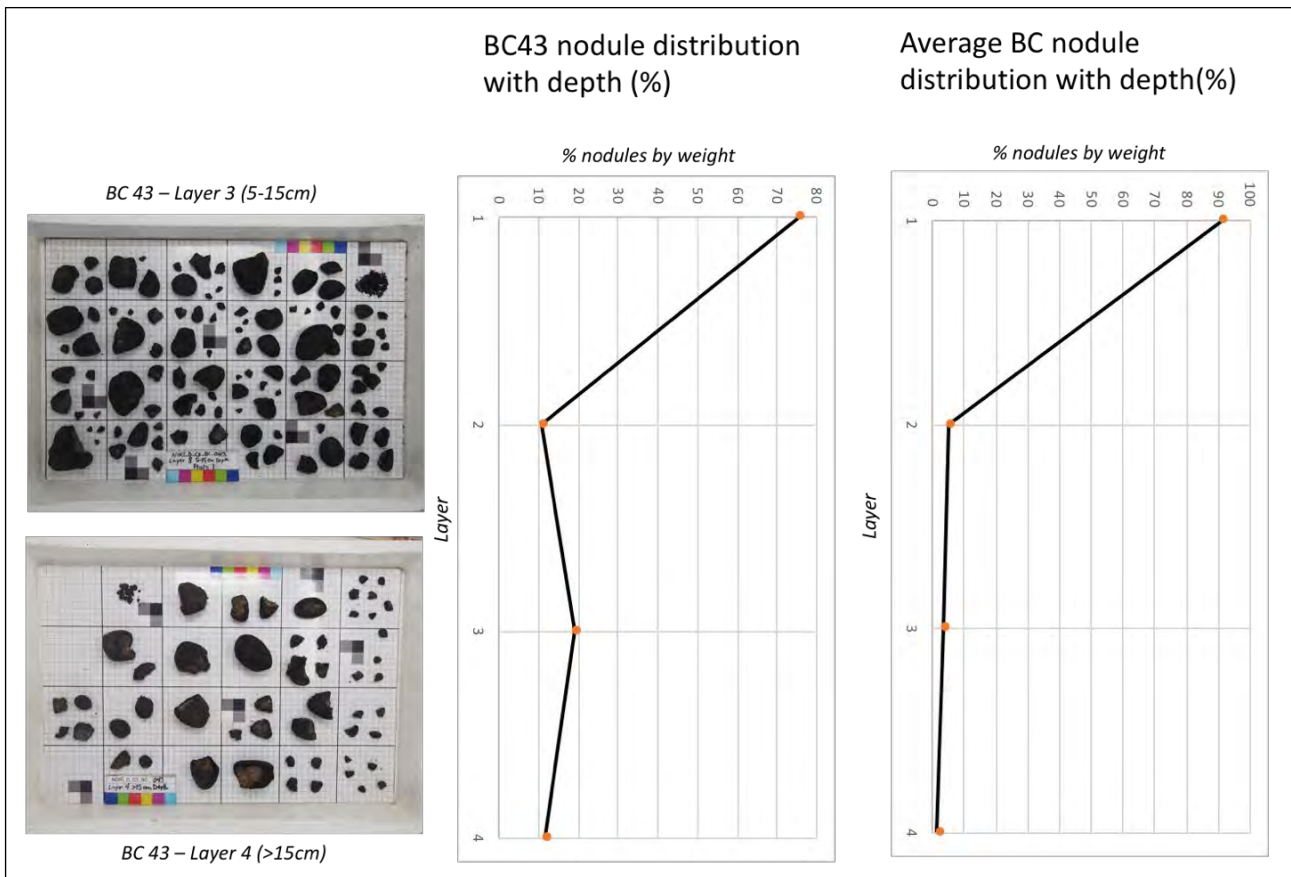
Note: Left – photo trays from layers 3 and 4, centre – nodule distribution with depth for BC43, compared to average nodule distribution with depth for all box cores (right).

7.3.8.3 AUV data

Reconnaissance AUV MBES traverses were conducted over the candidate Collector Test Sites to provide confirmation of topographic and geological features observed in the 2012 vessel-based MBES dataset, but at a higher level of detail and confidence. These traverses were then followed-up with low-altitude surveys using the AUV's camera payload to provide visual confirmation of nodule distribution. The reconnaissance lines also enabled calibration and refinement of the NORI Area D regional geological interpretation. Based on these revised interpretations a geomorphological domain interpretation was developed and preliminary relationships between backscatter and nodule distribution facies observed in camera data were established.

Figure 7.19 shows examples of AUV MBES data (ribbon) from reconnaissance traverses, shown against a background of EM122 vessel-based MBES background. The AUV data provides much finer-scale resolution than vessel-based bathymetry and shows good spatial correlation with macro-features. Figure 7.20 illustrates the fine geological detail provided by the AUV MBES. This type of detailed data will be useful for designing the operating path of the seafloor nodule collectors.

Figure 7.19 Comparison of AUV MBES data (ribbon) against EM122 vessel-based MBES
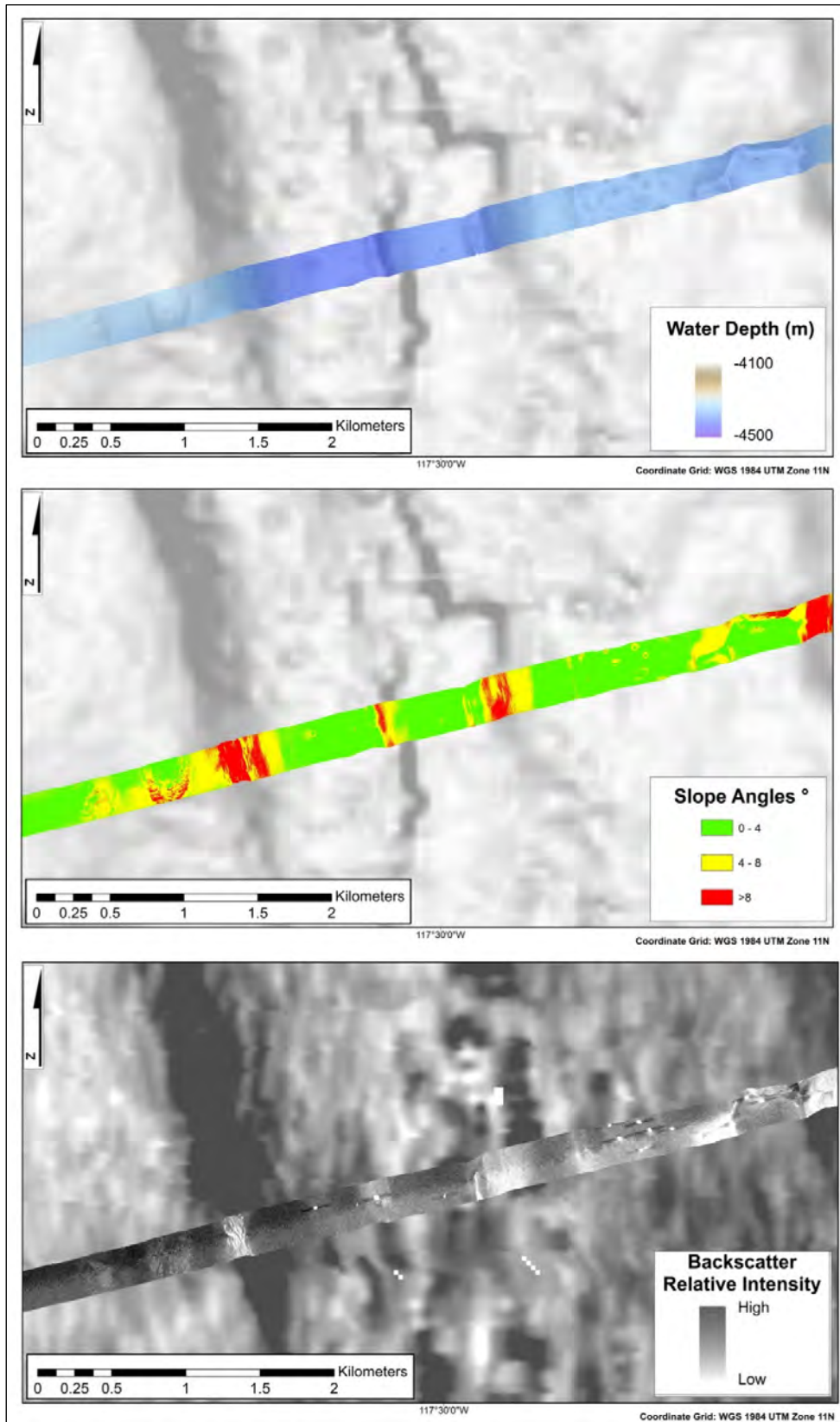
Note: Top – bathymetry; middle – bathymetric slope (hot colours indicate steeper slopes); bottom – backscatter.

Figure 7.20 Examples of AUV MBES data showing detailed-scale geological features
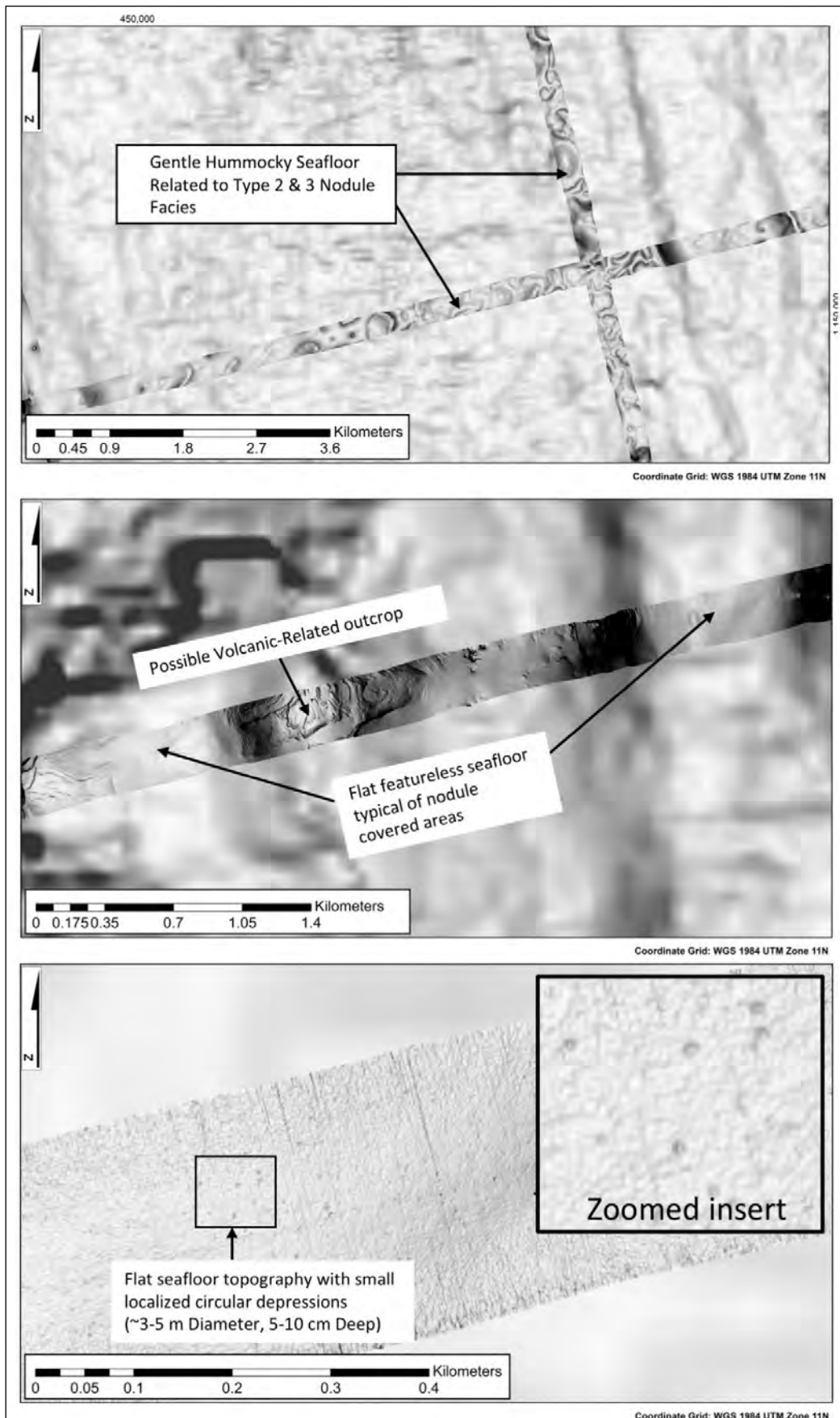
AUV camera data was acquired at 6 m altitude for 89% of the reconnaissance traverses, providing visual continuity of nodule distribution between the majority of the physical box core sample sites. In addition, a 3.5 × 3.5 km grid of camera data was acquired over the Collector Test Site. Camera data is near-continuous over the reconnaissance traverses. Photomosaic coverage along the 3.5 × 3.5 km spaced camera traverses over the selected Collector Test Site are continuous. Each camera frame is 6 m across-track and 4 m along-track. Figure 7.21 provides an example.

Figure 7.21   Example of AUV camera photo mosaic showing nodules
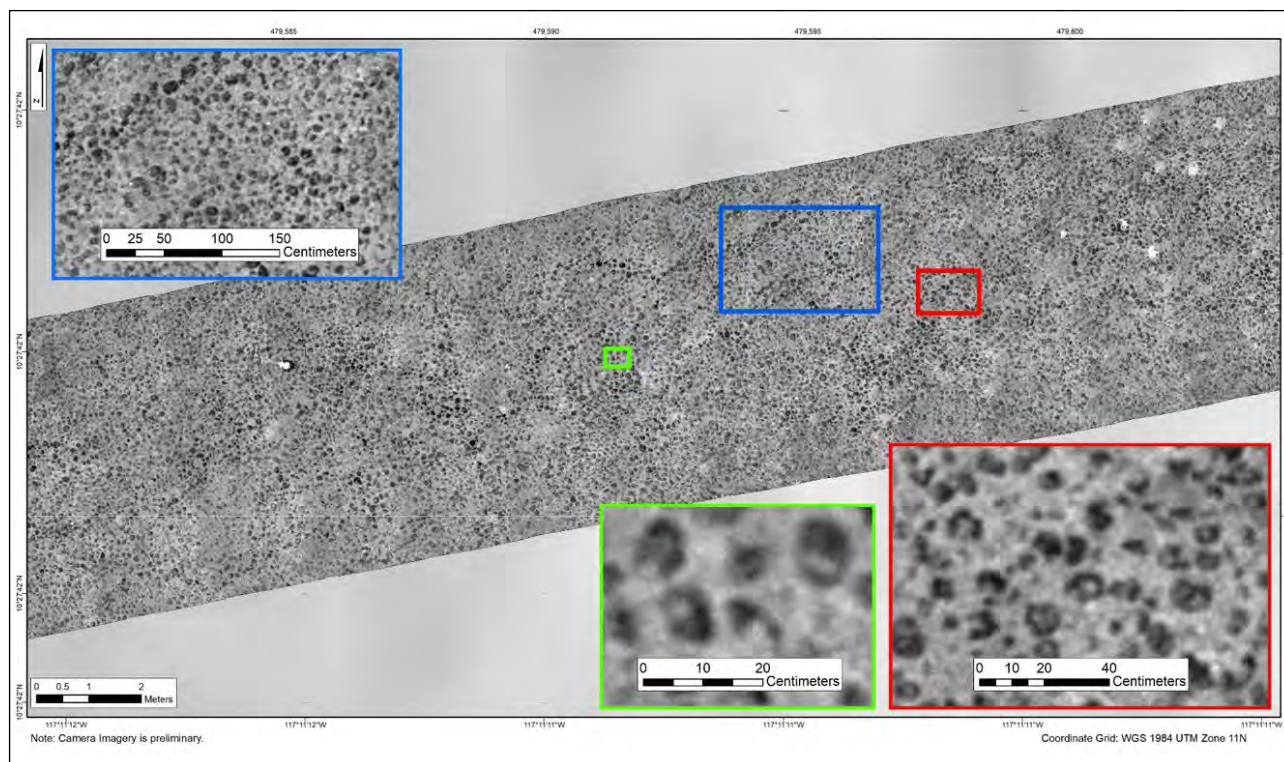
7.3.9   Nodule abundance estimation derived from AUV camera data

Although box coring is an effective method for measuring nodule abundance, it is slow and expensive. Therefore, it is advantageous if box core estimates can be supplemented by an alternative method.

There is a well-documented relationship between nodule length and wet weight (e.g., Felix, 1980). NORI confirmed this relationship by taking measurements of individual nodule length, using digital callipers, and wet weight, for nodules from box core samples BC001, BC002, BC003, and BC005 Figure 7.22.

In areas where nodules are not closely packed, image processing techniques can be used to identify each nodule unambiguously and measure its dimensions. In this case, it is possible to estimate nodule abundance from photographs. However, if nodules are closely packed and touch each other, image processing techniques are currently unable to reliably discriminate each individual nodule.

Photographic data acquired during the 2018 NORI campaign has shown the dominant nodule distribution in NORI Area D to be closely packed small-to-medium sized nodules (average long-axes length of 2.95 cm), averaging over 900 nodules per box core sample in the surface layer. It is therefore not possible to use image processing and not practical to use manual measurements of long axes for this facies.

Several estimation techniques were tested, and an alternative methodology was developed using a combination of long-axis measurement and percentage nodule coverage which was applied to the data.

Figure 7.22   Comparison of nodule long axis measurements, taken using digital callipers, and individual nodule wet weight for BC001, BC002, BC003, and BC005
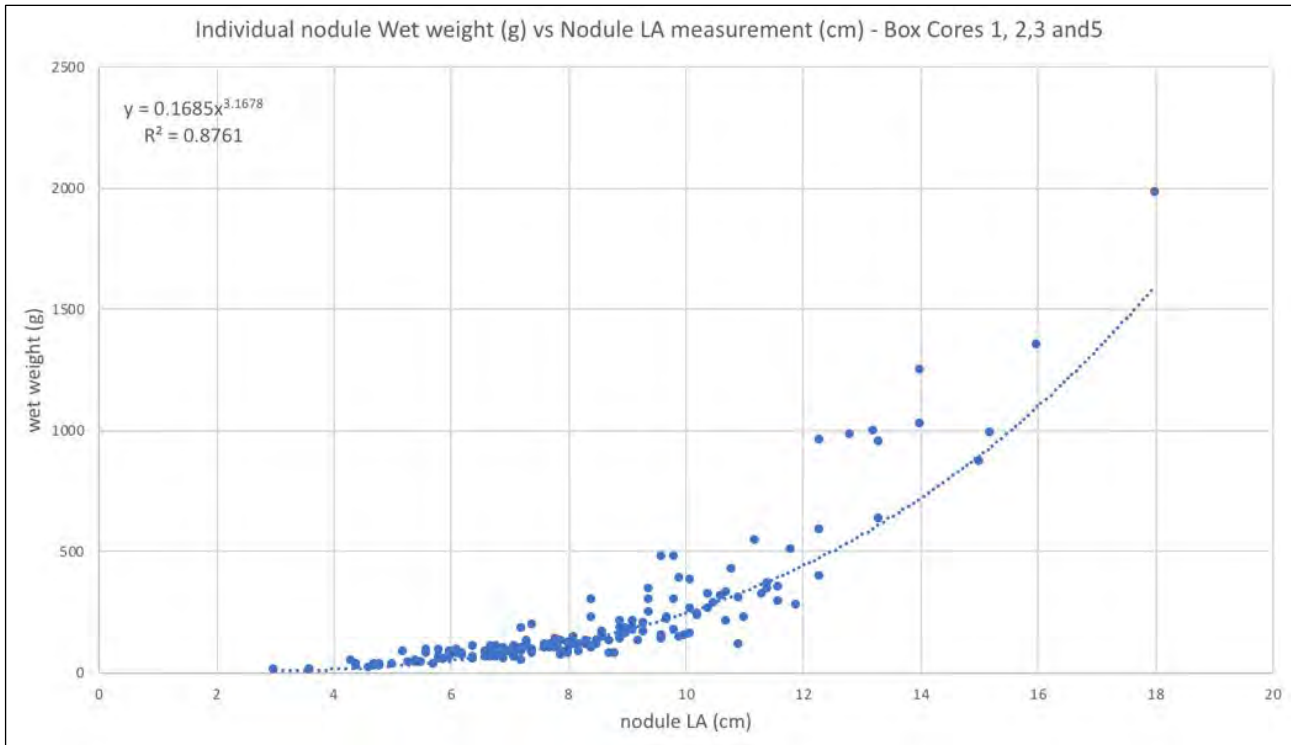
A multiple linear regression relationship between percentage nodule coverage estimated from the photographs and mean nodule long-axis measurement from six box core samples within the Collector Test Site was found to provide a good correlation with nodule abundance. The relationship is of the form:

$$Y = -15.20 + (0.24\ X_1) + (5.19\ X_2)$$

Where:

   Y is the estimated nodule abundance

   X_1 is the percentage nodule cover

   X_2 is the mean Long Axis measurement

The percentage nodule coverage was determined by thresholding the image and calculating the percentage area covered by nodules in the image. Nodule long-axes were manually measured where possible, for each nodule in the image Figure 7.23.

Figure 7.23   Detail of image processing
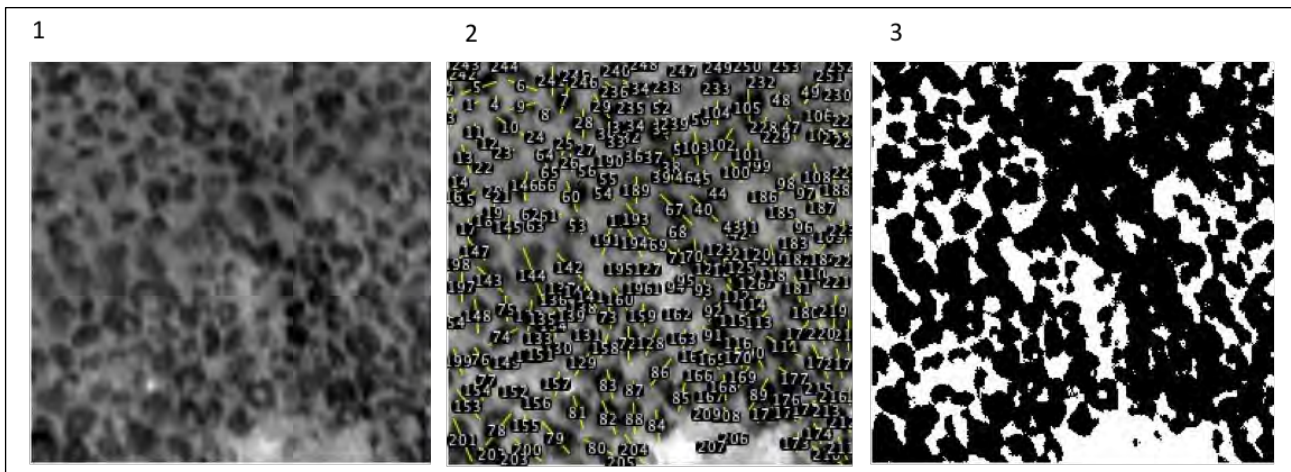
Notes:
1. Camera image.
2. Manual measurement of nodule long axes on calibrated image.
3. Image thresholding to determine percentage nodule coverage.

It was possible to obtain enough measurements to calculate representative mean long axis lengths which compared well with the mean long axis measurements from the actual box core samples Figure 7.24. Because photographs were not taken at the exact box core sites (due to loss of the camera laser-calibration system mounted on the box corer), 1 × 1 m subsets of the closest calibrated AUV camera data were used for this analysis. The average offset between the camera data and the actual box core site locations was 26 m. The offsets will have introduced some imprecision to the analysis, and it is expected that, in future, collocated photographs and box core samples will produce a better correlation.

Figure 7.24   Comparison of mean long axes lengths from AUV camera imagery and box cores
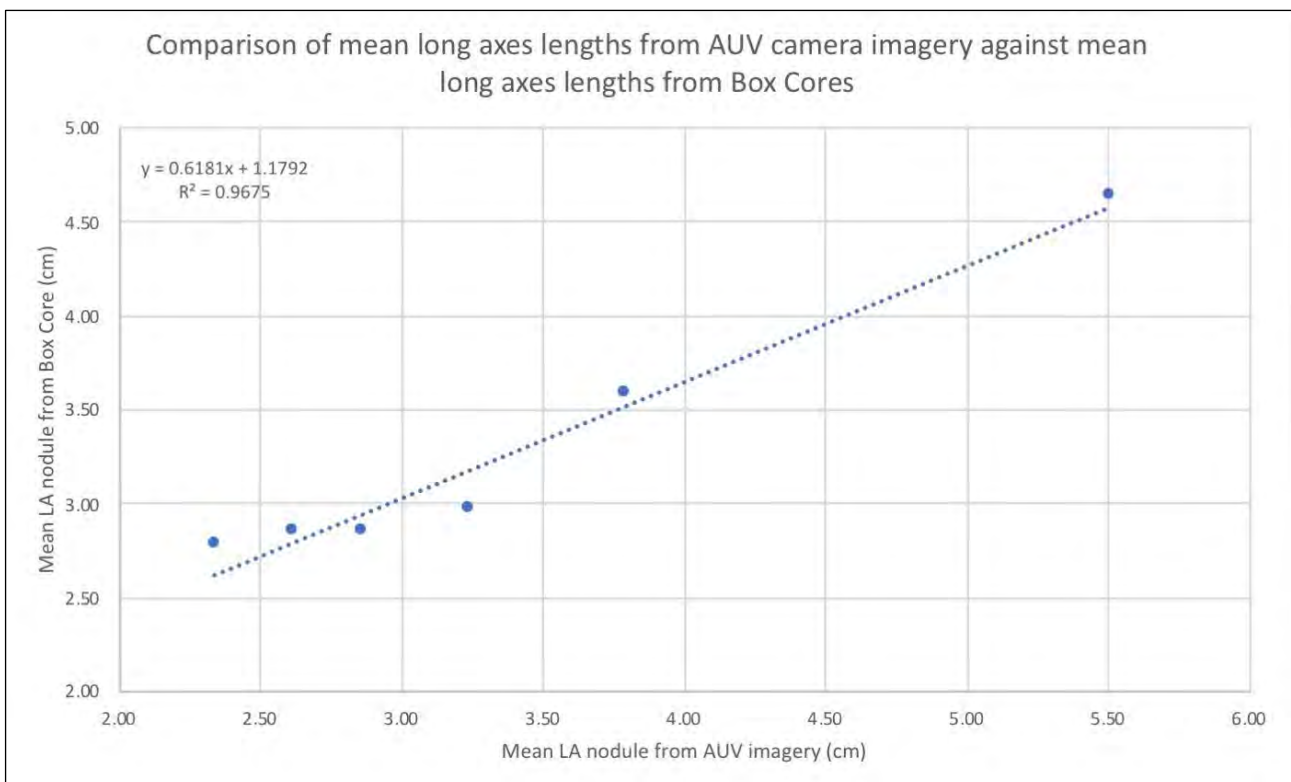
Figure 7.25 shows the estimated abundance vs. actual abundance for Felix method (top), and the multiple linear regression method (bottom) for six box cores in the Collector Test Site. Although the correlation is high for the Felix method, the multiple linear regression method provided a better correlation than the Felix method and estimates that are closer to the actual nodule abundances. This is because the method is not dependent on measurement of each-and-every nodule in the image, which is not possible with some of the images typical of Type 1 nodule facies.

Figure 7.25 Comparison of Felix method and multiple linear regression method
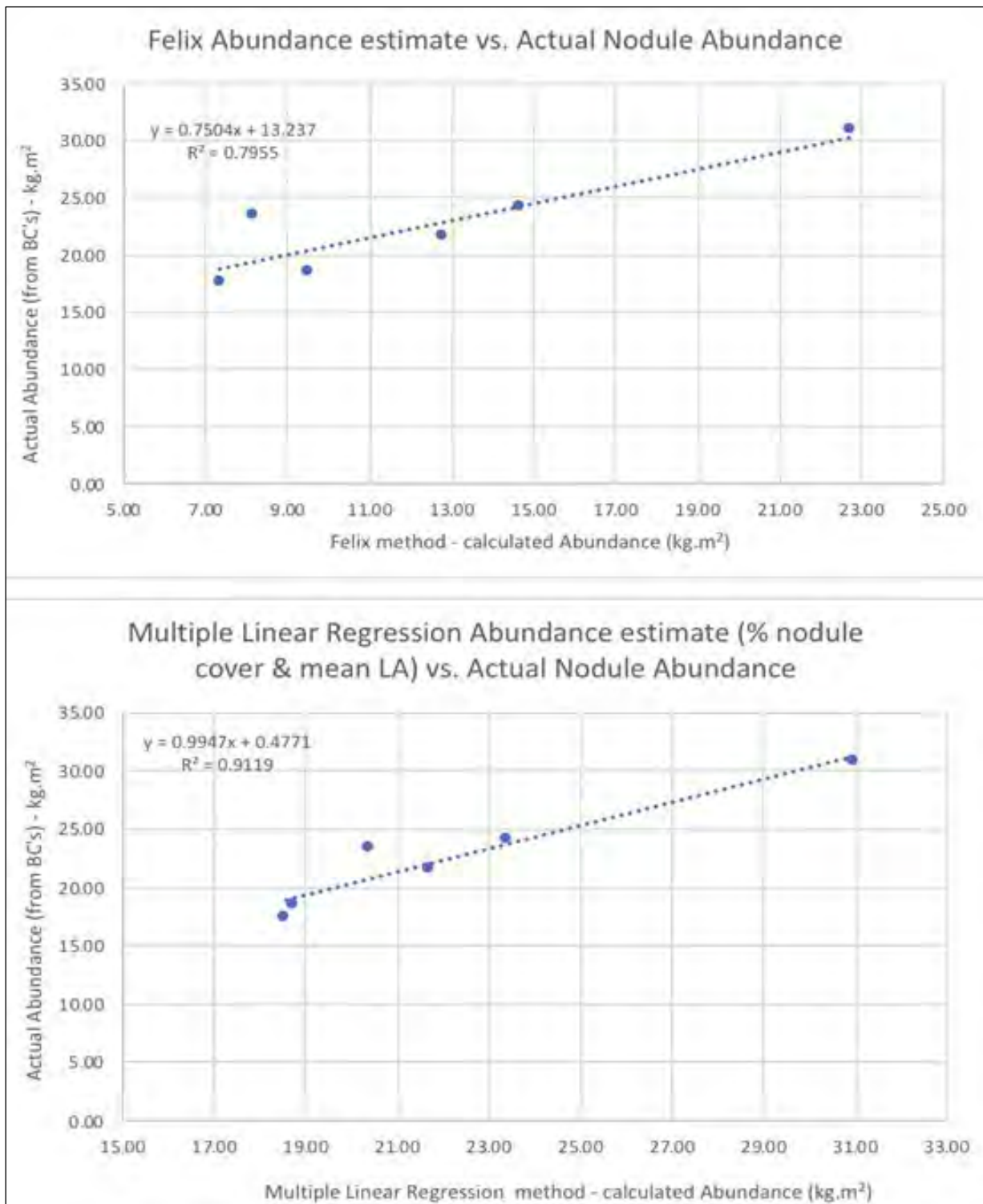
The multiple linear regression method was subsequently applied to the entire box core data set with associated AUV camera imagery (a total of 29 box cores used) to derive a more representative relationship using all available data. Extracted camera imagery was within an average offset of 15 m from actual box core site locations. The results are shown in Figure 7.26. An acceptable correlation (with an R^2 coefficient of 0.62) was obtained.

Figure 7.26   Multiple linear regression model for nodule abundance
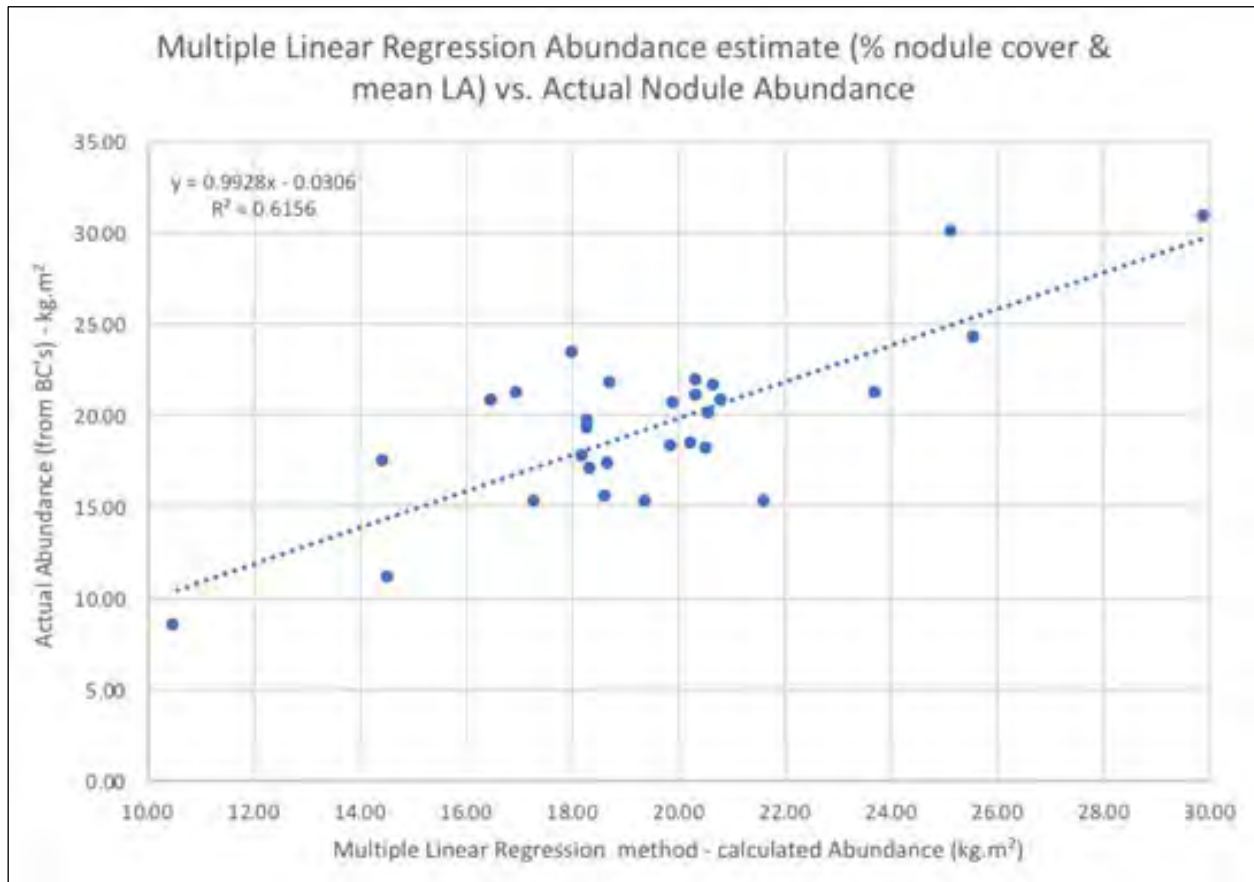
AUV camera transects were acquired on a 3.5 × 3.5 km grid pattern over the Collector Test Site. Subsets (1 × 1 m) of AUV camera data were extracted for each intersection point of the survey lines and the percentage nodule coverage was extracted as per the methods outlined above. Mean nodule long axis measurements were manually extracted from these images. This was necessary, as the majority of these extraction points are situated in Type 1 nodule facies, which were therefore not suited to the automated nodule detection method. Nodule abundance estimates were then derived for each of these intersection points, resulting in a 3.5 × 3.5 km grid of nodule estimation points over the Collector Test Site Figure 7.27. These estimates were used to supplement the Mineral Resource estimate.

Figure 7.27   Nodule abundance estimates at 3.5 × 3.5 km node spacing within the Collector Test Site
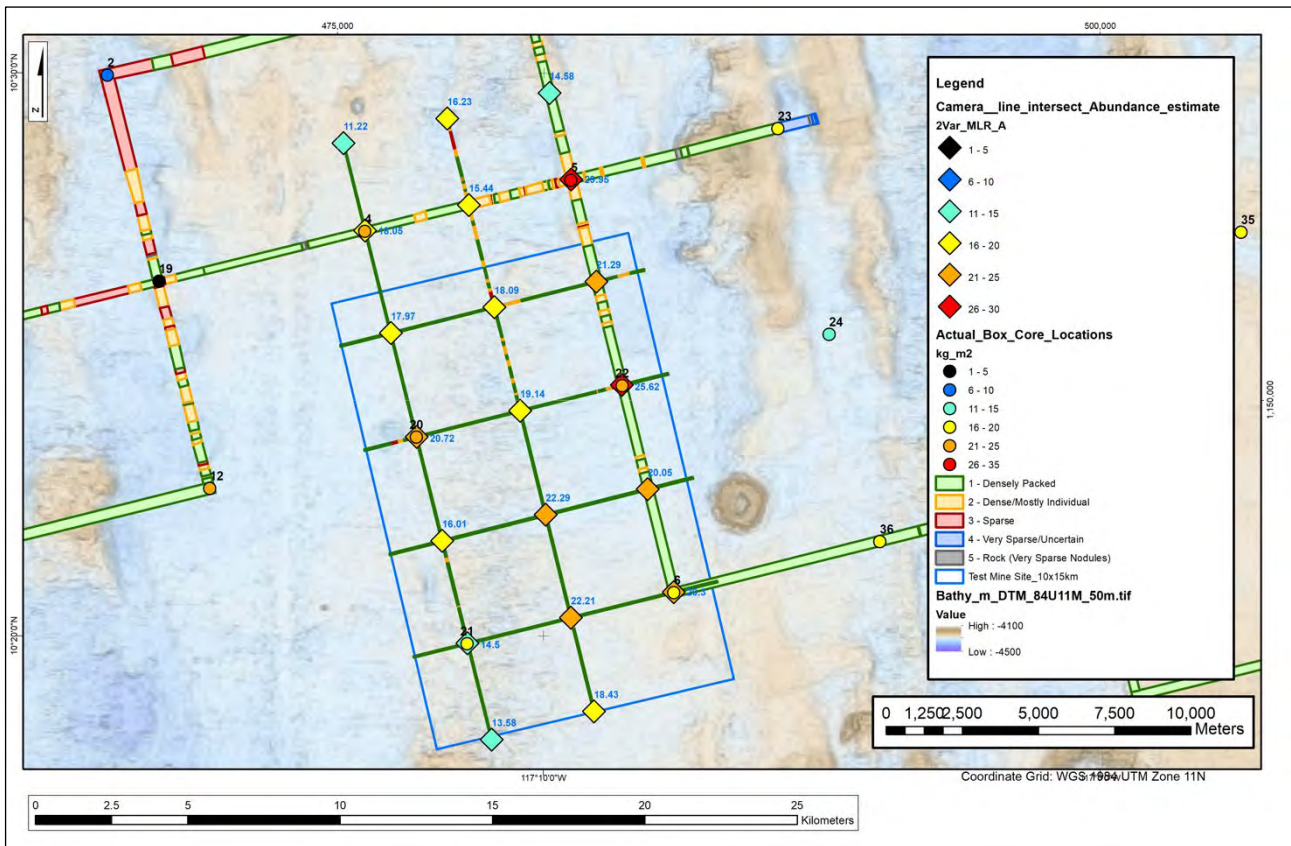
7.4   NORI 2019 campaign

Exploration in 2019 was divided into two campaigns (6A and 6B) due to the maximum duration of 45 days that OSV Maersk Launcher can remain out at sea. Campaign 6A was undertaken from 19/08/2019 to 03/10/2019 and Campaign 6B was undertaken from 10/11/2019 to 21/12/2019. The vessel was mobilised out of San Diego, California, USA.

Leap Energy was sub-contracted to provide geological support for the box coring operations. Bluefield Geoservices was subcontracted to provide the geotechnical logging and testing component of the programme, and ERIAS was sub-contracted to undertake environmental biological of the box cores.

7.4.1   Box coring

A 100 x 75 x 50 cm stainless steel box corer built by KC Denmark, and a Kongsberg Maritime HiPAP 501 Ultra Short Base Line (USBL) system were used for the sampling campaigns. The box corer was operated by an MSS marine crew and was fitted with a large Kongsberg USBL beacon for positioning Figure 7.28 and a sound velocity profiler (SVP) to monitor sound velocity variations in the water column. The positioning was monitored by two certified surveyors from the Leap Energy team. Fixes were taken during each box core landing and all sample coordinates were recorded in WGS84 UTM 11N.

Figure 7.28   Box corer on deck showing the USBL beacon mounting position
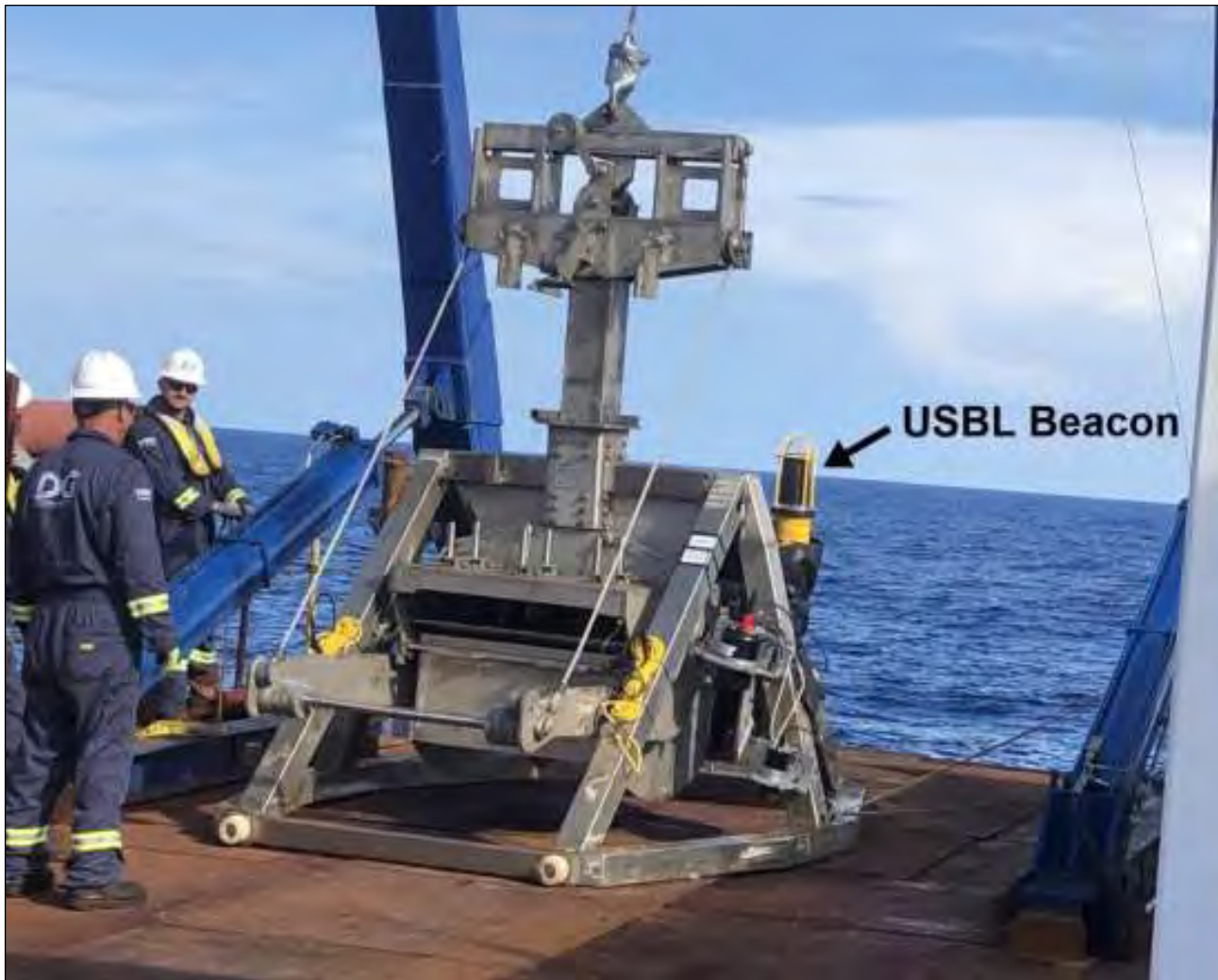
The procedures for sampling the nodules in Campaigns 6A and 6B were essentially the same as in 2018, with only minor changes in workflow to improve the efficiency of the process. The main changes were that the sampling intervals were simplified 0–1 cm, 1–15 cm, and the samples were not coned and quartered onboard the vessel. A flow chart of the sampling procedure is provided in Figure 7.29.

7.4.2   Nodule sampling

The dominant nodule shape, texture, degree of fragmentation, degree of botryoidal development together with the samples weight and nodule abundance was logged. The nodule facies classification system developed during the 2018 campaign was used. For the clay footwall succession, the sediment lithology and colour were recorded.

The dominant nodule facies in the NORI Area D license area for the samples recovered during Campaigns 6A and B was Type 1 (82%).

The nodule description and measurement procedures were the same as used in 2018.

Sample preparation procedures were the same as used in 2018, with the exception that they were coned and quartered at the on-shore laboratory, rather than onboard the vessel.

Figure 7.29   Box core processing flow sheet for Campaign 6B
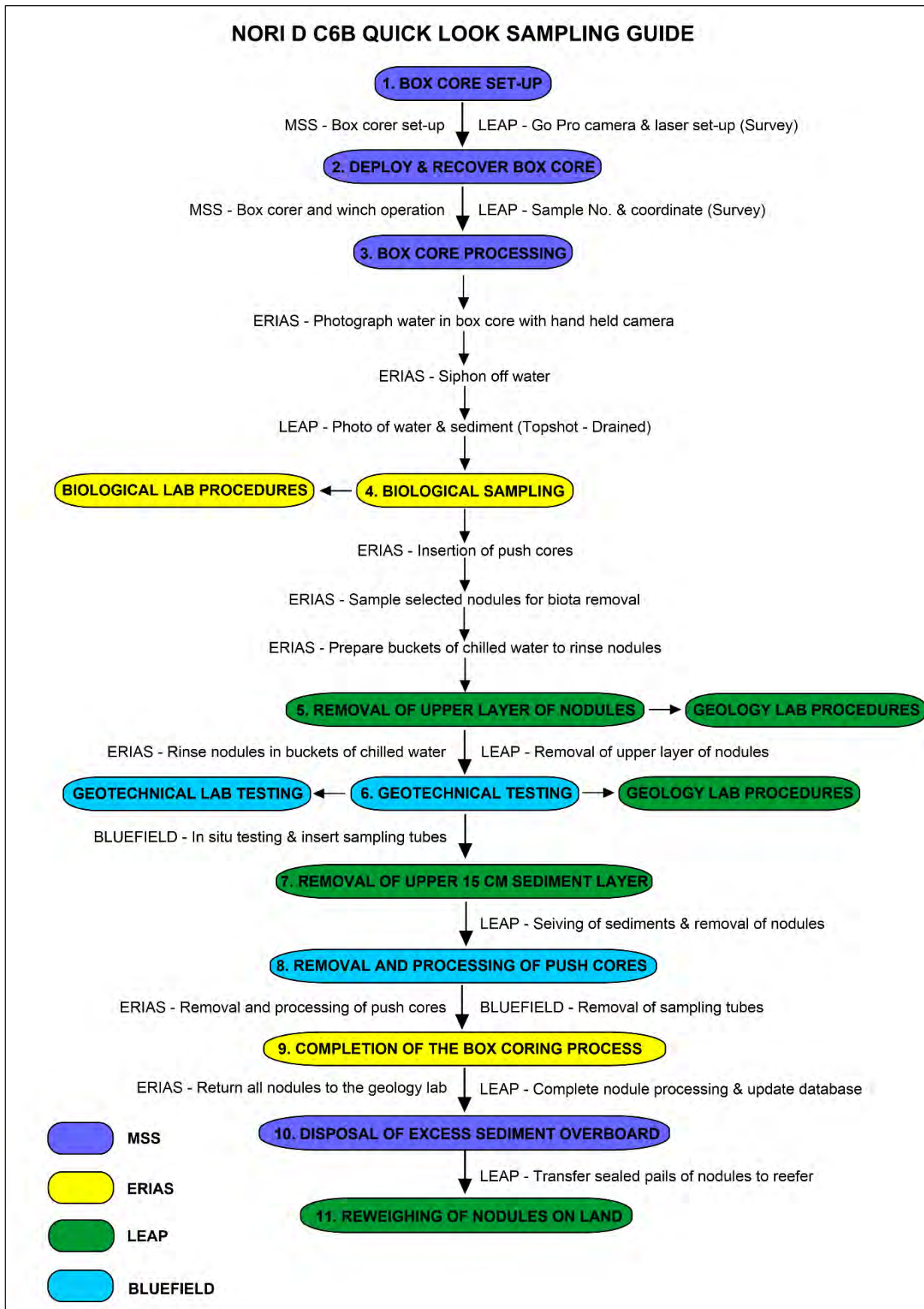
Note for Campaign 6A the processing flow was similar, with the absence of biological push-cores.

7.4.3 Biological sampling

Biological sampling involved the collection of specimens of mega, macro, meio and microfauna from the samples of nodules and underlying sediments collected in the box cores during the 2019 campaigns. Specimens of biota were collected from a number of horizons in the box core sample, including sieving of the water layer overlying the sediments to collect motile specimens; physical removal of specimens of megafauna from sediment and attached to nodules and preserving them for later analysis; washing nodules to dislodge macro fauna; and using cores pushed into the sediment to collect meio and macro fauna from different sediment horizons. Sediment samples were also retained and preserved for environmental DNA (eDNA) analysis.

Biological material was collected and preserved from 100 box cores during Campaign 6A adding to the samples collected from 45 box cores during Campaign 3. All the samples and specimens collected during the campaigns have been appropriately preserved and are stored for identification and analysis at a later date.

Marine mammal observations were made from the bridge of the vessel and logged in a data base.

7.4.4 Geotechnical sampling

Bluefield Geoservices performed geotechnical testing on 206 box core samples to a maximum depth of 0.50 m below sea floor. These were performed as part of the work-flow once the box cores were landed out on deck. All samples were subject to cone penetrometer testing and a subset of samples were subject to a comprehensive series of tests, including shear vane and plate load tests, using a purpose-built geotechnical rig provided by Bluefield Geoservices. Coring and geotechnical logging were also completed off-shore. Three (3) push cores collected from each box core for laboratory analysis. A comprehensive campaign of laboratory testing was also undertaken.

The soils encountered were very soft clays. Off-shore geotechnical analysis consisted of cone penetration test (CPT), laboratory vane, Torvane and plate load testing Figure 7.30. Push core and bulk density samples were taken from the box core opportunistically to aid sample description. Samples were also collected for subsequent on-shore laboratory testing Figure 7.31. In addition, eight (8) gravity cores were collected.

Figure 7.30   Photographs of geotechnical plate load test (left) and CPT (Right)
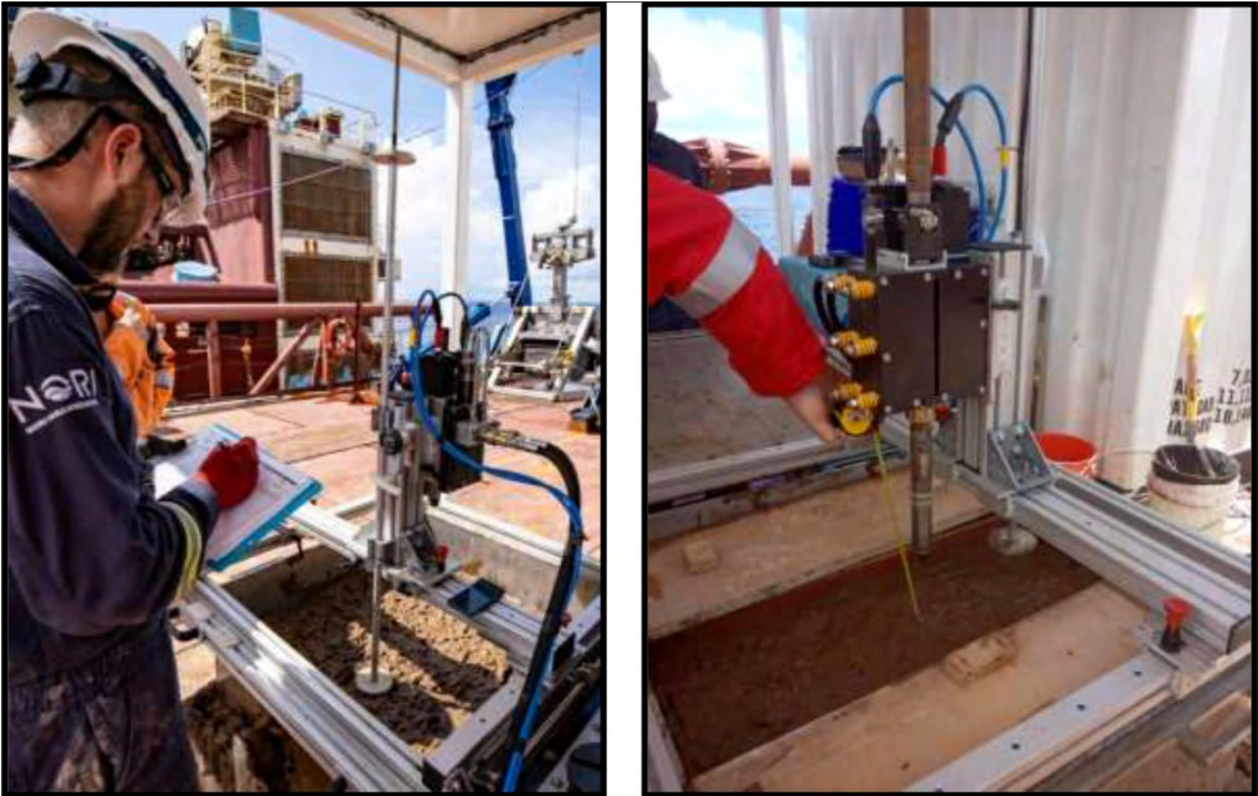
Figure 7.31   Photographs of biological & geotechnical tube sampling

7.4.5   Exploration results

Box core sampling was attempted at a total of 106 sites in the NORI Area D license area during Campaign 6A and 107 sites during Campaign 6B. Disturbed samples, considered to be unreliable, were omitted from the sample sequence.

A total of 106 box cores (BC046–BC151) and four gravity cores were acquired in the NORI Area D license area during Campaign 6A and 101 box cores (BC176–BC280) and four gravity cores were acquired during Campaign 6B. Disturbed samples, considered to be unreliable, were omitted from the sample sequence. Table 7.6 lists box core sample coordinates and polymetallic nodule weights and Figure 7.32 shows the location of the box cores.

The majority of the polymetallic nodules (92%) were found on the sediment surface (0 cm to 1 cm interval), with the remainder being predominantly encountered buried in the sediment at depths between of 1 cm and 15 cm. Occasionally, nodules were found buried deeper in the box core (15 cm to 30 cm), but these were generally in advanced stages of breakdown and were very easily broken when any attempt was made to recover them. The nodules from the deeper sedimentary layers (15 cm to 30 cm) were noted but were not collected or processed along with the nodule samples destined for the assay laboratory.

The nodules collected during the sampling campaign ranged in size from 10 mm to 250 mm in diameter. The dominant nodule shape encountered were discoidal in shape, whilst polynucleic shaped nodules were confined to the smaller Type 1 nodules.

The soils encountered in the box cores generally consisted of a lower sedimentary unit of very soft, pale brown clay, becoming dark brown with depth, and showing evidence of bioturbation.

The two sampling campaigns returned similar average nodule abundances, with the NORI_D_C6A campaign at 18.1 kg/m^2 and the NORI_D_C6B campaign at 17.0 kg/m^2. In general, nodule abundance is higher in the north and west of NORI Area D and diminishes towards the southeast. Topographic or geological controls may control nodule type/nodule facies on a more local scale.

Table 7.6 Box core sample coordinates and polymetallic nodule weights

Box Core Number	Campaign	Actual Location		Weight (kg)		Abundance (kg/m2)		Nodule Facies
		Easting (E)	Northing (N)	Offshore (kg)	Onshore (kg)	Offshore	Onshore	
046	6A	516607.65	1222981.94	16.02556	16.0642	21.37	21.42	1
047	6A	494699.86	1224747.78	13.78932	13.891	18.39	18.52	1
048	6A	511534.73	1214549.64	23.9472	24.0276	31.93	32.04	2
049	6A	519947.78	1209474.13	16.62136	16.604	22.16	22.14	1
050	6A	523284.31	1195972.15	11.88762	11.842	15.85	15.79	1
051	6A	514872.31	1201070.85	17.10605	17.0536	22.81	22.74	2
052	6A	506434.69	1206129.37	15.71338	15.6634	20.95	20.88	2
053	6A	498012.48	1211234.86	12.26207	12.2216	16.35	16.30	1
054	6A	489587.78	1216348.68	14.2689	14.2255	19.03	18.97	1
055	6A	481141.59	1221418.01	22.27297	22.3188	29.70	29.76	3
056	6A	459186.71	1223177.39	14.00777	13.945	18.68	18.59	1
057	6A	467625.44	1218090.78	13.5955	13.5602	18.13	18.08	1
058	6A	476068.70	1212995.08	11.80235	11.7452	15.74	15.66	1
059	6A	484494.43	1207897.25	16.26776	16.2132	21.69	21.62	1
060	6A	501354.11	1197701.54	14.59081	14.522	19.45	19.36	1
061	6A	509744.18	1192623.25	14.17769	13.7906	18.90	18.39	3
062	6A	529959.77	1168937.39	11.92477	11.9114	15.90	15.88	1
063	6A	521539.08	1174008.22	11.18427	11.1644	14.91	14.89	1
064	6A	504687.57	1184187.24	11.99619	11.9978	15.99	16.00	2
065	6A	496247.62	1189262.13	12.86045	12.8506	17.15	17.13	1
066	6A	479387.41	1199464.57	16.49672	16.4812	22.00	21.97	1
067	6A	470959.14	1204558.24	18.9512	18.947	25.27	25.26	2
068	6A	462522.78	1209648.28	13.16105	13.1526	17.55	17.54	1
069	6A	454099.31	1214738.71	17.5744	17.5698	23.43	23.43	2
070	6A	445655.22	1219855.64	10.34846	10.3302	13.80	13.77	1
071	6A	423700.42	1221601.55	11.30465	11.283	15.07	15.04	1
072	6A	432117.69	1216503.17	13.69547	13.674	18.26	18.23	1
073	6A	440560.66	1211410.19	12.90316	12.9	17.20	17.20	1
074	6A	448984.92	1206313.30	17.04071	17.0428	22.72	22.72	1
075	6A	457429.71	1201201.58	17.31903	17.3008	23.09	23.07	2
076	6A	465872.41	1196137.90	10.49147	10.424	13.99	13.90	3
077	6A	491182.38	1180846.76	14.74507	14.7456	19.66	19.66	1
078	6A	499123.23	1175721.79	14.2055	14.1934	18.94	18.92	1
079	6A	508024.00	1170680.10	10.85474	10.8406	14.47	14.45	1
080	6A	502935.60	1162237.17	11.64862	11.6512	15.53	15.53	1
081	6A	494488.51	1167334.36	14.57712	14.5718	19.44	19.43	1
082	6A	486070.94	1172431.49	14.53504	14.5266	19.38	19.37	1
083	6A	477643.41	1177492.78	11.09514	11.0816	14.79	14.78	1
084	6A	469212.18	1182594.20	0.22081	0.2152	0.29	0.29	3
085	6A	460772.24	1187696.49	12.0924	12.0718	16.12	16.10	1
086	6A	452336.33	1192782.56	16.59518	16.5884	22.13	22.12	1
087	6A	443900.13	1197890.45	16.30036	16.295	21.73	21.73	1
088	6A	435462.90	1202979.23	14.60069	14.4481	19.47	19.26	2
089	6A	427028.99	1208062.11	22.62526	22.3786	30.17	29.84	2
090	6A	418571.39	1213165.55	16.29064	16.2818	21.72	21.71	1
091	6A	413487.58	1204727.92	12.08875	12.0572	16.12	16.08	1
092	6A	421917.19	1199644.93	11.26413	11.237	15.02	14.98	1
093	6A	430365.98	1194549.71	22.07454	22.0586	29.43	29.41	2
094	6A	438798.78	1189430.79	12.82568	12.7992	17.10	17.07	1
095	6A	447230.62	1184361.20	13.48456	13.473	17.98	17.96	1
096	6A	455676.00	1179261.70	14.37345	14.3573	19.16	19.14	1
097	6A	464120.48	1174172.38	14.42651	14.4194	19.24	19.23	1
098	6A	472559.36	1169073.14	21.51717	21.3622	28.69	28.48	3
099	6A	459028.38	1165736.53	12.43137	12.3634	16.58	16.48	3
100	6A	442142.17	1175923.18	16.18182	16.168	21.58	21.56	1
101	6A	433707.25	1181010.15	12.45181	12.4348	16.60	16.58	1
102	6A	425252.79	1186103.71	12.98788	12.9608	17.32	17.28	1
103	6A	416833.40	1191215.07	11.2295	11.203	14.97	14.94	1
104	6A	428607.47	1172556.05	12.33715	12.3134	16.45	16.42	1
105	6A	437046.52	1167487.01	14.63293	14.614	19.51	19.49	1
106	6A	445500.53	1162398.24	8.57768	8.5522	11.44	11.40	1
107	6A	431972.50	1159031.23	11.92446	11.9074	15.90	15.88	1
108	6A	423515.81	1164114.75	12.42569	12.3972	16.57	16.53	1
109	6A	415075.99	1169212.06	13.13595	13.1134	17.51	17.48	1
110	6A	426873.12	1150607.91	12.73691	12.7186	16.98	16.96	1
111	6A	435327.90	1145511.28	12.14001	12.1106	16.19	16.15	1
112	6A	430226.54	1137045.40	12.63216	12.5962	16.84	16.79	1
113	6A	437965.37	1131586.20	12.29276	12.2552	16.39	16.34	1

Box Core Number	Campaign	Actual Location		Weight (kg)		Abundance (kg/m2)		Nodule Facies
		Easting (E)	Northing (N)	Offshore (kg)	Onshore (kg)	Offshore	Onshore	
114	6A	479116.50	1147163.22	15.95706	15.9884	21.28	21.32	1
115	6A	480444.37	1141434.45	11.41333	11.4294	15.22	15.24	1
116	6A	421777.08	1142152.38	12.06031	12.0862	16.08	16.11	1
117	6A	413318.88	1147228.51	16.52079	16.5528	22.03	22.07	1
118	6A	416702.07	1133703.33	13.72593	13.7608	18.30	18.35	1
119	6A	411614.90	1125256.57	12.21826	12.222	16.29	16.30	1
120	6A	414967.55	1111724.82	12.72899	12.7548	16.97	17.01	1
121	6A	420050.48	1120169.32	15.10089	15.1248	20.13	20.17	1
122	6A	425138.06	1128617.52	19.61851	19.6562	26.16	26.21	2
123	6A	433585.66	1123545.46	13.17885	13.203	17.57	17.60	1
124	6A	428507.42	1115095.64	11.919	11.9486	15.89	15.93	1
125	6A	423436.54	1106629.06	13.3223	13.336	17.76	17.78	1
126	6A	418331.13	1098177.44	13.47486	13.59	17.97	18.12	3
127	6A	431877.82	1101547.08	15.19952	15.1348	20.27	20.18	3
128	6A	436945.09	1109998.57	6.91858	6.91	9.22	9.21	3
129	6A	442029.06	1118448.01	8.43266	8.445	11.24	11.26	1
130	6A	447096.97	1126874.92	14.87212	14.8974	19.83	19.86	1
131	6A	452375.98	1135655.66	10.19886	10.2194	13.60	13.63	1
132	6A	465726.38	1138672.94	13.98023	14.0094	18.64	18.68	1
133	6A	460643.69	1130253.24	12.70846	12.7284	16.94	16.97	1
134	6A	455543.23	1121815.98	12.89784	12.9402	17.20	17.25	1
135	6A	450465.49	1113352.74	14.05746	14.0842	18.74	18.78	2
136	6A	445381.03	1104906.32	13.45611	13.4854	17.94	17.98	1
137	6A	440298.77	1096461.35	14.18014	14.208	18.91	18.94	1
138	6A	453831.90	1099841.45	10.87809	10.8968	14.50	14.53	1
139	6A	458910.51	1108271.81	14.7575	14.7822	19.68	19.71	1
140	6A	469079.49	1125145.80	9.44779	9.4656	12.60	12.62	1
141	6A	474166.09	1133580.71	21.84486	21.8806	29.13	29.17	1
142	6A	487678.37	1136931.37	14.11873	14.1478	18.83	18.86	1
143	6A	482613.51	1128514.00	13.49911	13.5304	18.00	18.04	1
144	6A	477520.76	1120066.87	9.59831	9.6198	12.80	12.83	1
145	6A	467366.44	1103210.54	12.54903	12.585	16.73	16.78	1
146	6A	462269.37	1094753.25	5.83656	5.8444	7.78	7.79	3
147	6A	475793.37	1098104.81	10.64722	10.6652	14.20	14.22	1
148	6A	480870.43	1106563.83	9.56179	9.5776	12.75	12.77	1
149	6A	485963.55	1114979.73	10.78484	10.8058	14.38	14.41	1
150	6A	491042.63	1123414.84	13.29108	13.317	17.72	17.76	1
151	6A	501214.83	1140282.91	10.38492	10.4166	13.85	13.89	1
176	6B	502418.14	1219582.70	11.54004	13.72970	15.39	18.31	1
177	6B	492165.51	1203027.33	14.60021	14.65020	19.47	19.53	1
178	6B	487723.34	1194277.13	16.00780	16.15610	21.34	21.54	2
179	6B	483224.08	1185931.07	11.14656	11.09160	14.86	14.79	1
181	6B	469612.58	1182708.01	0.19222	0.19140	0.26	0.26	3
182	6B	449011.77	1170456.99	13.27437	13.29930	17.70	17.73	1
183	6B	421474.25	1178380.02	10.93965	11.01570	14.59	14.69	1
184	6B	418645.62	1155452.39	8.82356	8.83100	11.76	11.77	1
185	6B	463750.70	1116692.88	10.38200	10.39870	13.84	13.86	1
186	6B	472185.88	1112042.30	6.83673	6.85280	9.12	9.14	1
187	6B	495681.84	1132079.90	14.03420	13.99820	18.71	18.66	1
188	6B	516031.76	1166786.72	9.80714	9.77200	13.08	13.03	1
189	6B	513218.81	1179435.87	11.50072	11.49160	15.33	15.32	1
190	6B	517597.21	1187822.19	12.37787	12.38550	16.50	16.51	1
191	6B	526154.72	1182536.17	10.58192	10.57820	14.11	14.10	1
192	6B	535083.05	1177206.95	14.50646	14.50970	19.34	19.35	1
193	6B	544069.68	1172577.00	14.92652	14.95270	19.90	19.94	1
194	6B	552336.85	1167991.04	13.35410	13.27920	17.81	17.71	1
195	6B	560928.71	1162375.98	11.43600	11.45130	15.25	15.27	1
196	6B	573820.21	1165454.13	11.99416	12.00280	15.99	16.00	1
197	6B	565398.99	1170534.36	11.69162	11.69590	15.59	15.59	1
198	6B	556962.56	1175622.59	9.29602	9.31230	12.39	12.42	1
199	6B	547798.50	1180216.72	8.82048	8.74950	11.76	11.67	1
200	6B	540137.69	1185771.66	9.65192	9.66100	12.87	12.88	1
201	6B	531718.84	1190879.71	15.60665	15.62500	20.81	20.83	1
202	6B	528382.18	1204379.93	17.56128	17.59670	23.42	23.46	1
203	6B	536982.07	1200221.05	12.10241	12.08520	16.14	16.11	1
204	6B	545479.10	1194520.87	14.06640	14.09410	18.76	18.79	1
205	6B	553642.77	1189125.33	14.47215	14.48590	19.30	19.31	1
206	6B	560423.45	1183620.69	15.88279	15.89460	21.18	21.19	1
207	6B	570491.07	1178957.69	20.45660	20.46870	27.28	27.29	1

Box Core	Campaign	Actual Location		Weight (kg)		Abundance (kg/m2)		Nodule
Number		Easting (E)	Northing (N)	Offshore (kg)	Onshore (kg)	Offshore	Onshore	Facies
208	6B	580315.46	1174714.26	15.68094	15.70670	20.91	20.94	1
209	6B	587324.63	1168794.39	13.52294	13.55710	18.03	18.08	1
210	6B	595751.30	1163719.65	11.41743	11.43540	15.22	15.25	1
211	6B	600796.45	1171870.83	2.10299	2.10700	2.80	2.81	3
212	6B	591732.46	1177389.59	12.94277	12.96020	17.26	17.28	1
213	6B	583989.66	1182277.47	18.71487	18.93940	24.95	25.25	1
214	6B	574436.49	1187355.09	12.59742	12.62280	16.80	16.83	1
215	6B	567154.67	1192456.64	12.88151	12.91070	17.18	17.21	1
216	6B	559694.23	1196570.59	10.16900	10.18430	13.56	13.58	1
217	6B	548810.93	1202550.23	13.27286	13.28510	17.70	17.71	1
218	6B	542208.73	1208372.45	10.80441	10.81310	14.41	14.42	1
219	6B	533463.71	1212793.71	19.10461	19.64000	25.47	26.19	1
220	6B	525043.93	1217890.82	12.55892	12.56290	16.75	16.75	1
221	6B	538555.15	1221240.58	13.65917	13.66380	18.21	18.22	1
222	6B	546971.72	1216147.52	9.86255	9.85740	13.15	13.14	1
223	6B	555398.86	1211052.66	20.69955	20.72350	27.60	27.63	2
224	6B	564054.77	1205256.71	22.38086	22.34700	29.84	29.80	2
225	6B	572221.70	1200875.38	17.19870	17.21670	22.93	22.96	1
226	6B	580647.66	1195781.78	11.72413	11.73510	15.63	15.65	1
227	6B	586058.88	1205747.69	2.33487	2.28760	3.11	3.05	3
228	6B	578405.69	1208794.06	11.56571	11.57990	15.42	15.44	1
229	6B	568914.77	1214387.60	0.06436	0.05870	0.09	0.08	3
230	6B	560490.86	1219464.34	22.76269	22.83590	30.35	30.45	2
231	6B	552569.22	1224867.76	15.83721	15.84900	21.12	21.13	1
232	6B	573974.86	1222797.89	18.21135	18.25390	24.28	24.34	2
233	6B	581162.85	1217819.97	15.54404	14.93740	20.73	19.92	1
234	6B	595905.10	1221029.60	10.22326	10.22780	13.63	13.64	3
235	6B	590812.89	1212611.81	0.07280	0.06800	0.10	0.09	3
236	6B	599245.09	1207536.70	15.76633	15.77690	21.02	21.04	2
237	6B	594141.85	1199119.57	15.14613	15.13090	20.19	20.17	1
238	6B	589718.56	1191576.21	12.87776	12.88160	17.17	17.18	1
239	6B	597473.20	1185632.05	16.33166	16.60740	21.78	22.14	1
240	6B	427521.58	1208175.68	24.68888	24.74570	32.92	32.99	2
241	6B	427181.38	1208336.73	23.96558	23.97810	31.95	31.97	2
242	6B	427026.80	1208053.74	21.66339	21.68060	28.88	28.91	2
243	6B	427372.60	1207869.27	19.79228	19.83340	26.39	26.44	2
244	6B	475892.75	1155507.57	15.43054	15.45830	20.57	20.61	1
245	6B	476075.26	1155822.88	14.91209	14.93730	19.88	19.92	1
246	6B	476383.82	1155639.43	16.44459	16.47350	21.93	21.96	1
247	6B	476221.61	1155336.85	20.57729	21.44420	27.44	28.59	1
248	6B	494570.63	1110107.21	10.87185	10.80680	14.50	14.41	1
249	6B	508506.11	1112715.00	10.74484	10.77530	14.33	14.37	1
250	6B	502703.96	1104576.73	11.25303	11.27970	15.00	15.04	1
251	6B	511267.52	1099766.40	12.49379	12.51860	16.66	16.69	1
253	6B	525492.22	1101354.00	10.66706	10.67910	14.22	14.24	1
254	6B	538281.77	1106479.92	9.11155	9.13100	12.15	12.17	1
255	6B	531570.91	1133475.91	9.22072	9.24050	12.29	12.32	1
256	6B	538131.10	1142242.69	9.58975	9.61210	12.79	12.82	1
257	6B	558767.44	1141508.87	10.28829	10.33230	13.72	13.78	1
259	6B	567441.46	1157040.38	9.30402	9.32910	12.41	12.44	1
260	6B	581121.73	1160276.52	11.07592	11.09250	14.77	14.79	1
261	6B	578322.44	1152403.20	10.80130	10.82450	14.40	14.43	1
262	6B	571914.91	1143656.28	11.13739	11.16800	14.85	14.89	1
263	6B	564367.04	1148482.10	14.13325	14.10520	18.84	18.81	1
264	6B	546195.42	1159070.82	11.85999	12.31040	15.81	16.41	1
265	6B	541265.30	1150568.10	14.68998	14.71810	19.59	19.62	1
266	6B	550937.75	1145366.82	14.23761	14.27500	18.98	19.03	1
267	6B	567009.16	1135090.99	10.33807	10.36310	13.78	13.82	1
268	6B	560576.99	1126326.33	12.70976	12.73120	16.95	16.97	1
269	6B	553508.53	1131754.58	9.75852	9.84910	13.01	13.13	1
271	6B	528228.26	1146990.38	10.17807	10.19650	13.57	13.60	1
272	6B	523132.39	1138565.91	9.51211	9.75400	12.68	13.01	1
273	6B	540012.64	1128404.50	9.36063	9.38670	12.48	12.52	1
274	6B	547906.56	1123487.95	11.03703	11.07510	14.72	14.77	1
275	6B	556862.35	1118254.55	9.40559	9.44960	12.54	12.60	1
276	6B	551793.40	1109834.92	10.00252	10.03040	13.34	13.37	1
277	6B	534693.27	1119985.85	10.01188	10.04040	13.35	13.39	1
278	6B	526496.86	1125044.81	9.88382	9.90200	13.18	13.20	1
279	6B	518071.02	1130133.75	12.37066	12.40100	16.49	16.53	1
280	6B	504544.16	1126772.68	9.89743	9.91170	13.20	13.22	1

Figure 7.32   Map of NORI Area D showing box core sample locations and bathymetry
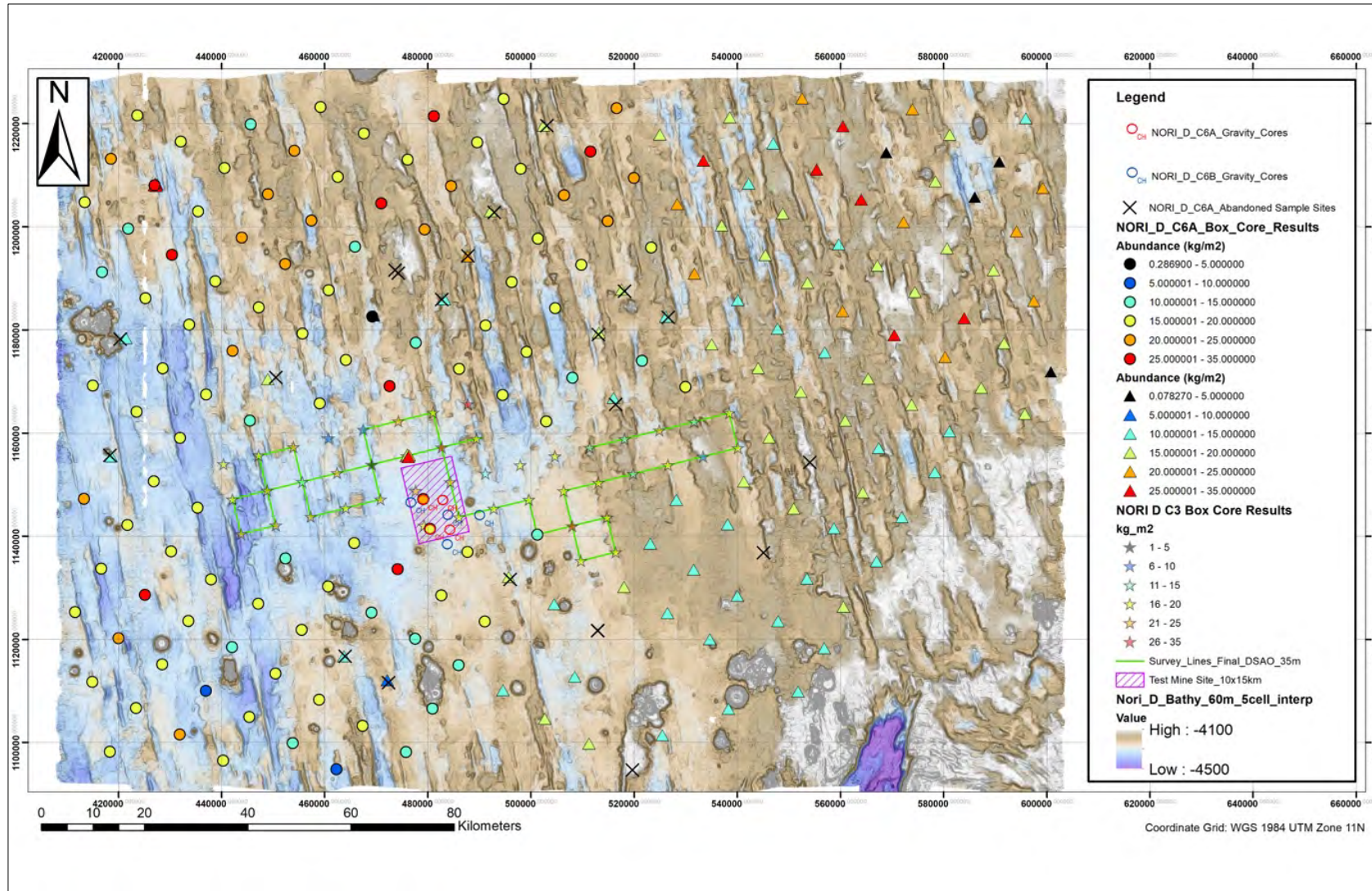
Note: Circles – Campaign 6A; triangles, Campaign 6B

7.4.6   Analysis of grade distribution by size fraction

As part of the Campaign 6A and 6B box core sampling programme, a preliminary examination of the relationship between polymetallic nodule size and grade was carried out. Twenty-four (24) nodule box core samples were separated into four size fractions (+50 mm, −50 mm + 25 mm, −25 mm +10 mm, and −10 mm) using sieves.

Plots of the relative difference in grade between the assays for individual size fractions and the weight-averaged grade of the whole sample are shown in Figure 7.33 to Figure 7.36. The masses of the size fractions, in relative percentage, are shown in Figure 7.37. In general the proportion of material less than 10 mm (the -10 mm fraction) is very small.

Twenty-four samples are too few to make firm statistical conclusions, but the data is sufficient to show that distribution of nickel, cobalt, copper and manganese is not uniform across particles of different sizes. The particles may be whole nodules or abraded pieces of larger nodules. The samples show that selection of the particle size range that will be recovered by the seafloor collection system, and loss of fines by abrasion in the ore handling systems, may have small impacts on the grade of the ore recovered to the production support vessel.

Figure 7.33   Relative difference of grade by size fraction – NiO (%)
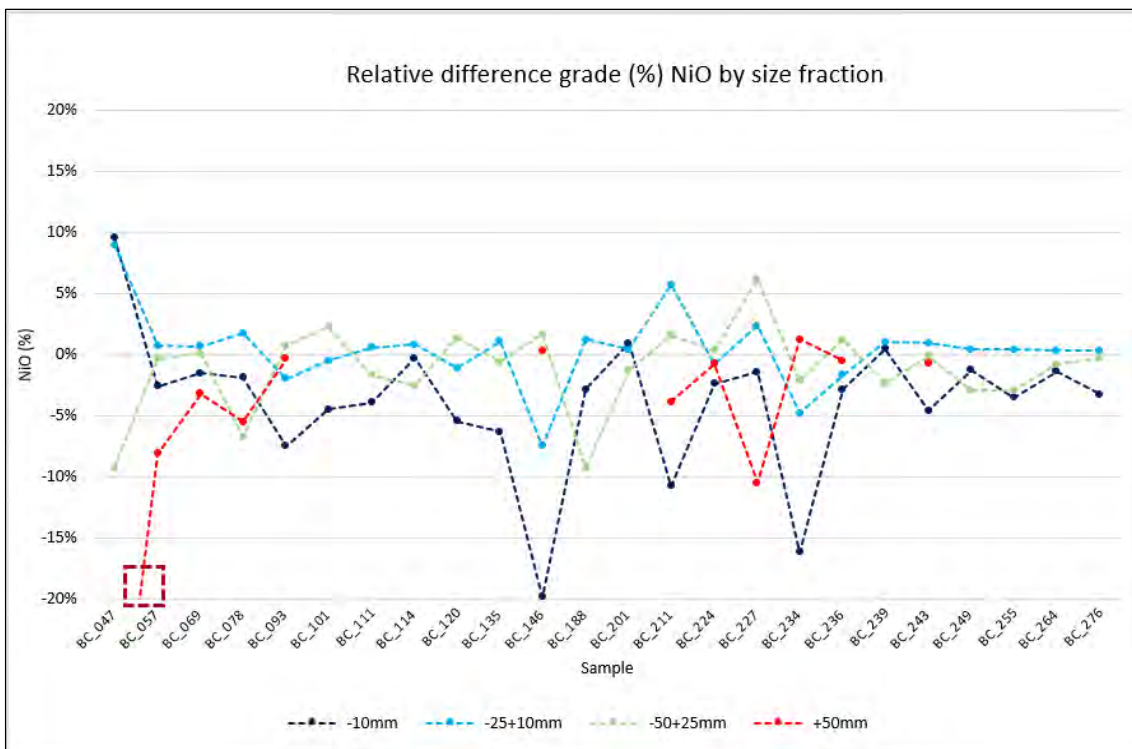
Note: Brown rectangle highlights anomalous grades in BC047

Figure 7.34   Relative difference of grade by size fraction – CuO (%)

Note: Brown rectangle highlights anomalous grades in BC047

Figure 7.35   Relative difference of grade by size fraction – CoO (%)

Note: Brown rectangle highlights anomalous value in BC227

Figure 7.36   Relative difference of grade by size fraction – MnO (%)

Note: Brown rectangle highlights anomalous grades in BC047

Figure 7.37   Proportions of size fractions by mass (relative percentage)

8 Sample preparation, analysis, and security

This Section describes the methods used for preparing and assaying the box core samples from the 2018 and 2019 exploration campaigns. The methods used in 2019 were not materially different from those used by NORI in 2018. In the opinion of the Qualified Person the sample preparation, security, and analytical procedures were adequate for estimation of Mineral Resources. The assays produced from this programme, supplemented by Pioneer Investor data, were used for estimation of Mineral Resources in NORI Area D.

8.1 Security

8.1.1 Box core samples

The geoscience laboratory on board the Maersk Launcher was manned by a team of qualified geoscience staff rotating on 12-hour shifts during box coring operations. All samples were weighed at the weighing stations. Reference weights were used to periodically check the accuracy of the electronic scales. All weights and associated nodule descriptions were recorded in logbooks (also digitally scanned) and captured in a digital (Excel) database. A digital photographic archive of all samples was also compiled. Data was stored on a computer and backups to external disks were regularly made.

On completion of processing, samples were stored in polythene bags placed in gasket-sealed plastic pails. All nodule pails were assembled in the geoscience laboratory and temporarily stored there until they were transported to a refrigerated container (reefer). The reefer was secured with a tag-in, tag-out system.

Sample bags were prepared with triple redundancy- numbered zip tie, printed bar code, and hand-written in permanent ink. Tracking of samples was maintained with a bar-code scanner and digital database.

Following checking of the nodule count in each box core against the photographic record and reweighing of the nodules, the samples from the depth layers were recombined. These samples were assembled into respective storage pails depending on sample type and destination. Each sample was scanned and recorded on the sample master spreadsheet, and sample pails sealed with tamper-proof tape, and carried to the secured storage reefer Figure 8.1.

Figure 8.1   Sample storage

Source: NORI. Note: (Left to right) sealed pail containing samples, secured refrigerated container, tag-in tag-out logbook, and seal.

All samples were taken out of the reefer and reweighed on land upon arrival in San Diego. The sealed pails were reopened by geoscientists, weighed, scanned, replaced in pails, sealed with tamper-proof tape and returned to the secured storage reefer. Regular email communications were conducted with the Qualified Person for the Mineral Resource estimate during the sample acquisition operations.

8.1.2   Camera imagery

Camera imagery and data acquired by the Fugro ESVII AUV in 2018 was logged to the AUV's internal payload processing data storage disk. This data is co-registered, and time-date stamped with the vehicle's other geophysical sensors (e.g., SSS) and navigation systems and resultant navigation data. The vehicle was positioned with a combination of INS and USBL navigation.

Once each dive was completed and the AUV returned to deck, the data was transferred across from the payload data disk bottle to the Fugro data processing server and backed-up.

Preliminary processing of the data was undertaken on board to aid follow-up survey site selection and optimisation. Review of the data was undertaken by the Fugro Geoscience team and NORI Client Representative on the vessel. The data was fully processed post campaign completion at Fugro's Layfette offices in Louisiana.

Additional image classification and nodule long-axes automated extraction was undertaken by the same Fugro 2018 NORI campaign Geoscience members at Fugro's offices in Houston, Texas.

8.2   Sample preparation and assaying

All samples were freighted to ALS Laboratory Group (ALS) in Brisbane, Australia. ALS has a biosecurity quarantine facility approved by the Australian Quarantine and Inspection Service (AQIS). All samples were irradiated before clearing quarantine. The samples were not heat-treated as this would have resulted in breakdown of some of the hydroxide minerals.

The samples were inspected by AMC staff to confirm that there had been no tampering since despatch from San Diego.

Each box core sample was divided into four: a primary sample, a duplicate (primary laboratory), a duplicate (secondary laboratory) and a reference sample. For the 2018 campaign this was carried out onboard the vessel, as described in Section 9.3.8. For the 2019 campaigns, the division was carried out by cone and quartering at the on-shore laboratory.

The primary samples were submitted to ALS. For the 2018 sampling campaign, the duplicates (secondary laboratory) were submitted to Bureau Veritas laboratory in Perth, Australia. For the 2019 sampling campaigns, the duplicates were assayed at ALS and a separate set of pulps was later sent to BV for independent analysis. Reference samples were retained by NORI and stored in Brisbane.

ALS in Brisbane was selected as the primary laboratory as it has extensive experience in the analysis of high manganese samples and polymetallic nodules. ALS operates quality systems based on international standards ISO/IEC17025:1999 "General requirements for competence of calibration and testing laboratories" and ISO9001:2000 "Quality Management Systems Requirements".

The sample preparation and assaying procedure at ALS was as follows:

- Samples were transferred to barcode-labelled aluminium trays and dried in an oven at 105 °C for three (3) days. This was a higher temperature than use in the 2018 programme but there appear to be no significant differences between the assays as a consequence. Moisture loss was measured.

- After drying, samples were jaw crushed in a Jacques jaw crusher to reduce particle size to less than 10 mm.

- The crushed samples were then pulverised in an LM5 mill to a powder with typical particle size >85% passing 75 μm. Very small samples were pulverised in a smaller bowl using an LM2 mill. A sieve test was conducted for every 20th sample to check the particle sizes.

- Pulps were analysed by a fusion/XRF method (ME-XRF26s) using a small aliquot (0.33 g) to avoid fusion problems. The following oxides were reported:
  — LOI, Al_2O_3, BaO, CaO, Cr_2O_3, CoO, Fe_2O_3, K_2O, CuO, MgO, MnO, Na_2O, P_2O_5, SO_3, SiO_2, NiO, TiO_2, PbO, ZnO.

- Pulps were fused with lithium borate to create a bead that was dissolved with acid and analysed by inductively-coupled plasma emission mass spectroscopy (ICP-MS) (method ME-MS81) for:
  — Ba, Ce, Cr, Cs, Dy, Er, Eu, Ga, Gd, Hf, Ho, La, Lu, Nb, Nd, Pr, Rb, Sm, Sn, Sr, Ta, Tb, Th, Tm, U, V, W, Y, Yb, Zr.

- Pulps were analysed for:
  — As, Cd, Li, Mo, Sb by four acid ICP-AES method (ME-ICP61).
  — Bi, Ge, Se, Te, Tl by four acid digest ICP-MS (method ME-MS62s).
  — Hg by low temperature digestion in aqua regia and ICP-MS (method Hg-MS42).
  — B by ICP-MS (method B-ICP69.
  — F by KOH fusion and ion selective electrode (method F-ELE81a).
  — Loss on ignition (LOI) at 1000 °C.

Manganese can exist in different oxidation states. AMC checked the totals of all the oxides plus LOI for each sample. The totals were generally about 96%. The shortfall of about 4% appears to arise because some of the manganese occurs in higher-valence states. A more realistic conversion of elemental manganese to manganese oxide would be approximately $MnO_{1.85}$.

ALS also reported a calculated total, being the sum of the reportable analytes plus LOI. Manganese was included in this calculation as Mn_3O_4 but was reported on the certificate of analysis as MnO. This leads to the sum of analytes reported plus LOI, calculated by AMC, adding up to a lower value than the total calculated by ALS. The ALS calculation using Mn_3O_4 is aimed at covering the middle ground of MnO and MnO_2.

BV was used as the secondary laboratory, to provide an independent check on the accuracy of the sample preparation and assaying by ALS. BV operates quality systems based on international standards ISO/IEC17025:1999 and ISO9001:2000. Each sample batch included internal quality control samples (certified reference materials).

The sample preparation and assaying procedure at BV was as follows:

- Samples were dried in an oven at 105 °C. Moisture loss was measured.
- Samples crushed and split, if required, then pulverised in a vibrating pulveriser

- Pulps were cast using a 12:22 flux with added sodium nitrate to form a glass bead. The beads were analysed by XRF for: TiO2, Fe, Al2O3, SiO2, Mn, CaO, MgO, S XRF, P XRF, BaO, K2O.
- Pulps were analysed by Laser Ablation Inductively Coupled Plasma Mass Spectrometry for:
  — Ag, As, Ba, Be, Bi, Cd, Ce, Co, Cr, Cs, Cu, Dy, Er, Eu, Ga, Gd, Ge, Hf, Ho, In, La, Lu, Mn, Mo, Nb, Nd, Ni, Pb, Pr, Rb, Re, Sb, Sc, Se, Sm, Sn, Sr, Ta, Tb, Te, Th, Ti, Tl, Tm, U, V, W, Y, Yb, Zn, Zr.
- Pulps were analysed for LOI at 1000 °C.

8.3 Quality assurance and quality control procedures 2018

Certified reference materials (CRMs), blank samples (crushed rock samples with very low Mn, Ni, Co and Cu) and duplicate samples were used for quality control and quality assurance during the NORI 2020 campaign.

8.3.1 Certified reference materials

The CRM called NOD-P-1, manufactured by the U.S. Geological Survey (USGS), was used for the NORI 2020 campaign. Material used in the preparation of the CRM was collected from the Pacific Ocean (14°50′ N, 124°28′ W) at a depth of 4,300 m.

Six CRMs were inserted into the NORI 2018 campaign sample submissions at a rate of 1 in 14. Table 8.1 shows the assayed oxide values for manganese, cobalt, nickel and copper for the CRMs and the certified values for NOD-1-P.

There was a slight positive bias in the manganese oxide assays and the BV (Bureau Veritas Minerals Pty Ltd) assays for nickel, manganese and cobalt were slightly elevated relative to those from ALS but these differences are not significant. The CRM results indicate that the NORI 2018 assay results are satisfactory.

Table 8.1 CRM assays from NORI 2018 campaign

Sample	NiO (%)	CuO (%)	MnO (%)	CoO (%)	Laboratory
Certified value	1.71	1.44	37.6	0.28	-
0367075A	1.720	1.430	38.040	0.280	ALS
0367108A	1.730	1.450	38.240	0.280	ALS
0367175A	1.720	1.420	38.000	0.280	ALS
0367177A	1.720	1.410	37.920	0.280	ALS
0367109A	1.781	1.440	38.865	0.294	BV
0367183A	1.794	1.452	38.865	0.296	BV

8.3.2 Blanks

The blank samples were composed of dolomite gravel or granite, which were expected to have very low content of manganese, cobalt, nickel and copper. The blank material was not assayed prior to insertion in the NORI sample batches. A total of 11 blank samples were inserted into the NORI 2018 sample assay batches at a rate of 1 in 8. Table 8.2 shows the assayed oxide values for the blanks. The assays for the blank samples indicate slightly elevated manganese (deliberate as some of the blanks had manganese mixed in with the blank) and negligible nickel, copper and cobalt.

Table 8.2 Blank sample assays from NORI 2018 campaign

Sample	NiO (%)	CuO (%)	MnO (%)	CoO (%)	Laboratory

0367116A	0.010	0.010	0.380	0.010	ALS
0367089A	0.030	0.030	0.630	0.010	ALS
0367091A	0.010	0.010	0.230	0.010	ALS
0367118A	0.010	0.010	0.380	0.010	ALS
0367200A	0.010	0.010	0.060	0.010	ALS
0367202A	0.020	0.010	0.420	0.010	ALS
0367241A	0.010	0.010	0.460	0.010	ALS
0367052A	0.006	0.004	0.181	0.001	BV
0367088A	0.010	0.007	0.232	0.001	BV
0367149A	0.009	0.009	0.284	0.001	BV
0367239A	0.003	0.002	0.142	0.002	BV

8.3.3 Duplicates

Duplicate samples were prepared by cone and quartering the box core samples, as described in Section 9.3.8.

A total of 44 samples were assayed at ALS paired with duplicate samples also assayed at ALS. Figure 8.2 presents the results. The precision of the results is very good and there is no evidence of significant biases or errors.

A total of 43 samples were assayed at ALS paired with duplicate samples assayed at BV. Figure 8.3 presents the results. The precision of the results is good. There are very small high bias for nickel and manganese compared with the ALS assays Table 8.3 but this is not significant.

These results are consistent with the observation for the assays of the NOD-P-1 standard.

The maximum half absolute relative difference for the ALS paired data is NiO = 1.95%, CuO = 4.76%, MnO = 1.99%, CoO = 4.35% and for the BV assays paired with the ALS primary samples is NiO = 3.22%, CuO = 2.49%, MnO = 2.31%, CoO = 6.35%. The precision in the nodule sample assays is acceptable.

Figure 8.2 Comparison of primary samples assayed at ALS and duplicate samples assayed at ALS
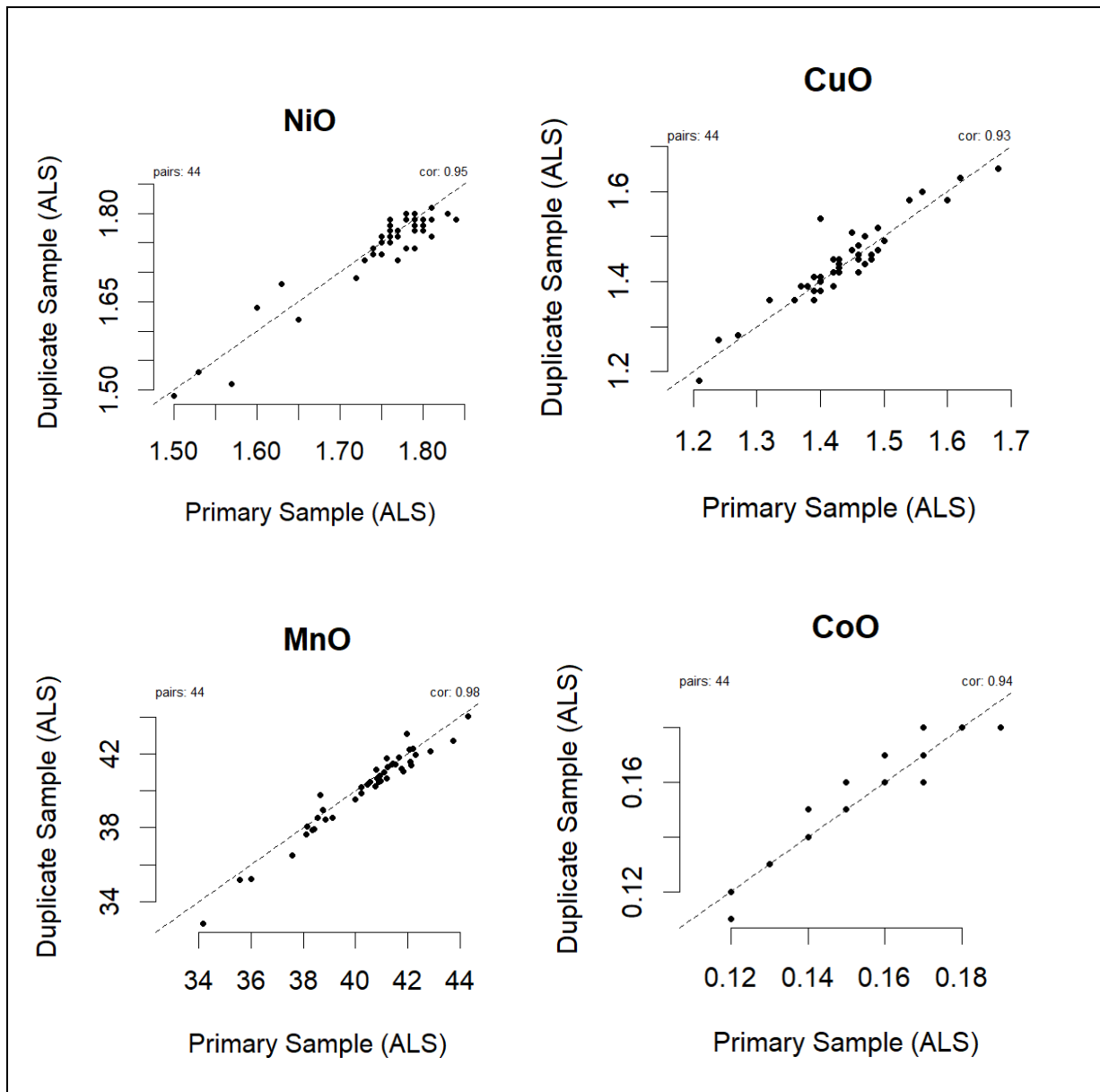
Figure 8.3   Comparison of primary samples assayed at ALS and duplicate samples assayed at BV
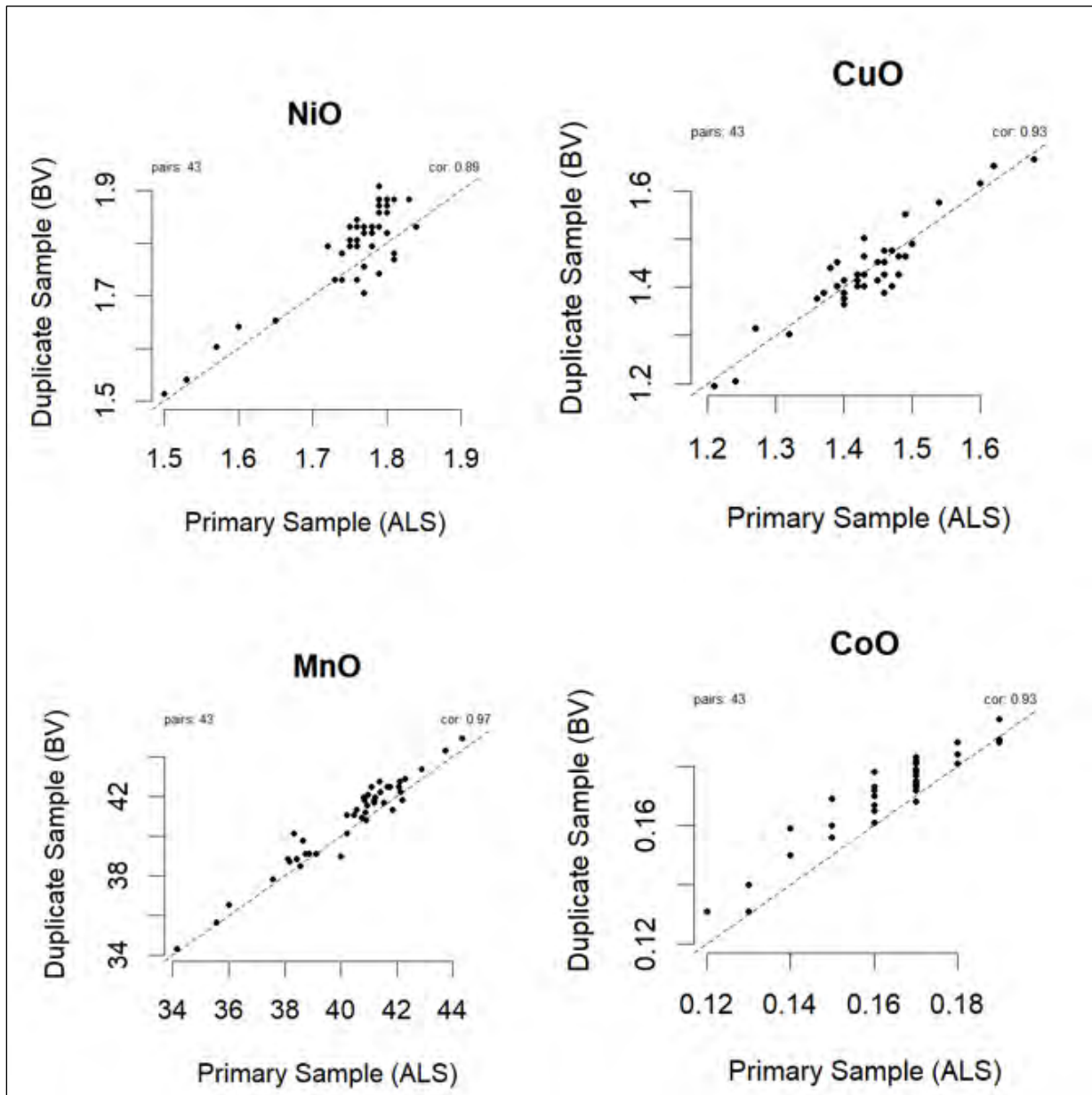
Table 8.3   Duplicate average sample grades by laboratory

Variable	ALS Primary	ALS Duplicate	BV Duplicate
NiO (%)	1.75	1.74	1.79
CuO (%)	1.44	1.44	1.43
MnO (%)	40.39	40.11	40.82
CoO (%)	0.16	0.16	0.17

8.4 Quality assurance and quality control procedures 2019

Certified reference materials (CRMs), blank samples, and duplicate samples were used for quality control and quality assurance during assaying of the samples collected in the 2019 campaigns.

8.4.1 Certified reference materials

The CRM called NOD-P-1 was used. A total of 22 CRMs were inserted into sample submissions at a rate of 1 in 10. Table 8.4 shows the assays for the CRMs and the certified values for NOD-1-P.

There was a slight positive bias in the manganese oxide assays and the BV (Bureau Veritas Minerals Pty Ltd) assays for nickel, manganese and cobalt were slightly elevated relative to those from ALS but these differences are not significant. The CRM results indicate that the NORI 2019 assay results are satisfactory.

All the assays for Nod-1-P from ALS were within two standard deviations of the certified values and were satisfactory. The single Nod-1-P sample assayed at BV returned assays for nickel, copper, manganese and cobalt that were all biased slightly high.

Table 8.4   CRM assays from NORI 2019 campaigns

Sample	NiO (%)	CuO (%)	MnO (%)	CoO (%)	Laboratory
Certified value	**1.71**	**1.44**	**37.6**	**0.28**	**-**
STD11	1.73	1.43	37.86	0.28	ALS
STD12	1.72	1.43	37.79	0.28	ALS
STD1	1.73	1.45	37.3	0.29	ALS
STD2	1.72	1.42	37.29	0.28	ALS
STD3	1.71	1.42	37.14	0.28	ALS
STD4	1.71	1.41	37.13	0.28	ALS
STD5	1.72	1.44	37.43	0.28	ALS
STD6	1.73	1.44	37.54	0.28	ALS
STD7	1.73	1.47	37.73	0.29	ALS
STD8	1.71	1.44	37.39	0.28	ALS
STD9	1.72	1.45	37.59	0.28	ALS
STD10	1.71	1.42	37.7	0.28	ALS
STD13	1.73	1.43	38.07	0.29	ALS
STD14	1.73	1.43	37.94	0.29	ALS
STD15	1.73	1.44	37.93	0.29	ALS
STD16	1.71	1.42	37.49	0.28	ALS
STD17	1.72	1.43	37.74	0.28	ALS
STD18	1.72	1.42	37.67	0.28	ALS
STD19	1.72	1.43	37.85	0.28	ALS
STD20	1.72	1.43	37.82	0.29	ALS
STD21	1.71	1.43	37.72	0.28	ALS
STD4	1.82	1.54	38.87	0.30	BV

8.4.2 Blanks

The blank samples were composed of recycled glass, which were expected to have very low content of manganese, cobalt, nickel and copper. The blank material was not assayed

prior to insertion in the NORI sample batches. A total of 11 blank samples were inserted into the NORI 2019 sample assay batches at a rate of 1 in 19. Table 8.5 shows the assays for the blanks. The assays for the blank samples indicate negligible contamination in the sample preparation.

Table 8.5   Blank sample assays from NORI 2019 campaign

Blank name	Sample	NiO (%)	CuO (%)	MnO (%)	CoO (%)
UUM_3	Blank1	<0.01	<0.01	<0.01	<0.01
UUM_3	Blank2	0.01	<0.01	0.13	<0.01
UUM_3	Blank3	0.01	0.01	0.13	<0.01
UUM_3	Blank4	0.01	0.01	0.12	<0.01
UUM_3	Blank5	0.02	0.01	0.57	<0.01
UUM_4	Blank6	<0.01	0.02	<0.01	<0.01
UUM_4	Blank7	<0.01	0.03	<0.01	<0.01
UUM_4	Blank8	0.02	0.02	0.2	<0.01
UUM_4	Blank9	0.01	0.03	0.22	<0.01
UUM_4	Blank10	0.01	0.02	0.16	<0.01
UUM_4	Blank11	0.02	0.04	0.42	<0.01

8.4.3   Duplicates

Duplicate samples were prepared by cone and quartering the box core samples, as described in Section 9.3.8. A total of 19 samples were assayed at ALS paired with duplicate samples also assayed at ALS. Figure 8.4 and Table 8.6 presents the results. The precision of the results is very good and there is no evidence of significant biases or errors.

Figure 8.4   Comparison of primary samples assayed at ALS and duplicate samples assayed at ALS
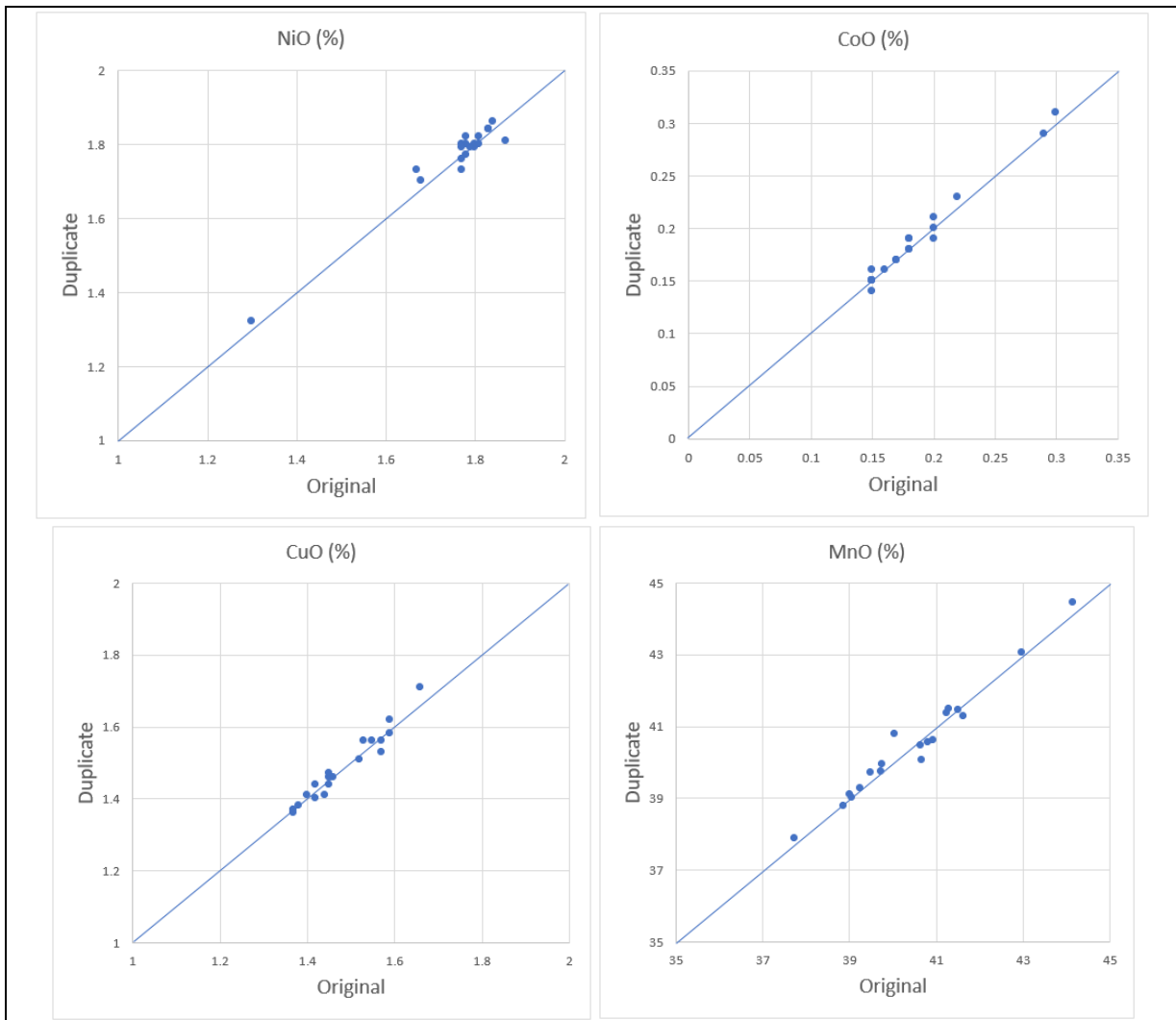
Note: Diagonal blue line at 1:1 ratio

Table 8.6   Duplicate average sample grades from ALS

Variable	Number	ALS Primary	ALS Duplicate
NiO (%)	19	1.76	1.77
CuO (%)	19	1.48	1.49
MnO (%)	19	40.47	40.47
CoO (%)	19	0.19	0.19

The pulps of 27 pulp samples assayed at ALS were resubmitted for assay at BV. Figure 8.5 presents the results. The results for nickel, copper, cobalt and manganese are all biased high by approximately3% to 5%, compared with the ALS assays Table 8.7.

These results are consistent with the observation for the assays of the NOD-P-1 standard which indicated that the BV results were biased slightly high.

Figure 8.5   Comparison of primary samples assayed at ALS and duplicate samples assayed at BV
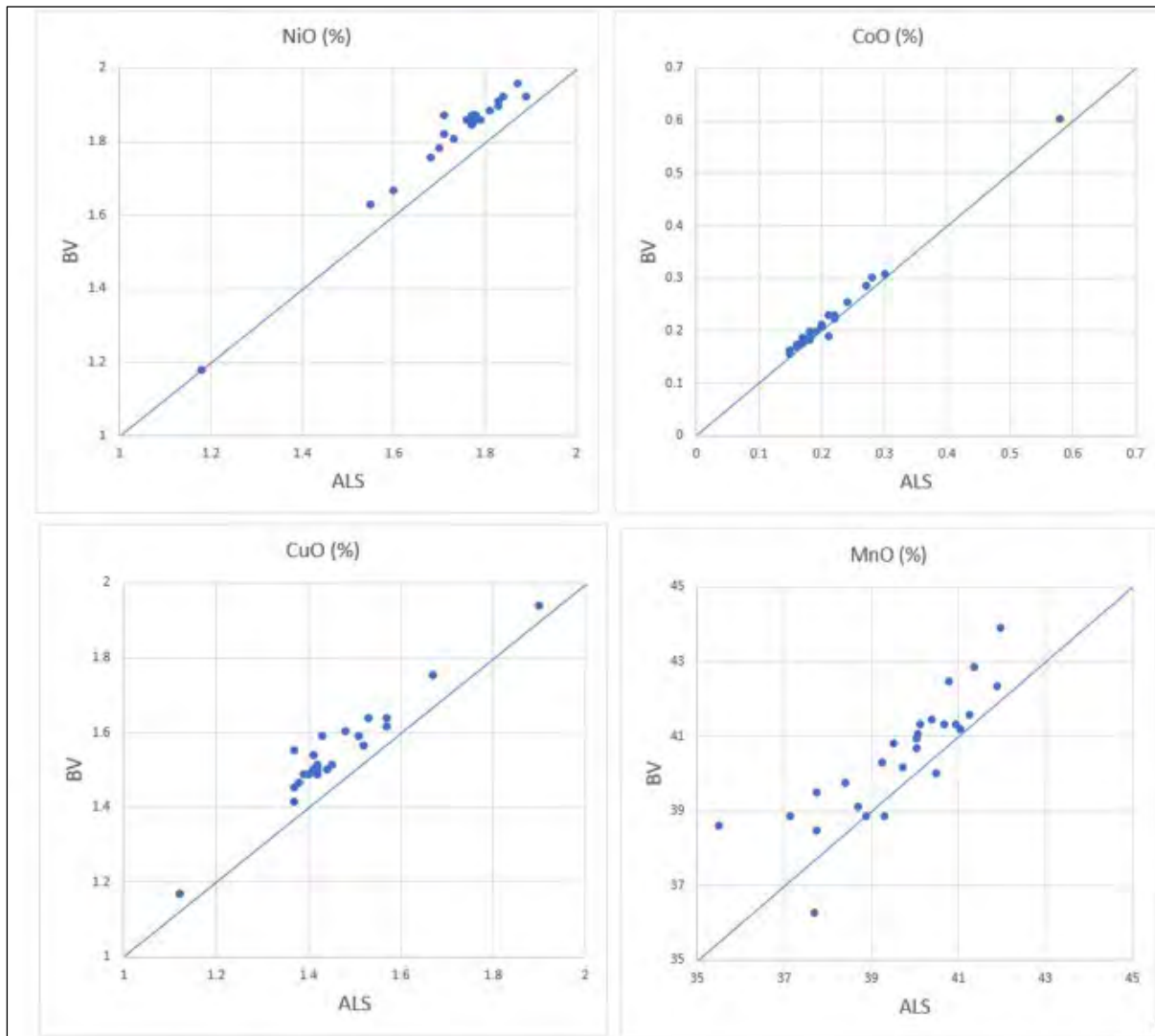
Note: Diagonal blue line at 1:1 ratio

Table 8.7   Duplicate average sample grades from ALS and BV

Variable	Number	ALS Primary	BV Pulp Duplicate
NiO (%)	27	1.74	1.82
CuO (%)	27	1.47	1.56
MnO (%)	27	39.4	40.5
CoO (%)	27	0.21	0.22
SiO2 (%)	27	12.6	12.9

8.5   Moisture content

The moisture content of polymetallic nodules consists of two main types of water: free water occurring with pore spaces and water of crystallisation which forms part of the mineral structure of many of the iron and manganese minerals in the nodules. There may also be moisture held in meta-stable mineral phases.

Manganese minerals with various types of crystalline lattice have different levels of thermal stability. Layered manganese minerals (buserite I, asbolane-buserite, and birnessite) are stable up to 120 °C–150 °C; asbolane up to 180 °C, vernadite, up to ~500 °C; todorokite and pyrolusite, up to 600° and 670 °C, respectively (Novikov and Bogdanova, 2007). Measures of the moisture content of polymetallic nodules are therefore highly dependent on the temperature and the length of time to which the nodules are heated.

Published data on the moisture content of polymetallic nodules is commonly inconsistent. The following moisture content information was obtained from samples collected in the NORI Areas:

- A drying test undertaken on a nodule sample collected during the NORI 2012 campaign indicated moisture loss of 24% at 120°C (Golder, 2015).
- Average moisture content of four Campaign 2 samples dried for 12 hours at 120 °C was 28.7% (Golder, 2015).
- Average moisture content of the Campaign 3 (2018) box core samples dried for three days at 60 °C (at ALS) was 19.3% and LOI at 1,000 °C was 16.8%.
- Average moisture content of the Campaign 3 (2018) box core samples dried for at 105 °C (at Bureau Veritas) was 17.0% and LOI at 1,000 °C was 16.6%.
- Average moisture content of the Campaign 6A and 6B (2019) box core samples dried for at 105 °C (at ALS) was 28.1% and LOI at 1,000 °C was 15.6%.

Ambient conditions, such as air temperature, humidity, evaporation rate and exposure time, during the handling of the nodules prior to sealing in sample bags were not recorded in these programmes. Also, the impact of drying time and oven temperature on the removal of pore water from the nodule samples has not been quantified. Consequently, the average moisture contents measured in different campaigns may not be directly comparable.

The loss on ignition data, which are measures of water of crystallization, are better controlled and show a reasonable degree of consistency.

9 Data verification

The original assay sheets for the individual samples collected by the Pioneer Investors from within the NORI Area are not available for auditing against the values in the database. Neither AMC nor DeepGreen nor NORI have had access to the original assay sheets for the individual samples that are within the Area, nor the quality control procedures used by the laboratories and the ISA. However, the consistency between the abundance and grade data collected by the Pioneer Investors, as presented in Section 9.1, supports the contention that the quality of the Pioneer Investor data is satisfactory.

It is also reasonable to infer that the Pioneer Investor data are of sufficient quality for resource estimation because the ISA is an independent agency with significant accountability under the Law of the Sea. Part of its mandate is the receipt and storage of seafloor sampling data suitable for the estimation of nodule resources and the legally binding award of licenses. It is reasonable to assume that a reasonable level of care was applied by the ISA.

Data collected by NORI is well-documented and was subject to satisfactory QA/QC processes. Documentation verified by the Qualified Person includes photographs, daily exploration reports, digital logging sheets and original assay reports. In the opinion of the Qualified Person the NORI data is of high quality and suitable for estimation of Measured Mineral Resources.

Assaying of nodules collected by NORI in 2012, 2013, 2018, and 2019 confirm the mean grades of the historical grab samples and support the contention that the quality of the Pioneer Investor data is satisfactory for inclusion in resource estimation. The main limitation with the Pioneer Investor data is the likelihood that some of the abundance values were too low, due to loss of nodules from the FFG. Estimates of abundance that include Pioneer Investor data are therefore likely to be conservative.

In the opinion of the Qualified Person the sample preparation, security, and analytical procedures were adequate for estimation of Mineral Resources.

10Mineral processing and metallurgical testing

10.1 Introduction

A combined pyro- and hydro-metallurgical flowsheet was evaluated for these IA. Similar flowsheets were investigated at various times over the last several decades. NORI initially relied on the significant body of information in the literature for process development. Subsequently, they have embarked on an extensive program of small and pilot-scale pyrometallurgical test work that has further informed definition of that part of the flowsheet. The work to date is discussed in Section 10.3.

The literature on test work for this process was reviewed and interpreted by Kingston Process Metallurgy in their report to NORI in October 2017. In turn, that report was reviewed as part of the current study, with important aspects from it being adopted for the purposes of process modelling and definition. Relevant extracts from the report are reproduced below in Section 10.2 shown in *italic* font. Comments from the Initial Assessment Section 13 author are shown as footnotes where applicable.

10.2 Literature review (from KPM concept study, 12 October 2017)

10.2.1 Studies on the pyrometallurgical processing of polymetallic nodules

Pyrometallurgical processing of nodules has been extensively studied from the early 1970s until the present day and appears to be the preferred process for most of the other currently active nodule processing research groups. Many groups including: Kennecott; Inco; Cuban / Bulgarian; German; Indian; Japanese; and Korean have studied pyrometallurgical processing of nodules at a laboratory scale. The nodule samples for these tests were collected from their respective license areas in the Clarion Clapperton [sic] Zone (CCZ). The composition of the nodules used in each of the studies is compared in Table 10.1 with that of the NORI Area D resource nodules. [Note: the NORI assays are from samples collected prior to 2017, not the current resource estimate].

Table 10.1 Comparison of sea nodule composition

Element	NORI	Inco	German	Japan	Indian	USBM
Ni	1.36%	1.14%	1.36%	1.36%	1.15%	1.33%
Cu	1.14%	0.80%	1.17%	1.04%	1.10%	1.20%
Co	0.13%	0.22%	0.16%	0.18%	0.08%	0.23%
Mn	28.40%	23.20%	31.23%	28.40%	24.30%	29.70%
Fe	6.68%	6.90%	6.20%	5.07%	5.36%	5.50%
Mo	-	0.06%	0.06%	0.06%	-	-
Zn	0.15%	0.11%	0.15%	0.14%	-	0.15%
SiO_2	18.40%	18.43%	12.64%	12.20%	13.14%	13.40%
Al_2O_3	3.89%	5.80%	4.29%	4.35%	4.5%	4.76%
MgO	2.92%	2.90%	3.20%	-	2.70%	3.12%
CaO	2.16%	1.81%	2.27%	2.19%	0.76%	1.79%
Na_2O	2.40%	5.12%	2.74%	-	1.02%	2.97%
K_2O		-	1.19%	-		1.13%
P		0.17%	0.21%		0.01%	0.10%
MnO / SiO_2	1.99	1.63	3.19	3.01	2.39	2.86

It should be noted that while in general the different nodule samples have similar compositions, there are subtle variations that can have significant implications for

pyrometallurgical processing. Of particular importance is the ratio of MnO:SiO2 in the nodules as this impacts the choice of process operating parameters for the electric furnace smelting operation. This issue is discussed further in the Sections below.

Based on a review of the data found in the nodule smelting literature, it was concluded that the best data for designing a preliminary pyrometallurgical flowsheet for treating NORI nodules was provided by the Inco, Japanese and German references.

10.2.1.1 Inco

Inco[1] did extensive test work in the early 1970s on smelting nodules using a conventional Rotary Kiln Electric Furnace (RKEF) flowsheet for FeNi production from laterite, as shown in Figure 10.1.

Inco carried out laboratory tests using as received nodules (30% moisture) to simulate drying and reduction in a rotary kiln at 1,000 °C using a reducing gas containing: 14.7% CO, 8.2% H$_2$, 6.7% CO$_2$, 6.7% H$_2$O and 63.2% N$_2$ from combusting Bunker C oil with 60% stoichiometric air. Most of the Ni, Cu and Co oxides (70–90%) were reduced together with about 25% of the Fe oxides to a metal. With the addition of 4.5% anthracite coal, the extent of Fe oxide reduction to metal increased to about 45%. Inco also carried out tests to study the behaviour of the nodules in a 15 cm diameter pilot scale rotary kiln and reported that the amount of dust generated was similar to that observed in a commercial laterite rotary kiln and that the maximum temperature of operation for a kiln would be about 1,000 °C before the reduced nodules became sticky and caused plugging of the kiln. Unfortunately, no other data was reported from the pilot kiln tests.

---

[1] R. Sridhar, W. E. Jones, and J. S. Warner, "Extraction of copper, nickel and cobalt from polymetallic nodules", JOM, April 1976, p 32.

Figure 10.1   Schematic flow diagram of the Inco process for treating polymetallic nodules
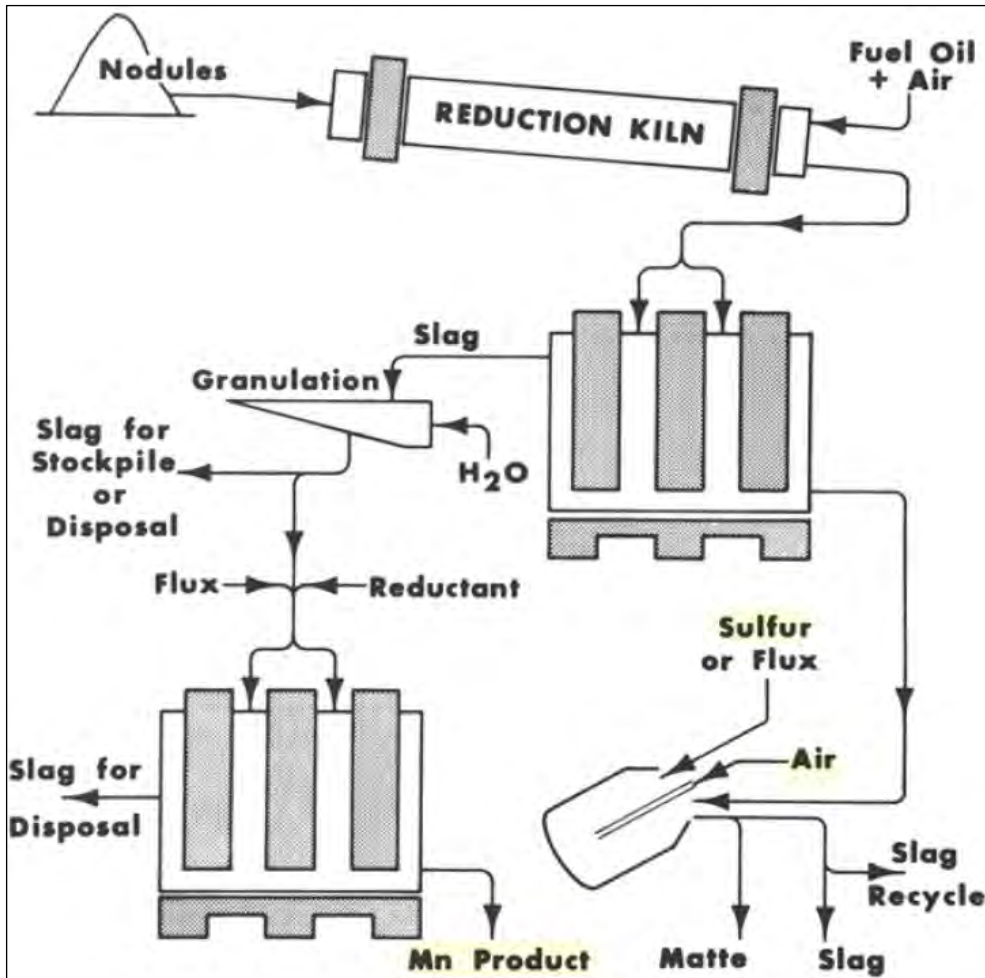
The Inco nodules had a low MnO:SiO$_2$ ratio of 1.6 with an estimated liquidus temperature of only about 1,300 °C. The Ni-Cu-Co-Fe alloy has a similar liquidus temperature so that no fluxes were needed to be able to smelt the nodules to produce a fluid slag and alloy at a reasonable temperature of about 1,400 °C. The pre-reduced nodules were blended with coal and smelted in crucibles at 1,380-1,420 °C for 1 hour to produce a metal phase, typically containing >90% of the Ni, Cu and Co, and a slag phase containing >97% of the Mn. No fluxes were added. Typical results are shown in Table 10.2 and Table 10.3.

Table 10.2   Results from Inco smelting tests

Element	Alloy[1] - Wt %	Slag[2] - Wt %	Recovery in Alloy Wt %
Nickel	12.5–21.0	0.05–0.15	93–98
Copper	8.5–11.5	0.04–0.12	85–95
Cobalt	2.0–3.0	0.006–0.015	90–98
Iron	60.0–70.0	0.7–1.7	80–90
Manganese	0.3–6.0	25–33	0.5–2.5

Pre reduced at 1000 °C for 1 hour and smelted at 1400 °C.
[1] 6–8.5% of dry nodule weight.
[2] 72–80% of dry nodule weight.

Table 10.3   Distribution of Elements During Reduction Smelting (Inco)

Element	Alloy[1] - Wt %	Slag[1] - Wt %	Recovery[2] in Alloy, Wt %
Nickel	13.7	0.05	98
Copper	8.7	0.02	95
Cobalt	2.3	0.006	98
Iron	70.7	1.26	87
Manganese	1.2	32.0	0.5
Molybdenum	0.56	< 0.01	>86
Vanadium	0.002	0.04	0.5
Titanium	0.02	0.45	0.5
Zinc	0.09	0.01	6
Lead	0.01	0.003	2
Phosphorus	0.99	0.13	36
Sodium	< 0.003	2.76	1
Arsenic	0.04		64
Antimony	0.03		~100

[1] Alloy was 8% of dry nodule weight and slag was 72% of dry nodule weight.

[2] Recovery from nodules.

The molten Ni-Cu-Co-Fe alloy from the smelting furnace was converted using air to oxidise the Mn and about 15% of the Fe to slag. The alloy was then sulphidised by injecting elemental sulfur to form Ni_3S_2, Cu_2S and Co_9S_8 and the resulting highly metallised (Fe) matte was converted using air to form a high-grade (HG) matte (about 5% Fe) and a low Ni-Cu-Co slag with minimal SO_2 generation.

The ground matte was oxygen pressure leached at 110-160 °C in sulfuric acid to extract 99% of the contained Ni, Cu and Co and precipitate most of the Fe. In the Inco flowsheet, it was proposed to recover the Cu by SX/EW and the Ni and Co as metals or salts by any of the many available conventional processes. A high Mn slag (44% MnO) from one of the smelting tests was reduced with coke in an electric furnace to produce a ferro-manganese (82% Mn) alloy, the main form of Mn alloy used by the steel industry at that time.

10.2.1.2   Sumitomo

In the 1990s, Sumitomo[2] investigated a smelting flowsheet similar to Inco's for processing nodules. The nodules used had a high MnO: SiO₂ ratio of 3 giving an estimated slag liquidus temperature of about 1,530 °C. The nodules were crushed, dried at 110 °C to remove water not chemically bound, mixed with coal and flux and heated at 900 °C for two hours. The calcine was then smelted at 1,400 °C using 5% fixed carbon addition, as coal, and with additions of 12% SiO₂ and 7% CaO to minimise the liquidus. The results of the laboratory smelting tests are shown in Table 10.4.

---

[2] Tetsuyoshi Kohga et al, "Recovering Iron, Manganese, Copper, Cobalt, and High Purity Nickel from Polymetallic nodules", JOM, December 1995, p 40.

Table 10.4   Results of Sumitomo smelting tests

Element	Alloy (wt. %)	Recovery (%)	Slag (wt. %)
Ni	22.3	98.5	0.02
Cu	16.7	97.5	0.03
Co	5.4	96.8	0.01
Mn	0.22	0.05	31.3
Fe	55.0	62.1	2.79
Zn	0.01	3.2	<0.01
Mo	1.01	80	<0.1

The Ni, Cu and Co recoveries to the alloy were very high together with very little Mn reduction. After partial oxidation of the alloy to slag off the Mn and part of the Fe, the residual alloy was fully sulphidised with sulfur to convert all the Fe to FeS and then further converted to a purified matte and SO2, as shown in Table 10.5.

The purified Ni-Cu-Co matte was leached with Cl_2 gas and to extract 99% of the metals into a chloride pregnant liquor solution (PLS) containing: 145 g/L Ni, 74 g/L Cu, 11 g/L Co and 19 g/L Fe and a sulfur residue that would be recycled back to the converter for sulphidisation. Ni, Cu and Co metals were recovered from the chloride PLS by SX/EW and the Cl_2 gas recycled to the leach using the same processes as used at Sumitomo's Ni refinery.

Table 10.5   Composition of matte produced by Sumitomo

Element	Alloy (wt. %)	Recovery (%)
Ni	20.0	34.2
Cu	14.7	25.3
Co	4.83	4.05
Mn	<0.1	<0.1
Fe	34.7	10.8
S	33.2	25.7

The Mn slag from smelting was reduced in two stages: a first stage to remove Fe and P to produce a Fe-Mn alloy followed by a second stage to produce a SiMn alloy.

10.2.1.3   German Federal Institute for Geosciences and Natural Resources

Most recently, a German group conducted a study with the aim to develop "a sustainable, zero-waste process route to extract valuable metals from marine Mineral Resources" from the German licensed territory in the CCZ[34]. After reviewing historical work conducted on possible hydrometallurgical and pyrometallurgical flowsheets, it was concluded that the pyrometallurgical flowsheet developed by Inco offered the most promise to treat manganese containing nodules.

Subsequently, a preliminary thermodynamic model of the first smelting step of the Inco flowsheet was developed and validated against experimental data. The sample of the German nodules under investigation had a very high MnO: SiO_2 ratio of 3.2 with an

---

[3] D. Friedmann, A. K. Pophanken and B. Friedrich, "Pyrometallurgical Treatment of High Manganese Containing Deep Polymetallic nodules", J. Sustain. Metall., Published Online 18 July 2016.

[4] Friedmann, D, et al, "Optimized slag design for maximum metal recovery during pyrometallurgical processing of polymetallic deep-polymetallic nodules", MOLTEN16, TMS 2016, p. 97-104.

estimated (FactSage) slag liquidus temperature of about 1550 °C. The thermodynamic model further estimated that the slag liquidus temperature decreases with MnO: SiO_2 ratio, as shown in Figure 10.2. The implications for the smelting step was that additions of silica could be used to lower the slag liquidus, allow the smelting to be conducted at a lower temperature and minimise the reduction of manganese.

Smelting tests were carried out using a 50 kW electric furnace with 3 kg mixtures of nodules, silica flux and carbon using MnO: SiO_2 ratios of 1.0, 2.0 and 3.2. The alloy and slag compositions from the tests are summarised in Table 10.6.

Figure 10.2 Estimated Slag Liquidus as a function of MnO_2/SiO_2 ratio
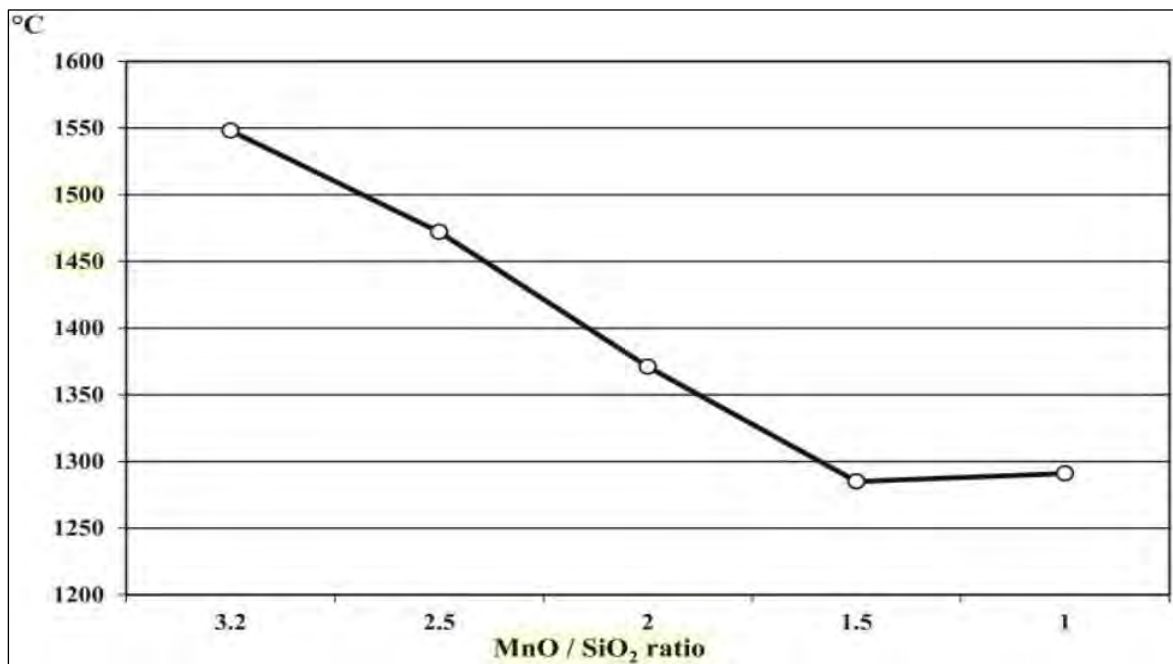
Table 10.6 Results from the German smelting tests

MnO / SiO2	Ni (%)	Cu (%)	Co (%)	Fe / FeO (%)	Mn / MnO (%)	SiO2 (%)	Temperature (°C)
3.2 – alloy	13.4	9.1	0.7%	54.3	18.5	-	1650
3.2 - slag	0.5	0.7	-	9.4	55.3	14.7	
2.0 – alloy	17.0	12.7	1.9%	62.4	2.2	-	1450
2.0 - slag	-	-	-	3.5	47.4	31.0	
1.0 – alloy	17.8	10.8	2.0%	60.4	2.5	-	1400
1.0 - slag	0.1	0.2	-	3.0	38.0	41.0	

The results showed good general agreement with the predictions of the thermodynamic model and indicated that SiO_2 flux additions could be used to operate the smelting process at a temperature of 1400–1500ºC with minimum MnO reduction. The Ni recovery in all tests was >95%. Using the nodule, matte and slag compositions and assuming a Ni recovery to matte of 96.5%, the matte and slag weights and compositions were estimated together with the Ni, Cu, Co, Fe and Mn recoveries to alloy and the partition coefficients, as shown in Table 10.7. The estimated Cu and Co recoveries, based on the assumptions used to generate the mass balances, were significantly lower than the other data ranging from 76–84% for Cu and 43–92% for Co. These recoveries are hard to explain especially

since the Ni recoveries to alloy and the Fe contents of the alloy and the amount of FeO reduced were consistently high in all tests.

Table 10.7   Partition coefficients from the German smelting tests

Stream	Wt.	Ni	Cu	Co	Fe	Mn
Nodules	100	1.36%	1.17%	0.16%	6.2%	31.2%
R=3.2 – alloy	9.8	13.4%	9.1%	0.7%	54.3%	18.5%
R=3.2 – slag	68.6	0.07%	0.41%	0.13%	1.3%	42.8%
R=3.2 – recovery to alloy		96.5%	76.2%	42.8%	85.8%	18.5%
R=3.2 – Dm/s		193	22	5	-	-
R=2.0 – alloy	7.7	17.0%	12.7%	1.9%	62.4%	2.2%
R=2.0 – slag	84.5	0.06%	0.22%	0.016%	1.6%	36.7%
R=2.0 – recovery to alloy		96.5%	83.8%	91.7%	77.7%	0.5%
R=2.0 – Dm/s		302	57	120	-	-
R=1.0 – alloy	7.4	17.8%	10.8%	2.0%	60.4%	2.5%
R=1.0 – slag	105.4	0.05%	0.37%	0.012%	1.7%	29.4%
R=1.0 – recovery to alloy		96.5%	68.1%	92.2%	71.8%	0.6%
R=1.0 – Dm/s		395	30	168	-	-

10.2.1.4 United States Bureau of Mines

The USBM studied smelting of nodules in the laboratory and carried out 35 reduction tests on 1.9 kg samples of nodules blended with 350 g silica and 100 g coke in SiC crucibles[5]. The reduction temperature was 1400 °C and the holding time was 1.5 hours. Two tests were also conducted on reducing the smelting test slag with lime flux additions at 1450 °C to form FeMn. The results of these tests are summarised in Table 10.8.

Table 10.8   Results of USBM Smelting Tests

Stream	Ni	Cu	Co	Fe	Mn
Nodules	1.33%	1.20%	0.23%	5.46%	29.7%
Smelted alloy	14.6%	12.4%	2.54%	48.6%	9.2%
Smelted slag	0.02%	0.03%	0.009%	0.3%	29.7%
FeMn alloy	0.17%	0.24%	0.03%	6.1%	75.1%
FeMn slag	<0.01	0.07	<0.001	0.07	5.35%

The USBM also tested 4 hydrometallurgical processes: Fluid-bed reduction; Cuprion ammoniacal leach process; High temperature pressure oxidation and Fluid-bed reduction & HCl leach. EPA toxicity tests were carried out on all the leach residues and slags from the processes. It was concluded that all the slags and tailings produced would be classified as non-hazardous as defined by the EPA toxicity test[6]. Although this is a very encouraging conclusion, it should be noted that this work was conducted in 1985 and it is recommended

---

[5] Haynes, B.W., "Laboratory processing and characterization of waste materials from manganese nodules", USBM RI 8938, 1985b.

[6] Note by author: The EPA toxicity test and conclusions referenced above were based on the then current testing procedure and toxicity limits (from 1985).

that further investigation of the current relevant regulatory guidelines be conducted and, as required, specific testing NORI materials be conducted.

10.2.1.5 Indian National Metallurgical Laboratory

The Indian nodule smelting tests were carried out in a 50 kVA rectangular electrode furnace using 20 kg batches of nodules blended with coke and silica[7]. After melting an initial charge, the two graphite electrodes were immersed in the slag and the remaining charge gradually added. At the end of the test, the molten slag and alloy were tapped into a clay-graphite crucible and allowed to cool. The tests were carried out at slag temperatures in the range 1350-1450ºC and with the amount of coke in the charge varying between 5 and 15%. The optimum conditions were found to be 7.5% coke at 1400 °C giving the highest recoveries to alloy of 94% Ni, 91% Cu and 78% Co, as shown in Table 10.9. These tests probably represent the best simulation for a potential commercial nodule smelting operation available from the literature.

Table 10.9   Results of Indian smelting tests

Stream	Wt.	Ni	Cu	Co	Fe / FeO	Mn / MnO	Si / SiO2
Nodules	100	1.15%	1.10%	0.08%	5.4%	24.3%	13.1%
Alloy	7	15.4%	14.5%	0.8%	61.5%	3.9%	0.3%
Slag	71.8	0.04%	0.08%	0.01%	5.60%	43.20%	29.20%
Recovery to alloy		94%	91%	78%	80.6%	1.1%	
Dm/s		385	181	84			

10.2.2   Ni, Cu, and Co partition coefficients

The concept of partition coefficients is useful for assessing the efficiency of metallurgical processes. In the case of smelting reduction processes, the partition coefficient is the ratio of concentrations of a specific element in the metallic and slag (or matte and slag) phases. A high partition coefficient indicates efficient recovery of that element to the metallic phase and vice versa for a low partition coefficient.

10.2.2.1 Experimental test work

The Ni, Cu, and Co partition coefficients from the nodule smelting studies reviewed above are compared in Table 10.10 together with the recovery of iron to the alloy.

Table 10.10   Partition coefficients from sea nodule smelting tests

Partition coefficients				
Study	Ni	Cu	Co	Fe to alloy
Inco	396	154	194	87%
Japan	1115	557	540	70%
German	302	57	121	86%
Indian	385	181	84	80%
USBM	730	413	282	81%
Average	586	272	244	81%

The partition coefficients for Ni, Cu and Co from these tests are very high ranging between 302–1115 for Ni, 57–557 for Cu and 84–540 for Co. These values are for well-controlled

---

[7] Agarwal, S., et al, "Studies on recovery of Ni, Co, Cu from polymetallic polymetallic nodules by direct reduction smelting", COM 2009, Sudbury, p. 509-517.

laboratory conditions with slow cooling in-situ that promotes excellent settling of the small alloy prills from the slag. The partition coefficients in a commercial operation, with less ideal settling conditions, would be expected to be lower.

Barnes[8] investigated the smelting of cobalt in a small-scale (120–250 kW) DC furnace from a fayalitic reverberatory furnace slag that contained approximately 0.75% Co and 1.2% Cu. The results showed a correlation between the Co and Fe recoveries to the metal, as illustrated in Figure 10.3.

10.2.2.2 Commercial furnace operation

Solar[9] studied Ni/Co recovery from 11 FeNi smelting furnaces and found that Ni recoveries averaged 93.5% (range 89.6–97.0%) and Co recoveries averaged 71.9% (range 56.5-85.3%) corresponding to average partition coefficients of about 220 for Ni (range 155–264) and about 41 for Co (range 20–92). Solar also showed that Ni recovery to FeNi correlated well with the Fe recovery to the FeNi (range 13–65%), as shown in Figure 10.4.

Figure 10.3   Relationship between Co and Fe recoveries to alloy from Co smelting tests (Barnes)
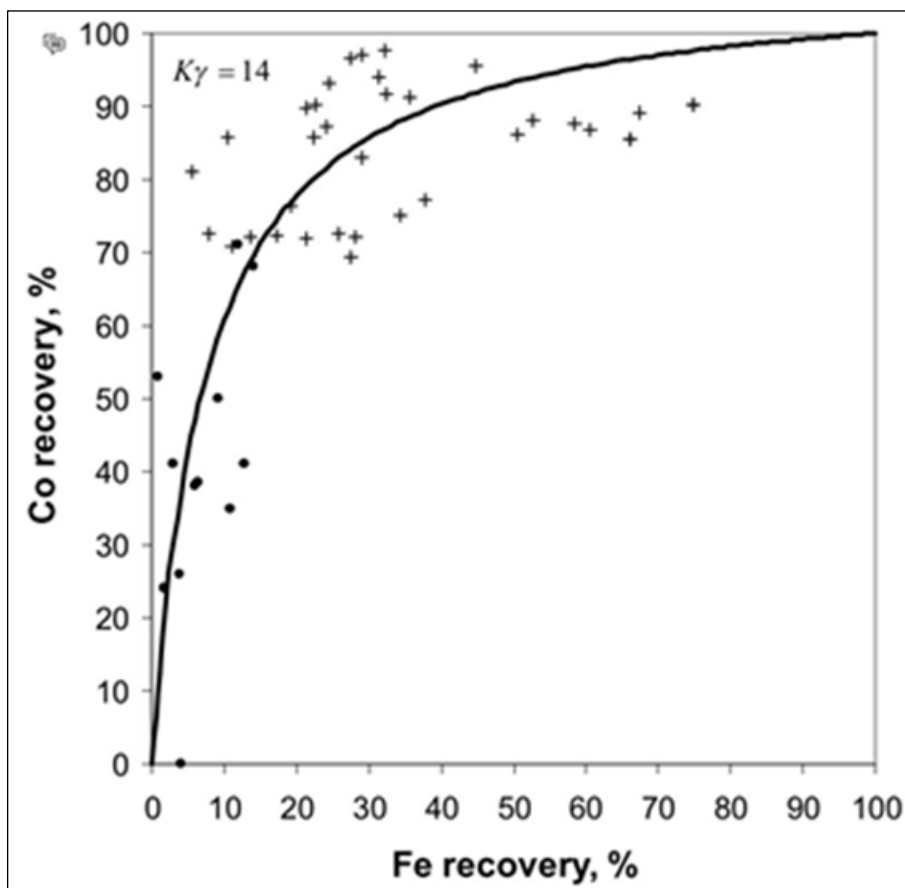
[8] Barnes, A., et al., "Cobalt from slag – Lessons in transition from laboratory to industry", COM 2011, Montreal.

[9] Solar, M., "Mechanical slag losses in laterite smelting – nickel", COM 2009, Sudbury, p. 277-291

Figure 10.4 Relationship between Ni and Fe yields in laterite smelters, actual vs theoretical
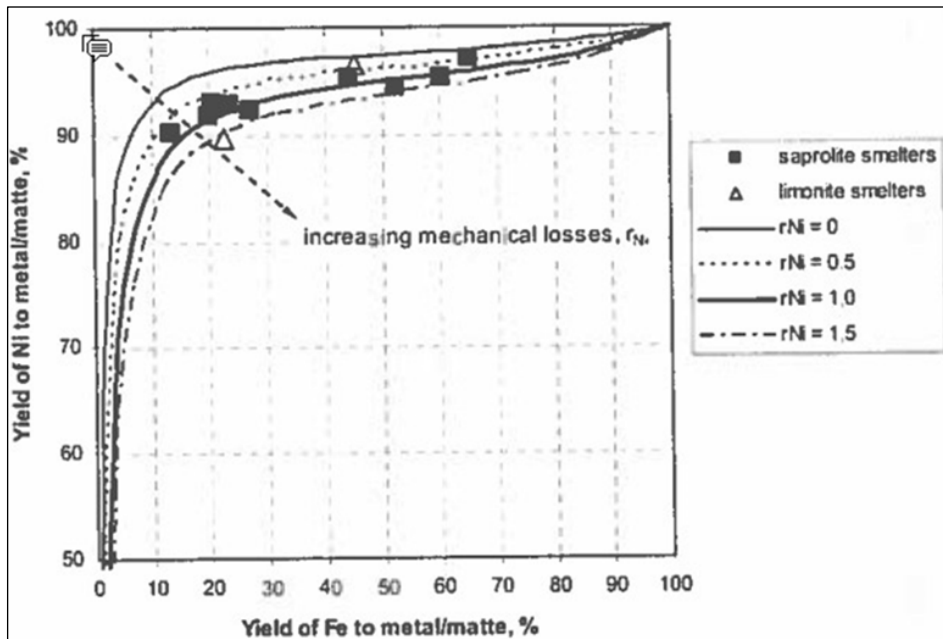
There are insignificant amounts of Cu in the laterite feeds to FeNi furnaces and the best data for the partition coefficient for Cu is from various Cu and Ni smelter slag reduction electric furnaces. The most pertinent data that could be found from Cu and Ni smelter slag reduction furnaces is summarised in Table 10.11.

Table 10.11 Partition coefficients from various Cu and Ni slag reduction electric furnaces

Data from	EF matte/alloy (%)					EF slag (%)				Partition coefficient		
Harjavalta smelter10	Ni	Cu	Co	Fe	S	Ni	Cu	Co	Fe	Ni	Cu	Co
Harjavalta Old Ni smelter EF	45	12	-	25	8	0.2	0.3	-	40	225	40	-
Harjavalta DON smelter EF	52	5	-	30	8	0.3	0.1	-	43	173	50	12
Mintek EF11	42	19	1.5	33	1	0.3	0.5	0.12	37	140	38	12
Konkola 2nd EF12	-	65	5	20	8	-	0.5	0.3	40	-	130	17
Amax Carteret EF13	8	25	-	60	-	0.1	0.3	-	30	80	83	-

The Cu partition coefficients range from 40 to 130 with an average of about 75. The Ni and Co partition coefficients are lower than those from FeNi smelters presumably because of the significantly lower Fe recovery to the alloy / matte phase.

---

[10] Mackinen, T., et al, "Physical chemistry of direct nickel matte smelting", Sulphide Smelting '98, TMS, p. 59-68.

[11] Jones, RT., "CONROAST – DC arc smelting of dead-roasted sulphide concentrates", Sulphide Smelting 2002, TMS, p. 435-56

[12] Masanza, M.K., et al., "Commissioning of a second cobalt recovery furnace at Nchanga smelter", 5th International Symposium on high-temperature metallurgical processes, TMS 2014, p. 217-27.

[13] Rajcevic, H., et al., "Development of electric furnace slag cleaning at a secondary copper smelter", J. Metals, March 1982, p. 54-56.

10.2.2.3   Partition coefficients assumed for plant design criteria

Based on Solar's and Barnes evaluations, the % of Fe input reduced to Fe in alloy in the nodule smelting tests should give the best correlation for Ni and Co recovery. The average % Fe reduction in the nodule smelting tests summarised in Table 10.10 was about 80%. This is higher than any of the FeNi plants. Using Solar's correlation at 80% Fe recovery to alloy, the Ni recovery should be about 97%, equivalent to a partition coefficient for Ni of about 285 based on a preliminary nodule smelting mass balance. This is about half of the average Ni partition coefficient from the laboratory nodule smelting tests, shown in Table 10.10, and in agreement with the assumption that mechanical Ni losses in an industrial furnace will be roughly equal to the chemical NiO losses. Based on a similar mechanical loss assumption for Cu and Co, their partition coefficients would be 130 and 120 respectively.

10.2.3   Mn reduction during smelting

The recovery of Mn to the alloy for most of the nodule smelting tests was in the range 0.5-1.0% except for the USBM tests (2.8% Mn reduction), where CaO flux was added, and the German test without flux (5.8% Mn reduction) that required a temperature >1600 °C. The conditions used in both of these tests would have significantly increased MnO reduction.

The nodule smelting tests suggest that to minimise reduction of Mn and to produce the highest Mn grade in slag, only sufficient SiO_2 flux should be added to the nodules to produce a MnO/SiO_2 ratio in slag of about 2.2, giving a slag liquidus of about 1400 °C, such that the smelting furnace can be operated at a temperature of about 1500 °C to minimise MnO reduction and produce a fluid slag to reduce mechanical metal losses and facilitate tapping.

Based on the results of the nodule smelting tests it is reasonable to assume that reduction of MnO could maintained at < 1%.[14]

10.2.4   Processing of the EF alloy in Peirce-Smith converters

Both the Inco and Japanese studies proposed processes where the alloy would be converted into a HG[15] Ni-Cu-Co matte containing 5–10% Fe using Peirce Smith (PS) converters. To maintain high sulfur usage efficiency during this process, the manganese must first be eliminated prior to sulphiding the alloy. This is achieved by oxidising the molten alloy to lower its manganese content to <0.1% and fluxing with silica. The alloy is then sulphided with elemental sulfur and the sulphided bath converted using the standard method to eliminate iron as an iron silicate slag. It was found that the nickel and copper values in the slag in the early stages of converting were low enough that the slag could be discarded. The cobalt recovery in the matte was found to depend on the level of Fe remaining in the matte. The HG matte after converting typically contained: ~25% Cu, ~40% Ni, ~5% Co, ~% Fe, ~20-25% S, <0.01% Mn. There was insufficient data on converting in the Inco nodule smelting paper to determine metal distributions, but the paper reported 80% Co recovery to a 5% Fe matte and very high Ni and Cu recoveries.

The Inco study demonstrates that it is possible to produce a 5% Fe HG matte from polymetallic nodules. However, it is believed that HG matte containing 1% Fe would be more readily marketed and would receive higher contained metal valuation. The best industrial plant data for converting highly metallised Ni mattes is from the PT Vale

---

[14] Note by author: For the purposes of the PEA, MnO reduction of 1% was assumed as a reasonable basis.

[15] Note by author: HG = High Grade.

Indonesia Soroako nickel smelter[16] and the converter balance is summarised in Table 10.12. The matte is processed in 3 PS converters (9 m long × 4 m dia.) blowing at about 18,000 Nm³/h. A typical converter cycle takes about 7 hours to produce about 50 t of HG matte (1% Fe). It should be noted that the recovery of Co to the matte at the Soroako smelter is purposely maintained low as Co is not desired in the product.

Table 10.12　Converter mass balance from Soroako nickel smelter

	tpd	Ni	Co	Fe	S
Matte	909.2	26.0%	0.80%	63.0%	10.0%
Partition coefficient		236	7.3	573	91
Slag	900	2.0%	0.60%	53.0%	
Partition coefficient		18.0	5.4	477.0	
HG matte	280	78.0%	1.00%	1.0%	20.0%
Partition coefficient		218.4	2.8	2.8	2.8
Recovery		**92.4%**	**38.5%**		

The best industrial plant data for Cu distribution in metallised Ni-Cu matte converting is from Glencore's Falconbridge Ni-Cu smelter[17]. This data is shown in Table 10.13 and is compared with the partition coefficients calculated from the laboratory converting data in the Japanese nodule smelting paper and data from Vale's Thompson Ni smelter[18].

Table 10.13　Comparison of partition coefficients during matte converting

% Fe in matte	Partition coefficients							
	Falconbridge			Thompson		Japanese		
	Ni	Cu	Co	Ni	Co	Ni	Cu	Co
40%	-	-	-	-	-	230	150	75
30%	40	30	3.5	250	-	150	70	15
20%	40	30	3.5	150	7.5	36	18	6
10%	30	25	2.5	75	3.4			
5%	20	20	1.5	40	1.4	13	5	3

The Thompson Ni data is for oxidic Ni only. The Ni, Cu and Co partition coefficients for the Japanese laboratory study were estimated from their metal recovery data presented in Figure 10.5. These were adjusted to account for higher entrained losses in industrial practice to give recoveries to alloy of 99.0% Ni, 98.5% Cu and 97% Co when converting the alloy down to about 40% Fe.

[16] Crundwell, F., et al., "Extractive metallurgy of nickel, cobalt and platinum group metals", Elseveir 2011, p. 103.

[17] Bustos, A., et al., "Converting simulation at Falconbridge Limited", Extractive metallurgy of nickel and copper, TMS, 1988, p. 335-53.

[18] Diaz, C., et al., "A review of nickel pyrometallurgical operations" Extractive metallurgy of nickel and copper, TMS, 1988, p. 211-39.

Figure 10.5   Metal   recovery   versus   iron   content   in   alloy   during   converting
(Japanese study)
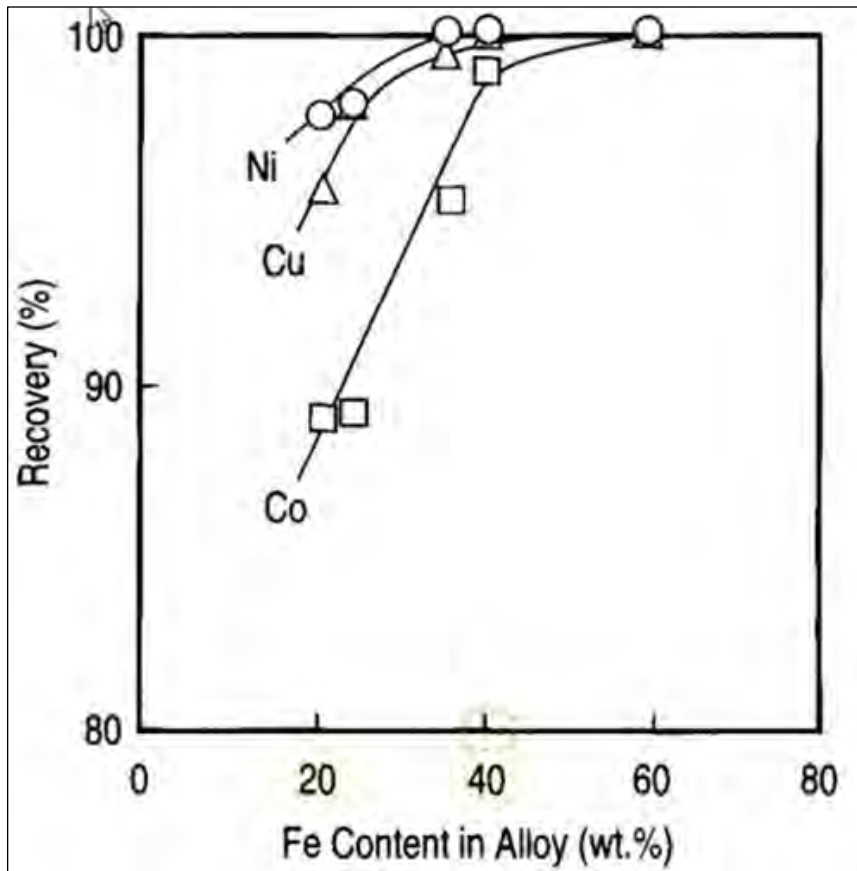
Overall, it is concluded that it would be feasible to produce a HG matte with 1% Fe from
the NORI polymetallic nodules and that data from analogous industrial operations can be
used to prepare preliminary design criteria.

10.2.5   Hydrometallurgical processing of Ni-Cu-Co matte

There are several methods of leaching Ni-Cu-Co mattes to recover the valuable metals.
The simplest process is that proposed by Inco[19] in which the finely ground matte (99%
minus 45 microns) would be leached with sulfuric acid an autoclave operating at about 110
°C to dissolve the Ni, Cu, Co, and Fe. In the laboratory batch leach tests, Inco used the
following conditions:

*   Matte solids density of 9%.
*   150 psi O_2.
*   100 g/L of acid (85-90% stoichiometric acid requirement).

These tests achieved 99% extraction of Ni, Cu, Co and Fe in 2 hours with 99% S conversion
to sulfate. The PLS contained about 20 g/L acid and 5 g/L Fe (50% Fe^{2+}). This was
neutralised with limestone to pH 3.5 and SO_2/air injection used to oxidise all the Fe to
Fe3+ and to precipitate Fe down to about 10 mg/L Fe as a stable ferrihydite / gypsum

[19] R. Sridhar, W. E. Jones, and J. S. Warner, "Extraction of copper, nickel and cobalt from polymetallic nodules",
JOM, April 1976, p 32.

precipitate. After solid-liquid separation and washing, this residue could be ponded. The PLS after Fe removal contained: 40 g/L Ni, 24 g/L Cu and 5 g/L Co.

The Fe in the PLS can also be precipitated in the autoclave as jarosite or hematite under different operating conditions and both alternatives have been operated commercially in Ni refineries. For example, the Rustenberg refinery[20] used to precipitate its Fe as sodium jarosite but it now operates its pressure oxidation process at a slightly higher temperature of about 150ºC to precipitate the Fe from solution as hematite. This process gives a higher 99% Ni, Ci, Co extraction, a small amount of high Fe residue (>50% Fe) as well as lower Fe and acid in the resultant PLS. The leach residue could be recycled to the converters to maximise residual metal recovery.

There are two several proven methods for extracting the Ni, Cu and Co values from the PLS. Firstly, treatment with H_2S could be used to precipitate a pure Cu sulphide and a mixed Ni/Co sulphide. Alternatively, the PLS could be processed using solvent extraction (SX) and electrowinning (EW) to recover Cu as cathode copper before recovering the Ni and Co from solution as a mixed sulphide precipitate.[21]

10.3 NORI Test Work and Piloting

NORI has embarked on an extensive program of test work at various scales in support of process development for the project. To date, small scale pyrometallurgical tests (of the order of up to kilograms of material) have been undertaken and larger scale piloting of the pyrometallurgical process has commenced with calcining approximately 70 t of nodules. Hydrometallurgical test work will follow once sufficient matte has been generated to provide feed.

NORI has retained the services of three main facilities to conduct the pyrometallurgical work:

- Kingston Process Metallurgy (KPM): Small scale calcining and smelting work
- FLSmidth: Preliminary material characterization and calcining; pilot scale calcining (0.9 m diameter x 15 m long)
- Expert Process Systems (XPS): Preliminary converting tests, pilot scale smelting, sulfidation and converting.

The over-arching objectives of the program are:

- To demonstrate at small and pilot scale the viability of the chosen process
- To measure important parameters for engineering design.

To date, results do not appear to be in any significant disagreement with the process definition as originally based on the literature review. One of the more notable findings arising from test work and investigation performed to date is that the higher oxides of manganese thermally decompose, even in the presence of carbonaceous reductant, thus reducing the amount of reductant required. In addition, the test work program has generated information that was not previously available (e.g., certain elemental deportments). Where appropriate, this information has been incorporated into the process design.

---

[20] Hofirek, Z. et al., "Pressure leach capacity expansion using oxygen-enriched air at RBMR Rustenburg Base Metal Refiners", Hydrometallurgy, 39, 1995, 91-116.

[21] Note by author: A third option is to remove copper via EW and separate the nickel and cobalt via SX. Supplementary purification can be done to allow the nickel and cobalt streams to be processed either via EW to create nickel and cobalt cathode, or with crystallization to produce nickel and cobalt sulphates.

10.3.1   Preliminary Work at FLSmidth

Early work at FLSmidth included:

- Measurement of physical properties, e.g.,
  — Free moisture content
  — Specific gravity
  — Bulk density
  — Particle size distribution
- Differential Thermal Analysis (DTA)
- Sintering tests
- Batch kiln reduction calcining (0.3 m diameter x 1 m long)
- Speciation (oxidation states) of manganese, iron, nickel in nodules and calcine
- Tumble tests.

Some of the key findings have been:

- Both the batch kiln and sintering tests indicate that sintering temperatures are well above the target commercial operating temperature of 900 °C.
- A high degree of reduction of iron and nickel (to metal) can be achieved during calcination as well as almost complete decomposition and reduction of manganese oxides to Mn^{2+}.
- Results from the tumble test suggest that calcining the nodules in a commercial rotary kiln should incur less dust generation than a nickel laterite operation.

10.3.2   KPM Work

The test work at KPM has been supplemented by thermodynamic modelling, which is providing very useful insights into the process as well as calculation of important parameters.

The primary work at KPM involved calcining and smelting at two relatively small scales:

- 100 g, using a small batch kiln for calcining and a small induction furnace for smelting.
- 1–1.5 kg using a larger induction furnace for both calcining and smelting.

Additional work was completed to further understand the speciation, thermal decomposition and reduction behaviour of manganese oxides in the nodules.

Alloy liquidus temperature was measured using DTA and the slag liquidus was mapped out by thermodynamic modelling.

Some of the key findings have been:

- The calcining and smelting work at KPM has demonstrated that, in addition to making an alloy of the expected composition for further processing, it is possible to make a slag phase that is low in Cu, Ni and Co and, importantly for saleability as a product, low in phosphorus.
- Tests were carried out under various conditions—in particular the amount of reductant was varied and this revealed that:
  — Less reductant was required than had been predicted by the process model. This led to the investigation into manganese oxide behaviour.
  — The metallurgical outcome is quite sensitive to the amount of reductant added and design of the commercial plant must recognize this.

- One of the best-outcome tests was reviewed for metal deportments, which were found to be in reasonable agreement with the process model values. Some key additional information was added to the model.
- The slag and metal liquidus' were such that the process model design temperatures could be confirmed.
- The understanding gained from the manganese investigation has been incorporated into the process model, resulting in a prediction of lower reductant requirements.

10.3.3 Small Scale Work at XPS

The preliminary work at XPS focused on the converting part of the proposed process. A significant part of the objectives for this early work is to establish experimental techniques that can be carried into the pilot scale work for this challenging part of the process flowsheet.

Two types of testing have been carried out so far:

- Converting an artificial matte.
- Removing manganese and adding sulphur to make matte, using an artificial alloy (corresponding to the electric furnace product in the proposed process).

A 30 kW induction furnace was used for the work, melting charges in the 2–10 kg range.

10.3.3.1 Converting of Artificial Matte

An artificial matte was made by melting various components such as pig iron, local nickel matte, manganese powder, etc. Only the main elemental components of metallurgical significance were included in the recipe. The target matte composition was calculated to subsequently pass along the expected converting path for the matte targeted in the commercial operation. The matte was successfully made in an induction furnace and it was then blown down (converted) to a matte containing only 5% iron using a silicon carbide lance immersed in the melt. Silica flux was added to form a fayalite slag of an appropriate iron/silica ratio.

In addition to establishing experimental methodologies, the work provided valuable information on the deportment of elements of interest between matte and slag. While there is deportment information on elements such as Ni, Cu and Co from the non-ferrous industry, others, such as Mn and phosphorus, are not as well understood. The work generated preliminary partition coefficients for elements of interest as a function of iron in matte that were included in the process model. This improves understanding of the implications of different set points for intermediate and final matte iron levels on pay-metal recovery and residual unwanted elements.

10.3.3.2 Manganese Removal and Sulphidation

The proposed pilot-scale work at XPS is to receive calcined nodules from FLS and first smelt them to an alloy, then to sulphidize to a matte and convert to a final matte for hydrometallurgical processing. In the proposed commercial operation, sulphur will be introduced to the molten material in liquid form, per the practice at SLN's Doniambo operation prior to 2016. This was considered to be impractical with the proposed equipment set-up available at XPS. Instead, sulphur can be added in the form of sulphur-bearing compounds. Both pyrrhotite and pyrite were tested, with additions being to the surface and by submerged injection via a lance.

Addition of pyrrhotite via lance injection was the most successful in terms of sulphur efficiency. The additional iron units will simply lengthen the converting time somewhat.

The alloy from the smelting process is expected to contain a few per cent manganese. Manganese is known to form a separate phase (in addition to matte and slag) in the presence of significant amounts of sulphur. This phase is described as 'mushy' at converting temperatures and may pose some complications for the pilot work. It may be desirable to remove the manganese from the alloy before adding sulphur. (It is unlikely that this will be an issue for the proposed commercial operation, with alloy addition being made to intermediate matte.)

Tests were conducted to blow out the manganese using a lance and silica flux prior to adding sulphur. The work demonstrated that manganese levels can be lowered in metal and captured in slag, however, if the slag remains in the vessel when sulphur is then added, the 'mushy' phase will still manifest.

11 Mineral Resource estimates

Mineral Resources were first estimated for NORI Areas A, B, C and D by Golder Associates in late 2012 (Golder, 2013), primarily using data collected by the Pioneer Investors. Data collected by NORI in 2018 was used by AMC Consultants Pty Ltd to update the Mineral Resource estimate for NORI Area D in 2018, and data collected in 2019 was used to update the Mineral Resource estimate in 2020. The estimates of the combined Mineral Resources in NORI Areas A, B, C, and D are summarized in Table 11.1. This IA only considers development of NORI Area D. The cut-off of 4 kg/m^2 abundance is derived from the estimates of costs and revenues presented in this Initial Assessment.

Table 11.1   NORI 2020 Mineral Resource estimate, in situ, for the NORI Areas within the CCZ at 4 kg/m^2 nodule cut-off.

NORI Area	Category	Tonnes (Mt (wet))	Abundance (wet kg/m^2)	Nickel (%)	Copper (%)	Cobalt (%)	Mn (%)	Silicon (%)
D	Measured	4	18.6	1.42	1.16	0.13	32.2	5.1
D	Indicated	341	17.1	1.4	1.14	0.14	31.2	5.5
D	Measured + Indicated	345	17.1	1.40	1.14	0.14	31.2	5.5
D	Inferred	11	15.6	1.38	1.14	0.12	31.0	5.5
A	Inferred	72	9.4	1.35	1.06	0.22	28.0	-
B	Inferred	36	11	1.43	1.13	0.25	28.9	-
C	Inferred	402	11	1.26	1.03	0.21	28.3	-

The estimates for NORI Areas A, B and C are the NORI 2012 estimates (Golder 2015). Note: Tonnes are quoted on a wet basis and grades are quoted on a dry basis, which is common practice for bulk commodities. Moisture content was estimated to be 24% w/w. These estimates are presented on an undiluted basis without adjustment for resource recovery.

Abbreviations used for statistical terms in this section are: Min = minimum, Max = maximum, Var = variance, CV = coefficient of variation.

11.1 Polymetallic nodule sample data

All polymetallic nodule sample data (historic box-core and free-fall grab samples, and the NORI 2018 box-core) and the abundance estimates derived from photographs were combined into a single data set. The data set contains assays for nickel (%), copper (%), manganese (%), cobalt (%), silicon (%), iron (%) and phosphorus (%), and measurements of nodule abundance (kg/m^2).

11.1.1   Historic sample data

Historic data provided by the ISA and BGR to NORI included 392 samples (Table 11.2). The data includes measurement of nodule abundance (kg/m^2) and the assays manganese (%), cobalt (%), nickel (%) and copper (%). The data were checked for anomalous or erroneous data and cross-checked with data supplied directly by the ISA.

Table 11.2   Summary statistics of historic polymetallic nodule data within NORI Areas A, B, C and D used for the 2012 Mineral Resource estimate

Variable	Samples	Missing	Min	Max	Mean	Var	CV	Median
Ni (%)	360	32	0.68	1.75	1.30	0.016	0.10	1.31
Co (%)	360	32	0.05	0.33	0.17	0.004	0.35	0.19

Variable	Samples	Missing	Min	Max	Mean	Var	CV	Median
Cu (%)	360	32	0.40	1.50	1.10	0.028	0.15	1.13
Mn (%)	360	32	12.84	33.90	29.45	8.406	0.10	30.20
Abundance (wet kg/m^2)	392	0	0	52.2	11.9	64.303	0.67	12.00

Source: Golder 2015. Var = variance; CV = coefficient of variation

11.1.2   TOML sample data

TOML Area F is adjacent to the western border of NORI Area D. In 2020, NORI acquired the data from this area, including 26 nodule samples (1 historic sample and 25 samples collected by Nautilus Minerals Inc.). The TOML data includes measurements for abundance (kg/m^2) and assays for manganese (%), nickel (%), copper (%) and cobalt (%). All assays were converted from oxides to elemental values. AMC included this data for estimating the NORI Area D mineral resource because it provides more control of abundance and grade estimates along the western margin of NORI Area D. Summary statistics are presented in Table 11.3.

Table 11.3   Summary statistics of TOML Area F polymetallic nodule assays

Variable	Samples	Missing	Min	Max	Mean	Median	Var	CV
Ni (%)	26	0	1.05	1.51	1.41	1.42	0.008	0.06
Co (%)	26	0	0.09	0.17	0.13	0.13	0.000	0.14
Cu (%)	26	0	1.10	1.35	1.24	1.23	0.005	0.06
Mn (%)	26	0	30.1	33.6	32.2	32.4	0.813	0.03
Abundance (wet kg/m^2)	26	0	1.2	29.1	17.9	18.1	45.359	0.38

11.1.3   NORI 2018 sample data

NORI Campaign 3, in 2018, focused on collecting close spaced (7 km by 7 km spacing) box core samples, supplemented by seafloor photography in an area selected for trial mining.

Forty-five sites were sampled with a box core. The assay data set includes 45 primary box core samples Table 11.4 and a further 87 duplicates, standards, blanks and other samples. The data includes a suite of multivariate assays which including manganese, copper, nickel, cobalt, silicon, iron and phosphorus. The primary sample assays were used for resource estimation. The duplicate sample data were included in the variography because they provide information about the nugget variance.

During the NORI 2018 campaign, seafloor photographs were captured along with the box-core sampling. The photographs were used to estimate nodule abundance from the relationships between nodule long-axis length, the percentage of the photo covered by identified nodules, and nodule weight. Fourteen (14) seafloor photographs within the Measured Mineral Resource boundary were used to estimate nodule abundance.

Table 11.4   Summary statistics of the 2018 NORI Area D primary assay data.

	Number	Missing	Min	Max	Range	Mean	Median	Var	CV
Abundance (wet kg/m²)	45	1	6.50	29.90	23.40	18.00	18.10	23.694	0.2700
Nickel (%)	45	0	1.18	1.45	0.27	1.37	1.39	0.004	0.0455
Copper (%)	45	0	0.97	1.34	0.38	1.15	1.14	0.005	0.0614
Cobalt (%)	45	0	0.09	0.15	0.05	0.13	0.13	0.000	0.1010
Manganese (%)	45	0	26.44	34.33	7.88	31.28	31.69	2.557	0.0511
Silicon (%)	45	0	4.81	8.06	3.25	5.53	5.34	0.420	0.1170
Iron (%)	45	0	4.27	8.21	3.94	6.66	6.86	0.696	0.1250
Phosphorus (%)	45	0	0.12	0.25	0.13	0.16	0.15	0.001	0.1460

11.1.4   NORI 2019 sample data

NORI Campaigns 6A and 6B, in 2019, focused on upgrading the NORI Area D Inferred Mineral Resource to Indicated Mineral Resource by collecting close spaced (10 km by 10 km spacing) box core samples.

Box core sampling was attempted at a total of 106 sites in the NORI Area D license area during Campaign 6A and 101 sites during Campaign 6B. Disturbed samples, considered to be unreliable, were omitted from the sample sequence. Summary statistics for the remaining 207 primary box core samples are presented in Table 11.5.

The data includes a suite of multivariate assays which include manganese, copper, nickel, cobalt, silicon, iron, and phosphorus.

Table 11.5   Summary statistics of the 2019 NORI Area D primary assay data.

	Number	Missing	Min	Max	Range	Mean	Median	Var	CV
Abundance (wet kg/m²)	207	0	0.08	32.99	32.92	17.55	17.13	28.98	0.3070
Nickel (%)	207	4	0.91	1.49	0.57	1.38	1.40	0.006	0.0558
Copper (%)	207	4	0.77	1.41	0.65	1.15	1.14	0.007	0.0721
Cobalt (%)	207	4	0.09	0.45	0.36	0.14	0.13	0.001	0.2130
Manganese (%)	207	4	24.23	34.46	10.24	30.95	31.19	2.543	0.0515
Silicon (%)	207	4	4.74	8.97	4.23	5.61	5.39	0.472	0.1220
Iron (%)	207	4	3.81	11.16	7.35	6.73	6.81	0.704	0.1250
Phosphorus (%)	207	4	0.11	0.51	0.40	0.16	0.15	0.002	0.2640

11.1.5   Representativeness of sampling

Comparison of the seafloor photographs at the box core sites and the observed distribution of nodules in the box cores indicated that the box core samples were largely undisturbed and representative of the sampled locations.

Sampling in 2018 and 2019 confirmed the earlier assessment of continuity of grade and nodule abundance. Continuity of grades and abundance between sample points can be reasonably assumed for the following reasons:

- Statistics of the nodule samples within the reserve blocks of the CCZ show a very low coefficient of variation, which indicates a low risk in estimating and interpolating grades.
- Variography of the samples within the NORI Area shows reasonable spatial continuity with ranges greater than the average sample spacing for nickel, copper, cobalt, and manganese. Abundance has a more erratic variogram with shorter ranges.
- The continental scale of the deposit and mode of formation leads to the expectation of low variability.

The sample density and spacing within the NORI Area are sufficient to demonstrate continuity of nickel, copper, cobalt, and manganese. The reprocessed backscatter data and the low-level seafloor photography from the 2018 campaign indicate strong continuity of nodule abundance across NORI Area D.

11.1.6   Data integration

The historic, TOML and NORI nodule sample data were combined into a single data set. The combined data set (Areas A, B, C and D) contains 1299 records. This data includes both the primary assays and duplicated primary assays.

Summary statistics for all manganese nodule data within NORI Areas, including the nodule abundance estimated from photographs for NORI Area D and the duplicate samples, are listed in Table 11.6. Note the very low coefficient of variation for nickel, copper, manganese and cobalt.

Table 11.6   Summary of all manganese nodule data within NORI Area D

	Number	Missing	Min	Max	Mean	Median	Var	CV
Abundance (wet kg/m^2)	763	1	0.00	52.20	14.77	15.50	54.898	0.5020
Nickel (%)	763	50	0.68	1.75	1.34	1.37	0.012	0.0833
Copper (%)	763	50	0.40	1.50	1.12	1.14	0.018	0.1180
Cobalt (%)	763	50	0.05	0.45	0.16	0.14	0.003	0.3220
Manganese (%)	763	50	12.84	34.80	30.27	30.84	6.217	0.0824
Silicon (%)	763	410	4.70	9.00	5.60	5.40	0.463	0.1210
Iron (%)	763	410	3.80	11.20	6.70	6.80	0.720	0.1260
Phosphorus (%)	763	410	0.10	0.50	0.20	0.20	0.001	0.2300

Cumulative probability plots of the polymetallic nodule sample data within the NORI Areas are provided in Figure 11.1. The plots show that the distributions for nodule abundance and the assays manganese, cobalt, nickel and copper are different across the NORI Areas. The biggest differences are exhibited in the cobalt distributions with Area D being significantly lower than Areas A, B and C. The plots also show that there are only a couple of potential outliers (extreme values) including a high nickel assay (>1.6% Ni) from Area A and low manganese values (<15% Mn) from Area C. NORI Areas A, B and C show very similar distributions for abundance, manganese, cobalt, nickel and copper.

Figure 11.1   Cumulative probability plots of abundance and assays for the integrated sample data
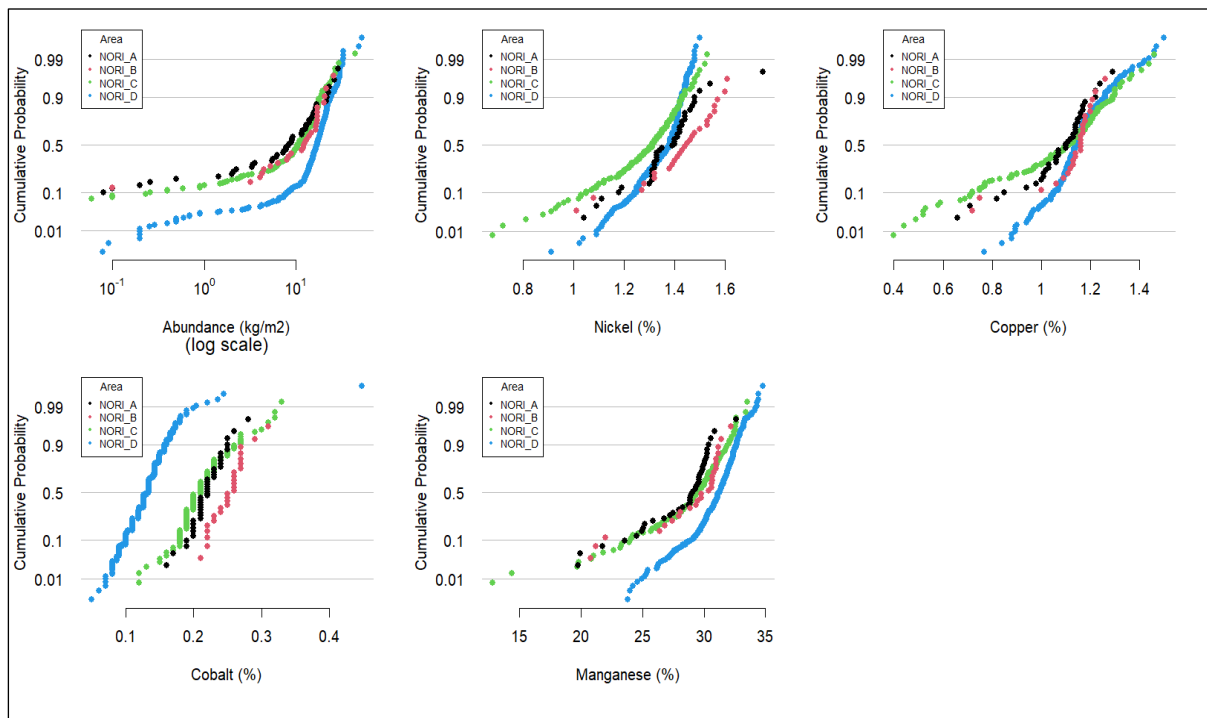
11.2 NORI Area D

11.2.1   Geological domains

Geological interpretation and definition of geological and geomorphological domains were completed by Ian Stevenson of Margin - Marine Geoscience Innovation, using the bathymetry and backscatter data sets.

Domains include abyssal plains, abyssal hills, high seafloor slope, volcanic outcrops and discrete volcanic cones. The abyssal hills and slope domains have been separated on the basis of whether the box core sampling indicates a hard substrate or not.

Analysis of land-out video footage, AUV camera data and AUV sub-bottom profiler showed a good correlation between slopes steeper than 6° and the presence of hard ground where there were a high number of failed box core recoveries (21 sites). Areas where the slope gradient exceeds 6° were assumed to be too steep for nodule collection and were excluded from the Mineral Resource estimate, as shown in Figure 11.2. The steep slope domain covers only 6% of NORI Area D.

Volcanic outcrop occurs frequently along and parallel to the ridges and frequently occur along the margins between the abyssal hill and abyssal plain domains. Volcanic cones are found mostly along the southern margin of NORI Area D, in a line running roughly east-west. The volcanic domains are interpreted to be rugged and to carry few nodules. They have been excluded from the Mineral Resource.

NORI Area D is dominated by the abyssal plains domain which covers 68.6% of the area. The areas that are considered unlikely for harvesting (high slope and volcanic domains) cover 16.9% of NORI Area D. The proportions of the various domains are shown graphically in Figure 11.3.

Figure 11.2 Map of NORI Area D geological domains.
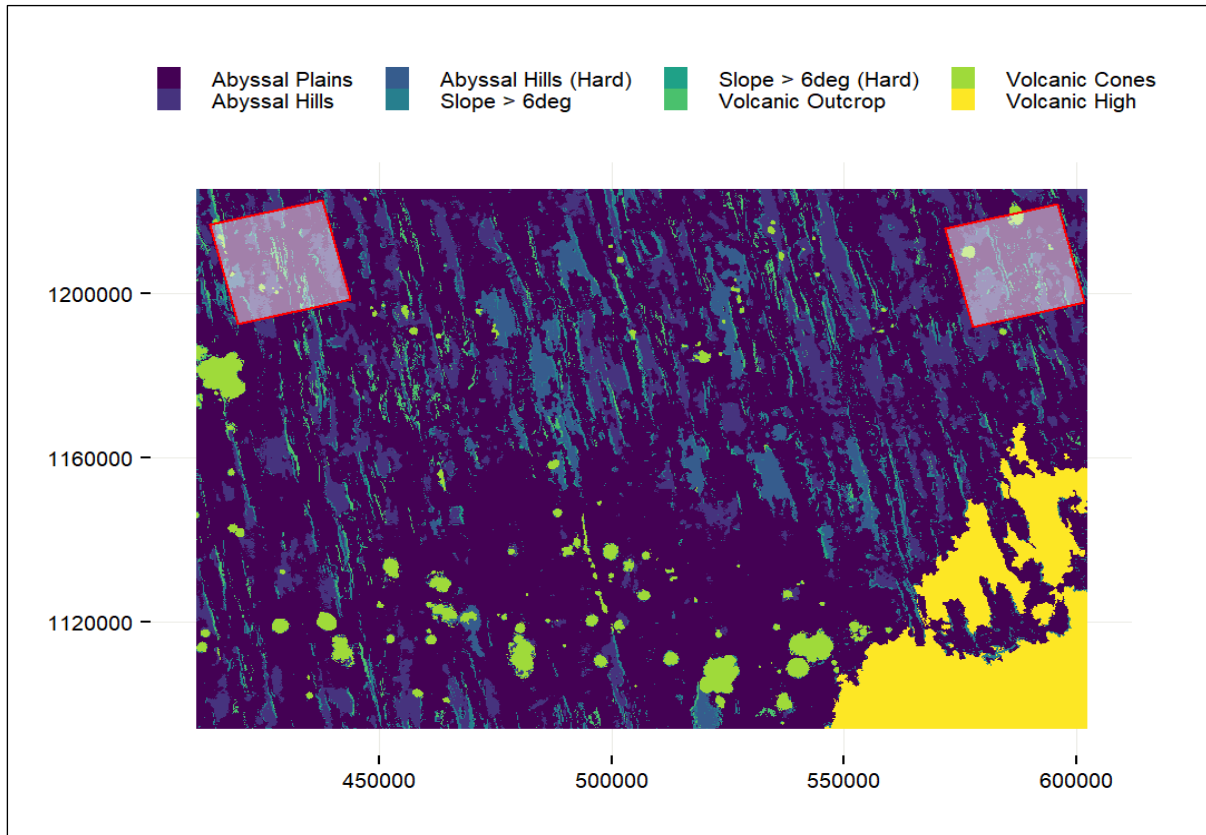
Figure 11.3 Proportions of geological domains in NORI Area D
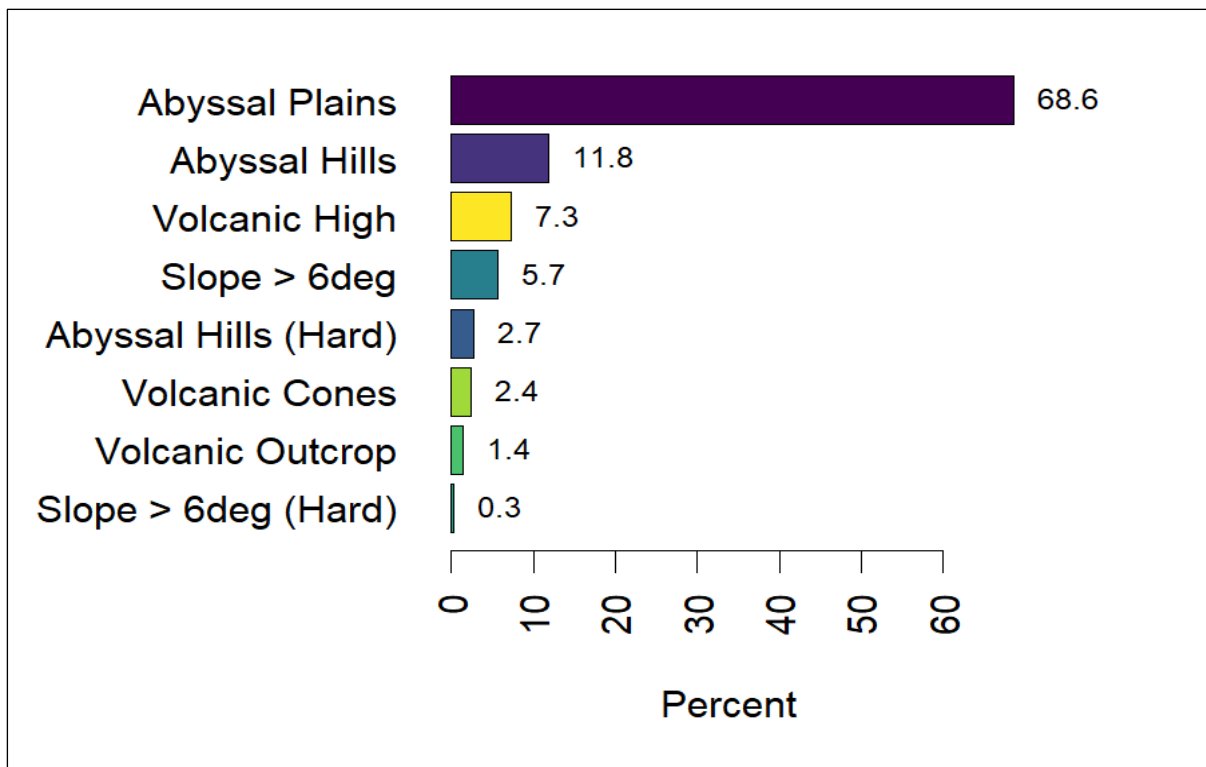
11.2.2   Nodule type and sediment drift

Nodule type (Type 1 and Type 2/3) areas and areas covered by sediment drift were interpreted from the backscatter data and the box core land out videos and box core logging. The distribution of nodule types is shown in Figure 11.4. The areas marked as "NA" are volcanic areas where the presence of nodules is not confirmed.

Figure 11.4   NORI Area D nodule type domains.
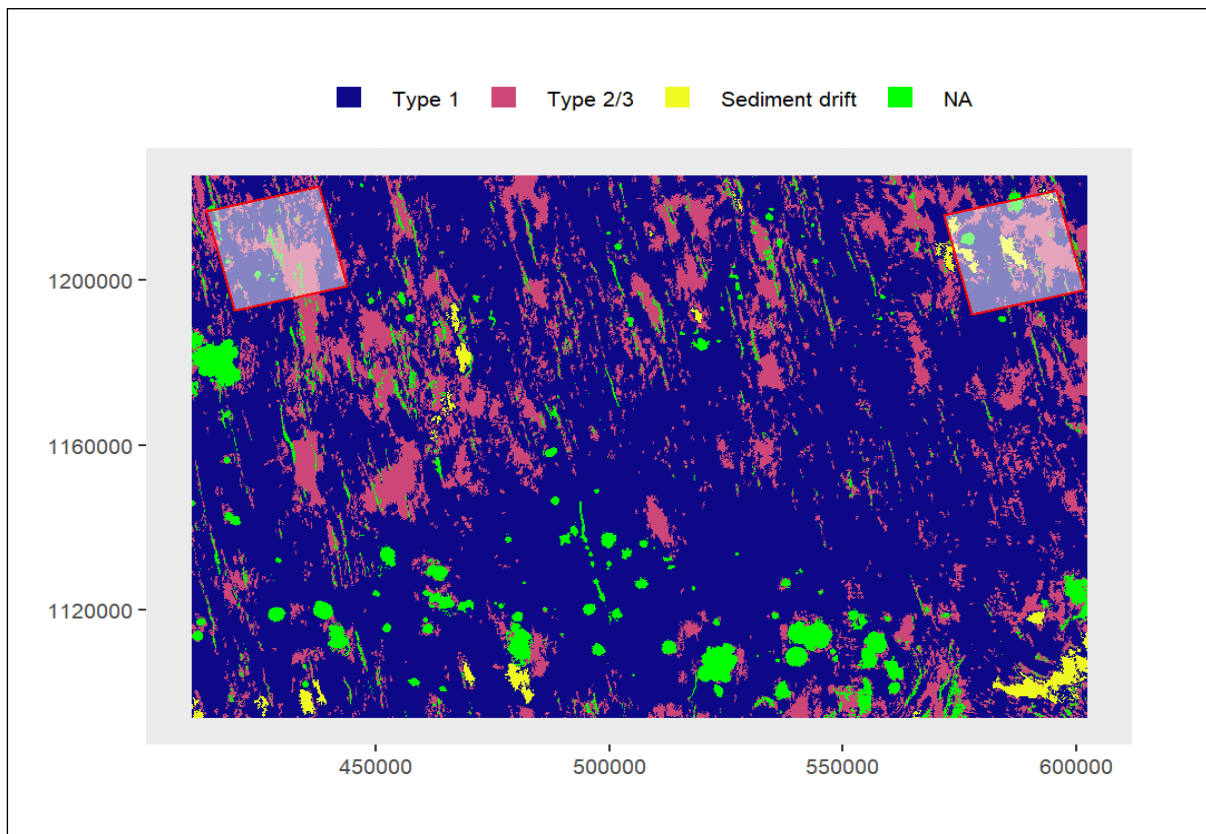
The larger Type 2 and 3 nodules only cover approximately 17% of NORI Area D. The smaller Type 1 nodules are the most common nodule type across NORI Area D, covering approximately 78% of the area. The sediment drift domain, a soft sediment ooze with low backscatter, is rare within NORI Area D. A large proportion of the sediment drift occurs in the volcanic high areas. The impact of the sediment drift domain on the mineral resource estimate is considered to be negligible. The areas marked as "NA" are volcanic areas where the presence of nodules is not confirmed.

11.2.3   Backscatter

The backscatter data was collected during 2012 and reprocessed in 2018. The data was collected on 20 m by 20 m resolution over the area from 405215.4 mE to 606235.4 mE and from 1087387 mN to 1240007 mN. The backscatter data was converted to the same resolution and extent as the interpreted geological domains to allow direct comparison between datasets.

11.2.4   Bathymetry

The bathymetry data was collected during 2012 and reprocessed in 2018. The data was collected on 50 m by 50 m resolution over the area from 405694.2 mE to 606294.2 mE and from 1086099 mN to 1240249 mN. The bathymetry data was converted to the same

extent as the interpreted geological domains to allow direct comparison between datasets. Additional layers representing slope angle Figure 11.5 and aspect, in degrees, were calculated from the bathymetry and then added as separate raster layers to the bathymetry raster.

Figure 11.5   NORI Area D slope angle
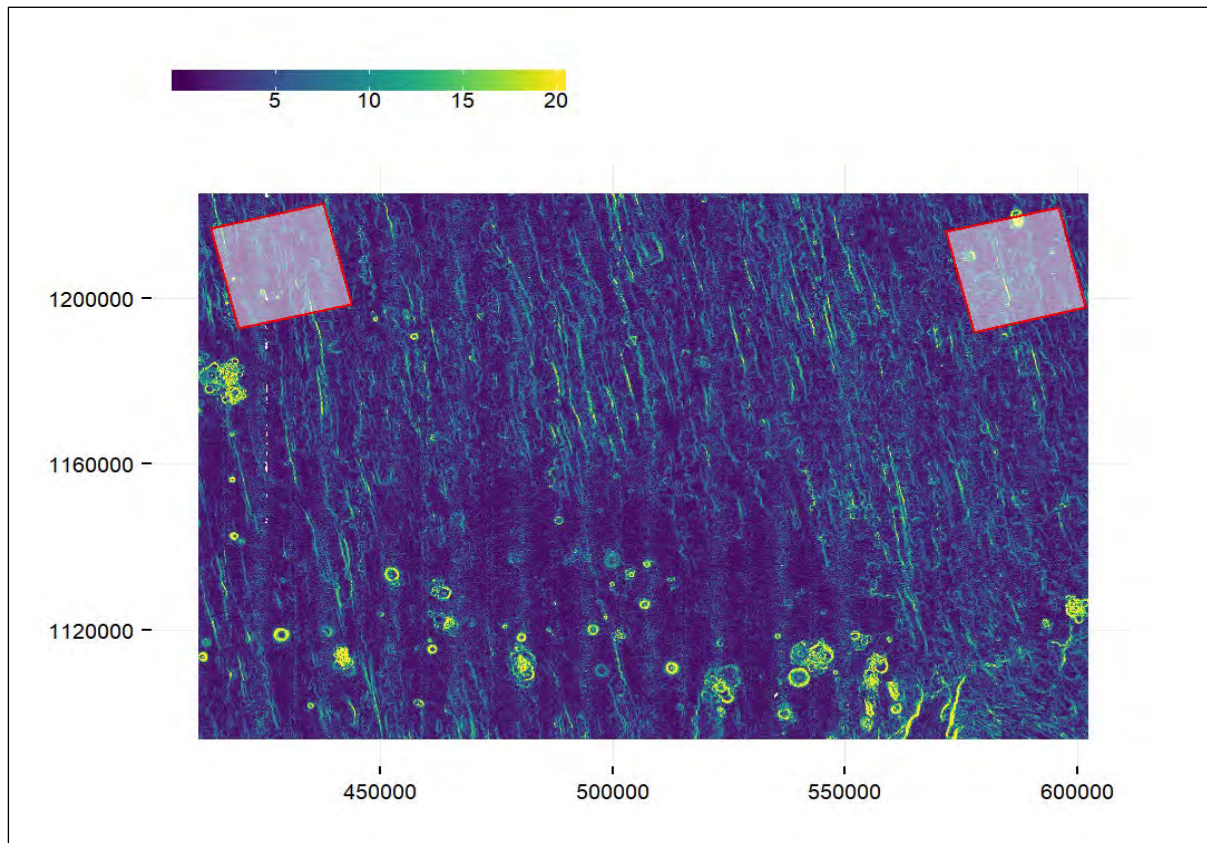
11.2.5   PRZ areas

NORI is considering the location of areas that may, in future, be designated as Preservation Reference Zones (PRZ) for the preservation of biological diversity. Two possible locations for PRZs are shown on the Figures in this report e.g., Figure 11.5. Their locations are not yet finalized, and they may be repositioned. For this reason. the PRZ areas are included in the resource estimate. It is anticipated that the areas finally selected as PRZs will be excised from the Mineral Reserves when they are estimated.

11.2.6   Data processing

For estimation of resources in the NORI Area D, the integrated NORI data was filtered to only include NORI Area D and TOML Area F samples. The combined data set contains 556 records of which 26 records are from TOML Area F Figure 11.6. Further preparation of the nodule sample data included:

- Calculate average values for duplicate pairs of box core samples.
- Combine clustered historic samples.
- Check for outliers.
- Assign domains.
- Apply top cuts.

The grades that comprise the polymetallic nodules have a unit sum constraint. That is, the sum of the elements (including oxygen and hydrogen) is 100%. Consequently, the elements of interest in the Mineral Resource are not entirely independent. Conventional estimation methods are based on the assumption of independence. For the 2020 estimate of Mineral Resources, AMC decided to use a mathematical transformation to generate a set of independent variables that could be estimated into a block model and then back-transformed to grade estimates. To prepare the data it was necessary to:

- Impute (replace) missing values for silicon, iron and phosphorus.
- Apply projection pursuit multivariate transform (PPMT) to manganese, copper, nickel, cobalt, silicon, iron and phosphorus values.
- Apply normal scores transform to abundance values.

These preparation steps are discussed below. The backscatter, slope, aspect (slope dip direction) and geological domain features were extracted from the GIS raster data at the nodule sample locations. This data was combined with the nodule sample data for analysis.

Figure 11.6   Plan showing location of data points and the NORI Area D boundary.
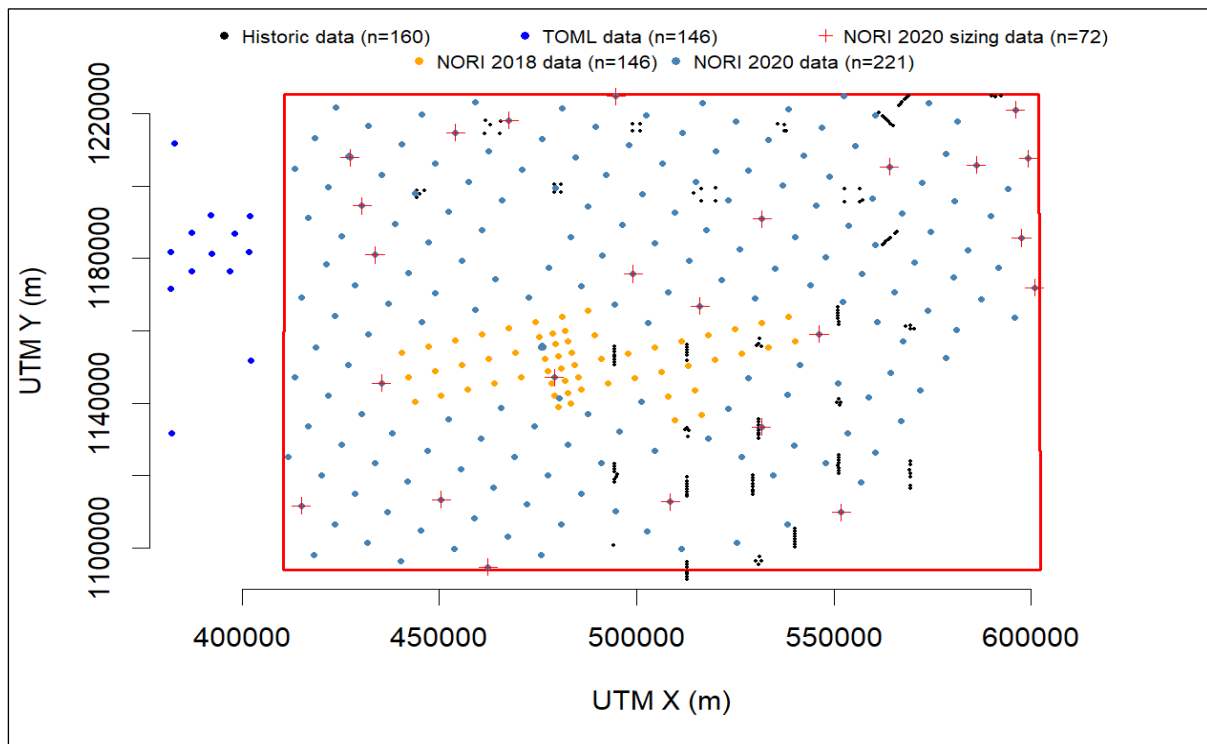
11.2.7   Declustering

The historic data exhibits two forms of spatial clustering Figure 11.6. Along the northern boundary of NORI Area D there are locations with multiple historic samples (up to 5 samples) collected within a tight square 'X' configuration (separation distances of ~1800 m to ~3600 m). While in the south of NORI Area D, the historic sample locations are arranged in strings of multiple samples in linear configurations. These are likely to be free-fall grab samples. Both forms of clustered data may introduce bias during grade estimation with methods that use spatially weighted averages, such as kriging.

A cell declustering algorithm was used to decluster the sample data. The spatially weighted (declustered) means and unweighted means for nodule abundance, nickel, copper and

cobalt are compared in Table 11.7. The original and declustered means are very similar due to the low variance and high spatial continuity of the abundance and assay data.

Table 11.7   Spatially weighted mean assays for NORI Area D samples

	Mean	Weighted Mean
Abundance (kg/m^2)	17.42	16.7
Nickel (%)	1.37	1.37
Copper (%)	1.15	1.15
Cobalt (%)	0.136	0.135
Manganese (%)	31.07	31.01
Silicon (%)	5.62	5.62
Iron (%)	6.73	6.67
Phosphorus (%)	0.16	0.16
MnO:SiO$_2$ (%)	3.4	3.36

11.2.8   Outliers within the sample data

Outliers (extreme values) detected using the Local Outlier Factor algorithm are highlighted (black crosses) in the pairs plot shown in Figure 11.7 and listed in Table 11.7. All identified outliers are historic nodule samples. The location of these outliers relative to all samples within NORI Area D is shown in Figure 11.8. The identified outliers appear to be low in manganese and/or high in abundance.

The plot also reveals that nickel is moderately positively correlated with abundance and cobalt, while manganese is moderately positively correlated with copper and moderately negatively correlated with cobalt. Abundance also shows a weak correlation with copper and cobalt. Copper shows a weak correlation with nickel. Silicon shows a strong negative correlation with manganese.

The sample with anomalously high assay of 0.58% Co is the +50 mm fraction of NORI box core 227. The assay was confirmed by reanalysis of the sample pulp. The mass weighted cobalt assay for sample BC 227 is 0.29%.

Figure 11.7 Pairs plot showing correlations between NORI Area D sample values
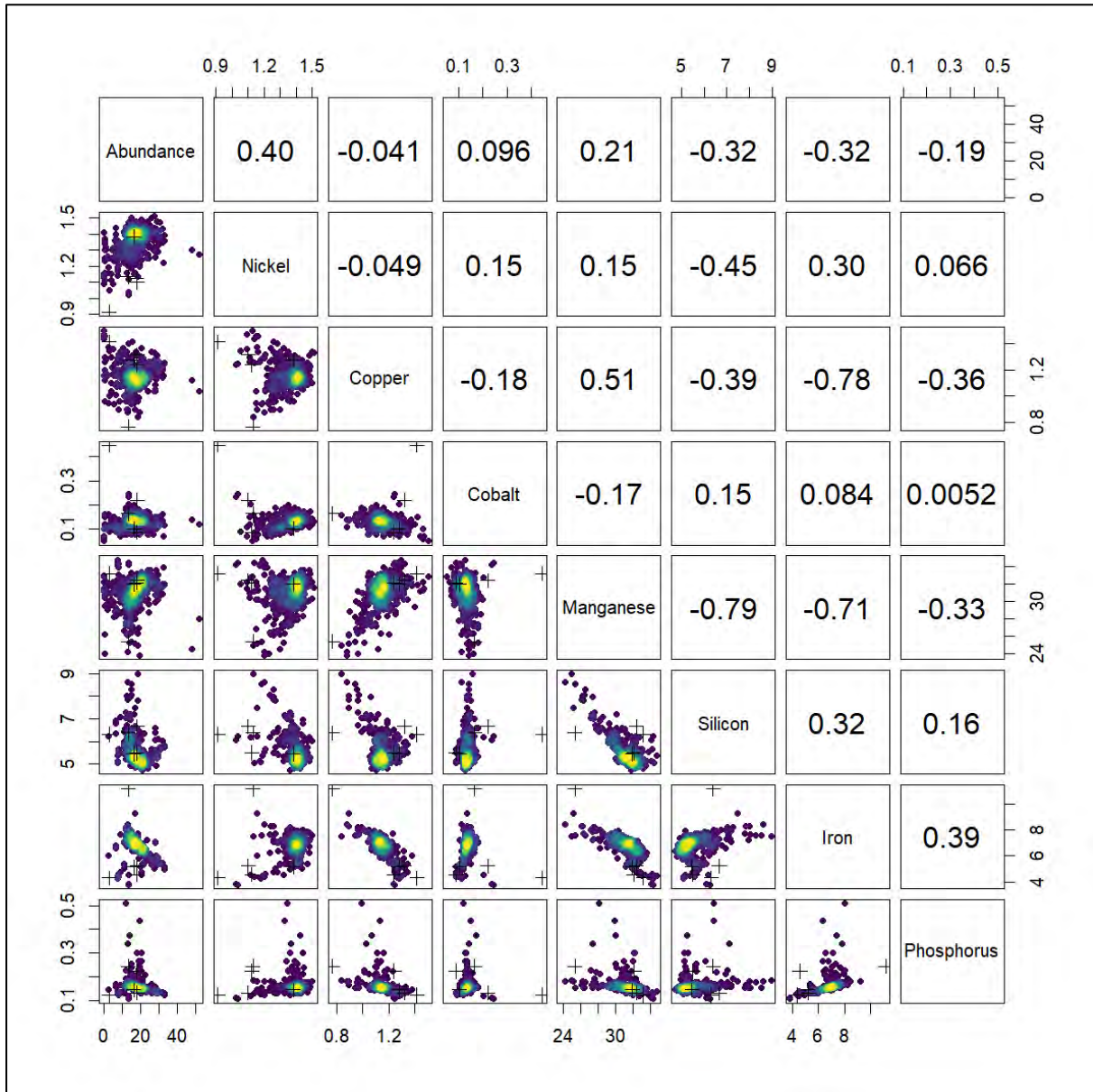
Note: Axes labelled in percentage. Potential outliers are shown as a red cross. The upper panels show the Pearson correlation coefficient. Averaged co-located data point values.

Table 11.8 Detected polymetallic nodule sample outliers

UTM X (m)	UTM Y (m)	Abundance (kg/m²)	Nickel (%)	Copper (%)	Cobalt (%)	Manganese (%)	Silicon (%)	Iron (%)	Phosphorus (%)
586058.9	1205748	3.1	0.9	1.4	0.4	33.2	6.3	4.3	0.1
459028.4	1165737	16.5	1.4	1.3	0.1	32.0	5.5	5.2	0.1
418331.1	1098177	18.1	1.1	1.2	0.1	32.2	5.5	4.6	0.2
452376.0	1135656	13.6	1.1	0.8	0.2	25.4	6.4	11.2	0.2
509744.2	1192623	18.4	1.1	1.3	0.2	32.4	6.7	5.2	0.1

Figure 11.8   Location of identified outliers
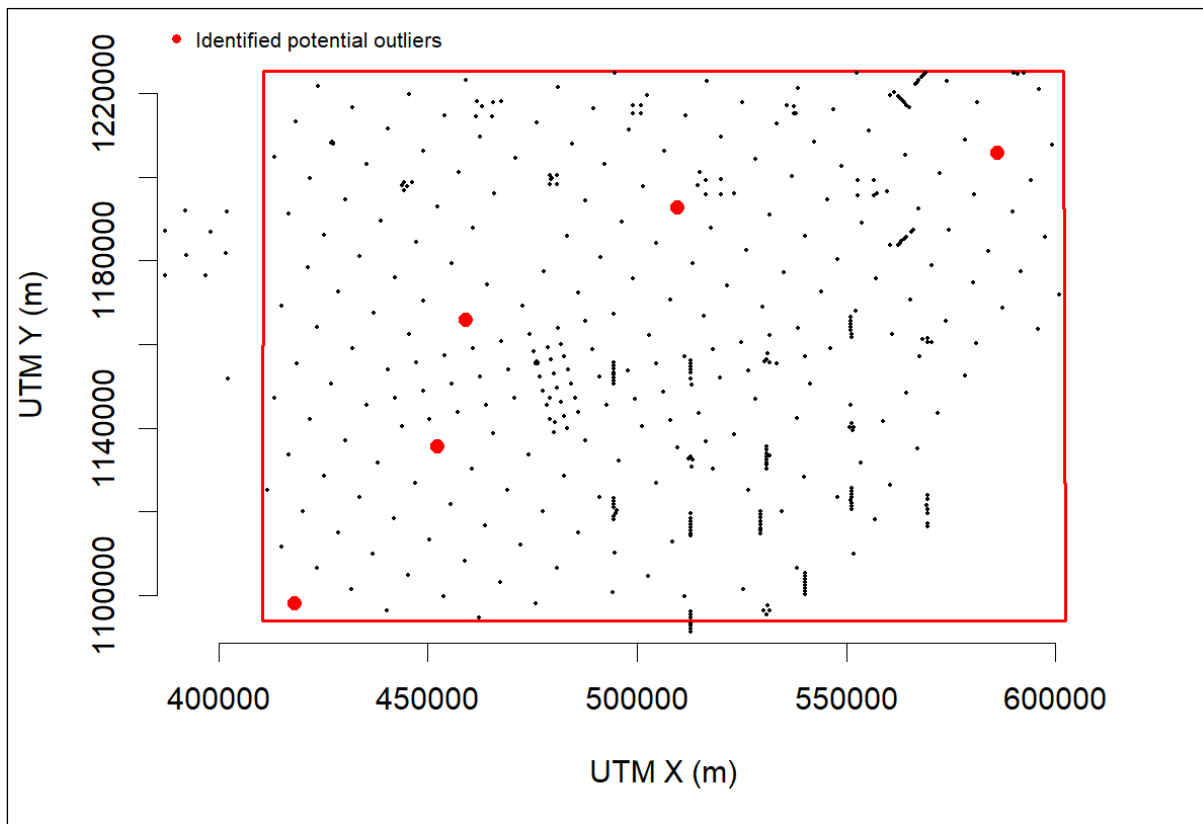
11.2.9   Top-cuts

To reduce the influence of outliers on the estimation of local grades the most common approach is to trim those outliers to some arbitrary value (typically the 97.5, 98 or 99 percentile or mean plus twice standard deviation). Table 11.9 shows the top-cuts that could be considered using these methods. Other methods include selecting the top-cut value by inspecting log-probability plots and looking for where the distribution breaks down in the high values or looking at the inflection point in a mean-variance plot.

Table 11.9   Potential top-cut values for abundance, nickel, copper, manganese and cobalt values

	97.5%	98.0%	99.0%	Mean+2*sd	Median+1.5*IQR
Abundance (wet kg/m^2)	29.80	29.90	30.54	28.44	26.32
Nickel (%)	1.48	1.48	1.49	1.53	1.46
Copper (%)	1.32	1.33	1.34	1.31	1.26
Cobalt (%)	0.17	0.17	0.21	0.19	0.16
Manganese (%)	33.59	33.73	34.31	34.38	34.20
Silicon (%)	7.54	7.85	8.16	6.98	6.53
Iron (%)	7.99	8.03	8.27	8.41	8.05
Phosphorus (%)	0.25	0.26	0.32	0.24	0.18

The top-cuts applied to the nodule sample data are listed in Table 11.10 and are shown as red lines in the plots provided in Figure 11.9. The mean-variance curves by top-cut value

Figure 11.9 show that the top-cut values were selected where the tails of the distributions become unstable.

Table 11.10   Top-cut values applied to abundance, nickel, copper, manganese and cobalt values

Variable	Top-cut
Abundance	33
Nickel (Ni)	1.48
Copper (Cu)	1.45
Cobalt (Co)	0.197
Manganese (Mn)	34.2
Silicon (Si)	8.2
Iron (Fe)	8.4
Phosphorus (P)	0.31

Figure 11.9   Histogram, cumulative probability and mean-variance plots of abundance and grades for NORI Area D nodule samples
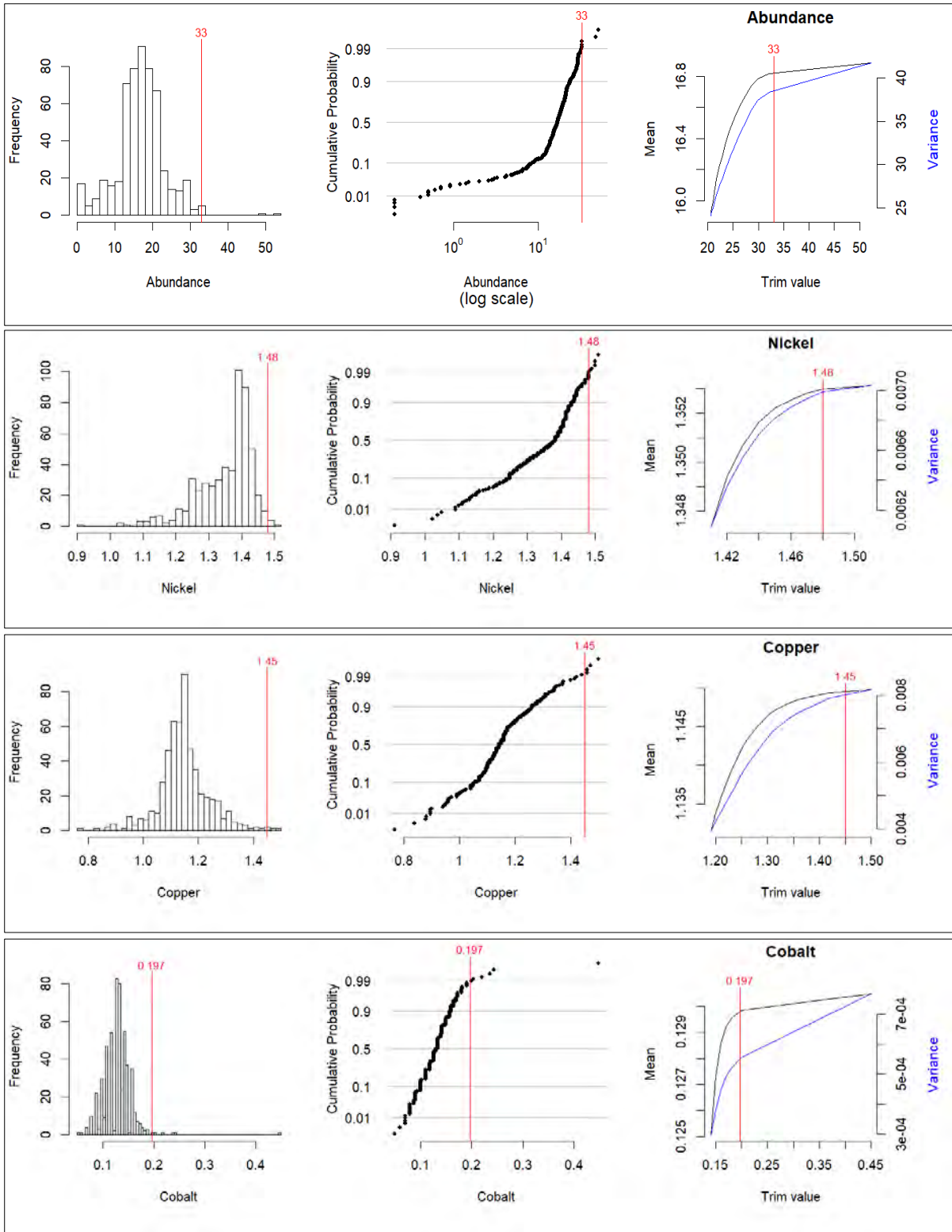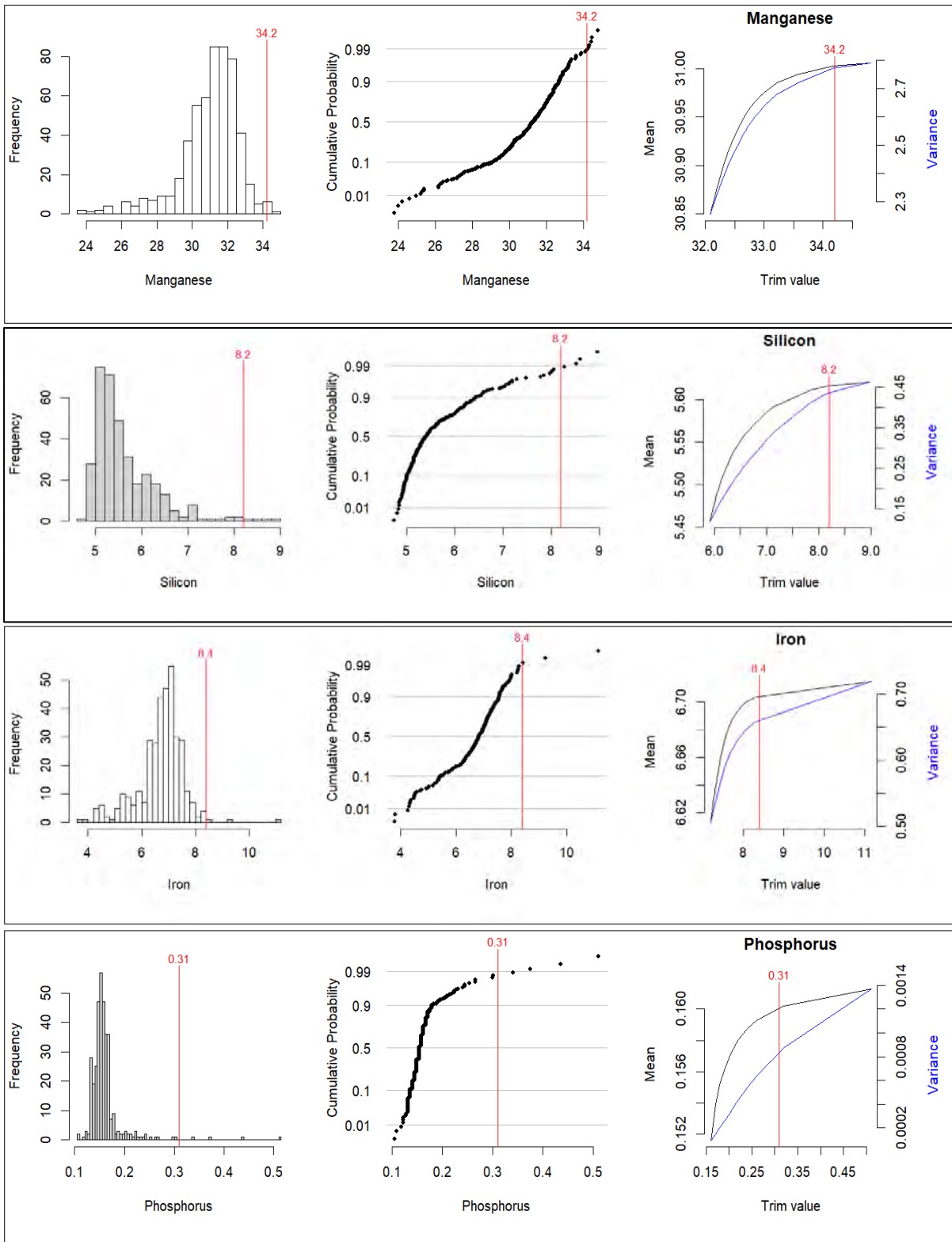
11.2.10   Missing value imputation

Silicon, iron and phosphorus assays are only present in the NORI and TOML data. The historic data only contains assays for manganese, nickel, copper and cobalt. To be able to apply a multivariate transform to the data, it is necessary that there are no missing values.

Where there are missing values either the sample must be removed from the transform or the missing values must be imputed.

Linear regression models were developed to predict silicon (R^2 = 0.758), iron (R^2 = 0.788), and phosphorus (R^2 = 0.758), using the manganese, nickel, copper, and cobalt data. Histograms and cumulative probability plots of the silica to manganese oxide ratio Figure 11.10 show that imputing the missing silicon values did not alter the distribution of the silica to manganese oxide ratio significantly.

Figure 11.10 Histogram and cumulative probability plots of MnO:SiO$_2$ ratio for NORI Area D nodule samples
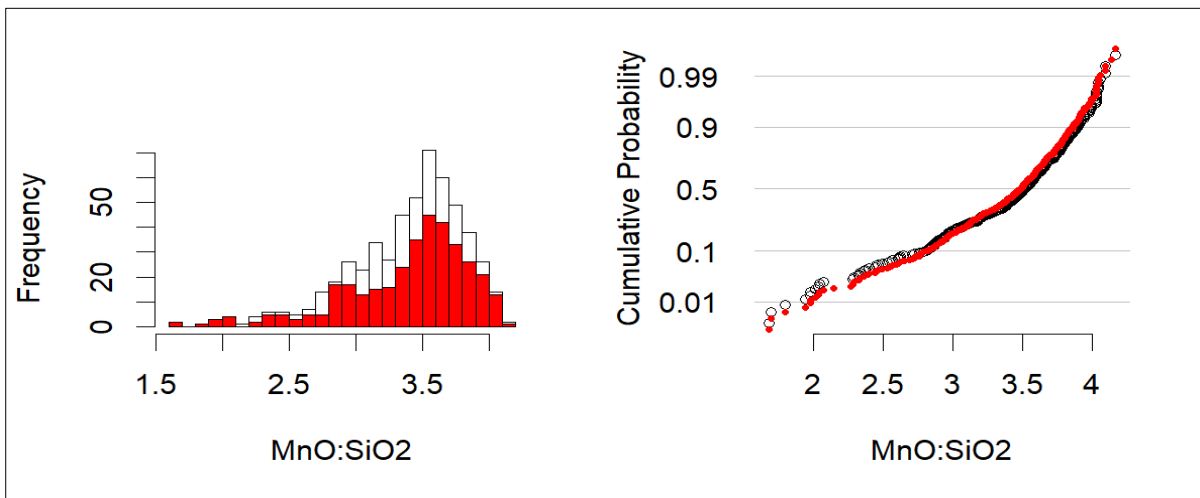
Note: Black data series is the original NORI Area D data. Red data series is NORI Area D data with missing silicon values imputed using linear regression.

11.2.11   Domain modelling

Geological domains were assigned to the NORI Area D samples by extracting the values from the geological domain raster at the sample UTM locations. The TOML Area F samples were all assigned to abyssal plains domain. The majority of the samples (367 samples, 82.1%) fall within the abyssal hills/plains domains. The proportions of nodule samples by geological domain are shown graphically in Figure 11.11.

Figure 11.11 Frequency of NORI Area D nodule samples by geological domains
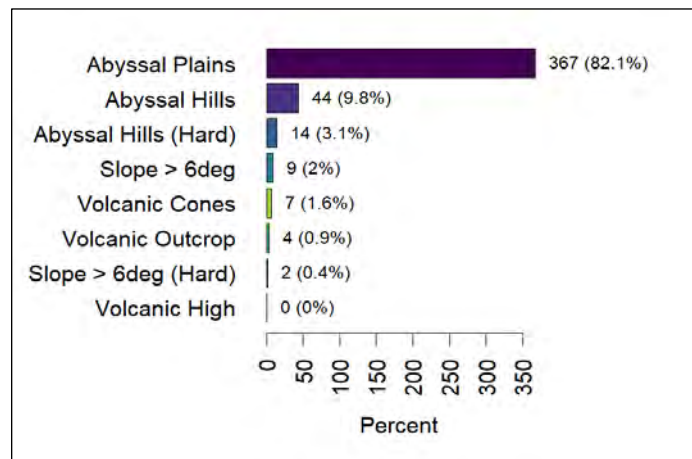
Nodule type domains were assigned to the NORI Area D samples by extracting the values from the nodule type domain raster at the sample UTM locations. The TOML Area F samples were all assigned to Type 1 domain. The majority of the samples (379 samples, 84.8%), fall within the abyssal hills/plains domains. Due to the small size of the sediment drift domain, there is only one sample that falls within this domain. This is insufficient to describe the grade and nodule distributions for this domain. The proportions of nodule samples by nodule domain are shown graphically in Figure 11.12.

Figure 11.12 Frequency of NORI Area D nodule samples by nodule type domains
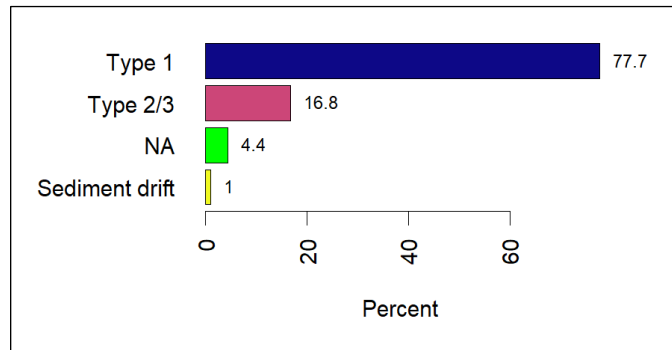
Boxplots of abundance and grades by domain Figure 11.13 suggest that as the slope increases the silicon content in the nodules increases, iron slightly increases and the manganese decreases. Also, the nickel and copper grades appear to decrease with increasing slope. This suggests that the nodules forming on the hills may be influenced by hydrothermal fluids from fissures/fractures associated with the hills or by the chemistry of the footwall rocks and sediment.

The high-slope (>6°) domains have very different distributions for all assays compared with the abyssal hills/plains domains which comprise bulk of the NORI Area D area. Because of this difference it is necessary to exclude the samples from the high-slope domains when estimating grades for the abyssal hills/plains domains. Also, because of the low number of samples in the high-slope domains and the volcanic domains it will be necessary to assign average grades to the resource model for these domains.

The boxplots of abundance and grades by nodule type Figure 11.14 suggest that the three samples within the sediment drift domain are significantly different from the Type 1 and 2/3 nodules. This domain contains an outlier cobalt value. Nodules within the sediment drift domain are low in nickel, high in copper, high in manganese and silicon and low in iron and phosphorus, compared with the other nodule domains. Comparison of Type 1 and Type 2/3 nodule grades indicates small differences. Type 1 nodules show higher nickel, iron, phosphorus and lower copper and silicon than the Type 2/3 nodules. These differences are also reflected in the nodule sizing analysis.

Due to the anomalous grade and abundance values for the sediment drift domain, these samples were excluded from the resource estimate. The low nodule abundance samples within the abyssal hills/plains domains, classified as either Type 1 or Type 2/3 nodules, may actually be occurring within unidentified sediment drift areas or on volcanic outcrops.

Figure 11.13 Boxplots of NORI Area D nodule abundance and assays by geological domain
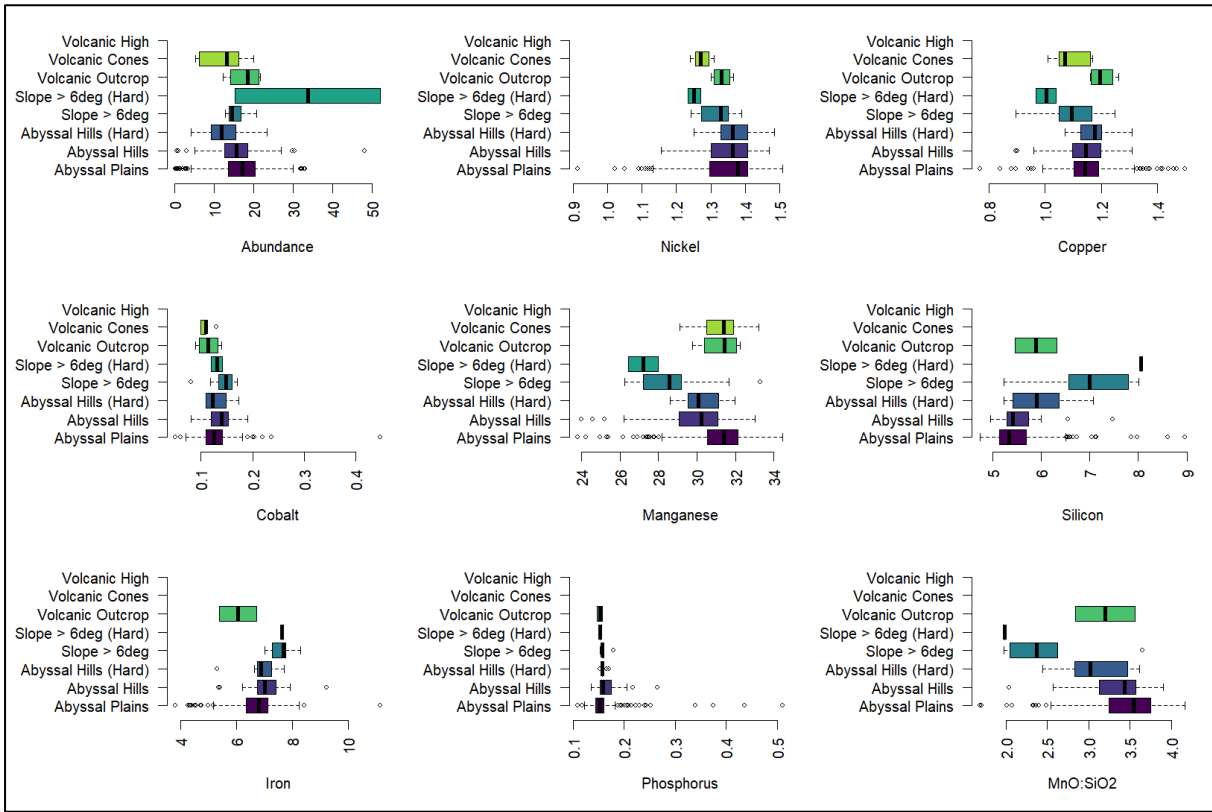
Figure 11.14 Boxplots of NORI Area D nodule abundance and assays by nodule type domain
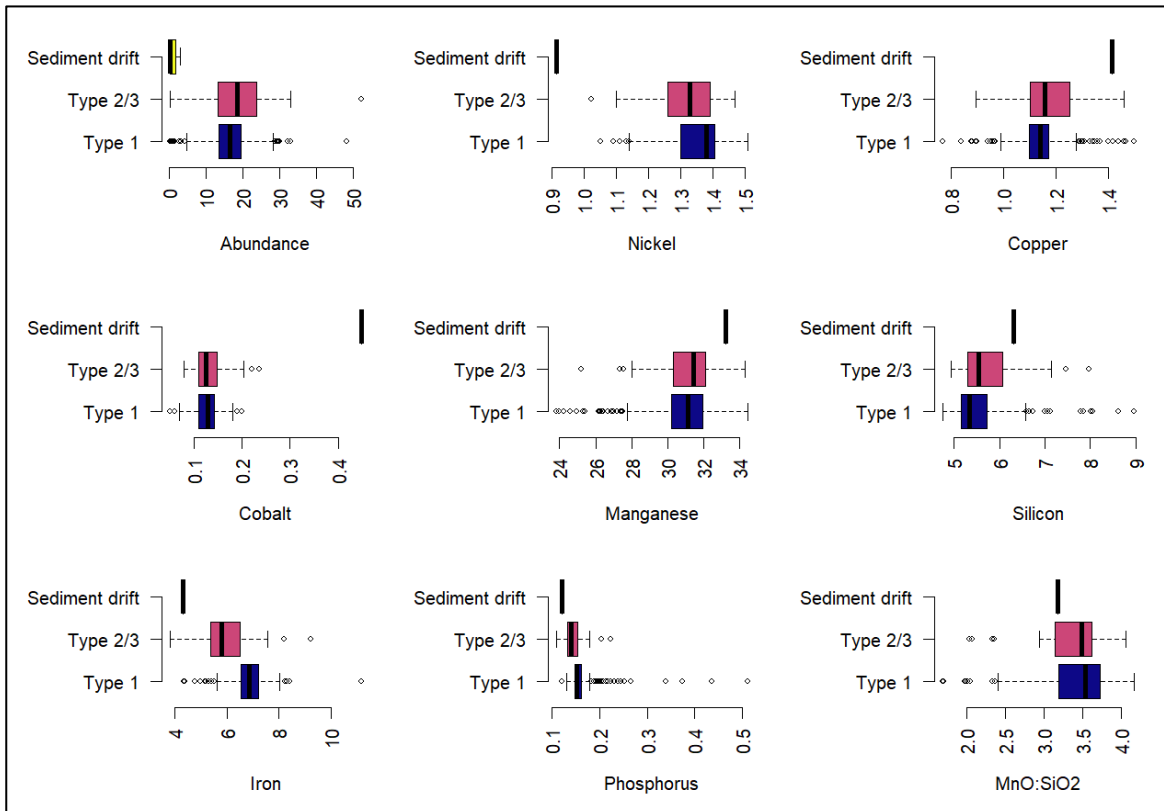
Comparison of nodule abundance with backscatter, slope and aspect was undertaken to assess the influence of these features on the distribution of nodules and nodule abundance. Scatter plots of nodule abundance versus backscatter, slope and aspect are provided in Figure 11.15. Also shown are scatter plots of manganese and silicon versus slope.

The plots suggest that there is linear relationship between backscatter and abundance which has a Pearson correlation coefficient of 0.35. Abundance does not appear to be influenced by slope or aspect. However, there are few samples in areas with a slope greater than 4°. Also note that there appears to be slightly lower abundance in areas where the aspect ranges from 125° to 175°. Silicon appears to increase with increasing slope (Pearson correlation coefficient of 0.38).

Figure 11.15 Scatter plots of NORI Area D nodule abundance versus backscatter, slope and aspect and manganese and silicon versus slope.
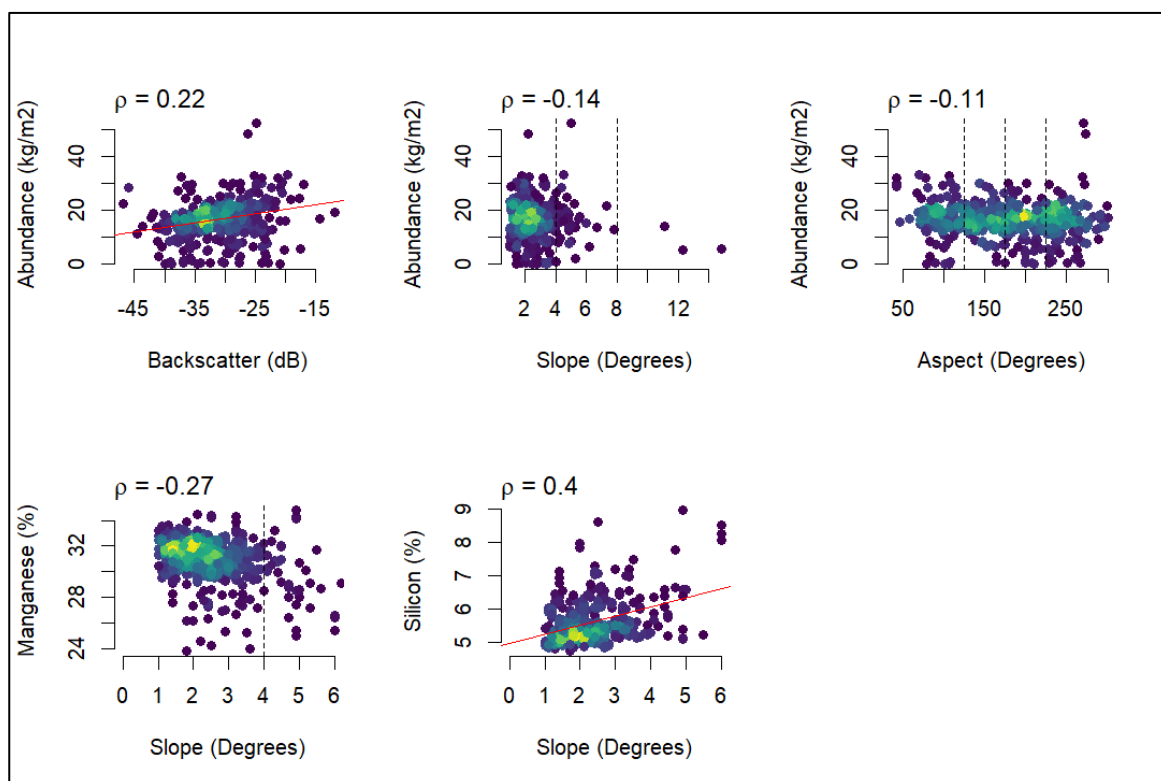
Boxplots Figure 11.16 were also generated to help visualize the trends seen in the scatter plots. The boxplot of abundance versus slope suggests that abundance is lower in areas with a slope greater than 6°. The trend in abundance versus backscatter is clear but also highlights a much higher variance in abundance in areas with higher backscatter.

Figure 11.16 Boxplots of NORI Area D nodule abundance versus backscatter, slope and aspect and manganese and silicon versus slope.
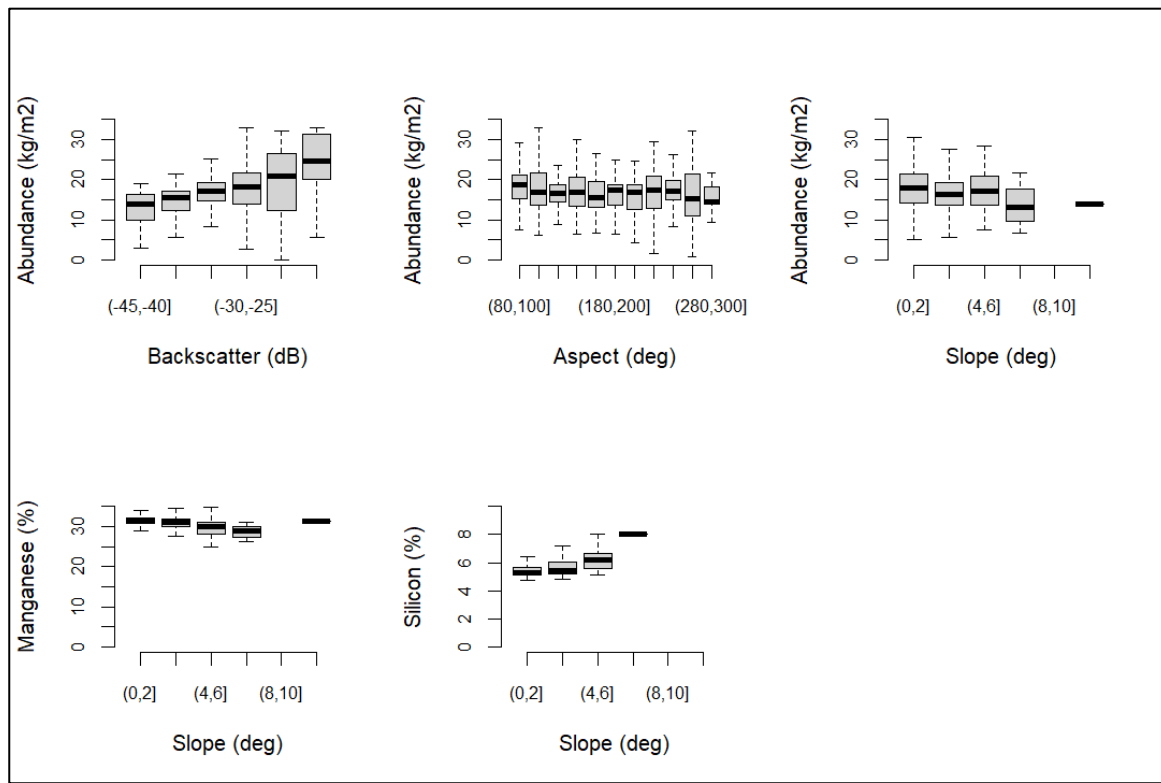
11.2.12   Data transformations

Missing values for silicon, iron and phosphorus were imputed using linear regression models. A Projection Pursuit Multivariate Transformation was then performed on the data. PPMT is a method to transform multivariate numeric data into multigaussian data. The transform aims to remove all bivariate correlations between the variables making them independent and to transform each variable to a normal distribution. The transform allows for independent random estimation or simulation of gaussian variables using simple kriging. The kriged estimates are then back-transformed into the original multivariate space, where all bivariate correlations and trends are restored. The transform is useful for simple kriging and sequential gaussian conditional simulations, where the variables are required to be independent and gaussian. The transform ensures that, even when using different variograms for each transformed variable, the bivariate relationships are maintained.

11.2.13   Summary statistics of processed sample data

Summary statistics for the data used for the NORI Area D resource estimate are provided in Table 11.11 to Table 11.15.

Table 11.11   Summary of samples within NORI Area D used for resource estimation

	Number	Missing	Min	Max	Mean	Median	Var	CV
Abundance (wet kg/m^2)	320	1	0.08	32.99	17.42	17.07	28.861	0.3080
Nickel (%)	320	18	0.91	1.51	1.37	1.40	0.006	0.0572
Copper (%)	320	18	0.77	1.41	1.15	1.14	0.007	0.0732
Cobalt (%)	320	18	0.07	0.45	0.14	0.13	0.001	0.2030
Manganese (%)	320	18	24.23	34.46	31.07	31.35	2.520	0.0511
Silicon (%)	320	72	4.74	8.97	5.62	5.41	0.466	0.1210
Iron (%)	320	72	3.80	11.16	6.73	6.82	0.703	0.1250
Phosphorus (%)	320	72	0.11	0.51	0.16	0.15	0.002	0.2430

Note the 14 missing values for nickel, copper, manganese and cobalt are the photo samples where only abundance is recorded and 4 box core samples with low abundances that were not assayed. The samples with missing silicon, iron and phosphorus are comprised of TOML samples, historic samples and NORI samples derived from photography.

Table 11.12   Summary statistics of historic (declustered) samples within NORI Area D and TOML Area F

	Number	Missing	Min	Max	Mean	Median	Var	CV
Abundance (wet kg/m^2)	29	0	6.73	28.10	14.88	14.01	25.396	0.3390
Nickel (%)	29	0	1.18	1.34	1.29	1.29	0.001	0.0280
Copper (%)	29	0	0.98	1.37	1.14	1.12	0.008	0.0804
Cobalt (%)	29	0	0.07	0.18	0.12	0.11	0.001	0.2420
Manganese (%)	29	0	25.88	32.90	30.55	30.86	2.175	0.0483
Silicon (%)	0	29						
Iron (%)	0	29						
Phosphorus (%)	0	29						

Note 28 samples are within NORI Area D and 1 sample is within TOML Area F.

Table 11.13   Summary of NORI 2018 nodule box-core and photo samples within NORI Area D used for resource estimation

	Number	Missing	Min	Max	Mean	Median	Var	CV
Abundance (wet kg/m^2)	59	1	6.50	29.90	17.90	18.00	20.387	0.2520
Nickel (%)	59	14	1.18	1.44	1.38	1.40	0.004	0.0468
Copper (%)	59	14	0.96	1.33	1.15	1.15	0.005	0.0618
Cobalt (%)	59	14	0.09	0.15	0.13	0.13	0.000	0.0967
Manganese (%)	59	14	26.15	34.41	31.35	31.83	2.702	0.0524
Silicon (%)	59	14	4.96	8.28	5.66	5.45	0.444	0.1180
Iron (%)	59	14	4.36	8.14	6.71	6.96	0.695	0.1240
Phosphorus (%)	59	14	0.13	0.21	0.16	0.16	0.000	0.1220

Note the 14 missing values for nickel, copper, manganese and cobalt are the photo samples where only abundance is recorded.

Table 11.14   Summary statistics of NORI 2019 nodule box-core samples within NORI Area
D used for resource estimation

	Number	Missing	Min	Max	Range	Mean	Median	Var	CV
Abundance (wet kg/m²)	207	0	0.08	32.99	32.92	17.55	17.13	28.98	0.3070
Nickel (%)	207	4	0.91	1.49	0.57	1.38	1.40	0.006	0.0558
Copper (%)	207	4	0.77	1.41	0.65	1.15	1.14	0.007	0.0721
Cobalt (%)	207	4	0.09	0.45	0.36	0.14	0.13	0.001	0.2130
Manganese (%)	207	4	24.23	34.46	10.24	30.95	31.19	2.543	0.0515
Silicon (%)	207	4	4.74	8.97	4.23	5.61	5.39	0.472	0.1220
Iron (%)	207	4	3.81	11.16	7.35	6.73	6.81	0.704	0.1250
Phosphorus (%)	207	4	0.11	0.51	0.40	0.16	0.15	0.002	0.2640

Table 11.15   Summary statistics of TOML Area F nodule box-core samples adjacent to
NORI Area D used for resource estimation

	Number	Missing	Min	Max	Mean	Median	Var	CV
Abundance (wet kg/m²)	25	0	1.19	29.13	18.14	18.30	46.448	0.3760
Nickel (%)	25	0	1.05	1.51	1.41	1.42	0.008	0.0621
Copper (%)	25	0	1.10	1.35	1.23	1.23	0.005	0.0584
Cobalt (%)	25	0	0.09	0.17	0.13	0.13	0.000	0.1400
Manganese (%)	25	0	30.11	33.62	32.17	32.30	0.845	0.0286
Silicon (%)	0	25						
Iron (%)	0	25						
Phosphorus (%)	0	25						

Note: these are the 25 samples collected by Nautilus Minerals Inc.

11.2.13.1 Spatial continuity

Spatial continuity of abundance and the grades of manganese, nickel, copper, cobalt, silicon, iron and phosphorus were assessed using semi-variograms. For convenience, semi-variogram is abbreviated to variogram in the following discussion.

A variogram is a graphical representation of the variance between pairs of points at different separation distances. For data that is spatially correlated, it is expected that closely-spaced pairs of data will have lower variance than widely-spaced pairs. At a particular distance, known as the range, the pairs become uncorrelated and the variance no longer increases. Experimental variograms are generated from the data in different orientations to see if there is greater continuity in a particular direction (anisotropy). If there is no strong evidence of anisotropy, the directional variograms can be combined into an omnidirectional variogram for ease of interpretation. The experimental variogram can be fitted with a mathematical model (the variogram model) from which spatial weights can be determined during the kriging estimation process.

11.2.13.2 Polymetallic nodule abundance and nodule grades

All NORI box-core samples and nodule abundances derived from photos within NORI Area D were used for analysis of spatial continuity. The PPMT transformed data was used for calculating the experimental variograms.

The direction of greatest continuity suggested by the variogram maps Figure 11.17 is approximately 075° or 165°. This direction is an artefact of the sparseness of the sampling and the orientation of the sampling grid which is oriented 075°, roughly parallel to the broad regional trend of the CCZ.

Figure 11.17 Variogram maps of NORI Area D nodule sample assays
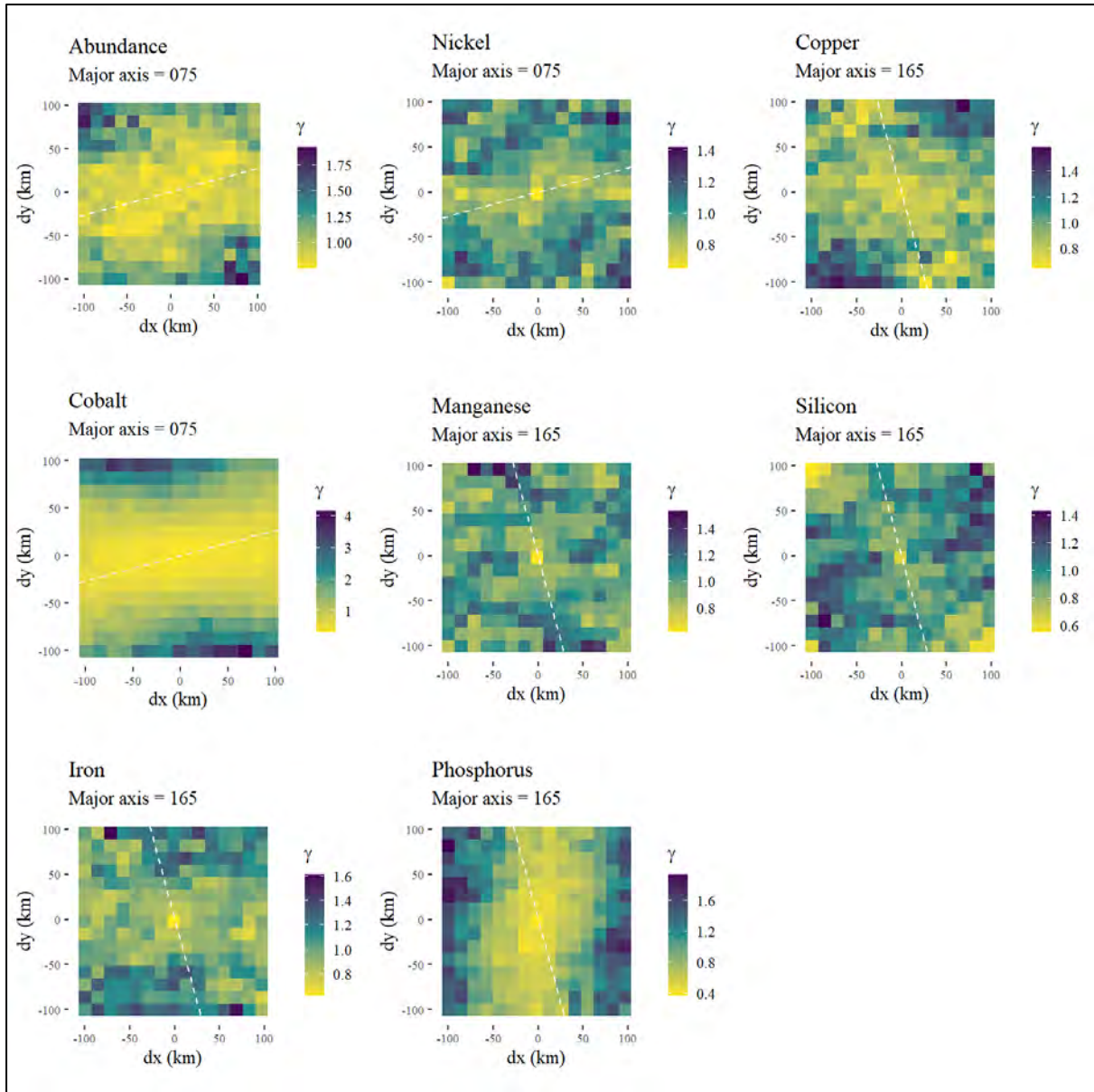
Two-structure, spherical models were fitted to the experimental variograms for abundance, nickel, copper, and manganese, while cobalt was fitted with only one structure. The experimental variograms for cobalt suggest very long ranges in the 075° direction.

The variogram models used for estimating block nodule abundance and grades are listed in Table 11.16 and illustrated in Figure 11.18 to Figure 11.25.

Table 11.16   Variogram models

	Abundance	Nickel	Copper	Cobalt	Manganese	Silicon	Iron	Phosphorus
Nugget	0.1	0.1	0.10	0.10	0.10	0.10	0.10	0.10
Sill 1	0.6	0.7	0.60	0.20	0.35	0.50	0.60	0.30
Range 1 Omni	3.0	12.0	2.00	20.00	6.00	6.00	6.00	12.00
Range 1 Major	3.0	20.0	12.00	20.00	10.00	16.00	9.00	18.00
Range 1 Minor	3.0	12.0	9.00	7.00	4.00	6.00	6.00	12.00
Sill 2	0.3	0.2	0.30	0.70	0.55	0.40	0.30	0.60
Range 2 Omni	80.0	100.0	80.00	80.00	40.00	50.00	50.00	100.00
Range 2 Major	60.0	100.0	80.00	170.00	50.00	80.00	60.00	140.00
Range 2 Minor	60.0	60.0	60.00	60.00	30.00	30.00	40.00	100.00
Major Dir.	75.0	75.0	165.00	75.00	165.00	165.00	165.00	165.00
Anisotropy	1.0	0.6	0.75	0.35	0.60	0.38	0.67	0.71

Figure 11.18 Abundance omni-directional, 065° and 165° directional variograms
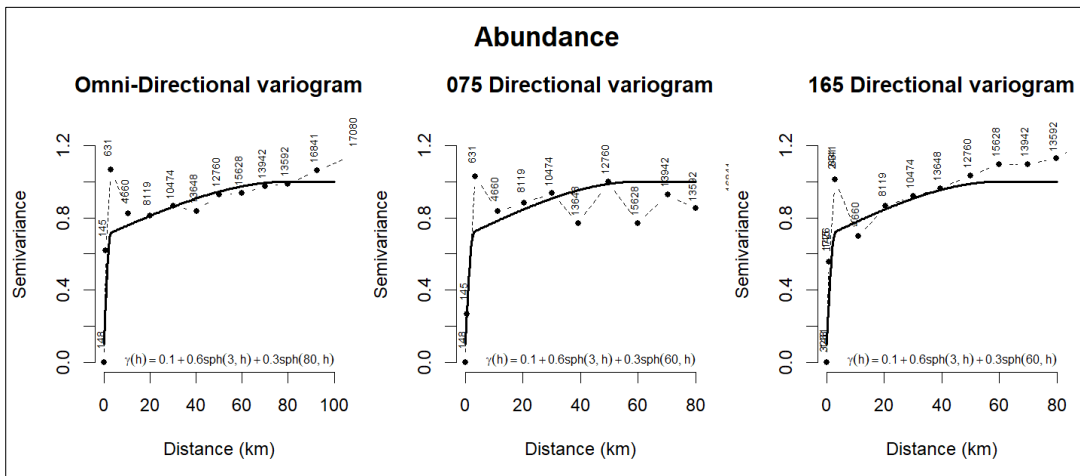
Figure 11.19 Nickel omni-directional, 065° and 165° directional variograms
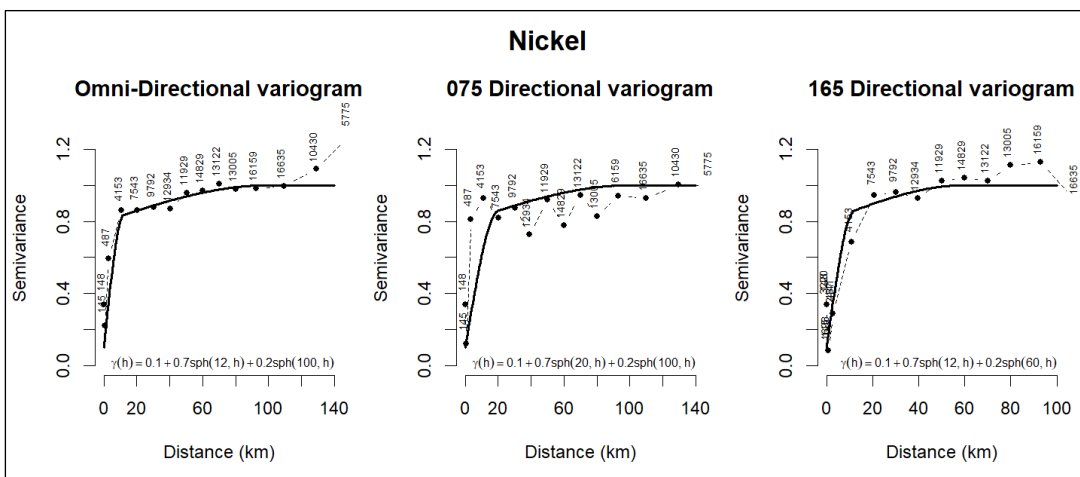
Figure 11.20 Copper omni-directional, 065° and 165° directional variograms
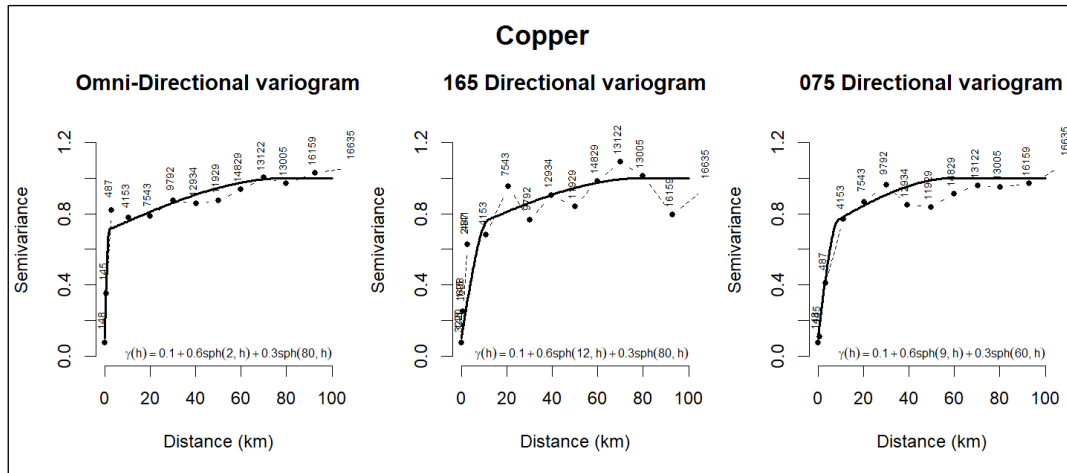
Figure 11.21 Cobalt omni-directional, 075° and 165° directional variograms
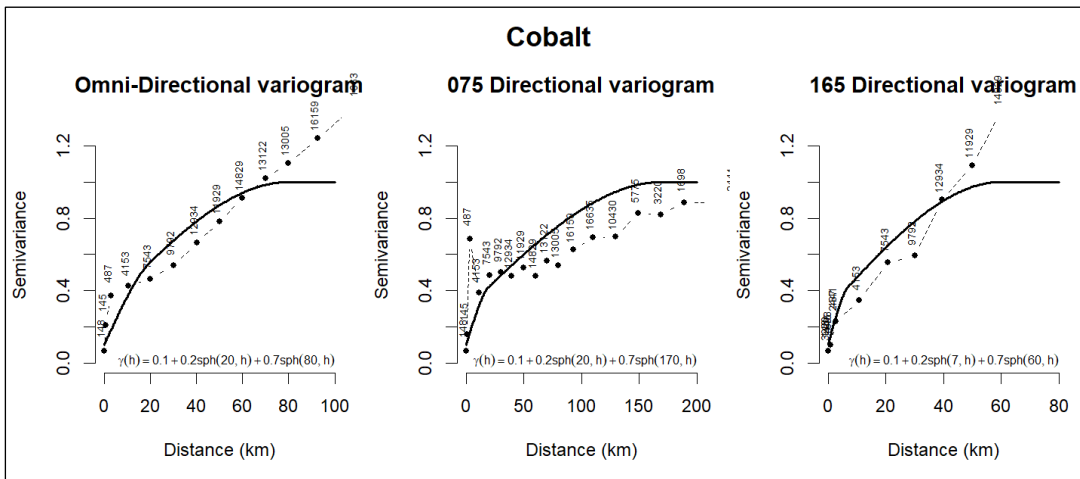
Figure 11.22 Manganese omni-directional, 075° and 165° directional variograms
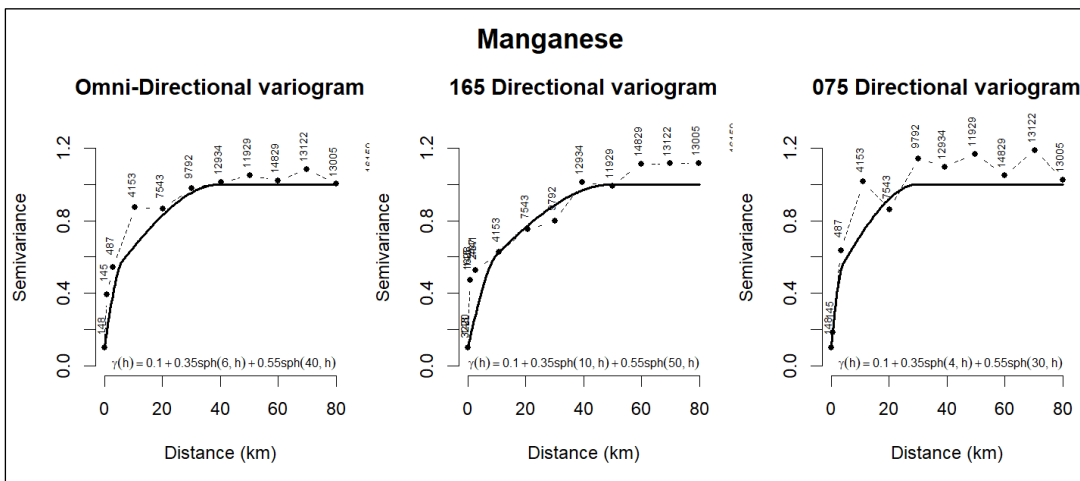
Figure 11.23 Silicon omni-directional, 075° and 165° directional variograms
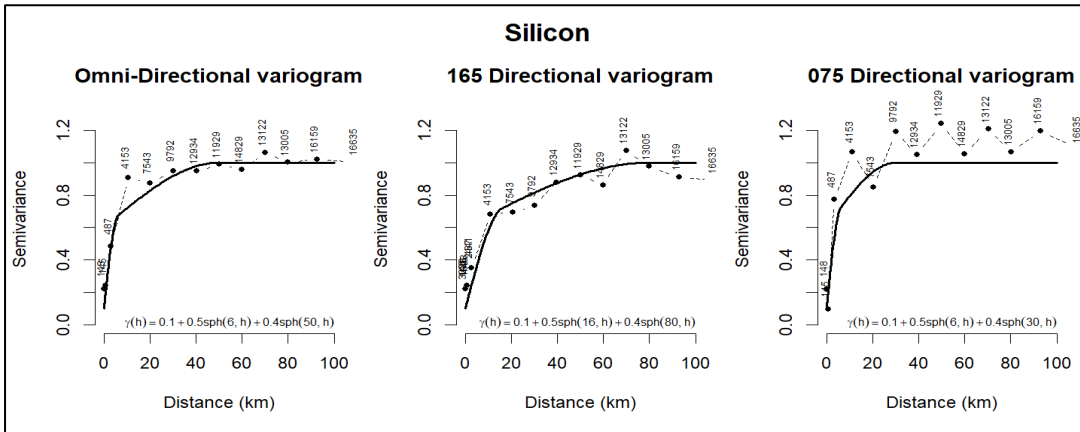
Figure 11.24 Iron omni-directional, 075° and 165° directional variograms
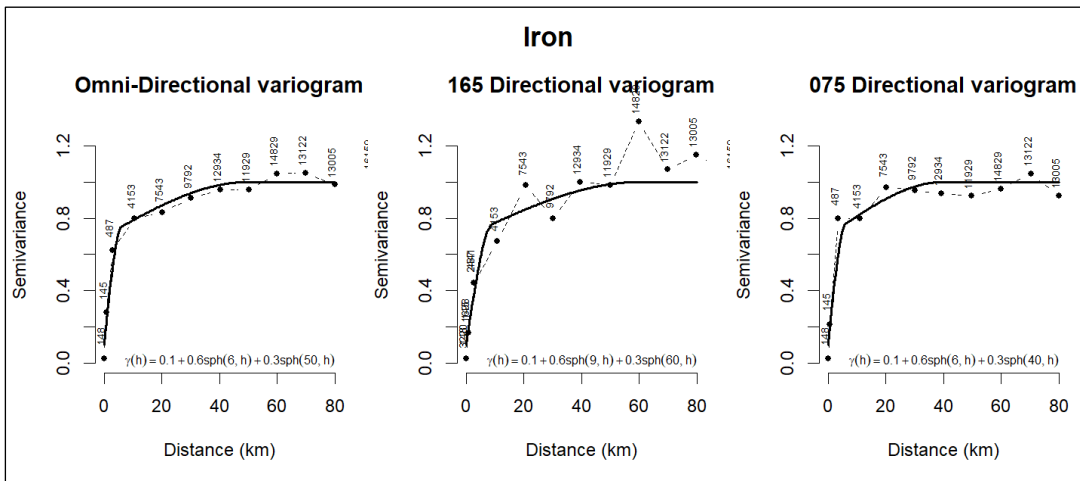
Figure 11.25 Phosphorus omni-directional, 075° and 165° directional variograms.
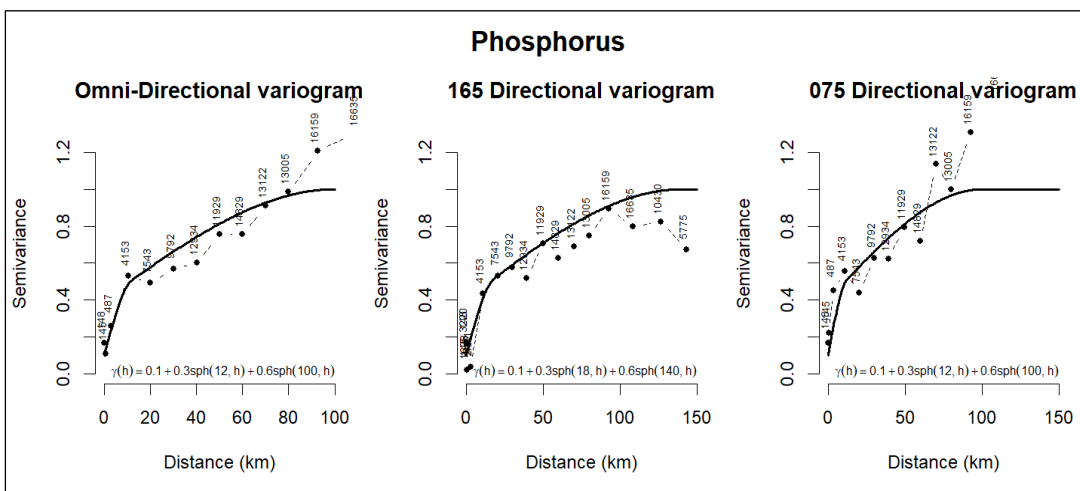
11.2.13.3 Backscatter

Acoustic backscatter is considered to reflect the substrate hardness of the seafloor. Absorption of the acoustic signal is expected to occur highest in areas covered by soft

sediment (ooze) and lowest in areas of hard outcropping volcanics. The presence of nodules on the seafloor is expected to influence local absorption and be dependent on nodule packing which is a function of nodule abundance and nodule type.

Continuity of abundance is expected to be reflected in the backscatter data. Experimental variograms Figure 11.26 were calculated from the backscatter data and fitted with spherical variogram models. Omni-directional and directional variograms (065° and 155°) were calculated. The variograms are well-structured and consistent with the variograms of abundance.

Figure 11.26 Backscatter omni-directional, 065 and 155 directional variograms.
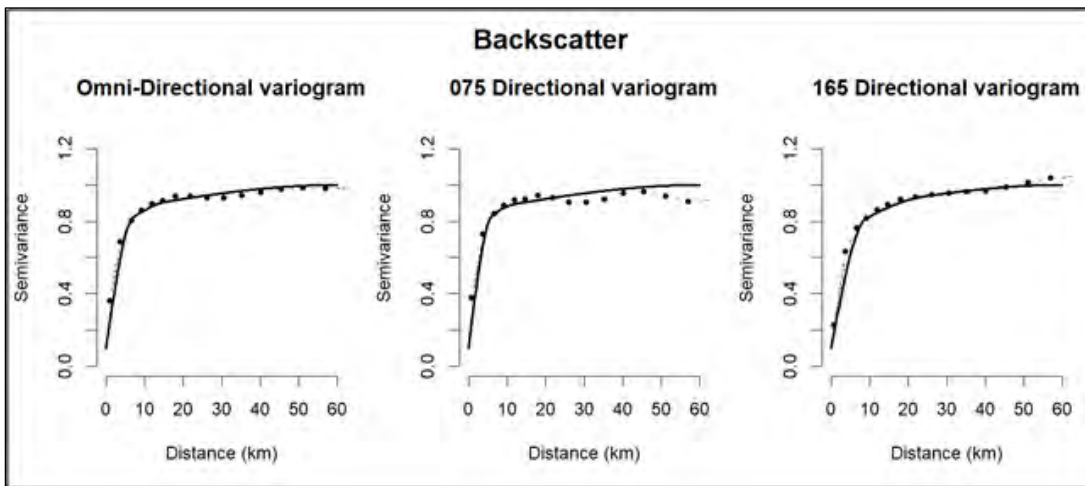
11.2.14   Estimation of nodule abundance and grades

A geological raster grid model of NORI Area D was constructed from the geological domaining GIS raster data by aggregating the raster by a factor of 10. This expanded the raster cell size from 50 m to 500 m. The origin, extent and cell size are outlined in Table 11.17.

Table 11.17   NORI Area D grid model extents

	Easting	Northing
Model origin	410444.2110	1093899.210
Model limit	602444.2110	1225399.210
Cell size	500	500
Number of cells	263	263

The geological grid model contains a layer (NOD) which identifies the percent coverage of nodules within the 500 m by 500 m panel. This layer was constructed by aggregating the 50 m by 50 m reclassified geological domain raster. The geological domain raster was reclassified by assigning a value of 1 for the abyssal plains, abyssal hills and abyssal hills (hard) domains. All other domains were assigned a value of 0. The 500 m by 500 m geological grid model is shown in Figure 11.27.

Figure 11.27 NORI Area D 500 m by 500 m grid model, showing percentage coverage of nodules
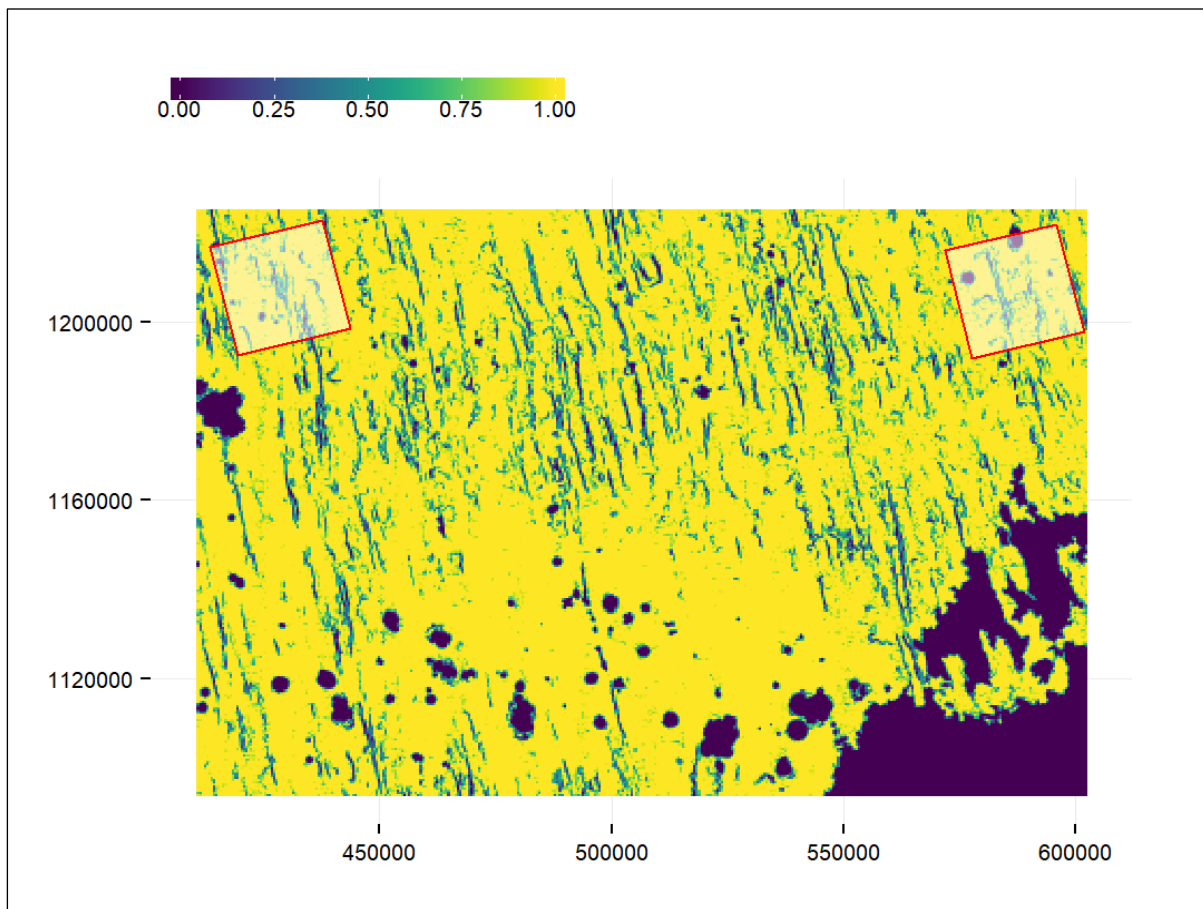
Points coloured by percent nodule coverage

The geological grid model was used as the discretization points for 3.5 km by 3.5 km sized panels. Inverse distance weighting (power of 2) and simple kriging were used to estimate nodule abundance and nodule grades into the geological grid model. Simple kriging was selected because ordinary kriging is not suited to the transformed grade variables. The 500 m by 500 m point estimates were aggregated to a grid with dimensions of 3.5 km by 3.5 km.

The prepared and transformed data was used for estimating nodule abundance and nodule grades. Samples falling within the high-slope (> 6°) geological domains were excluded from the estimation. A minimum of 1 and a maximum of 10 samples were used in informing the estimates.

Comparison of the inverse distance (IDW), ordinary kriging (OK) and simple kriging estimates with nodule sample data are illustrated in Figure 11.28. The cumulative probability plots show, as expected, that the simple kriging panel estimates are smoother (lower variance) than inverse distance panel estimates which are smoother than the nodule samples. The smoothing for the simple kriging estimates of nodule abundance is higher than the smoothing exhibited by the nodule grades. This is interpreted to be due to 70% of the sill in the spatial variogram for nodule abundance occurring at 3 km. The medians for the three distributions are very similar for nodule abundance and nodule grades.

Figure 11.28 Cumulative probability plots comparing nodule samples with IDW and SK estimates.

11.2.15   Cut-off grade

Due to the extremely low variance in the grades and the high metal content of the nodules, a cut-off based on abundance is appropriate for determining the limits of economic exploitation. A cut-off of 4 kg/m^2 abundance was chosen for the NORI Contract Area, based on the estimates of costs and revenues presented in this report, generalized as follows:

- 1.7 Mt minimum annual tonnage mined;
- $0.25 Million/km^2 for offshore operating costs;
- 1,036 km^2 collected area processed;
- $95/ dry tonne for transport costs;
- $119/dry tonne for processing costs;
- $15/dry tonne for corporate, general and administrative costs;
- $33/dry tonne for ISA and state royalties;

- 95% recovery of nickel at an assumed price of nickel metal $16,472/t;
- 86% recovery of copper at an assumed price of $6,872/t copper metal;
- 77% recovery of cobalt at an assumed price of $46,333/t cobalt metal;
- 99% recovery of manganese at an assumed price of $4.50/dmtu manganese in manganese silicate

The method of calculation for the cut-off determines the minimum average nodule abundance needed during steady state operations such that the revenue minus costs (excluding capital) is greater than zero. Revenue includes metal pricing and metallurgical processing recoveries, and the costs include the collection, transport, processing, corporate costs, and royalties.

The price estimates are long term (2034 – 2046) forecasts provided in a report by CRU International Limited (CRU, 2020). The Qualified Person considers that this timeframe is reasonable in view of the likely time required to bring the majority of the NORI mineral resources into production.

11.2.16   Mineral Resource classification

The limiting factor for Mineral Resource classification for NORI Area D is confidence in the estimates for abundance. Confidence in the resource estimate was assessed using the probability of abundance being greater than ±15% of mean abundance over one quarter production (Measured) and one year's production (Indicated) at 90% confidence.

The risk in quarterly production estimates was assessed by using Conditional Gaussian simulation was used to simulate abundance. Each simulation was an equiprobable realization of the modelled data. The simulation was run 100 times using the same data and same estimation parameters and variogram model as used for kriging.

Assuming an annual production rate of 8 Mt (wet) of nodules per year (240 Mt over 30 years), the panel size for a quarter of a year's production is 10,846 m by 10,846 m assuming an average abundance of 17 kg/m^2. To simplify the conditional simulation, the area covered by a quarter of a year's production was set at 10 km by 10 km while one year's production was set at 20 km by 20 km. This equates to a yearly production rate of 6.4 Mt and one quarter of a year's production of 1.6 Mt with an average abundance of 16 kg/m^2.

The conditional simulations of 500 m by 500 m panels were aggregated up to 10 km by 10 km and 20 km by 20 km panels. The probability of abundance being greater than +/-15% of mean abundance over one quarter production (Measured) and one year's production (Indicated) is shown in Figure 11.29.

The conditional simulation of abundance Figure 11.29 suggests that in the small area near the centre of NORI Area D where sample spacing is 3.5 km by 3.5 km the estimates are of high confidence and could be classified as Measured Mineral Resource. In the rest of NORI Area D, where there are samples at a spacing of 7 km by 7 km and 10 km by 10 km, the estimates are of sufficient confidence to be classified as Indicated Mineral Resource. The south-east corner of NORI Area D where there are generally no samples, and which is mostly covered by the volcanic high domain is considered to be estimated with low confidence. Note that there are some areas covered by 10 km by 10 km spacing that have high confidence.

Figure 11.29 Abundance: Probability of exceeding 15% of mean at 90% confidence for quarterly and yearly production.
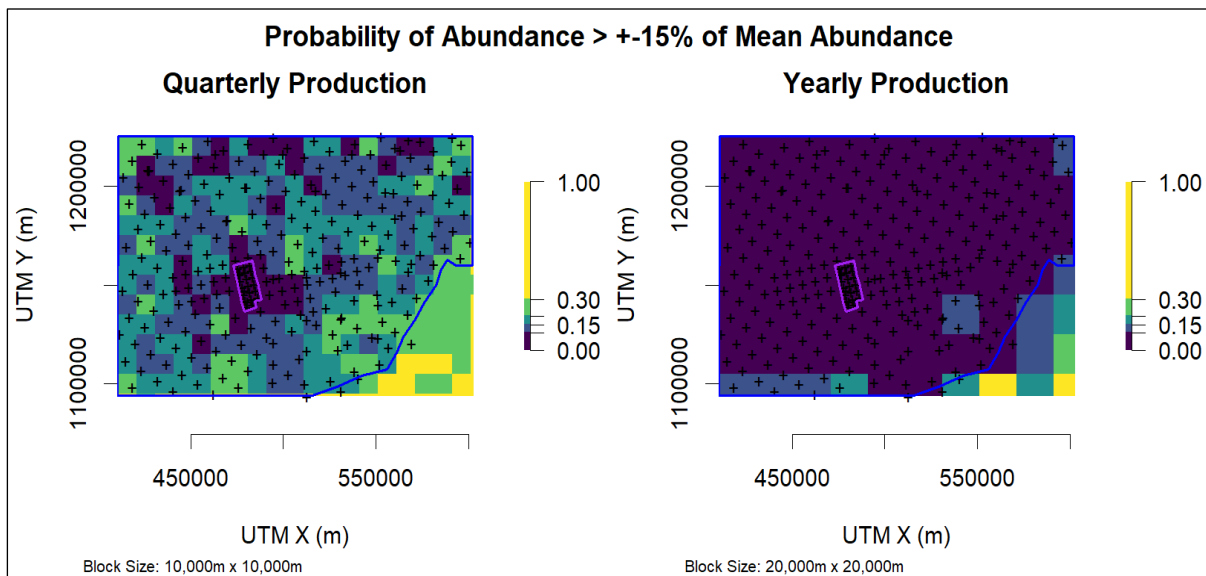
Perimeters: (purple) Area of high confidence = Measured Mineral Resource; (blue) Area of moderate confidence = Indicated Mineral Resource.

The Mineral Resource was classified on the basis of the quality and uncertainty of the sample data and sample spacing, in accordance with SEC Regulation S-K (subpart 1300).

The Measured Mineral Resource was assigned to the area within NORI Area D where box-core sampling was conducted on a nominal 7 km by 7 km spacing and infilled with estimates of nodule abundance from seafloor photography to a spacing of 3.5 km by 3.5 km.

The Indicated Mineral Resource was assigned to the area within NORI Area D where box-core sampling was conducted on a nominal spacing of 7 km by 7 km but without additional photo-estimates of nodule abundance, or 10 km by 10 km.

The Inferred Mineral Resource was assigned to the areas of abyssal plain in the southeast corner of NORI Area D that are largely unsampled. The volcanic high in the southeast corner was excluded from the mineral resource estimate due to the high level of uncertainty about nodule abundance and grades in this domain. Mineral Resource classification boundaries are shown in Figure 11.30.

Figure 11.30 Mineral Resource classification boundaries
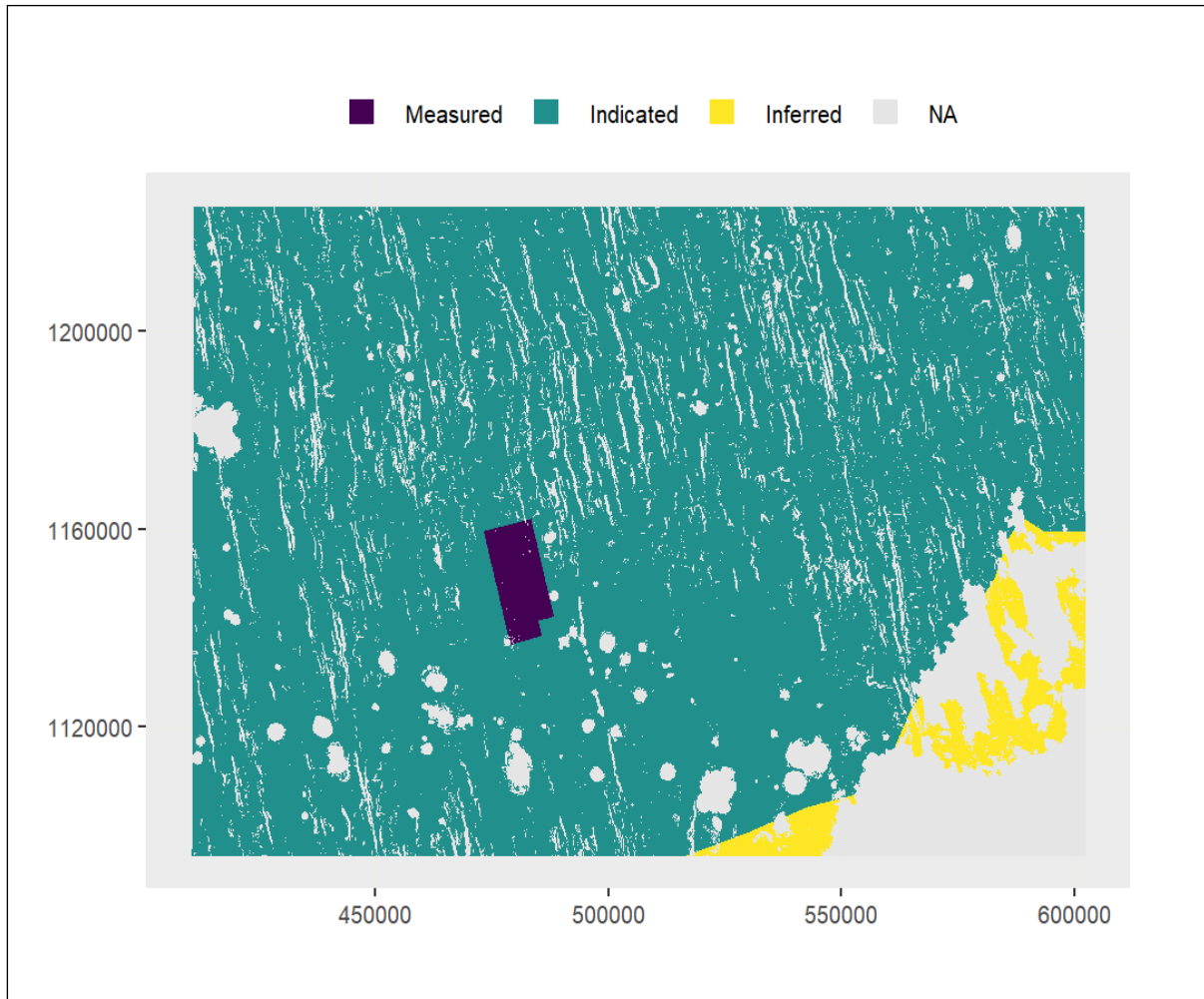
The reasons for excluding the Volcanic High from the Mineral Resource include:

- Uncertainty in distinguishing between volcanic outcrop and high abundance nodules using the backscatter data.

- No nodule samples have yet been collected within the volcanic high and as such it is unknown whether there are any nodules occurring within the domain.

- The geological domain interpretation used for this resource update is based on significant supporting data compilation and re-interpretation of all existing license-scale data. In addition, it considers integration of associated basin-scale geological and geophysical data and interpretations. The previous resource estimation (2018) and data interpretation primarily focused on interpretation of AUV data over the small, closely-sampled area near the centre of NORI Area D.

- The volcanic high is interpreted as a relic volcanic intersection high, which also includes a relic transform parallel trough. Both are volcanic related features related to the Clipperton transform zone. The volcanic high is interpreted to have formed when the Clipperton transform fault was active, at a time when the seafloor was situated at the East Pacific Rise mid-ocean ridge. This is supported by comparison of backscatter texture, outcropping structural fabric within this domain and the associated bathymetric geomorphology.

- The terrain across the volcanic high is extremely rugged and is at a much shallower depth than the rest of NORI Area D. The volcanic high is less than 50 km from a

significant CaCO$_3$ anomaly seen in the compilation of basin-scale surficial sediment lithology data. This strongly suggests that the volcanic high sits above the carbonate compensation depth in a region that is therefore not favorable for nodule formation.

- The evidence that nodule chemistry is affected by substrate means that it is not reasonable to infer the grades of nodules that might occur in the Volcanic High domain from grades of nodules in other domains.

In the Qualified Person's opinion, the Mineral Resources have reasonable prospects of economic extraction. No fatal flaws have been identified. It is reasonable to expect that, with further engineering design and testwork, the technical and economic factors relevant to the collection of nodules and the extraction of nickel, cobalt, copper and manganese products from the nodules can be resolved. Accordingly, it is the Qualified Person's opinion that all issues relating to all relevant technical and economic factors likely to influence the prospect of economic extraction can be resolved with further work.

11.2.17   Estimation results

The 3.5 km by 3.5 km panel estimates were added back onto the 50 m by 50 m geological domaining GIS raster model. Nodule abundance and nodule grades for cells identified as either high-slope (> 6°) or volcanic outcrop domains were set to the mean values from the nodule samples. Cells identified as volcanic cone or volcanic high or sediment drift were set to null.

Resource categories were added to the 50 m by 50 m raster grid model using the perimeters defined by conditional simulation.

Results of the simple kriging (SK) estimates are shown in the spatial plots Figure 11.31. Note the two very small spots of high silicon estimated in the abyssal domains. These two spots are interpreted to be the result of miss-labelling of high slope domains which have high silicon. Also note the high phosphorus in the south-eastern near the volcanic high domain. Cobalt is relatively high in the north of NORI Area D and relatively low in the south while manganese, nickel, copper and iron are relatively uniformly distributed across NORI Area D. Abundance and cobalt grade appears to be higher in the north.

Figure 11.31 Nodule abundance and nodule grades 3.5 km by 3.5 km SK panel estimates for NORI Area D
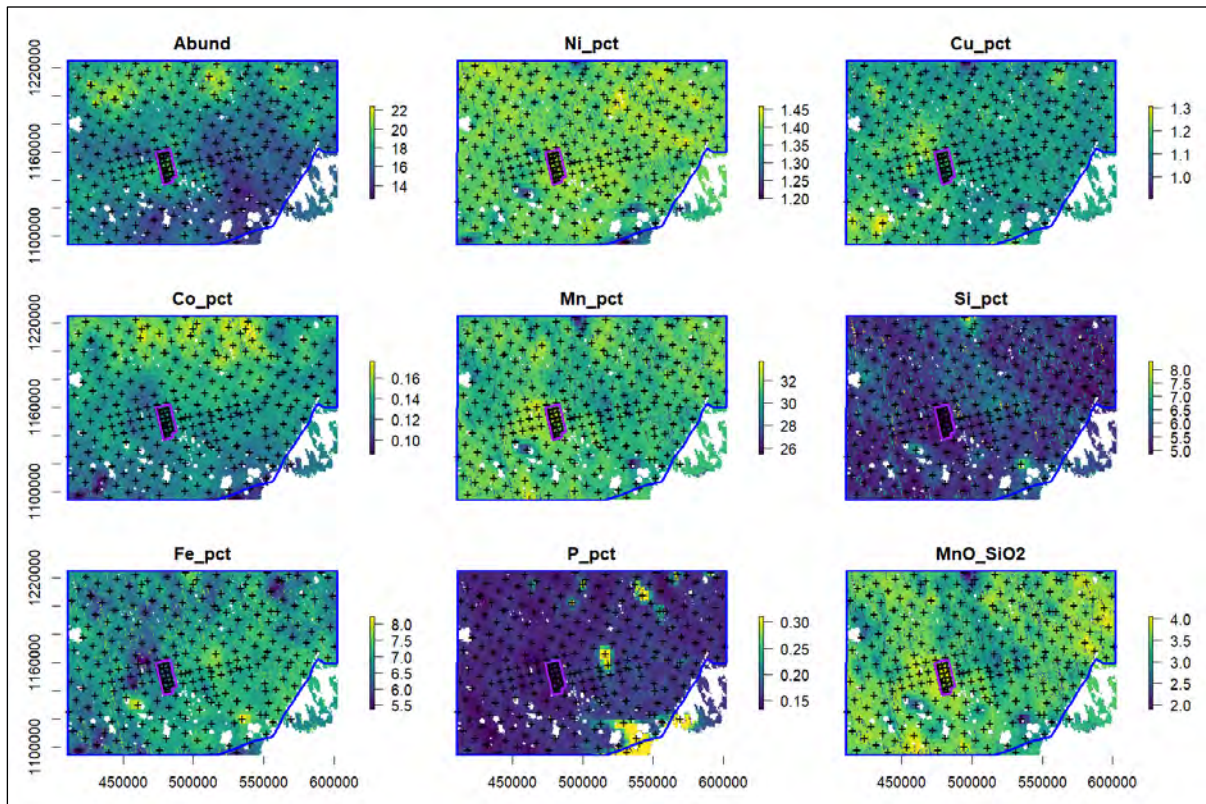
The nodule abundance and tonnage curves for NORI Area D at various nodule abundance cut-offs are shown in Figure 11.32. The curves indicate that there are no 3.5 km by 3.5 km panels with abundance of less than 12 kg/m^2. The volcanic outcrop, volcanic high, volcanic cones and high-slope (>6°) domains were excluded from the estimate.

Figure 11.32 NORI Area D abundance-tonnage curve.
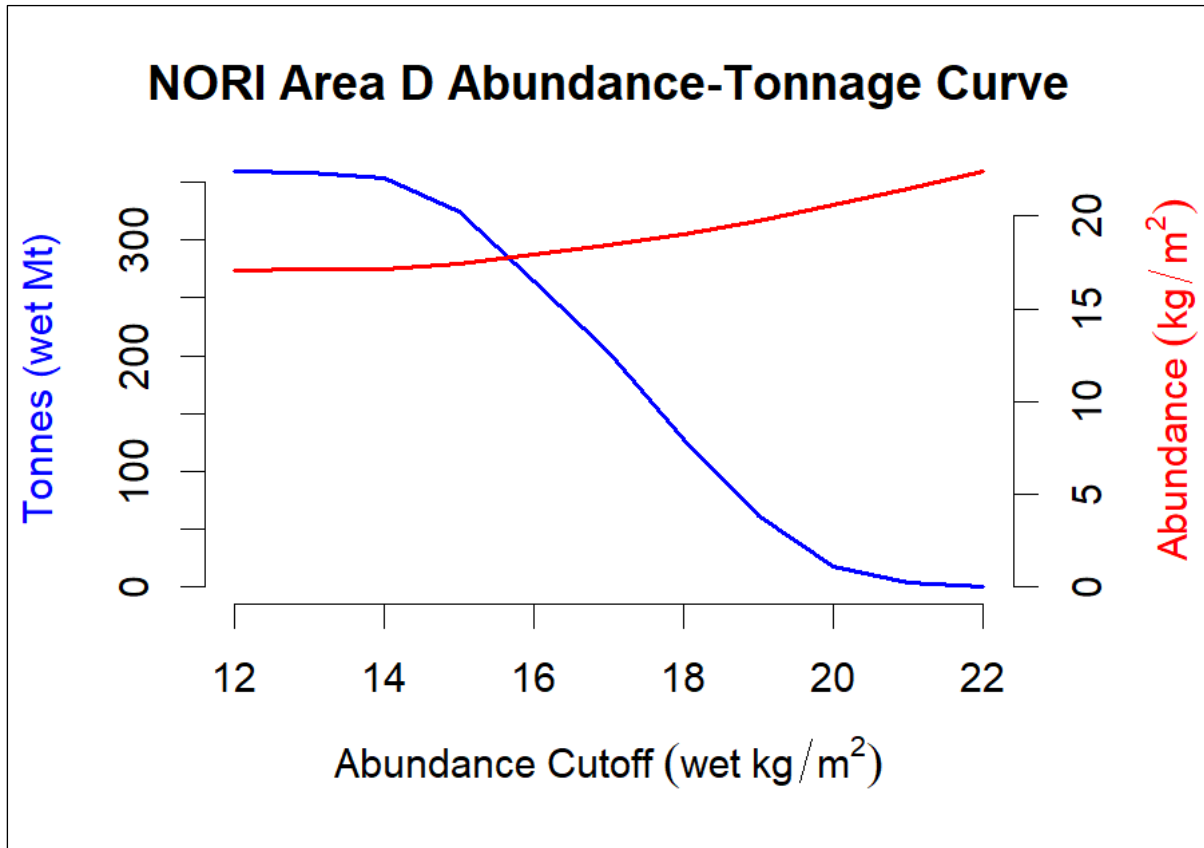
The Mineral Resource is reported in Table 11.18 at a nominal abundance cut-off value of 4kg/m^2.

Table 11.18   2020 Mineral Resource estimate, in situ, for NORI Area D at 4 kg/m^2 abundance cut-off

NORI Area	Category	Tonnes (Mt (wet))	Abundance (wet kg/m^2)	Nickel (%)	Copper (%)	Cobalt (%)	Manganese (%)	Silicon (%)
D	Measured	4	18.6	1.42	1.16	0.13	32.2	5.13
D	Indicated	341	17.1	1.40	1.14	0.14	31.2	5.46
D	Measured + Indicated	345	17.1	1.40	1.14	0.14	31.2	5.46
D	Inferred	11	15.6	1.38	1.14	0.12	31.0	5.50

Note: Tonnes are quoted on a wet basis and grades are quoted on a dry basis, which is common practice for bulk commodities. Moisture content was estimated to be 24% w/w. These estimates are presented on an undiluted basis without adjustment for resource recovery.

Figure 11.33 shows the panels coloured by abundance, with the colour intervals corresponding to seven sequential 40 Mt (wet) increments, ranked from highest abundance to lowest abundance. The figure shows that abundance is highest along the northern margin of NORI Area D, which is also high in cobalt.

Figure 11.33 2020 Mineral Resource model coloured by abundance, in seven 40 Mt (wet) increments
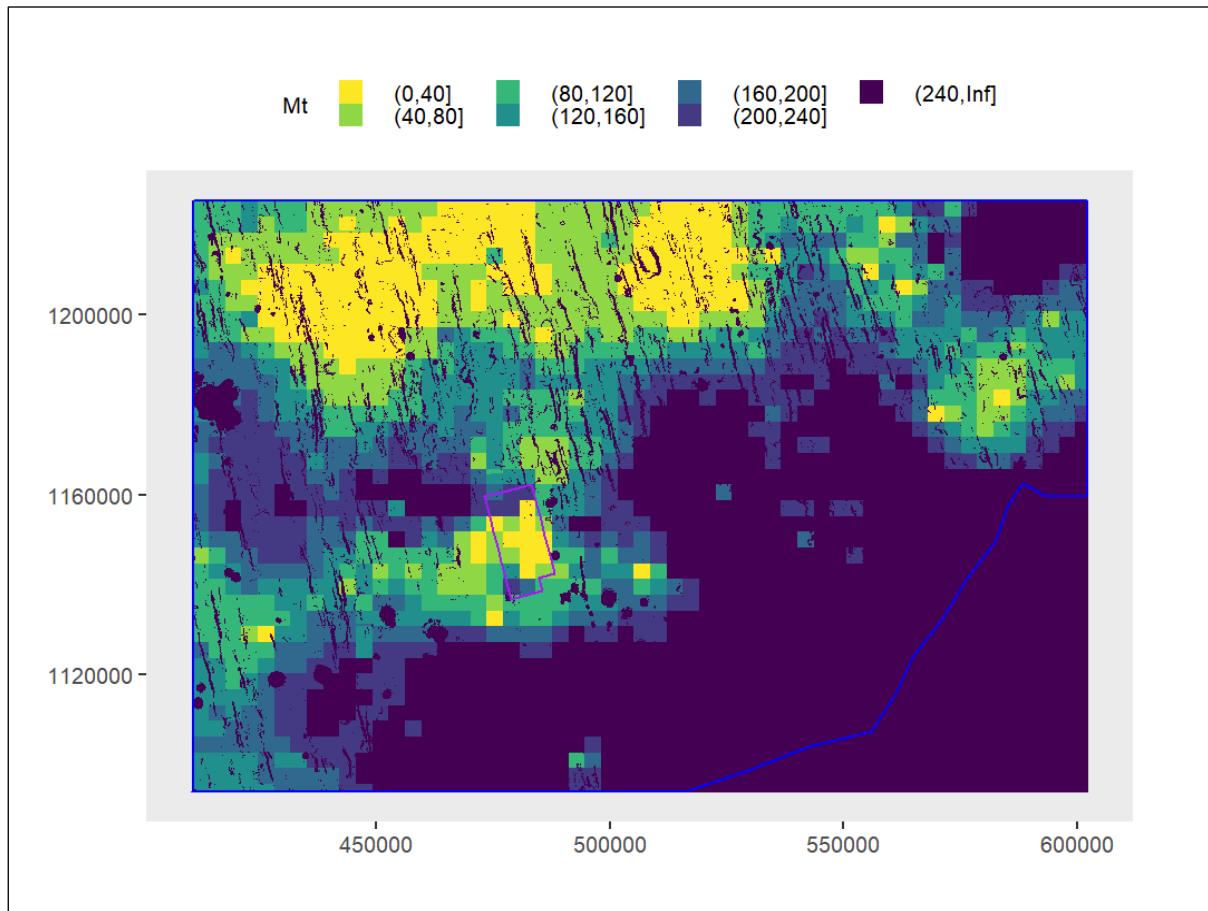
11.2.18 Comparison with previous resource estimates

The first resource estimate for NORI Area D, completed in 2012, was 399 Mt (wet) of polymetallic nodules and was based solely on historic samples.

In 2018 NORI completed a box core sampling campaign that focused on a small area near the centre of Area D which was selected as a potential trial mining site. Where box core sampling was conducted on a nominal 7 km by 7 km spacing and infilled with estimates of nodule abundance from seafloor photography on a 3.5 km by 3.5 km grid the Mineral Resource was classified as Measured. Where sampling was at a nominal spacing of 7 km by 7 km but did not have any additional photo-estimates of nodule abundance, the Mineral Resource was classified as Indicated. The additional samples resulted in an updated resource estimate of 383 Mt (wet), consisting of 4 Mt Measured and 34 Mt Indicated and 345 Mt Inferred Mineral Resources.

The latest exploration campaigns (2019) added box core sampling at a spacing of 10 km by 10 km across most of the remainder of NORI Area D. The latest Mineral Resource estimate (2020) is 356 Mt (wet), consisting of 4 Mt Measured and 341 Mt Indicated and 11 Mt Inferred Mineral Resources. Taking into account the conversion of the majority of Inferred to Indicated Mineral Resources, the remaining Inferred Mineral Resource has decreased by 26 Mt as a result of excluding the Volcanic High domain in the south-eastern corner of NORI Area D, due to uncertainty about the occurrence of nodules in this area. The 2020 resource estimate is also slightly higher in abundance (5.4% higher), and nickel

(6.1% higher), cobalt (5.4% higher) and manganese (2.2% higher) grades than the 2018 estimate.

Comparison of the area covered by Inferred, Indicated and Measured Mineral Resource for the 2020 estimate and the same area in the 2018 model shows that nickel grade has increased by 6% (1.32% to 1.40% Ni) while abundance has increased by 6% (16.0 to 17.0 kg/m^2). Mineral Resource tonnage has increased by 10% (from 10 to 11 Mt) in the Inferred area and 7% (from 320 to 341 Mt) in the Indicated area. The positive conversion rates arising from infilling the sampling grid with high quality box core sample data (rather than extending the area sampled) are exceptionally high compared to the typical outcomes from infill sampling of terrestrial mineral deposits.

To allow direct comparison between the 2018 and 2020 resource estimates the 2018 block model was converted to polygons, one rectangular polygon for each block, and then rasterized to match the 2020 raster model. The two models were combined by dividing the 2020 estimate of abundance at each raster pixel location by the 2018 estimate of abundance to obtain a conversion rate from the 2018 estimate to the 2020 estimate. The abundance conversion rate from the 2018 model to the 2020 model is shown in Figure 11.34. A value below 1.0 indicates a reduction in abundance and a value above 1.0 indicates an increase in abundance for the 2020 model over the 2018 model. Overall, the area previously identified as Measured and Indicated Mineral Resource has not changed other than some slight changes along the margins due to the addition of the 2019 Campaign 6A and 6B sampling. The biggest change is along the western margin where the area previously identified as Inferred_2 (not supported by sampling) has increased in abundance. Also, the abundance along the western margin of the Inferred_1 boundary (red dashed line on the plot) has decreased in abundance due to better constraint of higher abundance, historic sampling in the area. The biggest increase in abundance is in the north-eastern corner where it has increased by nearly a factor of 2.

Figure 11.34 Ratio 2020:2018 abundance estimates, showing the 2018 resource classification boundaries
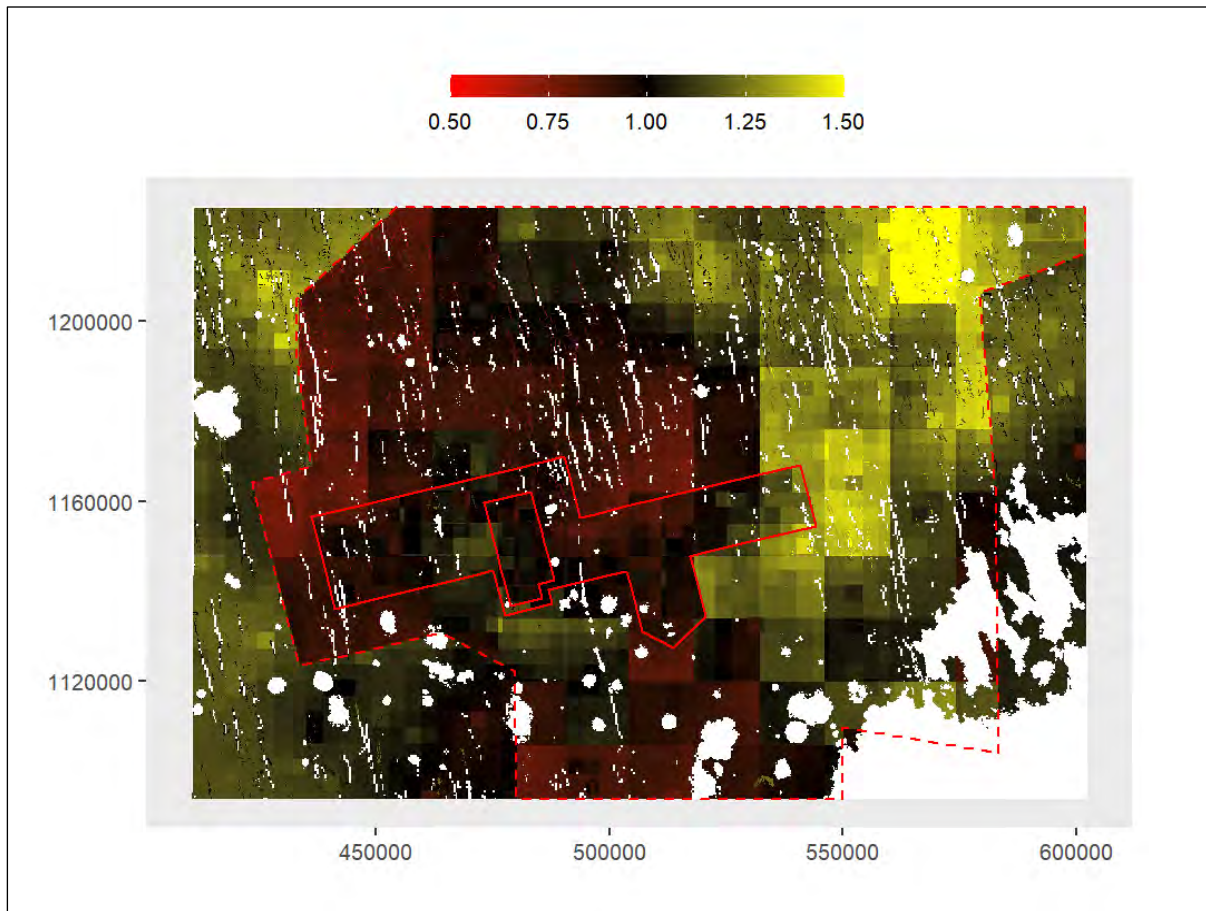
Note: Measured Resource: inner red solid polygon, Indicated Resource: outer solid red polygon, Inferred_1 Resource: dashed red polygon, Inferred_2 Resource: remainder

11.3 NORI Area A, B and C

The Mineral Resource estimates for NORI Areas A, B and C have not been updated. The existing Mineral Resource estimate generated by Golder in 2012 remains the current estimate. There has been no new exploratory work conducted in the areas to warrant an update to the estimates.

All information for this section has been summarized from Golder 2015 technical report. The information presented for NORI Area D in this section, is superseded by the information presented in Section 11.2.

11.3.1   Boundaries and geological domains

Based on the geophysical interpretation of the NORI multibeam there are areas identified as low nodule density and possible lava flows and outcrops in NORI Area C. These areas cover a lower percentage of NORI Area C than the areas identified as high, medium, or indeterminate nodule density. The areas identified as low nodule density and possible lava flows and outcrops are numerous, discontinuous, and are generally smaller than the average sample spacing. As such, no domaining was done using the mapped areas of potential lava flow and outcrop.

Since the NORI Area falls within a single bathymetric domain (abyssal hill province) and entirely within the CCZ deposit boundary, it was not considered necessary to domain the data for an Inferred Mineral Resource.

11.3.2   Nodule sample data

The polymetallic nodule data for NORI Areas A, B and C have not changed since the 2012 Mineral Resource estimate (Golder 2015). The nodule data used for the 2012 resource estimate included only the historic polymetallic nodule sample data. The summary statistics for this data is listed in Table 11.19. Note that this summary includes NORI Area D.

Table 11.19   Summary statistics of samples within the NORI Area used for the 2012 Mineral Resource estimate.

Variable	Samples	Missing	Min	Max	Mean	Var	CV	Median
Ni (%)	360	32	0.68	1.75	1.30	0.016	0.10	1.31
Co (%)	360	32	0.05	0.33	0.17	0.004	0.35	0.19
Cu (%)	360	32	0.40	1.50	1.10	0.028	0.15	1.13
Mn (%)	360	32	12.84	33.90	29.45	8.406	0.10	30.20
Abundance (wet kg/m^2)	392	0	0	52.2	11.9	64.303	0.67	12.00

Source: Golder 2015. Var = variance; CV = coefficient of variation; Ni = nickel; Co = cobalt; Cu = copper; Mn = manganese

11.3.3   Data processing

The data were checked for anomalous or erroneous data and cross-checked with data supplied directly by the ISA. Data preparation steps included in order:

- Data validation.
- Conversion of latitude/longitude coordinates to UTM coordinates using WGS 84 datum:
  — These areas cover several UTM zones but were overlaid to facilitate modelling of all areas in one model.
  — The minimum and maximum UTM coordinates for each of the NORI areas are listed in Table 11.20.
- A plan of the tenement or Area locations is presented in Figure 11.35.
- Resetting 0 assay values to missing and 0 abundance values to 0.01 where there are assay values.
- Application of top cuts (see Table 11.22).

Figure 11.35 NORI Areas A, B, C and D, showing location of historic data
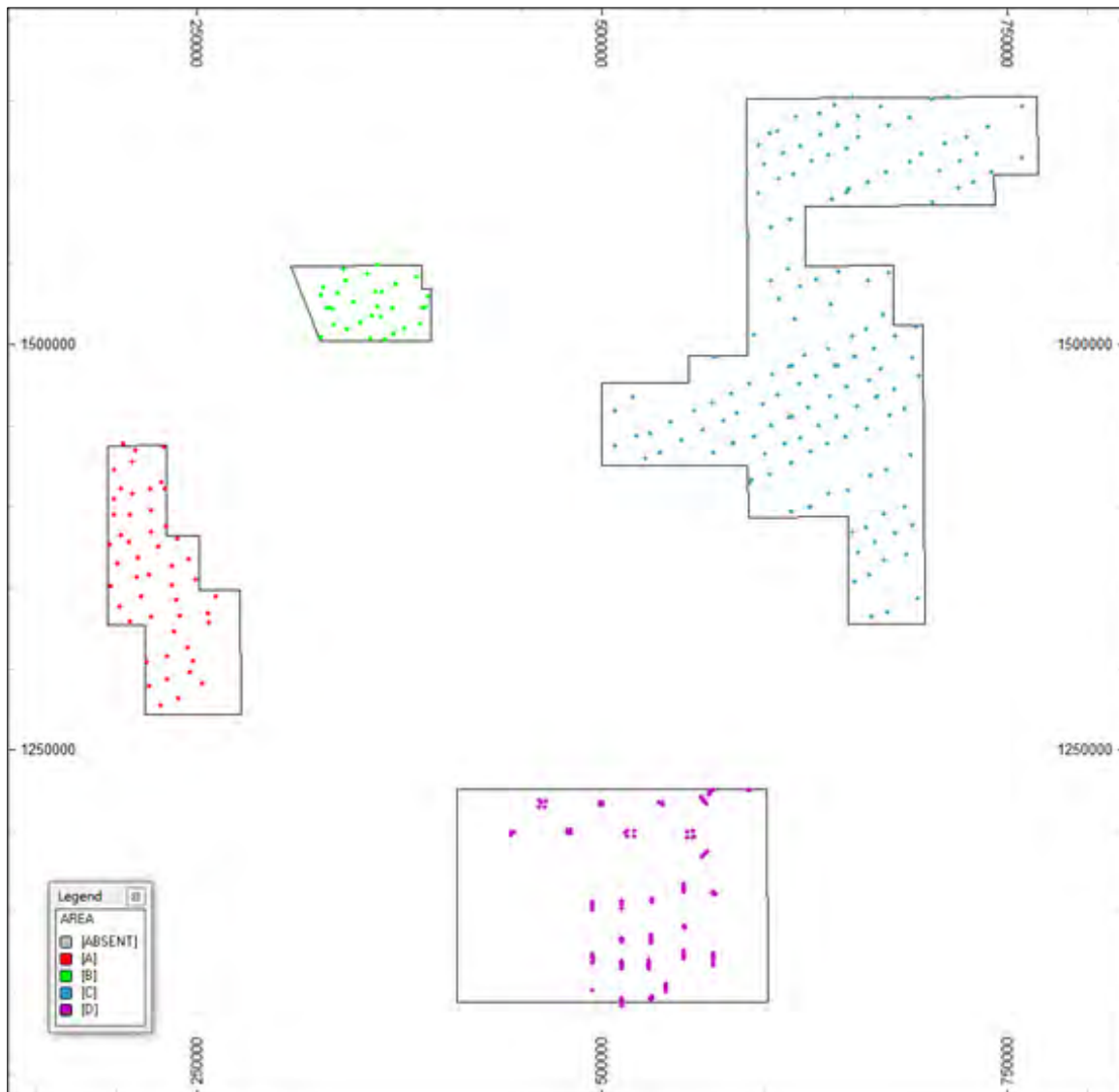
NB: Areas A, B, C and D cover several UTM zones but were overlaid to facilitate modelling of all areas in one model. The apparent distances between the Areas in this figure are not real distances.

Table 11.20   Minimum and maximum UTM coordinates for NORI Exploration Areas

NORI Area	Pioneer Investor		UTM Easting	UTM Northing	UTM Zone
A	Yuzmorgeologiya	Minimum	546318.6	1276704.2	8
		Maximum	612250.2	1438373.8	
B	Yuzmorgeologiya	Minimum	627009.7	1502544.4	8
		Maximum	693143.2	1548239.6	
c	IOM	Minimum	508307.5	1651913.6	10
		Maximum	759829.0	1331443.7	
D	BGR	Minimum	444252.3	1091225.8	11
		Maximum	592471.8	1224898.2	

Source: Golder 2015.Yuzmorgeologiya = State Enterprise Yuzhmorgeologiya (Russian Federation). IOM = Inter Ocean Metal Joint Organisation; AMR = Arbeitsgemeinschaft Meerestechnisch Rohstoffe.

11.3.4 Declustering

Declustering was used to remove potential biases in statistics that can arise from variable sample spacing, which can arise from the multiple sampling at close locations as the ship undertakes its voyage.

Normal cell declustering without any boundaries can present issues where the edge cells become overweighted as the cell size is increased. A modified cell declustering algorithm was used that weights the cells to the block model volume within each cell. The process provides a declustering weight which is used to weight the univariate statistics Table 11.21. For this method, the cell size was optimized for a square window size of 30 km and the origin offset 10 times.

Table 11.21   NORI Areas A, B, C and D declustered statistics (historic data only).

Variable	Samples	Min	Max	Mean	Var	CV	Median
Ni (%)	360	0.68	1.75	1.29	0.021	0.11	1.32
Co (%)	360	0.05	0.33	0.19	0.003	0.27	0.20
Cu (%)	360	0.40	1.50	1.08	0.035	0.17	1.12
Mn (%)	360	12.84	33.90	28.91	10.524	0.11	29.81
Abundance (wet kg/m^2)	392	0	52.20	11.57	66.736	0.71	11.00

Source: Golder 2015 Var = variance; CV = coefficient of variation

11.3.5 Top-cuts

The coefficient of variation is very small for nodule abundance, nickel, copper, manganese, and cobalt, suggesting that the application of top-cuts is not necessary. However, due to the wide spacing of samples, a top-cut was applied to trim the high (99.5th percentile) values to reduce the likely impact of the high-grade outliers.

The presence of outliers (extreme values) and the need to apply "top-cut" values or "capping" (where samples above a certain threshold are assigned the top-cut value) to sample populations was assessed using a number of techniques:

- Examination of grade distributions using cumulative probability plots.
- Statistical assessment of the grade distributions.
- Examination of the spatial locations of identified outlier samples.

Top cuts defined in Table 11.22 are roughly equivalent to the 99.5th percentile of the mineralized samples and do not have a significant impact on the average grade. Application of top cuts reduced the mean only for manganese, which was reduced by a very low 0.2% of the uncut mean. This is simply because the grades within the CCZ are very consistent due to the deposit's hydrogenetic and diagenetic origin.

Table 11.22   NORI Areas A, B, C and D top cuts used for NORI 2012 Mineral Resource estimate.

Variable	Top-Cut Value (%)
Ni	1.56
Co	0.31
Cu	1.46
Mn	33
Abundance	32

Source: Golder 2015

11.3.6   Spatial continuity

The variograms for NORI Areas A, B and C were not updated as there has been no new sampling collected from these areas since 2012. This Section is summarised from the Golder 2015 technical report.

The samples with top-cuts applied were used for variogram analysis. Traditional variograms showed good structure and were used for all variogram modelling. The variograms were scaled to the population variance. Variogram maps were calculated for the purpose of determining direction of greatest continuity. An example variogram (nickel) shown in Figure 11.36. Variogram models are presented in Table 11.23.

Table 11.23   Variogram models, NORI Area A, B and C

Variable	Nugget	Sill	Range Along Strike(km)	Range Cross Strike(km)
Ni	0.2	0.8	20	20
Co	0.2	0.8	30	30
Cu	0.2	0.8	30	30
Mn	0.2	0.8	50	50
Abundance	0.2	0.8	30	30

Figure 11.36 Variogram map for nickel, NORI Areas A, B and C
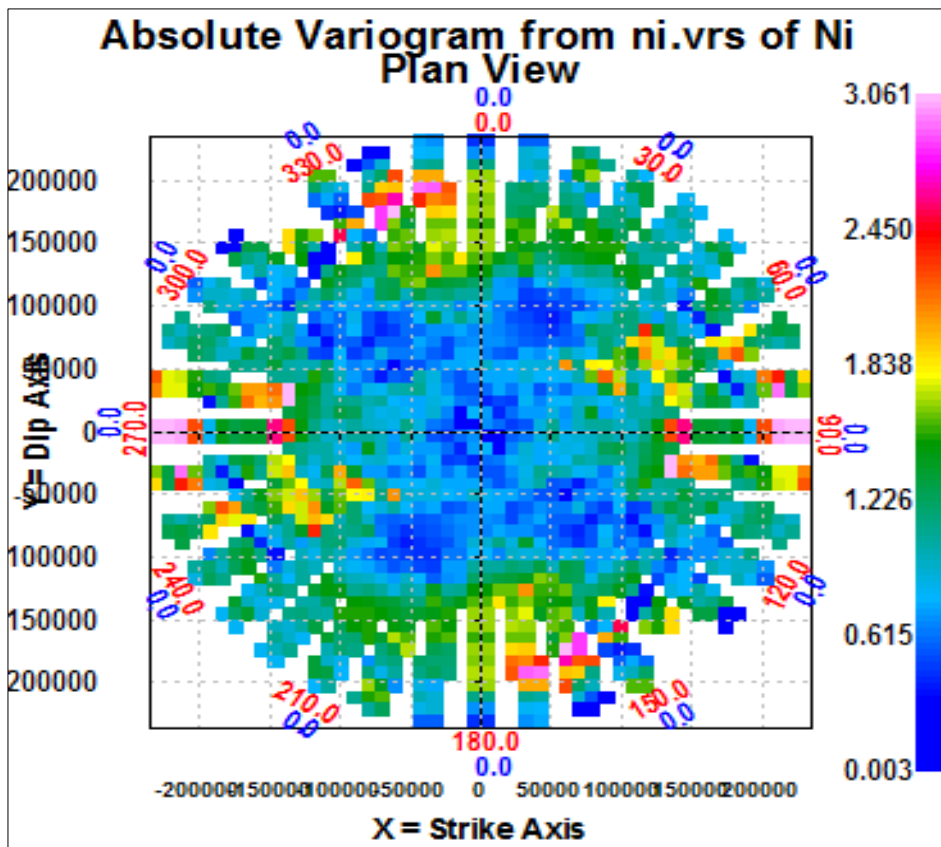
Where possible, variogram model parameters were retained at similar values between orientations, and between the different variables, so as not to produce artefacts in the estimations. This was done to ensure element relationships or correlations evident between samples were respected implicitly during estimation and reflected in the resource estimate. Also, the same type of variogram model was fitted to the experimental variograms.

Gaussian variogram models were fitted to the experimental variograms. Typically, spherical models are sufficient for modelling the spatial continuity, but in this case the Gaussian model better fit the data. Gaussian models give greater weight to the very close samples (in the range of 0 to 5 km) and then rapidly decay to the sill compared with the spherical model. This fits in with the likely short-range variability possibly being controlled by the ridges, which are of the frequency of 3 to 5 km and oriented approximately north-northwest.

The directions of greatest continuity from the variogram maps is 060° and 150°, which are roughly parallel and orthogonal to the broad regional trend of the CCZ. Smaller scale local trends oriented parallel with ridges are not visible in the wide-spaced data. The long-range experimental variograms for abundance are erratic with an almost nugget model.

Additional variogram parameters used in most cases for variogram calculation include:

- Single structure Gaussian models with common nugget and incremental sill levels.
- Lag distance of 5 km.
- Horizontal search angle of 15°.
- Vertical search angle of 15°.
- Horizontal distance of 30 km.

Major and semi-major variograms for nickel are shown in Figure 11.37.

Figure 11.37 Major and semi-major variograms for nickel (red line is actual data and blue line is modelled curve)
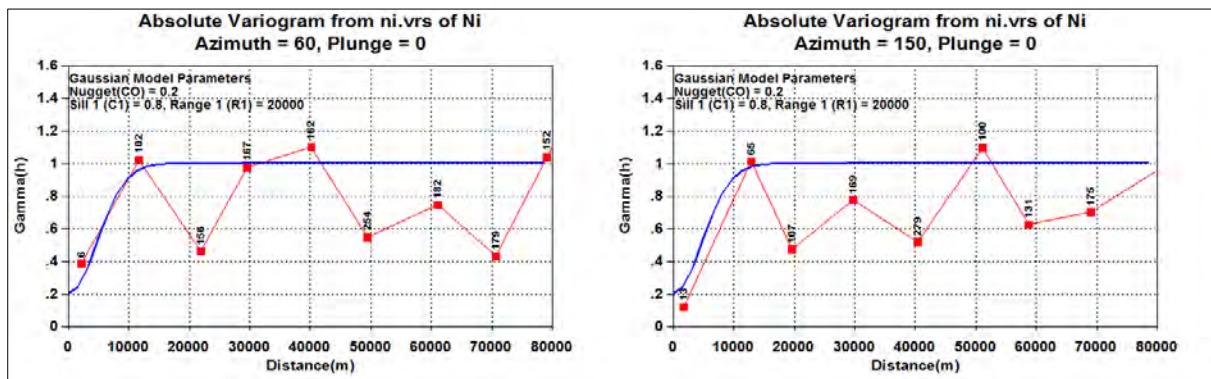
11.3.7   Geological block model

The block model contains 931 blocks, representing nickel, cobalt, copper, manganese, and abundance of polymetallic nodules. The model was built using the model framework defined in Table 11.24 and with additional block attributes listed in Table 11.25. A vertical block size of 1 m was used, essentially creating a two-dimensional model. The 1 m thickness is simply to give the blocks a default value. The tonnage of nodules in each block was estimated from the surface area of the block multiplied by the abundance estimate.

Blocks were added to the model using the limits of the NORI Areas. Parent blocks were split into sub-blocks to ensure reasonable resolution of the tenement boundaries.

Table 11.24   NORI Area A, B and C block model framework (UTM coordinates).

	Easting	Northing	Elevation
Model origin (m)	195000	1093000	−0.5
Model limit (m)	775000	1653000	0.5
Model extent (m)	580000	560000	1
Parent block dimensions (m)	10000	10000	1
Number of parent blocks	58	56	1
Minimum sub-block size	500	500	1

Table 11.25   NORI Area A, B and C model variables.

Variable	Type	Description
AREA	alphanumeric	Tenement area (A to D)
Ni	numeric	Estimated Ni weight % value
Co	numeric	Estimated Co weight % value
Cu	numeric	Estimated Cu weight % value
Mn	numeric	Estimated Mn weight % value
Abundance	numeric	Estimated nodule abundance wet kg/m^2

The total area of the block model is 74,840 km^2 which is 100.01% of the actual total area of the NORI Area of 74,830 km^2. This indicates that the sub-blocks were adequate for estimating the NORI Area boundaries.

11.3.8   Estimation of nodule abundance and grades

Ordinary kriging (OK) was used to estimate nickel, cobalt, copper, manganese, and abundance in the block model. Grades were estimated on a parent block basis using block discretisation of 3 by 3 by 1. Grades were also estimated using IDW to the power of 2 and NN for validation of the OK estimates.

To ensure that all blocks in the model had values for nickel, cobalt, copper, manganese, and abundance, a three-pass elliptical search strategy was used for selecting the neighbouring samples for estimation. Dimensions of the search ellipse radii were based on the ranges of the variogram models and average sample spacing. The search pass ellipse radii that were used are:

- PASS 1: 30 km by 30 km.
- PASS 2: 60 km by 60 km (pass 1 expanded by a factor of 2).
- PASS 3: 90 km by 90 km (pass 1 expanded by a factor of 3).

A minimum of 1 and a maximum of 8 samples were allowed per octant for each search pass, with a minimum of 4 and maximum of 32 samples per estimate. The required minimum number of samples per estimate was relaxed to 1 sample for the third search pass. The relatively large number of samples used in the estimate will ensure the estimates are smoothed for this early stage of evaluation.

To complete the block estimates and avoid potential issues for missing grades the third and final search passes used large search radius to ensure most relevant blocks were assigned estimated grades. This ensured that nearly all mineralised blocks were assigned estimates. Any remaining unassigned grades were set to 0.01% for nickel, cobalt, and copper, and to 26.86% for manganese.

11.3.9   Cut-off grade

Due to the extremely low variance in the grades and the high metal content of the nodules, a cut-off based on abundance is appropriate for determining the limits of economic exploitation. A cut-off of 4 kg/m^2 abundance was chosen for the NORI Contract Area, based on the estimates of costs and revenues presented in this report, generalized as follows:

- 1.7 Mt minimum annual tonnage mined;
- $0.25 Million/km^2 for offshore operating costs
- 1,036 km^2 collected area processed
- $95/ dry tonne for transport costs;
- $119/dry tonne for processing costs;
- $15/dry tonne for corporate, general and administrative costs;
- $33/dry tonne for ISA and state royalties;
- 95% recovery of nickel at an assumed price of nickel metal $16,472/t;
- 86% recovery of copper at an assumed price of $6,872/t copper metal;
- 77% recovery of cobalt at an assumed price of $46,333/t cobalt metal;
- 99% recovery of manganese at an assumed price of $4.50/dmtu manganese in manganese silicate.

The method of calculation for the cut-off determines the minimum average nodule abundance needed during steady state operations such that the revenue minus costs (excluding capital) is greater than zero. Revenue includes metal pricing and metallurgical processing recoveries, and the costs include the collection, transport, processing, corporate costs, and royalties.

The price estimates are long term (2034 – 2046) forecasts provided in a report by CRU International Limited (CRU, 2020). The Qualified Person considers that this timeframe is reasonable in view of the likely time required to bring the majority of the NORI mineral resources into production.

11.3.10   Mineral Resource classification

Resource classification was done on the basis of the quality and uncertainty with the sample data. Accordingly, NORI Areas A, B and C are considered to have sufficient continuity to warrant Inferred Mineral Resource classification in accordance with SEC Regulation S-K (subpart 1300).

In the Qualified Person's opinion, the Mineral Resources have reasonable prospects of economic extraction. No fatal flaws have been identified. It is reasonable to expect that, with further engineering design and testwork, the technical and economic factors relevant to the collection of nodules and the extraction of nickel, cobalt, copper and manganese products from the nodules can be resolved. Accordingly, it is the Qualified Person's opinion that all issues relating to all relevant technical and economic factors likely to influence the prospect of economic extraction can be resolved with further work.

11.3.11   Estimation Results

The nodule abundance and tonnage curves for various nodule abundance cut-offs (kg/m^2) are presented in Figure 11.38. The curves indicate rapid reduction in global tonnage between abundance cut-offs of approximately 6 to 20 kg/m^2, which brackets the mean abundance for the NORI Area.

Figure 11.38 NORI Area A, B and C Mineral Resource abundance tonnage curves
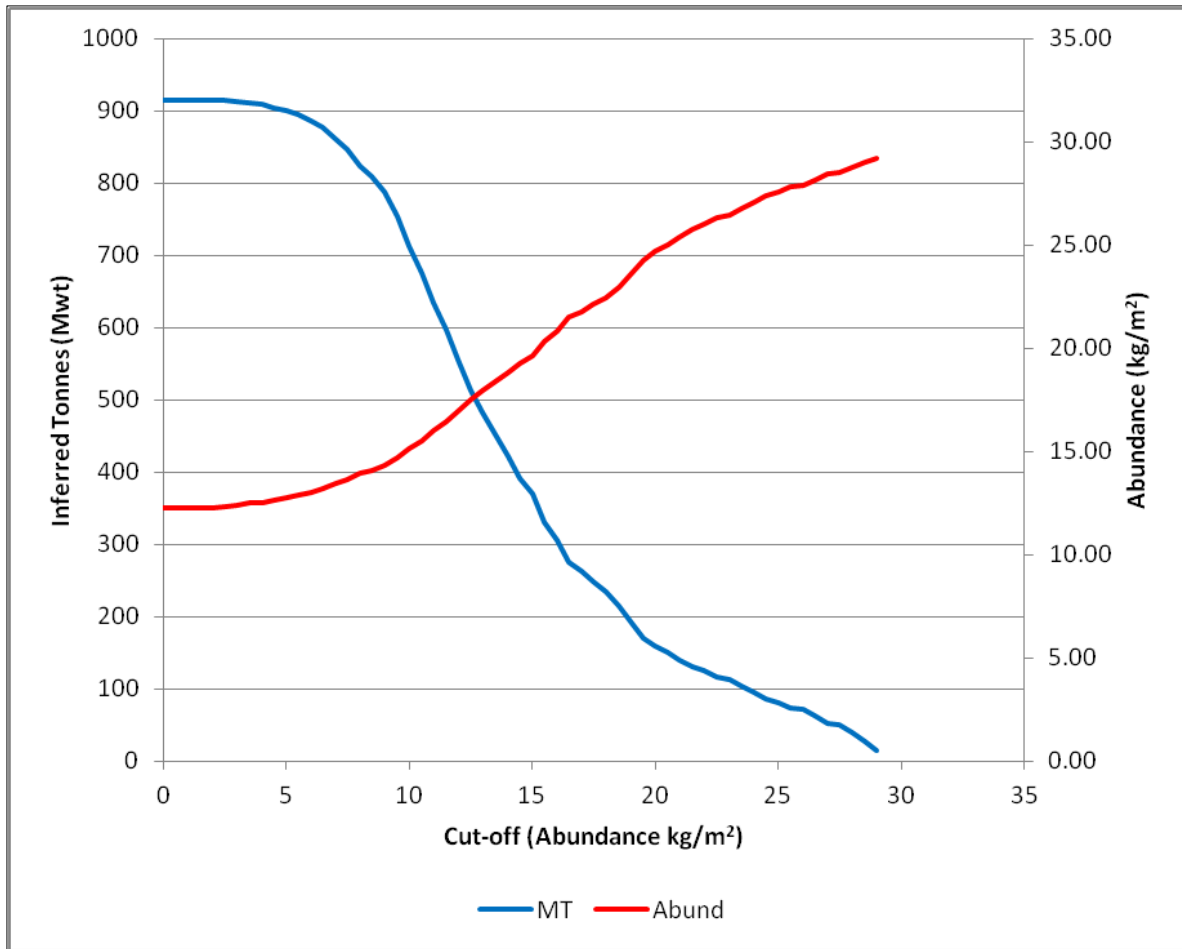
The Mineral Resource, with an effective date of 31 December 2020, is reported in Table 11.26 at an abundance cut-off value of 4 kg/m^2. This cut-off is justified by the estimates of costs and revenues presented in this Initial Assessment.

Table 11.26   NORI Area A, B and C Mineral Resource estimate, in situ, at 4 kg/m^2 abundance cut-off

NORI Area	Category	Nodule tonnage (Mt (wet))	Abundance (wet kg/m²)	Ni (%)	Cu (%)	Co (%)	Mn (%)
A	Inferred	72	9.4	1.35	1.06	0.22	28.0
B	Inferred	36	11	1.43	1.13	0.25	28.9
C	Inferred	402	11	1.26	1.03	0.21	28.3

Source: Golder 2015. Note: Tonnes are quoted on a wet basis and grades are quoted on a dry basis, which is common practice for bulk commodities. Moisture content was estimated to be 24% w/w. These estimates are presented on an undiluted basis without adjustment for resource recovery.

Figure 11.39 shows sample locations and estimated block grades for nickel (similar plots for copper, cobalt, and manganese are included in Appendix C). Figure 11.40 shows sample locations and abundance within the NORI Area. The figures indicate there is continuity of grade and abundance at ranges (40 to 80 km) several times greater than the average sample spacing. The patterns in distribution appear consistent between nickel, copper, cobalt, and manganese, reflecting the homogenous nature of the nodule chemistry across the NORI Area.

Figure 11.39 Map of sample distribution and block model estimates of nickel, NORI 2012 estimates
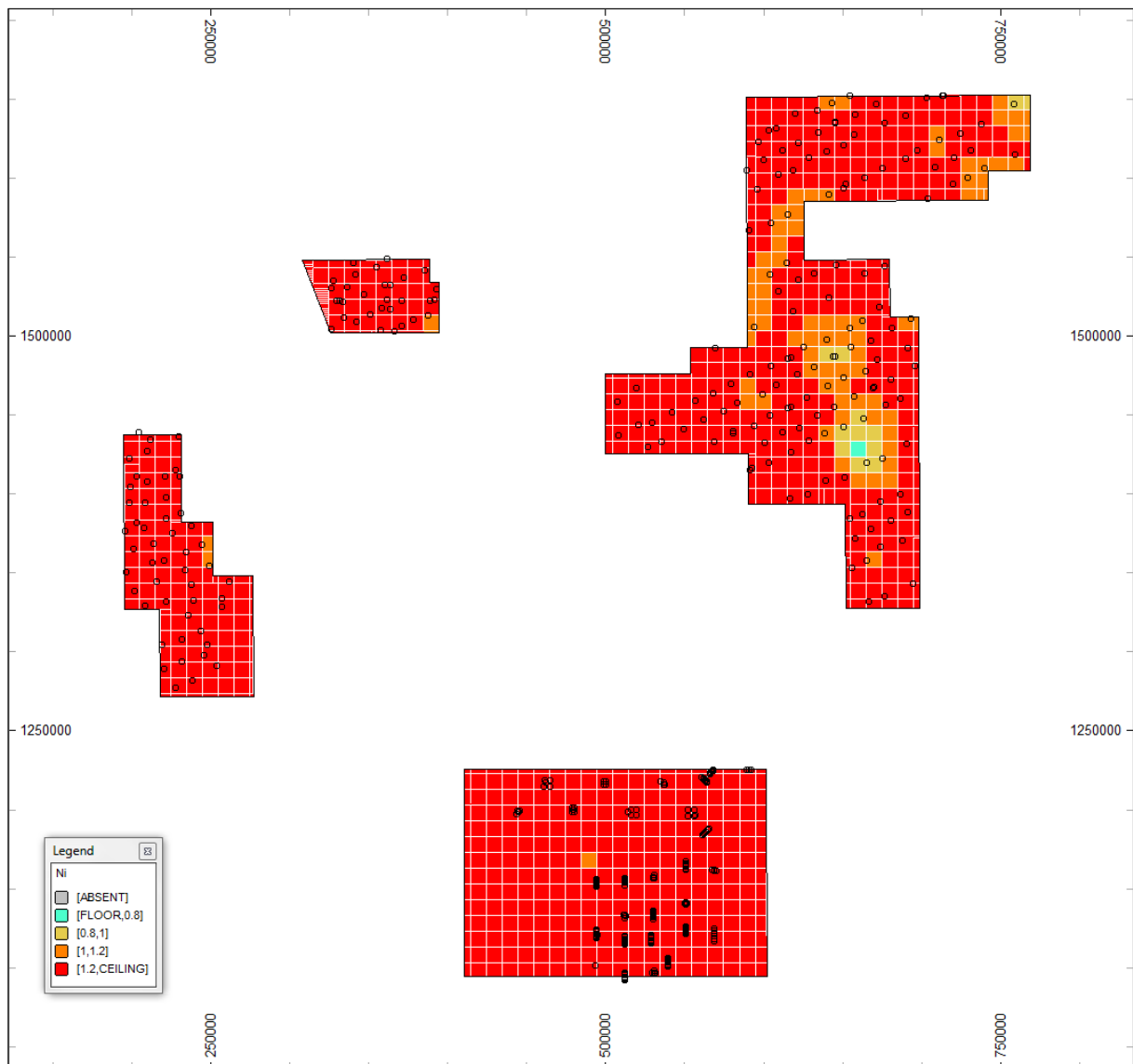
NB: Areas A, B, C and D cover several UTM zones but were overlaid to facilitate modelling of all areas in one model. The apparent distances between the Areas in this figure are not real distances.

Figure 11.40   Map of sample distribution and block model estimates of abundance, NORI 2012 estimates
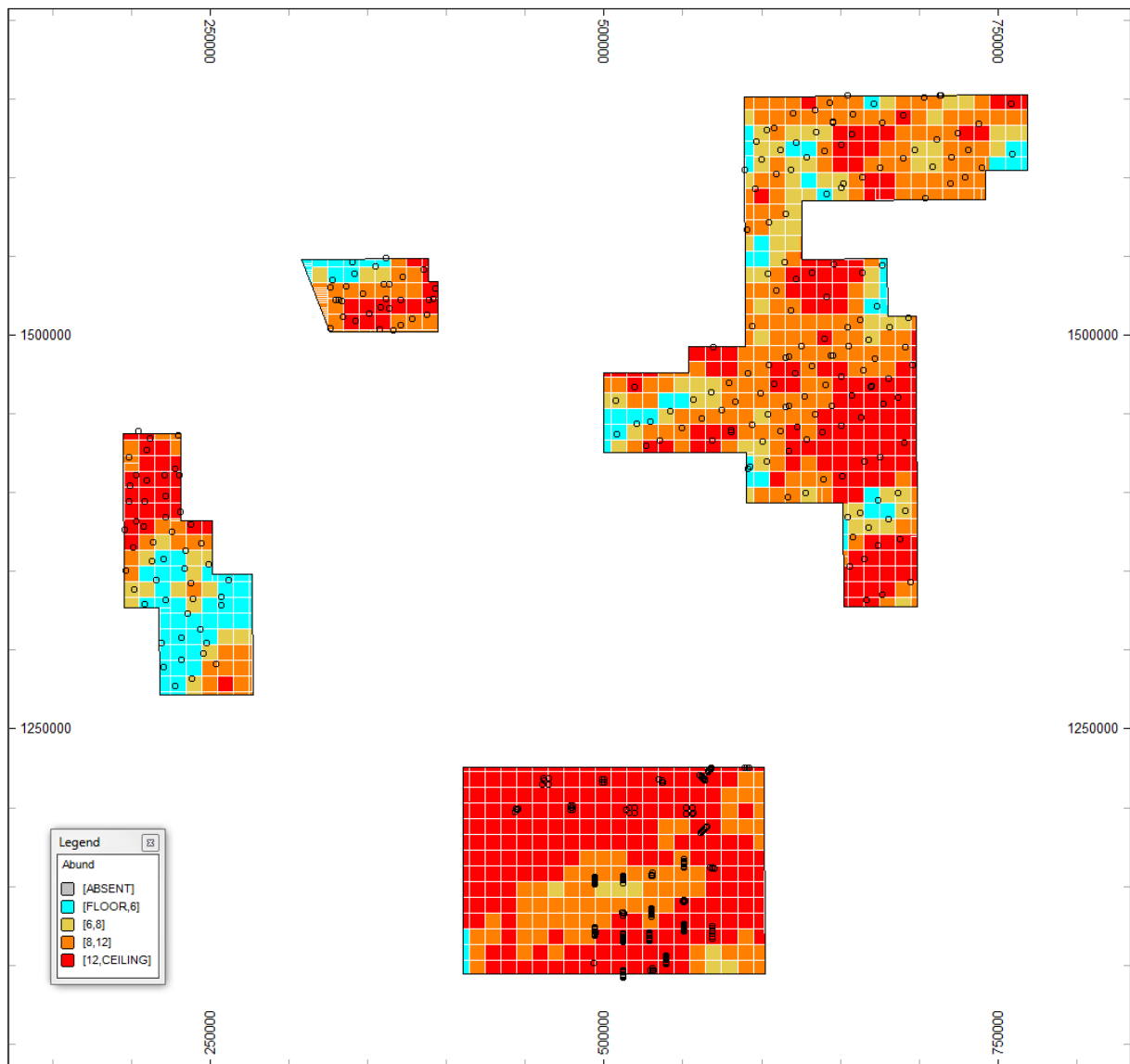
12 Mineral Reserve estimates

There are no Mineral Reserve estimates for the NORI Property, and the potential viability of the Mineral Resources has not yet been supported by detailed mine design or optimization processes nor a pre-feasibility study or a feasibility study.

13 Mining methods

This Section provides a description and operating concept for the proposed nodule collection at NORI Area D. The seabed system is an extrapolation of existing technologies in deep ocean operations and previous seabed development activities. Much of the technology is a direct derivative of previous experience in nodule developments, such as consortium activities in the 1970s, including significant pilot testing, and advances in deep water oil and gas development. There still remain particular component and sub-systems that are not "off-the-shelf" and require further development. The technical readiness of some of the described components and assumptions need to be verified by further testing.

13.1 Development plan

NORI proposes to implement the project in multiple phases that will allow the seafloor production systems to be tested and then nodule production to be gradually ramped up. The phased approach will facilitate de-risking of the project for relatively low initial capital investment. The proposed development phases are as follows:

- The Collector Test is designed to perform proof of concept for the methods of collecting and lifting the nodules while acquiring sufficient data to design a commercial system. Nodule collected during the Collector Test would be stored on the Hidden Gem and brought to shore for use in large scale process pilot testing. The Collector Test would use a converted sixth generation drillship, the Hidden Gem. The Collector Test would not demonstrate the transhipment of nodules to a shore-based facility.
- Project Zero would be an extension of the Collector Test using an upgrade of the converted drillship to produce a sufficient and continuous quantity of nodules to support a relatively small commercial operation of about 1.3 Mtpa (wet) nodules delivered to a shore-based facility. This operation would demonstrate a more continuous mining operation at a larger scale than the Collector Test and would demonstrate the transhipment of nodules to a processing facility. This initial commercial system would operate for five years.
- Project One would increase production in a further three steps:

  — a further upgrade of the Hidden Gem for up to 3.6 Mtpa (wet) production, for a 20-year production life.
  — introduction of a second converted drillship (Drill Ship 2) with a capacity of up to 3.6 Mtpa (wet), designed for a 20 year production life.
  — construction of a new purpose-built production support vessel (Collector Ship 1) with capacity of up to 8.2 Mtpa (wet). Project One would benefit from lessons learned on the Collector Test and Project Zero.

All projects involve similar methods for collection of nodules: a self-propelled collector using hydraulic methods to pick up the nodules from the seafloor, and an airlift driven riser and lift system (RALS) to raise the nodules to the surface. Project Zero and Project One would both deliver nodules in the form of a slurry to a bespoke converted bulk mineral carrier positioned aft of the production support vessel (PSV) and connected by floating slurry hoses. The nodules delivered to the transport vessels would be dewatered and placed in the cargo holds, while the water would be returned to the PSV via separate floating hose and disposed of at some depth through a special riser fall pipe.

The main differences are in the specific vessels (converted drillship or new build), the number of collectors operating in tandem and the scale of the operation.

13.2 Off-shore system concept

The off-shore system concept for Collector Ship 1 is illustrated in Figure 13.1. Nodule collection will be managed from PSVs on the surface. The nodules will be collected from the seafloor by self-propelled, tracked, collector vehicles. The collector design includes technology for reducing or eliminating the introduction of sediment into the lift system. This technology is being developed by Deep Reach Technology, Inc. under funding from the U. S. Department of Energy. Deep Green is participating in this research by contribution sediment samples from the NORI Area D box cores.

Material collected by the collector vehicles will be pumped into a concentrator / hopper where fine material and excess water will be separated, yielding a higher concentration slurry, which will be transferred via flexible hoses to the RALS. The RALS consists of steel riser pipe engineered with varying diameter and bundled with buoyancy and other auxiliary lines. The sub-sea flexible hose and RALS architecture is based almost entirely on standard deep-water components from the upstream oil and gas industry.

Lifting will be accomplished using an airlift method. Compressed air will be inserted in the riser pipe at approximately 1,500 m depth, resulting in low density in the mixture above this point. The density difference causes suction in the lower section of the RALS, which results in lift of the nodule slurry. Airlift systems were proven during trial nodule recovery operations at site in the 1970s (Lecourt & Williams, 1971, Kaufman, Latimer, & Tolefson, 1985, Shaw, 1993) and are currently used in shallow off-shore diamond mining operations in South Africa at approximately 120 m depth (MHWirth, 2020).

To achieve a high-efficiency airlift operation, and to limit the exit velocities, the discharge of the airlift mixture will be pressurised to 800 kPa. The slurry will first be discharged into a pressurised surge tank and subsequently fed to a pressure let-down system to reduce the pressure to atmospheric. The flow from the pressure let-down system will be either pumped to a transport vessel or, if a transport vessel is not connected, to buffer storage tanks on board the PSV.

The collector vehicles will make parallel, linear traverses of the seafloor. Long collection paths are regarded as favourable as that will minimize the number of turns required to start a new collection path. The collector vehicles will turn 180° in a wide arc, by operating the inner and outer tracks at different speeds. The PSV will adjust its position and the position of the RALS in coordinated movements.

Figure 13.2 is a schematic diagram of the overall flow process in the extraction operation.

Figure 13.1   Overall extraction operation
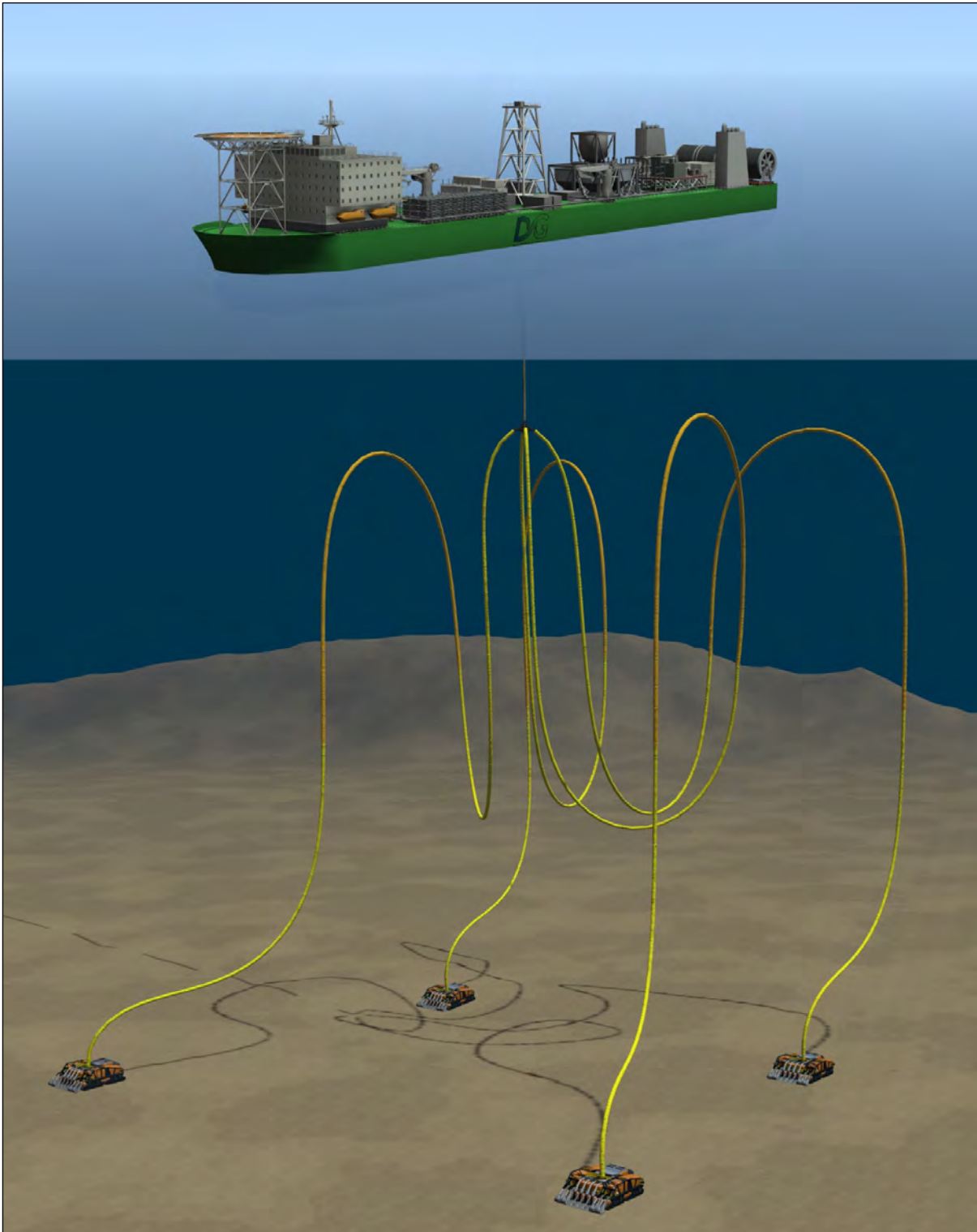
Source: NORI

Figure 13.2   Flow of nodule material
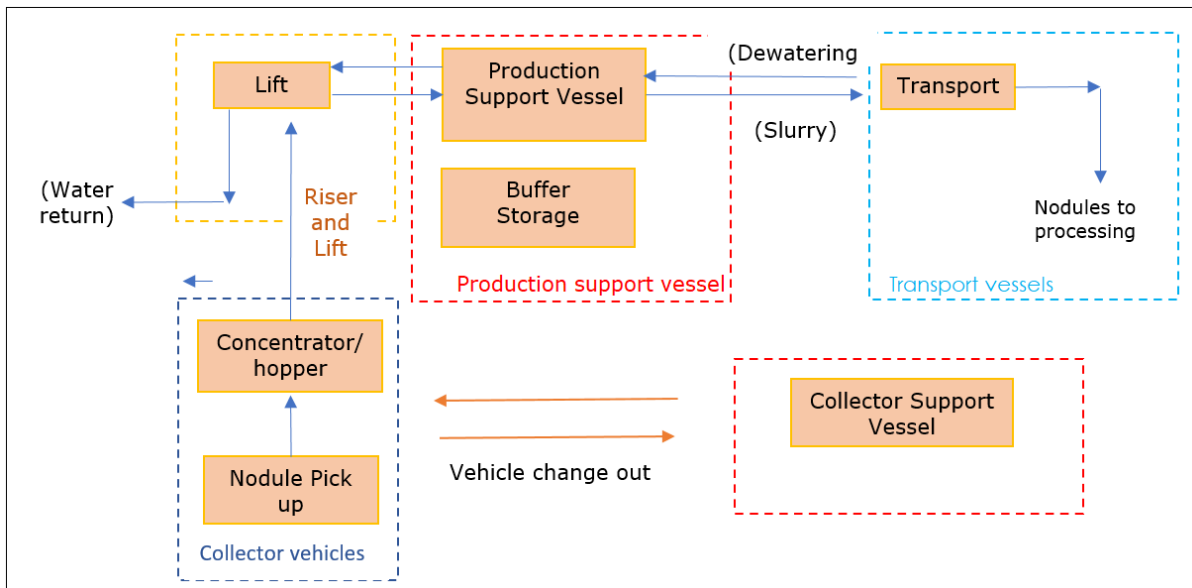
The basic design parameters adopted for the off-shore systems are presented in Table 13.1. The parameters are updated from a scoping study by Deep Reach Technology, Inc. (2015). The nodule recovery efficiency is based, in part, on tests performed in the 1970s for KCON by Marconaflo Corporation on a decanted sample of a nodule slurry produced in a pump loop simulating comminution in a lift pump system. System availability is an average including allowances for periodic (5-year) special surveys of the vessel requiring drydocking. The nodule production sequence and the financial model consider the timing of these surveys.

Table 13.1   Key design data for off-shore systems

Parameter	Project Zero	Project One	
Maximum annual production (Mtpa (wet))	1.3	3.6	8.5
Nodule abundance (kg/m^2 (wet))	20	20	20
Mining recovery efficiency (%)	77%	77%	77%
Annual system availability (days)	229	229	267
Maximum seabed slope	6°	6°	6°
Moisture content of dewatered cargo	10%	10%	10%
Size distribution of dewatered cargo	95% minus 16 mm, 5% minus 0.5 mm	95% minus 16 mm, 5% minus 0.5 mm	95% minus 16 mm, 5% minus 0.5 mm

13.3 Geotechnical considerations

The physical characteristics of the seafloor sediments will have important influence on the mobility of the collector vehicles, the detailed design of the collection path, and the volume of sediment that will be disturbed by production activities. Little data was available for NORI Area D prior to 2018 but, as described in Section 9.35 and 9.4.4, NORI systematically collected geotechnical measurements from box core samples in Campaigns 3, 6A and 6B (Fugro, 2019). Analysis of the data is still at an early stage.

UTEC Geomarine (UTEC) completed a review of the track selection and sizing of the collector vehicle, as part of the scoping study project completed by DRT. For the purpose

of the scoping study, it was assumed that the subsea collector will be self-propelled and use either a tracked system with skid steering or an Archimedes Screw Driven (ASD) system. UTEC noted that tracked systems have been proven reliable and versatile system for subsea vehicles such as mining vehicles and trenching machines, whereas ASD vehicles have only been proven for land-based usage.

The geotechnical parameters used as input to the study were based on a report on the sediments cored on Leg 86 of the Deep-Sea Drilling Project (Schultheiss, 1985), this document was not sighted by AMC as part of this review. The report considered the track designs for sea floor clays with the material strength parameters presented in Table 13.2.

Table 13.2   Geotechnical properties of clays defined by UTEC, 2015.

Depth (m)	Shear Strength (kPa)	Submerged Unit Weight (kN/m^3)
0–5	2–7	2.74

Using the parameters in Table 13.2 UTEC calculated:

- Maximum bearing pressures, for clays with a uniform shear strength of 2kPa and 10kPa.
- Mobility envelopes for clays with a uniform shear strength of 2kPa and 10kPa.
- Immediate settlement was only calculated for clay with a uniform shear strength of 10 kPa.
- The effect of the collector vehicle loading on slope stability for slopes between 2° and 20°.

A range of vehicle loads were studied over a range of slopes, both in roll and in pitch, in varying soil strengths. UTEC noted that it was difficult to draw any firm conclusions although it appeared that slopes of greater than about 3° to 5° have the potential to generate stability difficulties for the collector vehicle.

UTEC provided recommendations to DRT for the track area and submerged weights for the collector vehicle, based on estimates of the ultimate and dynamic bearing capacities. UTEC also recommended further investigation into the efficiency of skid-steering, and the dynamic effects of the collector vehicle on the bearing capacity of the sea floor clays.

During the Campaign 3 box coring program, undisturbed samples were brought to the surface and either sent for laboratory testing or were subject to testing on board the ship. The Campaign 3 data suggests that below the top 400 mm the shear strength range considered in the UTEC report is valid. Very low residual shear strengths were also recorded, with undrained shear strengths between 0.5 and 1.5 kPa below 400 mm. These very low residual strengths would result in soft or boggy conditions in high traffic areas depending on ground disturbance. At the mine design stage, the collector paths are to be designed to minimize movement over previously disturbed areas.

Submerged unit weights below 400 mm were estimated to vary between 1.65 and 2.25 kN/m^3. These values are lower than the 2.75kN/m^3 used by UTEC in their stability analysis work. Potentially this could reduce slope stabilities further when a loading is applied to the slope.

The geotechnical data collected during Campaign 6A and 6B provided more detailed characterization of the seafloor sediments and produced results broadly consistent with the earlier testing.

Based on the geotechnical reports provided, the seabed will comprise around 110 mm of dark brown clayey silt sludge overlying a very soft yellow brown, clayey silt. The yellow brown clayey silt has a typical undrained shear strength between 3–10 kPa, which is consistent with the assumptions in the 2015 UTEC study.

Further stability analysis and 3D numerical modelling are required to improve the reliability of the geotechnical assessment. The Collector Test will provide critical information and allow calibration of performance of the collector vehicle on a range of slope angles. This will provide a basis for improvement of design and operating parameters.

13.4 Collector Test and Hidden Gem conversion

NORI plans to conduct a Collector Test in 2022. This will test the systems for nodule collection and will have a design production rate of 1800 tpd (wet), or about 75 tph, but it will not transport nodules to shore.

NORI entered into a contract with Allseas Group S.A. (Allseas), in July 2019, to develop and deliver the Collector Test. DeepGreen also entered into a strategic alliance agreement with Allseas, where Allseas will undertake the development and operation of a system to collect 200 Mt of nodules from NORI Area D. In February 2020, Allseas acquired the Hidden Gem, a Samsung 10,000 drillship, to undertake the Collector Test and with the aim of supporting Project Zero Figure 13.3.

Figure 13.3   Hidden Gem drillship (courtesy Allseas)

Source: NORI

Allseas (Bosland, 2020)proposes to convert the Hidden Gem from 6th generation drillship to a vessel to support the Collector Test, as follows:

- The Hidden Gem would be refurbished and recertified for the Collector Test under Lloyds Rules. Thrusters will be removed and seals replaced during the docking period, before reinstalling.

- The main derrick and associated riser handling equipment will be reactivated and certified. All equipment for handling drill pipe and perform drilling operations that is obsolete for the intended prototype test will systematically be isolated from the operating systems, maintenance seized and ultimately be removed from the vessel. This will include drill pipe, top drive, marine riser, mud pumps etc.

- All cranes will be certified and operations including man riding certificates.

- For mining operations, the Hidden Gem will be equipped with a prototype mining collector and 4.2 km 8″ airlift riser, corresponding to a 20% prototype scale. The system will have a production capacity of 420 ktpa (wet).

- The collector dry weight is 75 t. The collector nozzle array spans 6 m width and can travel at maximum 0.5 m/s.

- The collector comes with a dedicated launch and recovery system (LARS) rated 90 t safe working load (SWL) that can deploy a <10m wide collector. For the deployment it will use its 1MW aramid reinforced umbilical, with a 35 t SWL. The LARS will be installed on portside aft between frames 49 and 55.

- Nodule collection operations will be supported by a dedicated deep-water WROV from Schilling rated for operational water depths up to 4,500 m. Launch and recovery will be from starboard aft between frames 30 and 35.

- The crude oil tank between frames 67 and 76, with 5910 m^3 capacity will be converted to store the 3,600 t of nodules that will be collected during the Collector Test. This tank will have a top hatch that allows access after Collector Test to offload the 3600t nodules using bulk grab and mobile bob cat lowered onto the tank top.

- Nodule dewatering and separator placed on main deck on top of nodule storage tank. Separator will be a double shaker deck that can process 80t/hr. It includes the permanent work consisting of piping from riser head and to storage tank.

- Flexible TCP jumper hose ID 7″, including connectors and buoyancy to connect the collector to riser base in a submerged lazy-S configuration. Jumper hose has dedicated reel and a LARS for deployment over the vessel side starboard aft of drill tower between frames 75 and 80.

- Containerised air compressor spread will be demobilised after the Collector Test. The base case for the Collector Test is to rent three containerised sets. Piping to connect and supply will remain as part of the permanent work.

13.5 Project Zero

NORI plans to commence commercial operations on a small scale (Project Zero) with low capital cost, using the Hidden Gem with further modifications after the Collector Test.

Project Zero would initially deliver up to 1.3 Mtpa (wet) of nodules to a shore based processing or stockpiling location (transportation and logistics are discussed in Section 18). This project phase will serve as a proof of concept of the entire mining operation (including pyrometallurgical processing).

Project Zero will be designed to produce for up to 5-years before dry docking for refurbishment. The results of initial operations will be used to optimize the design for Project One.

NORI asked DRT to evaluate upgrade of the Hidden Gem from the Collector Test to Project Zero. DRT's evaluation (Deep Reach Technology, Inc., 2020) is based on the information received from Allseas (Bosland, 2020), regarding the conversion of the Hidden Gem from 6th generation drillship to a vessel to support the Collector Test. Based on this information and assessment of the drawings and specifications of the original Vittoria 10,000 Samsung

drillship, DRT assumed that upgrading the Hidden Gem for Project Zero, would involve these steps:

- Addition of collector heads and modifications to the existing Collector Test collector to achieve 8.7 m effective collection width.
- Upgrade of the LARS umbilical winches to accommodate a larger umbilical for deploying the collector and powering it.
- Adding airlift pressure let-down system.
- Adding a compressor module to drive the airlift.
- Replacing the Collector Test 8″ riser with a 12″ riser with appropriate larger diameter sections for the airlift.
- Adding a decanting weir to the buffer storage for gravity separation.
- Adding a hopper and re-slurrying equipment (in-tank Dyna-Jets) to the buffer storage tank for offloading.
- Adding a material handling system including piping, pumps, offloading reels with hoses to transfer nodules to a transport vessel.

Other than the information presented above, DRT has not participated in any design reviews nor is DRT privy to detailed information about the Collector Test design. The assumptions DRT has made need to be verified.

The transport model for Project Zero indicates that two 35,000 dwt bulk mineral carriers are required assuming the nodules will be transported to a port on the west coast of Mexico. Under the assumed conditions the loading time is greater than eight days, and the queuing model indicates a returning vessel would arrive while the other vessel is being loaded. The loading time includes interruptions for collector maintenance. The minimum buffer storage, to avoid shut down for transport unavailability, would be the time to break a connection and makeup a new connection, or about 6 – 8 hours. This corresponds to about 2,700 t minimum buffer capacity required, which is within the capacity given above for the Collector Test.

13.6 Project One

Project One would be the progressive implementation of larger scale operations to ultimately achieve nodule production of up to 14 Mtpa (wet) from three vessels.

The Hidden Gem would be upgraded to include two 12 m collector vehicles and a larger riser to achieve a nominal capacity of up to 3.6 Mtpa.

A second modified drillship, Drill Ship 2, would also be commissioned with two 12 m collector vehicles.

Hidden Gem and Drill Ship 2 would be joined by a new purpose-built PSV, Collector Ship 1, that would commence production in 2026 with two 12 m wide collectors. A third collector would be added at the end of 2026 and a fourth at the end of 2027. All collectors would operate in tandem and would be connected to a single production riser as illustrated in Figure 13.1 for four collectors. Operations would also be boosted by the introduction of a Collector Support Vessel dedicated to maintenance of the collector vehicles deployed by Collector Ship 1. When fully operational, there will be eight collectors in production supported by three PSVs (Hidden Gem, Drill Ship 2 and Collector Ship 1). Project One will benefit from lessons learned on the Collector Test and Project Zero.

13.6.1   Upgrade of the Hidden Gem

After the Hidden Gem has operated for five years at 1.3 Mtpa, it would be upgraded to be capable of producing up to 3.6 Mtpa for a 20-year design life. The upgrade includes engineering, procuring and integrating the following changes/additions:

- Increasing riser diameter from 12″ to 16″ and adding buoyancy to maintain the top tension withing the derrick capacity of the drillship.
- Increased air compressor capacity to operate the air lift riser for the design production rate.
- Refurbishment of the hull structure and coatings to achieve the design life of 20 years with minimal steel renewal at special survey drydockings.
- Providing collector equipment redundancy to provide the reliability and availability to achieve the total annual nodule production tonnage required.
- Providing additional electrical switchgear and motor control centres (MCCs) to operate the additional redundant mining equipment.
- Relocate and upgrade the collector LARS system from the port side aft to the starboard side forward of the moonpool where space exists to handle, store, and maintain larger collectors on deck. Figure 13.6, Figure 13.7 and Figure 13.8 illustrate the proposed changes to the Hidden Gem deck plan.
- Providing two additional 7 MW power generation units to provide additional power for larger air compressor capacity.

Two 12 m wide collectors will be operated in tandem. The existing flexible jumper hose power reel and collector umbilical system will be used but a second new flexible jumper hose reel, and collector umbilical system will be purchased to enable the installation and operation of a second subsea collector.

The collector umbilicals will be integrated with the riser. The concept of operations for collector maintenance in Project One will require adding the capability to make and break umbilical connections on the seafloor, whereas in the Collector Test and Project Zero the collector umbilical will be used for lowering and raising the collectors. Both Project Zero and Project One will require a subsea disconnectible connection between the collector and flexible jumper, and the riser and flexible jumper.

The 12″ riser will be replaced with a 16″ riser to accommodate 3.6 Mtpa production (about 16,000 tpd wet). Larger upper sections will be added for more air volume. The flexible jumper and riser from the 1.3 Mtpa case will be replaced with a larger flexible jumper.

Additional buffer storage will be required to meet the minimum storage requirements for transport. Tanks that could potentially be used for buffer storage are identified in Table 13.3. Tanks aft of the moonpool would provide the most accessibility. For this IA we assume that two additional crude oil tanks between frames 67 and 76 will be converted to buffer storage tanks to achieve approximately 15,000 m^3 of storage. Sloping sides and nodule re-slurrying equipment will be added. Further surveys would be required to determine the suitability of these tanks.

Figure 13.9 shows a process flow diagram for the material handling and offloading system.

Figure 13.4   Hidden Gem – original drillship profile

Figure 13.5   Hidden Gem - original drillship deck plan

Figure 13.6   Hidden Gem - converted for Project Zero - profile
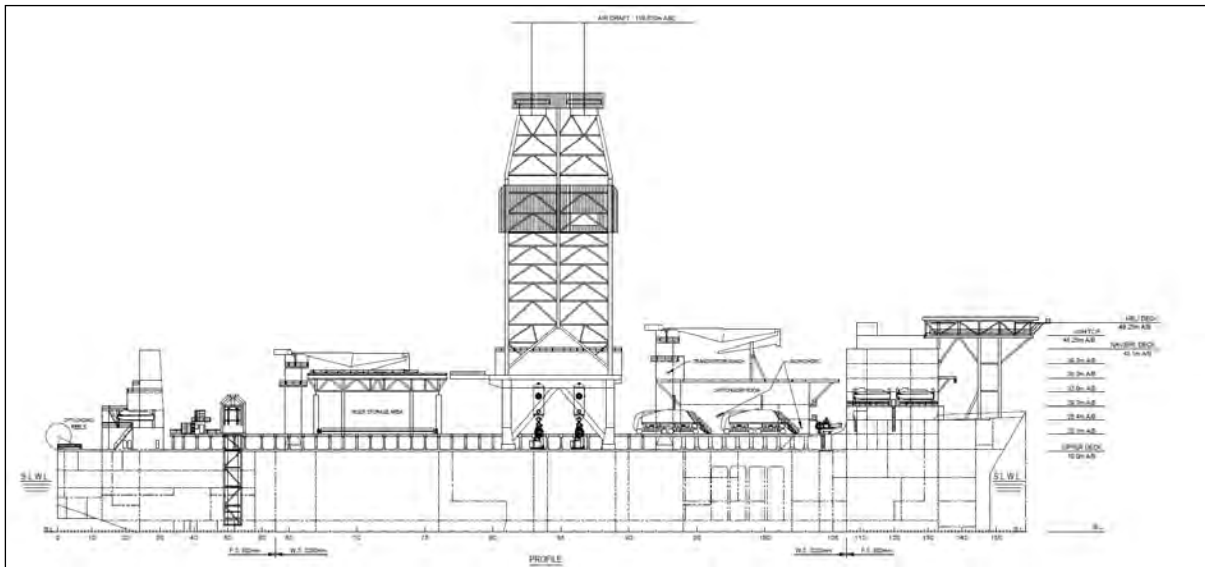
Figure 13.7   Hidden Gem - converted for Project Zero - deck plan
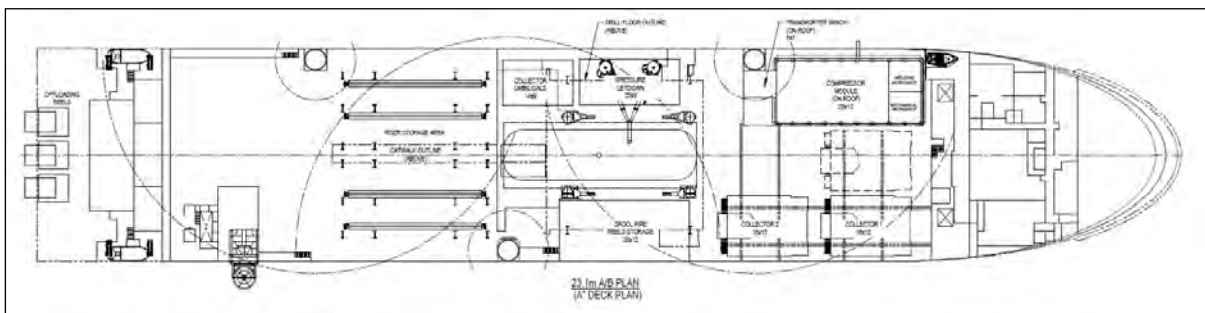
Figure 13.8   Hidden Gem - converted for Project Zero - sections
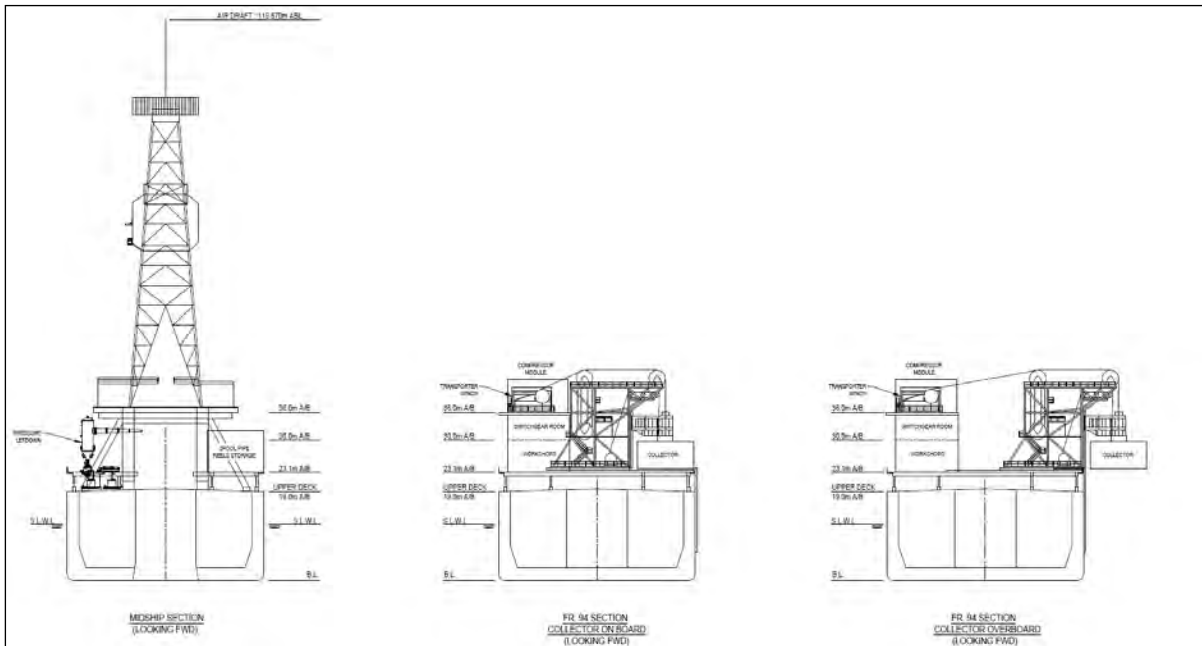
Table 13.3   Available Volume for storage of nodules on the Hidden Gem

Location	Length (m)	Width (m)	Height (m)	Volume (m3)
Tanks Below Riser Rack Area (FR67 to FR 76)				
C.O.T. Port	29	11	16	5,104
C.O.T. Center	29	12	16	5,568
C.O.T. Starboard	29	11	16	5,104
Tanks Moonpool Sides (FR76 to FR82)				
No.4 HOLD Port	22	11	16	3,872
No.4 HOLD Starboard	22	11	16	3,872
Tanks Moonpool Sides (FR82 to 89)				
No.3 HOLD Port	23	11	16	4,048
No.3 HOLD Starboard	23	11	16	4,048
Tanks Forward Moonpool (FR90 to 94)				
No.2 HOLD Port	13	11	16	2,288
No.2 HOLD Center	13	11	16	2,288
No.2 HOLD Starboard	13	11	16	2,288
		Volume Available (m3)		**38,480**

Figure 13.9   Material handling, dewatering and offloading systems
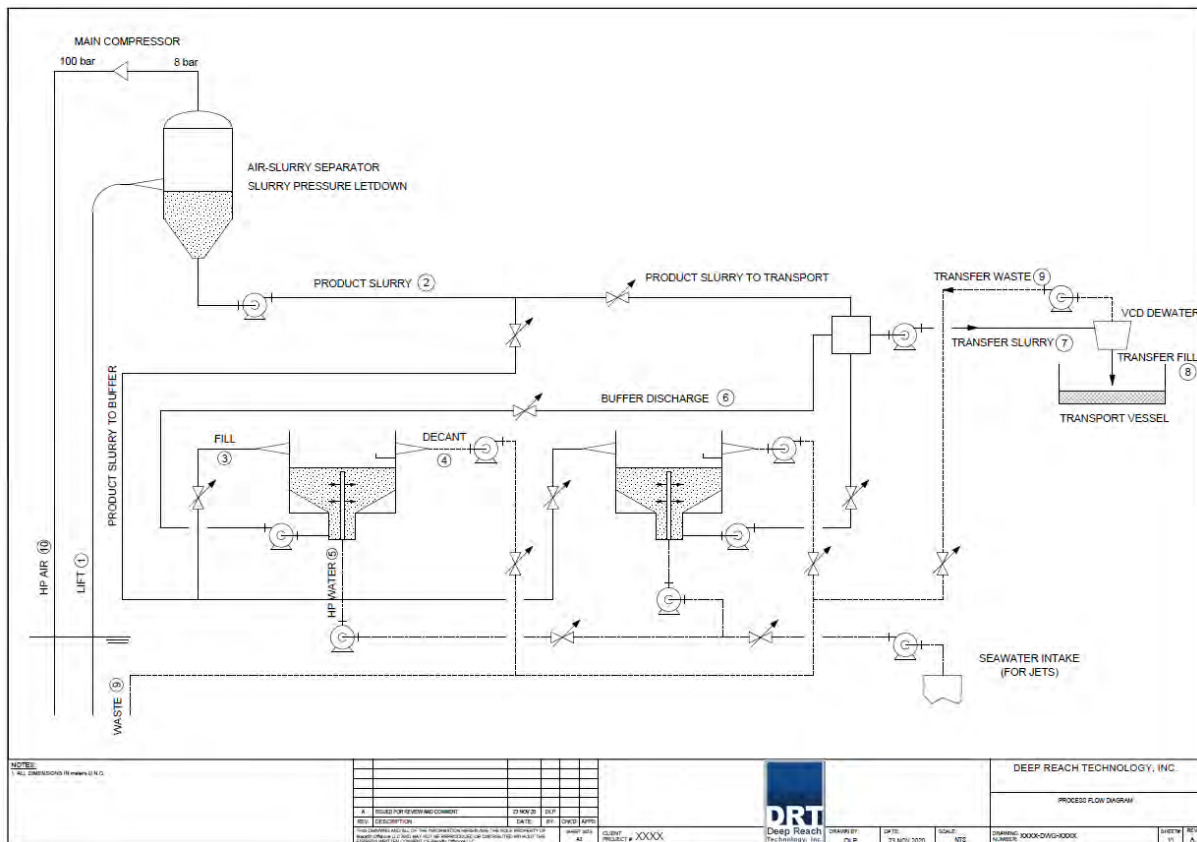
13.6.1   Conversion of Drill Ship 2

Conversion of Drill Ship 2 to a PSV assumes the same design as for the upgraded (3.6 Mtpa) Hidden Gem. However, the costs include refurbishment and conversion work that was performed on the Hidden Gem prior to the Collector Test.

It should be noted that vessel refurbishment and conversion costs are a function of the state of the vessel at the time of purchase and cannot accurately be estimated without a vessel survey and assessment. It is recommended that for the PFS or DFS phase specific candidate vessels be chosen for evaluation.

13.6.2   Collector Ship 1

The purpose-built PSV used in the cost estimate for Project One (Collector Ship 1) has been sized specifically for the NORI Area D project. The conceptual design is shown in Figure 13.10.

Figure 13.10 Collector Ship 1, production support vessel

Source: DRT

The Collector Ship 1 specifications are shown in Table 13.4. Collector Ship 1 will be similar in size to an Aframax or New Panamax class of tanker.

Table 13.4   Specifications for Collector Ship 1 PSV for Project One

Parameter	Value
Length	225 m
Beam	38 m
Depth	20 m
Design draft	13.5 m
Displacement	103,000 t
Deadweight tonnage	79,000 t
Nodule buffer storage	60,000 t cargo ~ 48,000 t nodules
People on board	120
Installed power (approx.)	100 MW

All the PSVs will be equipped with controllable thrusters and will be capable of dynamic positioning (DP), which will allow the vessel and riser to track the collectors. The airlift system will include a main compressor and makeup and booster compressors, which will be integrated on the PSV. All power for off-shore equipment, including the nodule collecting vehicles, will be generated on the PSV.

13.6.3   Collector vehicle

The off-shore system will incorporate self-propelled, tracked, collecting vehicles Figure 13.11. The collectors will traverse the seabed in a pre-determined pattern at a speed of up to 1,800 meters per hour (up to 0.5 m/s). Suction dredge heads on each collector will recover a dilute slurry of nodules, sediment, and water from the seafloor. A hopper or slurry concentrator on each vehicle will allow the larger, heavier nodules to fall into the underflow where they are to be pumped as a higher concentration slurry (in terms of nodule density) to the riser through flexible hoses. Excess water and sediment will pass out of the hopper overflow.

Figure 13.11 Preliminary design for the collector vehicle
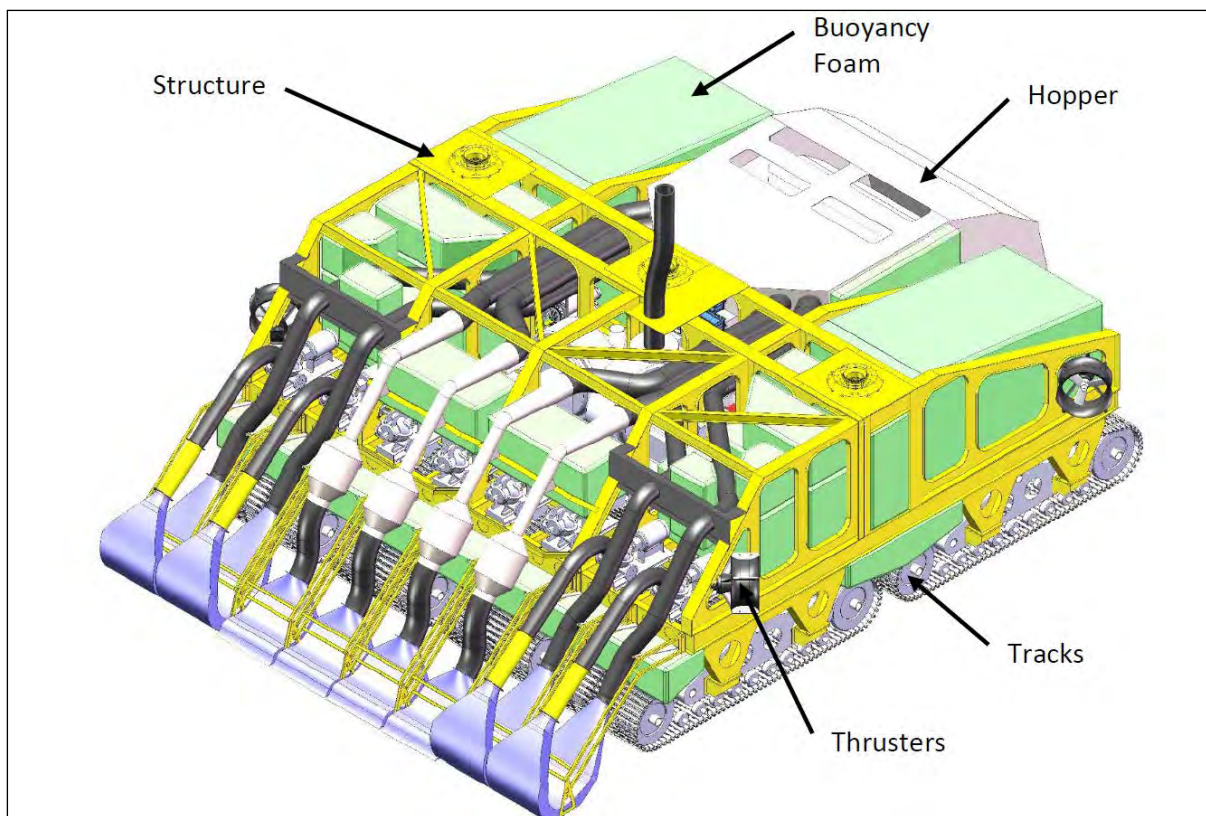
The vehicles will be of comparable size and weight to the largest pipeline trenching machines used in deep water in the upstream oil and gas industry. Trenching machines have been used for years for the trenching, burial, and maintenance of pipelines and power cables, and for ploughing operations for burial depths greater than 1.5 m. The collectors will also be of comparable size and weight (in air) to the large machines that were built for seafloor massive sulphide mining in deep water, off-shore Papua New Guinea (for Nautilus Minerals Inc., in 2015), albeit that those machines are designed to operate on a seafloor composed of hard rock.

The specifications of the collector vehicles are summarised in Table 13.5 and compared to an oil and gas trenching machine and Nautilus's bulk cutter. Several tests have been performed, and are being planned, for tracked vehicles in soft pelagic clays including in the CCZ. The NORI collectors will carry a substantial volume of buoyancy foam to control the machine's weight in water and therefore the bearing pressure.

Table 13.5   Collector vehicle specifications

Parameter	NORI's collector	Perry XT1500 trencher	Nautilus's bulk cutter
Length	18.4 m	9.4 m	15.0 m
Width	12.8 m	6.1 m	4.2 m
Height	5.75 m	3.9 m	
Weight in air	256 t	30.1 t	275 t
Weight in water	25 t	2.2 t	
Bearing pressure	1.5 kPa	2.8 kPa	
Undrained shear strength	2.0 kPa	2.5 kPa	-
Maximum transit speed	0.5 m/sec	0.7 m/sec	
Operating depth	5,000 m	1,500 m	2,500 m
Operating power	1,500 kW	1,100 kW	
Installed / peak power	2,050 kW	-	

During normal operations, the collectors will follow a predetermined path based on the analysis of site survey data and such considerations as nodule abundance, nodule grade, seabed topography, and any obstructions. Normal collecting operations are illustrated in Figure 13.12.

Figure 13.12   Normal collecting operations
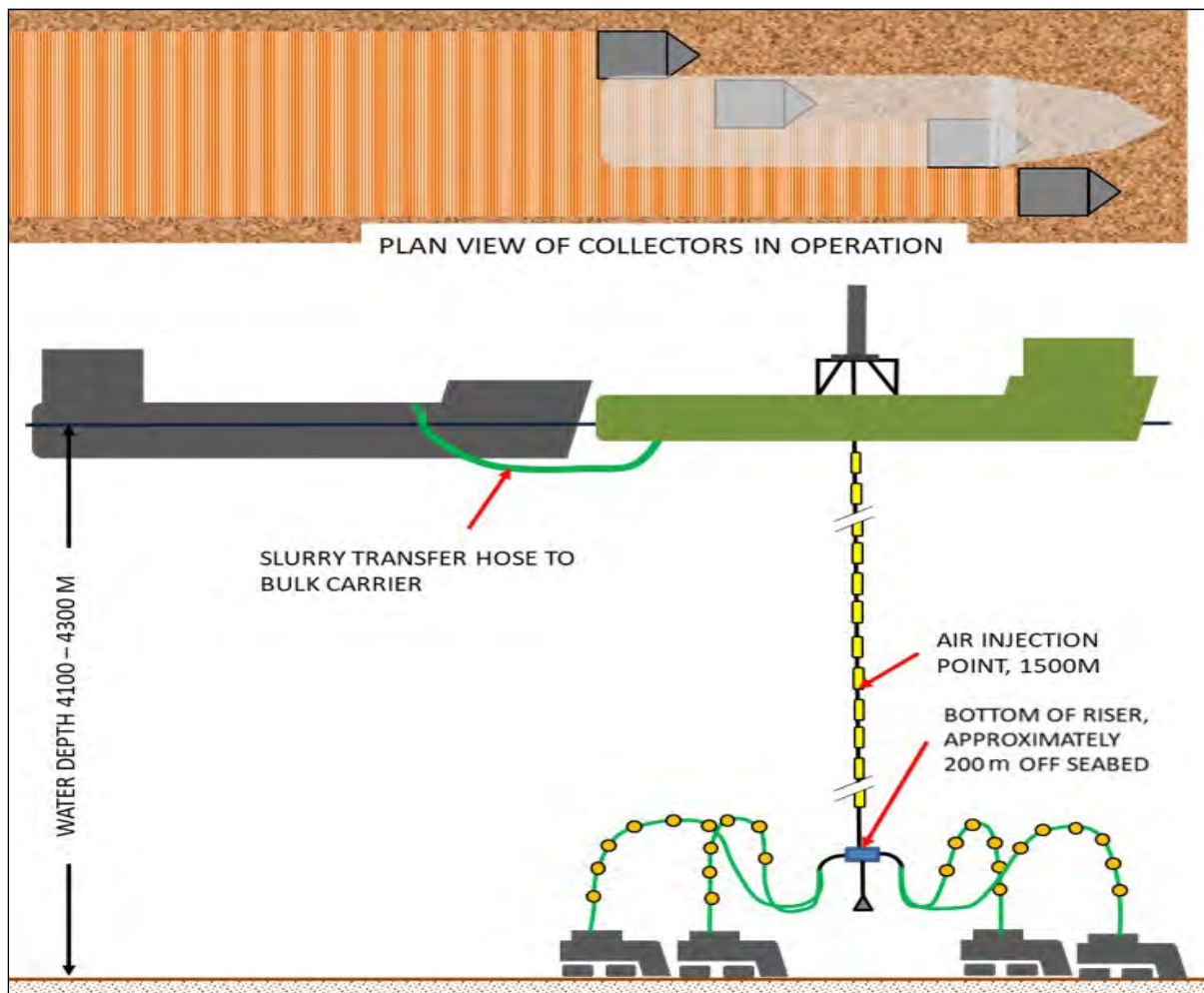
The collectors will generally operate in semi-autonomous mode. However, an array of forward-looking obstacle avoidance imaging systems will process and report approaching terrain in real time and manual/supervisory control will be returned, as and when required.

In Project One, maintenance for the collector vehicles deployed by Collector Ship 1 will be performed by a separate collector support vessel (CSV). When a collector requires repair, either planned or unplanned, it will be disconnected from the jumper hose and power umbilical (which connect it to the RALS) by a remotely operated vehicle (ROV). The CSV will maintain a spare collector, which will be deployed by a wireline hoist to reconnect with the seafloor spread. The collector requiring maintenance will be hoisted to the surface by the CSV. The storyboard procedure for collector change out is shown in Figure 13.13.

Figure 13.13   Collector change-out operations concept

1. A new vehicle is connected to the lift system

2. Vehicle to be serviced is disconnected from the jumper
3. Mining system can operate with three harvesters

4. ROV connects hoist line to vehicle to be serviced

5. Vehicle hoisted to surface for servicing
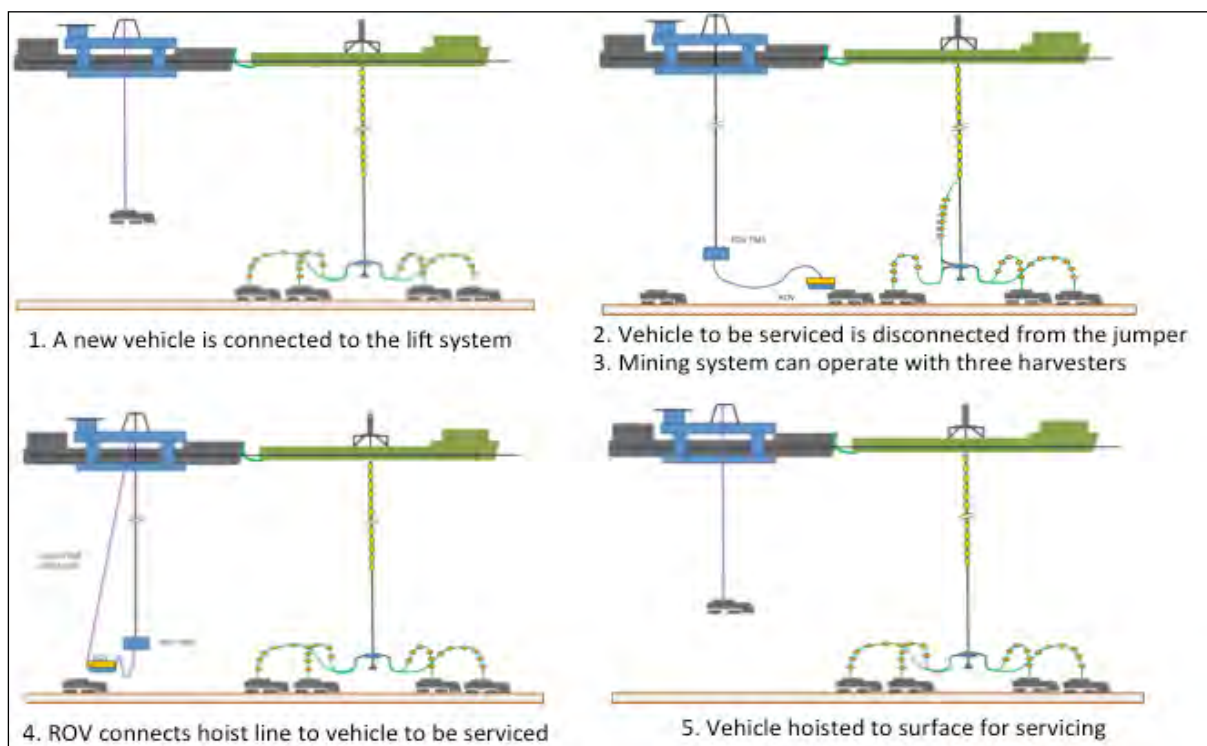
13.6.4   Plume mitigation

The collector described above picks up seafloor sediment along with the nodules it collects. The fine-grained sediment consists primarily of either the microscopic, calcareous or siliceous shells of phytoplankton or zooplankton; clay-size siliciclastic sediment; or some mixture of these. When the water and sediment are discharged from the nodule concentrator, or as excess water from shipboard dewatering of the nodules, a plume will be generated in the water column.

DRT was recently awarded a research grant by the U. S. Department of Energy, Advanced Research Projects Agency – Energy (Deep Reach Technology, Inc., 2021), to advance a concept for mitigating or eliminating the sediment plumes by:

- Preventing all the sediment laden water from entering the lift system, thus eliminating sediment in the wastewater produced by dewatering (except for sediment and nodule fines released by nodule attrition, and
- Active flocculation of the sediment discharged from the collector using electrocoagulation.

NORI is participating in this research by providing sediment samples from NORI Area D for electrocoagulation tests.

The work to date has shown, in theory, that sediment can be eliminate from the riser by adding an additional pump to collect clean water for conveying nodules to the riser, and by implementing a special underflow mechanism that will allow control of a small amount of upflow in the separation hopper to prevent water from the pick-up head from entering the riser, while nodules (greater than about 5 mm) will pass to the riser. Figure 13.14 is a conceptual illustration of a collector with this concept. The collector costs used in this IA all have an allowance for adding this feature to the collectors. The addition of electrocoagulation, while showing promise, adds complexity to the collector and is still the subject of evaluation. Further government support is expected in 2021 to perform testing of both these concepts at a laboratory scale.

Figure 13.14   Illustration of collector vehicle with plume mitigation (patent pending)
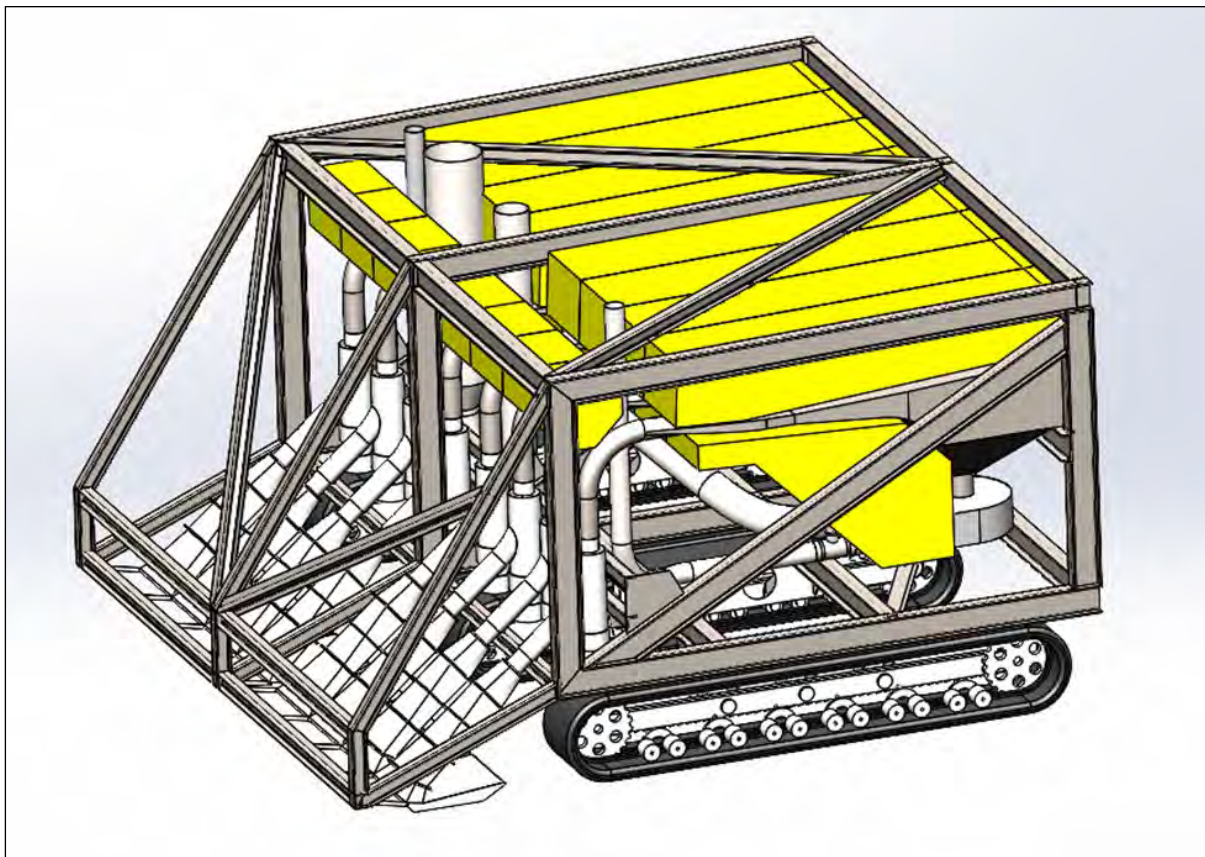
13.6.5   RALS

13.6.5.1   Riser

The RALS will take in the combined slurry from the collector vehicles and deliver the slurry to the PSV via airlift. The main riser pipe will consist of three main sections. The lower section (RALS-1) will carry the two-phase slurry in nominal 28″ outside diameter (OD) pipe from the collectors to the airlift injection location. The second section (RALS-2) will carry a three-phase mixture of slurry and air in 28″ OD pipe. This section will also include three 12 ¾″ OD auxiliary pipes. The former will carry the compressed air for the airlift system. The latter will carry the effluent from dewatering of the slurry to the discharge point. The depth of the discharge point is yet to be selected and will depend on plume modelling and other environmental considerations. The upper section of pipe (RALS-3) will have a larger

diameter to account for the expansion of air in the airlift. It will also include the discharge and air supply piping. Umbilical cables for powering the collectors and carrying data will be attached to the riser.

The entire riser string will be supported on a detachable buoy that is latched into the moon pool of the PSV (an opening in the floor or base of the ship's hull giving access to the water below). The buoy may be detached during a hurricane emergency. When this is necessary, the lower riser manifold will rest on the ocean floor on an emergency ground anchor and the riser string will be supported by the buoy about 100 m below the sea surface. This position is below the depth of high wave energy. This will enable the PSV to transit away from the storm area. After the hurricane has passed, the PSV will re-engage with the buoy. This process is identical to the operation of disconnectable risers on off-shore floating production and storage vessels in the Gulf of Mexico. The specifications of the RALS are shown in Table 13.6.

13.6.5.2 Airlift system

The airlift power will be derived from three compressors: a main compressor, a booster compressor, and a make-up compressor. The specifications of the airlift compressors for Project One Collector Ship 1 are shown in Table 13.7. These parameters are based on a nominal production rate of 6.4 Mtpa (wet) (Deep Reach Technology, Inc., 2015) and need to be upgraded for the modified design basis in this IA (up to 8.2 Mtpa). CAPEX and OPEX estimates in Section 21 have been scaled to account for this increased capacity. The main compressor used as a basis for the IA cost estimate is shown in Figure 13.15. It is an Elliott Group model 46M6I two-stage centrifugal compressor with inter-cooling. To control the compressor performance for varying loads due to variable nodule abundance on the ocean floor, for example, the compressor is equipped with adjustable inlet guide vanes.

Table 13.6   Riser pipe stack up

Riser Joint Type	Description	Weight In Air (mt)	Weight In Water (mt)	OD (m)	Number of Joints	Water Depth (m)
RALS-1	• Main Pipe 28" OD x 0.625" wt • 3" typ. Umbilical (4 each)	5.1	4.4	0.86	130	1500 to 4000

RALS - 2	• Main Pipe 28" OD x 0.625" wt
	• 3" typ. Umbilical (4 each)
	• Discharge Pipe (3 each)
	   ○ 12-3/4" OD x 0.5 wt
	• Air Supply Pipe
	   ○ 12-3/4" OD x 0.5 wt
	• Buoyancy Modules (4 each)
	   ○ 1.53 m OD
		23.7	0.4	1.53	47	600 to 1500

RALS – 3	• Main Pipe 36" OD x 0.75" wt
	• 3" typ. Umbilical (4 each)
	• Discharge Pipe (3 each)
	   ○ 12-3/4" OD x 0.5 wt
	• Air Supply Pipe
	   ○ 12-3/4" OD x 0.5 wt
	• Buoyancy Modules (4 each)
	   ○ 1.68 m OD
		28.4	-1.4	1.68	31	0 to 600

Total Rigid Riser System		2708.2	552.5	-	208	4000

Source: Deep Reach Technology, Inc., 2015. Notes: RALS-1 = main riser pipe, lower section; RALS-2 = main riser pipe, middle section; RALS-3 = main riser pipe, upper section.

Table 13.7   Nominal airlift compressor specifications

Parameter	Main compressor		Booster compressor	Make-up compressor
	Peak production	Normal operation		
Mass flow of air (kg/s)	84	56	15.2	10.1
Volumetric flow of air (m^3/h at standard temperature and pressure)	252,000	168,000	45,544	30,207
Inlet pressure (kPa)	780	780	9,400	100
Outlet pressure (kPa)	8,460	9,430	15,000	800
Estimated power (MW)	26.0	18.1	0.74	2.4

Figure 13.15 Main air compressor (Elliott Group model 46M6I)

Source: Provided by Elliott Group.

Airlift was successfully tested in three deep-water pilot tests in the 1970s: two by the Ocean Mining Associates consortium, and one by Ocean Management Inc. There have also been several large terrestrial tests and at least one successful use of airlift for hoisting coal in a Soviet mine. Table 13.8 shows the main parameters of relevant airlift operations and tests for comparison with those proposed for this project.

The proposed airlift design discharges the 3-phase slurry under an 800 kPa pressure. The compressed air is dried and recycled in the compressors. This results in a reduced size of riser required at the discharge, and reduced compression ratio, compared to airlift systems with atmospheric discharge. It does require a specialize pressurized de-aeration tank and slurry depressurization on the production support vessel. Previous studies have shown that this approach results in a lower overall cost for the airlift system including the riser, but this conclusion needs to further be evaluated in the next study phase. The pressurized discharge has never been field tested, and the Collector Test is currently planned with one atmosphere discharge, hence large scale on-land testing of the pressurized discharge should be performed prior to its implementation on Project Zero or Project One.

Data from the KCON Tests (Doyle & Halkyard, 2007) have been used for validation of DRT's proprietary airlift simulation numerical model, which has been used for design of the airlift in this IA (Deep Reach Technology, Inc., 2019). The conclusion of this validation indicates the predicted flow rates were within ±10% for 3-phase flows (air-water-solids), and ±40% for 2-phase flows (air-water). DRT attributes the lower accuracy for 2-phase results to a difference in flow regimes, for example, slug flow for low air volumes, whereas the KCON model assumes froth flow (homogenous conditions). From observations made in the test work, particularly the KCON experiments, the presence of larger solids in the mixture results in breakup of air bubbles and a more stable froth flow. Although this data is based on smaller diameters and shorter lifts than the proposed deep ocean mining system, the experience with the Soviet mine is very close in terms of pipe diameters and flow rates,

albeit for a shorter lift. Lift column tests have been completed and the air-lift system will be tested during the Collector Test.

Table 13.8   Relevant airlift experience and tests

Reference	Vertical lift (m)	Pipe diameter (mm)	Lifting rate (tph)	Solids volumetric concentration (%)	Solids diameter (mm)
Collector Ship 1	4,400	679–870	1,600	16%	Up to 100
OMA, 1970, Blake Plateau Atlantic [LeCourt and Williams]	730	220	Unknown ("significant tonnages collected")	Unknown	Unknown
OMA, 1977, CCZ Pacific [Kaufman et al,1985]	4,400	160–240	0 to 75	20%	Up to 100
OMI, 1978 [Shaw, 1993] CCZ Pacific	5,200	200	30 (design)	unknown	Up to 100
KCON [Doyle & Halkyard, 2007] On-Land	30	305	Up to 400	0 to 44%	Up to 50
NRIPR, Japan [Saito et al, 1989] In Test Pit	200	151	Up to 96	0 to 15%	8–41
University of Karlsruhe Lab [Weber and Dedigel]	7.8	100	12	0 to 33%	
Mine shaft Rheinische Braunkohle AG [Weber and Dedigel]	441	300	115	0 to 8.6%	0.6–50 (Lignite)
Coal mine shaft Krasnoarmejsk-2, Donez Plateau (Ukraine), operated from 1966 to the 1970s [Heine, 1976]	460	400–1000	650	12–33%	15–25

The slurry from the RALS will pass through a diffuser to an airlift discharge system located on the deck of the PSV that will consist of a surge tank pressurised to 800 kPa and four lock hopper tanks operating in batch mode to reduce the pressure to atmospheric. Figure 13.16 is an illustration of this design. The high-pressure discharge system will allow optimum efficiency for the airlift operation.

Figure 13.16 Nodule and air discharge concept

Source: Feenan 2009

The airlift discharge, or pressure let-down, system shown in Figure 13.16 is a batch system. An alternate continuous flow system has been proposed Figure 13.17 which is considered potentially a more reliable method.

Figure 13.17   Continuous Flow Pressure Let-down System shown with dewatering equipment (patent pending)

13.6.6   PSV operations

A Dynamic Positioning (DP) system will keep the PSVs on a specified track using only propellers or thrusters and without external moorings or other physical restraints. The DP control system will be linked to the collector tracks to control riser loads on the collectors. The DP system will be composed of the power supply from the PSV main power system, the thruster systems, and the DP-control system. DP is used by the off-shore oil industry in locations such as the North Sea, Persian Gulf, Gulf of Mexico, West Africa, and off the coast of Brazil. There are currently more than 1,800 DP ships across the globe.

To accurately position the PSVs, a locating system will also be required. This will consist of a long baseline acoustic network set up with beacons spread out over the seabed and covering the site to be collected. The beacons will provide acoustic signals to each other and also the collectors, the bottom of the riser, and the PSV. The long baseline will also communicate with the differential GPS to ensure high precision geo-location for the system, at all times.

The same long baseline acoustic network for positioning the PSVs will be used to position the transport vessel, but likely enhanced with a telemetry system between the transport and the PSVs. The telemetry system will have functionality to execute disconnection of the transfer hoses, in the event of drive off or loss of power on either vessel.

If a transport vessel is connected to a PSV, the slurry from the RALS discharge system will be pumped directly to the transport vessel through floating hoses. The transport vessel, also dynamically positioned, will track in the wake of the PSV at about 100 m. Nodules will be dewatered by gravity settling in the holds of the transport vessel. Floating decanter weirs will recover the liquid containing water and sediment. This return water and sediment will be pumped back to the PSV through an additional floating hose to be returned to deep water via an auxiliary riser pipe that is part of the RALS.

If a transport vessel is not connected to a PSV, slurry from the discharge system will be pumped into buffer storage holds where it will also be dewatered by gravity settling. Figure 13.18 is a schematic diagram of the airlift discharge and slurry handling system for Collector Ship 1. Figure 13.9 shows the equivalent system for the drillship cases. When the transport vessel is subsequently connected, the buffer storage will be liquefied using a jetting system, and the slurry from the buffer will be combined with the slurry from the discharge system to be pumped to the transport.

Figure 13.18   Schematic of buffer storage and material handling on Collector Ship 1
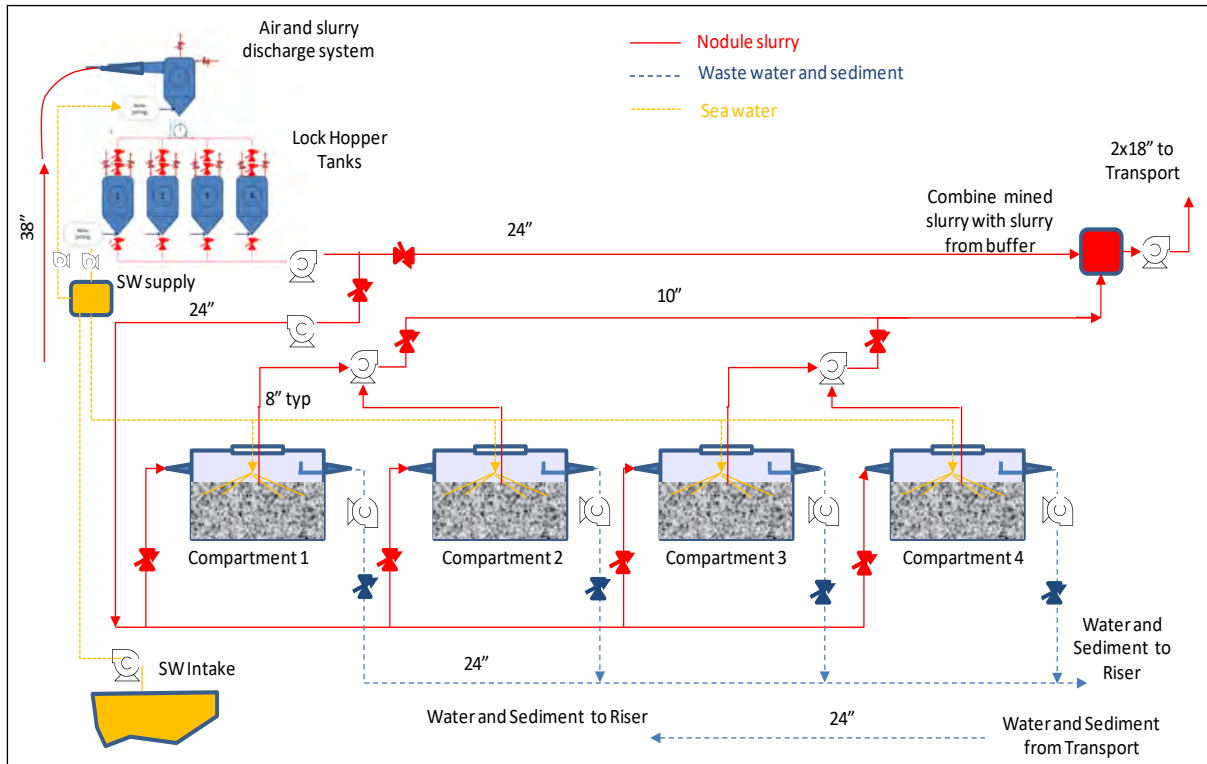
13.6.7   Collector support vessel

In Project One, in order to minimise the effect of collector maintenance on PSV operations, maintenance of the collectors deployed by Collector Ship 1 will be performed by a separate semi-submersible collector support vessel. Preliminary specifications of the CSV are listed in Table 13.9. The CSV will be similar to a subsea support platform such as the one shown in Figure 13.19.

When a collector requires repair, either planned or unplanned, it will be disconnected from the jumper hose and power umbilical (which connect it to the RALS) by ROV. The collector support vessel will maintain a spare collector that will be deployed by a wire line hoist to reconnect with the seafloor spread. The collector to be serviced will be hoisted to the deck of the collector support vessel. A preliminary deck plan for the collector support vessel is shown in Figure 13.20.

Table 13.9   Collector support vessel specifications

Parameters	Value
Draft	16 m
Column area	125 m^2
Column height	20 m
Column spacing (min)	50 m
Static air gap (freeboard)	10 m
Pontoon width	12.5 m^2
Pontoon height	5.65 m
Pontoon length	82.5 m
Deck length	80 m
Deck beam	50 m
Deck height	3.5 m
Displacement	17,250 t
Deadweight tonnage	9,750 t

Figure 13.19 Semi-submersible subsea oilwell support vessel, Q4000

Source: Helix Energy

Figure 13.20 Deck plan for collector support vessel
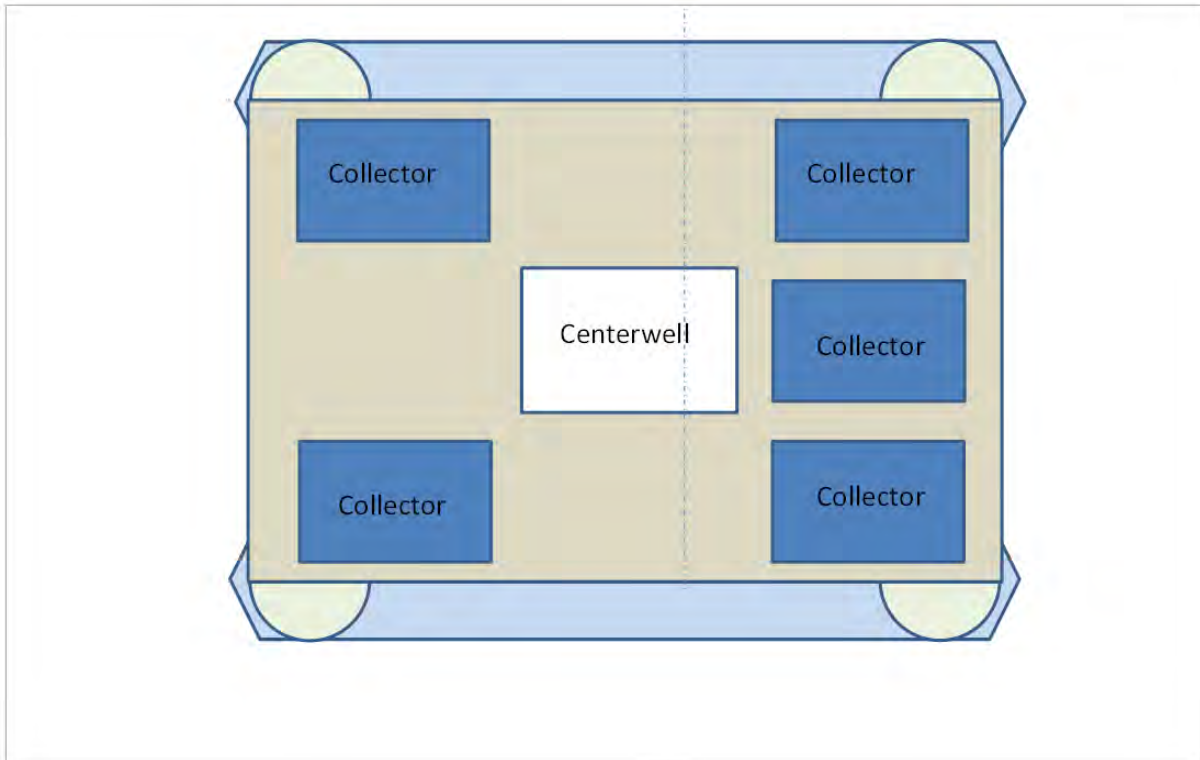
13.7 Life of Mine nodule production

13.7.1   Introduction

An assessment was conducted to prioritize the seafloor production, targeting areas of higher abundance. The assessment is not a detailed production plan but rather a conceptual plan of production increments linked to equipment operating schedules and the basis of design (BOD) production parameters. The mineral resource data has been adjusted using modifying factors and then accumulated into annual increments in accordance with the BOD parameters. The conceptual sequencing of production areas is summarized in Figure 13.21, showing the production blocks in five-year intervals over a life of mine (LOM) of over 27 years.

Figure 13.21 NORI 30-year potential production areas
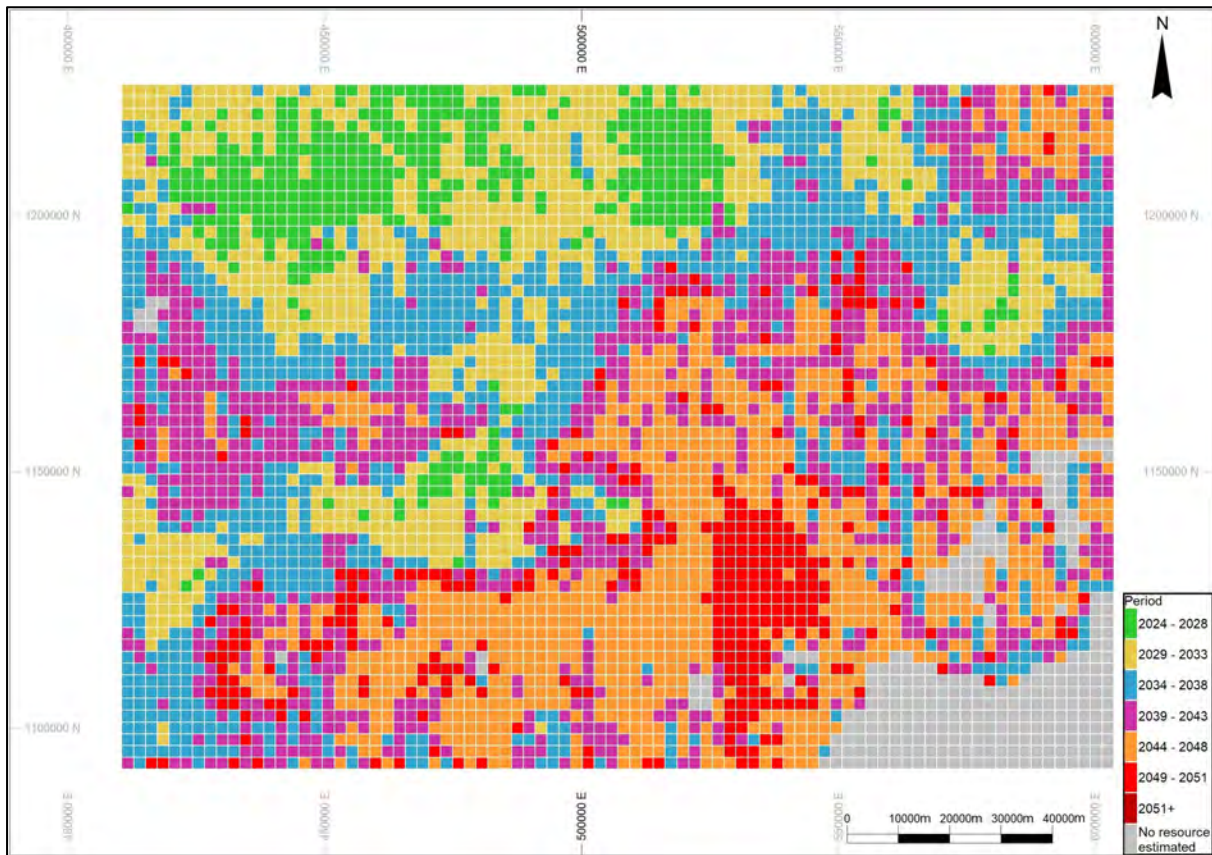
13.7.2   LOM basis of design

The nominal design parameters for the PSVs and their seafloor collector systems are summarized in Table 13.10 and Table 13.11. The tables distinguish between years in which the vessels dry dock and non-dry dock years. Every five years the production vessels (and collector support vessel in the case of Collector Ship 1) are required to dry-dock for Class special survey. Collector and riser replacement would also be conducted during this period. An allowance of 60 days is included for this based on experience with dry dockings for South African diamond mining vessels. Project Zero only operates for five years, so no allowance is required for dry docking the Hidden Gem. After five years, the Hidden Gem is upgraded.

Two utilization (operating days per year) values are tabulated. The nominal values assume 20 days downtime per year for manoeuvring. The "Utilization excluding manoeuvring" value is used below is estimating LOM production rates wherein a specific turning allowance is calculated for each year.

The BOD for the seafloor production systems is summarized in Table 13.12 to Table 13.14.

Table 13.10   Nominal engineering parameters for Hidden Gem and Drill Ship 2

Hidden Gem/Drill Ship 2 (no spare collector)	Pre-2030	Post 2030		
		Average	Dry dock Year	No dry dock
Dockings & scheduled outages (days)	0	12	60	0
Area moves	10	10	10	10
Available time at sea (days)	355	343	295	355
Collector mean time between repair (days)	14	14	14	14
Collector mean time to repair (days)	2	2	2	2
Planned maintenance, % (collector)	13%	13%	13%	13%
Planned maintenance, % (other)	5%	5%	5%	5%
Engineering downtime (days)	62	60	52	62
Engineering availability (%)	83%	83%	83%	83%
Engineering availability (days)	293	283	243	293
Other work (days)	10	10	10	10
Weather delays (days)	15	15	15	15
Process/transport delays (days)	10	10	10	10
Allowance for manoeuvring	20	20	20	20
Nominal utilization (%)	67%	66%	64%	67%
Nominal utilization (operating days per year)	238	228	188	238
Utilization excluding manoeuvring	258	248	208	258
Collector effective width (m)	8.7	12	12	12
Number of collectors (operating)	1	2	2	2

Table 13.11   Nominal engineering parameters - Collector Ship 1

Collector Ship 1 (Collector Support Vessel and spare collector)	Average	Dry dock Year	No dry dock
Dockings & scheduled outages (days)	12	60	0
Area moves	10	10	10
Available time at sea (days)	343	295	355
Collector mean time between repair (days)	30	30	30
Collector mean time to repair (days)	0.4	0.4	0.4
Planned maintenance, % (collector)	1%	1%	1%
Planned maintenance, % (other)	5%	5%	5%
Engineering downtime (days)	22	19	22
Engineering availability (%)	94%	94%	94%
Engineering availability (days)	321	276	333
Other work (days)	10	10	10
Weather delays (days)	15	15	15
Process/transport delays (days)	10	10	10
Allowance for manoeuvring	20	20	20
Nominal utilization (%)	78%	75%	78%
Nominal utilization (operating days per year)	266	221	278

Collector Ship 1 (Collector Support Vessel and spare collector)	Average	Dry dock Year	No dry dock
Utilization excluding manoeuvring	286	241	298
Collector effective width (m)	12	12	12
Number of collectors (operating)	4	4	4

Table 13.12   Seafloor production basis of design – Hidden Gem

Hidden Gem	Unit	Value
No dry dock years, four years continuous	days	238
Dry dock years, every fifth year	days	190
Average utilization (days per year)	days	229
Collector head width pre 2030	m	8.7
Collector head width post 2030	m	12
Collector speed	m/sec	0.5
Number of collectors pre 2030	Unit	1
Number of collectors post 2030	Unit	2
Pumping design rate set to average abundance	kg/m^2	20

Table 13.13   Seafloor production basis of design – Drill Ship 2

Drill Ship 2	Unit	Value
No dry dock years, four years continuous	days	238
Dry dock years, every fifth year	days	190
Average utilization (days per year)	days	229
Collector head width	m	12
Collector speed (maximum)	m/sec	0.5
Number of collectors	Unit	2
Pumping design rate set to average abundance	kg/m^2	20

Table 13.14   Seafloor production basis of design - Collector Ship 1

Collector Ship 1	Unit	Value
No dry dock years, four years continuous	days	278
Dry dock years, every fifth year	days	222
Average utilization (days per year)	days	267
Collector path Width	m	12
Collector speed (maximum)	m/sec	0.5
Number of collectors	Unit	2
Number of collectors 2026	Unit	2
Number of collectors 2027	Unit	3
Number of collectors 2028	Unit	4
Pumping design rate set to average abundance	kg/m^2	20

Turning of the PSV, collector vehicles and RALS has not yet been extensively investigated but will be assessed during the proposed Collector Test. Analysis of a towed system in the 1970s indicated a turn radius of greater than 1,000 m (KCON Feasibility report, 1976). For

this IA, a self-propelled turn with a radius of 500 m has been assumed Table 13.15. It has also been conservatively assumed that no nodules will be collected during the turns.

Table 13.15 Collector system turning parameters basis of design

	Units	Value
Turning interval assuming 180˚input	m	30,000
Seafloor collector availability		100%
Collector turning radius	m	500
Time to establish turn	h	0.25
Time to make 180˚turn	h	1.11
Total time to complete turn	h	1.36

Figure 13.22 shows the conceptual arrangement of collection paths. The path is developed as follows:

1) Collection path No 1 proceeds in a west to east direction.
2) Collection path No 2 is accessed by a 180˚ south turn and then proceeds in an east to west direction.
3) Collection path No 3 is accessed by a 180˚ north turn and then proceeds in a west to east direction with a 1.0 m offset from the edge of path No.1.
4) Collection path No 4 is accessed by a 180˚ south turn and then proceeds in an east to west direction with a 1.0 m offset from the edge of path No.2.
5) The extraction sequence progress in a southwards direction until the collection panel is completely traversed.
6) At this point the PSV, RALS, and collectors are relocated to the adjacent panel to the south and the sequence 1 to 5 is repeated.

Collector location will be guided by an array of long baseline (LBL) beacons on the seafloor. On completion of a rectangular panel, the equipment would repeat the operation in an adjacent panel.

Further studies will be required to optimise the collector paths and their orientation. The Collector Test is expected to provide essential information to inform these studies.

The annual production rate of each collector is a function of average nodule abundance (A), collector width (B), speed (C), number of days per year availability (D), and nodule recovery (E). The relationship is expressed by the following formula:

$$\text{Individual collector production rate (F)} = A \cdot B \cdot C \cdot D \cdot 24 \cdot E$$

A maximum velocity of 0.5 m/sec was assumed for the collector (DRT, 2015). Recovery includes factors to account for nodules that fail to be picked up (collector efficiency), nodules lost in the concentration process on the collector, and fine nodule material that is lost in the dewatering process on board the PSV and transport vessels (dewatering efficiency).

Figure 13.22 Conceptual nodule collection path sequencing
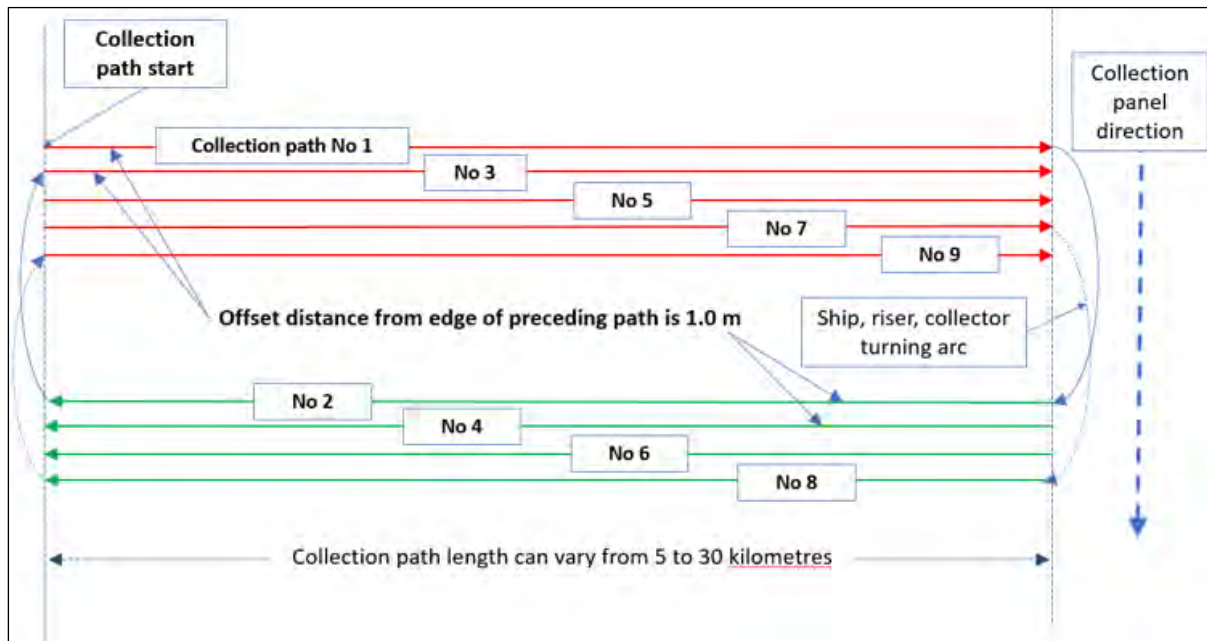
The mining system is designed to operate at a constant speed. Short scale variations in abundance on the seafloor will result in fluctuations in the flow through the collector and RALS. This is accounted for by designing for peak production of twice the average for the collector and 1.3 times the average for the lift system, taking into account the averaging times (nodule residence times) for these systems. This additional short-term capacity avoids the need to continually vary the speed of the collector.

The collecting operation is assumed to work 264 days per year. Estimates of annual availability of the production system were derived from an assessment of weather and mechanical downtime which indicated that 267 days could be expected.

Current experience with off-shore drilling and production suggests an uptime between 95 - 98% is possible with well-designed equipment, adequate redundancy, and planned maintenance. One of the most important factors for the deep-sea extraction project is the reliability and maintainability of the collectors themselves. The mean time between repairs, or service, of the collectors is uncertain until actual operations begin.

In order to mitigate the effect of this uncertainty, the collector change-out method described in Figure 13.13, has been adopted to minimise the time required to replace a collector for maintenance. It is estimated that the swap-out operation on Collector Ship 1 could be performed in as little as 12 hours. Figure 13.23 shows the effect of collector mean time between repair on overall utilisation based on this maintenance concept compared with other concepts for repair that do not involve spare collector swap out.

For this IA, the mean time between repair is assumed to be 30 days. Note that in comparison with the other strategies for collector repair shown in Figure 13.23, the total annual operating days for the proposed method is less sensitive to the mean time between repair. Crawler vehicles used for subsea diamond mining are typically recovered every 5–7 days for planned maintenance. The reason for such frequent maintenance of these vehicles is leakage of seals on hydraulic cylinders used for raising and lowering a large boom with a cutting head. The nodule collectors will not require any hydraulic cylinders.

Pilot test collectors in the 1970s succeeded in operating continuously up to about four days.

Figure 13.23 Impact of collector mean time between repair on overall utilisation - Collector Ship 1
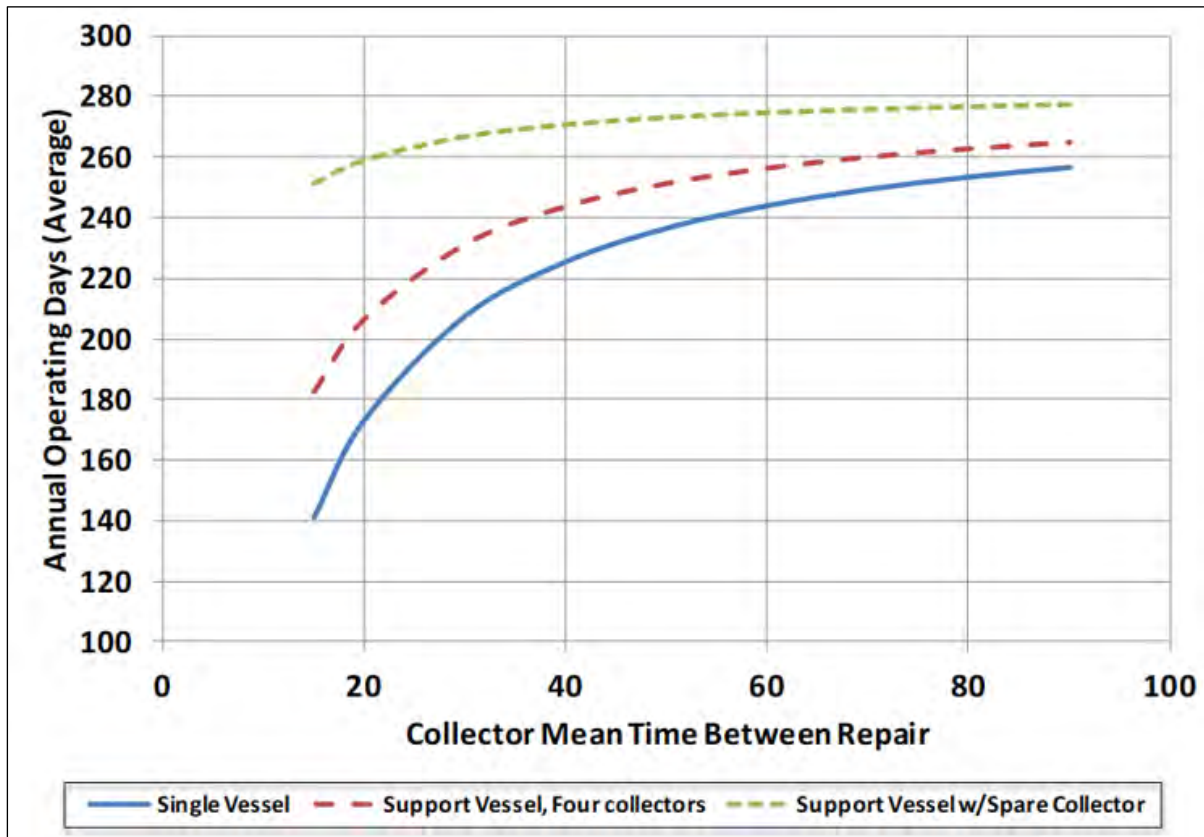
Aside from failures of lift pumps, collector failure was typically due to leakage of an oil filled electric motor (Shaw, 1993). This technology has subsequently been superseded by the advent of subsea water-cooled electric motors, which have recently been implemented in the subsea oil and gas industry and are achieving multiple years of life without maintenance (Millward, 2008). Reliability can now be greatly improved by employing direct electric drives, using water-cooled motors, for pumps and tracks instead of hydraulic power. Other measures to improve reliability include implementation of 100% redundancy for critical components such as suction pumps and instrumentation.

The overall nodule recovery efficiency is estimated at 80%. The recovery value is based upon test work conducted in the 1970s. Nodule recovery efficiency is the product of nodule entrainment efficiency, subsea concentrator recovery, and dewatering system efficiency. The estimate of dewatering recovery used in this IA is higher than indicated by the 1970s test work because data that has come to light recently suggests the amount of breakup during lifting the nodules up the RALS may be significantly less than previously assumed (Kennecott (1978), DRT (2015)).

The modifying factors applied to the mineral resource to estimate production tonnages are detailed in Table 13.16.

Table 13.16   Mineral Resource modifying factors

Modifying factors	Value	Description
Resource area efficiency	92%	The resource area efficiency factor is defined as the width of the collector divided by the width of the collector path. A 0.5 m undisturbed strip is to be left either side of the collector. For a 12 m wide collector, the resource area efficiency is calculated as 12 / 13.
Collector pick-up efficiency	90%	This is the percentage of nodule mass passed over by the collector that is pickup up by the collector head. Reference Table 6 Recovery efficiencies assumed for this study, DRT-1412-RP-02-R02: Seafloor Polymetallic Nodule Off-shore Scoping Study - Technical Report.
Collector underflow efficiency	95%	This is percentage of nodule mass that is pickup up that is passed to the collector underflow. Reference Deep Green Material Balance Summary, Preliminary for information only Thursday, November 28, 2020 (Collector nodule mass underflow/ Collector nodule mass picked up, 435.7/458.6).
Nodule attrition	0%	This is the percentage of mass of nodule lost through attrition from the sea floor to trans-shipment. It is included in the trans-shipment efficiency.
Trans-shipment efficiency	93%	This is the percentage of nodule mass transferred from the production vessel to trans-shipment. Reference Deep Green Material Balance Summary, Preliminary for information only Thursday, November 28, 2020. (Transport fill/ (Buffer fill + Buffer discharge), 508.8/ (435.7+129.6).
Overall collector efficiency	80%	This is the percentage of nodule mass passed over by the collector that is delivered to the transport vessel. It includes losses in the pick-up, overflow, attrition and trans-shipment (90%*95%*100%*93%).
Overall resource recovery factor	73%	Is the product of the resource area efficiency * collector pick-up efficiency * collector under flow efficiency * (1 - nodule attrition (%)), * trans-shipment efficiency (92%*90%*95%*100%*93%).

The resource accumulation excludes parts of each block that are considered not suitable for production, such as areas with volcanic rocks or where the sea floor slope is too steep. The collector was designed with a maximum operating slope of 8° but the Mineral Resource and production plan are based on a more conservative 6° limit.

The resource area efficiency factor includes a 0.5 m undisturbed strip either side of the collector path and encompasses an allowance for the collector turning zone at the end of each strip. The efficiency of the collector in the turning circle in unknown at this stage and nodules may be partially or non-recoverable. The 0.5 m strip either side of the collector is an allowance for inaccuracy in steering the collector. The proposed Collector Test is expected to provide valuable information on location control. The collectors will be turned at predefined points to avoid volcanic rocks, slopes greater than 6° and at the end of collection paths. The ability to recover nodules effectively in an area previously traversed and disturbed by turning needs to be evaluated. An estimate of 92% efficiency is considered reasonable for this high-level assessment.

Collector pick up efficiency of 90% was assumed, based on trials by the Kennecott consortium in 1976 (Kennecott Exploration Inc., 1976) and preliminary tank tests. The collector underflow efficiency of 95% accounts for the nodule mass that is to be pumped to the riser and nodule loss of 5% to the collector overflow. The collector overflow and nodule loss are ejected at the sea floor.

The mechanism of collecting and pumping of the nodules from the sea floor, through the airlift riser, to the surface vessel will cause nodules to collide with the collector system, riser walls and with other nodules. These collisions will result in attrition which will cause

some reduction in the nodule particle size. The nodules that report to the surface production vessel will be dewatered and depressurized prior to trans-shipment transfer to a transport vessel. During this process, nodule mass loss of 7% has been estimated, including the fine products of attrition in the riser. Lost nodules report to the dewatering discard flow.

The LOM incorporates the following parameters and processes:

- Block size selection was estimated to align with approximate one-week nodule production of 0.1 Mt. The block size is 2,300 m by 2,300 m with data being consolidated from the geological model, as is detailed in Figure 13.21.
- The following parameters (label, units) were accumulated into the LOM data set:
  — Nodule abundance (kg/m^2).
  — Nodule grades (%): Ni, Cu, Co, Mn, Si, Fe, P.
  — Manganese oxide silicon dioxide ratio.
  — Proportion of area covered by nodule domain (Nodule %).
  — Proportion of area covered by slopes greater than 6°.
  — Proportion of area covered by volcanic rocks.
  — Block designation by 5-year period (first 35 years).
- The following parameters were calculated and used in the LOM:
  — In situ nodule resource tonnes were calculated from the block area, nodule abundance and nodule area percentage.
  — Available nodule tonnes were calculated from the in situ nodule resources and the resource area efficiency factor and accumulated by 5-year periods.
  — Product tonnes were calculated from the available nodule tonnes, collector pick up efficiency factor, collector under flow efficiency factor, nodule attrition factor, and the trans-shipment efficiency factor.
  — Cumulative manganese oxide silicon dioxide ratio was determined from the weighted average block manganese oxide silicon dioxide ratios.
  — Travel distance for one collector was calculated from the block area, percentage nodule area, collector width and allows for the strip left in situ.
  — Pumping modifying factor was calculated to lower the travel speed of the collector when the nodule abundance is larger than the pumping maximum design rate. The pumping adjustment factor was used in determining the overall operated hours by multiplying the block time (travel distance / collector speed).
  — Collector operating hours were determined by:
    – Collector traverse distance divided by the average collector travel speed as defined in the BOD.
    – Additional time was estimated to take account of the turns required, as defined by the collection path. At this level of analysis there is no detailed collection path, hence an allowance was made for the number of turns and total time to complete a turn, as per the BOD. The number of turns per block was estimated by dividing the collector travel distance by the ship turning interval of 30,000 m. Figure 16-31, Figure 16-32 and Figure 16-33 details the LOM collector speeds and nodule abundance.
    – The collector operating time is for a single collector only and these hours were then multiplied by the number of collectors, as defined in BOD.

– The pumping adjustment factor was used in determining the overall operated hours by multiplying this factor by the block time (travel distance / collector speed).

13.7.3   LOM production summary

The LOM production sequence aims to maximize nodule production. It is a conceptual sequence based on mining the areas with the highest abundance first. Production blocks in each nominal 5-year production zone were ranked by abundance. The production sequence accumulates tonnage progressively down through the ranked blocks. Detailed collection paths for the PSVs and seafloor production systems were not developed nor was the production sequence optimized. The production blocks in the sequence are not necessarily spatially contiguous. Twenty (20) days were allowed in the LOM production summary for relocation between non-contiguous blocks. This approach would need to be evaluated through a rigorous mine design and optimization process.

The production summaries for the Hidden Gem, Drill Ship 2 and Collector Ship 1 are provided respectively in Table 13.17, Table 13.18, and Table 13.19. The consolidated LOM production is summarized in Table 13.18 and

Figure 13.24. Over the period 2024 to 2046 a total of 254 Mt is produced with annual production ranging from 0.96 Mt in 2024 to maximum of 14.32 Mt in 2031.

Figure 13.24 NORI Area D LOM production summary
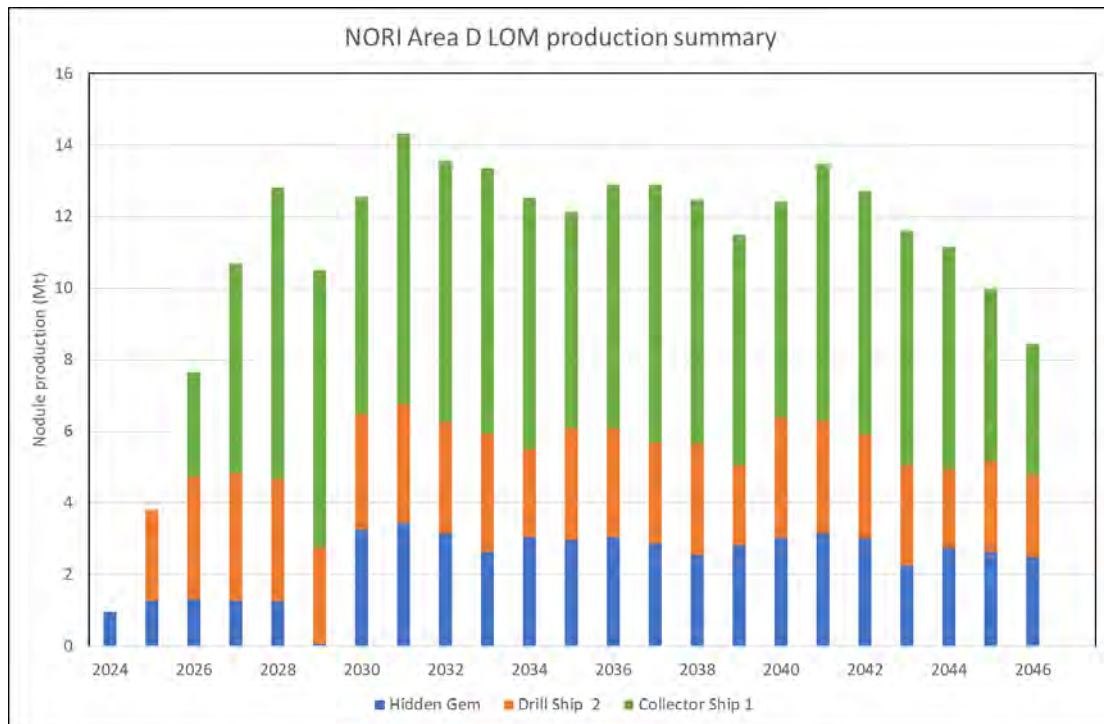
Table 13.17   Hidden Gem summary

Hidden Gem		2024	2025	2026	2027	2028	2029	2030	2031	2032	2033	2034	2035
Nodule Tonnage	Mt	0.96	1.26	1.31	1.27	1.25	0.07	3.25	3.44	3.14	2.63	3.05	2.96
Abundance	kg/m2	21.22	20.78	20.24	19.56	19.00	18.65	17.95	18.80	17.40	18.06	16.86	16.23
Ni Grade	%	1.39	1.40	1.40	1.40	1.38	1.43	1.40	1.39	1.40	1.39	1.40	1.40
Cu Grade	%	1.16	1.15	1.15	1.14	1.12	1.20	1.16	1.13	1.16	1.15	1.15	1.14
Co Grade	%	0.14	0.15	0.15	0.15	0.15	0.13	0.13	0.15	0.13	0.14	0.13	0.13
Mn Grade	%	31.49	31.54	31.47	31.06	30.86	31.46	31.41	31.05	31.29	31.22	31.18	31.23
Si Grade	%	5.58	5.48	5.45	5.58	5.81	5.56	5.34	5.68	5.38	5.51	5.39	5.41
Fe Grade	%	6.32	6.40	6.52	6.65	6.73	6.03	6.67	6.67	6.69	6.69	6.88	6.98
P Grade	%	0.15	0.15	0.15	0.15	0.15	0.15	0.15	0.16	0.15	0.16	0.16	0.16
MnO_SiO2	Ratio	3.42	3.48	3.50	3.37	3.24	3.42	3.56	3.33	3.52	3.44	3.51	3.49
Overall collector speed	(m/sec)	0.47	0.48	0.49	0.49	0.49	0.49	0.49	0.49	0.49	0.49	0.49	0.49
Annual operated hours	h	3,974	5,218	5,431	5,401	5,461	118	5,628	5,687	5,602	4,537	5,621	5,655
Travel distance	km	6,676	8,938	9,537	9,589	9,697	209	9,994	10,097	9,947	8,045	9,981	10,041
Ship Turns		211	283	302	304	307	7	317	320	315	255	316	318
Collected area	km2	62	82	88	88	89	5	247	249	246	199	247	248
Block sector		1	1	1	1	1	2	2	3	3	3&4	4	4

Hidden Gem		2036	2037	2038	2039	2040	2041	2042	2043	2044	2045	2046	Total
Nodule Tonnage	Mt	3.05	2.85	2.56	2.82	3.03	3.16	3.00	2.25	2.74	2.61	2.48	55.1
Abundance	kg/m2	16.88	15.75	17.45	15.38	16.60	17.34	16.36	15.58	15.02	14.42	13.59	16.93
Ni Grade	%	1.39	1.40	1.39	1.39	1.39	1.39	1.39	1.39	1.39	1.37	1.38	1.39
Cu Grade	%	1.16	1.13	1.14	1.13	1.14	1.14	1.13	1.12	1.13	1.13	1.12	1.14
Co Grade	%	0.13	0.13	0.14	0.13	0.13	0.14	0.14	0.14	0.13	0.12	0.13	0.14
Mn Grade	%	31.05	31.08	30.80	30.94	30.93	30.64	30.75	30.69	30.56	30.80	30.74	31.01
Si Grade	%	5.51	5.48	5.62	5.56	5.63	5.73	5.63	5.65	5.71	5.65	5.64	5.56
Fe Grade	%	6.78	7.05	6.84	7.07	6.86	6.87	6.99	7.14	7.18	7.03	7.11	6.86
P Grade	%	0.15	0.16	0.16	0.16	0.17	0.16	0.16	0.16	0.17	0.19	0.17	0.16
MnO_SiO2	Ratio	3.42	3.43	3.34	3.37	3.33	3.28	3.34	3.32	3.27	3.30	3.31	3.39
Overall collector speed	(m/sec)	0.49	0.49	0.49	0.49	0.49	0.49	0.49	0.49	0.49	0.49	0.49	0.49
Annual operated hours	h	5,605	5,629	4,555	5,685	5,641	5,660	5,698	4,495	5,674	5,629	5,671	118,276
Travel distance	km	9,952	9,995	8,088	10,094	10,016	10,050	10,116	7,982	10,074	9,995	10,070	209,186
Ship Turns		315	317	256	320	317	318	320	253	319	317	319	6,626
Collected area	km2	246	247	200	249	247	248	250	197	647	247	249	4,878

Note: Hidden Gem is upgraded in 2029

Table 13.18   Drill Ship 2 summary

Drill Ship 2		2024	2025	2026	2027	2028	2029	2030	2031	2032	2033	2034	2035
Nodule Tonnage	Mt		2.56	3.41	3.57	3.41	2.67	3.23	3.32	3.13	3.30	2.43	3.14
Abundance	kg/m2		20.49	19.99	19.45	18.81	18.51	17.81	18.19	17.27	18.10	16.65	17.24
Ni Grade	%		1.40	1.40	1.41	1.40	1.40	1.40	1.40	1.40	1.40	1.39	1.40
Cu Grade	%		1.14	1.15	1.13	1.14	1.15	1.15	1.14	1.15	1.14	1.16	1.13
Co Grade	%		0.15	0.15	0.15	0.14	0.14	0.13	0.14	0.13	0.14	0.13	0.14
Mn Grade	%		31.49	31.53	31.35	31.26	31.29	31.40	31.23	31.29	30.97	31.29	30.95
Si Grade	%		5.45	5.40	5.49	5.55	5.49	5.30	5.40	5.39	5.55	5.39	5.60
Fe Grade	%		6.56	6.54	6.68	6.63	6.62	6.77	6.71	6.81	6.76	6.74	6.93
P Grade	%		0.15	0.15	0.15	0.15	0.15	0.15	0.15	0.15	0.16	0.15	0.16
MnO_SiO2	Ratio		3.50	3.54	3.46	3.43	3.47	3.58	3.51	3.51	3.40	3.51	3.36
Overall collector speed	(m/sec)		0.48	0.49	0.49	0.49	0.49	0.49	0.49	0.49	0.49	0.49	0.49
Annual operated hours	h		3,970	5,316	5,704	5,636	4,481	5,634	5,665	5,629	5,664	4,535	5,655
Travel distance	km		6,890	9,422	10,128	10,008	7,956	10,004	10,058	9,994	10,057	8,053	10,039
Ship Turns			218	298	321	317	252	317	319	317	319	255	318
Collected area	km2		170	233	250	247	197	247	248	247	248	199	248
Block sector			1	1	1	1	2	2	3	3	4	4	4&5

Drill Ship 2		2036	2037	2038	2039	2040	2041	2042	2043	2044	2045	2046	Total
Nodule Tonnage	Mt	3.00	2.84	3.09	2.23	3.35	3.14	2.92	2.82	2.17	2.58	2.30	64.6
Abundance	kg/m2	16.37	15.59	16.90	15.26	18.24	17.13	16.15	15.44	14.88	14.28	12.65	17.23
Ni Grade	%	1.40	1.40	1.39	1.40	1.39	1.39	1.39	1.39	1.39	1.38	1.38	1.40
Cu Grade	%	1.14	1.13	1.15	1.13	1.14	1.13	1.13	1.12	1.13	1.13	1.13	1.14
Co Grade	%	0.14	0.13	0.14	0.13	0.14	0.14	0.14	0.14	0.13	0.13	0.13	0.14
Mn Grade	%	31.03	31.10	30.94	30.99	30.60	30.60	30.67	30.75	30.76	30.95	30.82	31.07
Si Grade	%	5.45	5.49	5.61	5.53	5.83	5.72	5.68	5.66	5.63	5.59	5.61	5.54
Fe Grade	%	6.95	7.07	6.82	7.11	6.76	6.90	7.00	7.04	7.11	7.00	7.05	6.83
P Grade	%	0.16	0.16	0.16	0.16	0.16	0.16	0.16	0.16	0.17	0.18	0.17	0.16
MnO_SiO2	Ratio	3.45	3.43	3.36	3.39	3.20	3.28	3.30	3.32	3.33	3.35	3.34	3.41
Overall collector speed	(m/sec)	0.49	0.49	0.49	0.49	0.49	0.49	0.49	0.49	0.49	0.49	0.49	0.49
Annual operated hours	h	5,694	5,653	5,674	4,530	5,707	5,698	5,617	5,667	4,538	5,610	5,638	117,916
Travel distance	km	10,109	10,037	10,074	8,044	10,133	10,118	9,973	10,063	8,057	9,962	10,011	209,191
Ship Turns		320	318	319	255	321	320	316	319	255	316	317	6,626
Collected area	km2	250	248	249	199	250	250	246	249	199	246	247	5,168
Block sector		5	5	6	6	7	7	7	7	7	7	7	

Table 13.19   Collector Ship 1 summary

Collector Ship 1		2024	2025	2026	2027	2028	2029	2030	2031	2032	2033	2034	2035
Nodule Tonnage	Mt			2.94	5.84	8.15	7.76	6.06	7.56	7.30	7.43	7.05	6.03
Abundance	kg/m2			19.71	19.20	19.08	18.19	17.70	17.70	17.01	17.39	16.45	17.71
Ni Grade	%			1.40	1.40	1.40	1.40	1.40	1.40	1.40	1.40	1.40	1.39
Cu Grade	%			1.14	1.14	1.13	1.15	1.16	1.15	1.16	1.15	1.15	1.14
Co Grade	%			0.15	0.15	0.15	0.13	0.13	0.14	0.13	0.14	0.13	0.14
Mn Grade	%			31.42	31.36	31.17	31.48	31.23	31.25	31.31	31.14	31.18	30.97
Si Grade	%			5.51	5.48	5.57	5.35	5.39	5.41	5.38	5.47	5.44	5.60
Fe Grade	%			6.61	6.64	6.70	6.61	6.72	6.71	6.77	6.77	6.85	6.76
P Grade	%			0.15	0.15	0.15	0.15	0.15	0.15	0.15	0.16	0.16	0.16
MnO_SiO2	Ratio			3.46	3.47	3.40	3.57	3.50	3.50	3.52	3.46	3.47	3.37
Overall collector speed	(m/sec)			0.49	0.49	0.49	0.49	0.49	0.49	0.49	0.49	0.49	0.49
Annual operated hours	h			4,633	6,297	6,642	6,626	5,321	6,635	6,662	6,641	6,657	5,284
Travel distance	km			8,226	11,181	11,783	11,765	9,447	11,781	11,828	11,792	11,819	9,382
Ship Turns				261	354	373	373	299	373	375	374	374	297
Collected area	km2			203	414	582	581	467	582	584	583	584	464
Block sector				1	1	1&2	2	2&3	3	3	4	4	5

Collector Ship 1		2036	2037	2038	2039	2040	2041	2042	2043	2044	2045	2046	Total
Nodule Tonnage	Mt	6.85	7.20	6.82	6.45	6.04	7.17	6.79	6.53	6.24	4.77	3.66	134.6
Abundance	kg/m2	15.99	16.83	15.93	15.05	17.67	16.75	15.84	15.23	14.64	14.01	8.56	16.67
Ni Grade	%	1.40	1.39	1.40	1.39	1.39	1.39	1.39	1.39	1.38	1.37	1.38	1.39
Cu Grade	%	1.14	1.13	1.14	1.14	1.13	1.14	1.12	1.13	1.13	1.11	1.13	1.14
Co Grade	%	0.13	0.14	0.13	0.13	0.14	0.14	0.14	0.13	0.12	0.12	0.13	0.14
Mn Grade	%	31.14	31.00	31.00	30.97	30.63	30.67	30.74	30.70	30.88	30.37	30.74	31.03
Si Grade	%	5.46	5.59	5.50	5.55	5.73	5.68	5.61	5.64	5.60	5.79	5.64	5.53
Fe Grade	%	6.96	6.91	7.01	7.08	6.84	6.93	7.08	7.12	7.03	7.19	7.05	6.87
P Grade	%	0.16	0.16	0.16	0.17	0.16	0.16	0.16	0.16	0.18	0.18	0.17	0.16
MnO_SiO2	Ratio	3.46	3.38	3.42	3.38	3.27	3.31	3.35	3.32	3.35	3.19	3.32	3.41
Overall collector speed	(m/sec)	0.49	0.49	0.49	0.49	0.49	0.49	0.49	0.49	0.49	0.49	0.49	0.49
Annual operated hours	h	6,650	6,644	6,644	6,656	5,307	6,649	6,656	6,656	6,616	5,291	6,559	131,726
Travel distance	km	11,807	11,797	11,798	11,818	9,423	11,806	11,817	11,818	11,747	9,395	11,645	233,877
Ship Turns		374	374	374	374	298	374	374	374	372	298	369	7,408
Collected area	km2	583	583	583	584	466	583	584	584	580	464	575	11,215
Block sector		5	5&6	6	6	7	7	7	7	7	7	7	

Table 13.20   NORI Area D production summary

Combined Summary		2024	2025	2026	2027	2028	2029	2030	2031	2032	2033	2034	2035
Nodule Tonnage	Mt	0.96	3.82	7.66	10.68	12.81	10.50	12.55	14.32	13.57	13.36	12.53	12.13
Abundance	kg/m2	21.22	20.58	19.93	19.33	19.00	18.28	17.79	18.08	17.16	17.70	16.59	17.23
Ni Grade	%	1.39	1.40	1.40	1.40	1.40	1.40	1.40	1.40	1.40	1.40	1.40	1.40
Cu Grade	%	1.16	1.15	1.14	1.14	1.13	1.15	1.15	1.14	1.16	1.15	1.15	1.14
Co Grade	%	0.14	0.15	0.15	0.15	0.15	0.13	0.13	0.14	0.13	0.14	0.13	0.14
Mn Grade	%	31.49	31.50	31.47	31.33	31.16	31.43	31.32	31.20	31.30	31.11	31.20	31.03
Si Grade	%	5.58	5.46	5.45	5.49	5.59	5.38	5.35	5.47	5.38	5.50	5.42	5.55
Fe Grade	%	6.32	6.51	6.56	6.65	6.69	6.61	6.72	6.70	6.76	6.75	6.84	6.86
P Grade	%	0.15	0.15	0.15	0.15	0.15	0.15	0.15	0.15	0.15	0.16	0.16	0.16
MnO_SiO2	Ratio	3.42	3.50	3.50	3.46	3.39	3.54	3.54	3.46	3.52	3.44	3.49	3.40
Overall collector speed	(m/sec)	0.47	0.48	0.49	0.49	0.49	0.49	0.49	0.49	0.49	0.49	0.49	0.49
Annual operated hours	h	3,974	9,188	15,379	17,402	17,740	11,225	16,584	17,986	17,893	16,842	16,813	16,594
Travel distance	km	6,676	15,828	27,185	30,898	31,488	19,930	29,445	31,936	31,770	29,894	29,853	29,462
Ship Turns		211	501	861	979	997	631	933	1,012	1,006	947	946	933
Collected area	km2	62	253	524	753	919	783	961	1,080	1,077	1,030	1,030	960
Block sector		HG=1 DS= CS=	HG=1 DS=1 CS=	HG=1 DS=1 CS=1	HG=1 DS=1 CS=1	HG=1 DS=1 CS=1&2	HG=2 DS=2 CS=2	HG=2 DS=2 CS=2&3	HG=3 DS=3 CS=3	HG=3 DS=3 CS=3	HG=3&4 DS=4 CS=4	HG=4 DS=4 CS=4	HG=4 DS=4&5 CS=5

Combined Summary		2036	2037	2038	2039	2040	2041	2042	2043	2044	2045	2046	Total
Nodule Tonnage	Mt	12.90	12.89	12.47	11.49	12.42	13.48	12.71	11.60	11.15	9.97	8.43	254.4
Abundance	kg/m2	16.29	16.32	16.48	15.17	17.56	16.98	16.03	15.35	14.78	14.19	11.15	16.87
Ni Grade	%	1.40	1.40	1.39	1.39	1.39	1.39	1.39	1.39	1.38	1.37	1.38	1.39
Cu Grade	%	1.14	1.13	1.14	1.13	1.13	1.14	1.13	1.12	1.13	1.12	1.13	1.14
Co Grade	%	0.13	0.14	0.14	0.13	0.14	0.14	0.14	0.13	0.13	0.12	0.13	0.14
Mn Grade	%	31.09	31.04	30.94	30.97	30.70	30.65	30.72	30.71	30.78	30.63	30.76	31.03
Si Grade	%	5.47	5.54	5.55	5.55	5.73	5.70	5.63	5.65	5.63	5.70	5.63	5.54
Fe Grade	%	6.92	6.98	6.93	7.08	6.82	6.91	7.04	7.10	7.08	7.10	7.07	6.86
P Grade	%	0.16	0.16	0.16	0.17	0.16	0.16	0.16	0.16	0.17	0.18	0.17	0.16
MnO_SiO2	Ratio	3.45	3.40	3.39	3.38	3.27	3.29	3.34	3.32	3.32	3.26	3.32	3.41
Overall collector speed	(m/sec)	0.49	0.49	0.49	0.49	0.49	0.49	0.49	0.49	0.49	0.49	0.49	0.49
Annual operated hours	h	17,948	17,927	16,874	16,871	16,655	18,008	17,970	16,819	16,828	16,531	17,868	367,917
Travel distance	km	31,868	31,830	29,960	29,956	29,571	31,974	31,907	29,863	29,879	29,353	31,726	652,253
Ship Turns		1,009	1,008	949	949	937	1,013	1,011	946	946	930	1,005	20,660
Collected area	km2	1,079	1,078	1,032	1,032	963	1,082	1,080	1,030	1,427	957	1,072	21,262
Block sector		HG=5 DS=5 CS=5	HG=5 DS=5 CS=5&6	HG=6 DS=6 CS=6	HG=6 DS=6 CS=6	HG=6&7 DS=7 CS=7	HG=7 DS=7 CS=7	HG=7 DS=7 CS=7	HG=7 DS=7 CS=7	HG=7 DS=7 CS=7	HG=7 DS=7 CS=7	HG=7 DS=7 CS=7	

Figure 13.25   LOM operational parameters
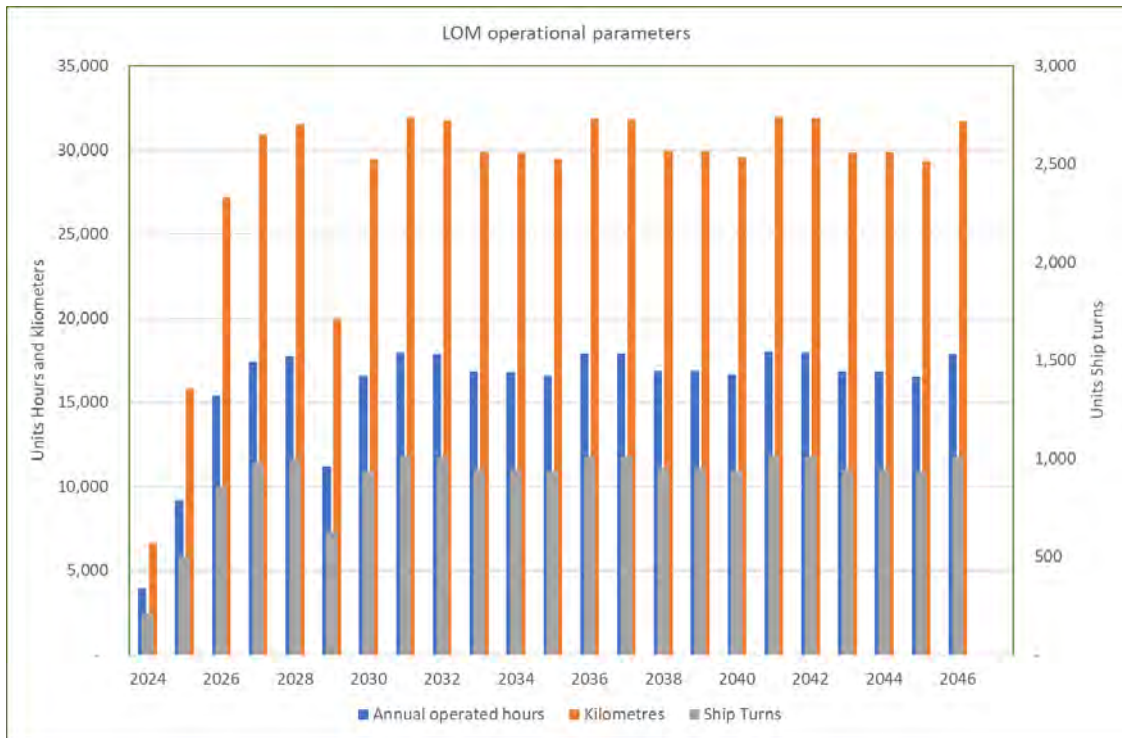
The LOM grades and manganese oxide silicon dioxide ratio are detailed in Table 13.20 and depicted in Figure 13.26 and Figure 13.27. All are relatively constant across the LOM period.

Figure 13.26   Variation in grades of nickel, copper, cobalt and phosphorus across LOM
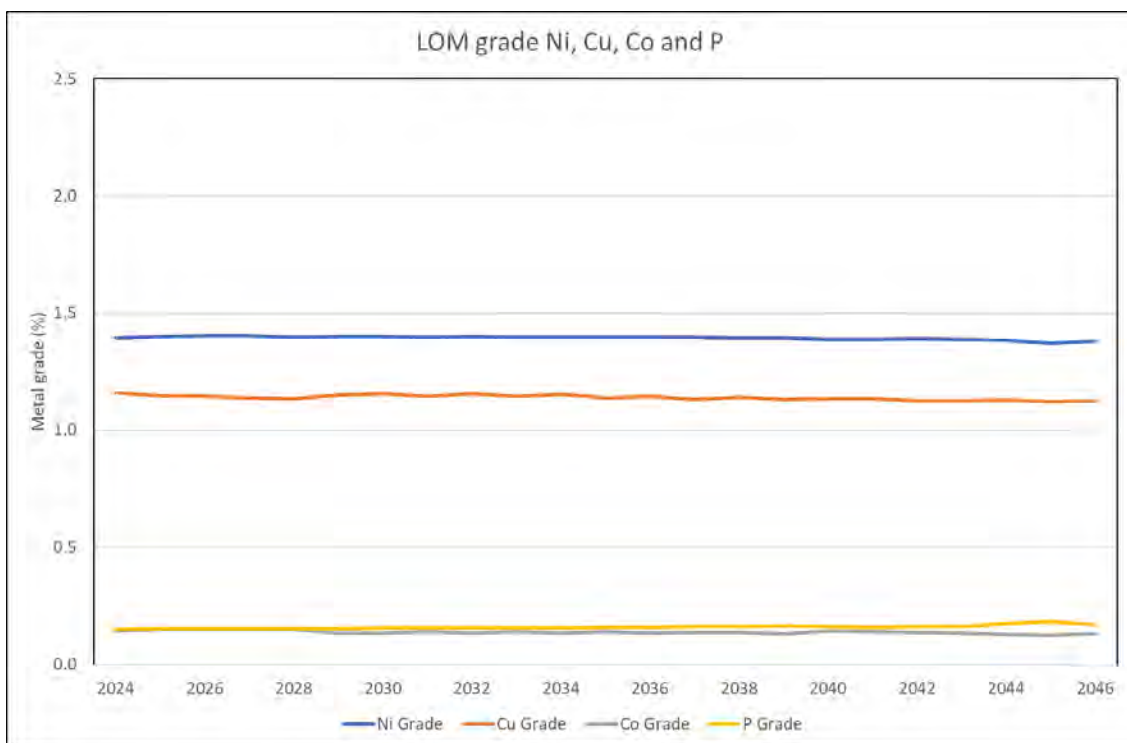
Figure 13.27 Variation in grades of manganese, iron, silicon and MnO:SiO$_2$ ratio across LOM
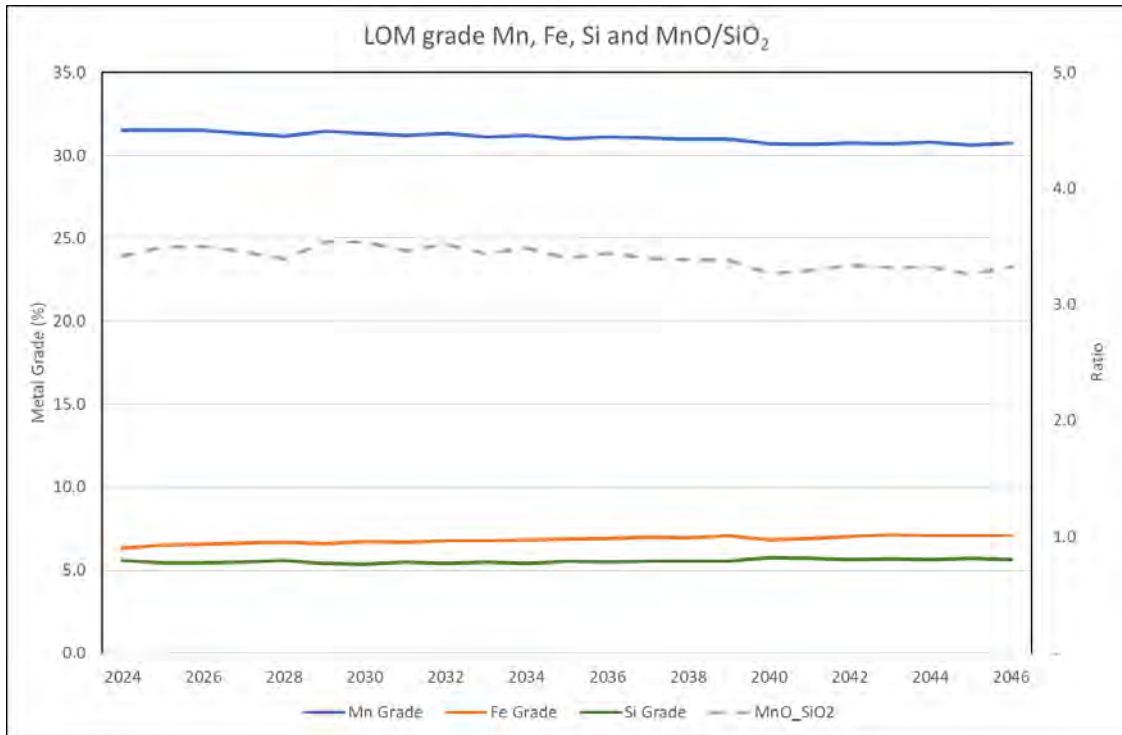
Figure 13.28 details the cumulative nodule product and cumulative abundance and Figure 13.29 shows the nodule product tonnages divided into abundance classes.

Figure 13.28 Cumulative LOM nodule production
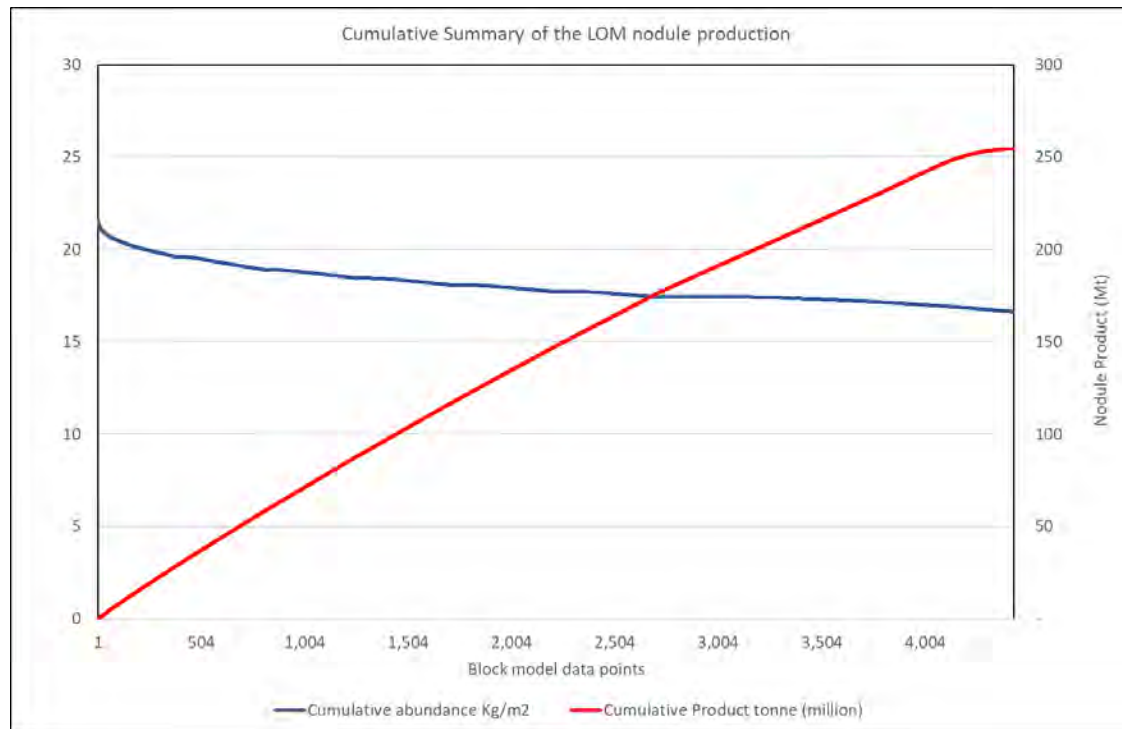
Figure 13.29 Histogram of nodule abundance
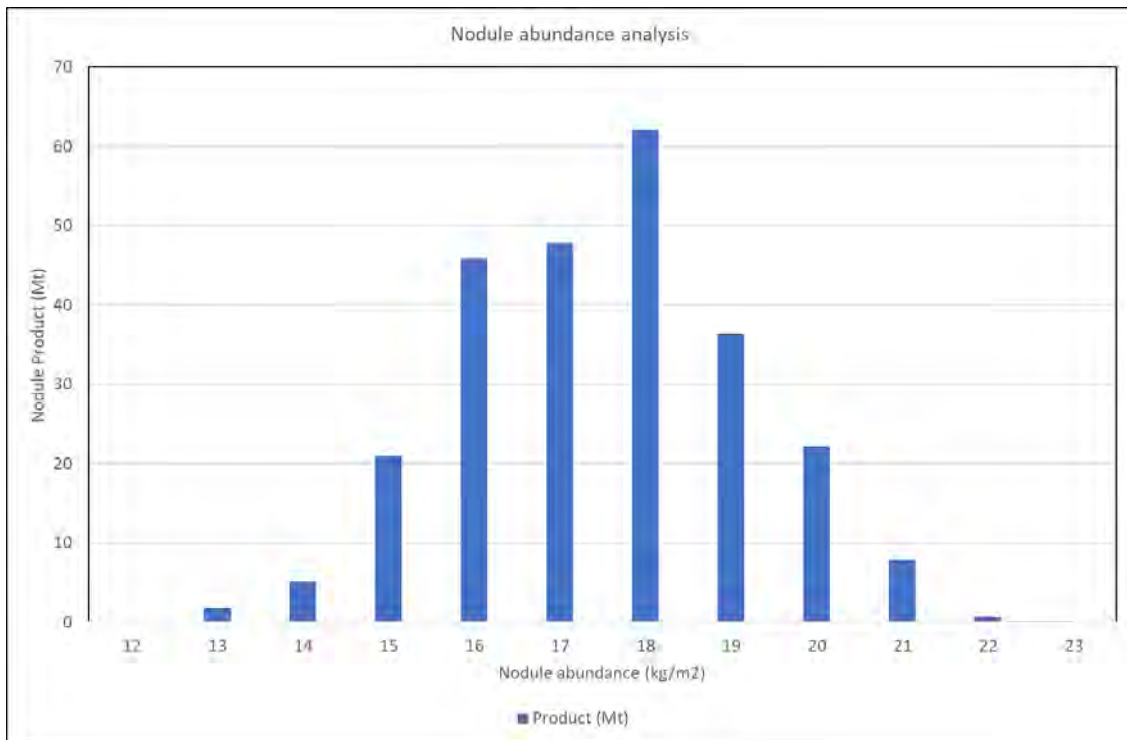
The LOM collector speed and nodule abundance over the LOM are detailed in Figure 13.30, Figure 13.31 and Figure 13.32.

Figure 13.30 Hidden Gem collector speed nodule abundance relationship
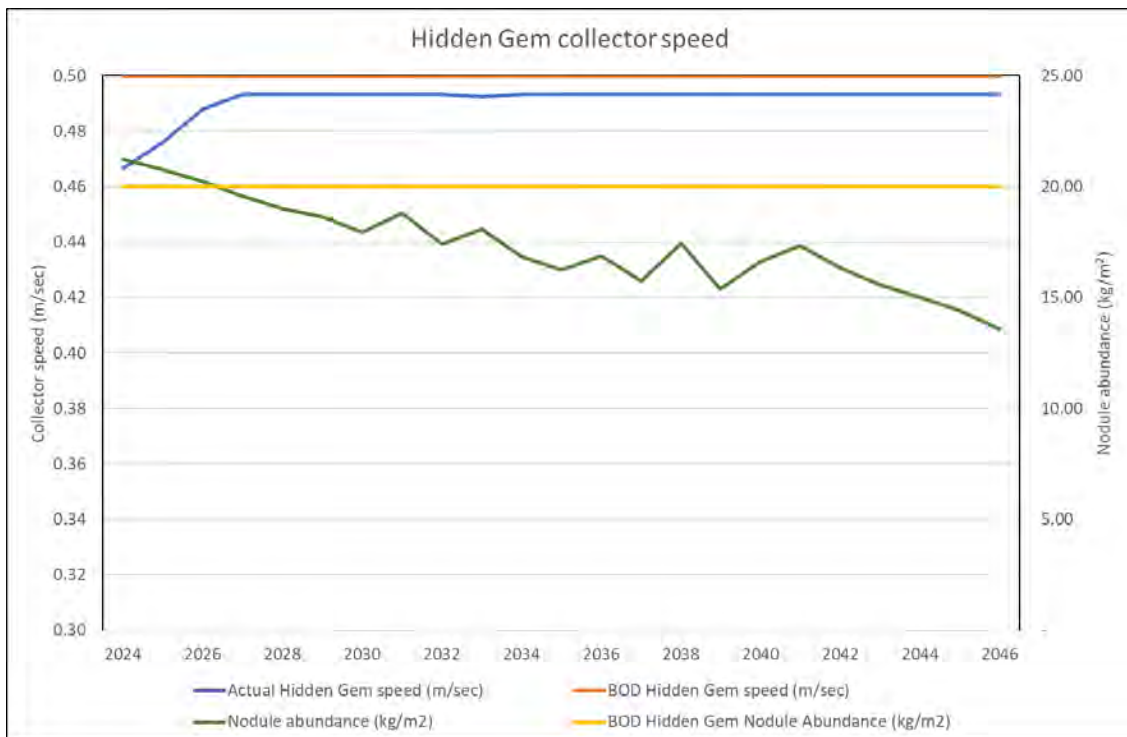
Figure 13.31   Drill Ship 2 collector speed nodule abundance relationship
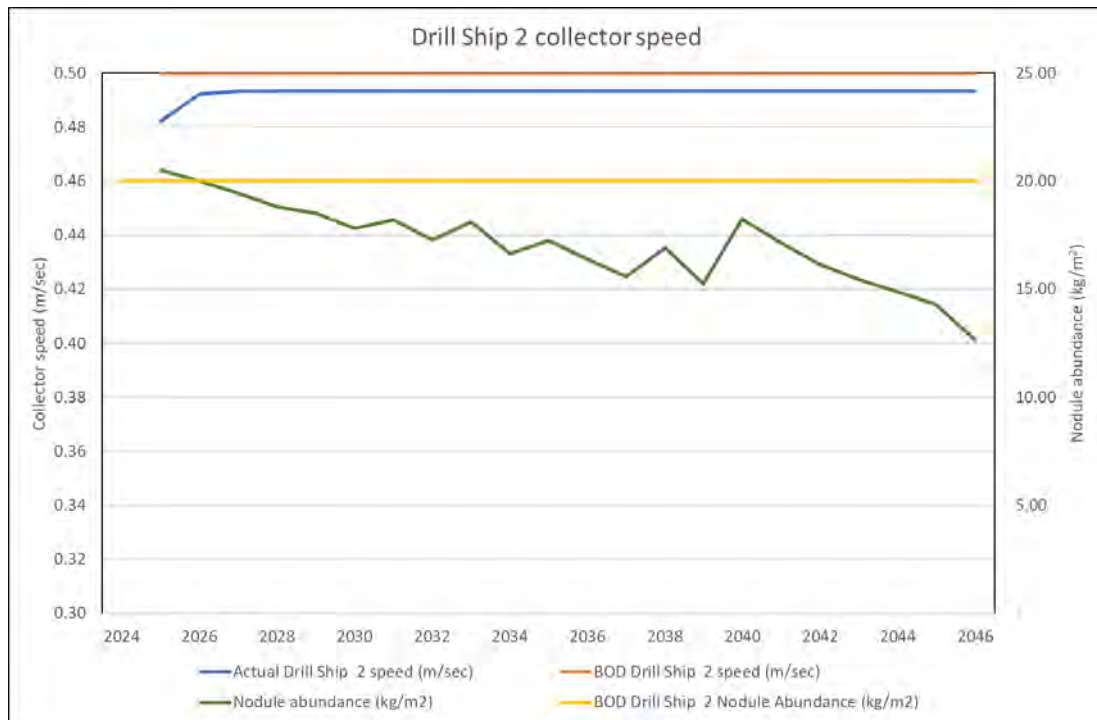
Figure 13.32   Collector Ship 1 collector speed nodule abundance relationship
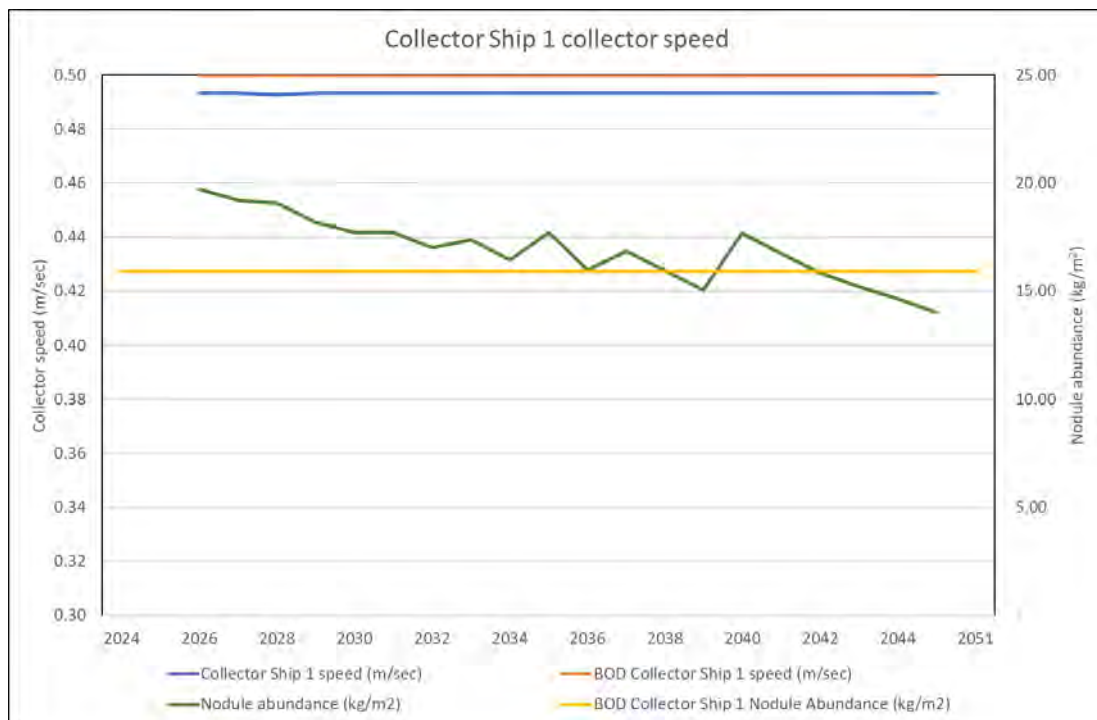
13.7.4   Inferred Mineral Resources

The LOM production sequence includes 6 Mt (wet) of nodules that are classified as Inferred Mineral Resources. This is approximately 2% of the total LOM production. Inferred Mineral Resources that are considered too speculative geologically to have the economic considerations applied to them that would enable them to be categorized as mineral reserves.

14 Processing and recovery methods

The following subsections with respect to process description, production rates and consumables were developed for a processing rate of 4.88 Mt/y (dry basis) of nodules. Subsequently, the resource definition has allowed for an increase in proposed processing rate and, with it, additional processing lines. The extrapolated production information, including toll processing at existing RKEF plants (Project Zero), is discussed in Sections 21 and 22 - this was developed by DeepGreen and forms the basis of the economic evaluation.

14.1 Process design basis

NORI has selected a combined pyro- plus hydrometallurgical process as the basis for the recovery of Ni, Cu, Co and Mn from polymetallic nodules for this IA. This is one of the process alternatives discussed in various literature sources (see Section 13). A pyrometallurgical front end of the plant uses the well-known nickel laterite process featuring rotary kilns and electric furnaces (RKEF) that respectively calcine and smelt the nodules to form an alloy and a slag. The alloy is then sulphidised to form a matte and then partially converted in a Peirce-Smith converter operation to remove iron, following the processing route that Societé Le Nickel used to operate at their Doniambo plant in New Caledonia. The matte from the sulphidation step will then be sent to the hydrometallurgical refinery.

The hydrometallurgical refinery design is based on a sulphuric acid leach flowsheet. A two-stage leach based on the flowsheets of the base metal refineries applied by several platinum producers in South Africa and the United States, particularly Lonmin and Sibanye Stillwater, will be used to produce copper cathode and a pregnant leach solution rich in nickel and cobalt, while low in copper. Further processing of the pregnant leach solution is based on mixed-sulphide precipitate processing flowsheets employing solvent extraction. The final production of battery-grade nickel and cobalt sulphates would use crystallisation.

The pyrometallurgical process generates a manganese silicate stream that can be sold to the manganese industry and a small slag stream that can be sold for construction, while the hydrometallurgical plant produces an ammonium sulphate by-product for sale to the fertiliser industry. Thus, together with the ability to recycle other hydrometallurgical side-streams to the pyrometallurgical process, the flowsheet has neither tailings ponds nor permanent slag repositories and does not generate substantial waste streams.

The following sections provide a description of the assumed process flowsheet and processing parameters.

14.1.1   Plant throughput and availability

The targeted processing rate for the proposed processing plant is 4.88 Mtpa of nodules, dry basis.

In RKEF plants, the kilns and furnaces are close-coupled due to the need to transfer hot calcine from the kilns to the furnaces, with only the transfer system and the furnace feed bins as a buffer between them. An Operating Factor of 85% was assumed for the pyrometallurgical facility based on typical RKEF design. Operating Factor considers planned and unplanned equipment outages and periods of slow-down. It relates the nominal hourly throughput (the rate at which the equipment should be able to operate) to annual throughput:

Annual Throughput = Nominal Hourly Rate × 8,760 hours per year × Operating Factor.

The hydrometallurgical process is decoupled from the pyrometallurgical process by intermediate storage and is assumed to operate for 8,000 hours per year at the nominal rate (equivalent to an Operating Factor of 91.3%).

Production values are reported in Section 14.3.2.2.13.

14.1.2   Feed properties

The nodules are expected to arrive at site largely intact and partially drained of excess sea water. They have a size distribution that is unspecified, but the majority are expected to be <50 mm, i.e., suitable for feeding to the kilns. Incoming nodules will be screened, and the oversize will be crushed.

14.1.3   Nodule composition, speciation, and assay reconciliation

Assay information based on recent (2018, NORI Area D Campaign 3 and 2020, Campaign 6A and 6B) core box samples was provided by NORI. A few adjustments were made to provide an input assay to process modelling that adds up to 100%. The assay as used in process modelling is given in Table 14.1.

Table 14.1   Nodule assay for use in process modelling

Component	Weight %
Loss on Ignition (LOI)	15.87
Oxygen in Mn Compounds	*5.14*
Crystalline Water	*10.73*
Al_2O_3	3.95
CaO	2.43
CoO	0.18
Cr_2O_3	0.01
CuO	1.43
Fe_2O_3	9.49
MgO	3.18
Mn_{Total}	31.2
MnO	0.0
MnO_2	39.44
Mn_2O_3	8.95
MoO_3	0.09
NiO	1.78
P_2O_5	0.36
S	0.11
SiO_2	11.68
ZnO	0.21
Other (assayed)	5.60
Other (unaccounted)	0.37
Total	**100**

The principal changes that were made were:

- Manganese was reported as MnO, but it is predominantly MnO_2 in polymetallic nodules. Recent test work (Section 13) has shown the manganese to be $MnO_{1.9}$. For the purposes of process modelling, this has been apportioned to the compounds MnO_2 and Mn_2O_3 as shown above.

- While LOI for nickel laterites is virtually all crystalline water, this is not the case for the nodules. Higher oxides of manganese decompose when heated to LOI measurement temperatures. Hence the reported LOI has been split into crystalline water and the oxygen that is expected to be lost upon heating as shown in Table 14.1.

- Molybdenum was added to the assay in accordance with measurements during recent test work. Although molybdenum is only present in small amounts, it increases in concentration during processing and becomes of metallurgical significance in the converting operation. The current refining flowsheet does not account for molybdenum. Additional processing steps are required to separate molybdenum and will necessitate additional capital and operating expenditure. While it may be possible to produce a marketable molybdenum by-product, further development would be required to determine the process requirements.

- Process modelling for the RKEF plant was based on using existing METSIM models for nickel laterite plants, modified for the abundance of manganese and copper (and the presence of molybdenum). The assay provided by NORI had a comprehensive list of elements, many at the ppm level, much of which would likely report to EF slag. This part of the assay was therefore assigned as 'Other (assayed)' and dealt with accordingly.

- The revised assay still did not add up to 100%. The missing assay was assigned to 'Other (unaccounted)' and also assumed to report to slag.

Free moisture content of well drained nodules is assumed to be 20% based on recent test work.

14.1.4   Final product specifications

The facility design is based on achieving the preliminary product specifications for nickel and cobalt sulphate products shown in Table 14.2.

Table 14.2   Preliminary Ni, Co product specifications

Component	Units	NiSO$_4$-6H$_2$O	CoSO$_4$-7H$_2$O
Ni	wt%	>22.0	<0.0001
Co	wt%	<0.001	>20.5
Cu	wt%	<0.0001	<0.0005
Fe	wt%	<0.0001	<0.001
Cr	wt%	<0.0001	<0.0005
Mn	wt%	<0.0001	<0.0001
Pb	wt%	<0.0001	<0.0001
Zn	wt%	<0.0001	<0.0005
Mg	wt%	<0.01	<0.01
Na	wt%	<0.02	<0.03
K	wt%	<0.0001	<0.0005
Ca	wt%	<0.0005	<0.005
Si	wt%	<0.002	<0.02

Copper is to be electrowon to cathode without a solvent extraction stage ahead of it. This is to maximise Ni and Co recovery in the subsequent stages. As a result, the Cu cathode quality is expected to be ≥99.9% for the assumed converter matte composition.

The slag produced by the EF operation is rich in manganese and would be marketed as feed to the ferro-manganese, silico-manganese industry.

Converter aisle slag that is not recycled internally may be sold as useful product, e.g., for road construction, sand blasting, or cement additive.

14.2 Project Zero

For Project Zero, NORI proposes to toll treat polymetallic nodules at existing RKEF smelters, utilizing excess industry capacity.

NORI has completed surveys of existing plants in China and Indonesia and commenced discussion with potential partners in Malaysia that are interested in Mn silicate offtake and interested in constructing and operating RKEF furnace lines. NORI advises there is significant interest from many parties in China to utilise RKEF plants which may become stranded as a result of the Indonesian government nickel laterite ore export ban restricting supply of the nickel laterite feedstock that they currently utilise or the general overbuilding of capacity for the nickel pig iron and ferronickel market. These RKEF plants were originally built to convert nickel laterite to nickel pig iron. A review by Kingston Process Metallurgy (Kingston Process Metallurgy, 2020) concluded that existing RKEF lines could be readily converted to process polymetallic nodules to marketable NiCuCo intermediate product(s) and a manganese silicate slag product for sale.

The availability of a total of four 1 Mtpa (wet) third party RKEF lines was assumed for the IA.

Options for toll treatment of matte in hydrometallurgical refineries were identified in Europe and Canada.

As part of Project Zero, NORI is also investigating the option of selling a nickel alloy product, which also contains copper and cobalt. The alloy would be produced at the end of RKEF process. Rather than reporting to the sulphidation stage of the pyrometallurgical plant, the alloy would be sold the market. This alloy is assumed to have a nickel grade of 15.5%.

14.3 Project One

14.3.1   Process description

14.3.1.1 Pyrometallurgical processing

Figure 14.1 shows the pyrometallurgical process flowsheet. It differs from most RKEF plants producing ferronickel in that:

- Dryers have been omitted. At 20% free moisture, the moisture content of the nodules is similar to dry ore discharged from the dryers at most nickel laterite plants. Nickel laterite ores have very variable moisture contents due to exposure to rainfall and can be muddy, sticky and difficult to handle and crush. The dryers therefore serve to render the ore easier to handle and provide a steady moisture feed to the kilns. These are not deemed to be issues for the nodules.

- Free moisture associated with the nodules is sea water.

- A converting operation is not normally part of a ferronickel plant (post tap-hole refining is typically performed in ladle operations). The proposed process follows SLN's former practice of adding molten sulphur to the ferronickel in Peirce-Smith converters and blowing out most of the iron. PT Vale Indonesia also has a converter aisle after the EFs, however they add the sulphur to the kiln discharge and use the converters solely for iron removal. (Sulphur addition to the kiln discharge is highly inefficient and releases substantial amounts of sulphur dioxide and was therefore not selected for this project.)

Figure 14.1   Pyrometallurgical process block flow diagram
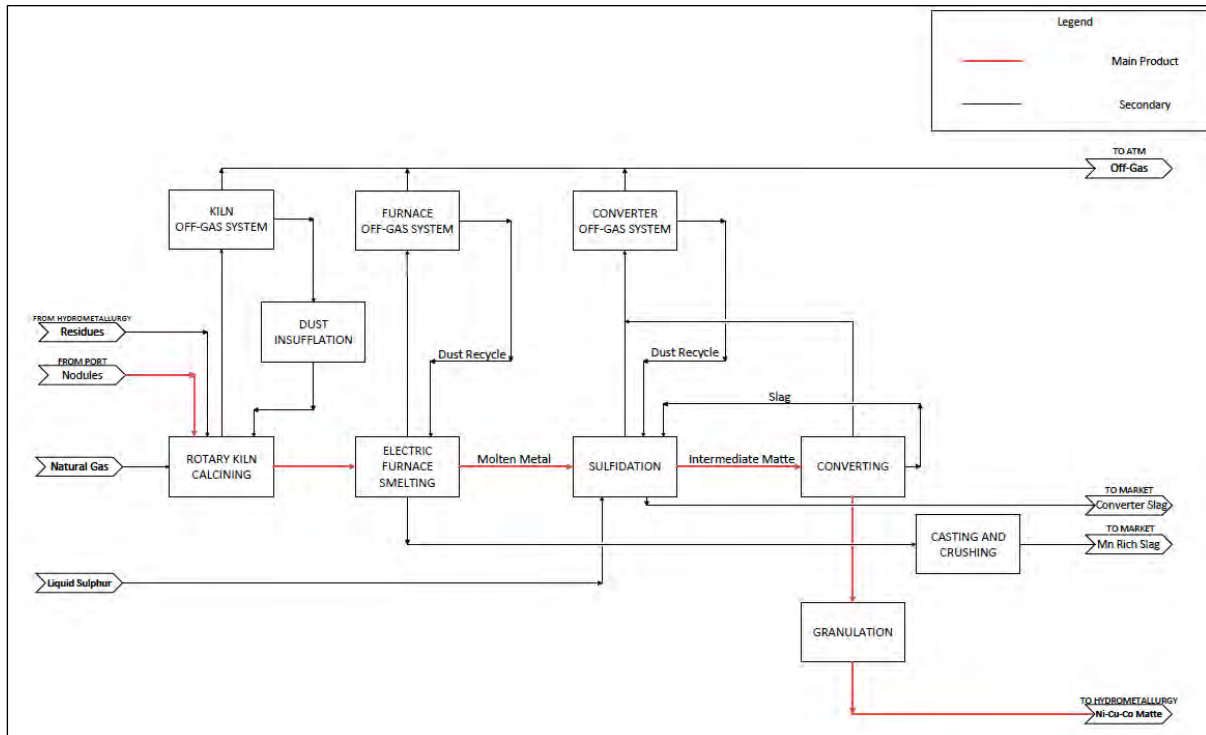
14.3.1.2 Pyrometallurgical process steps

Processing through the pyrometallurgical plant can be summarised as follows:

- Nodules are assumed to arrive at the plant on a continuous, 24-hour basis. Limited storage is therefore required at the plant—a 3-day stockpile has been allowed for.
- The nodules are screened at 2 inches and the oversize (expected 10–15%) are crushed.
- Nodules are conveyed to the kiln feed bins.
- Nodules are fed to the four, gas-fired kilns together with reductant coal, silica flux and residues from the hydrometallurgical refinery. Silica flux is added to target a given slag composition in the EF.
- The nodules are dried, calcined and partially reduced in the kilns.
- Off-gas from the kilns is taken from the feed end of the kilns and sent to particulate cleaning (electrostatic precipitators).
- Collected kiln dust is recycled dry via dust insufflation, i.e., by pneumatically conveying it via a carefully metered dosing system through a lance (pipe) placed through the hot end of the kiln and aimed at the burner flame.
- Hot calcine discharges continuously from the hot end of the kilns into hoppers that periodically discharge into refractory-lined calcine transfer containers.
- The calcine transfer container moves on rails away from the kiln and is hoisted up to the EF feed floor by crane where it is discharged to one of several furnace feed bins. It then returns to the kiln discharge hopper for the next load.
- With four kilns and three EFs, there is provision for cross-feeding.
- In the three, six-in-line (Soderberg electrodes) EFs, the calcine is smelted to produce a metal alloy and a large volume of manganese bearing slag.
- The manganese slag is cast, crushed and trucked to port for export.
- The metal alloy is tapped intermittently into ladles and taken to the converter aisle by crane.

- Off-gas from the furnace is cooled and cleaned of particulate. Collected dust is recycled back to the furnace via the kiln discharge hoppers.

- A large portion (e.g., 50%) of the molten alloy is sent to one of two pig casting machines, forming 20 kg ingots. The pig casters have enough capacity to cast the entire 60 t/h alloy production rate, allowing decoupling of the EF and converter aisle operations.

- In the converter aisle, molten alloy from the EFs is poured into one of two sulphidation vessels (SV). These are large Peirce-Smith converters (15′ diameter by 35′ long).

- Solid alloy ingots are added to the SVs as coolant to help maintain a suitable temperature.

- Silica flux is added to form slag with the iron that is being removed in the SV.

- As part of the converter aisle area, there is a sulphur melting facility where the sulphur is melted and warmed to 140 °C. It is then pumped to the Peirce-Smith vessels through heat-traced lines (steam). Although only two of the four Peirce-Smith vessels will be in use for sulphidation at any one time, there is provision for putting it into any of the vessels when one is down for maintenance/rebuild.

- In the SVs, liquid sulphur to transform the alloy to matte is pumped through a few of the tuyères in the barrel. Air is blown through the remaining tuyères at the same time. Before and after sulphur is pumped, i.e., during roll-in, roll-out, steam is passed through the sulphur tuyères.

- The SVs operate with a large heel in a semi-continuous mode, i.e., relatively small amounts of product matte are removed at a time. The matte is an intermediate matte containing around 30% iron. Slag from the SVs is relatively low in pay-metals and can be granulated.

- The intermediate matte from the SVs is taken to the third large finishing vessel (FV) (also with 15′ diameter by 35′ long). The fourth vessel serves as spare for use when another vessel is down for maintenance/reline.

- Silica flux is added to form slag with the iron that is being removed in the FV.

- When there is sufficient intermediate matte in the FV, blowing commences and continues until the iron in the matte is 5%. This is product matte and it is removed at the end of the batch and water-granulated. Granulated matte is then sent to the hydrometallurgical refinery.

- Slag from the FV is too rich in pay-metals to discard and it is therefore sent back to the SVs.

- Sulphur usage efficiency is assumed to be very high and as a result the matte is sufficiently sulphur-deficient (metallised) that very little sulphur dioxide is formed in the process. The gases from the Peirce-Smith vessels can therefore be treated for particulate capture only and discharged to stack. (It is understood that the one practitioner of this process, SLN in New Caledonia, did not require any sulphur dioxide scrubbing for their sulphidation process). Treatment for SO_2 will depend on the sulphur usage efficiency, but also on any limits on stack emissions and/or air quality in the smelter and nearby areas.

14.3.1.3 Hydrometallurgical processing

Figure 14.2 shows the hydrometallurgical process flowsheet. It consists of a unique combination of proven hydrometallurgical steps based on platinum base metal refineries and battery-grade sulphate production.

Figure 14.2   Hydrometallurgical process block flow diagram
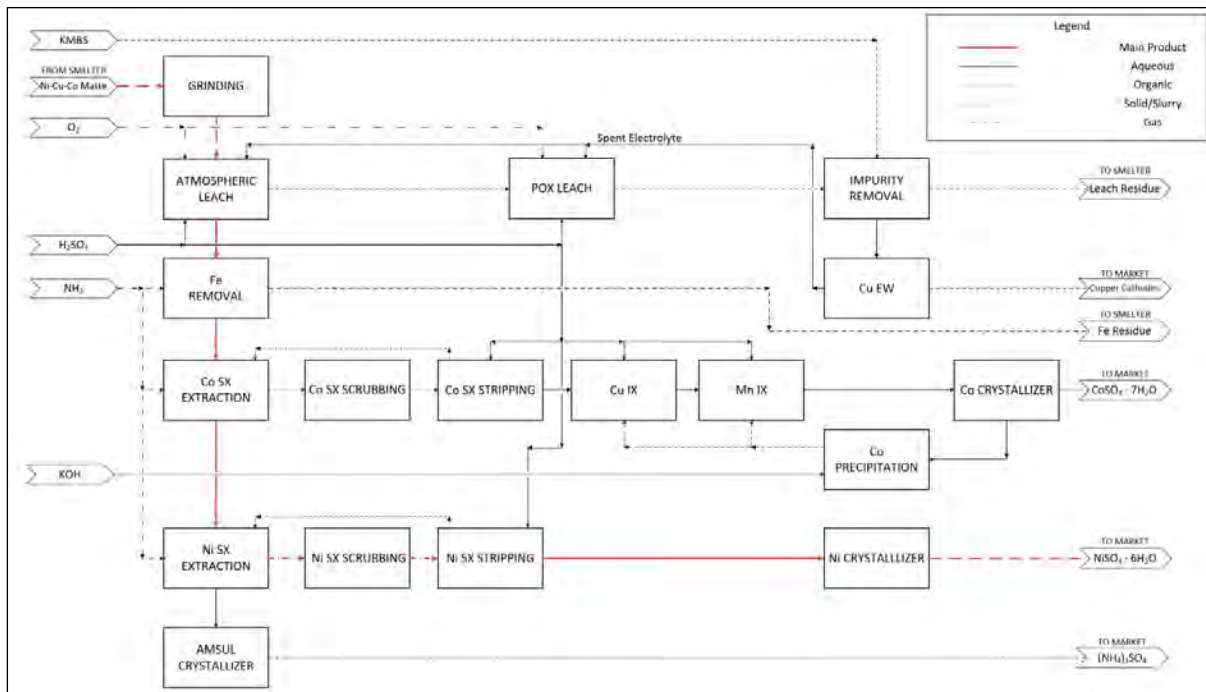
14.3.1.4   Hydrometallurgical process steps

Processing through the hydrometallurgical refinery can be summarised as follows:

- Ni-Cu-Co rich matte is transported from the pyrometallurgical facility to matte storage. An allowance of 3 days of storage space has been made.

- The matte is ground in a mill to reduce particle size before leaching. The ground matte is then pulped and stored with 8 hours of storage capacity.

- Pulped matte feed is then pumped to the first stages of atmospheric leaching, where oxygen and spent electrolyte from copper electrowinning leach the matte. In the final stages of atmospheric leaching, no oxygen is added, promoting metathesis reactions where copper in solution substitutes the nickel remaining in the matte. This leads to a solution high in nickel and low in copper, and a matte depleted in nickel and upgraded in copper.

- The remaining upgraded matte then proceeds to pressure leaching at 220 °C that uses autoclave technology to leach as much of the matte as possible using spent electrolyte, make-up acid and oxygen.

- Any residue remaining is collected and returned to the pyrometallurgical refinery for further recovery, while the copper rich solution from the autoclave is purified, cooled and sent to copper electrowinning to produce copper cathodes. Spent electrolyte is recycled to the atmospheric and pressure leach steps.

- Nickel solution from atmospheric leaching proceeds to iron removal, where ammonia is added to raise the pH and precipitate iron. The iron precipitate is separated and sent back to the smelter to recover any entrained pay metals and to avoid generating an iron waste stream.

- The iron free solution then proceeds to cobalt solvent extraction (SX), where cobalt is extracted using an organic solvent. The cobalt-free raffinate then proceeds to nickel SX, while the cobalt is stripped from the organic using dilute acid.

- The cobalt strip solution passes through purification, where copper and manganese Ion Exchange (IX) are used to purify any remaining impurities. Cobalt hydroxide

precipitated from the cobalt crystalliser bleed is used for pH control to avoid introducing potassium as an impurity.

- The pure cobalt solution is then sent to crystallisation to produce cobalt sulphate heptahydrate, which is bagged for sale.

- The cobalt free raffinate, which is rich in nickel then has the nickel extracted using a nickel selective organic extractant. The nickel is then stripped from the organic using dilute acid before being sent to crystallisation to produce nickel sulphate hexahydrate for sale.

- The remaining raffinate from nickel SX is sent to ammonium sulphate crystallisation to produce ammonium sulphate for use as a fertiliser.

- A small bleed from the ammonium sulphate crystalliser is sent to an effluent treatment system, where mixed-metal hydroxides are produced in the first step and magnesium and manganese hydroxides are produced in the second step. The mixed-metal hydroxides are recycled back to atmospheric leaching while the magnesium and manganese hydroxides are recycled back to the pyrometallurgical plant. The remaining solution is recycled back to ammonium sulfate crystallizer.

14.3.2   Key process parameters

Process parameters relating to throughput, stream assays, energy and reagent consumption are summarised in the tables shown in the following sub-sections.

14.3.2.1 Pyrometallurgical plant

14.3.2.1.1.   Calcining

Calcining has four large kilns 6 m in outside diameter and 135 m long. These are amongst the largest in use in the nickel laterite industry. The information given in Table 14.3 is for each kiln operating at nominal throughput.

Table 14.3   Kiln parameters

Parameter	Value
Nodules to kiln (dry basis)	164 t/h
Nodule moisture (wet basis)	20%
Silica flux to kiln	9.4 t/h
Insufflated recycle dust to kiln	10.3 t/h
Reductant coal to kiln (dry basis)	14.0 t/h
Calcine production	144 t/h
Calcine temperature	900 °C
Natural gas to kiln	8,271 Nm^3/h

14.3.2.1.2.   Electric furnace smelting

The design includes three high power EFs. They are rectangular with six Soderberg electrodes. Slag will be laundered to pits for solidification and subsequent reclaim. Alloy will be tapped intermittently into ladles—the hourly rates indicated are the average rates at which slag and alloy are made inside the furnace. The information given in Table 14.4 is for each furnace operating at nominal throughput.

Table 14.4   Electric furnace parameters

Parameter	Value
Calcine feed rate	192 t/h
Power input	87 MW
Average alloy production rate	18.7 t/h
Average slag production rate	165 t/h
Alloy temperature	1,450 °C
Slag temperature	1,500 °C
Metal composition (wt%)	15.8 Ni, 61.9 Fe, 12.5 Cu, 1.52 Co, 3.64 Mn
Slag composition (wt%)	52.6 MnO, 23.4 SiO_2, MnO/SiO_2=2.25

14.3.2.1.3.   Converter aisle

Alloy from the electric furnaces is tapped periodically into ladles and transferred by crane to the converter aisle. A large part of it (in the range of 50%) is cast into ingots to help with the converter heat balance in the SVs. The molten alloy is fed directly to the SVs. There are two SVs making an intermediate matte which is then transferred to a single operating FV. Unlike the information for the kilns and electric furnaces (per unit), the information given in Table 14.5 is for the entire production coming from the electric furnaces. Once again, while converter aisle operations are semi-continuous and batch, the production rates shown below are hourly average except for blowing rates, which are instantaneous.

Table 14.5   Converter aisle parameters

Parameter	Value
Total alloy to sulphidation	56.1 t/h
Sulphur to sulphidation	4.2 t/h
Silica flux to sulphidation	12.2 t/h
Air blowing rate (two vessels, instantaneous)	90,000 Nm^3/h
Operating temperature	1,300 °C
Intermediate matte production	32.7 t/h
Discard slag production	67.5 t/h
Intermediate matte composition (wt%)	27.3% Ni, 30.0% Fe, 20.6% Cu, 3.03% Co, 13.0% S
Silica flux to finish vessel	4.7 t/h
Air blowing rate (one vessel, instantaneous)	45,000 Nm^3/h
Operating temperature	1,300 °C
Final matte production	21.2 t/h
Recycle slag production	20.1 t/h
Final matte composition (wt%)	40.9% Ni, 5.0% Fe, 30.5% Cu, 3.35% Co, 20.0% S

14.3.2.2 Hydrometallurgical refinery

14.3.2.2.1.   Matte storage and grinding

This area consists of storage and stockpile space for the finished Ni-Co-Cu matte from the pyrometallurgical facility to allow decoupling of the hydrometallurgical refinery. An allowance of 3 days of storage space has been made. The matte is ground in a mill to reduce particle size to a P_{80} of 30 μm before leaching.

14.3.2.2.2.   Atmospheric leaching

Atmospheric leaching has two goals:

1.   The dissolution of the contained metals within the matte.
2.   Providing separation between the copper and nickel by producing:
    a.   A leach solution high in nickel and cobalt and low in copper.
    b.   A residual matte enriched in copper but depleted in nickel and cobalt.

The first step in atmospheric leaching consists of ground matte slurrying and storage, providing eight hours of surge capacity. This matte slurry is fed continuously to five atmospheric leach tanks operating at 85 °C, where it is mixed with spent electrolyte from copper electrowinning. Oxygen is sparged into the first three tanks, which promotes leaching of the matte. The nickel in the matte, which primarily exists as heazlewoodite (Ni_3S_2), reacts according to the following reaction:

$$2Ni_3S_2(s) + 2H_2SO_4(aq) + O_2(g) \rightarrow 2NiSO_4(aq) + 2H_2O(l) + 4NiS(s)$$
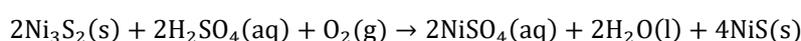
Note that solid millerite (NiS) is left as a by-product of the reaction. No oxygen is added in the final two tanks, allowing metathesis reactions between the copper in solution from electrowinning and any copper leached in the first three tanks and the remaining heazlewoodite. This process enhances the leaching extent of nickel and depletes the solution of copper. The principal metathesis reactions occur as follows:

$$2Ni_3S_2(s) + 2CuSO_4(aq) \rightarrow 2NiSO_4(aq) + 2Cu_2S(s) + 4NiS(s)$$

$$NiS(s) + CuSO_4(aq) \rightarrow NiSO_4(aq) + CuS(s)$$
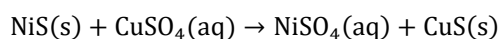
Similar reactions occur for cobalt leaching and metathesis as well. The nickel and cobalt rich solution are then separated from the remaining matte and proceeds to iron removal and then cobalt solvent extraction (SX). The remaining matte is sent to pressure oxidative leaching. See Table 14.6 for a summary of key process parameters. Note that the hourly values reported are on the basis of 8,000 operating hours per year (see Section 14.1.1).

Table 14.6   Atmospheric Leaching Parameters

Parameter	Value
Matte feedrate	19.75 t/h
Solids fraction of leach feed slurry	55%
Leach operating temperature	85-90 °C
Oxygen addition	1.72 t/h
Spent electrolyte addition	109.2 t/h
Nickel concentration in leach discharge solution	85 g/L Ni
Copper concentration in leach discharge solution	<1 g/L Cu
Iron Concentration in Leach Discharge Solution	<2 g/L Fe
Acidity of leach discharge solution	<1 g/L H_2SO_4

14.3.2.2.3.   Pressure oxidative leaching

Pressure oxidative (POX) leaching is intended to maximise the dissolution of the copper enriched matte from atmospheric leaching. The matte is first mixed with spent electrolyte from electrowinning and 93% sulfuric acid in a feed tank before being pumped to the autoclave operating at 2800 kPa and 220 °C. Oxygen and cooling water are added directly to the autoclave. After leaching, any residue remaining is separated from the solution and is sent to the pyrometallurgical refinery. The copper rich solution from the autoclave is

purified, cooled and sent to copper electrowinning. Key parameters for the POX leach are provided in Table 14.7.

Table 14.7   Pressure oxidative leaching parameters

Parameter	Value
Residence Time	1.5 hours
Pressure	2800 kPa
Operating temperature	220 °C
Oxygen utilisation	85%
Oxygen addition	11.2 t/h
Cooling method	Direct Injection
Cooling water addition	96.0 t/h
Spent electrolyte addition	127.4 t/h
93% sulfuric acid addition	3.2 t/h
Nickel concentration in POX discharge solution	34 g/L Ni
Copper concentration in POX discharge solution	72 g/L Cu
Acidity of POX discharge solution	10 g/L H_2SO_4

14.3.2.2.4.   Impurity removal and copper electrowinning

Copper solution from pressure oxidative leaching is purified and cooled before proceeding to copper electrowinning (EW). Impurities like selenium and tellurium are removed via reduction with potassium metabisulfite before EW. Note that this impurity removal step may not be necessary but has been left in as a cost allowance.

Purified copper solution from POX leaching proceeds to the electrowinning cellhouse. The electrowinning cellhouse is a well-ventilated building that houses two parallel rows of electrowinning cells. Ventilation serves to prevent the accumulation of acid mist, which is a health hazard and can result in electrical fires. A single overhead crane services the cells. Servicing activities include harvesting the copper cathode product, replacing them with fresh cathode sheets, replacing damaged anodes and maintenance. Rectifiers and transformers provide the power at the correct potential difference for effective operation.

In EW, guar and other trace additives are added to improve the properties of cathode produced, which form when electrical current is applied across the electrowinning cells.

Purified copper solution from POX leaching is combined with recirculated electrolyte in the electrowinning feed tanks. The resulting electrolyte feed solution then passes through the electrowinning cells where it comes into contact with the cathodes and anodes. The anodes have been assumed to be lead for the purposes of this estimate. The cathodes are comprised of stainless-steel starter sheets that accumulate copper as the electrowinning reactions proceed. Electrical current passing through the cells drives two reactions:

1.   At the cathode, an accumulation of electrons drives the reduction of Cu^{2+} in solution to Cu^0, causing the copper to plate on the stainless-steel starter sheets.
2.   At the anode, a deficit of electrons drives the decomposition of water into H^+ and O_2, causing the formation of sulfuric acid and the evolution of oxygen gas.

The current density is maintained at 200 A/m^2 to ensure controlled, even plating for a good quality cathode. The spent electrolyte is only depleted in copper by 3 g/L. A significant portion of the spent electrolyte is recirculated to the electrowinning feed tanks while the remainder exits the cellhouse and is sent to leaching for use as a lixiviant.

Table 14.8 provides the key parameters for impurity removal and copper EW.

Table 14.8   Impurity removal and copper electrowinning parameters

Parameter	Value
Impurity removal reagent	Potassium metabisulfite (KMBS)
Current density	200 A/m^2
Cell voltage	2.35 V
Electrowinning operating temperature	45 °C
Electrowinning copper bite	3 g/L Cu
Spent electrolyte copper concentration	40 g/L Cu
Spent electrolyte acidity	50–60 g/L H_2SO_4

14.3.2.2.5.   Iron removal

Iron is removed from the nickel rich solution that leaves the atmospheric leach by increasing the pH, using ammonia, in a series of continuous stirred-tank reactors. This causes the iron to precipitate as iron (III) hydroxide, allowing a series of thickeners and filters to separate the iron solids from the solution. The iron solids are sent back to the smelter to recover any entrained pay metals and to avoid generating an iron waste stream. The iron-free solution then proceeds to cobalt solvent extraction (SX).

Table 14.9 provides the key iron removal parameters.

Table 14.9   Iron removal parameters

Parameter	Value
pH control agent	NH_3
Target pH	5-5.5
Iron filter cake production rate	0.47 t/h
Solids fraction of the iron filter cake	60 wt%

14.3.2.2.6.   Cobalt solvent extraction

Cobalt SX consists of a series of mixer-settler units that facilitate the removal of cobalt from the iron-free solution. The circuit consists of three parts: extraction, scrubbing and stripping.

In extraction, the iron-free solution first contacts an organic solution that selectively removes cobalt via mixer tanks. The organic is comprised of bis (2,4,4 trimethylpentyl) phosphinic acid, an extractant with an affinity for cobalt, and a high flash point carrier solvent. After contacting the organic, the aqueous solution is separated using settler tanks. Extraction occurs in four mixer-settler stages. The cobalt free aqueous solution is pumped to nickel SX.

The cobalt-loaded organic from extraction then proceeds to scrubbing, where it is scrubbed with a weakly acidic, cobalt-rich aqueous solution to remove any impurities that may have loaded onto the organic. Scrubbing occurs in three mixer-settler stages. The spent scrubbing solution is recycled to extraction.

The scrubbed organic now proceeds to stripping, where the cobalt is stripped from the organic with sulfuric acid solution. Stripping occurs in three mixer-settler stages. A part of this cobalt strip solution is used to prepare the scrubbing solution and the remainder proceeds to cobalt purification. See a summary of the key parameters in Table 14.10.

Table 14.10   Cobalt SX Parameters

Parameter	Value
Extraction pH Control Agent	NH_3
Target Extraction pH	5.5
Target Operating Temperature	60 °C
Extractant	Bis (2,4,4 Trimethylpentyl) Phosphinic Acid (Cyanex 272 or equivalent)
Diluent	High flash point aliphatic solvent
Scrubbing Solution	Cobalt strip liquor and dilute H_2SO_4
Target Cobalt Concentration Exiting Scrubbing	25 g/L Co
Strip Acid	Dilute H_2SO_4
Target Stripping pH	3.4

14.3.2.2.7.   Cobalt purification

Cobalt purification serves to remove residual copper, manganese and other trace impurities that load in cobalt SX.

Copper is removed using ion exchange (IX) with an iminodiacetic acid resin. The copper loads onto the resin and is later stripped using sulfuric acid. Nickel present in solution will also load onto the resin. The stripped copper eluate is sent back to POX leaching. The copper-free cobalt solution proceeds downstream for manganese removal.

Manganese is also removed using IX, but with a Di-(2-ethylhexyl) phosphoric acid impregnated resin. Manganese, zinc and other base metals load onto the resin and are later stripped using sulfuric acid. The stripped manganese eluate is sent to effluent treatment. The purified cobalt solution is pumped to cobalt sulfate crystallization.

Cobalt hydroxide precipitated from the cobalt crystallizer bleed is used for pH control throughout cobalt purification to avoid introducing potassium as an impurity.

Table 14.11 summarises the key parameters below.

Table 14.11   Cobalt purification parameters

Parameter	Value
Copper IX resin	Chelating iminodiacetic acid (amberlite 718 or equivalent)
Copper IX design loading temperature	40 °C
Design product concentration	0.1 mg/L Cu
Design resin loading	0.05 mol Cu/L WSR
Copper IX elution reagent	Dilute H_2SO_4
Manganese IX resin	D2EHPA Impregnated (Lewatit VP OC 1026 or equivalent)
Manganese IX minimum loading temperature	20°C
Manganese IX maximum loading temperature	40°C
Resin loading capacity	13 g/L Zn
Manganese IX maximum operating pH	4
Manganese IX elution reagent	Dilute H_2SO_4

14.3.2.2.8.   Nickel solvent extraction

Nickel SX consists of five extraction stages and serves to remove the nickel from the cobalt free raffinate that is pumped from cobalt SX. Organic solution comprised of neodecanoic

acid, an extractant with an affinity for nickel, and a high flash point carrier solvent loads the nickel in extraction. The loaded organic is then scrubbed of any impurities that may have loaded before the nickel is stripped from the organic with sulfuric acid. A part of this nickel strip solution is then used for scrubbing and the remainder proceeds to nickel sulphate crystallisation.

To mitigate the risk of nickel-ammonium double salt precipitation, a portion of the nickel free raffinate from extraction is recirculated to the start of nickel SX. This serves to reduce the nickel concentration while increasing the ammonium sulphate concentration in the circuit. The remainder of the raffinate is pumped to crystallisation to produce ammonium sulphate. See a summary of the key parameters in Table 14.12.

Table 14.12 Nickel SX parameters

Parameter	Value
Extraction pH control agent	NH_3
Target extraction pH	6.85
Target operating temperature	60 °C
Extractant	Neodecanoic acid (commonly referred to as versatic acid 10)
Diluent	High flash point aliphatic solvent
Scrubbing solution	Nickel strip liquor and dilute H_2SO_4
Target nickel concentration exiting scrubbing	4 gpL Ni
Strip acid	Dilute H_2SO_4
Target stripping pH	5.2

14.3.2.2.9. Cobalt sulphate crystallisation and packaging

The purified cobalt solution from cobalt purification is sent to an evaporator where it is evaporated to saturation. The saturated solution is then fed to a crystalliser that uses steam, electricity and a vacuum to evaporate water at 38 °C and produce a $CoSO_4 \cdot 7H_2O$ slurry. For the purpose of this IA, the crystalliser design assumes the use of multiple effect evaporation, reducing steam consumption by using the evaporated water from the first stage of crystallisation to heat the second stage. The crystal slurry is then centrifuged before being dried to produce battery-grade $CoSO_4 \cdot 7H_2O$ crystals that are bagged in 1-tonne bags before delivery to market. Table 14.13 summarises the key parameters below.

Table 14.13 Cobalt sulphate crystallisation and packaging parameters

Parameter	Value
Target crystalliser operating temperature	38 ℃
Crystalliser bleed rate	5.5% of Cobalt in feed
$CoSO_4$ saturation concentration	31wt% in solution
Solids fraction at crystalliser outlet	45wt%
Target dryer operating temperature	40 ℃
Residual moisture in dryer	<0.25wt%
Product packaging type	1-tonne canvas bags

14.3.2.2.10. Cobalt Precipitation

The bleed from cobalt crystallization proceeds to a series of continuous stirred-tank reactors where potassium hydroxide is used to raise the pH of the solution and precipitate the cobalt as cobalt hydroxide.

Potassium hydroxide is used as a base instead of sodium hydroxide because it produces potassium sulfate when reacted with sulfuric acid while sodium hydroxide produces sodium sulfate. Potassium sulfate is a fertilizer and will not pose any problems when it eventually ends up in the ammonium sulfate product.

The precipitated cobalt hydroxide is filtered and washed using a belt filter before use as a pH modifier in cobalt purification. The remaining bleed stream is sent to effluent treatment. Table 14.4 summarizes the key parameters below.

Table 14.14   Cobalt precipitation parameters

Parameter	Value
pH Control Agent	KOH
Target pH	6–8
Solids fraction of the cobalt hydroxide filter cake	20wt%

14.3.2.2.11.   Nickel sulphate crystallisation and packaging

The nickel strip solution from nickel SX then proceeds to an evaporator where it is evaporated to saturation. The saturated solution is then fed to a crystalliser that uses steam, electricity and pressure to evaporate water at 65 °C and produce a $NiSO_4·6H_2O$ slurry. The crystallizer design assumes the use of multiple effect evaporation, reducing steam consumption by using the evaporated water from the first stage of crystallization to heat the second stage. The crystal slurry is then centrifuged before being dried to produce battery-grade $NiSO_4·6H_2O$ crystals that are bagged in 1-tonne bags before delivery to market. Table 14.15 summarises the key parameters below.

Table 14.15   Nickel sulphate crystallisation and packaging parameters

Parameter	Value
Target crystalliser operating temperature	65 °C
Crystalliser bleed rate	10% of Nickel in feed
$NiSO_4$ saturation concentration	36wt% in solution
Solids fraction at crystalliser outlet	45wt%
Target dryer operating temperature	40 °C
Residual moisture in dryer	<0.25wt%
Product packaging type	1-tonne canvas bags

14.3.2.2.12.   Ammonium sulphate crystallisation and packaging

The nickel SX raffinate is sent to an evaporator where it is evaporated to saturation. The saturated solution is then fed to a crystalliser that uses steam, electricity and pressure to evaporate water at 75 °C and produce an ammonium sulphate slurry. Like the nickel sulphate crystalliser, the ammonium sulphate crystalliser design assumes the use of multiple effect evaporation, reducing steam consumption by using the evaporated water from the first stage of crystallization to heat the second stage. The crystal slurry is then centrifuged before being dried to produce ammonium sulphate that is bagged in 1-tonne bags before delivery to market for use as a fertiliser. Table 14.16 summarises the key parameters.

Table 14.16   Ammonium sulphate crystallisation and packaging parameters

Parameter	Value
Target crystalliser operating temperature	75 °C
Crystalliser bleed rate	5% of ammonium sulphate in feed
$NiSO_4$ Saturation concentration	36wt% in Solution
Solids Fraction at crystalliser outlet	45wt%
Target dryer operating temperature	85 °C
Residual moisture in dryer	<0.25wt%
Product packaging type	1-tonne canvas bags

14.3.2.2.13.   Effluent Treatment

A small bleed from the ammonium sulfate crystallizer along with a few other minor streams from the overall process are sent to effluent treatment.

The first step of effluent treatment is mixed-metal hydroxide (MMH) precipitation, which consists of a series of continuous stirred-tank reactors. Potassium hydroxide is added to the reactors in order to raise the pH to between 7–9 and precipitate remaining base metals in solution as hydroxides. The resulting hydroxides are then filtered and washed before being recycled back to atmospheric leaching so that the contained nickel, cobalt and copper are recovered. The MMH-free solution proceeds to the second step of effluent treatment.

The second step of effluent treatment is magnesium and manganese precipitation. Again, the precipitation occurs in continuous stirred-tank reactors. This time, potassium hydroxide is added to raise the pH to between 10–12 to precipitate magnesium and manganese from solution as hydroxides. The resulting hydroxides are then filtered and washed before being sent to the pyrometallurgical plant. The remaining solution, now largely consisting of potassium sulfate and ammonium sulfate, is recycled back to the ammonium sulfate crystallizer for recovery as fertilizer. Table 14.17 summarizes the key effluent treatment operating parameters below.

Table 14.17   Effluent Treatment Parameters

Parameter	Value
MMH Precipitation	
pH Control Agent	KOH
Target pH	7-9
Filter cake production rate	0.03 t/h
Solids fraction of the filter cake	50%
Mg & Mn Precipitation	
pH Control Agent	KOH
Target pH	10-12
Filter cake production rate	0.01 t/h
Solids fraction of the filter cake	50wt%

14.3.3   Recoveries

Recoveries of Ni, Cu and Co through each major process step are shown in Table 14.18. The process models used for the study are not interlinked and, importantly, do not incorporate the recycle of hydrometallurgical residues back to the smelter. For the purposes of the IA, it has been assumed that the pay-metals in residues can be recovered by the recovery factor for the pyrometallurgical steps. This gives the final recoveries shown at the bottom of the table.

Table 14.18   Pay metal recoveries for combined plant

Process Step	Nickel		Cobalt		Copper	
	t/y	Recovery	t/y	Recovery	t/y	Recovery
Nodules in	68,300	-	6,830	-	55,600	-
Final matte	64,600	94.6%	5,290	77.4%	48,100	86.5%
Hydrometallurgical products before recycle	64,000	98.9%	5,190	98.0%	46,400	96.2%
Recycled residue	700	94.6%	100	77.4%	1,800	86.5%
Overall recovery	64,700	94.6%	5,270	77.2%	48,000	86.2%

In addition to the above base metals, approximately 3.7 Mtpa of manganese silicate is to be produced, containing 52.6% MnO (98.9% recovery of manganese).

14.3.4   Plant footprint

No layout of the proposed plant has been developed during this IA.

14.3.5   Infrastructure requirements: utilities, transportation and production

No site visit or specific site selection has been completed for the proposed plant, however potential sites are discussed in Section 18. An important aspect of site selection for the project is the assumption that it has good existing infrastructure in place, including appropriate port facilities, access roads, high voltage power supply, natural gas supply, etc. To assist with site selection, the following tables show utility requirements, major consumables and product quantities.

Table 14.19 shows major utilities required by the combined pyro- and hydro-metallurgical plant.

Table 14.19   Estimated Power, Natural Gas and Water Requirements

Commodity	Annual Requirement	Indicative Peak Demand
Electrical power	2,496,000 MWh	~330 MW
Natural gas	310,183,000 Nm^3	41,000 Nm^3/h
Water	5,741,000 m^3	770 m^3/h

In addition to the 6.1 Mt/y (wet) of nodules shipped to the plant, various other consumables will also be required. Table 14.20 Summarises consumable quantities in excess of 10,000 t/y.

Table 14.20   Major consumable requirements

Consumable	Approximate Annual Requirement
Coal	473,000 t (wet)
Silica flux	407,000 t
Sulphur	31,000 t
Sulphuric acid (93 wt%)	176,000 t
Anhydrous ammonia	48,400 t

Products and by-products from the process plant will have to be shipped to market. These are summarised in Table 14.21. For the contained pay-metal in each of the main products, refer to Table 14.18.

Unlike most mining processes, the proposed mineral processing flowsheet seeks to make by-products rather than substantial waste streams and is not expected to require tailings ponds or other long-term waste storage on-site.

Table 14.21   Annual product quantities

Product	Annual Production (tpa)
Nickel sulphate	289,300
Cobalt sulphate	25,100
Copper cathode	48,000
Manganese slag	3,690,000
Converter slag	503,000
Ammonium sulphate	192,000

14.3.6   Process plant ramp-up

Based on thorough resource assessment, engineering, test work and pilot-scale demonstration of the process with polymetallic nodules as the feedstock, the ramp-up performance of the integrated commercial facility could be analogous to similar metallurgical facilities that followed a full development program and invested in debottlenecking efforts during commissioning and ramp-up. Provided the project follows that course, it is reasonable to assume a modified Series 2 McNulty ramp-up (Wasmund et al, 2011) with 95% of design capacity after 2 years and 100% after 2.5 years.

15 Project infrastructure

15.1 On-shore infrastructure

The infrastructure requirements for the Project, apart from the minerals processing facility described in Section 17, are modest compared to terrestrial resources projects of similar production capacities.

The site and host country for the minerals processing facility has not yet been confirmed. The site must be serviced by grid power, reticulated water, and natural gas. A location will be selected that is close to an industrial port, and near an existing municipality from which labour can be sourced.

DeepGreen engaged Global Location Strategies (GLS) to carry out a global benchmarking study of potential sites for the minerals processing facility. The study considered the primary site location drivers for this facility including logistics costs (both inbound and outbound) and energy costs (electricity and natural gas) and port depth. The study also considered:

- Renewable energy availability
- Political stability of country
- Ease of doing business in region/country

The GLS study recommended 13 countries for further consideration.

The Project will require some warehousing capacity to store critical spares (for example, critical spares for the collectors and riser). It is likely that a suitable facility can be purchased or leased and need not be constructed. Reasonable land acquisition costs have been allowed for in the project evaluation model.

15.2 Nodule transport

DRT has performed a preliminary assessment of the transportation fleet for transfer of nodules from NORI Area D. The nodules will be landed at an existing deep-water industrial port equipped with bulk offloading facilities and depending on the location of the process plant areas for stockpiling and loading ore on a rail line for transport to the plant. For this study we have assumed the port of Lazaro Cardenas, Michoacan, Mexico, 960 nm from the NORI Area D reference site (11N, 117W). Lazaro Cardenas has an existing, bulk minerals unloading area (Figure 15.1) as well as fuel bunkering facilities. Alternately, the vessels could be equipped for self-unloading in bulk or slurry form. Facilities to receive the ore and dewater it (in the case of slurry offloading) would be required.

This IA assumes transportation of nodules will be by chartered vessels. For Project Zero, transport vessels with 35,000 t deadweight capacities will be sufficient. For the Project One drillship conversions (3.6 Mtpa), two 100,000 t deadweight trans-shipment vessels are required. For Collector Ship 1, the fleet consists of three vessels with deadweight capacities of 100,000 tonnes. The vessels will require DP capability to enable them to be loaded at sea astern of or alongside the PSV. Transhipment vessels will be converted bulk mineral carriers with dynamic positioning (DP) to allow tracking behind the PSV during operations Figure 15.2.

Nodules will be transferred at sea from the PSVs to transhipment vessels. The materials handling method has not yet been confirmed, but multiple options exist (for example, pumping as a slurry or conveying a solid product) and will be evaluated in future studies. This IA assumes the PSVs and the transhipment vessels will be equipped to facilitate the transfer of nodules at sea. This method of offloading, known as tandem offloading, is well

established for offloading of oil production vessels in remote areas of the world. DP tankers have been employed in this service for more than 20 years, see (Tannuri, et al., 2009).

The net transfer rate includes simultaneous unloading of the buffer tanks while transferring nodules directly from the lift system. An allowance is included for down time during collector maintenance cycles.

The interstitial moisture content of the nodule slurry during transportation is an important parameter in estimating transportation logistics and costs. Several dewatering methods have been studied previously in the 1970s (Kennecott Copper Corporation - Ledgemont Laboratory, 1977). This included evaluation of several dewatering methods using attrited nodule samples from pump loop tests. The results indicated the interstitial moisture of the cargo (excluding moisture contained in the nodule pores) could be between 5% (for centrifuge dewatering) to 20% (gravity separation). In addition to moisture content, the studies evaluated cut points and mineral recoveries in the dewatered ore. Based on these studies, gravity settling and decanting the wastewater was deemed the most practical and economic method of storage of nodules on the PSV, resulting in about 20% free moisture. The trans-shipment vessels would be equipped with vertical cuttings dryers to reduce the free moisture to 10% for shipping. Optimization of the material handling, dewatering and shipping requires reliable data on the attrition of nodules in the lift system, and on-board pumping. Losses of nodule material in the dewatering and handling process were estimated to be 7 - 10%. These estimates will need to be reassessed after the data collected during the Collector Test is analysed.

Any major on-shore maintenance for the off-shore equipment will be undertaken in third-party maintenance facilities.

Figure 15.1   Unloading bulk minerals at Mexican port of Lazaro Cardenas (Terminales Portuarias de Pacifico)

Figure 15.2   Offloading Operation: (left) with a conventional tanker; (right) with a DP tanker

16Market studies

On 25 May 2012, DeepGreen Engineering Pte. Ltd. (DGE) (a wholly owned subsidiary of DeepGreen Inc) and Glencore International AG (Glencore) entered into a copper off-take agreement and a nickel off-take agreement whereby DGE agreed to deliver to Glencore 50% of the annual quantity of copper material and 50% of the annual quantity of nickel material produced by DGE.

For LME Registered Grade "A" Copper Cathodes, the delivered price is the official LME Copper Grade "A" Cash Settlement quotation as published in the Metal Bulletin averaged over the month of shipping or the following month at Glencore's choice, plus the official long-term contract premium as announced annually by Codelco, basis CIF Main European Ports. For LME Registered Primary Nickel, the delivered price is the official LME Primary Nickel Cash Settlement averaged over the month of shipping or the following month at Glencore's choice. For other copper-bearing material and other nickel-bearing material, the parties shall agree a price annually for the forthcoming calendar year on the basis of prevailing market prices for such copper products and such nickel products.

Both the nickel and copper off-take agreements are for the life of the NORI Area, and either party may terminate the agreement upon a material breach or insolvency of the other party. Glencore may also terminate the agreement by giving 12 months' notice.

CRU International Limited (CRU) was commissioned by NORI to provide market overviews for the four main products from the NORI Area D Project: nickel sulphate ($NiSO_4$), cobalt sulphate ($CoSO_4$), copper, and a manganese product (CRU report dated October 23, 2020).

Over a five year horizon, CRU's price forecasts are based primarily on supply and demand fundamentals. These are established from CRU's detailed bottom-up analysis of supply by individual mine and finished product producer, and in-depth analysis of demand from individual applications. CRU also considers operating costs and inventories in its forecasts, as well as various other factors where relevant.

For the forecast beyond a five year horizon, cyclical supply-demand balances become hard to predict. Therefore, CRU's longer term price forecasts are based on the Long Run Marginal Cost (LRMC) concept. That is, that prices in the long term will trend towards, and fluctuate around, the full economic costs (i.e., operating costs including an allowance for a return on capital) of the marginal tonne required to meet long term demand. For example, when prices are above the LRMC, CRU would assume that supply would be added and prices would subside. Assets selected for the LRMC analysis are a representative sample that are likely to be in production to satisfy future demand. CRU uses its Project Gateway classification system to select projects. It is important to consider where these new assets will be located, how large they will be and what processing technology they will adapt. The composition of future capacity and accompanying demand levels will have a significant impact not just on the LRMC assessment, but also the upside and downside risk associated with that assessment.

One exception to this long term price forecasting methodology is the cobalt market. Since the majority of cobalt is produced as a by-product of copper or nickel mining, supply is inelastic to the cobalt price, with supply decisions instead more likely to be driven by the market environment for the operations' main copper or nickel product. This means that the Long Run Marginal Cost concept cannot readily be applied. Instead, CRU refers to historic pricing trends to establish a long term equilibrium price, taking into account longer term factors, such as the increasing importance of batteries as a cobalt end use, that might result in cobalt prices and product premia differing with historical trends.

Taking into account the foregoing assumptions and analysis, CRU expects $NiSO_4$ and $CoSO_4$ markets to undergo extreme growth from a relatively small current level of 181 kt nickel in sulphate and 35 kt of cobalt in sulphate in 2019, with markets to increase to 138 and 178 times their 2018 sizes respectively to 1.6 Mt nickel in sulphate and 500kt cobalt in sulphate by 2035, with much of this growth occurring post-2025. Electric vehicle production is the driver of this forecast growth.

In addition, copper and manganese ore markets are forecast to grow by 25% and 20% of their 2020 sizes by 2035, respectively. Copper and manganese demand will benefit from electric vehicle penetration, however the primary driver of growth for manganese ore will be steelmaking, and a variety of end use applications generally related to economic health for copper. A significant copper supply gap of around 5 Mtpa is expected by 2030 in the absence of new mine capacity, indicating that inducement pricing of greater than US$3.10/ lb Cu will be required to bring on new copper supply.

CRU expects $NiSO_4$ and $CoSO_4$ markets to undergo extreme growth from a relatively small current level of 181 kt nickel in sulphate and 35 kt of cobalt in sulphate in 2019, with markets to increase to 138 and 178 times their 2018 sizes respectively to 1.6 Mt nickel in sulphate and 500kt cobalt in sulphate by 2035, with much of this growth occurring post-2025. Electric vehicle production is the driver of this forecast growth.

Copper and manganese ore markets are forecast to grow by 25% and 20% of their 2020 sizes by 2035 respectively. Copper and manganese demand will benefit from electric vehicle penetration, however the primary driver of growth for manganese ore will be steelmaking, and a variety of end use applications generally related to economic health for copper. A significant copper supply gap of around 5 Mtpa is expected by 2030 in the absence of new mine capacity, indicating that inducement pricing of > US$ 3.10/ lb Cu will be required to bring on new copper supply.

CRU expects copper and $NiSO_4$ prices to rise in real terms by 2035, while manganese ore and $CoSO_4$ prices are forecast to remain flat, partly due to current prices being at or near a high point in the cycle, recent fall in prices, and expected modest growth in the global steel industry after the COVID 19 epidemic. The long-term cost of production is expected to rise for both copper and $NiSO_4$, helping to support prices.

The $NiSO_4$, $CoSO_4$ and copper to be produced by NORI are expected to be chemically and physically standard products and no marketability issues are expected. The sulphate forms ($NiSO_4$, $CoSO_4$) of these products are expected to be premium products and attract premia over pure nickel and cobalt.

The manganese silicate product differs in both physical and chemical specifications from standard forms of ore found in the market. NORI's manganese silicate is expected to have a manganese grade of around 40%, which matches neither the high grade (44% Mn) or low-grade (36–38% Mn) ore benchmarks. The product is expected to have SiO_2 and Al_2O_3 contents exceeding the most desirable levels for manganese products but a desirable high Mn to Fe ratio. NORI's processing route also reduces the oxidation state of the manganese oxide from MnO_2 to MnO, which will reduce the energy requirements for customers' downstream processing. On balance, CRU recommended adopting a small premium of 1- 3% of the 44% Mn ore benchmark price.

17 Environmental studies, permitting and social or community impact

NORI has commenced an Environmental and Social Impact Assessment (ESIA) process in support of an application for an exploitation license for the commercial development of deep-sea polymetallic nodules and has made significant progress with the baseline study program. Off-shore campaigns were completed over the period 2018 - 2020 to conduct oceanographic and sediment sampling activities. These provided the initial information to inform the scoping of baseline environmental studies required for the conduct of the ESIA investigations.

DeepGreen and NORI are seeking broad stakeholder consultation in the design and implementation of the ESIA program. In June 2019, NORI held a scoping study technical workshop with stakeholders in San Diego.

The development and status of the environmental program is described below. The baseline field study work commenced in 2012 and in October 2020 NORI began the first of six dedicated environmental baseline study off-shore campaigns in NORI Area D.

17.1 Permitting process

The ISA is mandated through UNCLOS to organize, regulate, and control all mineral related activities in the international seabed Area whilst preserving and protecting the marine environment. As NORI Area D is in the international seabed Area, the ISA is responsible for assessing any Environmental and Social Impact Assessment prepared by NORI and for granting the relevant contracts. NORI is currently one of 16 contractors with a license to explore for polymetallic nodules in the CCZ (refer ISBA/23/C/7, 5 June 2017).

Between 1998 and 2014, the ISA held workshops and developed a number of documents to provide guidance to contractors with respect to its expectations for responsible environmental management during the exploration and exploitation phases of mineral development. The ISA held a workshop "Towards an ISA environmental management strategy for the Area" over 20-24 March 2017 in Berlin Germany. The results of the workshop were published as ISA Technical Study 17 (ISA 2017).

The ISA has issued Regulations on Prospecting and Exploration for Polymetallic Nodules (adopted on 13 July 2000, updated on 25 July 2013). The regulations were complemented by the Legal and Technical Commission (LTC) recommendations for the guidance of contractors on assessing the environmental impacts of exploration (ISBA/25/LTC/6/Rev.1) which was most recently updated on 30 March, 2020. The draft exploitation regulations on deep-seabed mining were discussed at the 25th Session of the ISA (25 February to 1 March 2019 in Kingston Jamaica). The ISA had declared a target of 2020 to have the regulations approved but the COVID-19 pandemic disrupted the ISA program.

Although the environmental impact review process has not yet been finalised, the draft regulations outline the application process and the conditions that Contractors would need to implement during operations. All contractors have been made aware that the ISA requires the completion of the Environmental and Social Impact Assessment (ESIA) studies, culminating in an Environmental Impact Statement (EIS), in support of their applications for an exploitation license. Guidance for contractors in terms of what will be expected in the EIS has been provided in ISA Technical Study No. 10 (ISA 2012a). Further guidance will be provided with the completion of Standards and Guidelines for exploitation activities. The LTC has prioritized the development of six Standards and Guidelines, with three released for public comment in 2020 and the remaining three expected to be released in early 2021. The EIS, along with an Environmental Management System with subordinate Environmental Management and Monitoring Plans (EMMP), will be required as part of the application for an exploitation license within the Contract Area.

The environmental permitting process for the Area has been developed through a consultation program initiated by the ISA in 2013 and includes feedback obtained from multiple stakeholder groups. It is expected to involve a series of checks and balances, with reviews being conducted by the LTC with input from independent experts, as required. The recommendations of the LTC will then go before the ISA Council, which will then review the information provided and decide whether to approve the license application and, if so, what conditions should be applied.

NORI plans to conduct the ESIA studies largely in accordance with the draft ISA guidelines "Recommendations for the guidance of contractors for the assessment of the possible environmental impacts arising from exploration for marine minerals in the Area. Issued by the Legal and Technical Commission" ISBA/25/LTC/6/Rev.1 (ISA, 2020). A plan of work that addresses the requirements detailed in the draft guidelines has been developed.

NORI has progressed with the development of the scoping studies on the assumption that all of the detailed recommendations within this document will carry through to the final recommendations for the guidance of contractors.

The LTC has recommended seven key areas of information for the development of EIAs. These are physical oceanography, chemical oceanography, sediment properties, biological communities, bioturbation, sedimentation, and geological properties. These form the key investigation topics for surveys within the Area, including NORI Area D.

17.1.1   Role of sponsoring state

As sponsoring state, Nauru has a responsibility to ensure that NORI's activities in the international seabed area are carried out in conformity with Part XI of UNCLOS.

NORI is regulated by Nauru's International Seabed Minerals Act 2015 ("Nauru Act"), which requires NORI to, amongst other things, *"apply the Precautionary Principle, and employ best environmental practice in accordance with prevailing international standards in order to avoid, mitigate or remedy adverse effects of Seabed Mineral Activities on the Marine Environment"*.

The Nauru Seabed Minerals Authority, established under the Nauru Act, has a number of functions including to, *inter alia*:

- develop policies and institutional arrangements for the purpose of regulating and monitoring the development of seabed minerals in the international seabed area;
- develop standards and guidelines for Seabed Mineral Activities;
- conduct due diligence enquiries into Sponsorship Applicants or Sponsored Parties;
- assist the ISA in its work to establish, monitor, implement and secure compliance with the Rules of the ISA;
- undertake any advisory, supervisory or enforcement activities in relation to Seabed Mineral Activities or the protection of the Marine Environment, insofar as this is required in addition to the ISA's work in order for Nauru to meet its obligations under the UNCLOS as a Sponsoring State;

17.1.2   Compliance status

At the effective date of this report, NORI is in compliance with its exploration contract. NORI is required to submit 5-year work plans which it reports on annually to the ISA. Every 5 years the ISA and NORI review the work completed in the past 5 years. NORI then develops and submits a new 5-year work plan.

NORI has now commenced the exploitation permitting process. In addition to key engineering facets of the project such as designing the nodule collector and the dewatering facility, it is also planning and undertaking the following tasks:

• Characterising nodule mineralisation.

• Characterising the nature of the seabed, water column and biology.

• Conducting environmental baseline studies and impact assessments.

• Characterising the nature of any materials returned to the environment.

• Developing oceanographic and physical information to inform models (e.g., sediment plume models).

• Developing other plans, including the master environmental management plan (EMP) and the various subordinate plans.

17.2 Previous environmental studies

Historically, a significant amount of technical work has been undertaken within the CCZ by the Pioneer Investors. Each has developed work programs for their specific part of the Area with some cooperative campaigns undertaken where investigative work has been undertaken on multiple parts of the Area. In the last five to ten years there has been a rapid increase in the technical work undertaken within the CCZ. This work, which has included oceanography, seabed geology and geochemistry, and biological studies, has led to a rapid increase in independent published scientific studies based upon research from the technical studies carried out within the CCZ.

Examples of recent campaigns undertaken by other contractors and institutional research campaigns include:

• RV Sonne cruise SO239 (11 March 2015 to 30 April 2015), which carried out work to examine biological characteristics, genetics and geochemistry across a productivity gradient in the CCZ. The cruise visited six working areas in four ISA contractor areas (BGR, IOM, DEME, Ifremer) and the Area of Particular Environmental Interest (APEI) number 3, located to the north of NORI Area D. The IOM and BGR Areas are immediately adjacent to NORI Area D.

• RV Sonne cruise SO240 (3 May 2015 to 16 June 2015) was undertaken to examine low temperature fluid circulation in sediments. The work included seismic surveys, heat flow studies, pore-water, sediment and nodule sampling.

• UK Seabed Resources Ltd (UKSR) holds two licenses, one of these (UK-1) is located to the east of NORI Area D at the edge of the CCZ. UKSR funded two environmental baseline research cruises as part of the ABYSSLINE program in 2013 (AB01) and 2015 (AB02). AB02 was part-funded by Ocean Minerals Singapore (OMS), the Singapore-sponsored contractor for polymetallic nodules, and also visited OMS licence area as well as APEI-4, to the North.

• The RRS James Cook undertook a cruise (JC120) over 15 April to 19 May 2015 to undertake work at the north east APEI within the CCZ. The cruise was part of the Managing Impacts of Deep-seA reSource exploitation (MIDAS) European Union Framework Programme 7 Project, which was jointly funded by the Natural Environment Research Council.

Other EIS documents have also been completed for proposed nodule mining activities and submitted to the ISA. These include:

• Global Sea Mineral Resources (GSR) in 2018 for the development of a pre-prototype collector vehicle equipped with a launch and recovery system planned to be deployed and trialled in the GSR Contract Area in the Clarion-Clipperton Fracture Zone (NE Pacific Ocean)

- The German Federal Institute for Geosciences and Natural Resources (BGR) in 2018 for the testing of a pre-prototype manganese nodule collector vehicle in the Eastern German license area (Clarion-Clipperton Zone); and

- The Government of India's Ministry of Earth Sciences (MoES) in 2020 for a polymetallic-nodule collector pre-prototype deep-sea mining machine in the Indian Contract area of the Central Indian Ocean Basin.

NORI has conducted ten off-shore exploration campaigns in the CCZ between the granting of its exploration license in 2011 and the end of 2020. These have focussed on quantification of the mineral resource, with environmental studies included opportunistically, as follows:

- Campaign 1 in 2012 to NORI Areas C and D in the eastern part of the CCZ. Extensive multibeam geophysical surveying of the seafloor and bulk sampling was conducted. Approximately 4.5 t of nodules were recovered from the seafloor and evidenced by video footage.

- Campaign 2 in 2013 to NORI Areas A and B in the central part of the CCZ. Multibeam geophysical surveying of the seafloor along with recovery of approximately 270 kg of nodules from NORI Areas A and B. (collaboration with TOML). The 2012 and 2013 campaigns had a geological focus and the biological/environmental work carried out by NORI was opportunistic.

- Campaign 3 (26/04/18 to 5/06/18). The field work within NORI Area D included sampling to support environmental studies and to undertake geotechnical studies to inform collector vehicle and riser design, collect high-resolution imagery and environmental baseline studies. A total of 2,286 km of AUV data were collected that include potential reserve areas and camera traverses at 3 km line spacing to investigate nodule abundance and biota. Forty-five (45) box cores collected, with 35 used for environmental work. This included recovery of 239 nodule biota specimens, 62 megafauna (>20 mm) specimens, macrofaunal infauna (>0.25 mm) samples sieved from sediment to depth of 100 mm. Sediments were also collected for geochemistry.

- Campaign 6A (19/08/19 to 1/10/19). Seafloor sediment (box core) sampling for biota and sediment chemistry.

- Campaign 6B (22/11/19 to 21/12/19). Seafloor sediment sampling for biota and sediment chemistry.

- Campaign 4A (2/10/19 to 23/10/19). Deployment of oceanographic moorings and water quality investigations.

- Campaign 4B (6/01/20 to 4/02/20) – Bulk sampling and first stage of habitat disturbance studies.

- Campaign 4C (5/02/20 to 16/03/20) – Bulk sampling and first stage of habitat disturbance studies.

- Campaign 4D (16/06/20 to 15/07/20) – Mooring maintenance and data collection.

- Campaign 5A (16/01/20 to 30/12/2020) - Benthic biology and sediment geochemistry studies.

The availability of the vessel Pacific Constructor, operated by Ocean Infinity in NORI Area D provided NORI the opportunity to commission ROV/AUV surveys, from 23/05/20 to 30/05/20, of the collector site, a directly adjacent (expected) plume impact area, PRZ and intermediate control site. This resulted in the acquisition of approximately 250,000 images of the sea floor. This information will be used to start megafauna survey community characterization and inform survey planning for the forthcoming campaigns.

During Campaigns 6A, 6B, and 4A NORI collected a combined total of 8,673 seafloor biological samples and 267 sediment chemistry samples at 204 locations within NORI Area

D to provide initial baseline data for the project. During Campaign 4A, NORI deployed three oceanographic moorings for long term measurement of currents through the water column and other parameters such as turbidity and underwater acoustics. Five sites within NORI Area D were also set up for collection of water quality samples and ocean profiling data.

During Campaign 5A over 8000 sediment sub-samples and biological specimens were collected from boxcore and multicore samples retrieved from 46 seabed sites located in the proposed test mining area, plume deposition footprint and the PRZ. The samples are currently awaiting analysis at various analytical laboratories around the world.

The forward work plan over the next two years will involve several off-shore campaigns as follows[22]:

- Campaign 5B (15/01/21 to 280/2/21). Pelagic Biology. Campaign 5b will be supported by an ROV.
- Campaign 5C (1/04/21 to 14/05/21). Sediment analysis, surface biology, benthic biology will continue during this campaign. Campaign 5c will be supported by an ROV.
- Campaign 5D (15/10/21 to 30/11/21). Pelagic biology will continue during this campaign. Campaign 5d will be supported by an ROV.
- Collector Test (1/09/22 to 1/12/22). Disturbance studies before, during and after the Collector Test will be conducted during this campaign.

The combination of past, present and future studies in the CCZ and NORI Area D provides a significant body of information on the nature of the seabed, sampling procedures and potential environmental impacts of collecting nodules from the seafloor that can now be applied to provide the environmental information required for the ESIA. NORI's studies within the CCZ are being designed to provide data that will be collected using methods that meet international best practices. This will allow comparison with other CCZ technical studies and provide data that can be utilised by other parties. The ISA has hosted workshops for contractors with the aim of standardising methodologies.

NORI has committed to operation in accordance with the following international standards and best practices during the conduct of the ESIA:

- EPA WA (2016). Technical Guidance: Environmental Impact Assessment of Marine Dredging Proposals. Environmental Protection Authority, Perth, Western Australia. https://www.epa.wa.gov.au/policies-guidance/technical-guidance-environmental.
- IEC /ISO 31010 Risk Management Risk Assessment Techniques. https://www.iso.org/standard/51073.html.
- IFC (2013) Good Practice Handbook Cumulative Impact Assessment and Management: Guidance for the Private Sector in Emerging Markets. International Finance Corporation. https://www.ifc.org.
- MCA (2015). Cumulative Environmental Impact Assessment Industry Guide – Minerals Council of Australia. https://minerals.org.au/cumulative-impact-assessment.
- Rio Tinto. 2008a. Rio Tinto and biodiversity: Achieving results on the ground. Rio Tinto, London and Melbourne. Unpublished document available at: www. riotinto.com/documents/Reports Publications/ RTBidoversitystrategyfinal.pdf.
- Standards Australia. (2009). Risk management: Principles and guidelines (AS/NZS ISO 31000:2009). Retrieved from http://standards.org.au.

---

[22] Schedules are subject to revision depending on COVID-19 situation and other factors

- World Bank (2006) Environmental Assessment Sourcebook. Update Number 17. http://documents.worldbank.org.

All the data collected during the campaigns will be submitted to the ISA DeepData database and will be available to other contractors and researchers with interests in the CCZ.

17.3 Seabed physical environment

Sediment physical characteristics and geochemistry are important as sediments are disturbed during manganese nodule collection. Composition of sediments and sediment pore water has the potential to influence the natural environmental characteristics, principally water quality and potentially the flux of specific elements mobilised during this process. A range of studies associated with various Contract Areas have examined seabed cores and sediments and undertaken geophysical surveys.

As a result of a workshop conducted in May 2003, ISA developed a model of the geological environment within the CCZ (ISA, 2010). The CCZ geological setting has also been described in various ISA reports and Juan et al. (2018). The nature of sediments has been described by ISA (2010) and Halbach and Abrams (2013).

The detailed bathymetric data indicates that the key features are NNW orientated hills and valleys with relief in the order of a few hundred metres, a flat plain in the south-east of the Area and a series of volcanic cones mostly in the southern part of the Area. This relief will influence the distribution of benthic communities within the area.

Kazmin (2009) summarised that the CCZ is characterised by latitudinal distribution of sediment types in relation to climatic and biological zonation at the time of deposition. From the north to south there are red deep-sea clays, then argillaceous radiolarian ooze (siliceous clay), and then carbonaceous ooze (in the south) Figure 17.1.

Figure 17.1 Simplified surface sediment facies in the CCZ
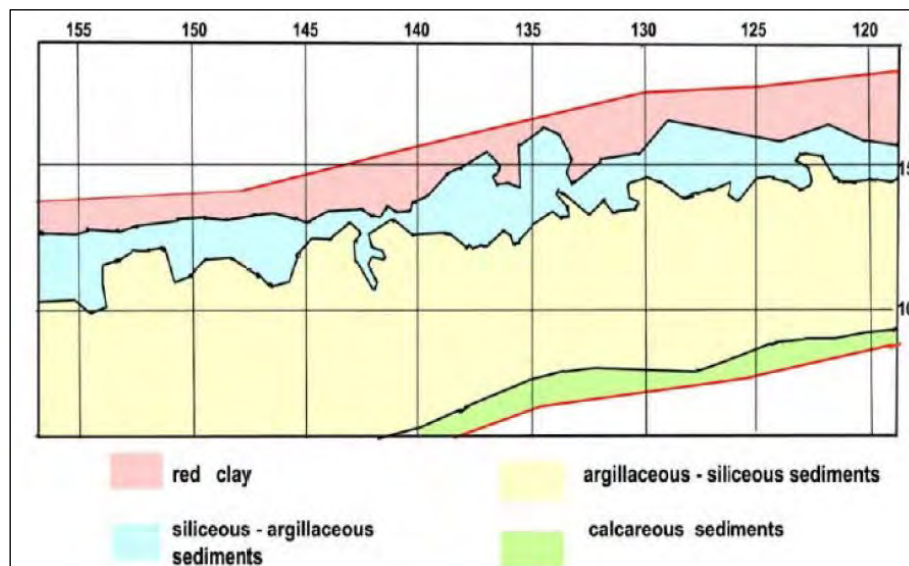
Source: Kazmin 2009 based on Yuzmorgeologiya (2002)

17.4 Sediment geochemistry and composition

ISA (2010) summarised the characteristics of the key sediment groups identifying the key lithic and authigenic components. Sediments are considered low in total organic carbon (TOC) reflecting the surface primary productivity. Halbach & Abrams (2013) included a

summary of sediment elemental analysis undertaken in areas adjacent to NORI Area D. Studies to date do not systematically include all key environmentally significant elements. Studies reported by Mewes et al (2014), De Smit et al. (2017), Volz et al. (2018) and Simon-Lledo et al. (2019) for adjacent part of the Area, provide information on grain size (site mean mud content up to 92.6%) and TOC content (0.2% (APEI3) to 0.5% (GSR and IOM Area)). TOC is lower below the surface of the sediments.

Studies have been carried out in the CCZ that examined sediment pore waters. Mewes et al. (2014) and Volz et al. (2018) reported on pore water chemistry (oxygen, manganese and nitrate) in sediments from a number of nearby Contract Areas including the BGR and IOM areas near NORI Area D.

During NORI Campaign 3, sediment samples of 100 mm diameter were taken from 31 box cores, in most cases at three depths (0–10 mm, 10–50 mm and 50–100 mm). Subsamples were frozen until analysed. A range of analysis were undertaken including:

- Total inorganic carbon, total organic carbon, and chlorophyll-a.
- Total phosphorus and soluble nitrite and nitrate.
- A range of total element analyses in sediment, including several environmentally significant elements.

Sediments sampled in the 2018 campaign were muds, classified as clay or calcareous clay. Cumulative particle sizes were all: <250 µm; 73–99% <32 µm and 13-88% <2 µm (defined as clay in the assessment).

Several elements (e.g., cadmium, copper, mercury and nickel) had concentrations higher than the ANZECC (2018) sediment quality guidelines. The concentrations of elements such as copper and nickel are similar to those measured in other parts of the Area in the east and middle of the CCZ (refer review by Halbach & Abram (2013).

NORI (2020b) collected additional sediment samples for chemical analysis during Campaigns 6a and 6b with samples taken from the 0 to 10 cm layer of each pushcore (10 cm in diameter). At the time of writing, sediment samples are being analysed for the physical and chemical characteristics.

17.5 Climate

Refer to Section 5.2.

17.6 Large-scale oceanography

The proposed nodule collection involves activities that will occur through the full water column, from the production support vessels (PSVs) at the surface to the collector vehicles on the seafloor. The RALS will convey the nodules from the seabed to the PSV, although the enclosed nature of the riser will separate nodules from the environment for most of the water column. Therefore, it is important to understand the physical oceanographic characteristics that will affect both the operational activities and the environmental impacts of those activities to the receiving marine environment.

The ocean is not uniform from surface to seafloor but stratified according to temperature, salinity and density gradients and oxygen levels. In clear oceanic conditions, light penetration is sufficient to support photosynthesis by phytoplankton to a depth between 100 and 200 m but is extinguished altogether below 1000 m. Water movements are also affected by tides, currents, and circulation on local and ocean-wide scales, as well as precipitation and wind. The depths and intensities of these layers are not constant but varies daily and seasonally, so frequent profiling is important to understand the extent of these natural variations.

17.6.1   Oceanic currents in NORI Area D

Upper ocean circulation within the CCZ is affected by trade winds and a system of large-scale currents (Gill 1982 in Demidova 1999). The north-easterly Trade Winds generate a westerly moving surface current, with waves having a height of 1 to 2 m. This is a broad current with an average speed of about 10 – 20 cm/s, decreasing with depth (NOAA 1981, ISA 2001, Tilot, 2006, GRS 2018). The surface currents extend down to a maximum depth of 500 m and form part of the North Equatorial Current directed towards the West. At intermediate depths (300-4800 m), the currents are weak (mean 0.08 knots [~4 cm/s]) and variable in direction (Tilot 2006). Three dynamic seafloor current regimes are evidenced in the region Morgan et al. (1999) and Demidova (1999):

- Calm periods, characterised by minimal current speeds (0 to 3 cm/s), moderate to low variance, and low tidal activity with time intervals lasting about 11 days.
- Intermediate, mostly inertial-tidal periods characterised by the alteration of current speed (0 to 5 or 6 cm/s) and velocity with a corresponding increase in the variance of data.
- Active periods, associated with an initial sharp increase in current speed, which can maintain relatively stable speeds to produce 24-hour means of as much as 8 cm/s (Demidova & Kontar 1989), and 1 hour means of between 13 and 15 cm/s (Hayes 1979). These events can be termed "benthic storms", which are regular, but not periodic, increases in the current speed lasting from about one or two weeks to five or six weeks.

The general scheme of deep oceanic circulation in the Pacific Ocean is related to the movement of cold and dense waters of Antarctic origin with high salinity and oxygen concentrations (Jaun et al., 2018) and the general direction of near-bottom currents is thought to be dominated by the flow of the Antarctic Bottom Water (ABW) (or Lower Circumpolar Water (LCPW)) from south to the north-east (Demidova 1999).

There are also suggestions from multi-beam bathymetric evidence that benthic currents in the CCZ may control movement and deposition of sediments along the seafloor valleys (Jaun et al. 2018; Morgan et al. 1999), with intermittent benthic storms considered capable of generating depositional and erosional features on the Pacific abyssal plains.

Overall, bottom current measurements at various locations through the CCZ show consistently low average near seabed current velocities (around 40–50 mm/sec). Site specific measurement of currents within NORI Area D in forthcoming campaigns is designed to characterise regional current velocity data through the water column to provide data to assist in sediment transport modelling (from disturbance and or discharge).

17.6.2   Oceanographic studies

Physical oceanographical studies in water depths of the CCZ are complex and necessarily long term (e.g., two to three years) to evaluate likely variations over time and location. During 2019, NORI initiated a long term oceanographic, sediment and benthic data collection program from Campaigns 6a and 6b, and deployment of three oceanographic moorings in Campaign 4A (NORI 2020b). The mooring locations and the water quality and Conductivity – Temperature - Density (CTD) profiling locations are shown in Figure 17.2. A diagram of the mooring arrays and sensor configuration is shown in Figure 17.3.

Scientific instrumentation attached to the moorings included:

- CTD, turbidity, transmissivity, and dissolved oxygen sensors.
- Acoustic Doppler Current Profilers (ADCPs) and Doppler Velocity Samplers (DVS).
- Acoustic hydrophone.

- Sediment traps.
- Seafloor camera system.

The data will be continuously recorded and accrue with each annual data recovery, equipment servicing and redeployment cycle, until October 2022.

Figure 17.2   NORI Area D mooring and water quality sampling locations
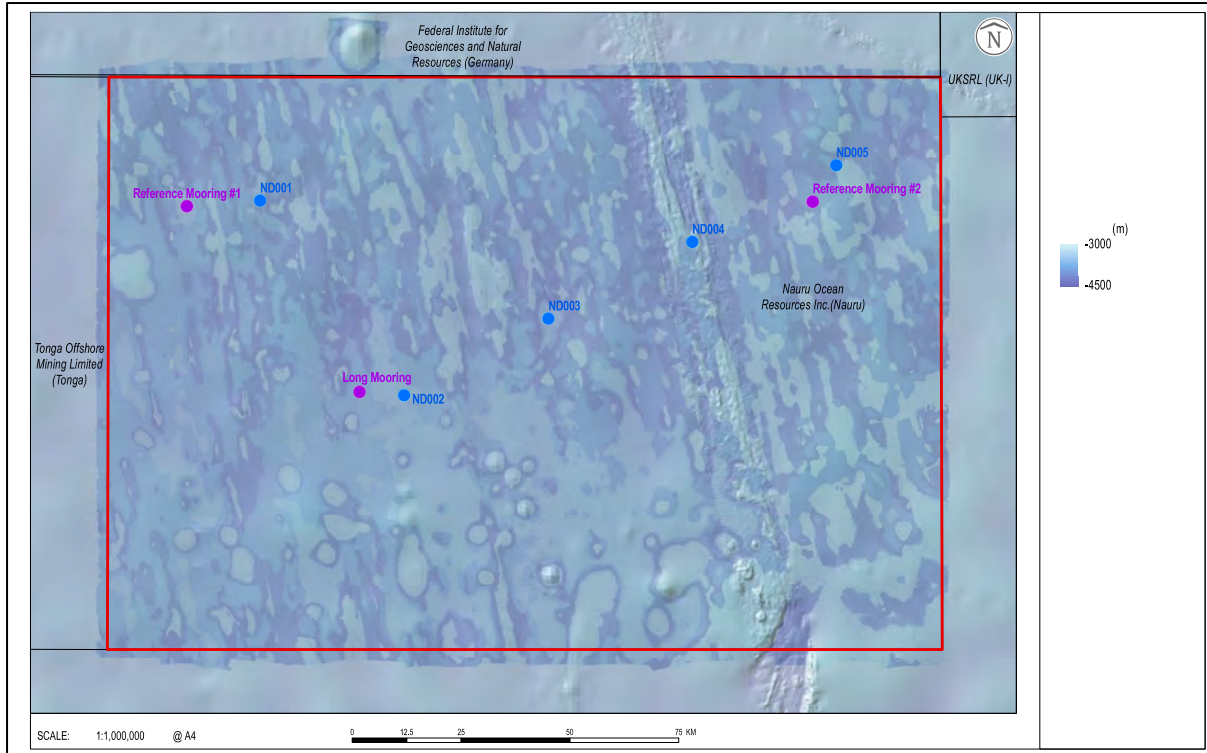
Figure 17.3   Equipment configuration on the mooring array
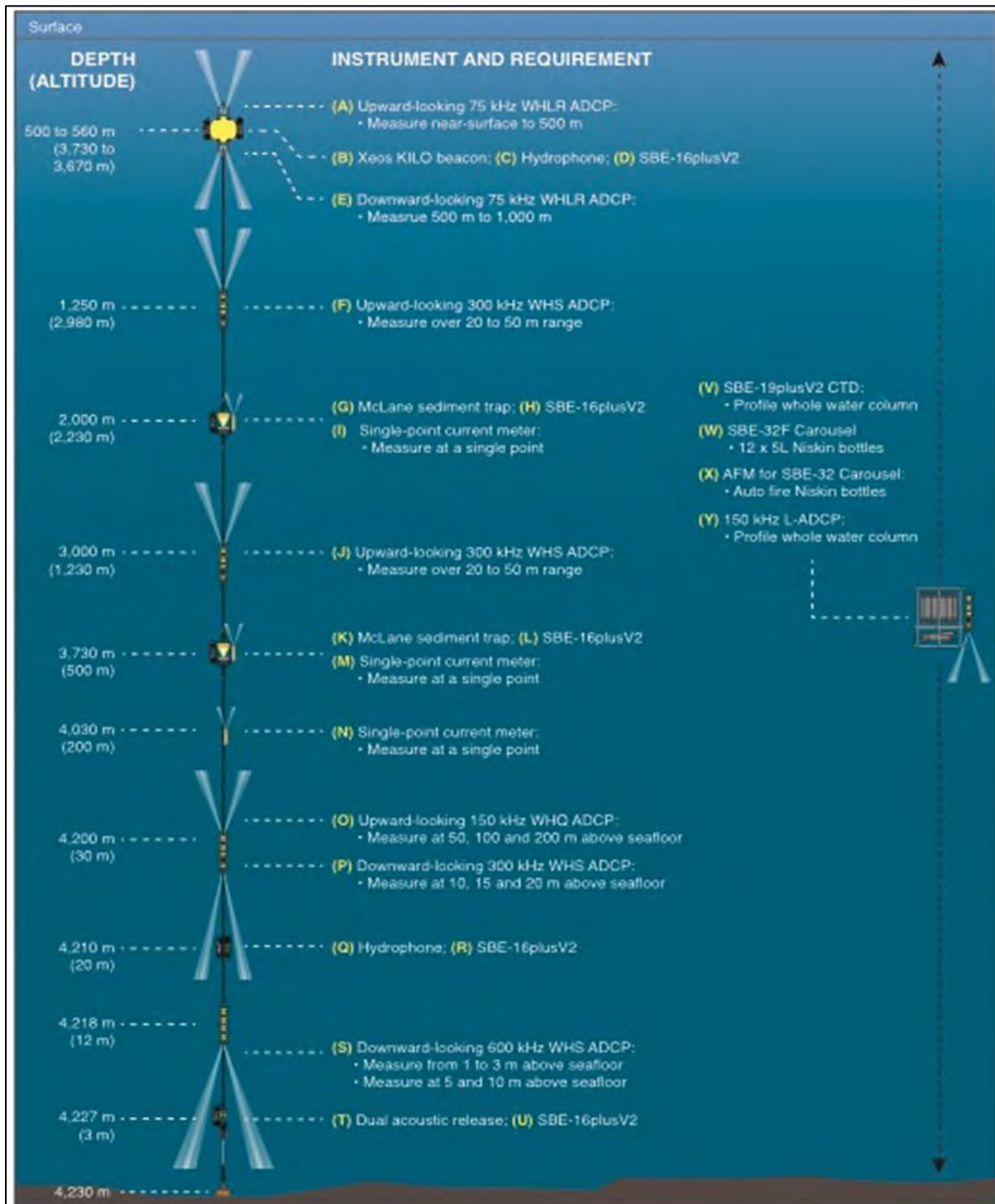
17.6.2.1   Surface currents

During Campaign 4A, six SOFAR surface drifters were deployed from within the NORI Area D Area. Initially, all drifted south-eastward to eastward across NORI Area D, with times of calm periods (circular drifting) until late-October 2019 when they left the block boundary, then drifted north-westward, with a net westerly displacement towards the central Pacific Ocean (Figure 17.4). The SOFAR spotters recorded wind speeds of between 3–19 knots and wave heights of between 1.4–2.8 m during their drift through the NORI Area D.

Figure 17.4   Surface currents recorded by SOFAR drifters
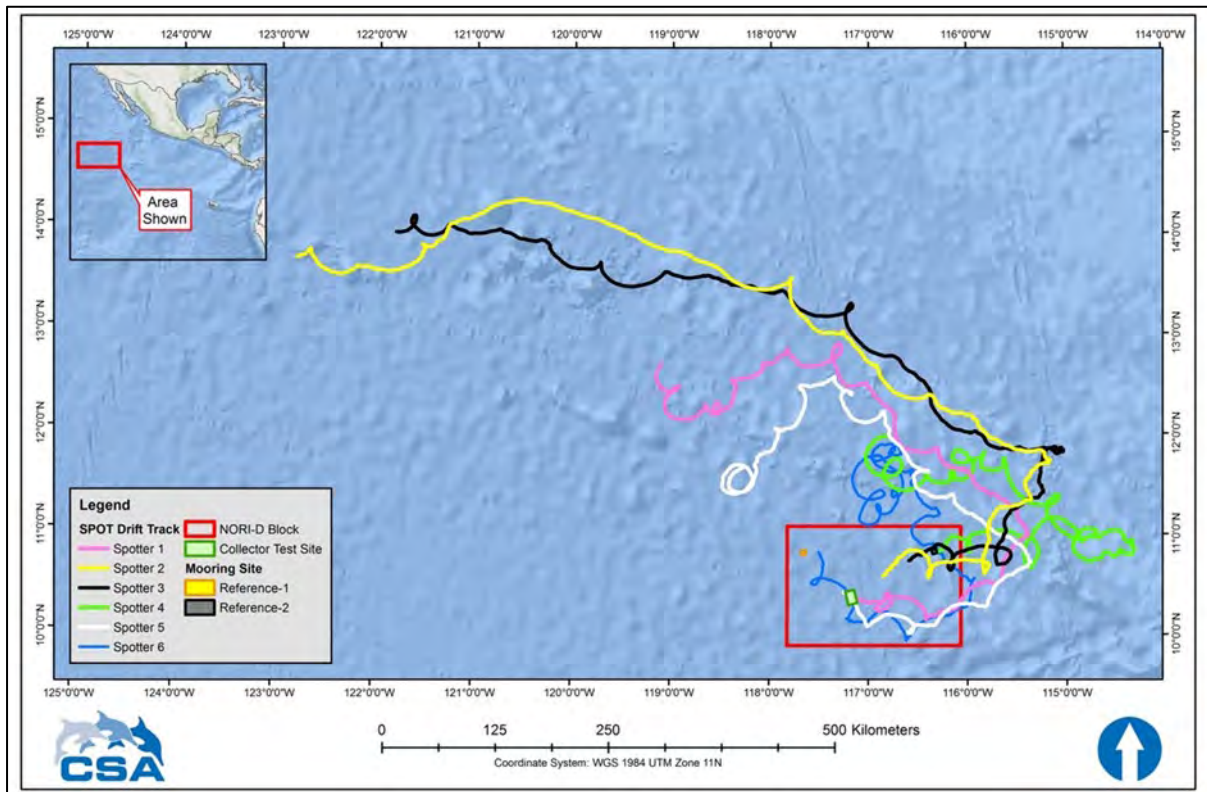
17.6.2.2   Water column vertical structure

Profiles of temperature, salinity, dissolved oxygen (DO), pH, turbidity transmissivity, and fluorescence measured in NORI Area D during Campaign 4A at each seawater sampling station are described below. Those for temperature, salinity, DO and pH also show interpolated cross-sections diagonally across the NORI AREA D block from the Collector Test Site (ND|002) to the Reference 2 location (ND|005).   Overall, these profiles are consistent with open ocean conditions. NORI's ongoing profiling of water column characteristics and faunal components will be instrumental for assessment of depths of discharge of riser water and selection of methods of achieving lowest environmental impact.

Figure 17.5 shows the temperature profile, typical of autumn conditions for deep water areas of the tropical north Pacific Ocean. There is a thin surface mixed layer (~50 m from surface) of near homogenous temperature (~27°C) formed by the mixing action of wind and waves, below which is the top of the thermocline, where temperatures drop sharply (~15°C) through the first 100 m of the water column. Seawater temperatures continue to decrease from 15°C to 2°C through the next 2,000 m and remain relatively stable and cold (1.5°C to 2°C) down to the seafloor. This pattern is consistent between the sampling sites.

Figure 17.6 shows the corresponding salinity profile within the water column, which range from approximately 33.5‰ in surface waters to 34.5‰ at the seafloor, with a halocline occurring in the upper 100 m of the water column. The maximum salinity (~34.75‰) was observed at approximately 100 m from which it gradually decreases and stabilizes through the water column to the seafloor. A slight depression in salinity was observed in the upper mesopelagic, coincident with the core of the oxygen minimum zone.

Figure 17.5   Temperature (°C) profile of NORI Area D during Campaign 4A
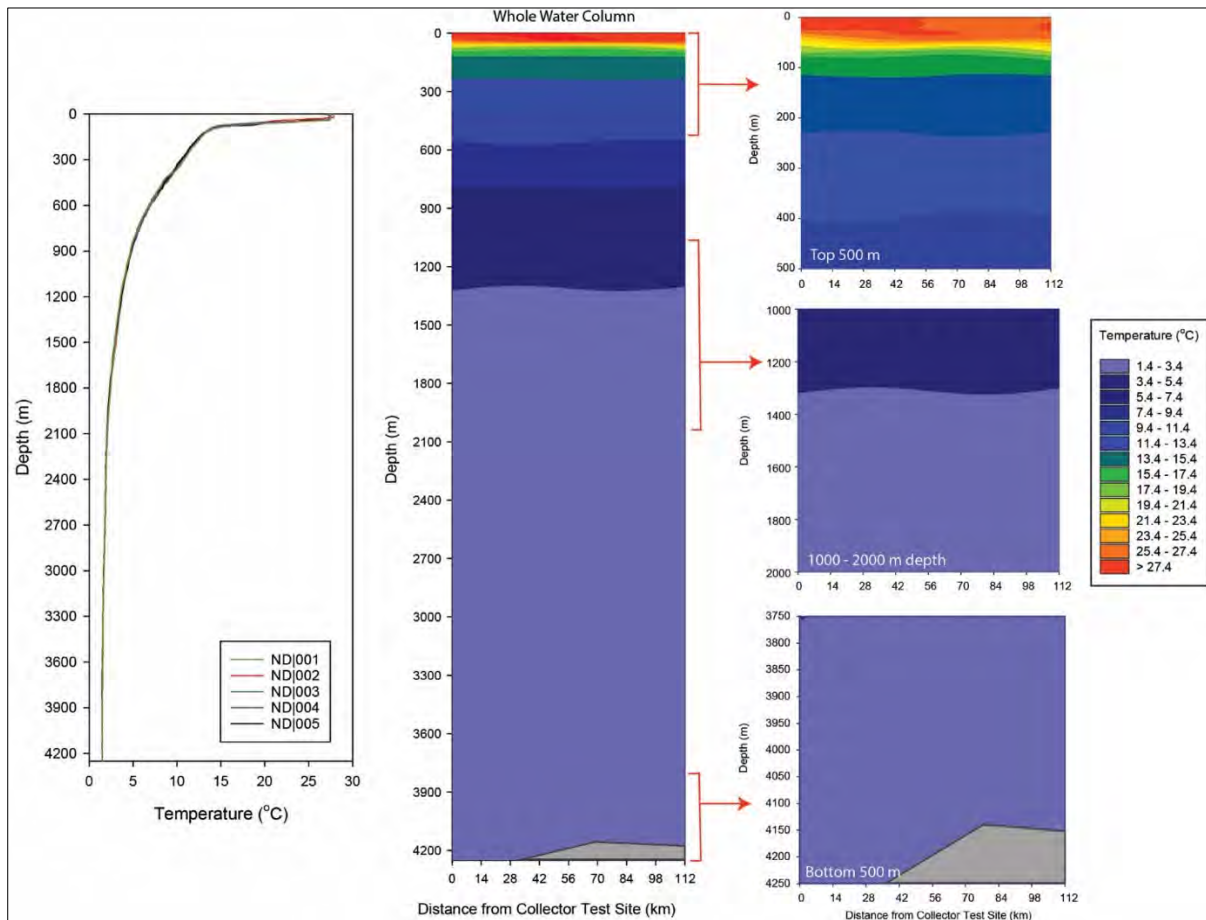
Note: Temperature (°C) profile of NORI Area D during Campaign 4A at each seawater sampling station (left). Interpolated cross-section of temperature diagonally across NORI Area D from the Collector Test Site (ND|002) to the Reference 2 location (ND|005) (right).

Figure 17.7 shows the profile of dissolved oxygen concentration that is typical for deep oceanic waters. There are high levels (6 to 7 mg/L) in the surface layers, where it is maintained from atmospheric and photosynthetic diffusion. There is an oxygen minimum zone, between 100 and 700 m, where respiration of oxygen by organisms exceeds renewal, resulting in very low oxygen concentrations (i.e., <0.5 mg/L). Below depths of 700 m, the dissolved oxygen concentration gradually increases to approximately 4.5 mg/L at the seafloor, with some slight differences between sites in the depth range of 700 to 1800 m. The source of this oxygen is generally believed to be from influx of oxygen rich waters from polar regions into the deeper parts of the ocean.

Figure 17.6   Salinity (psu) profile of NORI Area D during Campaign 4A
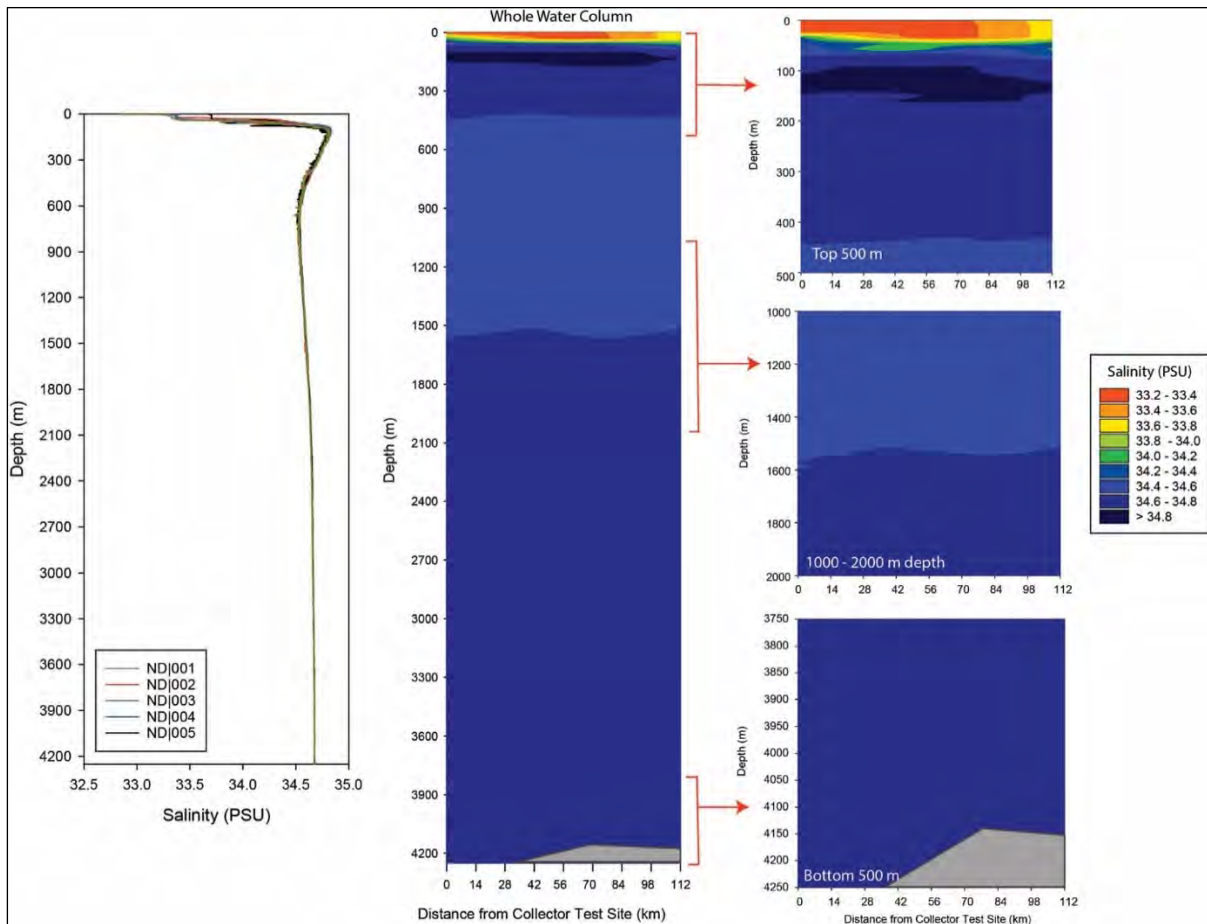
Note: Salinity (psu) profile of NORI Area D during Campaign 4A at each seawater sampling station (Left). Interpolated cross-section of salinity diagonally across NORI Area D from the Collector Test Site (ND|002) to the Reference 2 location (ND|005) (right).

Figure 17.7   Dissolved oxygen (mg L-1) profile of NORI Area D during Campaign 4A
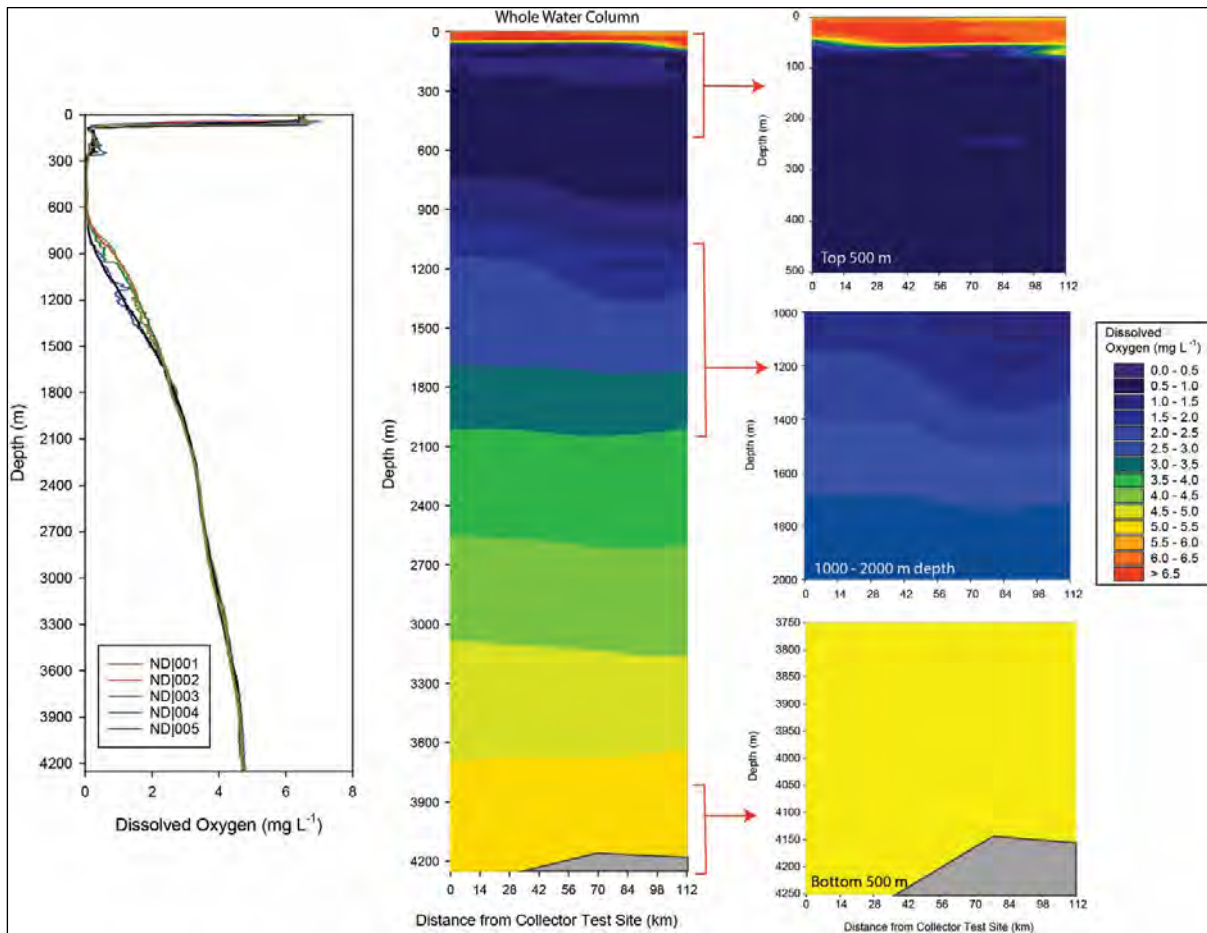
Note: Dissolved oxygen (mg L⁻¹) profile of NORI Area D during Campaign 4A at each seawater sampling station (Left) and interpolated cross-section of dissolved oxygen diagonally across NORI Area D from the Collector Test Site (ND|002) to the Reference 2 location (ND|005) (right).

Seawater pH values were generally uniform among the stations in the upper 100 m of the water column and between 2,000 m to the seafloor Figure 17.8 but showed some variability within the depth range of the oxygen minimum zone and showed a slight increase from west to northeast.

Figure 17.8   pH profile of NORI Area D during Campaign 4A
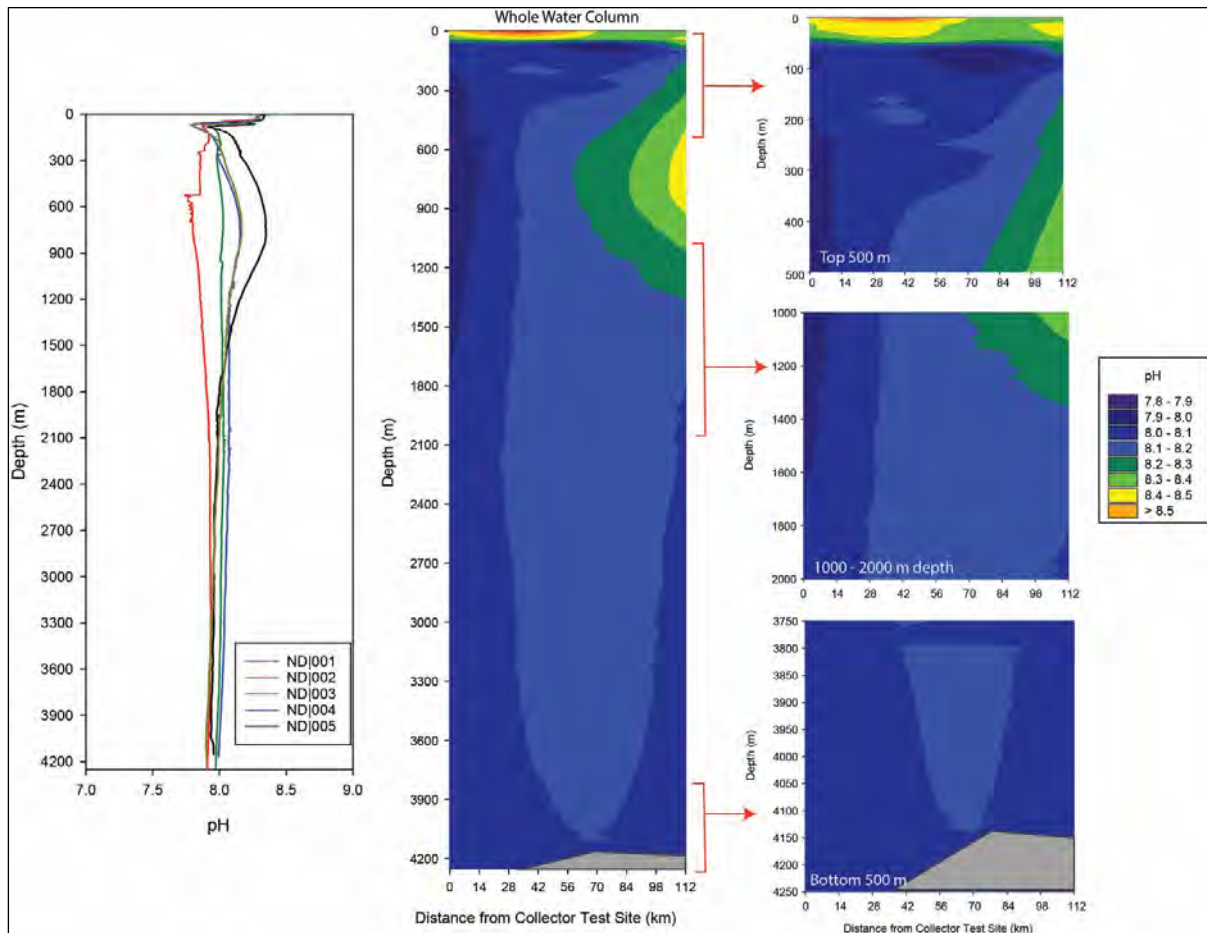
Note: pH profile of NORI Area D during Campaign 4A at each seawater sampling station (Left) and interpolated cross-section of pH diagonally across NORI Area D from the Collector Test Site (ND|002) to the Reference 2 location (ND|005) (right).

17.6.2.3   Suspended sediments, transmissivity and fluorescence

Turbidity and transmissivity (Figure 17.9) are fairly constant through the water column. Both measurements indicate that there is very little particle suspension at any depth, which is typical for open ocean systems remote from terrigenous inputs or upwelling regions. Fluorescence from chlorophyll showed that the deep chlorophyll maximum is found at a water depth of approximately 50 to 60 m depth, which coincides with the start of the oxygen minimum zone within the region. Fluorescence then rapidly decreased with depth to below detection through the remainder of the water column due to light limitation of growth.

Figure 17.9   Profiles of turbidity (NTU) (Left); percent transmissivity (centre) and fluorescence (mg m-3 Right), in NORI Area D during Campaign 4A
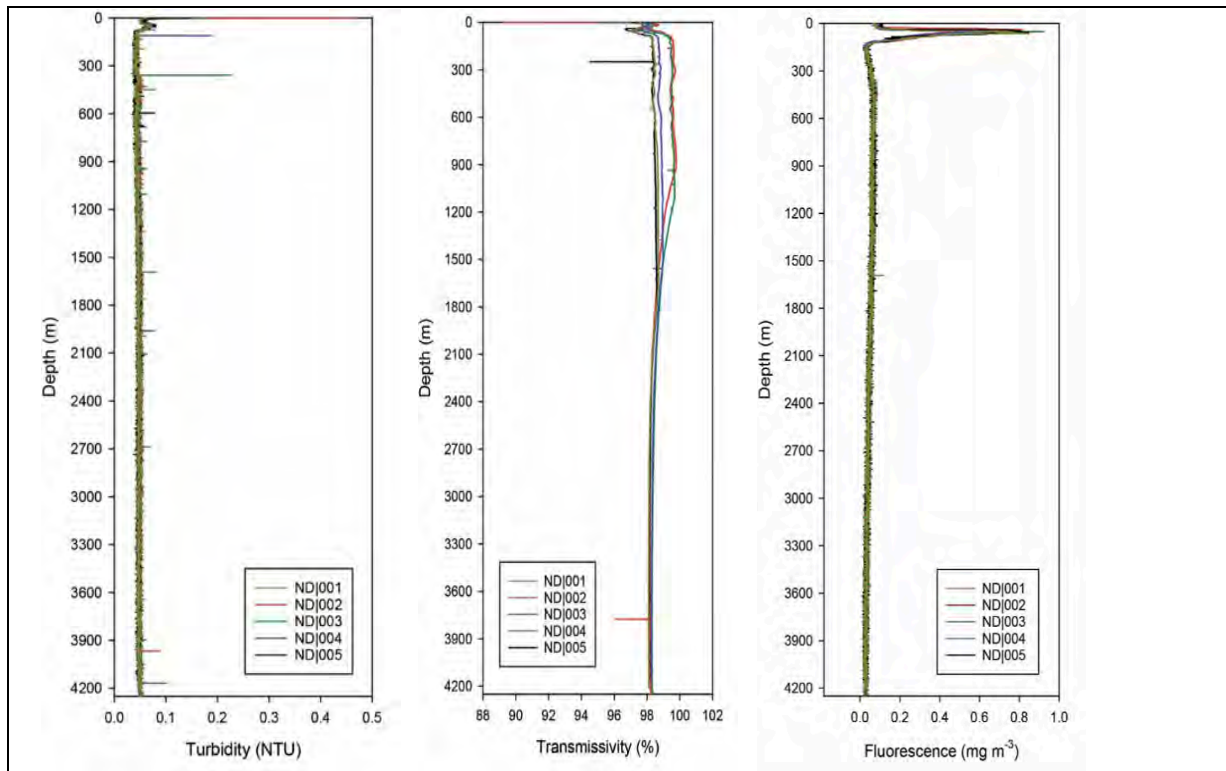
17.6.2.4   Water column chemistry

Sampling and measurements of water column chemistry included nutrients (nitrogen, phosphorus and silica), trace elements (metals and metalloids) and other major constituents was conducted at each of the five water quality sites in NORI Area D during Campaign 4A. The results available to date are tabulated in NORI Annual Report for 2019 (NORI 2020b) and, where possible, compared with Pacific Ocean reference concentrations (World Ocean Atlas WOA2018).   Planned further sampling campaigns during the ESIA study will provide progressively improved robustness of baseline characterization of water quality parameters and variations (e.g., with season) or consistent differences, if any, with results from other studies within the CCZ.

Nutrient concentrations throughout the water column in NORI Area D were generally similar to nutrient concentrations, vertical profile trends, variability, and nutrient maxima reported within the BGR License Area and to those reported within the generalized deep water Pacific Ocean (Johnson et al., 2020).

17.6.2.5   Sediment chemistry

During NORI AREA D Campaign 3, opportunistic seafloor sediment sampling for biological and EIA-related geochemical parameters was undertaken at 45 sites using box corers. Samples for sediment geochemical characterisation were obtained at 31 of these sites. In 2019, during NORI Campaigns 6A and 6B, NORI collected a further 267 samples from 204 sediment chemistry sites. The locations of all sampling sites are shown in Figure 7.32. The sediment samples were sent to ALS Environmental Laboratory in Kelso, Washington, USA for analysis, which is accredited by the State of Washington Department of Ecology. At the time of writing, sediments are being analysed for:

- Moisture content (to allow results to be expressed on a dry weight basis).
- Total carbon (TC), total organic carbon (TOC) and total inorganic carbon (TIC).

- Total organic matter.
- Alkalinity (after a 5:1 deionised water extraction).
- Chlorophyll-a and algal biomass.
- Total phosphorus.
- Nitrate-N and nitrite-N (after a 10:1 deionised water extraction).
- Total metals (aluminium, antimony, arsenic, boron, cadmium, calcium, chromium, chromium (VI), cobalt, copper, iron, mercury, lead, magnesium, nickel, selenium, silver, tellurium, thallium, uranium, vanadium, zinc).
- Silicon, silicon dioxide (by calculation).

Results for total metals have been compared against the Screening Quick Reference Tables (SQuiRTs) published by NOAA (Buchman, 2008), and the Australian sediment quality guidelines (Simpson and Batley, 2016). The SQuiRTs for inorganic variables in marine sediments include screening values ranging from nearly non-toxic to toxic levels, both the 'Effects Range-Low' (ERL) values and the 'Effects Range-Median' (ERM) values. All results for nickel concentrations and most copper concentrations exceeded the ERM range, with a maximum observed value up to ten times the EML for nickel and five times higher for copper. The majority of results for mercury and zinc were similar to, or less than the ERL range, and other metals were lower again or below the method reporting limit. The ESIA will need to assess the potential for remobilization of metals from the sediment during mining to affect the overlying water quality.

17.7 Ocean ecosystems

17.7.1   Overview of ecosystem compartments

The ISA draft guidelines (2020) recommend that all recognized size classes of biota from microbial (e.g., bacteria) to megafauna (organisms from 2 cm to whales) to be characterised in each zone of potential occurrence, from the atmosphere to the deep ocean seafloor. This section of the IA provides an overview of the expected faunal composition of each of these habitat compartments.   Much is drawn from literature sources but supplemented with initial findings from the three campaigns completed in 2019/2020 in NORI Area D. Information to meet all requirements of the ESIA is expected to be available by the completion of campaigns 5a to 5d and the Collector Test at the end of 2022. The key features of the epipelagic, mesopelagic and bathypelagic zones of the water column and faunal components are summarised below.

The epipelagic zone (0–200 m) comprises the near-surface, well-lit environment that includes the surface mixed layer, depth to thermocline and euphotic zone. This is the zone of primary production by phytoplankton, and the dependent food chains from zooplankton and micronekton to larger invertebrates, fish from baitfish to schooling tuna and sharks, marine turtles and mammals. Only within this zone is light sufficient for photosynthesis (by the phytoplankton). Downward transport of dead organisms and particulate organic matter contributes to the food chains in the deeper layers of the water column. However, the surface waters of the open ocean outside of the influence terrestrial run-off are oligotrophic (i.e., nutrient limited, low levels of primary production).

The mesopelagic zone (200–1,000 m) extends down to the lower limit of light penetration, where temperatures decline, and minimum dissolved oxygen levels are encountered. Bioluminescence plays an important ecological role for the many species of fish and invertebrates (e.g., shrimps and squids) and gelatinous organisms (e.g., jellyfishes). These communities also provide a significant proportion of the diets of tuna and other large species that dive into the mesopelagic zone to feed during the day or encounter through vertical migration of the plankton and other micronekton (small fish/invertebrates) into the epipelagic zone during night-time (Bertrand et al 2002).

The bathypelagic zone (>1,000 m) is characterized by the complete absence of light, very low temperature, low nutrients, low productivity, and dissolved oxygen concentrations that are intermediate between the oxygen minimum zone and epipelagic zone. Organisms living in this zone are mostly dependent on food descending from the upper photic zones as sinking marine snow (Polunin et al., 2001) and intermittent falling of large dead animals such as whales. The main characteristics of the abyssal ecosystems (see Smith 1999) are described as follows.

- Low productivity: Generally, biomass declines exponentially with depth (Marshall 1979, Herring 2002). Food availability on the CCZ seafloor is limited by a low flux of particulate organic carbon from the surface and low abundance of life at the abyssal seafloor, and flux from epipelagic zone may be seasonal.

- Low physical energy: Currents at the seabed are slow. Sediment erosion and redeposition from physical processes are uncommon, or intermittent as benthic storms. There is evidence from the eastern CCZ that on geological time scales, and possibly annually, re-suspension and sediment transport events may be occurring (Jaun et al. 2018; Morgan et al. 1999; Smith 1999).

- High species diversity: despite low biomass, diversity at local habitat and regional scales can be high and has been subject of study through CCZ with investigation of specific animal groups at both organism and genetic level. Diversity and genetic preservation are identified as key issues (by the ISA) in managing mineral development within the CCZ. This has led to the establishment of areas of particular interest (APEIs) within the CCZ, each with an area of 400 km by 400 km, which are intended to remain protected from the impacts of nodule collection (ISA 2011a, 2012b). In total, these areas contribute about 30% of the CCZ (Smith et al, 2010).

- Large and continuous habitat but with geographical variations in relation to seabed depth, topography (presence of seamounts and other features), geological variations (e.g., presence of lava) and biological variability.

17.7.2   Size classes of organisms

The following sections provide brief descriptions of some of the characteristic organisms found within each of the zones and habitats. The existing information, together with the results of the data currently being examined from the 2018 and 2019 campaigns and the proposed studies over the next four campaigns is expected to provide the required robust baseline data for quantitative assessment and comparison of the faunal populations within and between NORI Area D and other areas of the CCZ.

17.7.2.1 Benthic megafauna

Megafauna (>2 cm) within the CCZ include mobile and sessile organisms, mostly invertebrates that occur on soft and hard substrates. The epifaunal groups include those living at the sediment-water interface such as gastropods, crabs, sea urchins, as opposed to those living within the sediments such as the larger polychaete worms and burrowing crustaceans. Larger and more mobile species living close to the seafloor within the CCZ are likely to include omnivorous fish (primarily rattails), cephalopods (octopus, squid), scavenging amphipods, deep-sea shrimp, and large deposit feeders such as sea cucumber along with suspension feeding sponges and anemones.

Comparative information on abundance and diversity from other megafaunal studies in adjacent research or Contract Areas includes Tilot (2006), Stoyanova (2012), Amon et al. (2016; 2017), Simon-Lledo et al. (2019), and other international benthic research projects in the UK polymetallic nodule mining claim in the CCZ, such as ABYSSLINE http://abyssline.info/. The ISA has also created an Atlas of Abyssal Megafauna Morphotypes of the Clarion-Clipperton Fracture Zone (http://ccfzatlas.com/).

17.7.2.2   Benthic macrofauna

Macrofauna (>300µm <2 cm) include the organisms that live within and on the sediment and the semi-liquid layer of the sediment-water interface. Polychaete worms comprise 50% to 65% of the macrofauna found in the CCZ, and also crustaceans, echinoderms and bivalve molluscs. Most macrofauna feed on surface deposits. Other studies of sediment macrofauna, for example Yu et al. (2018), examined density and community structure between the areas, including preserve areas, and Janssen et al. (2015) investigated local and regional genetic diversity in isopods and polychaetes across the CCZ to assess connectivity and dispersal.

17.7.2.3   Benthic meiofauna

Meiofauna (>32 to 300 µm) are organisms that occupy the sediment interstitial space or the epibenthic semi-liquid layer at the sediment-water interface. They can also occur on nodule surfaces and other micro-habitat structures. They are ubiquitous and in greater abundance than macrofauna. The main marine taxa include foraminifera, nematode worms, copepods (crustacea), and several other phyla in lesser abundance (Higgins and Thiel, 1988). Due to their abundance, these animals play a key role in carbon cycling in the deep sea and are sufficiently numerous to allow robust statistical monitoring of indices of abundance and diversity over time or between sites in studies of impacts to seabed such as dredging operations (Clarke and Warwick, 1994).

A number of research programmes have sampled the abyssal North Pacific Ocean seafloor and collected data for multiple parameters of interest to biogeochemical modelling efforts. Overall, meiofaunal (63-300 µm) and macrofaunal (300 µm-3 mm) abundances and/or biomass represent the most widely sampled biological parameters in this region, and these data sets also exhibit the greatest consistency in collection methods across field programmes. Preliminary examination of the data indicates that the abundance of these benthic fauna is roughly proportional to the flux of nutrients available in particles settling from the surface (ISA 2010).

17.7.2.4   Benthic microbial communities

Microfauna (biota sized < 32 µm) include bacteria, archaea, protistans, fungi and viruses, which are expected to be present in the CCZ. A number of studies have been undertaken to understand the microbial communities present within sediment in the CCZ. Shulse et al. (2016) and Lindh et al. (2017), using rRNA gene sequencing, found that microbial community composition and diversity varied with habitat type, water column depth, and sediment horizon. Microbial communities in the sediments had the highest diversity, followed by nodules, and then by the water column with less than 1/3 the number of operational taxonomic units in the sediments.

17.7.2.5   Benthic nodule fauna

A key topic for study in the CCZ is the composition of the biological communities associated with seabed nodules, which provide the hard seabed substrate on which sessile organisms can attach. In the absence of nodules, there is relatively little other hard surface that provides substrate for organisms to attach themselves.

A research project by Tilot (2006) studied the distribution of benthic megafauna associated with nodules within the CCZ (NIXO-45, NIXO-41 and ECHO-1) sites. It includes an annotated photographic atlas for each phylum, and inventories, based on a collection of about 200,000 photographs of the ocean floor showing a taxonomic diversity of 240 taxa. Of these, 46 were echinoderms, and cnidaria (e.g., jellyfish and sea anemones) was the most diverse phylum with 59 different taxa. The study used a classification of eight nodule facies, based on nodule sizes, surface features and degree of burial to evaluate relative abundance and composition of fauna, by phylum, and trophic and functional groups from

analyses of photographic transects covered by towed and autonomous devices. Suspension-feeders were more abundant that detritus feeders regardless of the facies. The study also analysed spatial heterogeneity in distribution of populations across the eight different facies and facies gradients.

In 2019, NORI completed a habitat mapping project applying a clustering algorithm to NORI Area D data that resulted in an 8-cluster solution classification for geoforms (seamounts, bathymetric highs, bathymetric lows and flat plains), described in NORI (2020b). Within each of these geoforms, key compartments were identified (slopes associated with abyssal hills, depressions within bathymetric lows, seamount sub-features), where biological communities are expected to be distributed according to abiotic type. NORI's existing nodule distribution data is split between three nodule distribution types according to size and sediment gaps between nodules (or percentage cover by nodules). Overlaying the 8-cluster solution geoform classification for each nodule type was then used to determine whether a relationship exists between geoform and nodule distribution type. An example overlay of the eight geoforms for Type 1 nodules is shown in Figure 17.10.

Figure 17.10   Type 1 nodules coloured by their placement within the 8-Cluster geoform map of NORI Area D
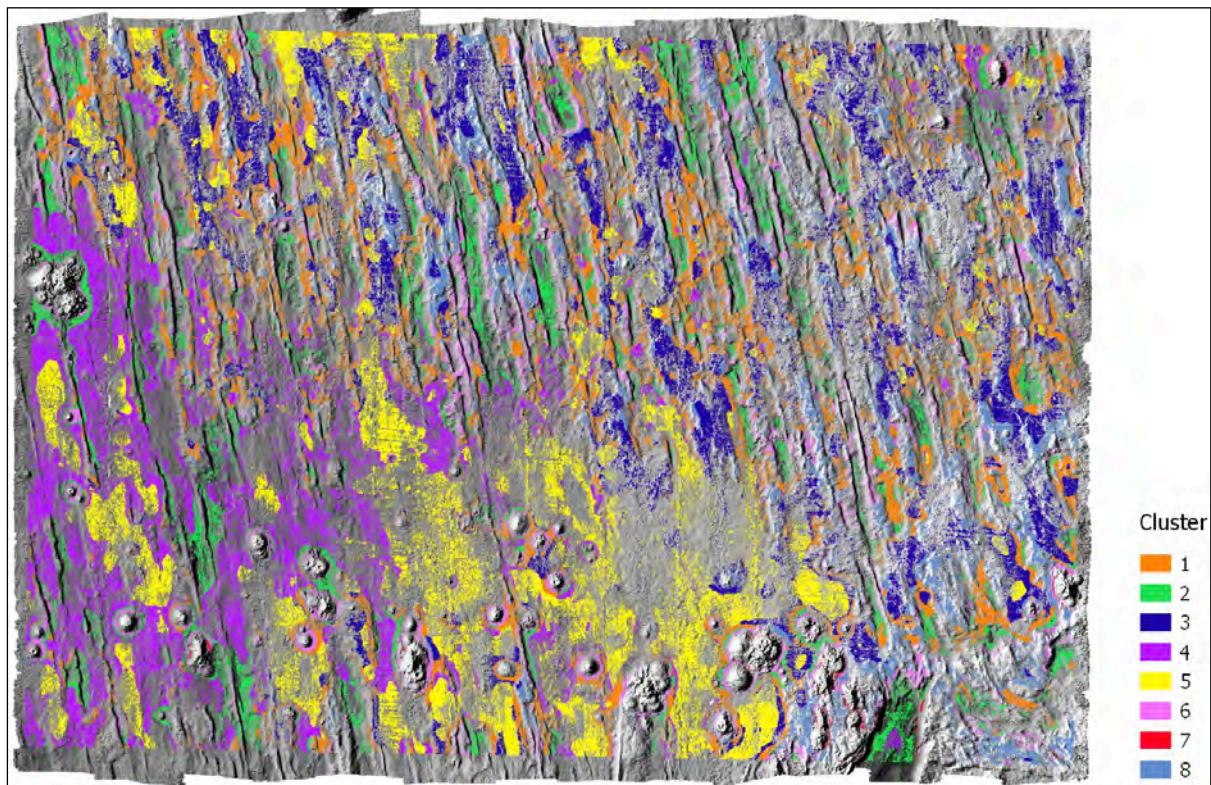
Results of the 8-cluster solution geoform classification were available prior to Campaign 6B, which enabled targeting of box core sampling to each of the 8-cluster geoforms. NORI collected 8,673 seafloor biological samples at 204 locations within NORI Area D. Four push-corer subsamples were taken from each box core for analyses of faunal class sizes and sediment chemistry. All samples were preserved using methods appropriate for the taxonomic and eDNA analyses required. Some examples of nodule-attached fauna and sediment megafauna from box core samples are shown in Figure 17.11. Analysis of these samples is yet to take place, however the degree of similarity between the respective eight facies identified in NORI (2020b) and Tilot (2006) will provide valuable comparisons of composition and distribution of nodule fauna over the wider CCZ area.

Figure 17.11   Examples of megafauna from NORI Area D (Note Each scale square is 1x1 cm)

Chitonidae *Chiton Carnosus* inhabiting nodule.

Crustacea *Chorocaris chacei* found in box core sample.

Echinoida *Echinus alexandri* found in box core sample.

Ophiuroid *Amphioplus daleus* (brittle star) found in box core sample.

Isididae Bamboo Coral and Polychaeta *Alaysia spiralis* inhabiting nodule.

Crustacea *Ventiella sulfuris* found on nodule.
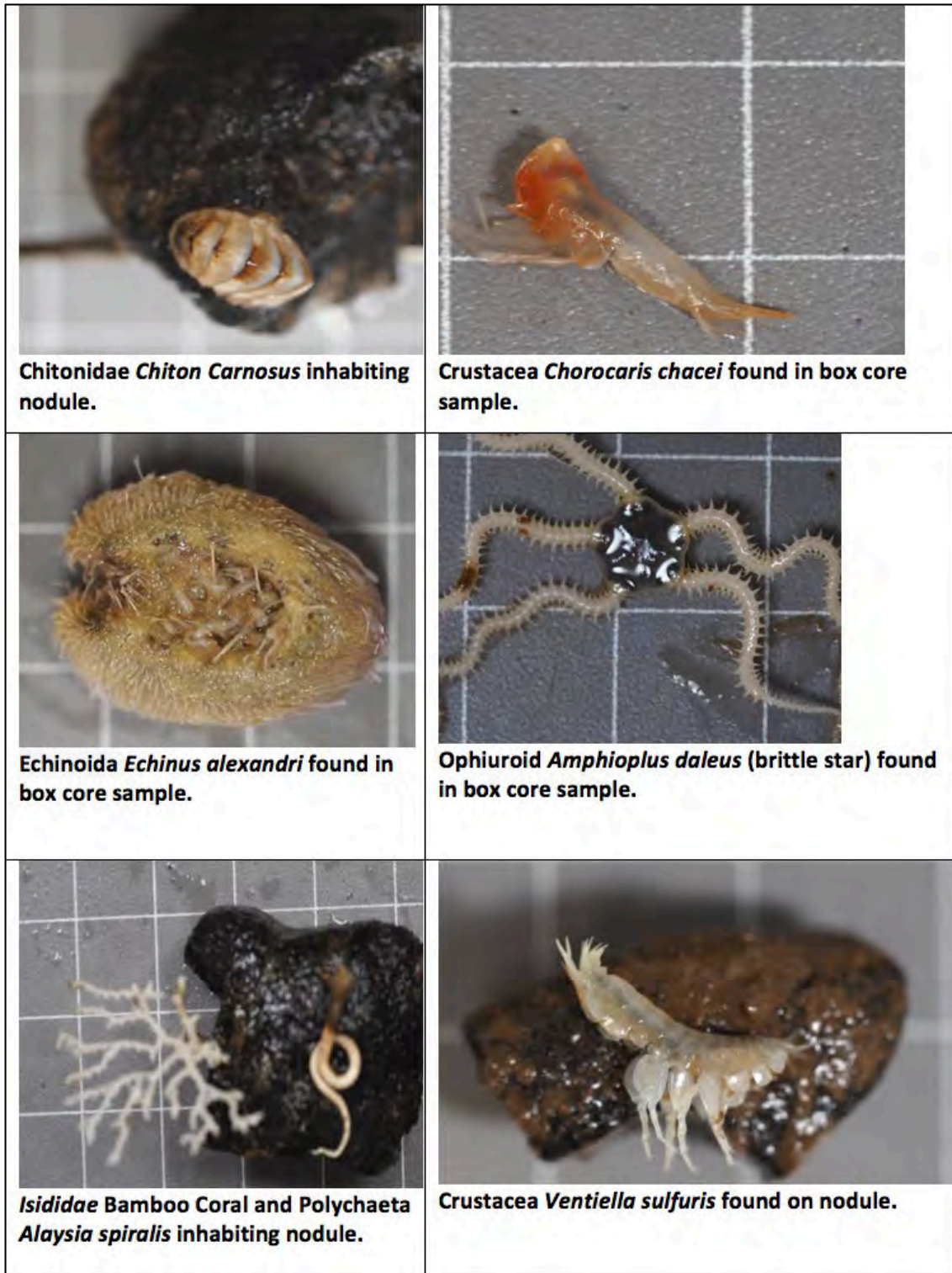
A number of other studies of nodule fauna have also been undertaken in the CCZ that provide background or analogous information and regional context of the types of benthic nodule fauna likely to be observed in NORI Area D, and the role that surface texture and microhabitat heterogeneity of nodules may play in the structure of these communities. These include Amon et al. (2016) Vanreusel et al. (2016), De Smet et al. (2017) Veillette

et al. 2007a, 2007b, Thiel et al. (1993) and Mullineaux (1987). Overall, much background information exists on the composition and distribution of nodule-associated fauna of the CCZ to compare and contrast with the findings from NORI Area D.

17.7.2.6 Benthic fish

Benthic fish species and their abundance can be assessed using techniques such as video surveys or video or camera bait stations. Although bait stations attract scavenging species, the method provides valuable information about a section of the fish community present at these depths. Many bathypelagic fish are opportunistic feeders, with large gaping jaws and stomachs adapted to feed on larger prey. Bioluminescence plays a role in feeding, predator evasion, reproduction and communication (Herring 2002). However, there are some more active bathypelagic fish such as families Macrouridae (rattails) and Morridae (cods). The AUV images collected to date, together with those that NORI will collect in the main study program, will provide images of fish present within NORI Area D and for comparison with other literature data for the CCZ.

17.7.2.7 Pelagic micro-organisms

Micro-organisms are found throughout the water column. Due to their size (and the size of their aggregates), they are an easily available substrate for filter feeders and selective feeders such as larval fish. Sorokin et al (1970) estimated that "bacterioplankton" are as important as algae as a primary food substrate. Work on bacterial communities within the UK-1 Area by Shulse et al. (2016) showed that diversity in the water column is lower than diversity in the sediment.

17.7.2.8 Pelagic Phytoplankton

In subtropical sea surface waters, nutrient concentrations are low and phytoplankton populations are sparse (Morgan et al. 1999). Algal productivity is driven by the availability of nutrients in surface waters, which is typically low in areas remote from the influence terrestrial runoff, and levels of light and depth of light penetration. Most publicly available CCZ plankton work appears to have originated from the Deep Ocean Mining Environmental Study (DOMES) sites. DOMES Sites A and B are located to the west of NORI Areas A and B. DOMES Site C is located between NORI Areas A/B and C (see ISA, 2010).

17.7.2.9 Pelagic zooplankton and micronekton

Research on zooplankton and micronekton carried out at the DOMES sites in the 1970s found concentrations to be highest in the upper 150 m, with highest densities of taxa within the upper 100 m of the water column (Morgan et al. 1999). However, many zooplankton only spend part of their time in the surface zone, descending into deeper water of the mesopelagic zone during daytime to escape predators, returning at night to feed on phytoplankton when they are less exposed to visual predators (Castro and Huber 2005). Some patterns of vertical distribution can be more complex with adaptation of species to live within the oxygen minimum zone (Fernandez-Alamo and Farber-Lorda 2006), highlighting the need to understand these processes and potential impacts at different depths within the water column.

17.7.2.10 Pelagic nekton

These include non-commercial species such as squid, lancet fishes, flying fishes, lantern fishes, rat-tail fishes, pelagic shrimp, and euphausiids as well as commercial fish species, such as tuna and billfishes. They are found throughout the Pacific Ocean at tropical and subtropical latitudes. Most of these surface schooling species are highly migratory, and their latitudinal range is seasonal. Many species of sharks are also expected to be found in the CCZ area, inhabiting all zones from surface to the seafloor.

17.7.2.11 Marine mammals, reptiles and birds

Several species of whales are likely to frequent or transit through the CCZ area, including large baleen whales: blue whales, fin whales, sei whales, and the toothed sperm whales. Dolphins such as the Pacific bottlenose and spinner dolphins are also likely to be present. Most sea turtles, particularly the leatherback have worldwide distributions that could transit through the project area.

Given the remote off-shore location of the CCZ, no bird breeding grounds occur at or near the NORI licence areas. However, a range of seabirds may occur in the wider CCZ environment, including those on a migratory pathway, or wandering seabirds, such as albatrosses, shearwaters and petrels.

During the 2019 campaigns, on board observations of marine fauna were made during the time sat NORI Area D and while transiting to and from the site, and this observing and recording program will continue on all NORI's future campaigns. Existing information available from other parts of the CCZ will also be utilised in conjunction with observational seabird research in and adjacent to NORI Area D to build a picture of seabird species present and their occurrence. Seabird observations will also be collated together with the marine mammal observation program.

17.7.3   Ecosystem biodiversity

Biodiversity includes the species and communities within each of the oceanographical zones and topographical habitats described above. It is an important measure of the overall ecosystem health and function, although it has no unifying metric for comparison. NORI's proposed studies are designed to describe the functioning of the CCZ seabed and overlying water column ecosystems, and the role played by different species to make definitive statements about biodiversity impacts in terms of maintenance, or the extent of any reduction or loss.

17.7.4   Ecosystem trophic interaction

Understanding how the components of the ecosystem interact and depend upon each other, through feeding and transfer of carbon is important in being able to understand effects that might occur within an ecosystem when any component of the system is disturbed.

The complexity of deep-water studies requires data on trophic interactions to come from multiple sources (Guenette et al. 2008; Pinkerton et al. 2010; Pinkerton & Bradford-Grieve 2014; Choy et al. 2015, 2017; Drazen & Sutton 2017). The biological dependencies and interactions are complex.

Understanding the ecosystem-scale deep-water trophic interactions within the NORI Area D block will require integration of studies (including trophic model development) undertaken across the CCZ. NORI's proposed sampling methods to be used during the proposed studies will allow for morphological taxonomy, environmental DNA (eDNA), molecular and stable isotope analysis to build up data on overall biodiversity and interactions.

17.7.5   Ecosystem interaction with existing economic activities

The key existing economic activities within the CCZ are the passage of cargo vessels and some fisheries activity.

17.7.5.1   Shipping

Although the NORI licence areas have the potential to overlap with some shipping routes, these do not appear to be major routes and the frequency of vessel passage is envisaged to be low, which is consistent with observations made by other ISA contractors operating in the CCZ.

NORI will require each vessel operating under its control to enter data into the ship's log related to ship sightings and activity within the NORI exploration areas. The draft EIS developed by NOAA for the Ocean Mining Associates CCZ manganese nodule exploration licence stated that only 50 vessel sightings were made over a non-continuous 10-year study period, and of these, only one was a fishing vessel (NOAA, 1984). During the NORI 2018 campaign, only one vessel (a fishing vessel) was seen in six weeks. Adherence to standard maritime navigational protocols and radio communications is expected of all vessels in the vicinity to avoid risks of collision.

17.7.5.2   Fisheries

The CCZ sits within Major Fishing Area Statistical Area 77 of the Food and Agriculture Organisation (FAO http://www.fao.org/fishery/area/Area77/en) of the United Nations, which covers a total surface area of 48.90 million km^2, including the area from 175°W to the west coasts of USA, Mexico and Central America between latitudes 5° and 40° N. Tuna and other larger pelagic fishes are important components of the marine fisheries and widely distributed in Area. The key countries fishing for tuna in Area 77 are Mexico and USA, followed by Venezuela, Japan, Korea, Spain, and other Asian nations. Over the period 2012 to 2018, total fish capture (including fish, crustaceans and molluscs) for the Eastern Central Pacific (Area 77) has ranged between 1.65 and 2.05 million tonnes (Food and Agriculture Organisation, 2018).

Distribution of catches of different species over smaller scales within Area 77 is provided by the Inter-American Tropical Tuna Commission (IATTC), which was established in 1950 and responsible for the conservation and management of tuna and other marine resources taken by tuna-fishing vessels in the eastern Pacific Ocean. The principal species of tunas caught are the three tropical tuna species (yellowfin, skipjack, and bigeye), followed by the temperate tunas (albacore, and lesser catches of Pacific bluefin). Other scombrids (mackerels), such as bonitos and wahoo, are also caught.

Access to the fishery is regulated by Resolution C-02-03, which requires vessels to be on the IATTC Regional Vessel Register in order to fish for tunas in the eastern Pacific Ocean. Vessels are authorized to fish by their respective flag governments, and only duly authorized vessels are included in the Register. The IATTC also has significant responsibilities for the implementation of the International Dolphin Conservation Program, as tunas are often associated with dolphin schools and such schools provide locational guidance on setting of the tuna purse seine nets.

Almost all the catches in the eastern Pacific Ocean are made by the purse-seine and longline fleets. Detailed catch data are available for the purse-seine fishery, which takes over 90% of the total catches reported. Figure 17.12 shows the average annual distributions of the purse-seine catches of yellowfin, by set type, caught in each 5° by 5° reporting area for the period 2013–2017 (IATTC, 2019). The sizes of the circles are proportional to the amounts of yellowfin caught. DEL denote nets set in location of dolphin schools; OBJ denotes nets set under floating objects and OBJ denotes nets set without associated objects / fish schools. This graph shows some purse seining for yellowfin occurs in the vicinity of NORI Area D (approximately 115° W and slightly north of 10°N). Figure 17.13 shows distributions of the average annual catches (metric tonnes) of bigeye and yellowfin tunas in the Pacific Ocean by Chinese, Japanese, Korean, and Chinese Taipei longline vessels, over the same period. The vast majority of this fishing effort takes place

to the south and west of the NORI Area D, with only minor contributions in the project area.

Overall, long term fishing activity within the CCZ near the Nori Area D appears low, based on monitored fishing vessel activity. Additional fisheries information on presence and sightings of fishing vessels will be collected as part of NORI's environmental work program.

Figure 17.12 Average annual distributions of the purse-seine catches in the Eastern Pacific Ocean of yellowfin tunas
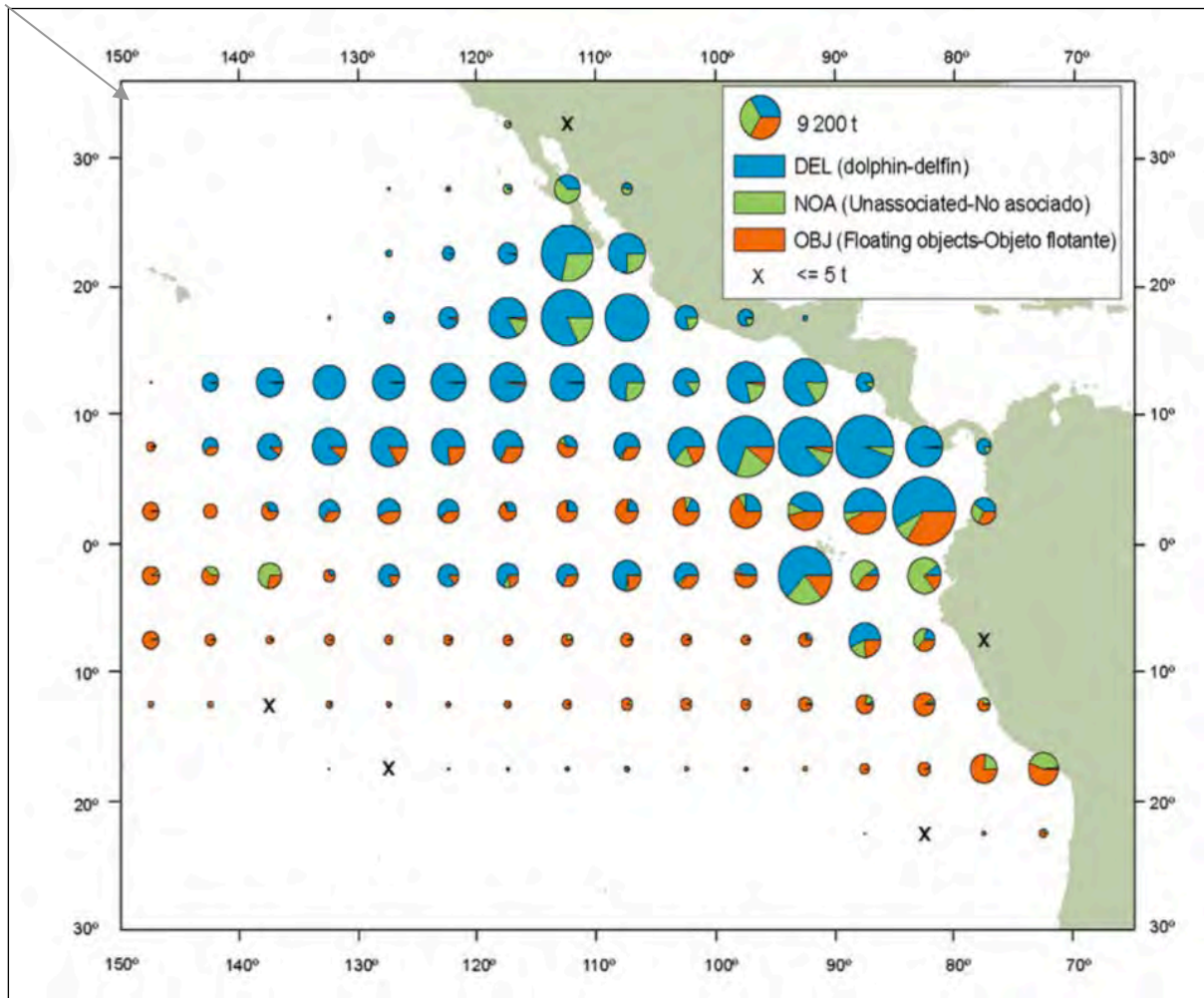
Source: IATTC

Figure 17.13 Average annual catches of bigeye (BET) and yellowfin (YFT) tunas in the Pacific Ocean
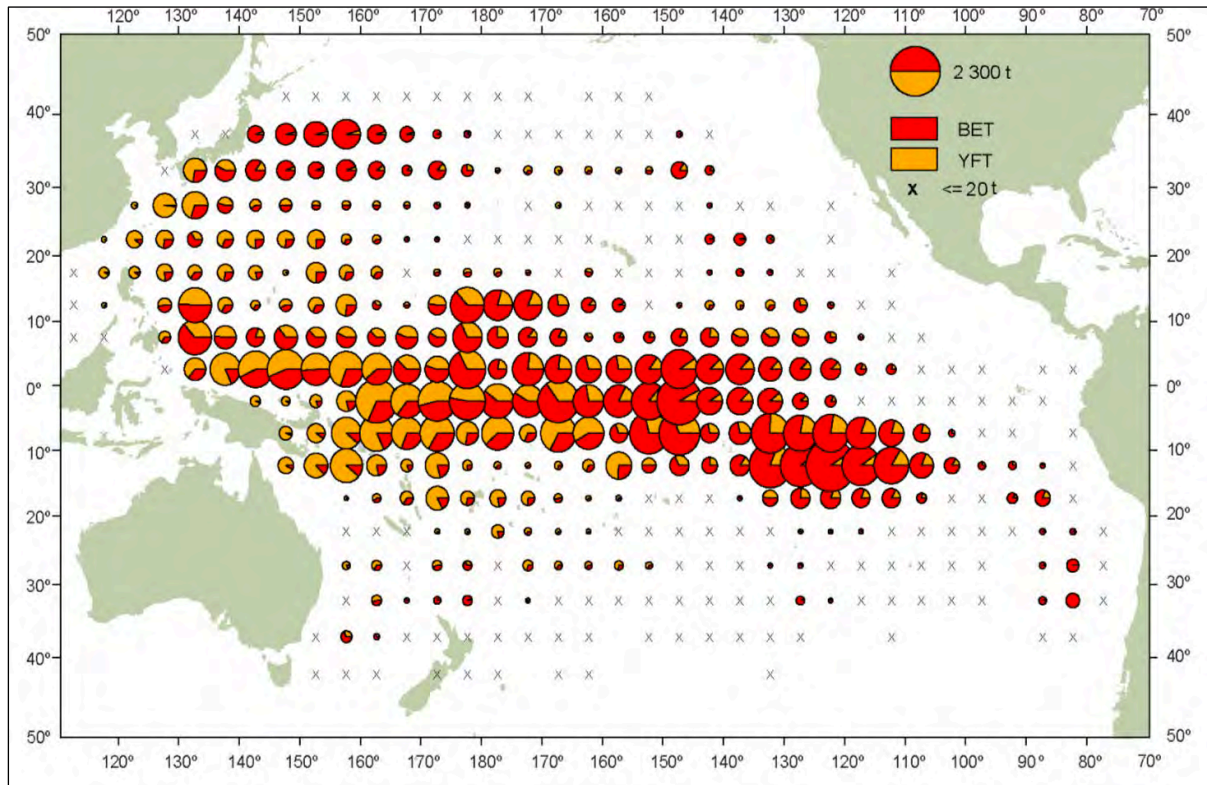
Source: IATTC

17.8 Environmental and Social Impact Assessment (ESIA)

NORI has commenced the ESIA process in support of an application for an exploitation license for the commercial development of deep-sea polymetallic nodules. The objective of the ESIA is to describe the project, its potential benefits and the predicted environmental and socioeconomic impacts of project-related activities during the development and operation of polymetallic nodule mining operations. The completed EIS will enable the regulator (ISA) to make an informed decision on the approval of the project and if approved, any further conditions deemed appropriate.

Progression of the ESIA now requires that a comprehensive program of oceanographic, biological and metocean data acquisition be conducted to characterize the baseline conditions at a designated Collector Test Site and control sites in NORI Area D, to enable future validation of the ESIA's predicted residual impacts (i.e., after all mitigation) during and after mining operations. To date, NORI has completed the initial scoping and has developed detailed study terms of reference to be undertaken by appointed experts. The first of several dedicated environmental campaigns started in October 2020. The stages of ESIA progress are described below.

17.8.1   Environmental Impact assessment scoping

Scoping is a critical early step in the preparation of the ESIA and is the point at which issues and impacts that will be important in the decision-making process are identified for investigation by the ESIA (Durden et al 2018).

In June 2019, NORI held a technical stakeholder scoping study workshop in San Diego. Participants included members of the ISA and Government of Nauru, environmental practitioners and academics from the fields of deep-sea mining and academia. The

participants followed a structured process of identification of zones of impact through the water column to the seafloor, then linking to each the impacting activities that are associated with polymetallic nodule harvesting. The output from this workshop formed the basis of a detailed scoping document and terms of reference for all the offshore environmental studies needed over the next two to three years to meet the regulatory requirements of the ISA (NORI 2020a).

In February 2020, NORI held a further multi-stakeholder workshop involving diverse stakeholders from academia, the regulator and industry, which focussed on the scoping of the NORI ESIA program. A number of NGO's which have advocated against nodule production were invited but declined to participate in the workshop.

The objectives of the Scoping Phase were to:

- Identify stakeholders and inform them of the proposed Project and the ESIA process.
- Provide stakeholders with the opportunity to identify any issues and concerns associated with the proposed Project.
- Identify areas of likely impact and environmental and social issues that may require further investigation by the ESIA.
- Develop the Terms of Reference (TORs) for specialist baseline and impact assessment studies in response to initial stakeholder input.
- Release the Scoping Report, including draft TOR for specialist studies, for stakeholder review and comment.

In principle, the main issues, in order of perceived priority and relevant to NORI Area D, were identified as:

- Seafloor – direct physical impact of mining/sampling equipment.
- Smothering/burying of fauna by sediment deposition.
- Change in seafloor sediment characteristics post mining (e.g., removal of solid surfaces, such as nodules suitable for attached species colonisation).
- Clogging of suspension feeders.
- Potential release of toxic trace metals and other contaminants.
- Loss of essential habitat (spawning/nursery grounds).
- Likely long time periods for recolonization and recovery of key species groups.
- Water column effects on behaviour of mammals, mesopelagic or migratory fish and plankton through changes in water composition (e.g., chemical contamination) and clarity.
- Surface increased vessel activities and potential pollution (includes risks associated with extreme weather events).
- Reduction in primary production through shading by discharges (if near-surface discharges occur in photic zone).
- Effects on behaviour of surface mammals, fish and birds through changes in water composition and clarity, noise and lights from vessel activity.
- Bioaccumulation of toxic metals through food chain.
- Sediment plume through water column from seafloor operations or midwater discharges.
- Local changes in pH.
- Nutrient and trace mineral enrichment (if near-surface discharges in photic zone).
- Potential oxygen depletion.

Figure 17.14 shows the zones through the water column to the seafloor, where the impacts of nodule harvesting are likely to occur.

Figure 17.14 Potential impact zones through the water column
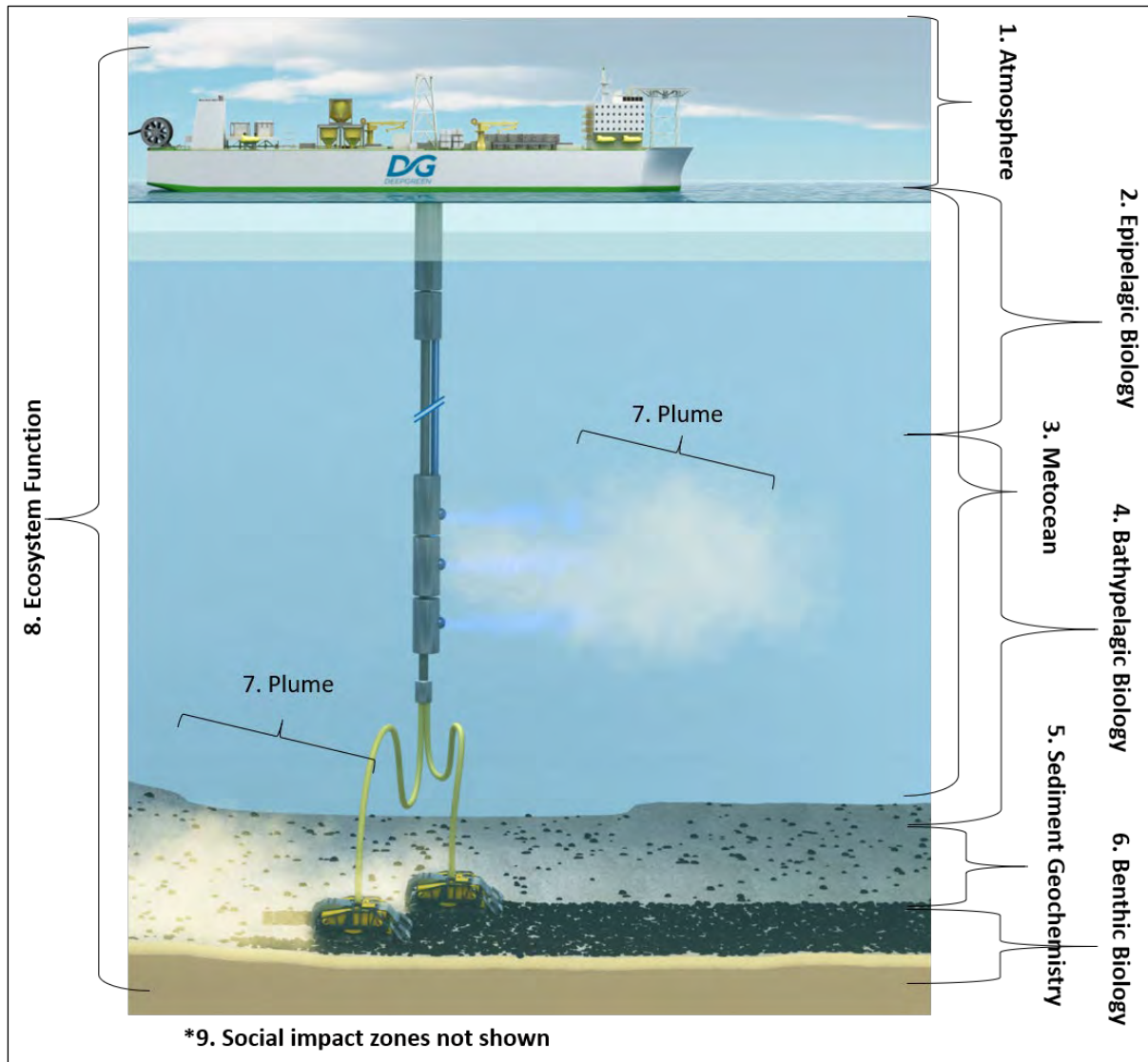
Source: NORI

After the impact zones were defined a suite of baseline studies was recommended as part of the ESIA to supplement the existing knowledge base and provide site specific data to inform the EIS. A list was developed by participants for each impact zone which described the focus and best available data collection techniques that should be employed. The outputs constitute a seabed-to-surface approach to conducting baseline studies as summarized in Table 17.1 and described in more detail in Section 20.8.2.

Table 17.1   Summary of outputs from June 3-5 workshop, San Diego, USA

Impact Zone	Study Focus	Data Collection Technique
Atmosphere	Meteorology	Desktop studies / At-sea met station
	Air quality	Desktop studies / Emissions incl. Greenhouse Gases
	Seabirds	Desktop studies / At-sea observations
	Light Environment	Desktop studies
	Noise environment (non-human impacts)	Desktop studies
Epipelagic Biology Bathypelagic Biology	Discharge vessels (surface)	Routine discharges / Process for transporting materials / Spills (behavior of material)
	Oil spills	Modelling / Post-impact response planning
	Wave climate	Desktop studies / Opportunistic vessel motion- wave height / Spotter buoys
	Noise environment (non-human impacts)	Moorings / Hydrophones / Engineering design – thrusters - RALS
	Biological environment	Cetaceans and other pelagic megafauna, debris, vessels – observations / Phytoplankton / Zooplankton / Micronekton / Bacterial collection and identification
	Water quality	Sample collection and laboratory analysis
Metocean	Upper, mid and lower water column noise	Hydrophones
	Cetacean presence	Hydrophones
	Sediment flux through water column	Sediment traps
	Sediment flux near seabed	Sediment traps
	POM flux through water column and near seabed	Sediment traps
	Isotope flux through water column and near seabed	Sediment traps
	Upper and midwater column physical oceanography	Moorings - CTD/ADCP
	Lower water column physical oceanography	Moorings - CTD/ADCP
	Vertical water movement	Moorings - CTD/ADCP
Sediment Geochemistry	Contaminant characterization	Screening study / Elutriate test / potential release of toxic metals
Benthic Biology	Habitat mapping	Desktop studies / Geomorphology mapping / Substrate mapping (nodule grades, distribution) / Mine plan development
	Biological communities – Microfauna, Meiofauna, Macrofauna, Megafauna, Demersal scavengers	Targeted taxonomic and distribution studies (AUV / Box cores / Multicores)
	Biotope characterisation	Biotope mapping and analysis
Plume	Upper and midwater column physical oceanography	Moorings - CTD/ADCP/ Hydrodynamic modelling

Impact Zone	Study Focus	Data Collection Technique
	Lower water column physical oceanography	Moorings - CTD/ADCP
	Sediment characterisation	Grain size / Physicochemical / Flocs
	Temporal water column physicochemical characterisation	CTD profiles / Niskin bottles
Ecosystem Function	Energy flows	Ecosystem modelling
Social	Stakeholders screening and mapping	Stakeholder screening / Mapping / Engagement Plan
	Training	Capacity building implementation plan
	Sponsoring state coordination	Communications and coordination plan
	Other marine users – Fishing, Subsea Cables, Military operations, Shipping, Cultural heritage	Desktop studies / Focused Studies
	Academic outreach	Communications and coordination plan

17.8.2   Project environmental impacts

The main impacts expected to occur during polymetallic nodule collection will involve removal from the seabed of material, with associated alterations to habitat and fauna. The lifting of nodules from the seabed will require the removal of water brought back to the surface with the nodules from the seabed. The separation of the seawater will likely occur immediately above or near to the collection site, either on the CSV or bulk carriers. The seawater that will be separated from the nodules will need to be discharged back to the sea. The discharge water will likely contain some fine material, made up primarily of residual sediment and fragments of nodules.

17.8.2.1 Impacts to surface waters

Impacts to surface waters will depend upon the type, number, and size of vessels and platforms deployed at the nodule collecting sites. Impacts associated with surface vessel operations are not exclusive to nodule collecting operations but will need to be considered. These include noise and lights with the main vessel operation, as well as support vessels and bulk carriers moving in and out of the area; vessel emissions to air; and routine discharges associated with vessels (noting that these will be governed by international legislation such as the International Convention for the Prevention of Pollution from Ships (MARPOL) and by specific management plans prepared in relation to particular aspects of operations from which impacts might arise (for example, the effects of lighting on seabirds).

17.8.2.2 Impacts to midwater column

Some noise and vibration of the riser are expected from the pumping of nodules to the vessel and may be detectable by organisms inhabiting or diving through those parts of the water column. The intensity and attenuation of generated noise will need to be assessed in the ESIA. The water and contained residual sediments returned to the sea will result in the generation of suspended sediments to which organisms in the vicinity will be exposed and potentially some temperature differences, depending on the extent of counter-current equilibration. NORI's guiding philosophy is to discharge riser water at a depth and in a manner that causes the least and shortest-lived disruption to the ocean's biology, physics, chemistry and ecosystem services. The selection of that depth will be informed by hydrodynamic modelling to determine the extent of sediment dispersion and by

identification of the organisms and their sensitivities to exposure to the sediment from the discharged riser water, including the physical and chemical composition of the sediments discharged.

17.8.2.3   Impacts to seafloor

Extraction of nodules will result in impacts to the fauna of the seafloor and overlying water column from the physical removal of habitat, the generation of suspended sediment, release of pore water and creation of new sediment surface with a physical structure and chemistry that may differ from that of the seabed prior to nodule extraction. The nodules are generally between 5 and 10 cm in diameter and lie half-buried in the sediment, and so some disturbance of substrate will occur. Mobile swimming or crawling animals may be able to move aside, but all sessile (immobile) benthic fauna in the path of the collecting operation will be affected. In areas of seafloor with soft sediment, much of the biodiversity is to be found in the top 5 to 8 cm of the sediment (Higgins and Thiel, 1988; Giere 1993); noting that, at the time of these references, size definitions of meiofauna extended to 300 or 500μ and into what are now included within the macrofauna.

As for the midwater impacts, NORI's guiding philosophy is for the development plan to include design features to minimise sediment escape to the water column and confine impacts of disturbed material within the collector paths as far as practicable, thereby minimising impacts to undisturbed areas.

17.8.2.4   Benthic disturbance and recovery studies

The return of the CCZ to its pre-impact state after removal of nodules from the mined areas is not likely to occur within any foreseeable timeframe, given that nodule formation is believed to be in millions of years. However other species and functions would recover over periods that are measurable. A number of experimental impact-recovery time series research have been carried out under several programs such those identified in Jones et al. (2017), who reviewed changes in faunal densities and diversity of benthic communities measured in response to the 11 simulated or test nodule mining disturbances undertaken in or relevant to the CCZ. Almost all studies showed some recovery in faunal density and diversity for meiofauna and mobile megafauna.

Twenty-six years after the 1989 disturbance and recolonization (DISCOL) experiment carried out in the Peru Basin nodule field, suspension-feeder presence remained significantly reduced in disturbed areas, while deposit-feeders showed no diminished presence (Simon-Lledó et al., 2019). Similarly Vonnahme et al. (2020), and Stratmann et al. (2018) found varying times of recovery for other indices such as: significantly reduced uptake of fresh phytodetritus by bacteria, nematodes and holothurians in plow tracks; microbial community diversity unchanged compared to unplowed reference areas, but microbial cell numbers were 30% lower; and taxonomic composition of meiofauna and macrofauna was not significantly different between plowed and reference sites, but carbon uptake by bacteria, nematodes and holothurians was significantly lower at plowed sites. Overall, these authors estimated that it could take up to 50 years for the more sensitive indicators to return to undisturbed levels.

17.8.3   Scopes of work and terms of reference

Based on the outputs from the June 2019 San Diego workshop, and to comply with ISA regulatory requirements, NORI prepared a Scoping Report including Terms of Reference for baseline environmental studies relating to all off-shore components of the project (i.e. nodule collection and transportation) to be conducted within NORI Area D (NORI 2020a). The compilation of this report was designed not only to comply with ISA regulatory requirements but also to address data gaps and reduce uncertainties in project options during progressive phases.

The 2020 Scoping Report provides:

- Identification of the key issues and concerns for consideration in the development of the ESIA study,
- Identification of resource areas that have the potential to be impacted and environmental issues that may require further studies in the ESIA,
- The regulatory body (the International Seabed Authority) with the full scope of the proposed studies and tasks that NORI proposes to undertake in order to comply as far as practicable with the combined regulatory recommendations, set out in ISA documents: i) Recommendations for the guidance of contractors for the assessment of the possible environmental impacts arising from exploration for marine minerals in the Area (ISBA/25/LTC/6; 2020), ii) Recommendations for the guidance of contractors for the assessment of the possible environmental impacts arising from exploration for marine minerals in the Area (ISBA/19/LTC/8 (2013) and iii) Recommendations for the guidance of contractors for the assessment of the possible environmental impacts arising from exploration for polymetallic nodules in the Area (ISBA/16/LTC/7; 2010); and
- Terms of Reference (TORs) for the ESIA studies that provide clear direction for the participating specialists on what needs to be assessed, how it will be assessed, and to what level of detail.

Several of these studies require long term information gathering using moored instruments or multi-year information collection to cover seasonal factors and to build robustness into hydrodynamic / plume modelling. As such baseline data collection in the NORI Area will require a multi-year program of work campaigns, spread over a three-year period. Key to this work is a comprehensive characterization and quantitative comparison of the baseline conditions at a designated Collector Test Site and control sites in the mining lease area.

The proposed campaigns planned for the NORI Area D Area (see Section 20.3) are designed and scheduled for the specialist consultants to complete their work in support of the preparation of the ESIA. Campaigns have been strategically timed to provide maximum time possible between consecutive sampling efforts, to coincide with known periods of seasonal variations in the water column, and to sample the Collector Test Site and a Preservation Reference Zone (PRZ)[23] twice before, and once following, the Collector Test.

17.8.4   Social license / stakeholder engagement

The NORI Area D project differs from a conventional land-based mining project in that there are no landowners or residents who would be directly impacted by the project through displacement or loss of assets. In this case, the key stakeholders include ISA member countries, sponsoring states, businesses in the fossil fuel replacement industries, and community groups with a range of interests in the deep sea and mining.

Engaging with these stakeholders early in the ESIA process is essential to understand their perspectives on the matters of importance to them. To this end, NORI has implemented a Communication and Stakeholder Engagement Plan (CSEP) to ensure that the communications and stakeholder engagement components of the ESIA are conducted in a structured manner, in accordance with international best practices, and that the outcomes of stakeholder engagement are aligned with the objectives of the ESIA and regulatory requirements.

---

[23] An area representative of the area to be mined but outside the mine area of influence

The CSEP demonstrates NORI's commitment to a program of genuine engagement with stakeholders (e.g., regulatory authorities, governments, NGO's, environmental groups and the media, which values their contribution and their involvement in the project. In the first instance the CSEP has been developed specifically for the ESIA study scoping phase of the project (as shown in Figure 17.15) with ongoing engagement guidance as the project transitions from the exploration to exploitation phases of the project. Managing relationships with key stakeholders, including regulatory authorities, governments, NGO's, environmental groups and the media, is critical - not just to the project's reputation and outcomes - but to the reputation of the proponents, investors and partner organizations responsible for bringing the project to fruition.

The objectives of the stakeholder consultation are to:

- demonstrate open and transparent communication.
- create awareness and understanding of the project.
- identify who needs to be aware of what information and when.
- ensure consultative opportunities are provided to ensure effective consideration and management of environmental issues throughout the ESIA.

The CSEP is intended to be a 'live' document and will be updated throughout the project lifecycle post the ESIA phase. A summary of communications and stakeholder engagement objectives as they relate to the Scoping Phase of the EISA is shown in Figure 17.15.

The key activities that have been initiated by NORI to date include:

- The June 2019, technical stakeholder scoping study workshop in San Diego, in which the participation of independent scientific institutions in the ESIA underscores the company's commitment to transparency during the exploration phase.
- Establishment of formalized partnerships with leading scientific research institutions and internationally renowned universities in a significant investment into its ongoing ESIA program of work.
- Organisation of the February 2020 two-day workshop in San Diego attended by more than 70 people from all over the world. Stakeholder meetings (in-person and online) to introduce NORI's environmental baseline thinking and initial planning and to seek feedback.
- February 2020 – Kingston, Jamaica – side event presentation at ISA Council meeting to stakeholders on NORI's environmental baseline thinking and initial plan.
- February 2020 – Kingston Jamaica – meeting with ISA Environment department to present Scoping Report and TOR concept and timelines.
- June/July 2020 – Submission of Scoping Report to LTC.
- October 2020 – response from LTC stating it did not have time to review Scoping Report and will provide feedback in the future.
- Funding of an independent, in-depth lifecycle assessment study that compares the cradle-to-gate impacts of two sources of metals – land ores and deep-sea polymetallic metals. The study produced a white paper, followed by three webinars in May and June 2020 on the white paper, where the lead authors presented the findings and answered questions live.
- Publication of life cycle climate change impacts of producing battery metals from land ores versus deep-sea polymetallic nodules (Paulikas et al, 2020).
- Production of news and media articles available via the DeepGreen website.
- Training opportunities, particularly for pacific island nations, and job advertisements via the website.

Initiatives planned over the next 6–12 months include:

- Release of the Scoping Report to workshop participants for feedback and review.
- Public release of Scoping Report for comments, revision based on public feedback, and submission of revised Scoping Report to LTC, noting public comments and changes incorporated.
- 2021 – submission of EIA to LTC and posting publicly for feedback for Collector Test in 2022 (must be submitted 12 months in advance).

Figure 17.15 Communications and Stakeholder Engagement objectives (scoping phase)
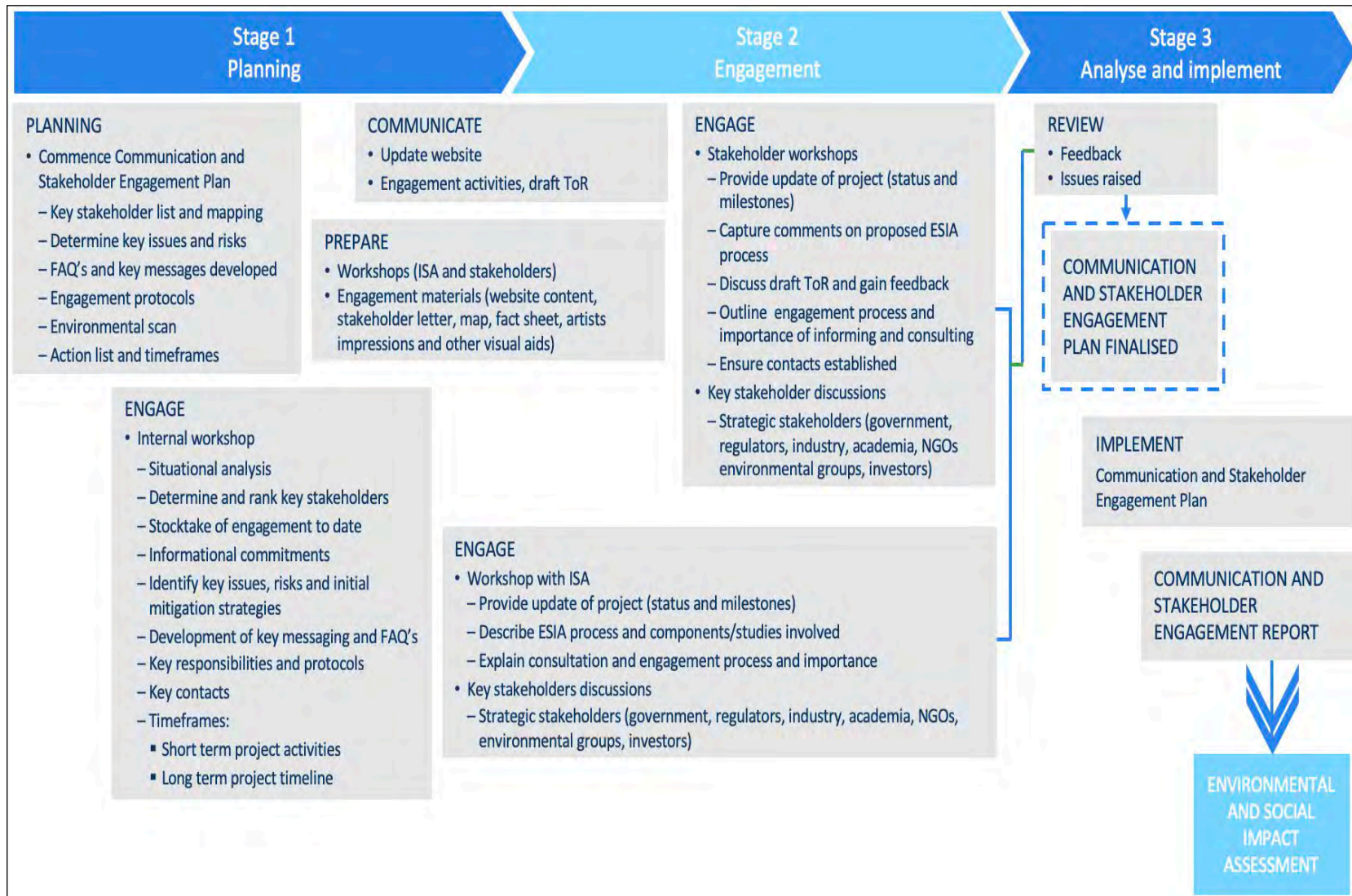
17.8.5   Project environmental impact assessment process

The impact assessment process predicts the likely changes to the existing environment that would arise as a result of the project activities and then evaluates the significance of those identified impacts, both in terms of the magnitude of impact (e.g., in duration or extent), and on the key environmental receptors, such as biodiversity, ecosystem services and conservation status of organisms. The initial screening is qualitative, based on secondary knowledge of the receiving environment and expert judgement of sources of impacts and impacts themselves. As the project's collection of primary environmental data progresses and greater definition of engineering details is available, so the assessment enables more quantitative estimates of the scales of impacts, thereby identifying the activities for which mitigation will be required.

The results of an initial qualitative Environmental Risk Assessment (ERA), seen as Step 1 of Figure 17.16, is based on secondary data that were used to inform the scoping process and develop a focused Plan of Work for the ESIA (NORI 2020a). The ERA will transition progressively from low, moderate and high in Step 1 to semi-quantitative and fully quantitative assessments in Steps 2 and 3, respectively, of Figure 17.16, as the information and feedback from the studies becomes available from the forthcoming campaigns.

Figure 17.16   Qualitative, semi-quantitative and fully quantitative risk assessments
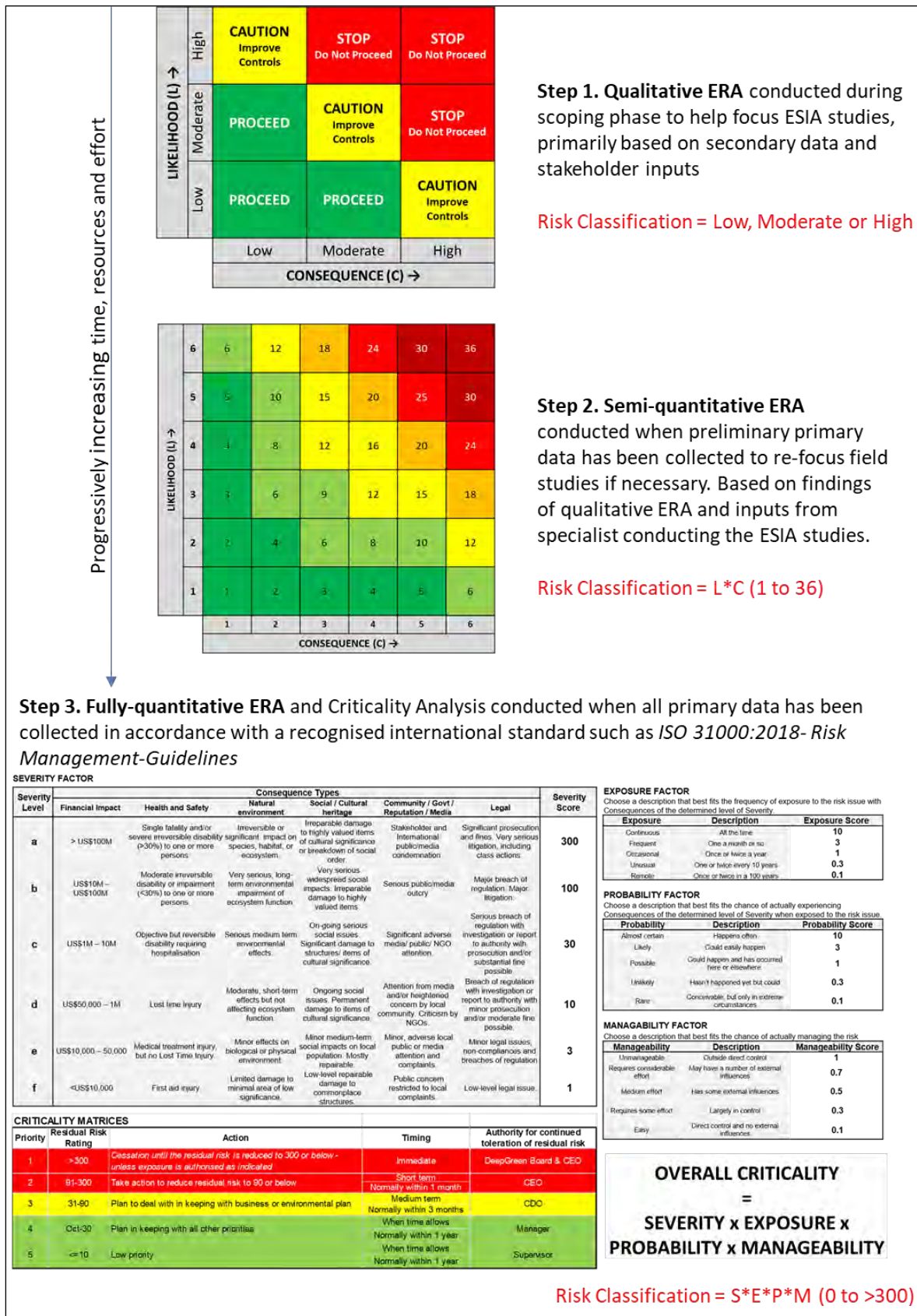
17.8.6   Ecosystem Based Management

The ISA document 'Draft regulations on exploitation of mineral resources in the Area' (ISBA/26/C/CRP.1; 17 December 2019) states that an 'ecosystem approach' should be adopted for the effective protection of the marine environment from the harmful effects arising from PMN mining in the CCZ. NORI anticipates that this requirement will be preserved in the final version of the regulations and is preparing terms of reference for the inclusion of an Ecosystem Based Management (EBM) approach to impact mitigation and management.

Internationally, the ecosystem approach to environmental management has emerged as the dominant paradigm for managing marine ecosystems, that aims to protect the health, productivity, and resilience of ecosystems as well as the ecosystem goods and services valued by human beings. According to the Convention on Biological Diversity (CBD), "the ecosystem approach is a strategy for the integrated management of land, water and living resources that promotes conservation and sustainable use in an equitable way".

EBM differs from conventional resource management in that it defines management strategies for entire systems, not simply individual components of the ecosystem. Importantly, EBM considers humans as an integral part of the ecosystem, since humans derive a portfolio of services from the ecosystem and also act as a driver influencing ecosystem processes. Thus, a key aspect of EBM is illuminating trade-offs among ecosystem services and management goals (see Levin et al. 2009).

17.8.7   Serious Harm

The ISA draft regulations define "*serious harm to the marine environment*" as "*any effect from activities in the Area on the marine environment which represents a significant adverse change in the marine environment determined according to the rules, regulations and procedures adopted by the International Seabed Authority on the basis of internationally recognized standards and practices informed by the best available scientific evidence.*

The definition of what constitutes "*significant adverse change*" or when harm becomes "*serious harm*" remains unclear. This is relevant in the context of the ESIA's needs to establish thresholds and targets against which serious harm can be benchmarked.

There are a number of references to workable definitions, e.g., Levin et al. (2016) narrowed the definition down by applying the FAO definition for "significant adverse impacts" as "those that compromise ecosystem integrity".

The FAO Guidelines provide that significant adverse impacts are "those that compromise ecosystem integrity" (Food and Agriculture Organisation, 2009, para 17). It lists six factors to consider:

1.   intensity and severity of the impact.
2.   spatial extent of the impact relative to habitat availability.
3.   sensitivity and vulnerability of the ecosystem to the impact.
4.   ability for the ecosystem to recover.
5.   the extent of ecosystem alteration.
6.   the timing and duration of the impact relative to species and habitat needs.

Operationalization of the definition of serious harm will be necessary to provide a practical benchmark against which success criteria can be developed for mitigation and monitoring purposes. This will require the identification of ecological thresholds and management targets for the critical components of the ecosystem that contribute to its integrity.

In practice, the impacts must first be identified and quantified, with mitigation measures then applied as necessary to reduce those residual impacts to as low as reasonably practicable (ALARP). Thereafter, only the regulatory authority can judge whether the benefits of the project justify acceptance of the residual impacts.

17.8.8   Precautionary Approach

ISA exploration regulations require that "*…sponsoring States (as well as the Authority) shall apply a precautionary approach as effected in Principle 15 of the Rio Declaration in order to ensure effective protection for the marine environment from harmful effects which may arise from activities in the Area…*" (Reg 31, para 2; Reg 33, para 2).

The Rio Declaration on Environment and Development, Principle 15 states:

"*in order to protect the environment, the precautionary principle shall be widely applied by States according to their capabilities, where there are threats of serious or irreversible damage, lack of full scientific certainty shall not be used as a reason for postponing cost-effective measures to prevent environmental degradation.*"

The precautionary approach indicates that positive action to protect the environment may be required before scientific proof of harm has been provided. The precautionary approach is triggered when, for a given action, there is a) potential for harm and b) uncertainty about causality and magnitude of impacts.

NORI will apply the Precautionary Approach throughout the ESIA process with continued adoption throughout the operational phase of the project. The application of a Precautionary Approach described by in ISA (2012) will be adopted.

17.8.9   Mitigation

NORI currently proposes to implement management and mitigation measures to minimise adverse environmental impacts in NORI Area D, in accordance with international best practices such as adherence to the Mitigation Hierarchy (Ekstrom et al., 2015; Holness 2018). The Hierarchy involves a sequence of four key actions - avoid, minimize, rehabilitate and offset— and provides a best practice approach to aid in the sustainable management of living, natural resources by establishing a mechanism to balance conservation needs with development priorities. It is acknowledged that application of the mitigation hierarchy framework in the deep-sea context presents different challenges, particularly when considering practicalities of rehabilitation and offsets in the deep-sea environment, (e.g., UNEP-WCMC, 2016; Niner et al., 2018). These potential limitations will be fully explored when applying the framework to the NORI Area D project. However, while relevant study information is being collected, NORI proposes in-principle mitigation design and activity that will include measures such as:

- Selection of a seabed production plan e.g., collector configuration, speed and sequential collection path to maximise collection efficiency and confine disturbance to the adjacent seabed and biodiversity.
- Engineering design options (e.g., hoods, screens or diffusers) to reduce impacts of sedimentation and deposition in adjacent areas.
- Minimisation of impacts to the water column by the use of a fully enclosed RALS.
- Conducting trial methods (e.g., plume flocculation) to minimise suspension of sediments from the collector, and to retain sediment deposition within the track of the collector, and not in adjacent mine tracks.
- Development of a hydrodynamic plume model to inform selection of the depth of the discharge point dewatering, taking into account environmental considerations, such as the:
  — Design of discharge to dilute to background as soon as possible.

— Minimisation of loss of particles in discharge from dewatering.

— Selection of discharge depth to minimise exposure to fauna and depth range of oxygen minima.

- The use of biodegradable fluids and oils in subsea equipment.

- The adoption of stray light and noise reduction strategies, while meeting essential surface and subsea operational safety requirements.

- The adoption of a waste management strategy that will address the management of sewage, chemical and hazardous materials to minimise the potential for contamination of the water column, including compliance with MARPOL.

- The development of emergency response plans to mitigate the effects of natural disasters and unplanned events.

- In addition to the PRZs and APEIs, it is estimated that approximately 27% of nodules will be left in the production areas after the collector has passed or between collector lines. These nodules may provide habitat for fauna dependent on hard surfaces.

17.8.10   Environmental management and monitoring plans

The ISA draft recommendations (ISBA/25/LTC/6/Rev.1) are that monitoring is conducted to ensure that no serious harm is caused to the marine environment from activities associated with the project. Environmental management of the project throughout the operational phase will require the implementation of the mitigation commitments in the ESIA to ensure that environmental targets are met and thresholds are not exceeded.

NORI will conduct monitoring during and after the operational phase of the project to validate predicted impacts and the effectiveness of mitigation measures applied. Its purpose is to include adaptive management of the project, and auditing of i) the accuracy of predicted impacts, ii) identification of any unexpected deviations from the predicted outcomes, iii) investigating reasons for any deviations, and iv) assessment of whether the mitigation measures have achieved their objectives of reducing or eliminating impacts.

The monitoring metrics and methods will be detailed in the Environmental Management and Monitoring Plan (EMMP). This is an important output of the ESIA process as it documents how NORI will implement, fund, and monitor the suite of mitigation measures described in the ESIA. The EMMP will demonstrate to the ISA that NORI has the technical knowhow, finances and will to minimize the residual impacts of the project to acceptable levels. The EMMP document will be issued as an attachment to the EIS.

A number of specific management plans will be required to support the NORI Area D project. These plans will be prepared as drafts and provided in support of the exploitation permit application. These plans may include but are not limited to:

- Conceptual closure plans.
- Emergency response plans.
- Waste management plans.
- Air quality management.
- Noise and vibration management.
- Lighting management.
- Marine mammal management.
- Biosecurity management (introduced species).

17.8.11   Environmental Management System

The Environmental Management System (EMS) is a set of internal rules which are defined by a collection of policies, processes, procedures and records. This system will define how NORI will identify, assess, monitor and maintain the interactions with the environment during the operational phase in order to prevent negative environmental impacts.

ISO 14001:2015 is the international standard for the development of an effective EMS framework. This will be applied to exploitation operations to help NORI run successfully without any harmful effects and impacts on the environment. The standard is designed to maintain profitability and reduce environmental impacts of an organization's products, services and processes.

The EMS will include provisions for adaptive management, utilising management and monitoring measures described in the EMMP in an iterative decision process to improve understanding and management of the system. Key components of the adaptive management system currently under development include:

- Ongoing monitoring programs to track the status of biological resources over time (through an appropriate indicator) to assess changes in response to management and mitigation actions.
- Decision points at which management responses are selected from a set of alternatives developed as a result of modelling and risk assessment.
- Assessment of information gathered through monitoring to inform decision making, environmental performance evaluation, and iterative learning.
- Feedback loops established so that information and understanding from monitoring and assessment can be used to inform the selection of management actions; as the level of understanding of the system evolves, so too does the quality of decisions.

This adaptive management approach will facilitate an iterative cycle of decision making, monitoring, and assessment leading gradually to improved management as a consequence of improved understanding.

17.8.12   Reporting

The output of the ESIA process is NORI's EIS, which will set out factual information relating to the project and all the information gathered relating to screening, scoping, baseline study, impact prediction and assessment, mitigation, and monitoring measures. With the formal submission of the EIS, the regulating authority (ISA) will be in possession of the information required about the potential benefits and residual impacts of the project on the environment to make an informed decision on the issuance of an exploitation license.

17.8.13   Permitting risks

This section outlines the potential risks of delay or refusal by ISA of environmental approval for the NORI Area D project. To date, there is no approved seabed mining operation in the Area, although other contractors are currently at various stages of the ESIA process.

There are some examples of permit applications for deep-sea mining projects in national jurisdictions, briefly summarized as follows. Proposals for three projects in the New Zealand EEZ have so far been refused: for Neptune Resources/NIWA (iron sands and phosphorite nodule extraction), Trans-Tasman Resources Ltd (TTRL) for seabed iron ore extraction, and Chatham Rock Phosphate Ltd (CRP) for phosphate nodules. Some of the critiques common to all have been inadequate assessment of impacts or scale of impacts, inadequate understanding of "whole ecosystems", insufficient safeguards and uncertainty of models.

Environmental approvals were granted in 2009 for Nautilus Minerals Solwara-1 EIS for proposed mining of polymetallic sea floor massive sulphide deposits in the Papua New Guinea EEZ. However, the project has not developed, mostly for technical and financial reasons. The project attracted NGO criticism post EIS for insufficient information on integrated benthic/pelagic ecosystems and lack of specific detail in the drafting of the Environmental Management and Monitoring Plan commitments.

Taking this information into consideration, NORI has followed a three-stage approach in developing the scope of work to ensure i) a rigorous and robust baseline is established to meet all ISA requirements, ii) a dynamic adaptive management system is implemented and iii) a staged approach to project implementation is followed.

At the time of writing, the ISA Regulations are in draft form, giving rise to a risk that the current terms of reference for the ESIA may not meet future (finalized) requirements with resultant information gaps. It is noted that the current (draft) content of the Regulations is comprehensive in coverage of the receiving ecosystem from microfauna to megafauna, and thereby quite onerous in comparison with typical requirements for terrestrial mining projects. In order to limit possible discrepancies developing over the period of the ESIA studies, NORI has developed the scope of work by systematically addressing each of the specific recommendations in the draft Regulations. NORI expects that recommendations for contractors for the assessment of the possible environmental impacts arising from exploration for polymetallic nodules in the Area will carry through from the draft to the final recommendations.

In addition, NORI will maintain frequent dialogue with ISA through the Legal and Technical Commission (LTC) as part of its Communication and Stakeholder Engagement Plan (CSEP) to ensure that any changes in requirements can be accommodated in a timely manner. It will also ensure that stakeholders (e.g., regulatory authorities, governments, NGOs, environmental groups and the media) are informed of project progress and lines of communication are maintained to address concerns arising.

17.9 Closure

The draft regulations on exploitation of mineral resources in the Area (ISBA/26/CRP.1) set out closure responsibilities that include preparation of Closure Plans within a prescribed time prior to planned closure, review of environmental performance guarantees, and post closure monitoring. There will therefore be some ongoing monitoring costs in fulfilment of the Closure Plans.

17.10   Onshore environmental and regulatory

Recovery of the target metals from the nodules will require on-shore processing. As yet, the processing plant has not been designed and its location and host country are not identified. The planned metallurgical process is not expected to produce solid wastes and the content of environmentally active trace metals such as cadmium and arsenic is low. However, NORI recognises that on-shore processing may have potential environmental impacts that should be formally assessed, in due course. NORI is committed to design the processing plant to achieve environmental performance consistent with best global practice and standards regardless of where the plant is built. A comprehensive environmental management plan to be compliant with EMS Standard ISO 14001:2004 will be developed during the Pre-feasibility Study Phase.

18 Capital and operating costs

The capital and operating costs have been split between on-shore and off-shore operations. The off-shore operations consist of all activity at sea, including the recovery of the nodules from the seabed, and transportation of the nodules to shore.

18.1 Project scale-up

NORI originally conceived development of NORI Area D with a production rate of 6.4 Mtpa (wet) of nodules, with processing of all the nodules in a new bespoke process plant. Early engineering studies and cost estimates were based on this scenario. For the current IA, NORI proposed a larger scale project, with processing of some of the nodule production under toll treatment arrangements. Toll treatment of nodules in the early years off the project would provide early cash flow without the need to bring forward capital expenditure on NORI's own plant.

In Project Zero, it is proposed that wet nodules will initially be processed in independent pyrometallurgical and hydrometallurgical plants a in toll treatment arrangement. NORI proposes that 4.1 Mtpa of nodules (wet) (3 Mtpa dry) will be processed in tolling arrangements each year (four pyrometallurgical plants by 0.75 Mtpa (dry)/plant). In Project One, once off-shore production increases above 3 Mtpa, the nodules will be processed in pyrometallurgical and hydrometallurgical plants operated and owned by NORI.

In Project One, the cost estimates off-shore property, plant and equipment are based on estimates prepared by DRT for NORI during the 2015 DRT scoping study and updated for this study. The scoping study cost estimates were generally derived from budget estimates supplied by original equipment manufacturers or engineering contractors that specialise in each of the items under consideration. DRT prepared new cost estimates for:

- Project Zero:
  — Upgrading the Hidden Gem drillship for commercial production at up to 1.3 Mtpa (wet) following the Collector Test.
- Project One:
  — Upgrading the Hidden Gem drillship to production at up to 3.6 Mtpa (wet).
  — Conversion of another drillship (Drill Ship 2) for production at up to 3.6 Mtpa (wet).
  — Construction of a bespoke PSV, Collector Ship 1, for production at up to 8.2 Mtpa (wet).

The costs are consistent with Class 4 estimates as defined by ASTM, AACE standards. Contingency is not included.

Estimates for Project Zero and Project One were prepared by DRT based on the assumption that the Hidden Gem sixth generation drillship being converted for the Collector Test would be upgraded to a commercial system following the Collector Test. Upgrading would take place in two stages:

1) Project Zero: would utilize the small collector vehicle (6 m width) from the Collector Test and its handling system (LARS).
2) Project One: would involve replacement of the small collector with two larger collectors and a new LARS to allow operation of the two larger collectors together.

To account for annual on-shore production that is higher than the 6.4 Mtpa (wet) of nodules baseline throughput values, the capital cost estimates were scaled up, pro-rata, based on capacity, with pyrometallurgical plant capacity 33% higher and hydrometallurgical plant capacity 80% higher. Limitations of the scaling approach include:

- Potential economies of scale are not considered.
- The 6.4 Mtpa (wet) baseline estimate is dated 2019, and the financial model 2020. No inflation adjustment was made.
- The 6.4 Mtpa (wet) baseline estimate was based on a single capital project execution approach, rather than a staged investment in multiple phases. Increased indirect costs for staged implementation of multiple projects were not considered.
- The forecast of construction duration for the 6.4 Mtpa (wet) baseline project is three years. The staged implementation for the larger project reflects shorter investment time periods which may be difficult to achieve for the initial stage.
- With respect to operating costs, no adjustments were made to the 6.4 Mtpa (wet) baseline estimate of unit production costs to reflect higher initial fixed costs (for partial production) and lower later fixed costs (for higher production) due to project staging.

The QPs consider that for the IA, which has an accuracy of the order of +/- 50%, the scaling factors are reasonable.

Based on the required production throughputs, NORI proposes to build and operate four RKEF lines and two hydrometallurgical refineries. The construction schedules of the RKEF lines are as follows:

- RKEF Lines 1 and 2: 2024 to 2026 with production commencing in 2027.
- RKEF Line 3: 2025 to 2027 with production commencing in 2028.
- RKEF Line 4: 2026 to 2028 with production commencing in 2029.

The construction schedules of the hydrometallurgical refineries are as follows:

- Hydrometallurgical refinery 1: 2024 to 2026 with production commencing in 2027.
- Hydrometallurgical refinery 2: 2027 to 2029 with production commencing in 2030.

Costs for NORI's proposed process plant have been considered from the arrival of the nodules at the facility to the production of final product and load out for transport from the facility.

Capital costs are divided into a pre-project period, construction costs during the project period, an operating period when sustaining capital expenditure (off-shore and on-shore) will be required and closure costs at the end of the operating period. All capital and operating costs are in US dollars.

Capital expenditure estimated at US$10.6 billion is required between 2021 and the completion of the project in 2046. A breakdown of the total is given in Table 18.1.

Table 18.1   Summary of all capital costs

Section	Cost estimate (US$ million)
Pre-project costs	$237
Project costs	
Off-shore project costs (including 25% contingency)	
Project Zero	$204
Project One	$2,244
Total	$2,448
On-shore project costs (including 25% contingency)	
Project One	$4,786
Total	$4,786
Total project costs	$7,234
Sustaining capital costs (on-shore and off-shore)	$2,637
Closure costs	$500
Total	$10,607

18.2 Pre-project capital cost estimates

NORI has estimated the costs that it expects to incur during study and engineering phases prior to construction. The pre-project period is expected to extend from 2021 until early 2024. The pre-project capital includes the costs of converting the Hidden Gem for the Collector Test, and the Collector Test itself. The pre-project cost estimates are summarised in Table 18.2.

Table 18.2   Pre-project capital costs

Section	Cost Estimate ($US million)
Equity Account	$37.5
Off-shore Development	$70.6
On-shore Operations	$36.3
Off-shore Operations	$32.7
Environment	$12.5
Geoscience & Mine Development	$0.4
Regulatory Approval	$2.4
Personnel costs	$36.8
Corporate costs	$1.7
Communications	$3.2
Business Development	$2.3
Total	$236.5

18.3 Project-period capital cost estimates

18.3.1   Off-shore capital costs

The offshore cost estimates were developed based upon the guidelines of the AACE (Association for the Advancement of Cost Engineering) International Recommended Practice No. 18R-97. Based on engineering studies performed previously by Deep Reach Technology (DRT) for Deep Green Resources and the experience in trial mining of deep sea nodules by DRT personnel, the cost estimate was considered to be a class 4. Off-shore capital costs were estimated to accuracy levels of -30% +40%.

18.3.1.1   Project Zero: Hidden Gem Upgrade

The Hidden Gem Drillship will be taken to a shipyard after it has been modified and used for the Collector Test and upgraded to be capable of producing up to 1.3 Mtpa, including one self-propelled collector and RALS. This system will have a design life of five years.

It has been assumed in the development of this cost estimate that the existing accommodation block, drilling and vessel systems on the Hidden Gem were either removed from the vessel, if not required, or refurbished and converted for use as a mining vessel for five years operation. The vessel will also be surveyed and classified by a recognized Class Society for operation as a Mining Vessel.

The capital expenditure (CAPEX) cost estimate for upgrading the Hidden Gem for up to 1.3 Mtpa operation includes engineering, procuring and integrating in a Singapore vessel conversion shipyard. The following changes/additions to the Hidden Gem used for the Collector Test are included:

- New air compressors to replace the leased units on the Collector Test with sufficient capacity to operate the air lift riser for the design production rate.

- Airlift discharge de-aeration and pressure let down system to provide an 8 bar pressurized discharge.

- Dewatering equipment and storage of the nodules in the vessel's existing Crude Oil Tanks.

- Slurrification and nodule offloading pumps and offloading hose reels and hawser to offload the nodules to a tandem moored Dynamically Positioned Transport Vessel.

- Slurry water return system from the Transport Vessel for subsurface disposal.

Note that equipment redundancy has been minimized to reduce CAPEX due the limited production time (five years) for this operation.

The cost includes reusing the collector umbilical system and modifying the collector vehicle used in the Collector Test. A completely new riser system and flexible jumper hose string between the collector and the steel riser will be purchased. It is assumed that the LARS purchased for the Collector Test and existing drillship ROV LARS modifications, will be suitable for Project Zero.

No allowance has been included in the CAPEX estimate for a mark-up by a contractor to execute the Engineering, Procurement and Construction/Commissioning (EPC) of the Hidden Gem upgrade. Therefore, the following are excluded from the CAPEX estimate:

- Taxes
- Duties
- Contractor costs for Letter of Credit, Bank Guarantee, and Performance Bond
- Owners costs for Program Management
- Cost of finance and project financing arrangements, if not neutral cash flow
- CAR Insurance
- Liability insurance
- Warranty / Repairs allowance
- Contractor profit
- Contractor overhead recovery (head office, bid preparation costs, etc.)
- Pre-project Engineering and Development Costs

CAPEX costs are summarized in Table 18.3. Transportation costs, including vessel charter, are included in the operating expenditure estimate (OPEX).

Table 18.3   Project Zero: CAPEX for Hidden Gem upgrade

2020 Costs (US$ million)	Collectors	Lift (Riser Only)	Production Vessel	TOTAL
Vessel Acquisition & Management	$0.0	$0.0	$0.5	$0.5
Single Unit Procurement including Vessel Acceptance Testing (excl. O&M Crew)	$18.5	$28.7	$42.7	$89.8
Initial Spares Inventory	$6.1	$4.3	$3.9	$14.3
Engineering & Subsystem Test	$4.5	$5.7	$9.5	$19.8
Project Management	$1.9	$2.9	$4.5	$9.3
Mobilisation to Site, Integration, Site Commissioning	$2.1	$6.2	$21.0	$29.3
TOTAL	$33.1	$47.8	$82.1	$163.0

18.3.1.2 Project One: Hidden Gem Upgrade

Following five years of operation, the Hidden Gem will be upgraded for production of up to 3.6 Mtpa with a design life of 20 years.

The CAPEX estimate for upgrading the Hidden Gem includes engineering, procuring and integrating, in a Singapore vessel conversion shipyard, including the following changes/additions to the 1 Mtpa mining vessel:

- Increased air compressor capacity to operate the air lift riser for the design production rate.
- Refurbishment of the hull structure and coatings to achieve the design life of 20 years with minimal steel renewal at special survey dry dockings.
- Providing mining equipment redundancy to provide the reliability and availability to achieve the total annual nodule production tonnage required.
- Provide additional electrical switchgear and MCCs to operate the additional redundant mining equipment.
- Relocate the Collector LARS system forward of the moonpool where space exists to handle, store and maintain larger collectors on deck.
- Provide two additional 7 MW power generation units to provide additional power for larger air compressor capacity.

The cost includes purchasing two new larger collector vehicles for simultaneous operation subsea. The existing flexible jumper hose power reel and collector umbilical system will be used but a second new flexible jumper hose reel and collector umbilical system will be purchased to enable the installation and operation of a second subsea collector.

The flexible jumper and riser from Project Zero will be replaced, due to wear and tear from the 5 years operation, and second flexile jumper hose string purchased for the second collector.

The riser and collector vehicles are considered to have a five-year service life, and their replacement every five years is considered Sustaining Capital. The actual service life may be greater or less than this and can only be determined after further engineering, testing and actual service experience.

The purchase of two new ROVs, complete with control cabin, have been included in the CAPEX for the 20-year design life with two collectors instead of leasing one as was done for Project Zero.

No allowance has been included in the CAPEX for a mark-up by a contractor to execute the EPC of the Hidden Gem upgrade. Therefore, the following are excluded from the CAPEX estimate:

- Taxes
- Duties
- Contractor costs for Letter of Credit, Bank Guarantee, and Performance Bond
- Owners costs for Program Management
- Cost of finance and project financing arrangements, if not neutral cash flow
- CAR Insurance
- Liability insurance
- Warranty / Repairs allowance
- Contractor profit

- Contractor overhead recovery (head office, bid preparation costs, etc.)
- Pre-project Engineering and Development Costs
- Contingency — 25% contingency was added in the economic analysis presented in Section 22 of this report

Table 18.4 provides a summary of the CAPEX for upgrading the Hidden Gem from 1 Mtpa to a 2.6 Mtpa production vessel.

Table 18.4   Project One: CAPEX for upgrade of Hidden GEM

2020 Costs ($US million)	Collectors	Lift (Riser Only)	Production Vessel	Total
Vessel Acquisition & Management	$0.0	$0.0	$2.3	$2.3
Single Unit Procurement including Vessel Acceptance Testing (excl. O&M Crew)	$67.4	$29.1	$111.8	$208.3
Initial Spares Inventory	$13.2	$3.6	$8.1	$24.9
Engineering & Subsystem Test	$4.8	$1.2	$9.7	$15.7
Project Management	$6.8	$2.4	$5.4	$14.6
Mobilisation to Site, Integration, Site Commissioning	$4.6	$4.8	$21.3	$30.7
TOTAL CAPEX	$96.7	$41.2	$158.6	$296.5

18.3.1.3 Project One: Drill Ship 2 Conversion

A second used drillship (Drill Ship 2) will be purchased and converted for use as second production vessel capable of producing up to 3.6 Mtpa for a 20-year design life. Since the vessel has not been previously used for mining operations, the existing hull structure and coatings, accommodation unit, and drilling and vessel systems will need to be removed if not being used for mining operations or refurbished and converted for an additional 20-year operation as a mining vessel.

An acquisition price of US$50 million was assumed for a used sixth generation drillship, based on current market information (Tomic, 2020).

The CAPEX estimate for converting Drill Ship 2 includes engineering, procuring, and integrating in a Singapore vessel conversion shipyard. The following changes are included:

- Air compressor module with capacity to operate the air lift riser for the design production rate.
- Refurbishment of the hull structure and coatings to achieve the design life of 20 years with minimal steel renewal at special survey dry dockings.
- Removal of the drilling equipment not to be used during the vessel operation as a mining vessel.
- Mining equipment redundancy to provide the reliability and availability to achieve the total annual nodule production tonnage required.
- Additional electrical switchgear and MCCs to operate the additional redundant mining equipment.
- New Collector LARS system forward of the moonpool where space exists to handle, store, and maintain larger collectors on deck.
- Dewatering equipment and storage of the nodules in the vessel's existing Crude Oil Tanks.
- Slurrification and nodule offloading pumps and offloading hose reels and hawser to offload the nodules to a tandem moored Dynamically Positioned Transport Vessel.

- Slurry water return system from the Transport Vessel for subsurface disposal.
- Two new ROVs and control cabin to support disconnection and retrieval operations of two operating subsea collectors, for maintenance and storm preparation operations.
- Refurbish existing drilling ROV LARS to support two mining ROVs.
- Provide two additional 7 MW power generation units to provide additional power for the larger air compressor capacity.

The cost includes purchasing two large new collector vehicles for simultaneous subsea operation, as well as two new flexible jumper hose powered reels with jumper hose strings and two collector umbilical systems.

A new RALS with steel nodule production riser, air lift injection line, seawater slurry disposal line, and buoyancy will be purchased.

No allowance has been included in the capital cost estimate for a mark-up by a contractor to execute the EPC of the Drill Ship 2 refurbishment and conversion. Therefore, the following are excluded from the CAPEX estimate:

- Taxes
- Duties
- Contractor costs for Letter of Credit, Bank Guarantee, and Performance Bond
- Owner's costs for Program Management
- Cost of finance and project financing arrangements, if not neutral cash flow
- CAR Insurance
- Liability insurance
- Warranty / Repairs allowance
- Contractor profit
- Contractor overhead recovery (head office, bid preparation costs, etc.)
- Pre-FID Engineering and Development Costs.
- Contingency – 25% contingency was added in the economic analysis presented in Section 22 of this report.

Table 18.5 presents a summary of the CAPEX for converting Drill Ship 2 to a production vessel.

Table 18.5 Project One: CAPEX for conversion of Drill Ship 2

2020 Costs (US$ million)	Collectors	Lift (Riser Only)	Production Vessel	Total
Vessel Acquisition & Management	$0.0	$0.0	$63.5	$63.5
Single Unit Procurement including Vessel Acceptance Testing (excl. O&M Crew)	$67.8	$29.3	$166.0	$263.1
Initial Spares Inventory	$13.3	$4.4	$15.7	$33.3
Engineering & Subsystem Test	$4.9	$5.8	$19.1	$29.8
Project Management	$6.8	$2.9	$7.7	$17.4
Mobilisation to Site, Integration, Site Commissioning, & Start-up	$4.6	$6.3	$31.1	$42.1
TOTAL	$97.4	$48.8	$303.0	$449.1

18.3.1.4   Project One: Collector Ship 1 construction

The Collector Ship 1 costs are based upon the previous Scoping Study performed in 2015 by DRT (DeepReach Technology Inc., 2015), revised in November 2020 as follows:

- Collector vehicle costs were adjusted to consider the commercial collector design developed by Cellula Robotics, Inc. (Cellula Robotics Ltd., 2015). This involved an addition of buoyancy material to maintain acceptable bearing load.
- Collector vehicle costs were adjusted to include capability to eliminate sediment entrained by the collector head from entering the riser. This includes additional ducting and clean water pumps. The design is based upon ongoing research into this improvement to the collector.
- CAPEX and OPEX costs were scaled to account for an increase in the nominal production rate to 8.2 Mtpa versus 6.4 Mtpa. This is to allow the project to take advantage of higher abundance (20 kg/m^2 versus 15.9 kg/m^2 assumed in the 2015 study).

Inflation of CAPEX was assumed to be zero in view of the current market situation for capital costs in the upstream energy markets (IHS Market, 2021). This data shows a 10% deflation in upstream capital costs since 2015. New build shipbuilding costs have been static since 2015.

Table 18.6 summarises the capital expenditure costs for the construction of Collector Ship 1 for 6.4 Mtpa production. Cargo ships to transfer nodules from the PSV to port are excluded from the estimate. These vessels will be chartered. In this table:

- "Single unit(s) procurement" refers to one production fleet consisting of five collectors, one RALS, one production vessel, and one collector support vessel.
- "Initial spares inventory" includes spare parts for the first year of operation. An allowance of 5% of single unit costs was used, except for 10% allowance for the collector.
- "Detailed engineering and subsystem testing" refer to the engineering and tests devoted to each sub-system. Design of the material handling and airlift system are included under the production vessel cost category. These include both non-recurring costs (for example, engineering) and recurring costs (for example, factory acceptance testing) associated with the design and test of each subsystem.
- "Project management" was estimated at approximately 2% of the single unit procurement cost.
- "Start-up, mobilisation, integration and commissioning" includes the activities of integrating all the equipment and performing trials in shallow and deep water prior to commencing ramp-up of extraction operations. An allowance of nine months of operations is included for this activity.

As was the case for the other vessels, no allowance has been included in the capital cost estimate for a mark-up by a contractor to execute the EPC of the refurbishment and conversion. Therefore, the following are excluded from the CAPEX estimate:

- Taxes
- Duties
- Contractor costs for Letter of Credit, Bank Guarantee, and Performance Bond
- Owners costs for Program Management
- Cost of finance and project financing arrangements, if not neutral cash flow
- CAR Insurance
- Liability insurance
- Warranty / Repairs allowance

- Contractor profit
- Contractor overhead recovery (head office, bid preparation costs, etc.)
- Pre-project Engineering and Development Costs
- Contingency – 25% contingency was added in the economic analysis presented in Section 22 of this report.

Table 18.6   Project One: CAPEX for Collector Ship 1

2020 Costs (US $million)	Collectors	Lift (Riser Only)	Production Support Vessel incl OFE	Collector Support Platform (PSS)	Total
Single Unit(s) Procurement	$164.4	$98.0	$384.1	$199.6	$846.0
Initial Spares Inventory	$16.4	$4.6	$19.2	$10.0	$50.2
Detailed Engineering & Subsystem Test	$14.2	$10.4	$17.3	$5.8	$47.6
Project management	$3.3	$2.0	$7.7	$4.0	$17.1
Startup, Mobilization, Integration & Commissioning	$0.0	$0.0	$65.9	$22.6	$88.5
Total	$198.3	$114.9	$494.1	$242.1	$1,049.4

18.3.1.5 Collector support vessel

A semi-submersible collector support vessel will maintain the collectors deployed by Collector Ship 1. The collector support vessel capital cost estimates were based on the actual costs for the Helix Deepwater Well Intervention platform Q4000, built in the Keppel AmFELS yard in Brownsville, Texas in 2002. The actual costs for this vessel were reportedly US$180 million. US shipbuilding price escalation is estimated at 150% (FRED, 2020) for an estimated cost of US$270 million in 2020. For this IA, a discount of 30% was estimated for Chinese versus US construction to estimate the cost for Chinese construction in 2020.

18.3.1.6 Project management

Project management costs represent an allowance for an integrated project team to manage and integrate the front-end engineering and design, which would be performed by one or more contractors. The cost estimates were based on engineer's estimates made by DRT, escalated by the US consumer price index (CPI) since 2015.

18.3.2   On-shore capital cost for Project One

Capital costs have been estimated for the construction of the processing facility to handle 4.88 Mt (dry) of nodules per year. The estimate has been developed according to Association for the Advancement of Cost Engineering Class 5 level of accuracy (−35% +50%) and is expressed in first quarter 2019 US dollars. A contingency of 32% has been applied to the estimate. Owner's costs and escalation beyond 2019 are excluded.

The on-shore capital cost estimates are summarised in Table 18.7. Further details of the estimate are provided in Table 18.8.

Table 18.7   Summary of project period on-shore capital costs

Section	Cost estimate (US$ million)
General	$179
Pyrometallurgical plant	$1,052
Hydrometallurgical refinery	$483
Total direct cost	$1,713

Indirect costs	$622
Total direct and indirect costs	$2,335
Contingency	$746
Total on-shore capital cost	$3,081

Table 18.8   Summary of project period on-shore capital costs by plant area

Section	Cost estimate (US$ million)
General	
Site development, roads and buildings	$46
Power supply and distribution	$46
Utilities	$76
Mobile equipment	$10
Total general	$179
Pyrometallurgical Plant	
General (building/substation)	$276
Feed handling	$106
Rotary kiln calcining	$216
Electric furnace smelting	$340
Converter aisle sulphidation	$113
Total pyrometallurgical plant	$1,052
Hydrometallurgical refinery	
Matte receiving and handling	$18
Leaching & Purification	$87
Copper EW	$107
Cobalt SX and Purification	$62
Nickel SX	$80
Crystallisation & Product Packaging	$82
Reagents and Utilities	$48
Total hydrometallurgical refinery	$483
Total direct on-shore costs	$1,713

Key assumptions that have been made in developing the estimate include:

- The processing plant will be situated on a flat site.
- Nodules will be delivered to the plant boundary, at the rate required by the process (any buffering to decouple ship unloading rates from conveying rates is assumed to be done at the port).
- Minimal storage of materials and reagents is provided at the plant.
- Utilities will be provided at the plant boundary, including power, water and natural gas.
- Oxygen will be supplied on a cost per tonne basis (sale of gas basis).
- The plant will be built near a major municipality, no camp infrastructure is assumed for construction or operating labour.

The following items are excluded from the capital cost:

- Sunk and legal costs.
- Special incentives and allowances.

- Owner's costs, including permitting and construction insurance.
- Escalation, interest and financing costs.
- Start-up costs beyond those specifically included.
- Additional exploration expenses.
- Delivery of utilities (power, water, natural gas) to the plant boundary. High voltage power lines would be supplied by others up to the plant main substation.
- Port facilities including storage.
- Equipment (permanent or mobile) required to transport feed materials from the port to the plant boundary.
- Equipment (permanent or mobile) required to transport products from the plant to port facilities.

18.4 Sustaining capital cost estimates

The sustaining capital costs (dry dock) for the vessels are:

- Hidden Gem Dry Dock: US$327 million (US$109 million per dry dock)
- Drill Ship 2 Dry Dock: US$349 million (US$109 million per dry dock)
- Collector Ship 1 Dry Dock: US$742 million (US$232 million per dry dock)
- Total: US$1,418 million

The sustaining capital includes replacement of collectors and risers during each 5-year dry docking cycle, as well as statutory maintenance required to maintain the vessels in class. The sustaining capital allowance was reduced for the last dry dockings for Drill Ship 2 and Collector Ship 1 because their remaining production life at those points is only two and one years, respectively.

For the process plant, sustaining costs of 1.25% of the total on-shore capital costs were applied from the first year of production (2024) to end of the scheduled project life (2046). Total sustaining capital for the on-shore components of the Project is estimated as US$1,219 million.

18.5 Closure cost estimates

A closure cost of US$500 million has been allowed in 2046 for remediation of the on-shore minerals processing facility.

Very little infrastructure is expected to be established in the seafloor production areas. Closure costs associated with off-shore activities, which will include post-closure monitoring, are not expected to be material to the IA cost estimates.

18.6 Operating cost estimates

The estimated operating costs, when production reaches steady state in 2030, are summarised in Table 18.9.

Table 18.9   Operating costs at steady state production

Section	Average Operating Cost over Life of Mine (US$ million/annum)	Average Unit Cost (US$/t - wet tonne nodules recovered)	Average Unit Cost (US$/t - dry tonne processed)
Off-shore	$240.7	$19.3	$25.40
Shipping	$254.4	$20.4	$26.84
On-shore	$1,286.2	$103.1	$135.71
Other	$25.0	$2.00	$2.64

Total	$1,806.3	$144.85	$190.59

18.6.1 Off-shore operating costs

The operating cost estimates used in this IA are based on estimates prepared by DRT for NORI during the 2015 DRT scoping study. The cost estimates were revised in February 2019. The US Department of Labor, Bureau of Labor Statistics Index CPI-U - Consumer Price Index for All Urban Consumers, increased by 5.848% from May 2015 to January 2019. For this IA, labor-related costs were escalated from 2015 estimates by this CPI value.

Operating expenses are dominated by the cost of fuel, originally based upon a cost of US$660 per tonne in the Los Angeles/Long Beach market. Since 2015, fuel prices have varied from a low of US$385 per tonne in early 2016, to a high of US$785 per tonne in Q4 2018. On 27 February 2020, the price was US$464 per tonne. This IA is based on a fuel price of US$500 per tonne, which is the same as the 2015 estimate, and is within the recent range of fuel prices in recent years. The qualified person considers this approach is reasonable.

The PSV crew is assumed to include 52 personnel of which 30 are devoted to mining operations, and the remainder marine crew. The collector support vessel crew includes 30 personnel of which eight would be devoted to collector and maintenance.

Maintenance costs have been factored from the initial capital expenditure at a rate of 5% per annum.

18.6.1.1 Project Zero operating costs

Off-shore operating costs estimated for Project Zero are shown in Table 18.10.

Owner's costs include on-shore staff for support of the operations, maintenance, mine planning and logistics of the mining operation, and operation of a separate chartered survey vessel for environmental monitoring and survey.

Table 18.10   Project Zero - Annual Off-shore operating cost

2020 Costs (US$ million/annum)	Collectors	Lift (Riser Only)	PSV	Total (w/o transport)
Personnel	$0.0	$0.0	$16.5	$16.5
Fuel (after start of mining operations)	$0.0	$0.0	$23.4	$23.4
Maintenance, Repair and Support Services	$1.6	$1.2	$9.0	$11.9
Insurance	$0.2	$0.2	$0.6	$1.1
TOTAL	$1.9	$1.5	$49.5	$52.9

18.6.1.2 Project One operating costs

Operating costs for the Hidden Gem and Drill Ship 2 during Project One are shown in Table 18.11

Table 18.11   Project One - Summary of annual off-shore operating costs for Hidden Gem and Drill Ship 2

2020 Costs (US$ million/annum)	Collectors	Lift (Riser Only)	PSV	Total

Personnel	$0.0	$0.0	$19.3	$19.3
Fuel	$0.0	$0.0	$26.7	$26.7
Maintenance, Repair and Support Services	$3.1	$1.3	$9.6	$14.1
Insurance	$0.7	$0.2	$1.6	$2.5
Total	$3.8	$1.6	$57.1	$62.5

The annual operating costs for Collector Ship 1 during steady-state production of approximately 7 Mtpa (wet) are summarised in Table 18.12.

Table 18.12   Project One - Summary of annual off-shore operating costs for Collector Ship 1

2020 Costs (US$ million/annum)	Collectors	Lift (Riser Only)	PSV	Total
Personnel	$0.0	$0.0	$15.7	$15.7
Fuel	$0.0	$0.0	$47.1	$47.1
Inspection, Repair and Support Services	$8.2	$4.7	$9.9	$22.8
Insurance	$0.0	$0.0	$3.4	$3.4
TOTAL	$8.2	$4.7	$76.0	$88.9

The annual operating costs for the CSV during steady-state production is summarised in Table 18.12.

Table 18.13   Project One - Summary of annual off-shore operating costs for CSV

2020 Costs (US$ million/annum)	Total
Personnel	$8.3
Fuel	$5.0
Inspection, Repair and Support Services	$5.5
Insurance	$0.9
TOTAL	$19.7

18.6.2   Transportation costs

This IA assumes transportation of nodules will be by vessels equipped with dynamic positioning (DP) and dewatering capabilities, utilizing vertical cuttings driers which can remove all but 10% of the free moisture in the vessel holds. DP capability will enable vessels to be loaded at sea, astern of the PSVs.

Transhipment cost estimates are based on estimates by DRT. Trans-shipment model parameters and costs are summarized in Table 18.14. The table indicates buffer storage capacity is adequate to cover the interval between vessel arrivals for Project Zero, however Project One has less buffer storage than this (1.6 days production in buffer storage versus 2.5 days between vessel arrivals, on average). This could be resolved by increasing size and number of vessels in the fleet or by increasing the buffer storage on the PSV, e.g., by converting a larger bulk mineral carrier. These estimates are considered adequate for the purposes of this IA, however further study and optimization of dewatering systems, buffer storage and transport fleet parameters should be performed during the pre-feasibility phase. Tests to determine the amount of attrition during collection and lifting of the nodules will be necessary to inform materials handling and dewatering studies.

In Project Zero, the nodules will be transported to toll-treatment facilities in China. DGM has estimated a cost of $11/t of nodule (wet) to transport the nodules from the transhipment to Chinese ports.

In-country costs to unload and transport the nodules from the Chinese ports to the toll treatment plants are included in the toll treatment figure estimate of US$100/tonne of nodule (dry). Estimates were based on initial market intelligence provided by Shanghai Metals Market (SMM, 2020).

In Project One, the IA assumes that nodules will be shipped from NORI Area D to a port on the west coast of Mexico in the state of Michoacán where a process plant would be located. NORI has also used a figure of $US11/tonne of wet nodules for transportation from the ports to the process plants, based on estimates by Global Location Strategies (Global Location Strategies, 2019) undertaken for NORI. This figure includes off-loading at the port and transportation to the plant.

Table 18.14   Summary of parameters and costs for transport between vessels and transhipment

Vessel	Project Zero	Project One	
	Hidden Gem	Hidden Gem/Drill Ship 2	Collector Ship 1
Annual Production (Mtpa (wet))	1.3	3.6	8.5
Vessel Size (DWT)	35,000	100,000	100,000
No. Vessels in Fleet	2	2	3
Average Cargo Loading Rate (tph)	185	456	1665
Cargo Loading Time (days)	8.3	9.1	2.5
Total Cycle Time (days)	15.5	17.4	10.8
Buffer Storage (days production)	0.8	0.3	1.6
Time between vessel arrivals (days)	−1.2	-0.7	2.5
Annual Costs (US$ million/annum)			
Personnel	$4.5	$4.9	$8.3
Fuel	$4.3	$6.7	$22.4
Inspection, Repair and Support Services	$3.8	$6.8	$9.8
Insurance	$0.0	$0.1	$0.1
Vessel Charter	$6.1	$12.6	$18.9
TOTAL OPEX	**$18.7**	**$31.1**	**$59.4**

18.6.3   Programme management and logistical costs

Estimates of programme management and logistical costs are provided in Table 18.15.

Table 18.15   Programme management and logistical cost

Section	Costs (US$ million/annum)
Personnel	$3.2
Travel, G&A	$0.9
Vessel Charter (Survey & Support)	$10.0
TOTAL	**$14.1**

18.6.4 Other operating costs

Estimates of annual corporate and administration costs are presented in Table 18.16.

Table 18.16   Annual corporate and administration costs

Section	Cost (US$ million/annum)
Nauru administration fee	$0.1
Kiribati administration fee	$0.1
Environmental monitoring	$1.5
Corporate costs	$10.0
Total	**$11.7**

18.6.5 On-shore operating costs — Project Zero

An overall operating cost of US$100/tonne dry nodules has been assumed for the toll treatment option in Project Zero and Project One. The figure covers the costs for a third party to treat the nodules in its processing facilities to produce the various products. This figure was based on benchmarked operations.

For the production of the nickel alloy, an alloy treatment charge of US$300/tonne of alloy produced has been assumed. This is based on benchmarked figures and discussions with traders.

18.6.6 On-shore operating costs — Project One

Operating cost estimates were developed assuming a throughput of 4.88 Mtpa dry nodules. Operating cost and production were subsequently scaled by DeepGreen for the projected increase in production, as discussed in Sections 19 and 22.

Project One Operating costs have been estimated for a normal, full operating year, not a ramp-up year or a major outage year (e.g., with the appropriate design features, furnace rebuilds are typically needed after 15–20 years) and are summarised in Table 18.17.

Major consumables (energy, reagents) have been taken from the mass and energy balances calculated in the process models. Other costs have been estimated by reference to other projects at more advanced stages of definition. Unit prices have been assumed based on previous projects, in-house data, or allowances. Plant management and general supplies for the complete facility have been assigned to the pyrometallurgical plant.

Further details for the pyrometallurgical operating costs, including unit prices, are shown in Table 18.18.

Table 18.17   Summary of on-shore annual operating costs for Project One

Section	Cost estimate (US$ million)
Pyrometallurgical plant (for 4.88 Mtpa of dry nodules)	
Electricity	$223.0
Coal	$47.3
Natural gas and diesel	$26.6
Maintenance materials	$35.5
Smelting and sulphidation consumables and slag handling	$28.6
Plant labor, management	$24.2
Water and water treatment	$5.5
Total pyrometallurgical operating costs	$390.8
Hydrometallurgical refinery (for 62 ktpa of produced nickel)	
Electricity	$26.6
Anhydrous liquid ammonia	$25.6
Maintenance materials	$18.4
Oxygen	$13.0
Other consumables	$12.0
Sulphuric acid	$11.5
Natural gas and diesel	$5.0
Plant labor	$8.9
Water and minor reagents	$4.0
Sodium hydroxide	$1.9
Total hydrometallurgical operating costs	$127.2
Total annual on-shore operating costs	$518.0

Table 18.18   Summary of pyrometallurgical operating costs for Project One (4.88 Mtpa of dry nodules)

Component	Annual Requirement	Unit	Unit price (US$/unit)	Annual Cost (US$ million)
Electricity				$223.0
Furnace power	1,967,301	MWh	$100	$196.7
Non-furnace power	262,800	MWh	$100	$26.3
Natural Gas				$26.0
Calcining	246,062,250	Nm^3	$0.1	$24.6
Kiln idling and start-up	12,303,113	Nm^3	$0.1	$1.2
Converter aisle	2,000,000	Nm^3	$0.1	$0.2
Diesel	941,176	L	$0.66	$0.6
Coal	473,048	t	$100	$47.3
Smelting Consumables				$13.6
Electrode paste	5,901	t	$572.6	$3.4
Silica flux	281,184	T	$31	$8.7
Minor smelting consumables	-	-	-	$1.5
Sulphidation Consumables				$9.0
Silica flux	125,897	t	$31	$3.9
Sulphur	31,020	t	$160	$5.0
Pig casting molds	-	-	-	$0.1
Slag Handling				$6.0
Water & Water Treatment				$5.5
Makeup water acquisition	5,182,416	m^3	$1.00	$5.2
Water treatment chemicals	-	-	-	$0.3
Plant Labor				$21.2
Supervisors and managers	21	Personnel	$40,000	$0.8
Engineers and laboratory	65	Personnel	$30,000	$2.0
Site workers and operators	738	Personnel	$25,000	$18.5
Maintenance Materials				$35.5
Laboratory Supplies				$1.0
Plant Management				$2.0
Total Pyrometallurgy Operating Costs				$390.8

Further details for the hydrometallurgical operating costs, including unit prices, are shown in Table 18.19.

Table 18.19   Summary of hydrometallurgical operating costs for Project One (62 ktpa of produced nickel)

Component	Annual Requirement	Unit	Unit price (US$/unit)	Annual Cost (US$ million)
Reagents				$54.7
Sulphuric acid	176,199	T	$65	$11.5
Potassium hydroxide	1,611	T	$1,200	$1.9
Anhydrous liquid ammonia	48,364	T	$530	$25.6
Potassium metabisulfite	2	T	$350	$0.0
Oxygen	104,275	T	$125	$13.0
Cobalt extractant	30	T	$34,770	$1.0
Nickel extractant	29	T	$3,210	$0.1
SX diluent	119	T	$1,040	$0.1
Copper IX resin	8	m^3	$10,730	$0.1
D2EPHA Impregnated Resin	4	m^3	$16,040	$0.1
Granular activated carbon	442	m^3	$2,380	$1.1
Flocculant and coagulant	35	T	$5,100	$0.18
Energy				$38.0
Electricity	266,200	MWh	$100	$26.6
Natural gas	49,817,098	Nm^3	$0.1	$5.0
Diesel	321,067	L	$0.66	$0.2
Other Consumables				$12
Product packaging	-	-	-	$11
Filtration consumables and additives	-	-	-	$1
Water				$1.4
Makeup water acquisition	558,990	m^3	$1.00	$0.6
Pretreated water	1,934,072	m^3	$0.29	$0.3
Demineralised water	809,743	m^3	$0.59	$0.5
Plant Labor				$8.9
Supervisors and managers	9	Personnel	$40,000	$0.4
Engineers and laboratory	27	Personnel	$30,000	$0.8
Site workers and operators	310	Personnel	$25,000	$7.8
Maintenance Materials				$18.4
Total Hydrometallurgy Operating Costs				**$127.2**

An allowance for plant management costs (labour and others) has been made for both the pyrometallurgical and hydrometallurgical facilities. This has been assigned to the pyrometallurgical plant. Operating labour cost accounts for plant operations only in both the pyrometallurgical and hydrometallurgical facilities. Expenses associated with corporate and administrative activities such as human resources, finance, accounting, marketing, permitting, insurance among others are excluded from the estimate.

No contingency has been included in the on-shore operating cost estimate. Any cost item not explicitly listed above has been excluded.

18.6.7   Sulphidization costs

NORI has assumed that some third party RKEF plants will be modified to produce nickel copper cobalt alloy. Some of the alloy production will be shipped to the NORI

hydrometallurgical plants to make use of spare capacity. This will require the alloy from the third party RKEF to be sulphidized. NORI has estimated a figure of US$3,000/t of nickel produced to account for the capital and operating costs of third party sulphidization treatment.

19 Economic analysis

A financial model based on estimates of future cash flows derived from extraction of nodules from the NORI Project has been developed in-house by DeepGreen. AMC reviewed the logic, input assumptions and integrity of the calculations and forecasts. The financial model is for NORI Area D only, which is at a preliminary level of planning and design.

The mining plan considered in this IA contemplates a 23-year production period. The expected production period is within the expected duration of a NORI Area D Exploitation Contract which would be thirty years (with possible extensions by periods of 10 years) as outlined in the current draft of the regulations for exploitation of Mineral Resources in the Area (ISBA /25/C/WP.1).

After the initial 23-year period, substantial resources will remain in the other NORI Areas that could support future mining (combined Inferred Mineral Resource in NORI Areas A, B and C of 510 Mt (wet) at 1.28% Ni, 0.21% Co, 1.04% Cu, 28.3% Mn, at an average abundance of 11 kg (wet)/m^2: Golder, 2013).

The project schedule is shown in the Gantt chart in Figure 19.1.

In Project Zero, NORI will toll treat the nodules in third party pyrometallurgical plants and sell the RKEF products into the alloy market. This will generate revenue whilst its pyrometallurgical and hydrometallurgical facilities are being built.

In Project One, NORI will stage the construction of its multiple pyrometallurgical and hydrometallurgical lines to flatten out capital expenditure requirements. Nodule production will be directed preferentially to the NORI pyrometallurgical plants as this is the lowest operating cost option. Whenever these facilities are at maximum capacity (particularly during the ramp-up phase), the surplus nodules will be sent for toll treatment.

NORI will ensure its own hydrometallurgical refineries are filled up to maximum capacity, as this produces the highest value products. Whenever its own hydrometallurgical refineries are at full capacity, NORI will sell the surplus product from its pyrometallurgical plant directly to the matte market. Whilst the matte is not as valuable as the refined products from the hydrometallurgical plant (nickel sulphate, cobalt sulphate, and copper cathode); it still provides a consistent revenue stream and assists for periods when the refineries are at full capacity.

Some of the alloy production from toll treatment of NORI nodules will be shipped to the NORI hydrometallurgical plants to make use of spare capacity. This will require the alloy from the third party RKEF to be sulphidized prior to hydrometallurgical treatment.

Based on discussions with buyers, NORI believes that there is sufficient demand for the alloy and matte over the life of the project.

Figure 19.1   Gantt chart showing proposed schedule of main project phases
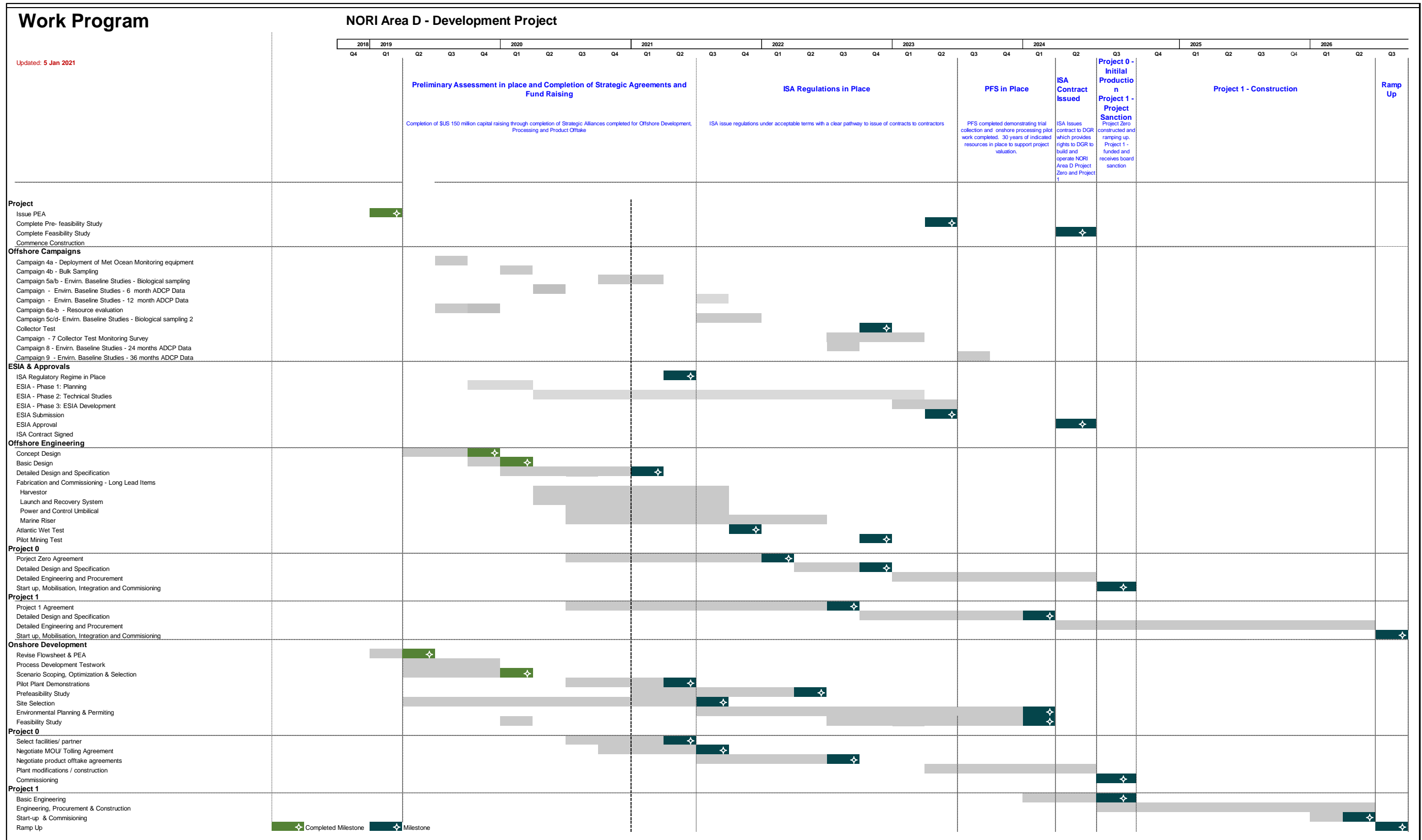
19.1 Inputs

Post-tax, real (uninflated) cash flows are discussed in this report. The valuation date is 1 January 2021. The analysis was performed on a 100% ownership basis and excludes consideration of financing costs and forward metal sales. The IA assumes the economic parameters listed in Table 19.1.

Table 19.1   Economic inputs

Parameters	Units	Values
Hydrometallurgical plant Ni recovery	%	94.6%
Mn recovery	%	98.9%
Hydrometallurgical plant Cu recovery	%	86.2%
Hydrometallurgical plant Co recovery	%	77.2%
Pyrometallurgical plant Cu recovery	%	96.8%
Pyrometallurgical plant Cu recovery	%	93.3%
Pyrometallurgical plant Co recovery	%	92.7%
Mn silicate grade	%	40.0%
Cu cathode grade	%	99.9%
Payability of Cu content in cathode	%	100%
Nodule moisture content	%	24%
On-shore tax rate	% of taxable income	20%
Average off-shore royalty	% of taxable income	6.7%

19.1.1   Commodity prices

Project revenues will come from the following sources:

- A nickel sulphate product
- A copper cathode product
- A cobalt sulphate product
- A manganese silicate product
- An ammonium sulphate product
- A nickel alloy product containing copper and cobalt.
- A matte product from the NORI pyrometallurgical plants containing nickel, copper and cobalt which would be sold to the matte market.

NORI has used the following payable percentages for the alloy:

- Nickel: 80% of in-situ value in the alloy.
- Copper: 40% of in-situ value in the alloy.
- Cobalt: 80% of in-situ value in the alloy.

The following treatment charges and refining charges for the alloy product were used in the NORI financial model:

- A refining charge of US$1,697/tonne of contained nickel in the alloy.
- A refining charge of US$800/tonne of contained nickel in the alloy.
- A refining charge of US$6,700/tonne of contained nickel in the alloy.
- A treatment charge $300/tonne of alloy.

For the matte product, NORI has used a used a payables figure of 83% of the market metal price of nickel, copper and cobalt.

The metal recoveries for the matte and alloy are those from the pyrometallurgical plant, whilst the refined products (nickel sulphate, copper cathode and cobalt sulphate) are from the hydrometallurgical refinery metal recoveries.

The prices forecast by CRU (CRU, 2020) and adopted for use in this IA are listed in Table 19.2.

Less than 1% of total revenue will be derived from production and sale of ammonium sulphate A price of US$90/t of ammonium sulphate has been assumed in this IA.

The Qualified Person considers the metal price assumptions underpinning the IA are reasonable.

Table 19.2   Commodity prices

	2024	2025	2026	2027	2028	2029	2030	2031	2032	2033	Average from 2034-2046
Ni metal (US$/t)	$14,067	$14,467	$14,868	$15,269	$15,670	$16,071	$16,472	$16,472	$16,472	$16,472	$16,472
Ni contained in Ni Sulphate (US$/t Ni)	$15,610	$16,027	$16,443	$16,860	$17,269	$17,678	$18,087	$18,087	$18,087	$18,087	$18,087
Mn contained in SiMn (US$/dmtu Mn)	$4.78	$4.73	$4.69	$4.64	$4.59	$4.54	$4.49	$4.49	$4.49	$4.49	$4.49
Cu metal (US$/t)	$6,435	$6,497	$6,557	$6,615	$6,673	$6,730	$6,787	$6,805	$6,822	$6,839	$6,872
Co metal (US$/t)	$52,881	$39,914	$38,204	$41,526	$45,137	$49,062	$51,106	$50,600	$49,126	$47,695	$46,333
Co contained in Co Sulphate (US$/t Co)	$64,250	$49,035	$46,933	$51,014	$55,450	$60,272	$62,784	$62,162	$60,351	$58,594	$56,920

19.1.2   Tax

In undertaking this economic assessment AMC has relied on DeepGreen's analysis of tax treatment of future revenue streams. AMC is not an expert in tax affairs.

The economic assessment is on a post-tax basis. Royalties payable to the ISA, and to the sponsoring state (Nauru) have been accounted for.

The ISA royalty has not been finalized, but discussions are focusing on a royalty that is calculated on an ad valorem basis that references LME pricing but excludes consideration of metallurgical recovery and pricing premia. It is at a rate of 2% for the first five years of production, and 6% thereafter. A further 1% environmental levy was added.

On-shore earnings consider a transfer pricing mark-up of 20% on off-shore operating costs. No off-shore corporate tax was applied.

NORI has not yet committed to locating its on-shore operations in any particular country. The Qualified Person considers it reasonable to expect that potential host nations (and provinces within potential host nations) will compete for the opportunity to host the on-shore operations and will offer favourable taxation arrangements. As a basis to selecting a corporate tax rate for use in this IA, AMC has referred to a publication titled International Comparison of Corporate Income Tax Rates, published by the Congress of the United States Congressional Budget Office (March 2017). The average tax rate (i.e., the total amount of corporate income taxes that companies pay relative to their income after excluding marginal enterprises) for companies operating in Mexico was reported to be 20.3%. Accordingly, AMC selected 20% as the corporate tax rate for this IA.

Straight-line depreciation of onshore and offshore assets was used to calculate the depreciation expense applicable. A depreciation period of 10 years was used for on-shore assets and a depreciation period of five years was used for off-shore assets.

The analysis indicates that the Project will generate approximately US$7.2 billion in undiscounted royalties payable to the ISA and Nauru, and US$9.1 billion in on-shore corporate tax payable to the host nation of the processing plant.

19.1.3   Production schedule

The production schedule on which the economic analysis is based was developed on an annual basis. The Qualified Person cautions that a prefeasibility study has not been undertaken and that the seafloor production schedule is preliminary in nature and should not be interpreted as a Mineral Reserve. Approximately 96% of the Mineral Resource within NORI Area D is classified as Indicated and a further 1% is classified as Measured Resource. The LOM production sequence includes 6 Mt (wet) of nodules that are classified as Inferred Mineral Resources. This is approximately 2% of the total LOM production.

The production schedule assumes staged operation initially of the Hidden Gem, then Drill Ship 2 and finally Collector Vessel 1, as out lined in Section 16.1.

The nodule metal grades and nodule abundance varying annually according to the life of mine schedule. The grades and nodule abundance for the mine plan were derived from a preliminary production schedule developed by AMC as outlined in Section 16.7. The higher abundance areas were targeted by the production schedule. The metal grades and abundance used in the schedule are compared to the averages (of all Mineral Resource categories) for NORI Area D in Table 19.3.

Table 19.3   Comparison of IA mine plan to Mineral Resource for NORI Area D

	Mineral Resource in NORI Area D (all categories)	Seafloor production plan	Difference (%)
Tonnage (Mt wet)	356	254	71%
Nodule abundance (kg/m^2)	17.0	16.9	99%
Ni grade (%)	1.40	1.4	100%
Mn grade (%)	31.2	31.0	99%
Cu grade (%)	1.14	1.1	100%
Co grade (%)	0.14	0.14	98%

The production ramp-up discussed in Section 17 was adopted for the production schedule. The Qualified Person considers the assumptions underpinning the IA are reasonable.

19.2 Results

All cash flows are denominated in millions of US dollars. The analysis excludes capital sunk prior to 1st January 2021 and excludes the value of the intellectual property that NORI will accrue during the operation. The total cash flows are summarised in Table 19.4.

The analysis indicates a positive economic outcome. Undiscounted post-tax net cash flow of US$30.6 billion is expected. An internal rate of return of 27% has been modelled. Discounted cash flow analysis of unleveraged real cash flows, discounting at 9% per annum, indicates a project net present value (NPV) of US$6.8 billion. Excluding the inferred mineral resources from the economic analysis, the post-tax project NPV is estimated at $6.7 billion, which is not a significant difference from the economic analysis that includes the inferred mineral resources.

The cumulative undiscounted cashflows are shown in Figure 19.2 and the discounted cash flows and progressive NPVs are shown in Figure 19.3. The project reaches its lowest cumulative undiscounted cash flow figure of US$4.0 billion in 2026. Undiscounted payback period is 6.6 years after commencement of production.

Table 19.4   Summary of cash flows

Cash flow item	Value (US$ million)
Nickel revenue	$44,106
Manganese revenue	$26,785
Copper revenue	$12,685
Cobalt revenue	$11,075
Ammonium sulphate revenue	$439
Total revenue	**$95,090**
Pre-project capital	$237
Off-shore construction	$2,448
On-shore construction	$4,786
Off-shore sustaining capital	$1,418
On-shore sustaining capital	$1,219
Closure costs	$500
Total capital	**$10,607**
Off-shore operating costs	$5,154
Shipping costs	$5,266
On-shore operating costs	$26,544
Corporate costs	$560
Total operating costs	**$37,524**
Royalties	$7,195
Onshore tax	$9,123
Taxes and royalties	**$16,318**
Net undiscounted cash flow	**$30,641**

Figure 19.2   Cumulative undiscounted cash flows
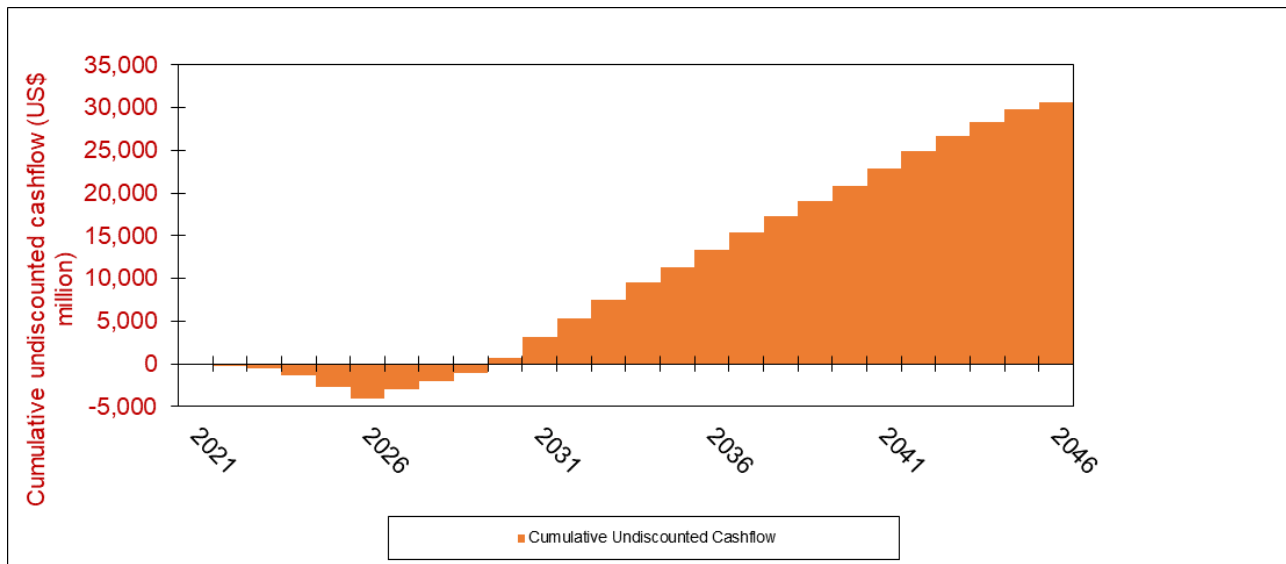
Figure 19.3   Project NPV$_{2021}$ and discounted cash flow
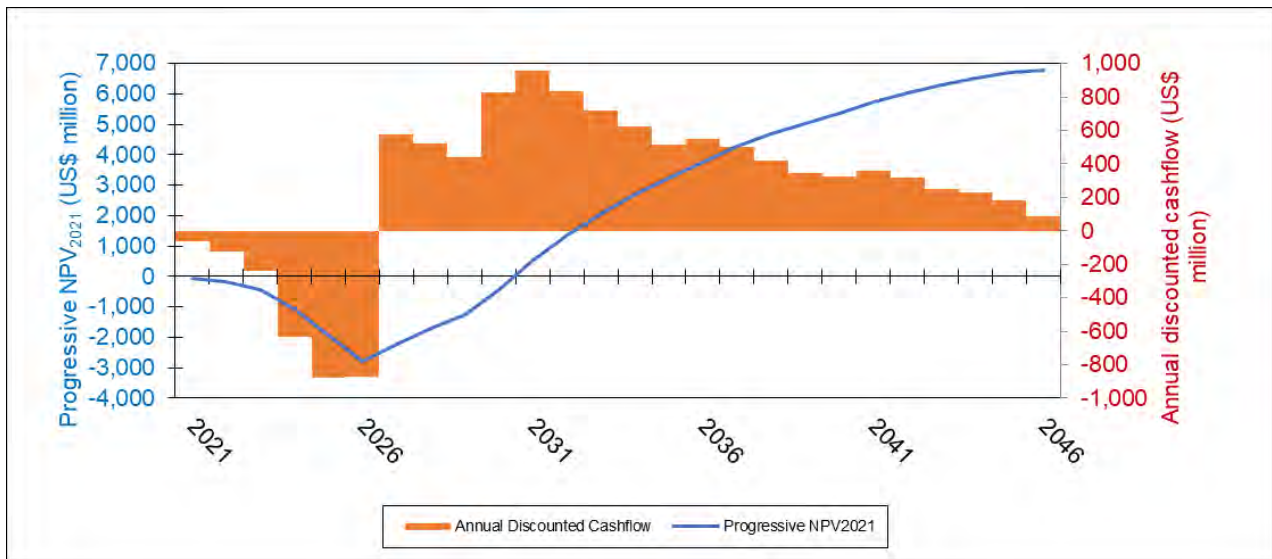
The analysis indicates that the Project will generate approximately US$7.2 billion in undiscounted royalties payable to the ISA and Nauru, and US$9.1 billion in on-shore corporate tax payable to the host nation of the process plant.

As outlined in Section 21, total project development capital required is $US7.5 billion, but because of the staged development approach, it is anticipated that revenue will be received prior to the finalization of project capital investment. The maximum negative cumulative undiscounted cash flow is expected to reach -$US4.0 billion in 2026. This is the level of capital finance that would be required to develop the project under the proposed development scenario and capital payback is expected 6.6 years after the start of production. The maximum negative annual discounted cash flow is -US$876 million.

The date of the investment decision (decision to mine) is 30th June 2023. NORI expects to spend $237 million on pre-project activities between 2021 and the date of the investment decision. The future value of the project on 30th June 2023 (after the pre-project expenditure is sunk and time has elapsed) will be US$8.6 billion and the IRR from that point will be 29%.

A summary of the revenues for the life of the project is shown in Table 19.5.

Table 19.5   Project revenues by year, over life of project

	Total	2024	2025	2026	2027	2028	2029	2030	2031	2032	2033	2034	2035	2036	2037	2038	2039	2040	2041	2042	2043	2044	2045	2046
Nickel in Alloy Revenue	604	94	-	242	113	112	-	-	44	-	-	-	-	-	-	-	-	-	-	-	-	-	-	-
Copper in Alloy Revenue	205	34	-	83	38	37	-	-	14	-	-	-	-	-	-	-	-	-	-	-	-	-	-	-
Cobalt in Alloy Revenue	62	14	-	21	11	12	-	-	5	-	-	-	-	-	-	-	-	-	-	-	-	-	-	-
Nickel in Matte to Market Revenue	3,625	-	467	675	443	734	577	9	201	150	119	4	0	54	51	-	0	0	121	19	-	-	0	-
Copper in Matte to Market Revenue	1,203	-	162	230	147	240	188	3	64	49	38	1	0	17	16	-	0	0	39	6	-	-	0	-
Cobalt in Matte to Market Revenue	876	-	115	153	106	186	141	2	52	35	29	1	0	12	12	-	0	0	29	4	-	-	0	-
Nickel Sulphate Revenue	39,877	-	-	-	1,059	1,084	1,110	2,272	2,272	2,272	2,272	2,272	2,201	2,272	2,272	2,260	2,084	2,240	2,272	2,272	2,092	2,007	1,779	1,516
Copper Cathode Revenue	11,277	-	-	-	306	310	317	641	637	645	642	648	622	645	638	640	586	634	644	637	587	566	503	428
Cobalt Sulphate Revenue	10,137	-	-	-	277	300	297	613	639	584	599	555	567	557	565	568	499	584	587	576	519	476	413	362
Manganese Silicate Revenue	26,785	108	428	849	1,166	1,377	1,126	1,326	1,508	1,433	1,403	1,320	1,270	1,353	1,350	1,302	1,201	1,286	1,394	1,318	1,202	1,159	1,030	876
Ammonium Sulphate Revenue	439	-	-	-	11	17	23	23	23	23	23	23	23	23	23	23	23	23	23	23	23	23	23	22
Total Nickel Revenue	44,106	94	467	918	1,614	1,931	1,688	2,281	2,517	2,422	2,391	2,275	2,201	2,326	2,323	2,260	2,084	2,240	2,393	2,291	2,092	2,007	1,779	1,516
Total Copper Revenue	12,685	34	162	313	491	586	505	644	716	693	680	650	622	662	654	640	586	634	683	643	587	566	503	428
Total Cobalt Revenue	11,075	14	115	174	394	498	438	616	696	619	627	556	567	569	577	568	499	584	616	580	519	476	413	362
Total Manganese Revenue	26,785	108	428	849	1,166	1,377	1,126	1,326	1,508	1,433	1,403	1,320	1,270	1,353	1,350	1,302	1,201	1,286	1,394	1,318	1,202	1,159	1,030	876
Total Ammonium Revenue	439	-	-	-	11	17	23	23	23	23	23	23	23	23	23	23	23	23	23	23	23	23	23	22
Grand Total	95,090	251	1,172	2,253	3,677	4,409	3,780	4,889	5,459	5,190	5,124	4,823	4,682	4,933	4,927	4,792	4,393	4,767	5,109	4,855	4,423	4,230	3,749	3,203

A summary of capital costs by year, for the life of the project is shown in Table 19.6.

The summary of operating costs for the life of the project is shown in Table 19.7.

Table 19.6   Capital costs by year, over life of project

	Total	2021	2022	2023	2024	2025	2026	2027	2028	2029	2030	2031	2032	2033	2034	2035	2036	2037	2038	2039	2040	2041	2042	2043	2044	2045	2046
Total Pre-Production Capital Costs	237	64	75	88	9	-	-	-	-	-	-	-	-	-	-	-	-	-	-	-	-	-	-	-	-	-	-
Total Off-Shore Conversion and Construction Capital Costs	2,448																										
Total Off-Shore Sustaining Capital Costs	1,418	-	-	-	-	-	-	-	-	109	232	-	-	109	109	232	-	-	109	109	232	-	-	109	22	46	-
Total Off-Shore Construction Capital Costs	4,786	-	-	-	491	631	1,708	563	810	582	-	-	-	-	-	-	-	-	-	-	-	-	-	-	-	-	-
Total Off-Shore Sustaining Capital Costs	1,219				6	14	35	42	52	59	59	59	59	59	59	59	59	59	59	59	59	59	59	59	59	59	59
Closure Costs	500																										500
Total Capital Costs	10,607	64	142	297	893	1,666	2,151	617	1,035	854	360	59	59	168	168	291	59	59	168	168	291	59	59	168	81	106	559
Total Development Capital Costs	7,470	64	142	297	887	1,652	2,116	575	983	685	69	-	-	-	-	-	-	-	-	-	-	-	-	-	-	-	-

Table 19.7   Operating costs by year, over life of project

	Total	2024	2025	2026	2027	2028	2029	2030	2031	2032	2033	2034	2035	2036	2037	2038	2039	2040	2041	2042	2043	2044	2045	2046
Offshore Vessel Operating Costs																								
Project Zero: Hidden Gem 1 Mtpa	264	53	53	53	53	53	-	-	-	-	-	-	-	-	-	-	-	-	-	-	-	-	-	-
Project One: Hidden Gem 2.6 Mtpa	1,063	-	-	-	-	-	-	63	63	63	63	63	63	63	63	63	63	63	63	63	63	63	63	63
Drillship 2	1,221	-	56	56	56	56	56	56	56	56	56	56	56	56	56	56	56	56	56	56	56	56	56	56
Collector Ship 1	1,867	-	-	89	89	89	89	89	89	89	89	89	89	89	89	89	89	89	89	89	89	89	89	89
CSV	414	-	-	20	20	20	20	20	20	20	20	20	20	20	20	20	20	20	20	20	20	20	20	20
Program Management and Logistics	324	14	14	14	14	14	14	14	14	14	14	14	14	14	14	14	14	14	14	14	14	14	14	14
Total	5,154	67	122	231	231	231	178	241	241	241	241	241	241	241	241	241	241	241	241	241	241	241	241	241
Shipping Operating Costs																								
Total	5,266	29	90	191	224	248	204	255	275	266	264	255	251	259	259	254	244	254	265	257	245	240	227	210
Onshore Operating Costs																								
Tolling	6,818	73	290	582	486	486	147	303	438	380	365	302	271	329	329	297	223	293	373	315	231	197	107	-
Sulphidisation	2,529	-	115	162	162	162	59	120	162	151	145	120	107	131	130	117	88	115	147	124	91	77	42	-
Refinery	5,229	20	79	159	221	264	217	259	295	280	275	258	250	266	265	256	236	254	276	261	237	228	202	172
RKEF Line	10,023	-	-	-	261	391	521	521	521	521	521	521	521	521	521	521	521	521	521	521	521	521	521	513
Product Logistics	1,945	7	30	59	82	98	81	97	110	105	102	96	93	99	99	95	88	94	102	96	88	85	75	64
Alloy Treatment Charge	113	19	-	46	21	20	-	-	7.4	-	-	-	-	-	-	-	-	-	-	-	-	-	-	-
Total	26,544	100	514	963	1,213	1,402	1,025	1,300	1,526	1,437	1,409	1,297	1,242	1,346	1,344	1,287	1,156	1,277	1,419	1,317	1,168	1,108	947	749
Corporate Costs																								
Total	560	10	25	25	25	25	25	25	25	25	25	25	25	25	25	25	25	25	25	25	25	25	25	25
Total Operating Costs																								
Total	37,524	206	751	1,410	1,693	1,906	1,432	1,821	2,067	1,969	1,939	1,818	1,758	1,870	1,869	1,807	1,665	1,797	1,950	1,840	1,678	1,613	1,439	1,225

The life of project taxes and royalties are shown in Table 19.8.

Table 19.8   Taxes and royalties by year, over life of project

	Total	2024	2025	2026	2027	2028	2029	2030	2031	2032	2033	2034	2035	2036	2037	2038	2039	2040	2041	2042	2043	2044	2045	2046
Royalties	7,196	10	46	88	140	168	306	396	443	420	415	390	379	399	399	388	355	386	414	393	358	342	303	259
Revenue	95,090	251	1,172	2,253	3,677	4,409	3,780	4,889	5,459	5,190	5,124	4,823	4,682	4,933	4,927	4,792	4,393	4,767	5,109	4,855	4,423	4,230	3,749	3,203
Offshore OPEX	10,420	96	212	422	456	479	382	496	515	507	505	496	491	500	500	495	484	495	506	498	486	481	468	451
Offshore Depreciation	3,739	133	337	418	407	400	365	221	140	137	124	104	90	90	90	90	90	90	90	90	90	73	35	35
Offshore Markup	2,832	46	110	168	173	176	149	143	131	129	126	120	116	118	118	117	115	117	119	118	115	111	101	97
Onshore Revenue Base	78,100	- 24	513	1,245	2,641	3,354	2,883	4,029	4,673	4,417	4,369	4,103	3,985	4,226	4,219	4,090	3,704	4,066	4,393	4,150	3,732	3,566	3,145	2,620
Onshore OPEX	26,544	100	514	963	1,213	1,402	1,025	1,300	1,526	1,437	1,409	1,297	1,242	1,346	1,344	1,287	1,156	1,277	1,419	1,317	1,168	1,108	947	749
Corporate Costs	560	10	25	25	25	25	25	25	25	25	25	25	25	25	25	25	25	25	25	25	25	25	25	25
EBITDA	50,995	- 134	- 26	257	1,404	1,928	1,833	2,704	3,121	2,955	2,935	2,781	2,718	2,855	2,850	2,779	2,523	2,764	2,949	2,807	2,540	2,433	2,173	1,846
Onshore Depreciation	5,737	50	114	288	349	435	499	505	511	517	523	479	421	253	198	118	59	59	59	59	59	59	59	59
EBIT	45,258	- 184	- 140	- 32	1,055	1,492	1,334	2,198	2,610	2,438	2,412	2,302	2,297	2,603	2,652	2,661	2,463	2,704	2,890	2,748	2,480	2,374	2,114	1,786
Tax	9,123	-	-	-	211	298	267	440	522	488	482	460	459	521	530	532	493	541	578	550	496	475	423	357

The summary of undiscounted cash flows for the life of the project is shown in Table 19.9.

Table 19.9   Undiscounted cash flows by year, over life of project

	Total	2021	2022	2023	2024	2025	2026	2027	2028	2029	2030	2031	2032	2033	2034	2035	2036	2037	2038	2039	2040	2041	2042	2043	2044	2045	2046
Revenue	95,090	-	-	-	251	1,172	2,253	3,677	4,409	3,780	4,889	5,459	5,190	5,124	4,823	4,682	4,933	4,927	4,792	4,393	4,767	5,109	4,855	4,423	4,230	3,749	3,203
Opex	-37,524	-	-	-	-206	-751	-1,410	-1,693	-1,906	-1,432	-1,821	-2,067	-1,969	-1,939	-1,818	-1,758	-1,870	-1,869	-1,807	-1,665	-1,797	-1,950	-1,840	-1,678	-1,613	-1,439	-1,225
Capex	-10,607	-64	-142	-297	-893	-1,666	-2,151	-617	-1,035	-854	-360	-59	-59	-168	-168	-291	-59	-59	-168	-168	-291	-59	-59	-168	-81	-106	-559
Taxes and Royalties	-16,318	-	-	-	-10	-46	-88	-351	-467	-573	-835	-965	-908	-897	-850	-838	-920	-929	-920	-848	-927	-992	-943	-854	-817	-726	-616
Undiscounted Net Cashflow	30,641	-64	-142	-297	-859	-1,291	-1,395	1,015	1,002	921	1,872	2,368	2,254	2,120	1,986	1,795	2,084	2,070	1,897	1,712	1,752	2,107	2,013	1,722	1,719	1,478	803
Cumulative Undiscounted Cashflow		-64	-206	-503	-1,361	-2,652	-4,047	-3,032	-2,031	-1,110	762	3,130	5,384	7,503	9,490	11,284	13,368	15,438	17,335	19,047	20,799	22,906	24,919	26,641	28,360	29,838	30,641

19.3 Inferred Mineral Resources

The IA is preliminary in nature and includes Inferred Mineral Resources that are considered too speculative geologically to have the economic considerations applied to them that would enable them to be categorized as mineral reserves. There is no certainty that the IA will be realized.

The LOM production sequence includes 6 Mt (wet) of nodules that are classified as Inferred Mineral Resources. This is approximately 2% of the total LOM production. Excluding the Inferred Mineral Resources from the economic analysis the project NPV is estimated to be $6.7 billion.

19.4 Sensitivity analysis

The sensitivity of project economics to changes in the main variables was tested by selecting high and low values that represent a likely range of potential operating conditions.

In terms of identifying high and low ranges:

- Grade and abundance ranges were based on the distribution throughout the resource.
- Onshore capital cost ranges were based on accuracy levels of +50%, -35%.
- Offshore capital cost ranges were based on Deep Reach Technology's accuracy levels of +40%, -30%.
- Other capital cost ranges were +/- 25%.
- Note, the collector speed is already at the BOD maximum of 0.5 m/s, so there was no high case value tested.
- Metal recoveries were based on realistic high and low values.
- For other variables ranges were +/- 20%.

The sensitivity analysis inputs are listed in Table 19.10. The impact of each variable on NPV (tested individually) is shown in Figure 19.4. The results are asymmetric for some variables. The variables with the biggest negative impact on NPV are all metal prices, total OPEX, collector speed, nickel sulphate price and development CAPEX. In general, revenue drivers have the biggest impact, followed by OPEX variables and then CAPEX variables.

Figure 19.4   Tornado diagram of NPV sensitivity to variables
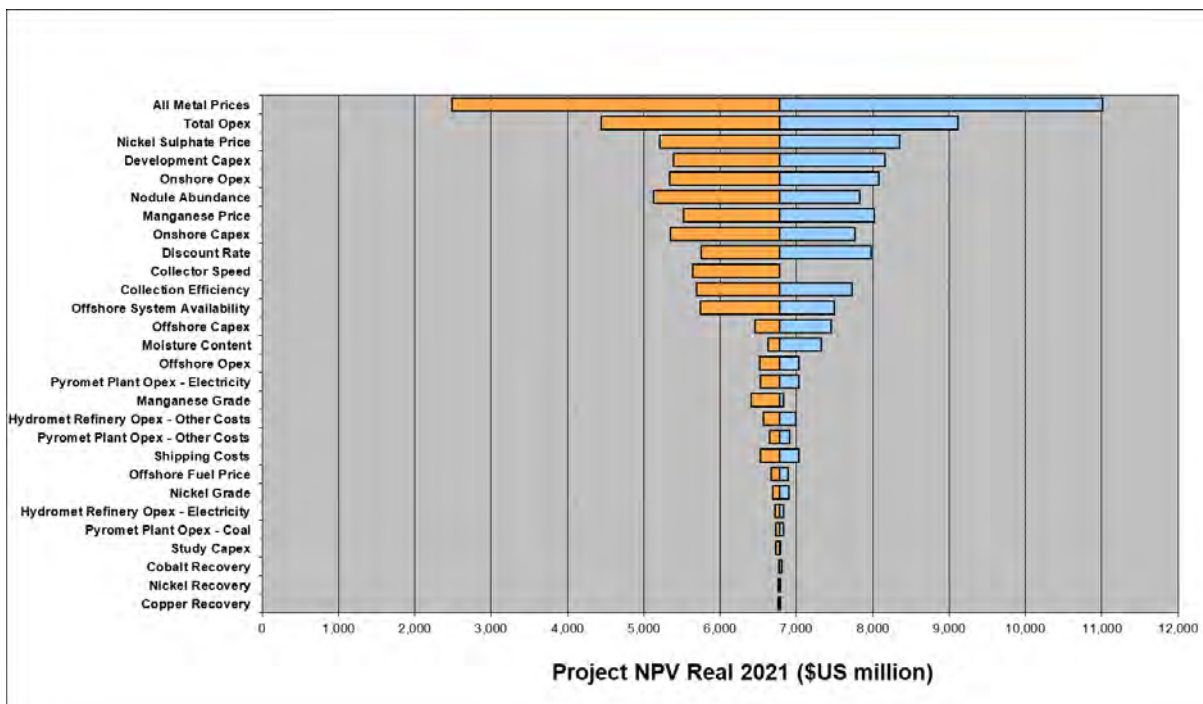
Table 19.10   Sensitivity analysis inputs

Parameters	Units	Values			Variation from Central Case Value	
		Low Case Value	Central Case Value	High Case Value	Low Case Value	High Case Value
Production and Revenue Parameters						
Nickel Grade	%	1.37	1.39	1.42	-1%	+2%
Manganese Grade	%	29.0	31.0	31.3	-6%	+1%
Nodule Abundance	kg/m^2	15.5	16.9	22.5	-15%	+16%
Collector Speed	m/sec	0.40	0.50	N/A	-20%	N/A
Collection Efficiency	%	81	90	99	-10%	+10%
Offshore System Availability	days/year	190	238	286	-20%	+20%
Moisture Content	%	25	24	20	+4%	-17%
Nickel Recovery	%	92.5	94.6	96.0	-2%	+1%
Copper Recovery	%	79.5	86.2	89.0	-8%	+3%
Cobalt Recovery	%	74.0	77.2	88.0	-4%	+14%
All Metal Prices					-20%	+20%
Nickel Sulphate Price	$US/t	$14,169	$17,711	$21,254	-20%	+20%
Manganese Price	$US/DMTU	$3.62	$4.53	$5.44	-20%	+20%
CAPEX Parameters						
Development CAPEX	$US Million	$9,338	$7,470	$5,603	+25%	-25%
Study CAPEX	$US Million	$296	$237	$177	+25%	-25%
Offshore CAPEX	$US Million	$3,427	$2,448	$1,713	+40%	-30%
Onshore CAPEX	$US Million	$7,179	$4,786	$3,111	+50%	-35%
Total CAPEX	$US Million	$13,259	$10,607	$7,955	+25%	-25%
OPEX Parameters						
Total OPEX	$US/tonne nodule (dry)	$232.9	$194.1	$155.3	+20%	-20%
Offshore OPEX	$US/tonne nodule (dry)	$32.0	$26.7	$21.4	+20%	-20%
Onshore OPEX	$US/tonne nodule (dry)	$164.8	$137.3	$109.8	+20%	-20%
Offshore Fuel Price	$US/tonne fuel	$600.0	$500.0	$400.0	+20%	-20%
Shipping OPEX	$US/tonne nodule (dry)	$32.7	$27.2	$21.8	+20%	-20%
Pyro Plant OPEX - Other Consumables	$US Million per RKEF line per annum	$96.3	$120.4	$144.5	+20%	-20%
Pyromet Plant OPEX – Electricity	$US Million per RKEF line per annum	$267.6	$223.0	$178.4	+20%	-20%
Pyromet Plant OPEX - Coal	$US Million per RKEF line per annum	$56.8	$47.3	$37.8	+20%	-20%
Hydromet Refinery OPEX - Electricity	$US Million per refinery per annum	$31.9	$26.6	$21.3	+20%	-20%
Hydromet Refinery OPEX - Other Costs	$US Million per refinery per annum	$120.7	$100.6	$80.5	+20%	-20%
Economic Parameters						
Discount Rate	%	10	9	8	+11%	-11%

20Adjacent properties

The NORI Area lies within the Clarion Clipperton Zone. Seafloor polymetallic nodules are distributed across the majority of the CCZ. Sections 7 and 20 discuss the relationship of the NORI Area to the other properties in the CCZ.

In 2020, DeepGreen acquired the polymetallic nodule exploration contract awarded by the ISA to TOML. TOML Area F is immediately west of NORI Area D.

21 Other relevant data and information

This section intentionally left blank.

22 Interpretation and conclusions

Exploration by several government-funded organisations and commercial consortia (the Pioneer Investors) from the 1960s onwards demonstrated a very large resource of polymetallic nodules, containing nickel, manganese, cobalt, and copper, located on the deep seafloor the CCZ, in the northeast Pacific Ocean between Hawaii and Mexico.

The nodules are located at depths of between 4,000 and 6,000 m and have been explored with considerable success using a variety of deep-sea technologies. Successful trial extraction in the CCZ has also been carried out to demonstrate that the nodules can be collected and pumped to a surface platform and subsequently processed to recover metals.

Exploration of the seafloor in international waters is now administered by the ISA and regulated by the UNCLOS. These institutions operate on the principle that the ocean floor beyond the limits of national jurisdiction, known as the Area, is the common heritage of mankind.

In July 2011, Nauru Ocean Resources Inc. (NORI), a subsidiary of DeepGreen Metals Inc. (DeepGreen), was granted an exploration contract over 74,830 km^2 in the CCZ consisting of four exploration areas (A, B, C and D) (the NORI Area or the Property). NORI's contract for exploration of polymetallic nodules was approved by the Council of the ISA on 19 July 2011, for a term of 15 years and then signed with the ISA on 22 July 2011.

NORI completed off-shore exploration campaigns in 2012, 2013, 2018, and 2019. During these campaigns a variety of data was collected including:

- Bathymetric mapping of the whole of NORI Area D using a hull-mounted MBES.
- Detailed seafloor survey work with an AUV, utilising an MBES, Side Scan Sonar (SSS), Sub-Bottom Profiler (SBP) and camera payload.
- Box core samples.

During this period NORI commissioned a variety of preliminary scientific and engineering studies into the exploitation of polymetallic nodules, with the primary focus on NORI Area D.

22.1 Mineral Resources

All the data indicates that both grades and abundance have remarkable continuity. Abundance is more variable than grades and is recognised as the primary control on classification of the Mineral Resource. Sufficient data was collected in NORI Area D to estimate Measured and Indicated Resources and define an area that is expected to be suitable for a trial of a mining system.

Sampling of NORI Area D at a spacing of 10 km by 10 km during the 2019 campaign confirmed that the nodules have low variability and high continuity. The latest Mineral Resource estimate (2020) is 4 Mt Measured and 341 Mt Indicated and 11 Mt Inferred Mineral Resources. Taking into account the conversion of the majority of Inferred to Indicated Mineral Resources, the remaining Inferred Mineral Resource has decreased by 26 Mt as a result of excluding the Volcanic High domain in the south-eastern corner of NORI Area D, due to uncertainty about the occurrence of nodules in this area. The 2020 resource estimate is also slightly higher in abundance (5.4% higher), and nickel (6.1% higher), cobalt (5.4% higher) and manganese (2.2% higher) grades than the 2018 estimate.

Comparison of the area covered by Inferred, Indicated and Measured Mineral Resource for the 2020 estimate and the same area in the 2018 model shows that nickel grade has increased by 6% (1.32% to 1.40% Ni) while abundance has increased by 6% (16.0 to 17.0 kg/m^2). Mineral Resource tonnage has increased by 10% (from 10 to 11 Mt) in the Inferred area and 7% (from 320 to 341 Mt) in the Indicated area. The positive conversion rates arising from infilling the sampling grid with high-quality box core sample data (rather than extending the area sampled)

are exceptionally high compared to the typical outcomes from infill sampling of terrestrial mineral deposits.

Whilst the IA focusses on the development of nodule production in NORI Area D, the other three areas (NORI Area A, B and C), are estimated to contain Inferred Mineral Resources of 510 Mt (wet) at 1.28% Ni, 0.21% Co, 1.04% Cu, 28.3% Mn, at an average abundance of 11 kg (wet)/m^2 at a 4 kg/m^2 abundance cut-off (Golder, 2013). The polymetallic nodule mineralisation in Areas A, B and C has similar characteristics to NORI Area D and it is likely that the technology proposed in the IA would be suitable for these additional areas.

22.2 Development plan

NORI proposes to implement the project in multiple phases that will allow the seafloor mining systems to be tested and then nodule production to be gradually ramped up. The phased approach will facilitate derisking of the project for relatively low initial capital investment. The proposed development phases are as follows:

- The Collector Test is designed to perform proof of concept for the methods of collecting and lifting the nodules while acquiring sufficient data to design a commercial system. Nodule collected during the test would be stored on the Hidden Gem and brought to shore for use in large scale process pilot testing. The Collector Test would use a converted sixth generation drillship, the Hidden Gem. The test would not demonstrate the transhipment of nodules to a shore-based facility.

- Project Zero would be an extension of the Collector Test using an upgrade of the converted drillship to produce a sufficient and continuous quantity of nodules to support a relatively small commercial operation of up to 1.3 Mtpa (wet) nodules delivered to a shore-based facility. This operation would demonstrate a more continuous mining operation at a larger scale than the Collector Test and would demonstrate the transhipment of nodules to a processing facility.

- Project One would increase production in a further three steps:

    — a further upgrade of the Hidden Gem for up to 3.6 Mtpa (wet) production, for a 20-year production life.

    — introduction of a second converted drillship (Drill Ship 2) with a capacity of up to 3.6 Mtpa (wet), designed for a 20 year production life.

    — construction of a new purpose-built production support vessel (Collector Ship 1) with capacity of up to 8.2 Mtpa (wet). Project One would benefit from lessons learned on the Collector Test and Project Zero.

NORI proposes that the processing of the polymetallic nodules would also be ramped up in phases. For Project Zero, NORI proposes to toll treat polymetallic nodules at existing RKEF smelters, utilizing excess industry capacity. In Project One, a purpose-built process plant would be constructed, including pyrometallurgical and hydrometallurgical circuits. Much of the nodule production would switch in phases from toll-treatment to treatment in this new plant. A portion of the nodule production would continue to be toll treated.

22.3 Off-shore operations

Preliminary design of an off-shore nodule collection system has been completed. The main items of off-shore infrastructure are the nodule collector vehicles, the riser, the production support vessel (PSV), and a collector support vessel.

The seabed system is an extrapolation of existing technologies in deep ocean operations and previous seabed development activities. Much of the technology is a direct derivative of previous experience in nodule developments, such as consortium activities in the 1970s, including significant pilot testing, and also advances in deep water oil and gas development.

The nodules will be collected from the seafloor by self-propelled, tracked, collector vehicles. No rock cutting, digging, drill-and-blast, or other breakage will be required at the point of collection.

The collectors will be remotely controlled and supplied with electric power via umbilical cables from the PSV. They nodules will be pumped as a slurry via flexible hoses to a riser, through which they will be transferred to the surface by means of an air lift. Nodules will be discharged to the PSV, where they will be dewatered and temporarily stored or transferred directly to ore transportation vessels. A separate collector support vessel will remain at sea to support the mining operation.

This IA assumes transportation of nodules will be by chartered vessels with deadweight capacities of up to 100,000 tonnes. The vessels will require DP capability to enable them to be loaded at sea alongside the PSV. Hydraulic offloading of the nodules from the PSV to the transport ships is assumed in this IA, but future studies will confirm the offloading mechanism.

There still remain particular component and sub-systems of the off-shore operations that are not "off-the-shelf" and require further development. The technical readiness of some of the described components and assumptions need to be verified by further design and testing. NORI plans to complete a Collector Test in 2022 which will address these issues.

22.4 On-shore operations

The overall flowsheet for the on-shore operations, i.e. smelting and sulphuric acid leach, is one of the options that have been considered in the literature. The first part of the pyrometallurgical process is the Rotary Kiln Electric Furnace (RKEF) process that is widely used in the nickel laterite industry. The second pyrometallurgical step (sulphidisation of the alloy produced in the first step to form a matte and then partially conversion in a Peirce-Smith converter to remove iron), while not widely practiced, also has commercial precedent at the Doniambo plant of Societe Le Nickel in New Caledonia.

Sulphuric acid leaching of matte from the pyrometallurgical process has precedent in the platinum group minerals (PGM) industry. Although copper producers typically have a solvent extraction step before electrowinning of their copper, direct copper electrowinning is done in most PGM refineries, where nickel and cobalt are also significant pay-metals. This is to maximise nickel recovery and minimise operating expenses. The nickel and cobalt are purified using solvent extraction, ion exchange and precipitation, which are all commercially proven hydrometallurgical processes. Battery grade nickel and cobalt sulphate are then crystallised from the purified solutions.

The pyrometallurgical process forms two by-products as well as the matte for the hydrometallurgical refinery:

- Electric furnace silicate product containing silica and 53% MnO that is intended to be sold as feed to the Si-Mn industry.
- A converter aisle slag that could be used for aggregate in road construction or other applications.

The hydrometallurgical refinery generates iron residues that would, for a stand-alone plant, require disposal. However, these streams can be recycled back to the pyrometallurgical plant for re-treatment and recovery of entrained pay metals.

Selection of ammonia as a principal reagent in the hydrometallurgical refinery means that an additional by-product—ammonium sulphate—is generated. This could be sold into the fertiliser industry.

The copper cathode quality from direct electrowinning, without a solvent extraction step, is expected to be ≥99.9% Cu. Quality of the matte produced in the pyrometallurgical plant will have an impact on this, including the potential carryover of impurities beyond values assumed for the purpose of the IA.

The production of battery-grade nickel and cobalt sulphates is targeted instead of nickel or cobalt cathodes or other intermediate products.

In summary:

- All parts of the proposed process have commercial precedents in similar or analogous industries, however not as a whole continuous flowsheet.
- Pay-metals are recovered in the following forms:
  — Copper cathodes with an expected quality of ≥99.9% Cu.
  — Battery-grade nickel sulphate.
  — Battery-grade cobalt sulphate.
- Rather than generating large waste streams, the process produces by-products including high manganese content furnace slag and ammonium sulphate.

The process assumptions used in this study will need to be verified as the project proceeds.

22.5 Environmental status

Historically, a significant amount of technical work has been undertaken within the CCZ by the Contractors and a significant body of information has been acquired during the past 40 years on the likely environmental impacts of collecting nodules from the sea floor.

NORI's off-shore exploration campaigns have included sampling to support environmental studies, collection of high-resolution imagery and environmental baseline studies. A number of future campaigns are planned to collect data on ocean currents and water quality to assist plume modelling, environmental baseline studies, box core and multicorer sampling focussed on benthic ecology and sediment characteristics.

NORI has commenced the ESIA process in support of an application for an exploitation license for the commercial mining of deep-sea polymetallic nodules. A comprehensive program of metocean and biological data acquisition is in progress to characterize the baseline conditions at a designated Collector Test site and control sites in the mining lease area.

NORI intends to manage the Project under the governance of an EMS, which is to be developed in accordance with the international EMS standard, ISO 14001:2004. The EMS will provide the overall framework for the environmental management and monitoring plans that will be required.

An EMP will be required. The plan will specify the objectives and purpose of all monitoring requirements, the components to be monitored, frequency of monitoring, methods of monitoring, analysis required in each monitoring component, monitoring data management and reporting. The plan will be submitted to the ISA as part of the exploitation contract application.

The social impacts of the off-shore operation are expected to be positive. The CCZ is uninhabited by people, and there are no landowners associated with the NORI Area D nodule project. No significant commercial fishing is carried out in the area. The Project will provide a source of revenue to the sponsor country, Nauru, and to the ISA.

The on-shore environmental and social impacts have not yet been assessed because the process plant has not been designed in detail, and the location and host country (and hence regulatory regime) not confirmed. The Project is not expected to require tailings ponds or other large-scale waste storage on-site. The deleterious elements (for example, cadmium and arsenic) content of the nodules is very low, indicating that with careful management the environmental impacts of the processing operation could be very low.

22.6 Economic analysis

The cost estimates used in this IA for off-shore property, plant and equipment are based on estimates prepared by Deep Reach Technology Inc. (DRT) for NORI during the 2015 DRT scoping

study. These were generally derived from budget estimates supplied by original equipment manufacturers that specialise in each of the items under consideration.

The estimates assume that the technologies proposed will be technically ready at the time the capital is spent. While much of the proposed technology is derived from previous experience in nodule development and from existing oil and gas technology, the concepts include substantial research and development, customisation, and bespoke engineering. Specific items that require development include field testing of collectors, airlift discharge systems, nodule attrition simulation; a mateable power connector in the megawatt range capable of operating at 5,000 m depth must be qualified. Accordingly, a budget allowance has been made for prefeasibility activities prior to commercial development of the project.

Off-shore capital costs were estimated to accuracy levels of -30% +40%. A contingency of 25% has been applied to the off-shore capital cost estimates.

On-shore capital costs were estimated according to an Association for the Advancement of Cost Engineering Class 5 level of accuracy (–35% +50%). For the 4.88 Mtpa case, a contingency of 32% was applied to the on-shore capital cost estimates. For the scaled-up throughput and economic analysis of Project One, 25% contingency has been applied. Owner's costs and escalation beyond 2019 are excluded.

The offshore cost estimates were developed based upon the guidelines of the AACE (Association for the Advancement of Cost Engineering) International Recommended Practice No. 18R-97. Based on engineering studies performed previously by Deep Reach Technology (DRT) for Deep Green Resources and the experience in trial mining of deep sea nodules by DRT personnel, the cost estimate was considered to be a class 4. Off-shore capital costs were estimated to accuracy levels of -30% +40%. On-shore capital costs were estimated according to an AACE Class 5 level of accuracy (–35% +50%). A contingency of 25% was applied to the off-shore and on-shore capital cost estimates.

Transportation cost estimates to an unspecified Mexican port are based on estimates by Global Location Strategies (Global Location Strategies, 2019) for NORI. The destination port has not yet been determined, nor has the location of the processing plant. Hence, the overland transport requirement cannot yet be estimated. Different vessel sizes will be considered in future studies.

The IA considers a mining plan for a 23-year production period. The draft regulations for exploitation of Mineral Resources in the Area (ISBA/23/LTC/CRP.3*), promulgated by the ISA, contemplate grant of an initial 30-year exploitation contract, with possible extension by periods of 10-years, subject to license re-applications and renewals. After the initial 23-year period substantial resources will remain in the other NORI Areas (A, B, and C) that could support future mining.

A financial model based on estimates of future cash flows derived from extraction of nodules from NORI Area D has been developed in-house by DeepGreen. AMC reviewed the logic, input assumptions and integrity of the calculations and forecasts and is satisfied that the outcomes of the model are reasonable for a IA.

The analysis indicates a positive economic outcome. Undiscounted post-tax net cash flow of US$30.6 billion is expected. An internal rate of return of 27% has been modelled. Discounted cash flow analysis of unleveraged real cash flows, discounting at 9% per annum, indicates a project net present value (NPV) of US$6.8 billion. Excluding the inferred mineral resources from the economic analysis, the post-tax project NPV is estimated at $6.7 billion, which is not a significant difference from the economic analysis that includes the inferred mineral resources.

The Qualified Persons caution that this IA is preliminary in nature. There is no certainty that the results presented in this IA will be realised. A prefeasibility study has not been undertaken. Mineral Resources are not mineral reserves and do not have demonstrated economic viability.

23 Recommendations

This IA indicates that the NORI Area D resource is potentially economic. The QPs recommend that further data gathering, analysis, design and cost estimation be undertaken to advance the Project.

The priorities should be undertaking the environmental baseline studies and compiling the ESIA required to facilitate timely permitting; obtaining a bulk sample of nodules for metallurgical testing and flowsheet optimisation; and the Collector Test to demonstrate proof of concept and to provide performance data to inform detailed engineering design.

Assuming these activities generate positive results, a prefeasibility study will be warranted.

DeepGreen has identified a program to advance the NORI Area D Project Figure 19.1. The program incorporates the activities recommended by the QPs. It also includes fabrication, commissioning and wet testing of long lead items required for the Collector Test, which is currently scheduled for Q2-3 2022.

Pre-project capital cost estimates, which cover these activities, are summarized in Table 18.2.

NORI estimates $70.6 million in pre-Project off-shore capital costs including $40 million for feasibility studies and engineering design. Approximately $60 million expenditure is expected for successful engineering, fabrication and completion of the Collector Test.

24References

Agarwal JC, Barner HEM, Beecher N. 1979. The cuprion process for ocean nodules, Chem. Eng. Prog 75(1):59-63.

Agarwal, S., et al, 2009. Studies on recovery of Ni, Co, Cu from polymetallic polymetallic nodules by direct reduction smelting, COM 2009, Sudbury, p. 509-517.

Allain V, Nicol S, Essington T, Okey T, Olson B, Kirby D 2007. An Ecopath with Ecosim model of the Western and Central Pacific Ocean warm pool pelagic ecosystem. Western and Central Pacific Fisheries Commission, Scientific Committee, Third Regular Session, 13-24 August 2007 Honolulu, United States of America. WCPFC-SC3-EB SWG/IP-8.

AMC, 2016. TOML Clarion Clipperton Zone Project, Pacific Ocean. Technical Report compiled under NI-43-101 by AMC Consultants Pty Ltd for Nautilus Minerals, March 2016.

AMC, 2018. Initial Assessment of Solwara Project, Bismark Sea, PNG, Technical Report compiled under NI-43-101 by AMC Consultants Pty Ltd for Nautilus Minerals Niugini Ltd.

AMC, 2018. NORI Area D, Clarion Clipperton Zone Mineral Resource Estimate, April 2019 Technical Report compiled under NI-43-101 by AMC Consultants Pty Ltd for DeepGreen Metals Inc.

American Society of International Law. 1975. DeepSea Ventures Inc: notice of discovery and claim of exclusive mining rights, and request for diplomatic protection and protection of investment. International Legal Materials 14(1) (January 1975): 51-68.

Amon DJ, Ziegler AF, Dahlgren TG, Glover AG, Goineau A, Gooday AJ, Wiklund H, Smith CR, 2016. Insights into the abundance and diversity of abyssal megafauna in a polymetallic-nodule region in the eastern Clarion-Clipperton Zone. Sci. Rep. 6, 30492.

Amon DJ, Ziegler AF, Kremenetskaia A, Mah CL, Mooi R, O'Hara T, Pawson DL' Roux M and Smith CR. 2017. Megafauna of the UKSRL exploration contract area and eastern Clarion-Clipperton Zone in the Pacific Ocean: Annelida, Arthropoda, Bryozoa, Chordata, Ctenophora, Mollusca. Biodiversity Data Journal 5: e14598 doi: 10.3897/BDJ.5.e14598.

ANZECC/ARMCANZ 2000. Australia and New Zealand Guidelines for Fresh and Marine Water Quality. Australian and New Zealand Environment and Conservation Council/ Agricultural and Resource Management Council of Australia and New Zealand. Canberra.

Arbizu P, Haeckel M 2015. RV SONNE Fahrtbericht / Cruise Report SO239 EcoResponse Assessing the Ecology, Connectivity and Resilience of Polymetallic Nodule Field Systems. The GEOMAR Helmholtz Centre for Ocean Research Kiel, Geomar Report 25.

Barnes, A., et al., 2011. Cobalt from slag – Lessons in transition from laboratory to industry, COM 2011, Montreal.

Bath, A. R. (1989), "Deep Sea Mining Technology: Recent Developments and Future Projects", Off-shore Technology Conference, Paper OTC 5998, Houston, Texas USA

Bernard, J., Bath, A. and Greger, B. (1987), "Analysis and Comparison of Nodule Hydraulic Transport Systems", Proceedings, Off-shore Technology Conference, paper OTC 5476, Houston

BGR 2018. Environmental Impact Assessment for the testing of a pre-protoype manganese nodule collector vehicle in the Eastern German license area (Clarion-Clipperton Zone) in the framework of the European JPI-O Mining Impact 2 research project.

Bertrand A, Bard F-X and Josse E, 2002. Tuna food habits related to the micronekton distribution in French Polynesia. Marine Biology 140: 1023-1037.

Bluhm H 2001. Re-establishment of an abyssal megabenthic community after experimental physical disturbance of the seafloor. Deep sea research 11(48):3841-3868.

Boschen RE, Collins PC, Tunnicliffe V, et al. 2015. A primer for use of genetic tools in selecting and testing the suitability of set-aside sites protected from deep-sea seafloor massive sulphide mining activities. Ocean & Coastal Management 122: 37-48.

Bosland, R. (2020, November 27). Email Subject: RE: Client Query No. 3A - Request for Info. Delft.

Brockett, F.H., Kollwentz, Walter M. (1977), "An International Project - Nodule Collectors", Off-shore Technology Conference, paper 2777 Houston, Texas.

Bustos, A., et al., 1988.Converting simulation at Falconbridge Limited", Extractive metallurgy of nickel and copper, TMS, p. 335-53.

Castro P and Huber ME, (Eds) 2005. Marine Biology. 5th Edition, McGraw Hill Publishers New York ISBN0-07-250934-1.

Cellula Robotics Ltd. (2015). Production Harvestor Design Report DCD15 CTR01/03.

Choy CA, Haddock SHD, Robison BH 2017 Deep pelagic food web structure as revealed by in situ feeding observations. Proc. R. Soc. B 284: 20172116. http://dx.doi.org/10.1098/rspb.2017.2116.

Clark M, Smith S 2013. Environmental management considerations. In: SPC 2013, Baker E, Beaudoin Y, editors. Deep sea minerals: manganese nodules, a physical, biological, environmental, and technical review. Vol. 1B, Secretariat of the Pacific Community. p. 27–38.

Clark MR, Rouse H, Lamarche G, Ellis J, Hickey C. 2017. Preparation of Environmental Impact Assessments: General guidelines for off-shore mining and drilling with particular reference to New Zealand. NIWA Science & technology Series. January 2007.

Clark MR, Durden JM and Christiansen S. 2019. Environmental Impact Assessments for deep-sea mining: Can we improve their future effectiveness? Marine Policy.

Clarke KR and Warwick RM, 1994. Change in marine communities: An approach to statistical analysis and interpretation. Plymouth Marine Laboratory, UK.

CRU, 2020. Updated PEA market input. Report for DeepGreen Metals. Dated 23/10/2020.

Crundwell, F., et al., 2011. "Extractive metallurgy of nickel, cobalt and platinum group metals", Elsevier, p. 103.

Cutter A 2018. US GEOTRACES Pacific Meridional Transect – GP15 Cruise Report 18 September – 24 November 2018. Seattle, Washington – Papeete, Tahiti (port stop in Hilo, Hawaii, 21-25 October 2018) R/V Roger Revelle. Available at geotraces.org.

Deep Reach Technology, Inc. (DRT) (2015) "Seafloor Polymetallic Nodule Off-shore Scoping Study – Technical Report", Report DRT-1412-RP-02-R02, 29 October 2015.

Deep Reach Technology, Inc. (2019). Theory and Validation of the DRT Airlift Model DRT-1907-RP-02-C01. Houston: Deep Reach Technology, Inc.

Deep Reach Technology, Inc. (2020). Drillship Conversion for Project Zero DRT-2009-RP-02-R01. https://www.deepreachtech.com/arpa-e-sbir-news-release

Deep Reach Technology, Inc. (2021). Improved Manganese Nodule Collector Design to Mitigate Sediment Plumes - Final Report Phase 1. Houston: Advanced Research Project Administration - Energy, U. S. Department of Energy.

Demidova T 1999. The Physical Environment in Nodule Provinces of the Deep Sea. In: Deep-seabed polymetallic nodule exploration: development of environmental guidelines. Proceedings of the International Seabed Authority 's Workshop held in Sanya, Hainan Island, People's Republic of China. June 1-5, 1998 (ISA/99/02). p. 79-116.

Demidova TA, Kontar EA 1989. On bottom boundary currents in the areas of development of manganese nodule deposits. Doklady Akademii Nauk SSSR 2(308):468-472.

De Smet B, Pape E, Riehl T, Bonifacio P, Colson L, Vanreusel A 2017. The Community Structure of Deep-Sea Macrofauna Associated with Polymetallic Nodules in the Eastern Part of the Clarion-Clipperton Fracture Zone. Front. Mar. Sci., 11 April 2017, https://doi.org/10.3389/fmars.2017.00103.

Diaz, C., et al., "A review of nickel pyrometallurgical operations" Extractive metallurgy of nickel and copper, TMS, 1988, p. 211-39.

Doyle, RL. and Halkyard, JE. (2007), "Large Scale Airlift Experiments for Application to Deep Ocean Mining", ASME, Proceedings of the 26th International Conference on Off-shore Mechanics and Arctic Engineering, OMAE 2007, June, San Diego, CA.

Drazen JC, Sutton TT, 2017. The feeding ecology of deep-sea fish. Annual Reviews Marine Science 9: 337-366.

Drazen JC, Leitner A, Morningstar S, Marcon Y, Greinert J, Purser A 2019a. Observations of deep-sea fishes and mobile scavengers from the abyssal DISCOL experimental mining area. Biogeosciences Discussions. https.//dio.org/10.5194/bg-2019-51.

Drazen J, Smith C, Gjerde K, Au W, Black J, Carter G, Clark M, Durden J, Dutrieux P, Goetze E, Haddock S, Hatta M, Hauton C, Hill P, Koslow J, Leitner A, Measures C, Pacini A, Parrish F, Peacock T, Perelman J, Sutton T, Taymans C, Tunnicliffe V, Watling L, Yamamoto H, Young E, Ziegler A 2019b. Report of the workshop Evaluating the nature of midwater mining plumes and their potential effects on midwater ecosystems. Research Ideas and Outcomes 5: e33527. https://doi.org/10.3897/rio.5.e33527.

Durden JM, Bett BJ, Jones DOB, Huvenne VAI, Ruhl HA, 2015. Abyssal hills – hidden source of increased habitat heterogeneity, benthic megafaunal biomass and diversity in the deep sea. Progress in Oceanography 137: 209-218.

Dymond J, Collier R 1988 Biogenic particle fluxes in the equatorial Pacific: evidence for both high and low productivity during the 1982-83 El Nino. Global Biogeochem. Cycles 2:129-137.

Earney FCF. 1990. Marine Mineral Resources. Routledge, p 387. Cited in: ISA. 2010. A geological model of polymetallic nodule deposits in the Clarion-Clipperton Fracture Zone and prospector's guide for polymetallic nodule deposits in the Clarion-Clipperton Fracture Zone. International Seabed Authority Technical Study: No. 6.

Ekstrom J, Bennun L and Mitchell R. 2015. A cross-sector guide for implementing the Mitigation Hierarchy. Cross Sector Biodiversity Initiative, Cambridge.

ERIAS 2018. NORI Area D, Campaign 3, Sediment Geochemistry Characterisation Report. Report prepared by ERIAS Group Pty Ltd for Maersk Supply Service/Nauru Ocean Resources Inc. Draft, December 2018.

Food and Agriculture Organization 2009. Management of Deep-sea Fisheries in the High Seas, FAO, Rome, Italy, 2009.[17]

Food and Agriculture Organization 2018. FAO Yearbook of Fishery and Aquaculture Statistics. http://www.fao.org/fishery/static/Yearbook/YB2018_USBcard/index.htm.

Feenan, J. P. (2009) "Seafloor Massive Sulphide Mining Concept", Off-shore Technology Conference, Paper 19823, Houston, Texas USA.

Fernandez-Alamo MA and Farber-Lorda J, 2006. Zooplankton and the oceanography of the eastern tropical Pacific: A review. Progress in Oceanography, 69: 318-359.

Felix, D. 1980. Some problems in making nodule abundance estimates from seafloor photographs. Marine Mining, Volume 2 Number 3, 293-302.

Flanagan and Gottfried, 1980. USGS nodule standard.

FRED, 2020. Producer Price Index by Industry: Ship Building and Repairing: Ship Repair, Nonmilitary (PCU336611336611A) | FRED | St. Louis Fed.

Fugro. (2019). Geotechnical Seafloor Sampling Survey: NORI Area D Area, Campaign 3; Report No. 1803-1344, Volume II Revision 0. Houston Texas: Fugro USA, Marine, Inc.

Giere O, 1993. Meiobenthology. Springer, Berlin. p. 328.

Gill AE. 1982. Atmosphere-ocean dynamics. New York: Academic Press. In Demidova T. 1999. The Physical Environment in Nodule Provinces of the Deep Sea. In: Deep-seabed polymetallic nodule exploration: development of environmental guidelines. Proceedings of the International Seabed Authority's Workshop held in Sanya, Hainan Island, People's Republic of China. June 1-5, 1998 (ISA/99/02).

Global Location Strategies, 2019. Deep Green Global Location Benchmarking Final Report. Report for DeepGreen, dated August 20, 2019.

Golder 2013. NI 43-101 technical report; Clarion-Clipperton Zone Project, Pacific Ocean. Report by Golder Associates Pty Ltd for Deep Green Resources Inc.

Golder 2015. Preliminary economic assessment, NORI Clarion-Clipperton Zone Area D Project, Pacific Ocean. Report prepared by Golder Associates for Deep Green Resources Inc.

GSR 2018. Global Sea Mineral Resources NV 2018. Environmental Impact Statement. Small-scale testing of nodule collector components on the seafloor of the Clarion-Clipperton Fracture Zone and its environmental impact (ISA_EIA_2018_GSRNOD2019)

Guenette S, Christensen V, Pauly D 2008. Trophic modelling of the Peruvian upwelling system: Towards reconciliation of multiple datasets. Progress in Oceanography 79: 326-335.

Halbach PE, Abram A 2013. Study Report about the surface sediments in the NE Pacific Clarion-Clipperton Zone (CCZ): Type of sediments, mineral and chemical composition and soil mechanical results of the surface layers. Prepared for DeepGreen Resources Inc. by FU Berlin. September 2018.

Hauquier F, Macheriotou L, Bezerra TN, Egho G, Martínez P, Arbizu PM, Vanreusel A 2018. Geographic distribution of free-living marine nematodes in the Clarion-Clipperton Zone: implications for future deep-sea mining Scenarios. Biogeosciences Discuss., https://doi.org/10.5194/bg-2018-492.

Hayes SP 1979. Benthic current observations at DOMES Sites A, B, and C in the tropical North Pacific Ocean. In: Bischoff YL, Piper DZ, editors. Marine geology and oceanography of the central Pacific manganese nodule province. New York: Plenum Press. 83-112.

Haynes BW, 1985. Laboratory processing and characterization of waste materials from manganese nodules, USBM RI 8938.

Hayton, B (2015) "Production Collector Design Report", Cellula Robotics, Ltd. Report CRL-DCD15-RP-09, 24 Dec.

Hein J, Mizell K, Koschinsky A, Conrad T. 2013. Deep-ocean mineral deposits as a source of critical metals for high- and green-technology applications: comparison with land-based resources. Manuscript Number: ORGEO-D-12-00079.

Heine, O. R. (1976), "Existing Large-Scale Air Lift Mining Operation and Air Lift Engineering Effort in the Soviet Union", Kennecott Exploration, Inc. Report TM-76-570

Hennigar, HF, Dick, RE, and Foell EJ, 1986, Derivation of Abundance Estimates for Manganese Nodule Deposits: Grab Sampler Recoveries to Ore Reserves, Off-shore Technology Conference, OTC 5237, May 1986, Houston.

Herring PJ, 2001. The Biology of the Deep Ocean. Oxford University Press, Oxford, England. ISBN-13: 978-0198549550

Higgins RP and Thiel H, (Eds) 1988. Introduction to the study of meiofauna. Smithsonian Institution Press. Washington DC.

Hofirek, Z. et al., 1995. Pressure leach capacity expansion using oxygen-enriched air at RBMR Rustenburg Base Metal Refiners, Hydrometallurgy, 39, pp 91-116.

Holness S, Stephens A, Ginsburg A, Botts EA, Driver A, Manuel J, & Mohasoa, P. 2018. Bridging the research-implementation gap: Mainstreaming biodiversity into the South African mining sector. Bothalia-African Biodiversity & Conservation, 48(1), 1-7.

IATTC 2019, https://www.iattc.org/PDFFiles/FisheryStatusReports/_English/No-17-2019

IFC 2013. Good Practice Handbook Cumulative Impact Assessment and Management: Guidance for the Private Sector in Emerging Markets. International Finance Corporation.

IHS Markit, 2021. Costs and Technology Indexes , accessed February 2021. https://ihsmarkit.com/Info/cera/ihsindexes/index.html

ISA, 1999a. Deep-seabed polymetallic nodule exploration: development of environmental guidelines. Proceedings of the International Seabed Authority's Workshop held in Sanya, Peoples Republic of China, June 1-5, 1998.

ISA. 1999b. Proposed technologies for mining deep-seabed polymetallic nodules. Proceedings of the International Seabed Authority's Workshop held in Kingston, Jamaica, 3-6 August 1999.

ISA. 2002. Standardisation of Environmental Data and Information: Development of Guidelines; Proceedings of the International Seabed Authority's Workshop, Kingston, Jamaica, June 25-29,

2001. Kingston Jamaica: Office of Resources and Environmental Monitoring, International Seabed Authority (ISA/02/02).

ISA. 2003. Establishment of a geological model of the polymetallic nodule resources in the Clarion- Clipperton Fracture Zone of the Equatorial North Pacific Ocean. Proceedings of the May 13-20, 2003, International Seabed Authority workshop held in Nadi, Fiji.

ISA. 2004. Marine Mineral Resources - scientific advances and economic perspectives. United Nations Division for Ocean Affairs and the Law of the Sea, Office of Legal Affairs.

ISA, 2008., Report on the International Seabed Authority's workshop on polymetallic nodule mining technology: current status and challenges ahead. Summary of Feb. workshop prepared by ISA Secretariat, Chennai, India.

ISA, 2010. A Geological Model of Polymetallic Nodule Deposits in the Clarion-Clipperton Fracture Zone and Prospector's Guide for Polymetallic Nodule Deposits in the Clarion- Clipperton Fracture Zone. International Seabed Authority Technical Study: No. 6 ISBN: 978-976-95268-2-2.

ISA, 2010. Recommendations for the guidance of contractors for the assessment of the possible environmental impacts arising from exploration for polymetallic nodules in the Area. ISBA/16/LTC/7. Issued by the Legal and Technical Commission.

ISA, 2012a. Environmental Management Needs for Exploration and Exploitation of Deep Sea Minerals. Kingston Jamaica: International Seabed Authority (ISA Technical Study No. 10).

ISA, 2012b. Decision of the Council relating to an environmental management plan for the Clarion- Clipperton Zone. Kingston Jamaica: International Seabed Authority. (ISBA/18/C/22; 26 July 2012).

ISA, 2013. Recommendations for the guidance of contractors for the assessment of the possible environmental impacts arising from exploration for marine minerals in the Area. ISBA/19/LTC/8. Issued by the Legal and Technical Commission.

ISA, 2014a. Deep sea macrofauna of the Clarion-Clipperton Zone. Kingston Jamaica: International Seabed Authority (ISA Technical Study No. 13).

ISA, 2014c. Developing a Regulatory Framework for Mineral Exploitation in the Area - Stakeholder Engagement.

ISA, 2015. Deep Sea Macrofauna of the Clarion-Clipperton Zone Taxonomic Standardisation Workshop. Uljin, the Republic of Korea, 23-30 November 2014. ISA Technical Study: No. 13, International Seabed Authority Kingston.

ISA, 2016. Review of the implementation of the environmental management plan for the Clarion-Clipperton Fracture Zone. Twenty-second session, Kingston, Jamaica, 11-22 July 2016. Legal and technical Commission, ISBA/22/LTC/12.

ISA, 2017a. Environmental assessment and management for exploitation of minerals in the Area. Report of an international workshop convened by the Griffith University Law School in collaboration with the ISA, Queensland Australia 23-26 May 2016. ISA Technical Study: No 16.

ISA, 2017b. Towards an ISA environmental management strategy for the area. Report of an international workshop convened by the German Environment Agency (UBA), the German federal Institute for GeoSciences and Natural Resources (BGR) and the Secretariat of the International Seabed Authority (ISA) in Berlin, Germany, 20-24 March, 2017. ISA Technical Study: No 17.

Initial Assessment of the NORI Property, Clarion-Clipperton Zone
Deep Green Metals Inc.

319002

ISBA/23/C/7, 5 June 2017 (ISA, 2017). Status of contracts for exploration and other matters. Twenty-third session Kingston, 7-18 August 2017. Report of the Secretary-General.

ISA, 2019. Draft Regulations on Exploitation of Mineral Resources in the Area (ISBA/25/C/WP.1).

ISA, 2020. Recommendations for the guidance of contractors for the assessment of the possible environmental impacts arising from exploration for marine minerals in the Area. ISBA/25/LTC/6/Rev.1 (Issued by the Legal and Technical Commission. Kingston, 4–15 March 2019. (Replaces ISBA/19/LTC/8).

Janssen A, Kaiser S, Meirner K, Brenke N, Menot L, Martinez Arbizu P (2015) A Reverse Taxonomic Approach to Assess Macrofaunal Distribution Patterns in Abyssal Pacific Polymetallic Nodule Fields. PLoS ONE 10(2): e0117790. doi:10.1371/journal.pone .0117790.

Jaun C, Van Rooij D, de Bruycker W 2018. An assessment of bottom current controlled sedimentation in Pacific Ocean abyssal environments. Marine Geology 403: 20-33.

Johnson K, Johnson B and Johnson H, 2020. Monterey Bay Aquarium Research Institute. Periodic Table of Elements in the Ocean. https://www.mbari.org/science/upper-ocean-systems/chemical-sensor-group/periodic-table-of-elements-in-the-ocean/ (accessed 15 Nov 2020).

Jones DOB, Kaiser S, Sweetman AK, Smith CR, Menot L, Vink A, et al. 2017. Biological responses to disturbance from simulated deep-sea polymetallic nodule mining. PLoS ONE 12(2): e0171750. https://doi.org/10.1371/journal.pone.0171750.

Jones, RT., "CONROAST – DC arc smelting of dead-roasted sulphide concentrates", Sulphide Smelting 2002, TMS, p. 435-56.

Jung H-S, Lee C-B, Jeong K-S, Kang J-K, 1998. Geochemical and mineralogical characteristics in two- color core sediments from the Korea Deep Ocean Study (KODOS) area, northeast equatorial Pacific. Marine Geology 144: 295-309.

Kaiser S, Smith CR, Arbizu PM, 2017. Editorial: Biodiversity of the Clarion Clipperton Fracture Zone. Marine Biodiversity, 47: 259-264.

Kamenskaya, O. E., Melnik, V. F. & Gooday, A. J., 2013. Giant protists (xenophyophores and komokiaceans) from the Clarion-Clipperton ferromanganese nodule field (eastern Pacific). Biology Bulletin Reviews 3, 388–398.

Karl DM, Letelier RM, Tupas LM, Dore JE, Christian JR, Winn CD, 1995. Ecosystem changes in the North Pacific subtropical gyre attributed to the 1991-92 El Nino. Nature 373:230-234.

Kaufman, R and Latimer, J. P., 1971. "The design and operation of a prototype deep ocean mining ship", Proceedings Society of Naval Architects and Marine Engineers, Spring Meetings, Honolulu, HI Vol. 3: 1-24.

Kaufman, R., Latimer, J. P., & Tolefson, D. C. (1985). The Design and Operation of a Pacific Ocean Deep-Ocean Mining Test Ship: R/V Deepsea Miner II OTC 4910. Offshore Technology Conference. Houston: SPE.

Kazmin Y 2009. Chapter 7 Geology of the Clarion Clipperton Zone: Existing geological information in respect of polymetallic nodules. In ISA 2009 (Establishment of a geological model of polymetallic nodule deposits in the Clarion-Clipperton Fracture Zone of the Equatorial North Pacific Ocean. Proceedings of the International Seabed Authority's Workshop held 13-20 May, 2003 in Nadi, Fiji).

Kennecott Exploration Inc., 1976. "Results of Air Lift Nodule Impact Simulation", Proprietary Report, TM-76-331.

Kennecott Exploration Inc., 1977. "The Air Lift Experiment", Proprietary Report, TAC-S-143.

Kennecott Exploration Inc., 1978. "Development of a Deep Ocean Manganese Nodule Collector System", Proprietary Report TAC-S-168.

Kennecott Exploration, Inc.,1978c. "Lift Pump Assessment and Comparison", Proprietary Report TAC-S-157.

Kennecott Copper Corporation - Ledgemont Laboratory. (1977). Shipboard Nodule Material Handling (proprietary report). Lexington, Massachusetts: Kennecott Exploration Inc.

Kim HJ, Hyeong K, Yoo CM, Chi SB, Khim BK, Kim D 2010. Seasonal variations of particle fluxes in the north eastern equatorial Pacific during weak El Nino and normal periods. Geosci J 14:415-422.

Kingston Process Metallurgy, 2020. Techno-economic evaluation of converting existing RKEF NPI facilities in China/Indonesia from processing Ni laterite ore to processing sea nodules. As part of KPM Project P1609 for DeepGreen Resources. February 21, 2020.

Kotlinski, R. and Stoyanova, V., 2006 Buried and surface polymetallic nodule distribution in the eastern Clarion–Clipperton Zone: main distinctions and similarities. Advances in Geosciences Vol. 9: Solid Earth, Ocean Science & Atmospheric Science (2006) Eds. Yun-Tai Chen et al. World Scientific Publishing Company, pp 67-74.

Kuhn 2015. RV SONNE S0240 Cruise Report I Fahrtbericht. Bundesanstalt tor Geowissenschaften und Rohstoffe (BGR).

Kukert H, Smith CR. 1992. Disturbance, colonisation and succession in deep-sea ecosystems. Trends in ecology and evolution 2:359-363.

LeCourt, E. J and Williams, D. W. (1971) "Deep Ocean Mining – New Application for Oil Field and Marine Equipment", Proceedings, Off-shore Technology Conference, Paper OTC 1412.

Lee, G.C, Kim, J., Chi, S.B., Ko, Y.T and Ham, D.J., 2008. Examination for correction factor for manganese nodule abundance using the free fall grab and box corer. The Sea: Journal of the Korean Society of Oceanography, Vol 13, No. 3 pp 280-285.

Leitner AB, Neuheimer AB, Donlon E, Smith CR, Drazen JC 2017. Environmental and bathymetric influences on abyssal bait-attending communities of the Clarion Clipperton Zone. Deep Sea Research Part I 125: 65-80.

Levin LA, Mengerink K, Gjerde KM, Rowden AA, Van Dover CL, Clark MR, Ramirez-Llodra E, Currie B, Smith CR, Sato KN, Gallo N, Sweetman AK, Lily H, Armstrong CW and Brider, J, 2016. Defining "serious harm" to the marine environment in the context of deep-seabed mining. Marine Policy, 74, 245-259.

Levin PS, Fogarty MJ, Murawski SA, Fluharty D 2009. Integrated Ecosystem Assessments: Developing the Scientific Basis for Ecosystem-Based Management of the Ocean. PLoS Biol 7(1): e1000014. https://doi.org/10.1371/journal.pbio.1000014.

Lewis, E. J. (1978), "Tapping the World's Deepest, Wettest Mine", Popular Mechanics, Nov. 1978.

Libralato S, Pranovi F, Stergiou K, Link J. 2014. Trophodynamics in marine ecology: 70 years after Lindeman. Mar. Ecol. Prog. Ser. 512, 1–7. (doi:10.3354/meps11033).

Lindh MV, Maillot BM, Shulse CN, Gooday AJ, Amon DJ, Smith CR, Church MJ 2017. From the Surface to the Deep-Sea: Bacterial Distributions across Polymetallic Nodule Fields in the Clarion-Clipperton Zone of the Pacific Ocean. Frontiers in microbiology https://doi.org/10.3389/fmicb.2017.01696.

Mackinen, T., et al, 1998. Physical chemistry of direct nickel matte smelting. Sulphide Smelting '98, TMS, p. 59-68.

Manheim FT, 1978. Book review of G. P. Glasby, Marine manganese deposits. Geochemica et Cosmochimica Acta 42(5):541. Cited in: ISA. 2010. A geological model of polymetallic nodule deposits in the Clarion-Clipperton Fracture Zone and prospector's guide for polymetallic nodule deposits in the Clarion-Clipperton Fracture Zone. International Seabed Authority Technical Study.

Marshall NB, 1979. Developments in Deep-Sea Biology. Blandford, Developments in Deep-Sea Biology. Poole. Dorset: Blandford Press 1979. ISBN 0-7137-0797-6. https://doi.org/10.1002/iroh.19810660416.

Masanza, M.K., et al., 2014. Commissioning of a second cobalt recovery furnace at Nchanga smelter, 5th International Symposium on high-temperature metallurgical processes, TMS 2014, p. 217-27.

Mero J, 1965. The Mineral Resources of the sea. Volume 1 (Elsevier Oceanography Series).

Mewes K, Mogollón J, Picard A, Rühlemann C, Kuhn T, Nöthen K, Kasten S 2014. Impact of depositional and biogeochemical processes on small scale variations in nodule abundance in the Clarion-Clipperton Fracture Zone, Deep Sea Res., Part I, 91(0): 125–141, doi:10.1016/j.dsr.2014.06.00.

MHWirth, 2020. 30 years subsea diamond mining with MHWirth drilling equipment. 30 Years Subsea Diamond Mining with MHWirth Drilling Equipment. Downloaded 18 February 2021.

Milligan RJ, Morris KJ, Bett BJ, Durden JM, Jones DOB, Robert K, Ruhl HA, Bailey DM 2016. High-resolution study of the spatial distributions of abyssal fishes by autonomous underwater vehicle. Sci. Rep. 6, 1-12.

Millward, B, 2008. Practical challenges of manufacturing a 2.5-MW subsea motor. https://www.offshore-mag.com/articles/print/volume-68/issue-10/subsea/practical-challenges-of-manufacturing-a-25-mw-subsea-motor.html.

Molodtsova TN, Opresko DM 2017. Black corals (Anthozoa: Antipatharia) of the Clarion-Clipperton Fracture Zone. Marine Biodiversity, 47: 349. https://doi.org/10.1007/s12526-017-0659-6.

Morgan CL, Odunton NI, Jones AT 1999. Synthesis of environmental impacts of deep seabed mining. Marine georesources and geotechnology 17:307-356.

Morgan C. 2009. Geological model project implementation. Presentation from the ISA geological model workshop December 2009, Kingston, Jamaica.

Mullineaux LS 1987. Organisms living on manganese nodules and crusts: distribution and abundance at three North Pacific sites. Deep-Sea Research 34(2): 165-184.

Niner HJ, Ardron JA, Escobar EG, Gianni M, Jaeckel A, Jones DO, … and Van Dover CL, 2018. Deep-sea mining with no net loss of biodiversity—an impossible aim. Frontiers in Marine Science, 5, 53. https://doi.org/10.3389/fmars.2018.00053

NORI 2020a. NORI AREA D Environmental & Social Impact Assessment, Scoping, Terms of Reference and Plan of Work

NORI 2020b. Nauru Ocean Resources Inc. Annual Report for year ended 31 December 2019

Novikov G.V. and Bogdanova O. Y., 2007, Transformations of Ore Minerals in Genetically Different Oceanic Ferromanganese Rocks, ISSN 0024-4902, Lithology and Mineral Resources, 2007, Vol. 42, No. 4, pp. 303–317.

Paulikas D, Katona S, IIves E, and Ali SH, 2020. Life cycle climate change impacts of producing battery metals from land ores versus deep-sea polymetallic nodules. Journal of Cleaner Production, https://doi.org/10.1016/j.jclepro.2020.123822.

Pape E, Bezerra TN, Hauquier F, Vanreusel A 2017. Limited Spatial and Temporal Variability in Meiofauna and Nematode Communities at Distant but Environmentally Similar Sites in an Area of Interest for Deep-Sea Mining. https://doi.org/10.3389/fmars.2017.00205.

Pinkerton MH, Bradford-Grieve JM, Hanchet SM 2010. A balanced model of the food web of the Ross Sea Antarctica. CCAMLR Science, 17: 1-31.

Pinkerton MH, Bradford-Grieve JM 2014. Characterising food web structure to identify potential ecosystem effects of fishing in the Ross Sea, Antarctica. CES Journal of Marine Science, Volume 71, Issue 7, September/October 2014, Pages 1542–1553, https://doi.org/10.1093/icesjms/fst230

Pinkerton MH 2013. Ecosystem Modelling of the Chatham Rise. Research report prepared for Chatham Rock Phosphate, April 2013. NIWA Client Report No: WLG2013-17. Pp 183.

Polunin NVC, Morales-Nin B, Pawsey WE, Cartes JE, Pinnegar JK and Moranta J, 2001. Feeding relationships in Mediterranean bathyal assemblages elucidated by carbon and nitrogen stable isotope data. Marine Ecology Progress Series, 220: 13-23.

Priede IG, Godbold JA, King NJ, Collins MA 2010. Deep-sea demersal fish species richness in the Porcupine Seabight, NE Atlantic Ocean: Global and regional patterns. Marine Ecology 31: 247-260.

Purser A, Marcon Y, Hoving H-jT, Vecchione M, Piatkowski U, Eason D, Bluhm H, Boetius A 2016. Association of deep-sea incirrate octopods with manganese crusts and nodule fields in the Pacific Ocean. Current Biology 26: R1247-R1271, December 19, 2016.

Rajcevic, H., et al., 1982. Development of electric furnace slag cleaning at a secondary copper smelter, J. Metals, March 1982, p. 54-56.

Rizea, S. (2018b), "Air Lift Simulation Model Developments – Validation Against Published Results", Technical Note DRT-IRAD-SR-TN-01, 20 December.

Saito, T., Usami, T., Yamazaki, Y. (1989), "Lifting Characteristics of Manganese Nodules by Air-Lift-Pump on 200 m Vertical Test Plant", Marine Technology Society, Proceedings, Oceans '89 Conference.

Schultheiss, P. J. (1985). Physical and Geotechnical Properties of Sediments from Northwest Pacific: DSDP Leg 86, in Initial Reports of DSDP. Washington DC: U.S. Government Printing Office.

Sharma, R, Khadge, NH, and Jai Sankar S, 2013. Assessing the distribution and abundance of seabed minerals from seafloor. Int. J. Remote Sens., vol.34; 2013; 1691-1706.

SMM, 2020. Market intelligence study for Deep Green. October 2020.

Shaw, JL. (1993) "Nodule Mining –Three Miles Deep!", Marine Georesources and Geotechnology, Vol. 11, pp. 181-197.

Shulse CN, Maillot B, Smith CR, Church MJ (2016) Polymetallic nodules, sediments, and deep waters in the equatorial North Pacific exhibit highly diverse and distinct bacterial, archaeal, and microeukaryotic communities. MicrobiologyOpen 1-16. https://doi.org/10.1002/mbo3.428.

Simon-Lledo E, Bett BJ, Huvenne VAI, Schoening T, Benoist NMA, Jeffreys RM, Durden JM, Jones DOB 2019. Megafaunal variation in the abyssal landscape of the Clarion Clipperton zone. Progress in Oceanography 170: 119-133.

Simpson S and Batley G, 2016. Sediment quality assessment: a practical guide. 2nd edition. Edited by S. Simpson and G Batley. CSIRO Publishing, Clayton South, Australia.

Smith CR. 1999. The biological environment in the nodule provinces of the seep sea. In: Deep-seabed polymetallic nodule exploration: development of environmental guidelines. Proceedings of the International Seabed Authority's Workshop held in Sanya, Hainan Island, People's Republic of China. 1–5 June 1998 (ISA/99/02). p. 41–68.

Smith CR, Galeron J, Glover A, Gooday A, Kitazato H, Lambshead J, Menot L, Paterson G, Rogers A, Sibuet M. 2008. Biodiversity, species ranges, and gene flow in the abyssal Pacific nodule province: predicting and managing the impacts of deep seabed mining. ISA Technical Study No. 3, International Seabed Authority, Kingston, Jamaica.

Smith CR, Tunnicliffe B, Colaço A, Sweetman AK, Washburn T and Amon D' 2020. Deep-sea misconceptions cause underestimation of seabed-mining impacts. Science July 31, 2020. https://doi.org/10.1016/j.tree.2020.07.002.

Smith CR, Gaines S, Watling L, Friedlander A, Morgan C, Thurnhurr A, Mincks S, Rogers A, Clark M, et al, 2010. Areas of Particular Environmental Interest (or "Protected Areas") for Ecosystem Based Management of the Clarion-Clipperton Zone: Rationale and Recommendations to the International Seabed Authority. 20 Expert participants in the workshop to Design Marine Protected Areas for Seamounts and the Abyssal Nodule Province in Pacific High Seas, Oct 23-26, 2007, University of Hawaii. https://www.isa.org.jm/files/documents/EN/Workshops/2010/Pres/SMITH.pdf.

Solar M, 2009. Mechanical slag losses in laterite smelting – nickel, COM 2009, Sudbury, p. 277-291.

Son J, Kim KH, Kim HJ, Ju S-J, Yoo CM 2014. Evaluation of Similarity of Water Column Properties and Sinking Particles between Impact and Preserved Sites for Environmental Impact Assessment in the Korea Contracted Area for Manganese Nodule Development, NE Pacific. Ocean and Polar Research 36(4): 423-435.

Sorokin YI. 1971. Quantitative evaluation of the role of bacteria-plankton in the biological productivity of tropical Pacific waters. In: Vinogradov ME, editor. Life activity of pelagic communities in the ocean tropics. pp 98-134.

Sorokin, Yu. I., T. S. Petipa, and Yeo V. Pavlova. 1970. Quantitative estimate of marine bacterioplankton as a source of food. Oceanology 10:253-260. (Cited in Turner 1984)

SPC 2013. Deep Sea Minerals: Manganese Nodules, a physical, biological, environmental, and technical review. Baker E, and Beaudoin Y. (Eds.) Vol. 1B, Secretariat of the Pacific Community.

Spickermann R, 2012. Rare earth content of manganese nodules in the Lockheed Martin Clarion-Clipperton Zone exploration areas. Proceedings Off-shore Technology Conference, Houston Texas.

Sridhar R, Jones WE, and Warner JS, 1976. Extraction of copper, nickel and cobalt from polymetallic nodules, JOM, April 1976, p 32.

Stoyanova V. 2012. Megafaunal diversity associated with Deep-Sea nodule bearing habitats in the eastern part of the Clarion Clipperton Zone, NE Pacific. 12th International Multidisciplinary Scientific GeoConference, www.sgem.org, SGEM2012 Conference Proceedings/ ISSN 1314-2704, June 17-23, 2012, Vol. 1, 645 - 652 pp.

Swaddling A 2016. Pacific ACP States, Regional environmental management framework for deep sea minerals exploration and exploitation. Suva, Fiji 2016 Prepared under the SPC-EU EDF 10 Deep Sea Minerals Project. SPC Noumea. http://dsm.gsd.spc.int/index.php/publications-and-reports.

Swaddling et al. 2016. Pacific-ACP states regional scientific research guidelines for deep sea minerals. Suva, Fiji 2016 Prepared under the SPC-EU EDF10 Deep Sea Minerals Project, by the Pacific Community (SPC) and the National Institute of Water and Atmospheric Research (NIWA) of New Zealand.

Tae-Kyeong Yeu ; Suk-Min Yoon ; Sup Hong ; Hyung-Woo Kim ; Chang-Ho Lee ; Jin-Ho Kim ; Cheon-Hong Min and Jong-Su Choi (2014) "Steering performance test of underwater mining robot" Proceedings Oceans 2014, IEEE, St. John's, 14-19 Sept.

Tannuri, E. A., Morishita, H. M., Simos, A. N., Saad, A. C., Correa da Silva, S. H., Matos, V. L., & Sphaier, S. H. (2009). DP Assisted Offloading Operations in Brazilian Water. Dynamic Positioning Conference. Marine Technology Society.

Tetsuyoshi Kohga et al, 1995. Recovering Iron, Manganese, Copper, Cobalt, and High Purity Nickel from Polymetallic nodules, JOM, December 1995, p 40.

Thiel H, Schriever G, Bussau C, Borowski C 1993. Manganese nodule crevice fauna. Deep-Sea Research I 40(2):419-423.

Thiel H, Schriever G, Ahnert A, Bluhm H, Borowski C, Vopel K. 2001. The large-scale environmental impact experiment DISCOL - reflection and foresight. DeepSea Research 11(48):3869-3882.

Tilot V, 2006. Biodiversity and distribution of megafauna. Vol. 1: The polymetallic nodule ecosystem of the Eastern Equatorial Pacific Ocean; Vol. 2: Annotated photographic atlas of the echinoderms of the Clarion-Clipperton fracture zone. Paris, UNESCO/IOC, 2006 (IOC Technical Series, 69).

Tilot V, 2006a. Biodiversity and distribution of faunal assemblages. Vol. 3. Options for the management and conservation of the nodule ecosystem in the Clarion-Clipperton Fracture Zone: scientific, legal and institutional aspects. Paris, UNESCO/IOC, 2010 (IOC Technical Series, 69).

Tilot V, Ormond R, Moreno Navas J, Catalá TS 2018. The Benthic Megafaunal Assemblages of the CCZ (Eastern Pacific) and an Approach to their Management in the Face of Threatened Anthropogenic Impacts. Frontiers in Marine Science. 5:7. doi: 10.3389/fmars.2018.00007.

Tomic B, 2020. Turkey expands drill fleet. Offshore Engineer, 21 February 2020. .https://www.oedigital.com/news/475897-turkey-expands-drillship-fleet.

Turner JT, 2002. Zooplankton fecal pellets, marine snow and sinking phytoplankton blooms. Aquatic microbial Ecology 27: 57-102.

Turner JT, 1984. The Feeding Ecology of Some Zooplankters That are Important Prey Items of Larval Fish. NOAA Technical Report NMFS 7. U.S. DEPARTMENT OF COMMERCE National Oceanic and Atmospheric Administration National Marine Fisheries Service.

UNEP-WCMC (2016). Marine No Net Loss: A Feasibility Assessment of Implementing no Net Loss of Biodiversity in the Sea. Cambridge.

United Nations, 1970. Declaration 2749 (XXV). Declaration of Principles Governing the Sea-Bed and the Ocean Floor, and the Subsoil Thereof, beyond the Limits of National Jurisdiction.

UTEC 2015. Deepsea nodule collector vehicle mobility study and track sizing. UTEC Geomarine Report No. SG-DRT0002-1-0, prepared for Deep Reach Technology.

Vanreusel A, Hilario A, Ribeiro P, Menot L, and Martínez Arbizu P, 2016. Threatened by mining, polymetallic nodules are required to preserve abyssal epifauna. Sci Rep 6, 26808. https://doi.org/10.1038/srep26808.

Veillette J, Sarrazin J, Gooday AJ, Galeron J, Caprais JC, Vangriesheim A, Juniper SK, 2007a. Ferromanganese nodule fauna in the Tropical North Pacific Ocean: species richness, faunal cover and spatial distribution. Deep-Sea Research. Part I, Oceanographic Research Papers, 54: 1912–1935.

Veillette, J, Juniper SK, Gooday AJ, Sarrazin J 2007b. Influence of surface texture and microhabitat heterogeneity in structuring nodule faunal communities. Deep-Sea Research. Part I, Oceanographic Research Papers, 54: 1936–1943.

Volz JB, Mogollon JM, Geibert W, Arbizu PD, Koschinsky A, Kaasten S 2018: Natural spatial variability of depositional conditions, biogeochemical processes and element fluxes in sediments of the eastern Clarion-Clipperton Zone, Pacific Ocean. Deep Sea Research Part 1 140: 159-172.

Wasmund B, Voermann N, Haneman B, Sarvinis J, Sheehan G, 2011. Implementing New Technologies in Metallurgical Processes: Building Plants that Work. Canadian Institute of Mining Conference (CIM / COM), 2011.

Washburn TW, Turner PJ, Durden JM, Jones DO, Weaver, P and Van Dover CL. 2019. Ecological risk assessment for deep-sea mining. Ocean & Coastal Management, 176, 24-39.

World Ocean Atlas 2018. (WOA18). https://www.nodc.noaa.gov/OC5/woa18/

Yu OH, Lee H-G, Kim D, Wi JH, Kim KH, Yoo CM 2018. Characterisation of deep-sea macrofauna in the Korean exploration claim area in the Clarion Clipperton Fracture Zone, Northeastern Pacific Ocean. Ocean Science Journal 53(2):301-314.

25 Reliance on information provided by the registrant

AMC has relied upon information provided by the registrant in preparing its findings and conclusions regarding the following aspects of modifying factors:

I.   Macroeconomic trends, data, and assumptions, and market studies as, for example, presented in Section 16;

II.   Marketing information and plans within the control of the registrant as, for example, presented in Section 16, 18.1, 18.2, 18.5;

III.   Legal matters outside the expertise of the qualified person, such as statutory and regulatory interpretations affecting the Project as, for example, described in Section 3, 13, and 20;

IV.   Environmental matters outside the expertise of the qualified person as, for example, described in Section 17;

V.   Accommodations the registrant commits or plans to provide to local individuals or groups in connection with its mine plans as, for example, described in Section 20; and

VI.   Governmental factors outside the expertise of the qualified person as, for example, described in Section 3, 19.1.2.

Date

The effective date of this Technical Report Summary is 31 December 2020.

Signature

AMC Consultants Pty Ltd

Canadian Engineering Associates Ltd

Deep Reach Technology Inc

MARGIN Marine Geoscience Innovation

Our offices

Australia

Adelaide

Level 1, 12 Pirie Street
Adelaide SA 5000 Australia

T +61 8 8201 1800
E adelaide@amcconsultants.com

Brisbane

Level 21, 179 Turbot Street
Brisbane Qld 4000 Australia

T +61 7 3230 9000
E brisbane@amcconsultants.com

Melbourne

Level 29, 140 William Street
Melbourne Vic 3000 Australia

T +61 3 8601 3300
E melbourne@amcconsultants.com

Perth

Level 1, 1100 Hay Street
West Perth WA 6005 Australia

T +61 8 6330 1100
E perth@amcconsultants.com

Canada

Toronto

TD Canada Trust Tower
161 Bay Street, 27th Floor
Toronto, ON M5J 2S1 Canada

T +1 416 640 1212
E toronto@amcconsultants.com

Vancouver

200 Granville Street, Suite 202
Vancouver BC V6C 1S4 Canada

T +1 604 669 0044
E vancouver@amcconsultants.com

Singapore

Singapore

30 Raffles Place, Level 17 Chevron House
Singapore 048622

T +65 6809 6132
E singapore@amcconsultants.com

Russia

Moscow

5/2, 1 Kazachiy Pereulok, Building 1
Moscow 119017 Russian Federation

T +7 495 134 01 86
E moscow@amcconsultants.com

United Kingdom

Maidenhead

Registered in England and Wales
Company No. 3688365

Level 7, Nicholsons House
Nicholsons Walk, Maidenhead
Berkshire SL6 1LD United Kingdom

T +44 1628 778 256
E maidenhead@amcconsultants.com

Registered Office: Ground Floor,
Unit 501 Centennial Park
Centennial Avenue
Elstree, Borehamwood
Hertfordshire, WD6 3FG United Kingdom